NASA/CP-2003-212403

National Educators' Workshop: Update 2002

Standard Experiments in Engineering, Materials Science, and Technology

Compiled by
Edwin J. Prior
Langley Research Center, Hampton, Virginia

James A. Jacobs
Norfolk State University, Norfolk, Virginia

W. Richard Chung
San Jose State University, San Jose, California

Proceedings of a workshop sponsored jointly by the National Aeronautics and Space Administration, Washington, DC; NASA Langley Research Center, Hampton, Virginia; Norfolk State University, Norfolk, Virginia; The ASM International Foundation; Air Force Office of Scientific Research; IBM Almaden Research Center; College of Engineering, San Jose State University; Seagate Technology, Inc.; Semiconductor Equipment and Materials International; and UltratechStepper and held in San Jose, California
October 13–16, 2002

National Aeronautics and
Space Administration

Langley Research Center
Hampton, Virginia 23681-2199

May 2003

Acknowledgments

We greatly appreciate the support provided by these organizations:

National Aeronautics and Space Administration – Langley Research Center
Air Force Office of Scientific Research
ASM International Foundation
College of Engineering, San Jose State University
School of Science and Technology, Norfolk State University
Seagate Technology, Inc.
Semiconductor Equipment and Materials International
UltratechStepper
American Ceramics Society, Northern California Section
American Society for Engineering Education
Columbia University
Ford Motor Company
International Council for Materials Education
Materials Science and Engineering Laboratories – National Institute of Standards and Technology
Mission College
National Aeronautics and Space Administration – Ames Research Center
Technology Commercialization Center
University of California – Davis
Workforce Silicon Valley

Available from:

NASA Center for AeroSpace Information (CASI)
7121 Standard Drive
Hanover, MD 21076-1320
(301) 621-0390

National Technical Information Service (NTIS)
5285 Port Royal Road
Springfield, VA 22161-2171
(703) 605-6000

PREFACE

The 17th Annual National Educators' Workshop, NEW:Update 2002, faced many challenges due to the slow economy; however, the hard work and creativity of the Organizing Committee, host institutions, and agencies resulted in a most successful event in fantastic venues. NEW:Update 2002 was built on themes, activities, and presentations based on extensive evaluations from participants of previous workshops as we continued efforts to strengthen materials and technical education. About 125 participants witnessed demonstrations of experiments, discussed issues of materials science and engineering (MS&E) with people from education, industry, government, and technical societies and heard plenary sessions on leading edge developments. As seen in this conference proceeding, participants were fortunate to engage in valuable mini workshops in state-of-the art laboratories. Faculty, from as far as Australia, were in attendance representing high schools, community colleges, smaller colleges, and major universities. Undergraduate and graduate students also attended and presented.

Our local hosts were key to quality events. Organizers from San Jose State University, IBM, Seagate, SEMI, and UltratechStepper coordinated the many scientists, engineers, professors and other staff by providing funding, opening their facilities, and developing presentations and activities. NEW:Update 2002 participants saw demonstrations of about fifty experiments and aided in evaluating them. We also heard updated information relating to materials science, engineering and technology presented at mini plenary sessions. Local faculty listed in this conference proceeding tackled numerous challenges to keep NEW:Update 2002 on track.

This publication provides experiments and demonstrations that can serve as a valuable guide to faculty who are interested in useful activities for their students. The material was the result of years of research aimed at better methods of teaching technical subjects. The experiments developed by faculty, scientists, and engineers throughout the United States and abroad add to the collection from past workshops. They include a blend of experiments on new materials and traditional materials.

Experiments underwent an extensive peer review process. After submission of abstracts, selected authors were notified of their acceptance and given the format for submission of experiments. Experiments were reviewed by a panel of specialists through the cooperation of the International Council for Materials Education (ICME). Comments from workshop participants provided additional feedback, which authors used to make final revisions, which were then submitted to the NASA editorial group for this publication.

The ICME encourages authors of experiments to submit their work to the *Journal of Materials Education (JME)*. The *JME* offers valuable teaching and curriculum aids including instructional modules on emerging materials technology, experiments, book reviews, and editorials to materials educators. See *JME* subscription information on pages xvii – xx.

Critiques were made of the workshop to provide continuing improvement of this activity. The evaluations and recommendations made by participants provide valuable feedback for the planning of subsequent NEW:Updates. NEW:Update 2003 will be held in Hampton and Newport News, Virginia, on October 19-22, 2003. Hosts include NASA Langley Research Center, Thomas Jefferson National Accelerator Facility, and Norfolk State University. Please see http://MST-Online.nsu.edu. Click on NEW:Update 2003 for developing information. Join us on the beautiful and historic Virginia Peninsula.

NEW:Update 2002 and the series of workshops that go back to 1986 are, to our knowledge, the only national workshops, or gatherings for materials educators that have a focus on the full range of issues on strategies for better teaching the full complement of materials. Displays by publishers, technical societies, and equipment suppliers added to the workshop's value.

We demonstrated the second edition of the CD-ROM *Experiments in Materials Science, Engineering and Technology 2* (EMSET2) with over 350 experiments from NEW:Updates. This CD-ROM is another example of cooperative efforts to support materials education. The primary contributions came from the many authors of the demonstrations and experiments for NEW:Updates. Funding for the CD came from both private industry and federal agencies. Please see the information on page xiii for obtaining the CD.

Special thanks goes to those on our national organizing committee, management team, hosts, sponsors, and especially those of you who developed and shared your ideas for experiments, demonstrations, and innovative approaches to teaching.

The Organizing Committee hopes that the experiments and technical updated material in this publication will assist you in teaching materials science, engineering and technology. We would like to have your comments on their value and suggestions for their improvment. Please send comments to Jim Jacobs, School of Science and Technology, Norfolk State University, Norfolk, Virginia 23504 or e-mail to dplaclaire@nsu.edu.

CONTENTS

ORGANIZING COMMITTEE

James A. Jacobs
Workshop Co-chairperson
Norfolk State University

W. Richard Chung
Workshop Co-chairperson
San Jose State University

Diana P. LaClaire
Assistant Director
Norfolk State University

Emily Allen
San Jose State University

Lisa Anderson
Semiconductor Equipment and Materials International

John E. E. Baglin
IBM-Almaden Research Center

Robert Berrettini
International Council on Materials Education

Susan S. Chang
Seagate Technology, Inc.

Hoffman Cheung
Seagate Recording Media

Jeanne Deatherage
ASM International Foundation

Rendee Dore
Mission College

Leonard W. Fine
Columbia University

James E. Gardner
Technology Commercial Center

Olivia Graeve
University of Nevada-Reno

Said Jahanmir
National Institute of Standards and Technology

Thomas F. Kilduff
Emeritus, Thomas Nelson Community College

Jeff J. Mack
Seagate Technology, Inc.

Ruth Madalena
Workforce Silicon Valley

Alfred E. McKenney
IBM Corporation, Retired

Mike Meier
University of California-Davis

Cliff Monroe
Mission College

Roy Okuda
San Jose State University

Mark Palmer
American Society for Engineering Education

Marite Pantangoo
Semiconductor Equipment and Materials International

Edwin J. Prior
National Aeronautics and Space Administration

Richard Ricker
Materials Science & Engineering Laboratory-NIST

Wayne H. Tobler
UltratechStepper

Richard Chung and Jim Jacobs

Jim Jacobs, Diana LaClaire, and Nikki Harris

The New EMSET2 CD ROM from Jim Jacobs, Al McKenney and Prentice Hall Publishing

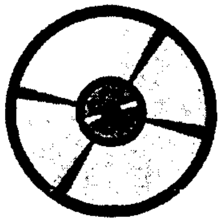

The CD ROM *Experiments in Materials Science, Engineering and Technology 2* (*EMSET2*) is now available!

For more than a decade, the National Educators' Workshops have enabled educators to participate in seminars of peer-reviewed experiments and demonstrations in materials science, engineering and technology. Following each workshop, these papers were published in an annual compendium, with the generous support of NASA.

Now, with the assistance from NASA and many other governmental, educational and industrial organizations, we have been able to publish thirteen yearly volumes of these papers in an easily used format, the *EMSET2* CD ROM. This is an expanded and updated version of the original *EMSET* CD ROM. This new version runs on all platforms and uses the universally-accepted Adobe Acrobat format for retrieval, display and printing.

To help the user, the nearly 350 experiments and demonstrations are indexed under the following seven categories:

- ✓ Structure, Testing and Evaluation
- ✓ Metals
- ✓ Polymers
- ✓ Ceramics
- ✓ Composites
- ✓ Electronic and Optical Materials
- ✓ Materials Curriculum

The user can find the material he or she wants by browsing the tables of contents or by searching for author, title, institution, or key word. Then the documents can be reviewed and used by displaying an exact image of the paper(s), including text, graphs, pictures, formulae, etc. or by printing the paper as written or even by copying the text and/or graphics into a word processor for editing.

To preview an individual demo version please reference ISBN 0-13-019475-1 and contact:
Melissa Orsborn
Prentice Hall
445 Hutchinson Ave. Fourth Floor
Columbus, Ohio 43235
1-800-228-7854 ext. 3622
Melissa_Orsborn@prenhall.com

Or to purchase the complete *EMSET2* CD ROM please reference ISBN 0-13-030534-0 and contact:
Prentice Hall Customer Service
1-800-922-0579

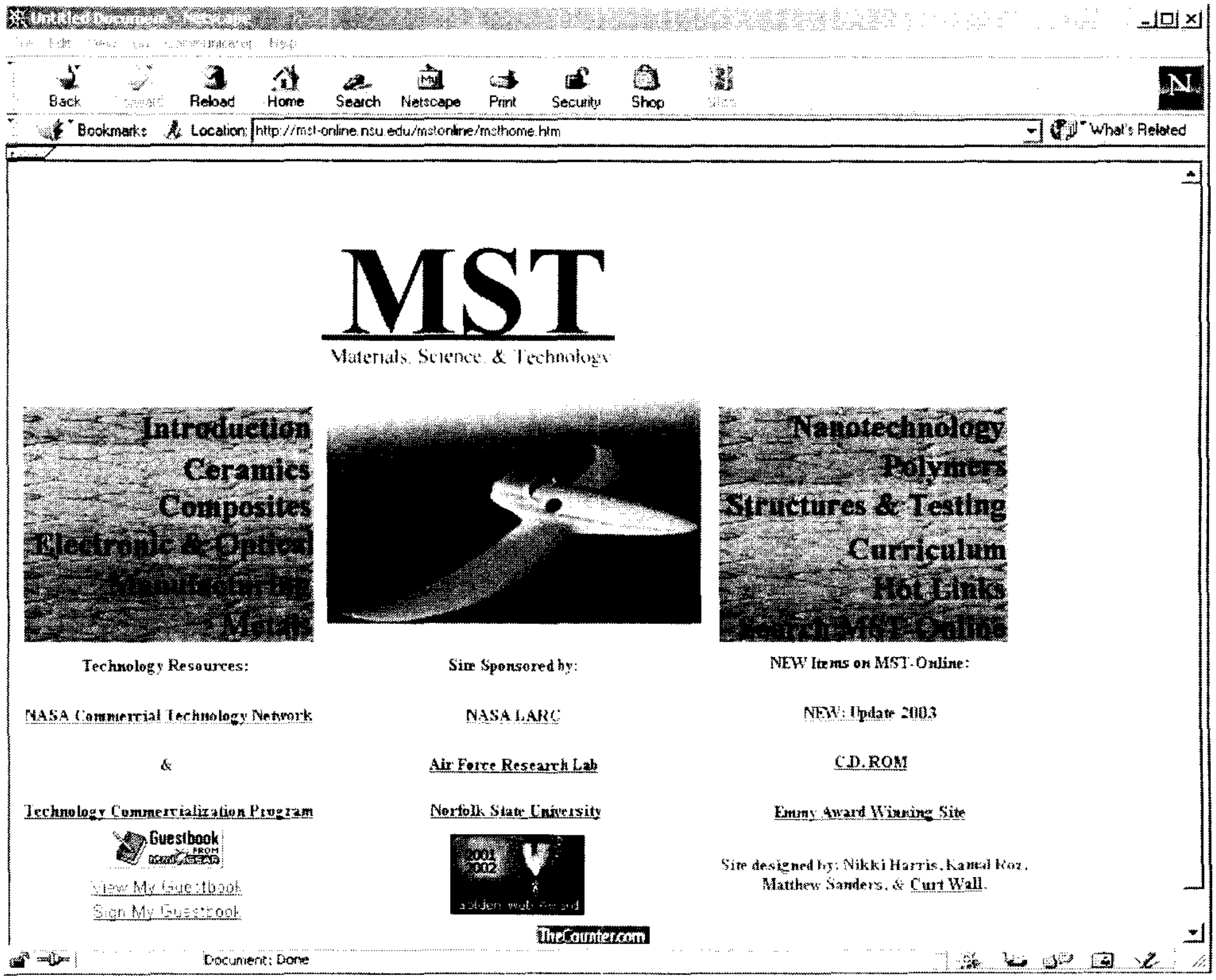

Technology Resources:

NASA Commercial Technology Network

&

Technology Commercialization Program

Site Sponsored by:

NASA LARC

Air Force Research Lab

Norfolk State University

NEW Items on MST-Online:

NEW: Update 2003

C.D. ROM

Emmy Award Winning Site

Site designed by: Nikki Harris, Kamal Roz, Matthew Sanders, & Curt Wall.

Click on, Http://MST-Online.nsu.edu> and

Link to the cool

World of Materials,

Science, & Technology

REVIEWERS

Harvey Abramowitz
Department of Engineering
Purdue University – Calumet

Alex O. Aning
Engineering Fundamentals
Virginia Tech

Aaron S. Blicblau
School of Engineering and Science
Swinburne University of Technology

Witold Brostow
Department of Materials Science
University of North Texas

L. Roy Bunnell
Material Science Department
Southridge High School

William Callister
Adjunct Professor of Metallurgy
University of Utah

G. Slade Cargill, III
Materials Science & Engineering Dept.
Lehigh University

Alexis G. Clare
NY State College of Ceramics
Alfred University

Michael Falk
Materials Science and Engineering
University of Michigan

Richard Griffin
MEEN Department
Texas A&M University

Peter Joyce
ME Department
U. S. Naval Academy

Isabel K. Lloyd
Materials & Nuclear Engr. Department
University of Maryland

Luz J. Martinez-Miranda
Dept. of Matls & Nuclear Engineering
University of Maryland

Mike Meier
Dept. of Chemical Engineering and
Materials Science
University of California, Davis

Devdas M. Pai
Mechanical Engineering
NC A&T State University

John M. Rusin
Department of Engineering
Edmonds Community College

Ronald E. Smelser
Department of Engineering
University of Idaho

Daniel Steinberg
Outreach Director
Princeton University

Mary B. Vollaro
Engineering Department
Western New England College

Edward L. Widener
Department of Mechanical Engineering
Purdue University

Registration

Diana LaClaire

Section title:

Subscriptions

Section contents :

Journal of Materials Education:

This price includes a handling fee of US$ 3, and air mail fourth class postage worldwide. Priority shipping is available for an additional US$6 per order, plus our shipping cost.

* $ 290/year for each of the years 2000 – 2002 (i.e. Vols. 22-24)
* $ 490/2 years for any two years in the 2000 - 2002 period
* $ 325/year for the year 2003 (Vol. 25)
* $ 550/2 years for the years 2003 - 2004

Back issues for 1999 and earlier years are available at US$ 50/issue

Payments should be made in the form of checks in US$ paid to
"University of North Texas"

with annotation
"for ICME"

and sent to:

Ms. Montserrat Salas
International Council on Materials Education
c/o University of North Texas
P.O. Box 305310
Denton, TX 76203-5310
USA

Journal of Materials Education - Spanish Edition

For subscription orders placed from within Mexico:
* Mexican pesos 1600/year for each of the years 2000 - 2003
* Mexican pesos 1750/year for the year 2004

Subscription orders within Mexico should be sent to:

Prof. Victor Sánchez Mendieta

Journal of Materials Education - Spanish Edition
Universidad Autónoma de Estado de México (UAEM)
Gómez Farias num. 200, esq. López Rayón, Col. Centro
C.P. 50000, Toluca, México

For subscription orders from all other countries, including air mail shipment:
* US $ 160/year for each of the years 2000 - 2003
* US $ 175/year for the year 2004

Subscription orders from all other countries must be accompanied by checks paid to
"University of North Texas"

with annotation
"for ICME"

and sent to:

Ms. Montserrat Salas
International Council on Materials Education
c/o University of North Texas
P.O. Box 305310
Denton, TX 76203-5310
USA

Journal of Materials Education
SUBMISSION OF PAPERS

Invitation to Authors

Authors are invited to submit manuscripts for publication in the ***Journal of Materials Education***. The Journal welcomes manuscripts on a wide variety of topics related to Materials Education, including pedagogical and technical subject areas. Articles will be carefully peer reviewed prior to acceptance for publication.

Format

Please refer to **Instructions for Authors**, at *http://www.unt.edu.icme/* or as published from time to time in the Journal. Manuscripts should be clearly written, and generally consistent with the Style Manual of the American Institute of Physics. Two (2) clear printed copies of the entire manuscript, including separate attached Figures and Tables, should be submitted, together with an "original". An electronic version of the manuscript, both text and graphics, is also required. In this version, the text should be in Microsoft Word, preferably for PCs, and objects or graphics files should be in standard, preferably editable, formats. Electronic files may be submitted as e-mail attachments, or mailed on diskette, CD or 100 MB Zip disk. They should be clearly labeled with all system and file information needed to facilitate handling. Authors who are unable to provide electronic files should so notify the Editor at the time of submission.

To facilitate the work of both reviewers and editors, please do not impose the Journal's 2-column layout in your manuscript/ file, and do not embed Figures and Tables in the body of the text.

Where to Send Manuscripts

All submissions will be carefully peer reviewed and must meet high standards for acceptance. Following revisions, if any, required by the editors, the article will be published.

Manuscripts may be submitted either in English or in Spanish, for inclusion initially in the corresponding edition of JME. Subsequent publication of articles selected for translation is also anticipated. The Journal appears also in Japanese, as a cover-to-cover translation of the English edition.

Send manuscripts in English to:

Prof. James A. Clum
Materials Science & Engineering Dept.
University of Wisconsin – Madison
1509 University Avenue
Madison, WI 53706-1595, USA

Tel.: 1 608 265 6067
Fax: 1 608 262 8353
jaclum@facstaff.wisc.edu

Send manuscripts in Spanish to:

Prof. Victor M. Castaño
Centro de Física Aplicada y Tecnología Avanzada
Universidad Nacional Autónoma de México
A. P. 1–1010
Santiago de Querétaro, Qro. 76000, México.

Tel.: (55) 56436150/51 or (442) 2381150/51
Fax: (55) 56234154/65 or (442) 2381154/65
meneses@servidor.unam.mx

Journal of Materials Education

PUBLICATION AND SUBSCRIPTION INFORMATION

Effective for orders placed after 1 January, 2003.

	English	Spanish**
Annual Subscription Rates		
a) For libraries and institutions	US$ 325 / yr	US$ 175 /yr
b) For individuals whose institution subscribes at the library rate	US$ 90 / yr	US$ 50 /yr
Single Issues *(Available only for Volume 21 and earlier)*	US$ 50 /issue	-

Prices include fourth class postage worldwide. Priority shipping is available for an additional US$ 15 per order.

Orders

Orders should be sent to the Publisher at the address below. Payment should be made by check in US$, paid to *"University of North Texas"*, and marked *"for ICME"*.

International Council on Materials Education
Attn: Ms. Montserrat Salas
University of North Texas
P.O. Box 305310
Denton, TX 76203-5310, USA

Tel.: +1 (940) 369-8336
Fax: +1 (940) 565-4824
e-mail: icme@marta.phys.unt.edu

We assume no responsibility for successful delivery of our shipments to addresses outside the USA. If you require shipping to a region of the world where receipt of goods is a problem, we recommend that you order via a subscription service or re-mailing service. Libraries in your area should be able to help you to locate a reliable U.S. agent.

****For Spanish Edition orders placed within Mexico:**

Annual Subscription Rates

a) For libraries and institutions	1750 Mexican pesos / year
b) For individuals whose institution subscribes	500 Mexican pesos / year

Orders placed within Mexico should be sent to the address below, together with checks in pesos, paid to *"Universidad Autónoma de Estado de México (UAEM)*:

Prof. Victor Sánchez Mendieta
Journal of Materials Education - Spanish Edition
Universidad Autónoma de Estado de México (UAEM)
Gomez Farias num. 200, esq. Lopez Rayon, Col. Centro
C.P. 50000, Toluca, México

REPRODUCTION RIGHTS

Purchase of a subscription automatically confers reproduction rights upon the subscriber and all members of the subscriber's institution. All other rights are reserved. Reproduction for use outside the subscribing institution is prohibited without permission of the copyright owner.

PUBLISHER

JME is published by the International Council on Materials Education, with offices at the address above, and also at the Center for Applied Physics and Advanced Technology Center, National Autonomous University of Mexico, A.P.I.-1010, Querétaro, Qro., Mexico 76000. meneses@servidor.unam.mx.

ISSN: 0738-7989

Printed and produced by the Autonomous University of the State of Mexico.

Row 1 front (L to R):
A.McKenney,. M. Vollaro, C. Monroe, B. Kawanami, E. Widener, R. Douglas, B. Callister, M. Zeng
Row 2 (L to R):
J. Jacobs, J. Deatherage, O. Graeve, R. Doré, K. Chen, R. A. Kimel, H. Rejali, F. Ekpo, S. Jahanmir, D. LaClaire
Row 3 (L to R):
R. Simoes, E. Allen, D. Vigliotti, N. Harris, A. Blicblau, E. Kedar, R. McCoy, V. Ravi, K. D. Song, D. Roylance
Row 4 (L to R):
D. Evans, J. Baglin, G. Holmes, J. Lumpp, S. Leach, A. Beattie, G. Lisensky, R. Chung, D. Palmgren, J. LaCombe
Row 5 (L to R):
E. Prior, S. Krause, B. Berrettini, J. Gardner, R. Griffin, G. Kridli, C. Graves. A. Wilkerson, D. Woodbury, M Meier
Row 6 (L to R)
D. S. Bethune, L. Geer, M. Rudes, R. Bunnell, A. Rowe

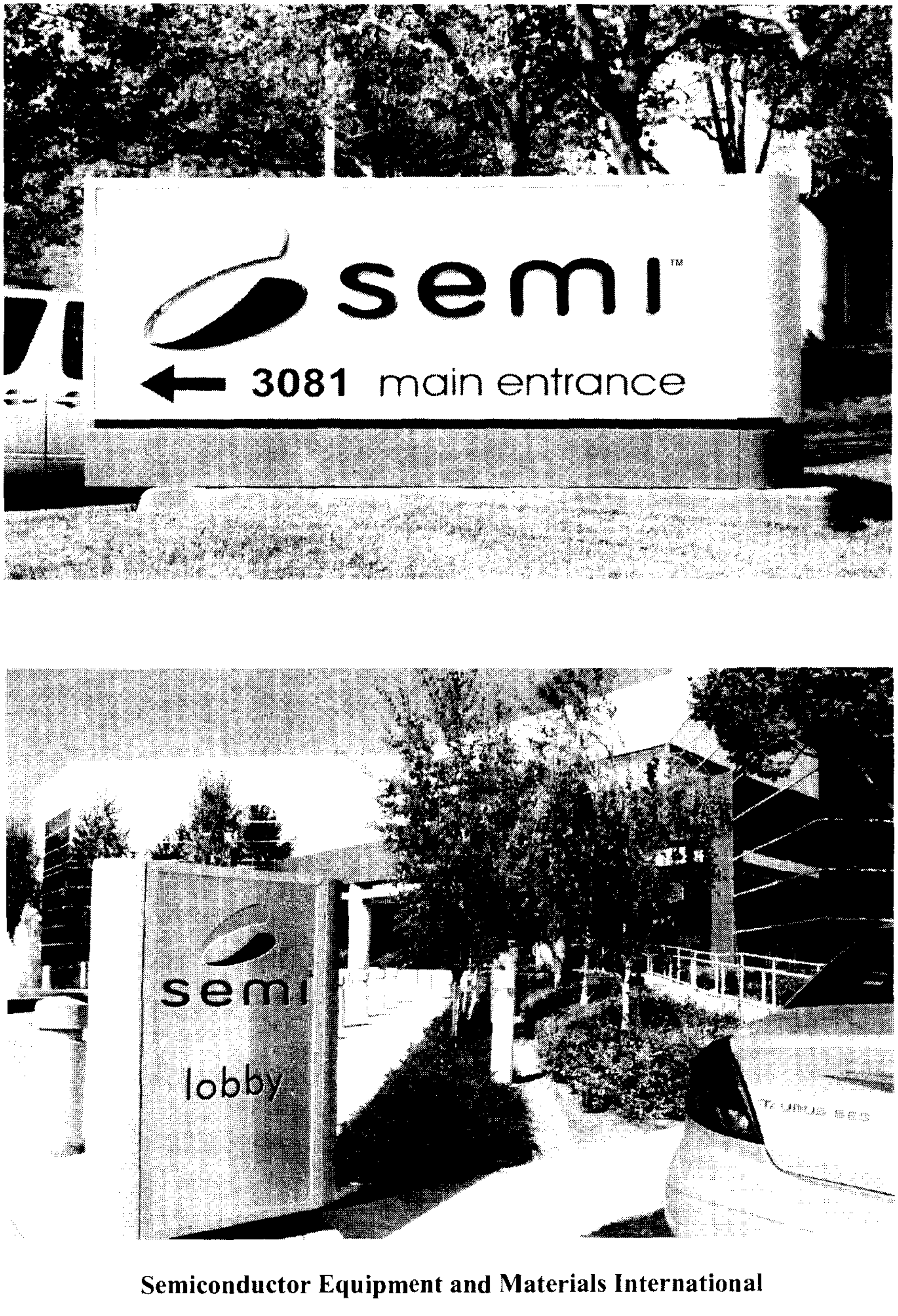

Semiconductor Equipment and Materials International

National Educators' Workshop 2002

PARTICIPANTS

Caroline Alexander
IBM Almaden

Emily L. Allen
Department of Chemical and Materials Engineering
San Jose State University
One Washington Square
San Jose, CA 95192-0086
408-924-4010
elallen@email.sjsu.edu

Aman Anand
1000 Towers Circle
Apartment South 718
Cape Girardeau, MO 63701
573-339-4376
amanfromcs@hotmail.com

Lisa Anderson
Semiconductor Equipment and
Materials International

John E. E. Baglin
IBM Almaden Research Center K19/D1
650 Harry Road
San Jose, CA 95120
408-927-2280
baglin@almaden.ibm.com

Alex D. Beattie
Modesto Junior College
435 College Avenue
Modesto, CA 95350
209-529-8735
beattiea@yosemite.cc.ca.us

Robert Berrettini
RR 1, 43 Lakeview Terrace
Harveys Lake, PA 18618
412-908-1884
E-mail berrettini@juno.com

Don Bethune
IBM

Aaron S. Blieblau
School of Engineering and Science
Swinburne University of Technology
P. O. Box 218
Hawthorn, Victoria
Australia 3122
+61 3 9214 8531 or 8372
ablieblau@swin.edu.au

L. Roy Bunnell
Materials Science Technology
Southridge High School
3320 Union Loop Road
Kennewick, WA 99338
509-734-3800
bunnro@ksd.org or roybunnell@aol.com

William D. Callister
University of Utah
2419 East 3510 South
Salt Lake City, UT 84109
801-278-8611
bill.callister@m.cc.utah.edu

Susan S. Chang
Seagate Technology, Inc.

Katherine C. Chen
Materials Engineering Department
California Polytechnic State University
San Luis Obispo, CA 93407
805-756-6634
kcchen@calpoly.edu

Hoffman Cheung
Seagate Recording Media
311 Turquoise Street
Milpitas, CA 95035
510-624-3585

W. Richard Chung
Department of Chemical and Materials Engineering
San Jose State University
San Jose, CA 95192-0082
408-924-3927
wrchung@email.sjsu.edu

Michelle Cotta
SEMI
3081 Zanker Road
San Jose, CA 95134
408-943-7989

Hans Coufal
IBM

Jai N. Dahiya
Professor of Physics & Associate Dean
College of Science & Mathematics
Southeast Missouri State University
One University Plaza, MS 6000
Cape Girardeau, MO 63701
573-651-2163
dahiya@physics.semo.edu

Jeane Deatherage
Administrator, Foundation Programs
ASM International Foundation
Materials Park, OH 44073
800-336-5152 ext 5533

Rendee Doré
Mission College
408-748-0927
DoreRendee@aol.com

Paul Doherty
The Exploratorium at San Francisco

Ransom W. Douglas
Design Technology
Norfolk State University
700 Park Avenue
Norfolk, VA 23504
757-823-8833
rdouglas@nsu.edu

Don Eigler
IBM

Efremfon Frank Ekpo
Bethune-Cookman College
640 Dr. M. M. Bethune Blvd.
Daytona Beach, FL 32114
386-481-2677
ekpoe@cookman.edu

Don Evans, Director
Center for Research on Education in Science
Arizona State University
Tempe, AZ 85287-5006
480-965-5350
devans@asu.edu

Leonard W. Fine
Department of Chemistry
Columbia University in the City of New York
Havemeyer Hall
New York, NY 10027
212-854-2017
fine@chem.columbia.edu

Jane Frommer
IBM

James Gardner
Technology Commercialization Center
12050 Jefferson Avenue, Suite 350
Newport News, VA 23601
757-269-0025
jgardner@teccenter.org

Larry Geer
Mission College and
Saratoga High School

Jerry Glembocki
Seagate Technology, Inc.

Marni Goldman
Stanford University
marni@chemeng.stanford.edu

Olivia Graeve
University of Nevada, Reno
1664 N. Virginia Street
MS 388
Reno, NV 89557
775-784-7098
oagraeve@unr.edu

Curtis M. Graves
NASA Langley Research Center
MS 400
Hampton, VA 23681-0001
757-864-3868
c.m.graves@larc.nasa.gov

Richard B. Griffin
Department of Mechanical Engineering
Texas A&M
College Station, TX 77843
rgriffin@mengr.tamu.edu

Nikki Harris
Norfolk State University
School of Science and Technology
700 Park Avenue
Norfolk, VA 23504
757-823-9421
neko08@excite.com

Craig Hawker
IBM

Dave Holmes
Senior VP Service Operations and Quality
Ultratech Stepper

Gale A. Holmes
National Institute of Standards and Technology
MS 8543, Polymers Division
Gaithersburg, MD 20899-8543
301-975-5280
holmes@enh.nist.gov

Jean-Paul Jacob
IBM

James A. Jacobs
School of Science and Technology
Norfolk State University
700 Park Avenue
Norfolk, VA 23504
757-823-8109
jajacobs@nsu.edu

Said Jahanmir
Ceramics Division
Materials, Room B 360
National Institute of Standards and Technology
100 Bureau Drive, MS 8520
Gaithersburg, MD 20899-8520
301-975-3671
said.jahanmir@nist.gov

Tony Jarrami
Seagate
47050 Kato Road
Freemont, CA 94538

Bruce Kawanami
Monta Vista High School
21840 McClellan Road
Cupertino, CA 95123
408-972-1753
bjkkb@hotmail.com

Eve Kedar
6121 Elmbridge Drive
San Jose, CA 95129
The Vega Girls Project
408-829-1163
evek@aol.com

Andrew Kellock
IBM

R. Allen Kimel
Pennsylvania State University
118C Steidle Building
University Park, PA 16802
814-863-8675
kimel@matse.psu.edu

Yulian Kin
Purdue University Calumet
2200 169th Street
Hammond, IN 46323
219-989-2684
kin@calumet.purdue.edu

Stephen Krause
Chemical and Materials Engineering Dept.
Arizona State University
Box 876006
Tempe, AZ 85287-6006
skrause@asu.edu

Ghassan Kridli
Department of Industrial and
Manufacturing Systems Engineering
University of Michigan-Dearborn
Dearborn, MI 48128-1491
gkridli@engin.umd.umich.edu

Diana P. LaClaire
School of Science and Technology
Norfolk State University
700 Park Avenue
Norfolk, VA 23504
757-823-9072
dplaclaire@nsu.edu

Jeffrey C. LaCombe
University of Nevada, Reno
Metallurgical & Materials Engineering
MS/388
Reno, NV 89557-0136
775-784-1797
lacomj@mines.unr.edu

Tin Lam
Seagate Recording Media

Sarah E. Leach
Mechanical Engineering Technology
Purdue University
1733 Northside Boulevard
South Bend, IN 46634-7111
574-237-4172
seleach@pusb.iusb.edu

David S. Licata
Lockheed Martin
111 Lockheed Martin Way
Sunnyvale, CA 94089
408-742-6390

Kathy Lin
Seagate
47050 Kato Road
Freemont, CA 94538

George Lisensky
Department of Chemistry
Beloit College
Beloit, WI 53511
608-363-2225
listnsky@beloit.edu

Bill Lu
Seagate Recording Media

Janet K. Lumpp
Electrical and Computer Engineering Dept.
University of Kentucky
453 Anderson Hall
Lexington, KY 40506-0046
859-257-4985
jklumpp@engr.uky.edu

Christopher Lutz
IBM

Jeff J. Mack
Seagate Technology, Inc.

Ruth Madalena
Workforce Silicon Valley

Robert A. McCoy
Mechanical Engineering Dept.
Youngstown State University
Youngstown, OH 44555
330-941-1736
ramccoy@cc.ysu.edu

Alfred E. McKenney
516 Fairfax Way
Williamsburg, VA 23185
757-221-0476
aem2@prodigy.net

Mike Meier
Department of Chemical Engineering and Materials Science
University of California, Davis
Davis, CA 95616
530-752-5166
mlmeier@ucdavis.edu
Meyya Meyyappan
Director, Center for Nanotechnology, MS 229-3
NASA Ames Research Center
Moffett Field, CA 94035
650-604-2616
Meyya@orbit.arc.nasa.gov

Dolores Miller
IBM Almaden
demiller@almaden.ibm.com

Cliff Monroe
Mission College

David Niebuhr
Materials Engineering
Civil & Environmental Engineering
California Polytechnic State University
1 Grand Avenue
San Luis Obispo, CA 93407
805-756-7163
dniebuhr@calpoly.edu

Stephen P. O'Brien
Dept. of Applied Physics & Applied Mathematics
Columbia University
200 S. W. Mudd, 500 West 120th Street
New York, NY 10027
212-854-9478
so188@columbia.edu

Roy Okuda
San Jose State University
okuda@sjsu.edu

Devdas M. Pai
NSF Center for Advanced Materials and Smart Structures
Department of Mechanical Engineering
North Carolina A&T State University
Greensboro, NC 27411
336-339-7620 ext. 316
pai@ncat.edu

Dale Palmgren
Arizona State University East
College of Technology & Applied Science
7001 E. Williams Field Road
Mesa, AZ 85212
480-727-1917
palmgren@asu.edu

Stuart Parkin
IBM

Ann Peterson
IBM

Edwin J. Prior
Office of Education
Mail Stop 400
Building 1216, Room 103
17 Langley Boulevard
NASA Langley Research Center
Hampton, VA 23681-0001
757-864-5800
E. J. PRIOR@LaRC.NASA.GOV

Vilupanur A. Ravi
California State Polytechnic University-Pomona
Chemical & Materials Engineering
3801 W. Temple Avenue
Pomona, CA 91768
909-869-6920
vravi@csupomona.edu

Hassan Rejali
California Polytechnic Institute-Pomona
3801 W. Temple Street
Pomona, CA 91768
909-869-2586
hmrejali@csupomona.edu

Charles Rettner
IBM

Phil Rice
IBM

H. Alan Rowe
Professor of Chemistry
Norfolk State University
Chemistry/Center for Materials Research
Norfolk, VA 23504
757-823-2248
harowe@nsu.edu

David K. Roylance
Massachusetts Institute of Technology
77 Massachusetts Avenue
Building 6, Room 202
Cambridge, MA 02139
617-253-3309
roylance@mit.edu

Merrill Rudes
Energy Concepts, Inc.
404 Washington Blvd.
Mundelein, IL 50050
847-837-8191
ecisales1@aol.com
mrudes@aol.com

Dan Rugar
IBM

Margaret Sam
San Jose State University

Campbell Scott
IBM

James F. Shackelford
Dept. of Chemical Engineering and
Materials Science
University of California
One Shields Avenue
Davis, CA 95616
530-752-4030
jfshackelford@ucdavis.edu

Mark Sherwood
IBM

Ricardo Simoes
Laboratory of Polymers
Department of Materials Science
University of North Texas
Denton, TX 76203-5310
940-565-3262
rsimoes@unt.edu

Kyo D. Song
Norfolk State University
700 Park Avenue
Norfolk, VA 23504
757-823-8105
ksong@nsu.edu

Jimmy Stephens
Prentice Hall
445 Hutchinson Avenue
Columbus, OH 43235
614-841-3725
jimmy_stephens@prenhall.com

N. Sundaresan
North Carolina A&T State University
Greensboro, NC 27410
336-33407620
mannur@ncat.edu

Wayne H. Tobler
UltratechStepper
3050 Zanker Road
San Jose, CA 95134
408-321-8835

Linda Vanasupa
California Polytechnic State University
San Luis Obispo, CA 93407
805-756-1537
lvanasup@tuba.calpoly.edu

Daniel P. Vigliotti
National Institute of Standards and Testing
Division 853
325 Broadway
Boulder, CO 80303-3328
303-497-3351
vigliotti@boulder.nist.gov

Mary B. Vollaro
Western New England College
1215 Wilbraham Road
Springfield, MA 01119
413-782-1490
mvollaro@wnec.edu

Charles Wade
IBM

Edward L. Widener
Purdue University
Knoy Hall 119
West Lafayette, IN 47907-1317
765-494-7521
elwidener@tech.purdue.edu

Amy Wilkerson
Applied Research Center
12050 Jefferson Avenue, Suite 713
Newport News, VA 23606
757-269-5760
alwilker@AS.WM.EDU

David Woodbury
Dept. Chemical Engineering and Materials Science
University of California-Davis
30 Oak Manor Court
Chico, CA 95926
530-345-6533
tekciw@aol.com

Deborah S. Yarnell
Prentice Hall
One Lake Street
Upper Saddle River, NJ 07458
201-236-7805
Debbie_Yarnell@prenhall.com

Ming Zeng
Department of Mechanical Engineering
The University of Akron
325 Sumner Street
Akron, OH 44325
Zengming168@yahoo.com

NATIONAL EDUCATORS' WORKSHOP

Update 2002: Standard Experiments in Engineering Materials, Science, and Technology

October 13–16, 2002 — San Jose, California

Sponsored by

National Aeronautics &
Space Administration
Langley Research Center

College of Engineering
San Jose State University

School of Science and Technology
Norfolk State University

Seagate Technology, Inc.

IBM-Almaden Research Center

UltratechStepper

Semiconductor Equipment
and Materials International

Air Force
Office of Scientific Research

ASM International

With the support of

American Ceramic Society
Columbia University
Lockheed Martin Space Systems Company
Prentice Hall
University of California-Davis

American Society for Engineering Education
International Council for Materials Education
International Council for Materials Education
Materials Science & Engineering Laboratories, NIST
Technology Commercialization Center
John Wiley & Sons

Don Evans

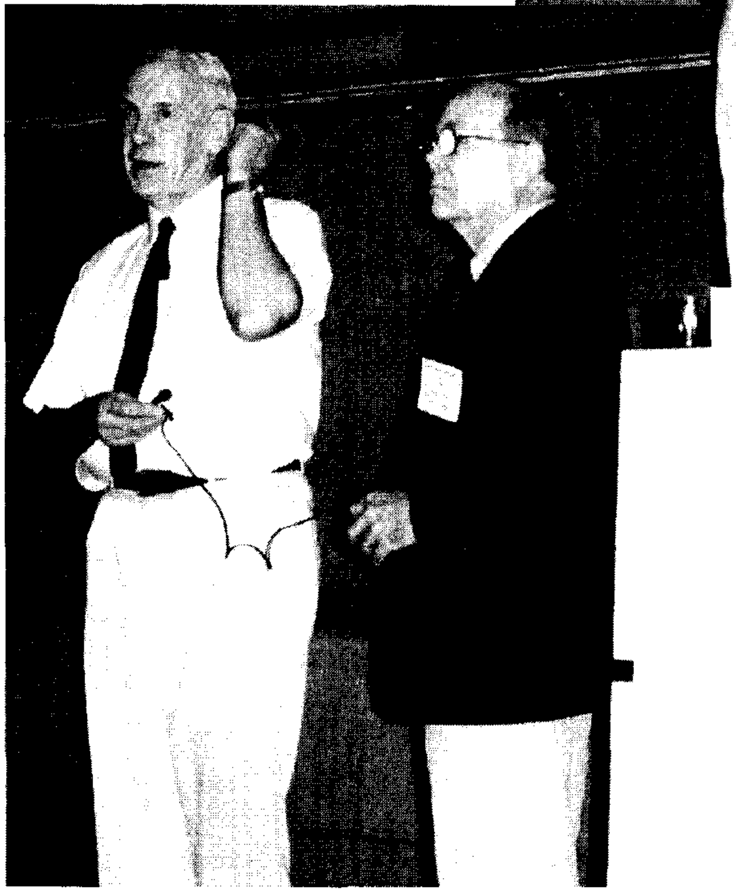

John Baglin and Don Evans

NATIONAL EDUCATORS' WORKSHOP

NEW:Update 2002

WORKSHOP AGENDA
AT
SAN JOSÉ STATE UNIVERSITY

SUNDAY, OCTOBER 13, 2002

1:00 – 3:30 p.m.	Lab Tours **Department of Chemical and Materials Engineering** *Materials Engineering Labs* *Microelectronics Process Engineering Lab* *Biochemical Engineering Lab* **Department of Technology, SJSU** *Product Design and Development Labs* *(Integrated instruction in Product Design, Materials and Processes*
3:30 – 3:45 p.m.	Welcome Remarks Dr. Belle Wei – Dean, SJSU College of Engineering
3:45 – 5:00 p.m.	**NANOTECHNOLOGY: OPPORTUNITIES AND CHALLENGES** Meyya Meyyappan – NASA Ames Research Center, Director, Center for Nanotechnology
5:00 – 7:00 p.m.	Reception sponsored by College of Engineering, San Jose State University

SUNDAY PROGRAM

San José State University

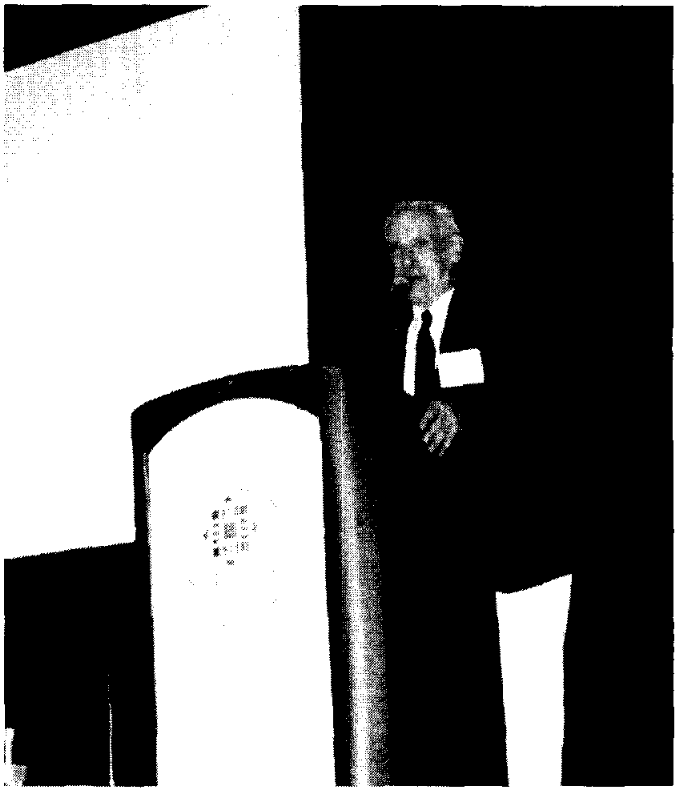

SUNDAY PROGRAM (Continued)

SUNDAY PROGRAM (Concluded)

Kyo Song, Jim Jacobs, Aaron Blicblau, Bill Callister and Ricardo Simões

MINI WORKSHOPS
MONDAY

SEAGATE

Group A – Fremont site:

Making a Magnetic Disk
1) Magnetic layer (MDP)
2) Carbon and lubricant
   Thin Film Characterization
3) Thin film composition and thickness (ESCA)
4) Lub type and carbon film composition (SIMS)

Group B – Milpitas site:

Reliability at Head-disk Interface
5) Mechanical tests (CSS, UMT, Flyability)
6) Electrical test (Discharge, voltage breakdown)
   Failure Analysis
7) Surface Analysis (AES, AFM)
8) Corrosion (FTIR, HC1, SO4 pickup)

SAN JOSE STATE UNIVERSITY

Solar cell fabrication workshop at SJSU's
Microelectronics Process Engineering Lab

LOCKHEED MARTIN

(open only to U. S. citizens who have previously registered and been cleared by security

1) Remote Sensing Space Sciences
2) Solar Array Product Center
3) Commercial Satellite Center

MINI WORKSHOPS

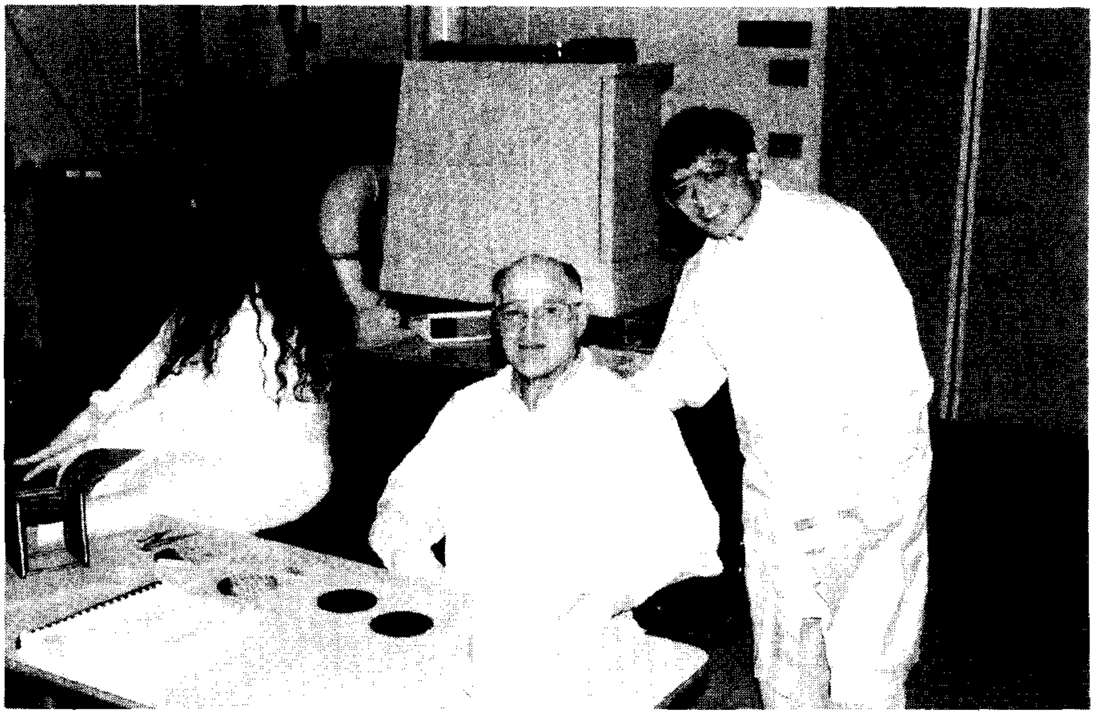

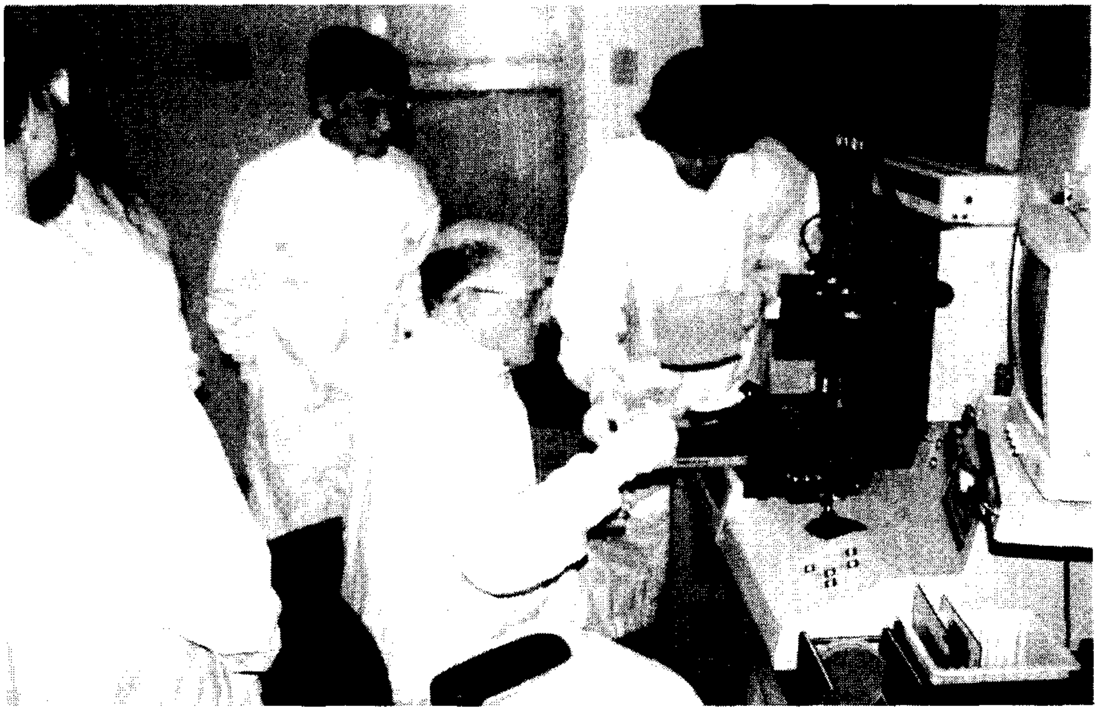

MINI WORKSHOPS (Continued)

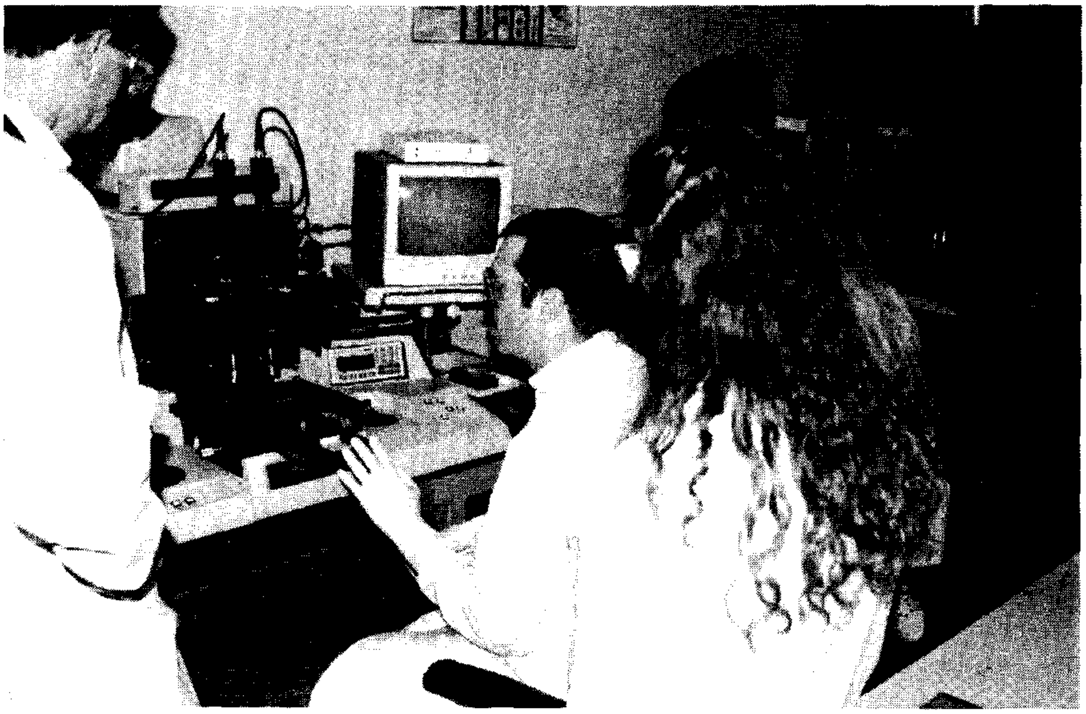

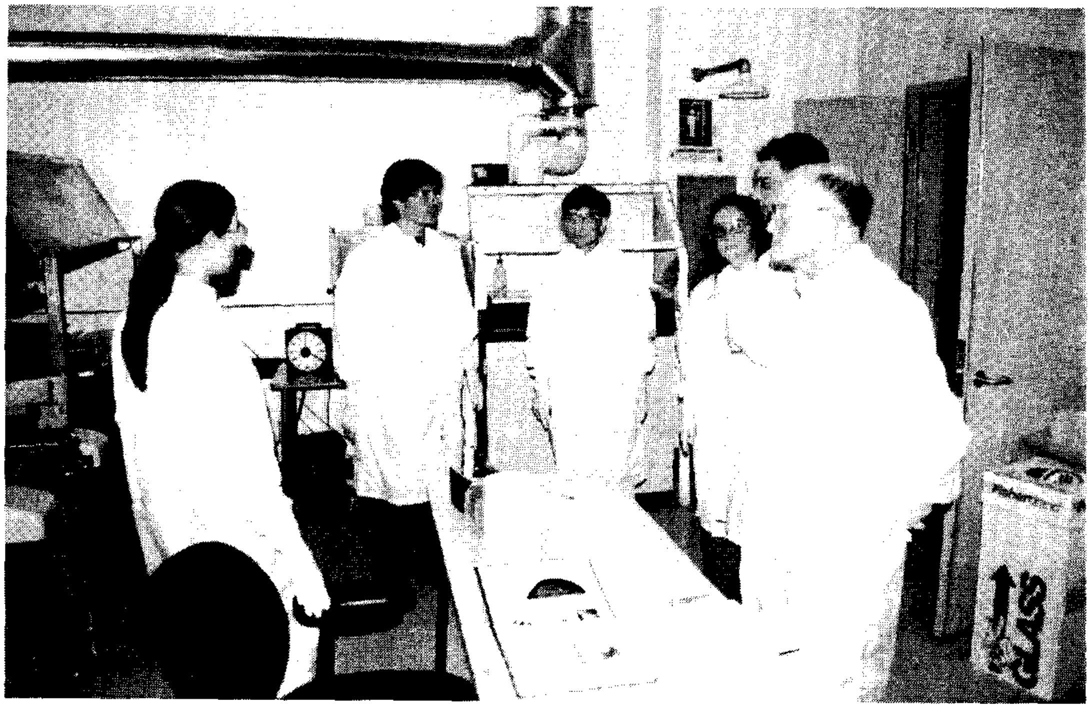

MINI WORKSHOPS (Continued)

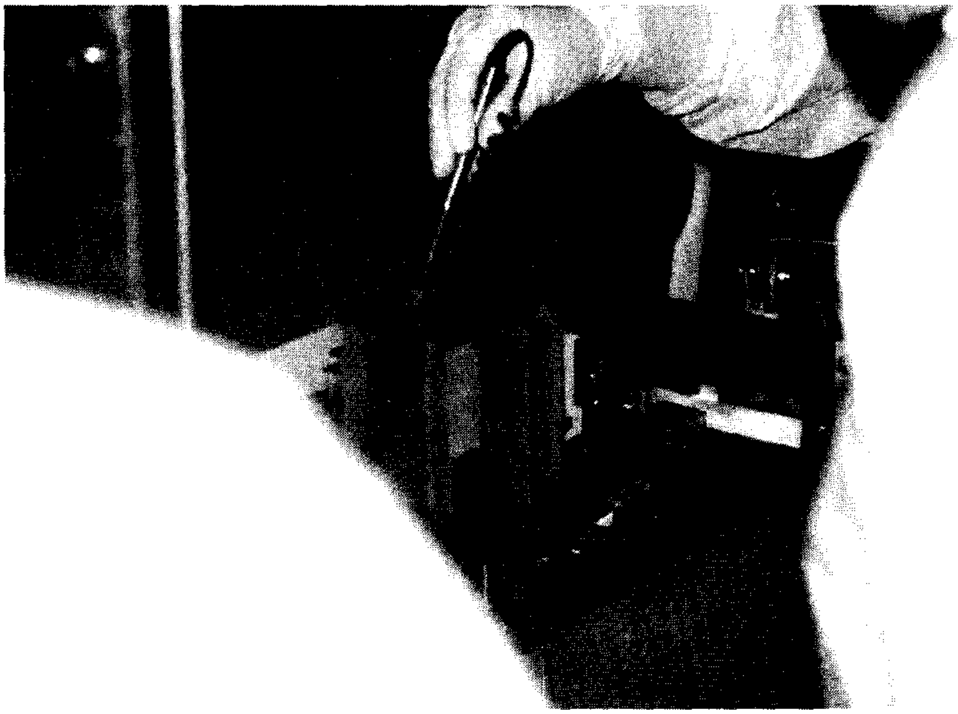

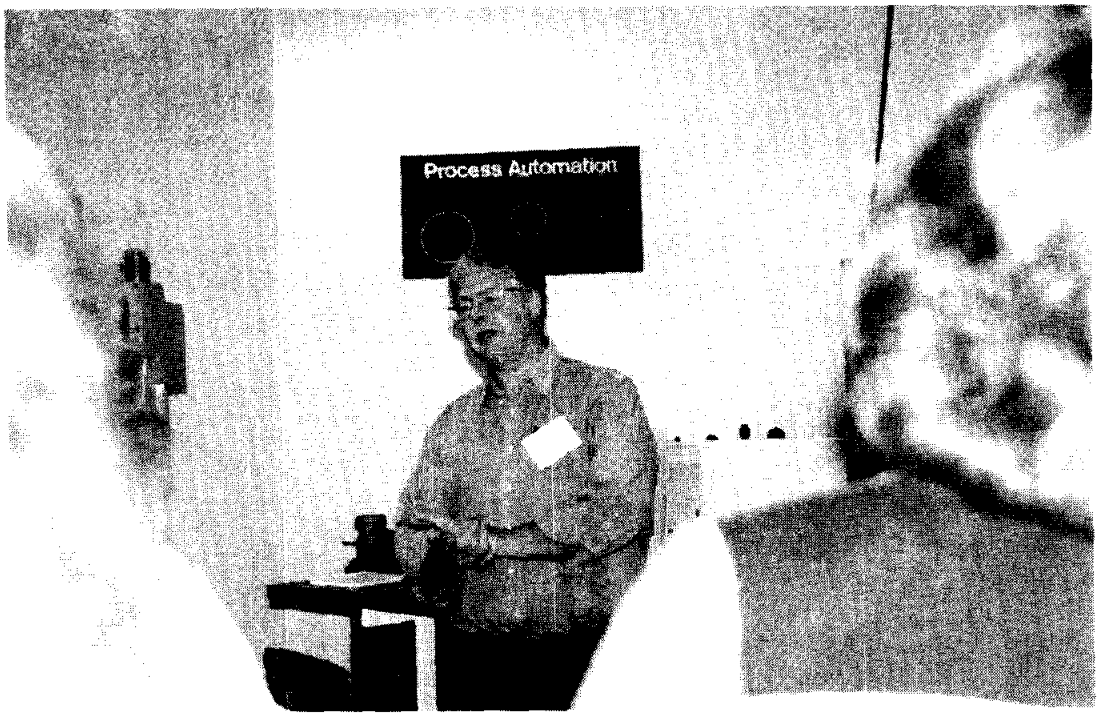

Seth Bates

MINI WORKSHOPS (Continued)

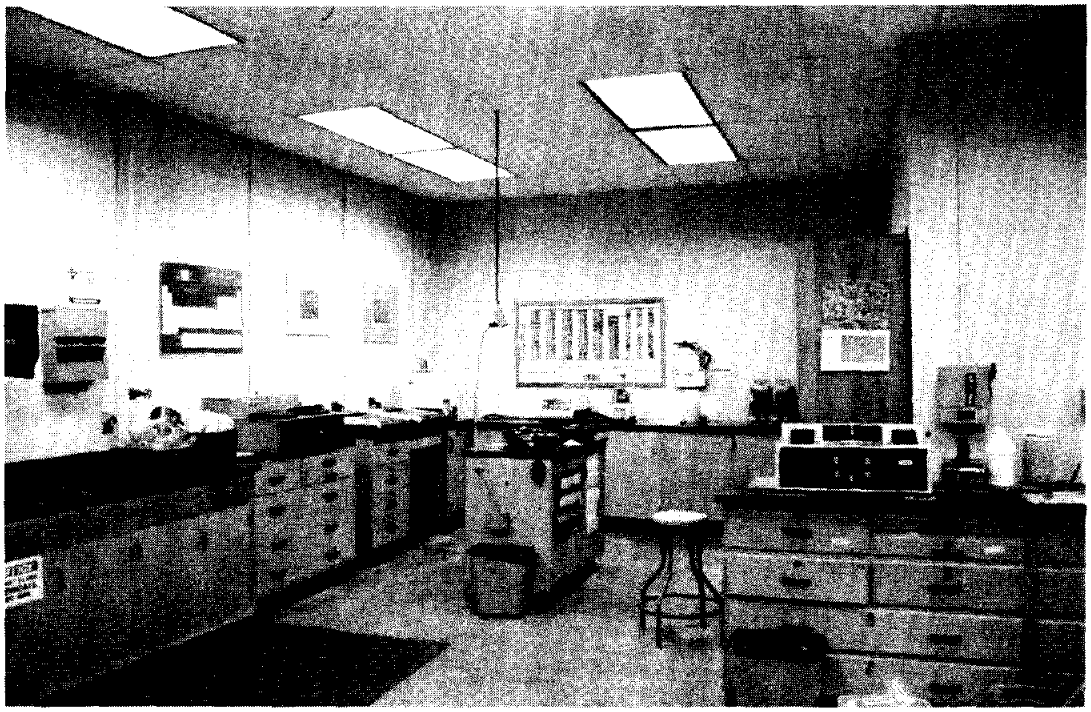

MINI WORKSHOPS (Continued)

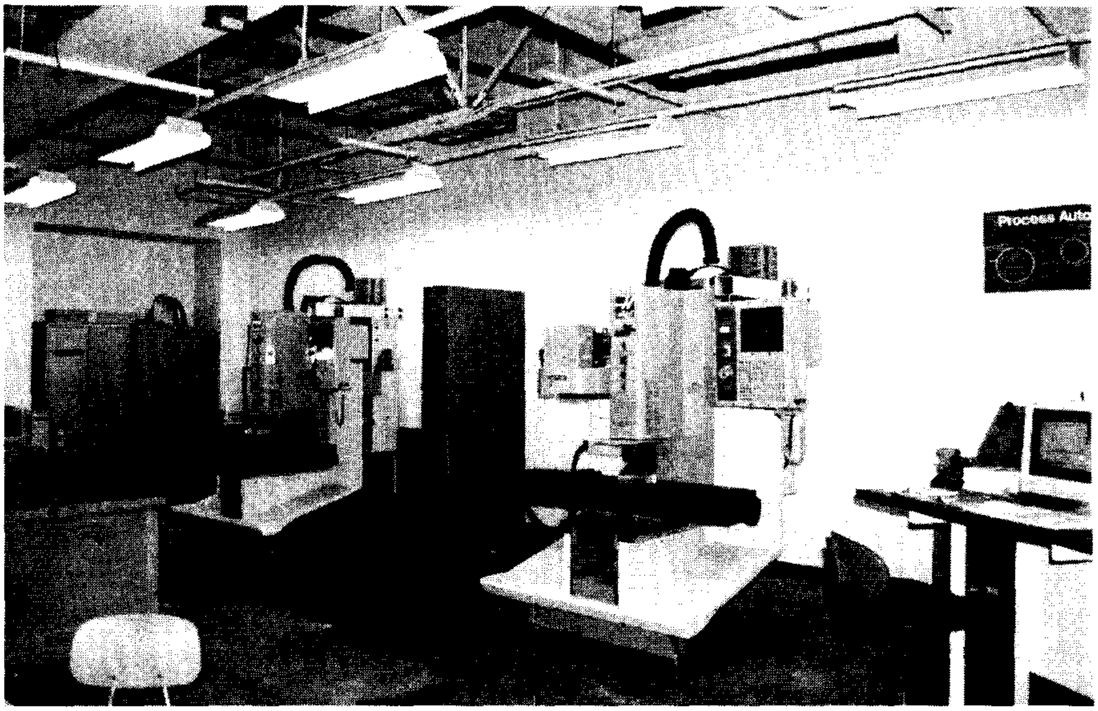

MINI WORKSHOPS (Continued)

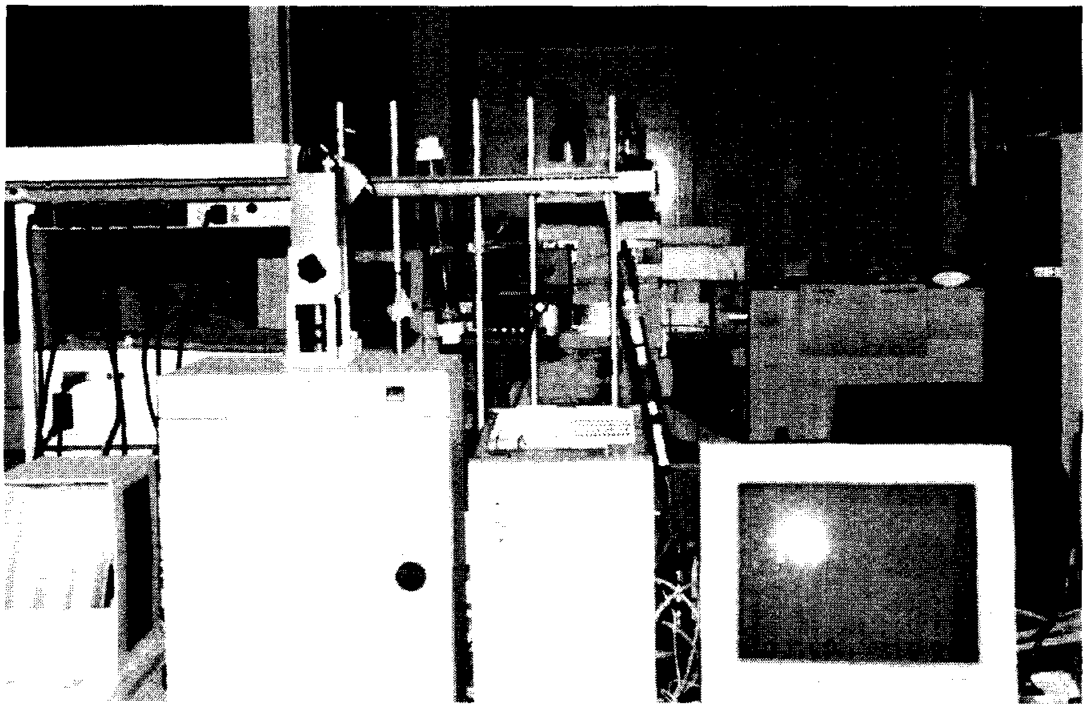

MINI WORKSHOPS (Concluded)

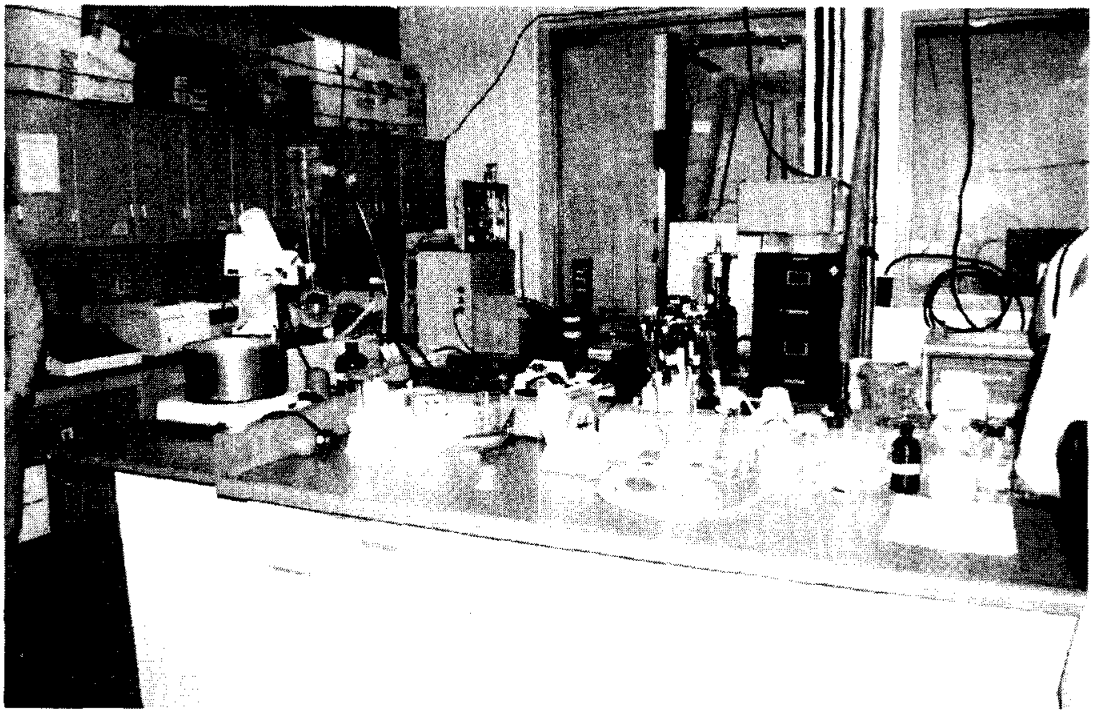

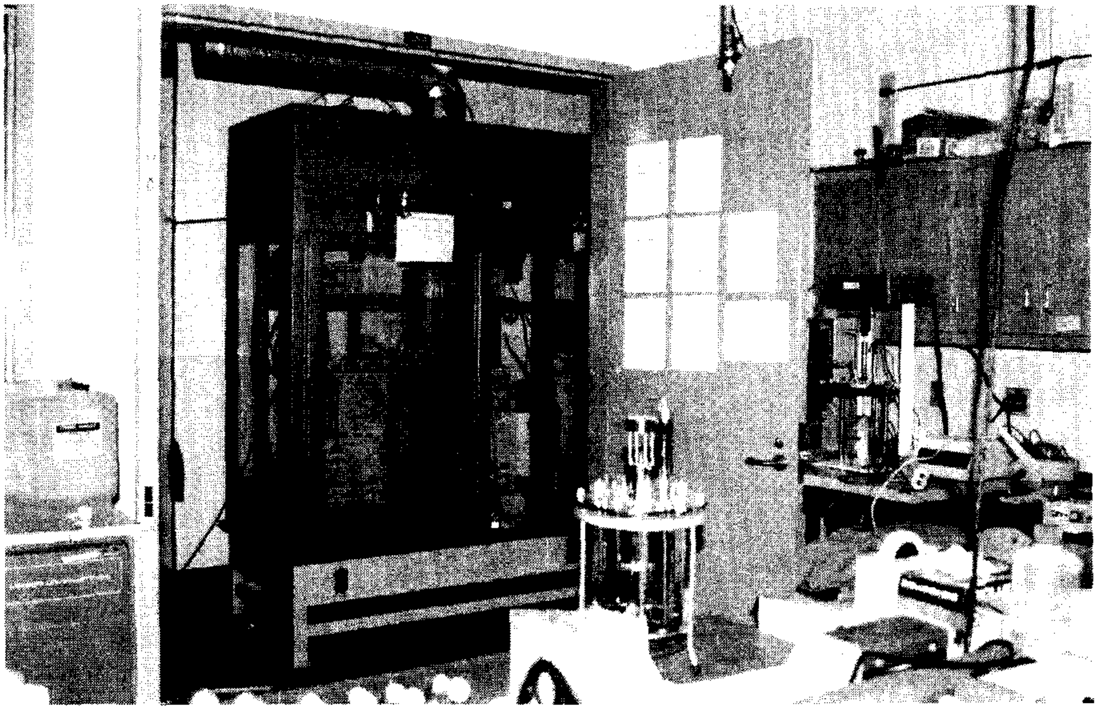

Seagate Educator's Workshop - Carbon and Lubricant

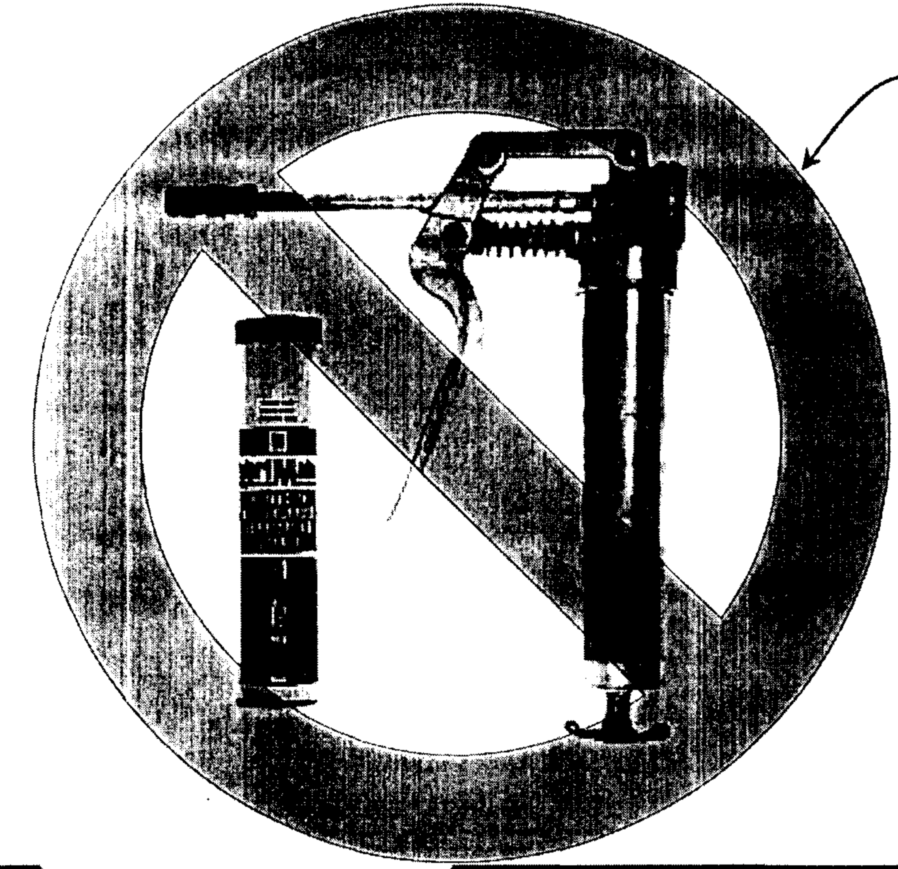

This is not how to lubricate the thin film media used in a hard disk drive

This is

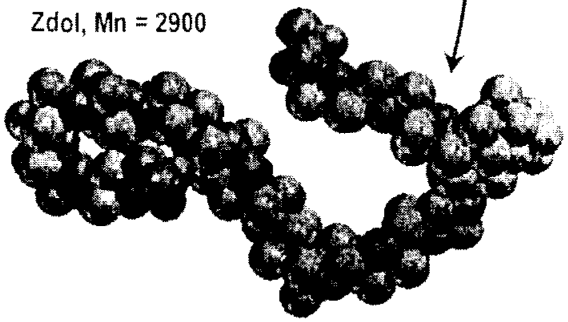

Mike Stirniman 10-14-02 Slide 1
Recording Media Operations

Seagate.
Information the way you want it.

Purpose of the lubricant is to protect your data

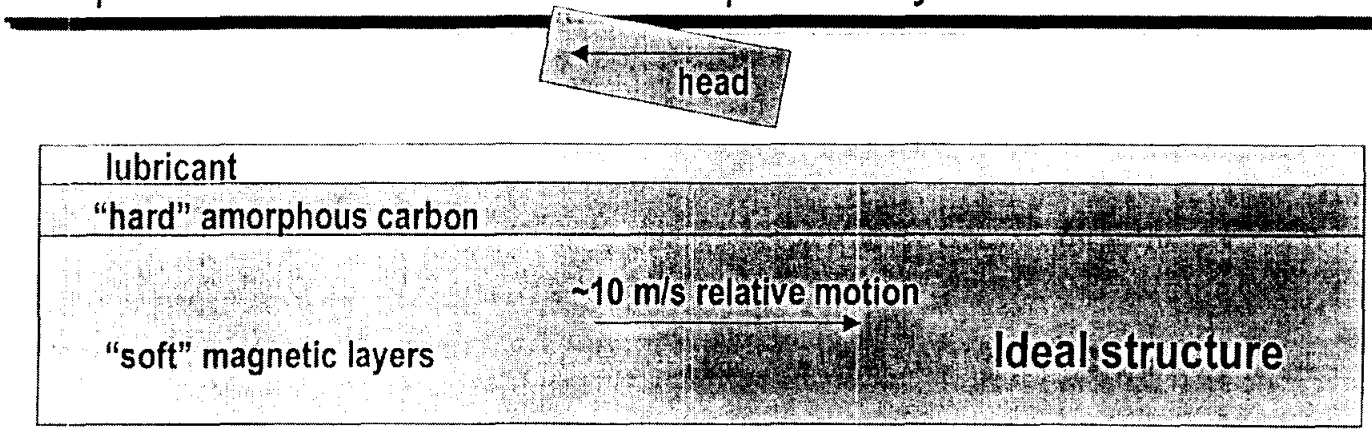

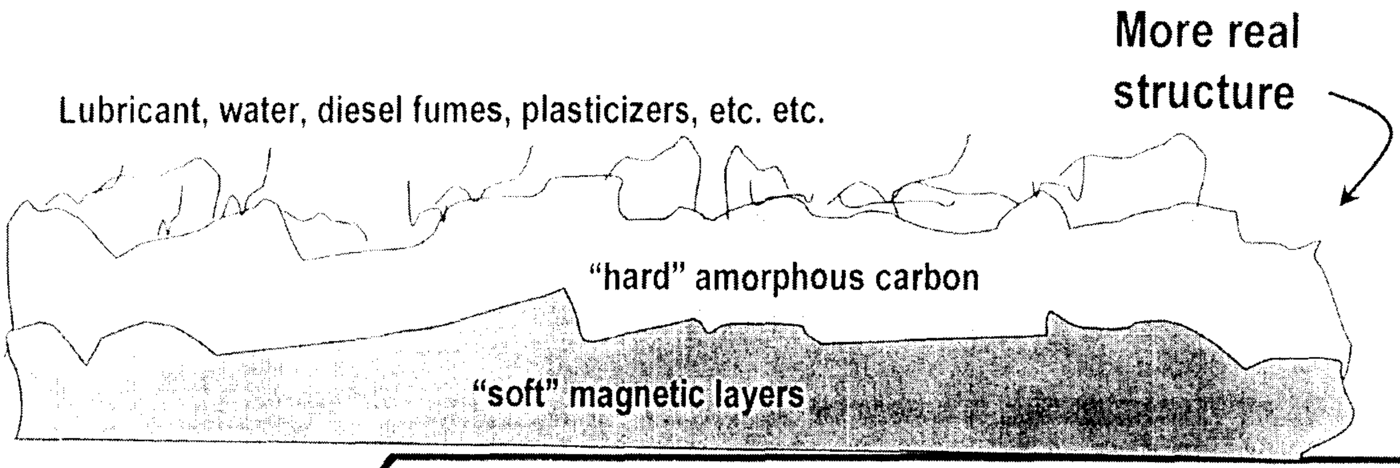

Lubricant physics

- Two regimes for lubrication:
  - Hydrodynamic (i.e. bearings): The surfaces are kept separated by a film of liquid, and bulk properties such as viscosity are used to describe the behavior through e.g. the Reynold's equation.
  - Boundary: A molecularly thin layer of material is used to reduce friction and prevent wear while the two surfaces are in intimate contact. Engine oil additives work in the boundary regime, and are designed to prevent wear during startup and before the parts are separated by the liquid film of oil.
  - Disk drive lubrication is always in the boundary regime, and understanding of the dynamics at the molecular level is required.

What is the lubricant?

- For many years, the most widely used lubricants have been some type of perfluoropolyether
- PFPEs are used as chemically inert vacuum pump fluids in the chip industry, and as ultra-low volatility lubricants in the space industry
- A chemically inert, low volatility lubricant is exactly what we need
    - Rubbing two surfaces together can cause many kinds of chemical degradation, including mechanical shear, triboelectrons, loacalized thermal degradation, etc.
    - The lubricant must be very thin, otherwise it increases the distance between the head and the magnetic layers - very bad
    - Because it is so thin (about 1-2 molecules), the vapor pressure of the lubricant needs to be in the 10^{-10} Torr range to prevent appreciable evaporation over the life of the drive

Application of a uniform monolayer film

1. Prepare a dilute (0.1% w/w) solution of PFPE in a volatile fluorinated solvent

2. Submerge the disc in the solution

3. Slowly withdraw the disc, dragging a thin meniscus of solution with it. After the solvent evaporates, a uniform film of the non-volatile lubricant remains

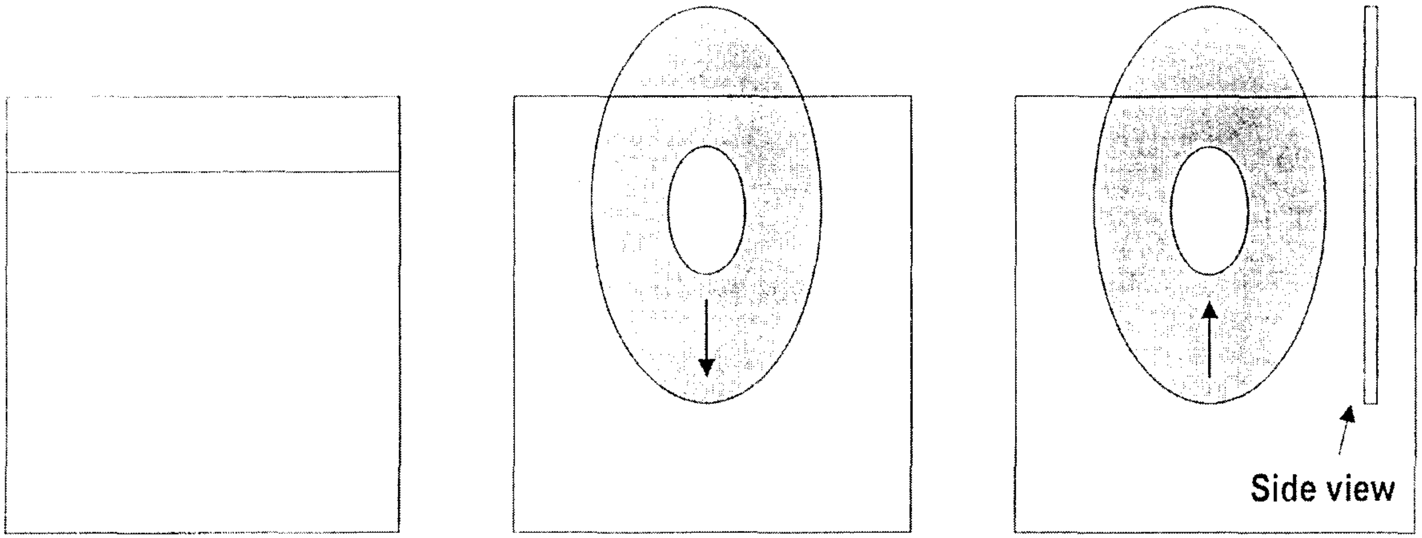

How is the molecularly thin layer measured?

- **Reflection Fourier transform infrared spectroscopy (FTIR) is used to measure the intensity of the stretch and bend modes of the carbon-fluorine bonds of the lubricant, and that intensity is compared to a calibration determined using X-ray photoelectron spectroscopy.**

1. Measure a background spectrum of an unlubricated disc

2. Measure the spectrum of a lubricated disc

3. Subtract the background spectrum from the lubricated disc spectrum, and the difference is the additional carbon-fluorine bond modes of the lubricant

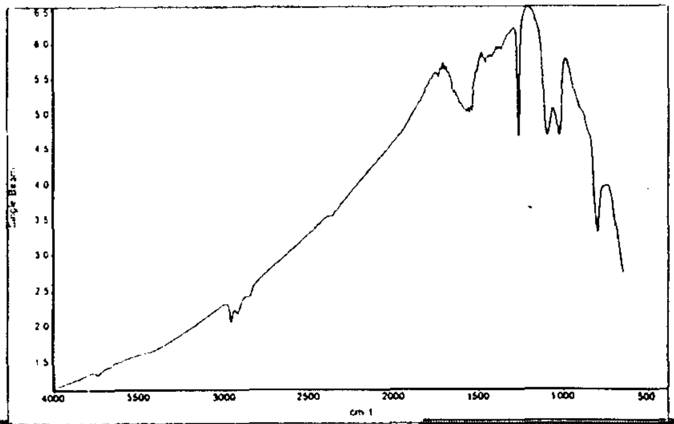

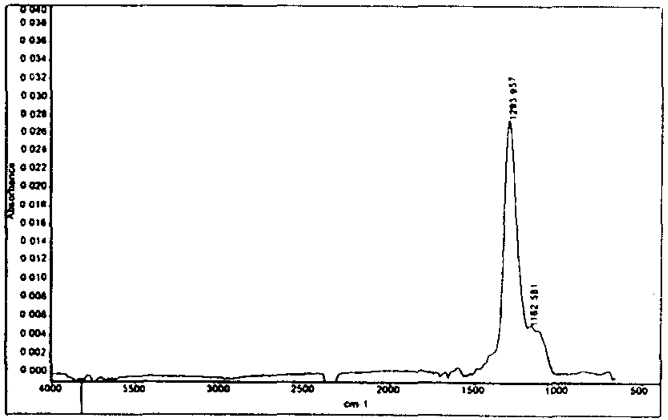

Media Sputter Technology

Alex S Rou

Oct 14, 2002

Outline

1. Magnetic Storage (HDD) Industry
2. Magnetic Media Technology
3. Sputter Technology
4. Opportunity & Challenge for Magnetic Material Scientists and Engineers

1. Hard Disc Drive Industry Over View

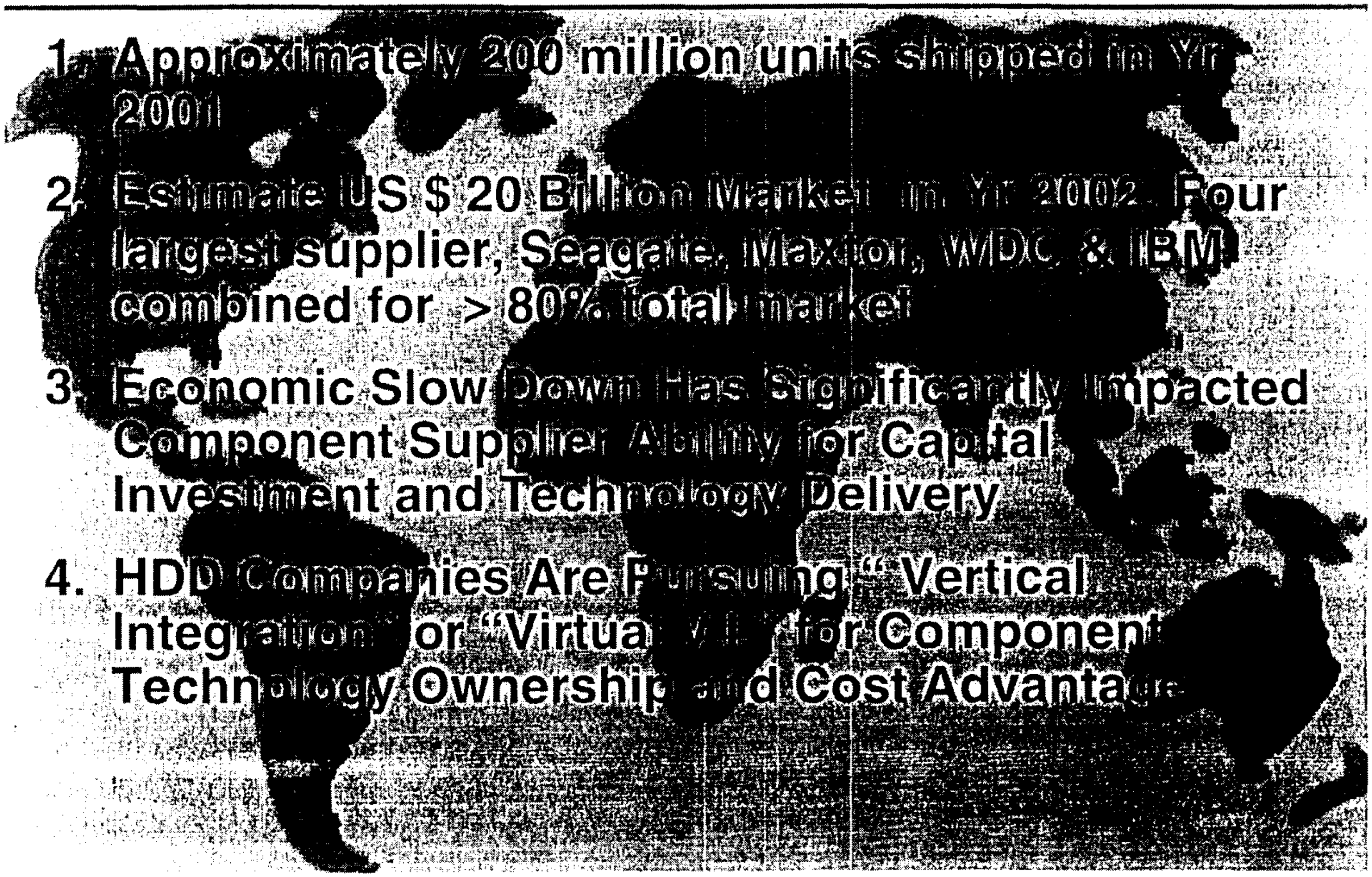

1. Approximately 200 million units shipped in Yr 2001
2. Estimate US $ 20 Billion Market in Yr 2002. Four largest supplier, Seagate, Maxtor, WDC & IBM combined for > 80% total market
3. Economic Slow Down Has Significantly Impacted Component Supplier Ability for Capital Investment and Technology Delivery
4. HDD Companies Are Pursuing " Vertical Integration" or "Virtual V.I." for Component Technology Ownership and Cost Advantage

Recording Head and Media

* Relationship of Reader and Writer

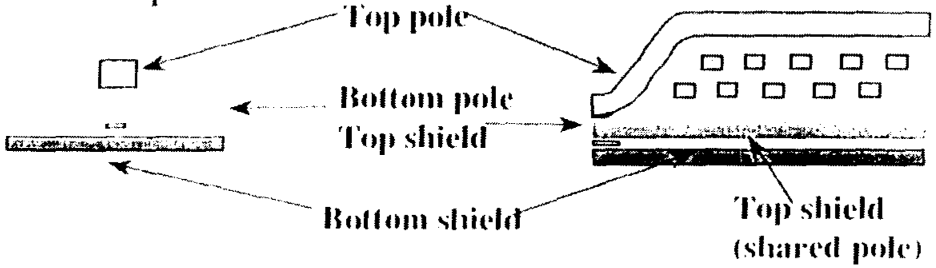

Top pole

Bottom pole

Top shield

Bottom shield

Top shield
(shared pole)

* Geometrical Relationship of the Head and Media

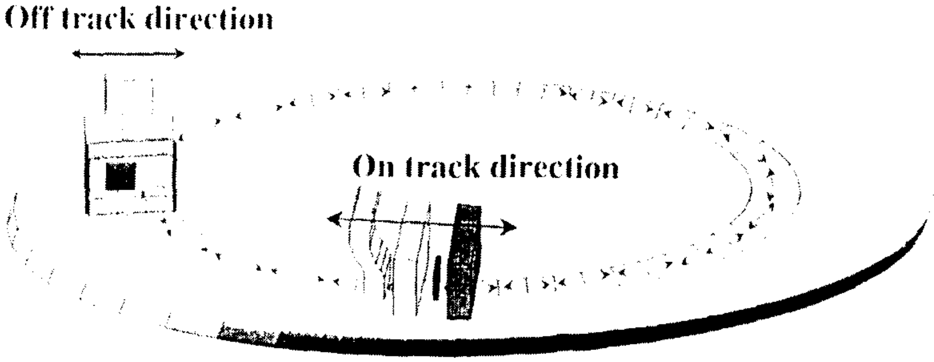

Off track direction

On track direction

Areal Density Demonstrations

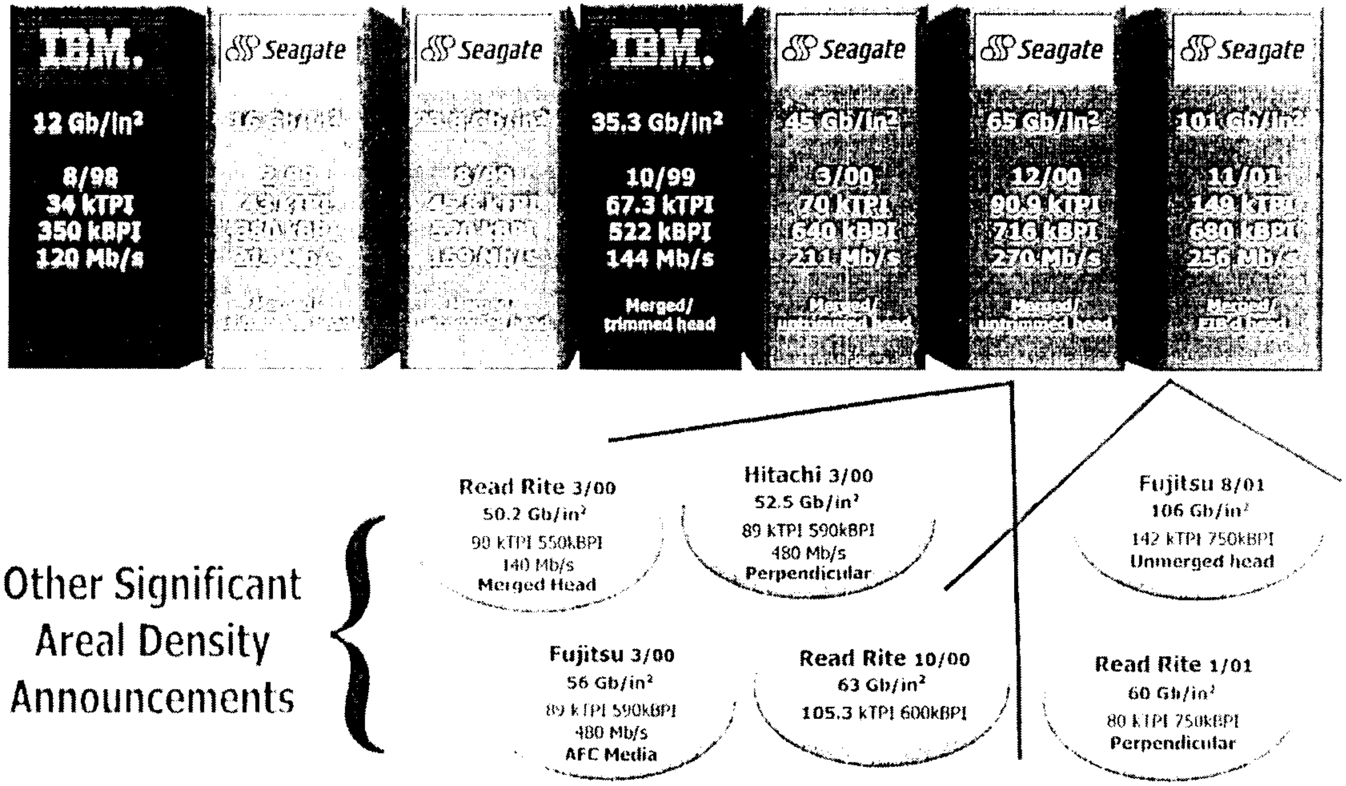

IBM.
12 Gb/in²
8/98
34 kTPI
350 kBPI
120 Mb/s

Seagate
[illegible]
[illegible]
[illegible]
[illegible]
[illegible]
[illegible]

Seagate
[illegible]
8/99
[illegible]
[illegible]
150 Mb/s
[illegible]

IBM.
35.3 Gb/in²
10/99
67.3 kTPI
522 kBPI
144 Mb/s
Merged/
trimmed head

Seagate
45 Gb/in²
3/00
70 kTPI
640 kBPI
211 Mb/s
Merged/
untrimmed head

Seagate
65 Gb/in²
12/00
90.9 kTPI
716 kBPI
270 Mb/s
Merged/
untrimmed head

Seagate
101 Gb/in²
11/01
149 kTPI
680 kBPI
256 Mb/s
Merged/
FIB'd head

Other Significant
Areal Density
Announcements

Read Rite 3/00
50.2 Gb/in²
90 kTPI 550kBPI
140 Mb/s
Merged Head

Hitachi 3/00
52.5 Gb/in²
89 kTPI 590kBPI
480 Mb/s
Perpendicular

Fujitsu 8/01
106 Gb/in²
142 kTPI 750kBPI
Unmerged head

Fujitsu 3/00
56 Gb/in²
89 kTPI 590kBPI
480 Mb/s
AFC Media

Read Rite 10/00
63 Gb/in²
105.3 kTPI 600kBPI

Read Rite 1/01
60 Gb/in²
80 kTPI 750kBPI
Perpendicular

Trajectories - Areal Density

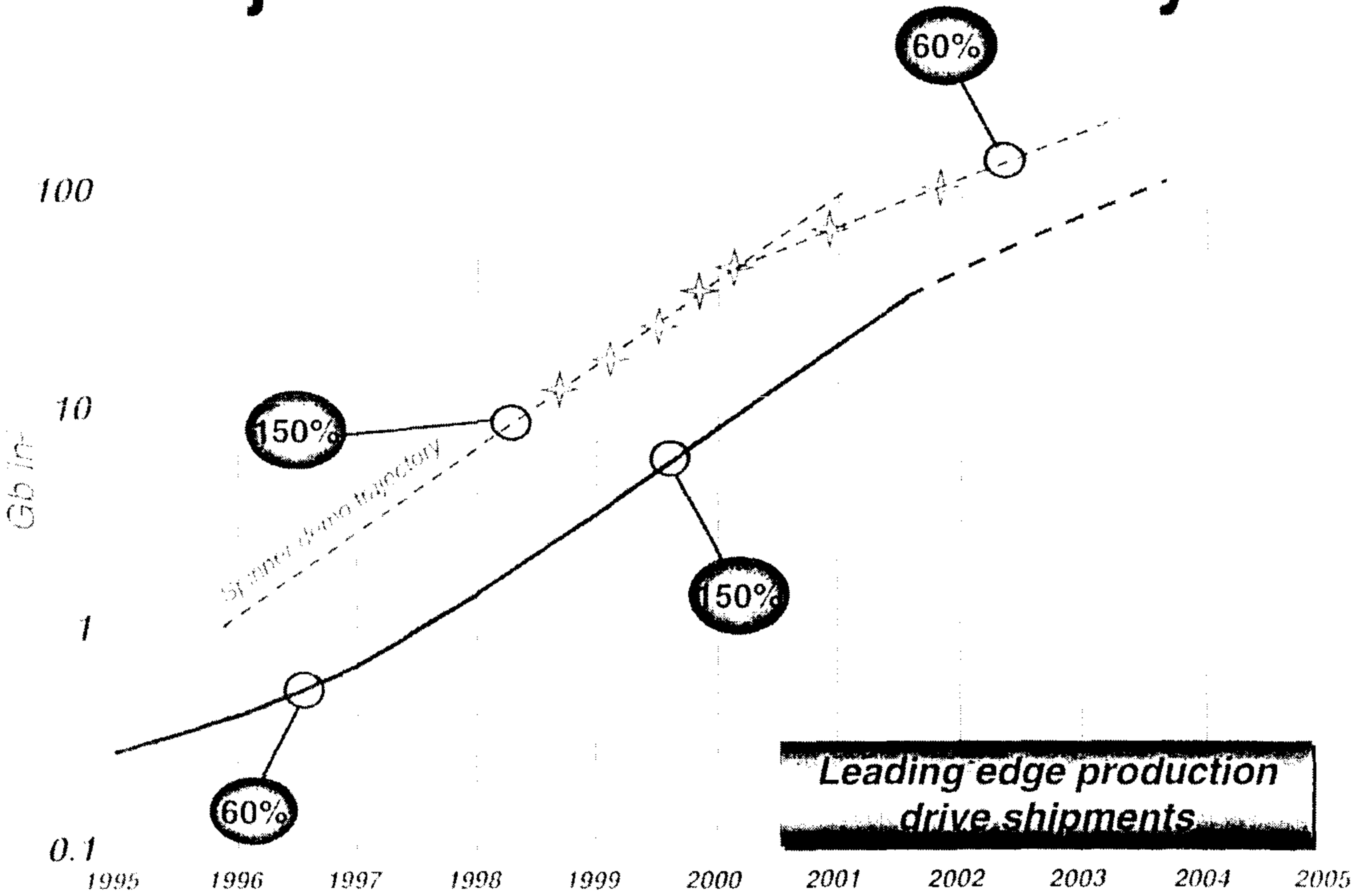

Leading edge production drive shipments

Recording Media Process Flow

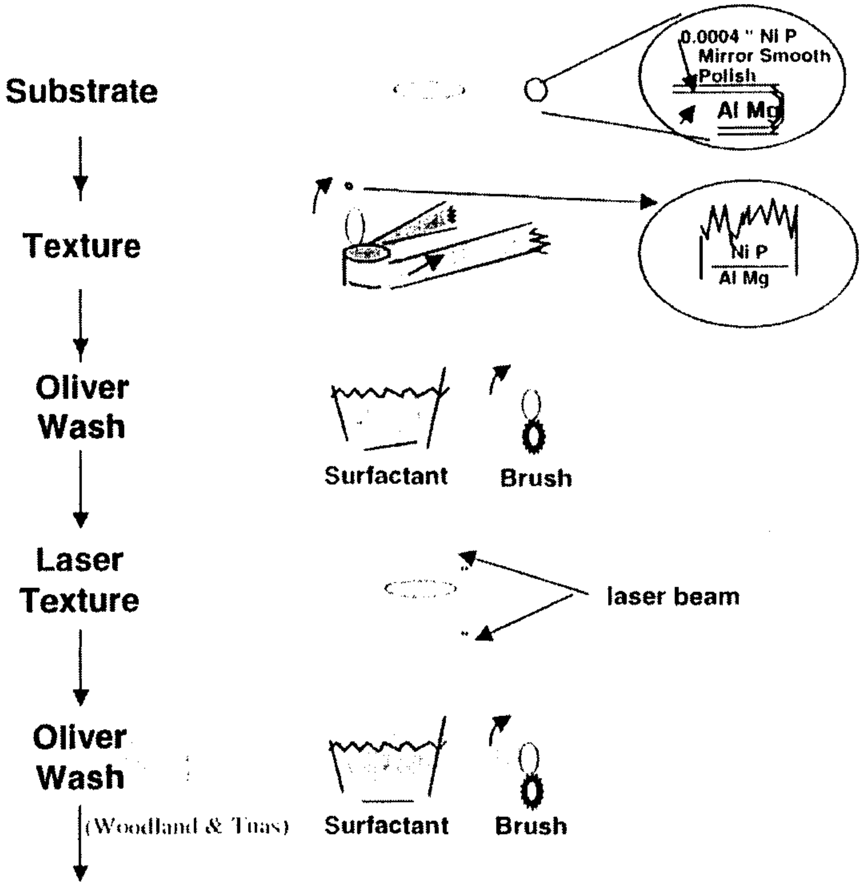

Substrate

Texture

Oliver Wash

Laser Texture

Oliver Wash

(Woodland & Tuas)

Recording Media Process Flow

Final Clean

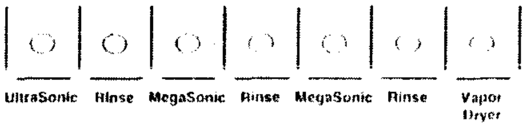

Sputter

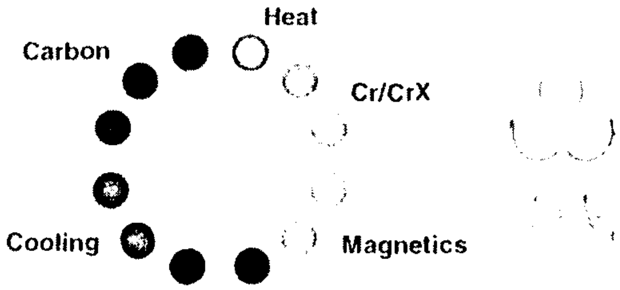

Lube

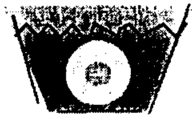

Tape Burnish

Recording Media Process Flow

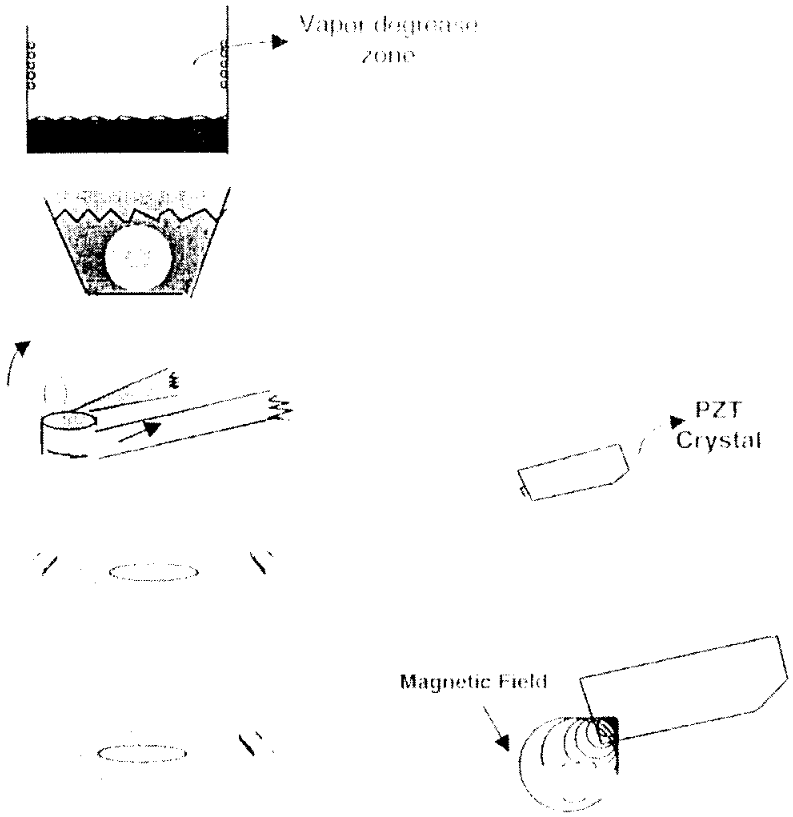

Degrease

2nd Lube

Wipe

Burnish GHT

Certify

Structure of Magnetic Thin Film Media

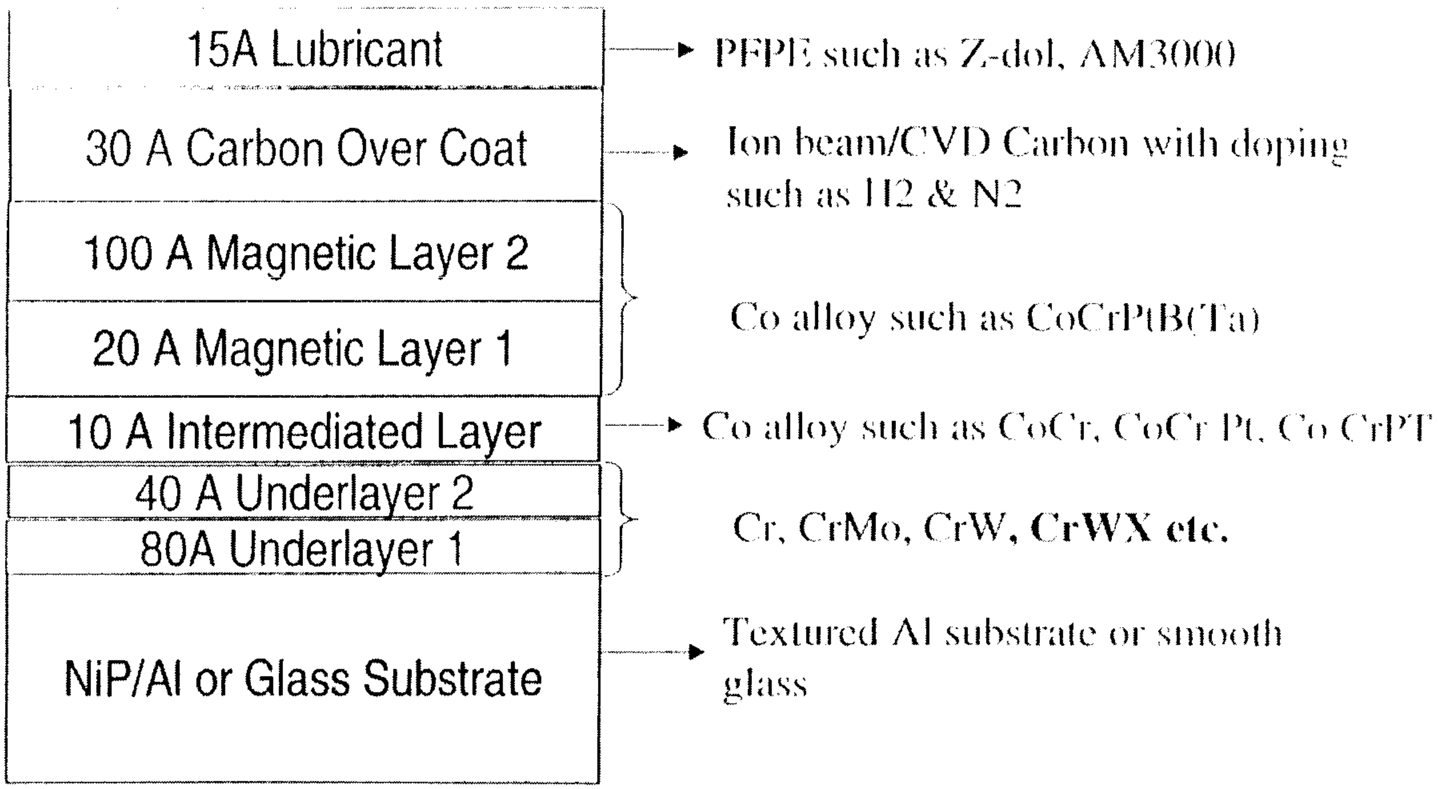

15A Lubricant → PFPE such as Z-dol, AM3000

30 A Carbon Over Coat → Ion beam/CVD Carbon with doping such as H2 & N2

100 A Magnetic Layer 2
20 A Magnetic Layer 1
} Co alloy such as CoCrPtB(Ta)

10 A Intermediated Layer → Co alloy such as CoCr, CoCr Pt, Co CrPT

40 A Underlayer 2
80A Underlayer 1
} Cr, CrMo, CrW, **CrWX etc.**

NiP/Al or Glass Substrate → Textured Al substrate or smooth glass

Cross-section TEM image:Glass Media

Grain Boundary Segregation

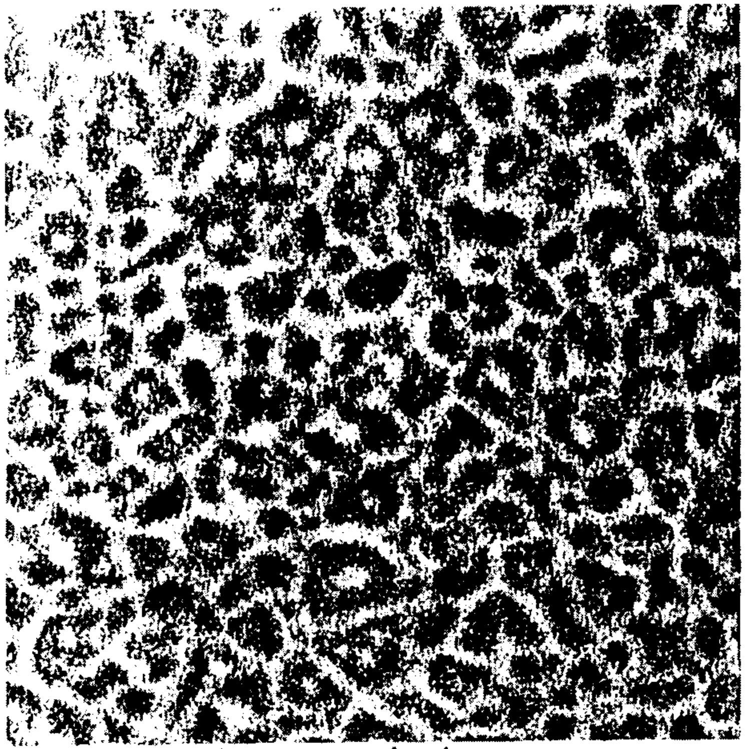

Cr jump ratio image

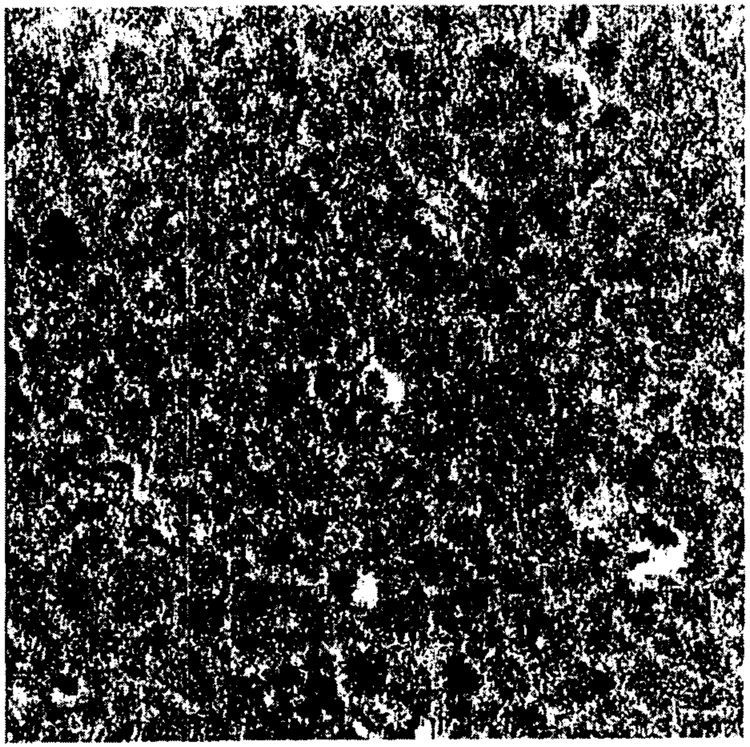

Boron jump ratio image

Courtesy NCEM Lawrence Berkeley Lab

Carbon Overcoat: 30 Å

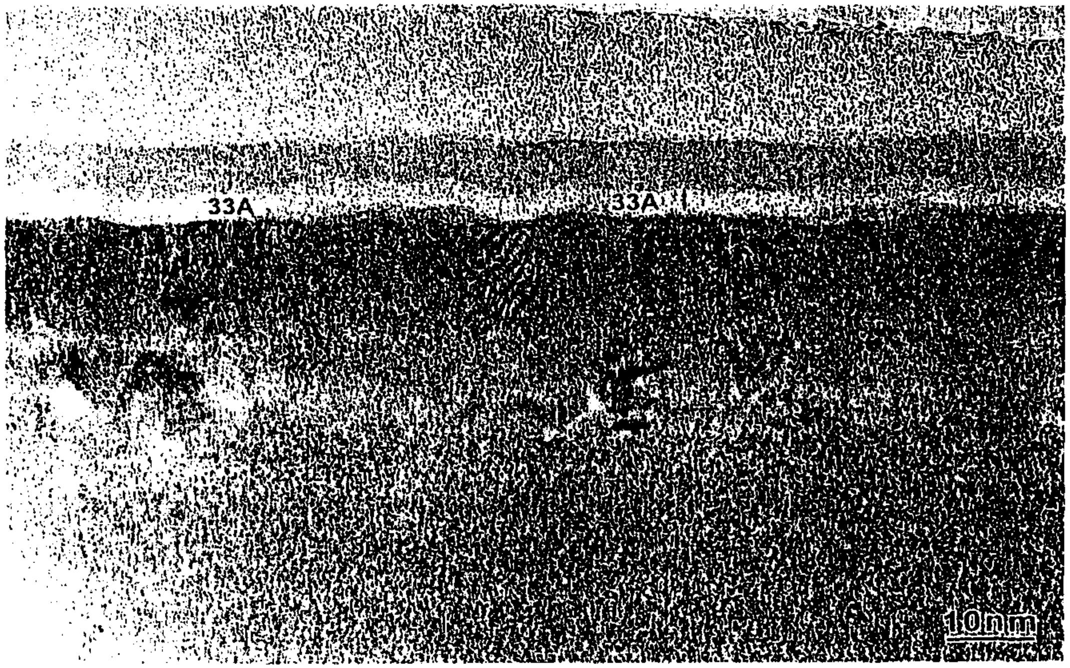

2023-1

Precision TEM Inc. (408) 980 8898

Critical Role of Each Layer

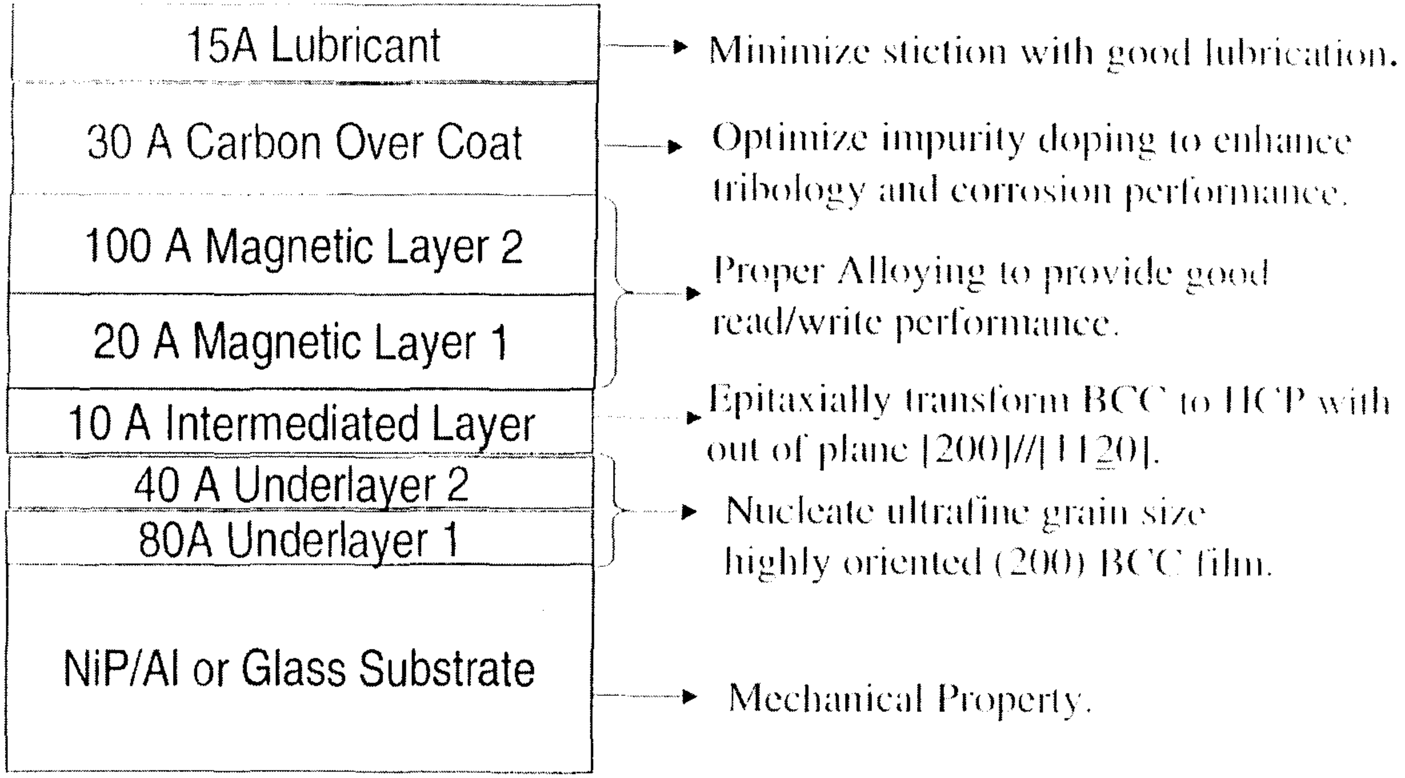

15A Lubricant → Minimize stiction with good lubrication.

30 A Carbon Over Coat → Optimize impurity doping to enhance tribology and corrosion performance.

100 A Magnetic Layer 2
20 A Magnetic Layer 1
→ Proper Alloying to provide good read/write performance.

10 A Intermediated Layer → Epitaxially transform BCC to HCP with out of plane $[200]//[11\bar{2}0]$.

40 A Underlayer 2
80A Underlayer 1
→ Nucleate ultrafine grain size highly oriented (200) BCC film.

NiP/Al or Glass Substrate → Mechanical Property.

MDP sputter Machine Configuration

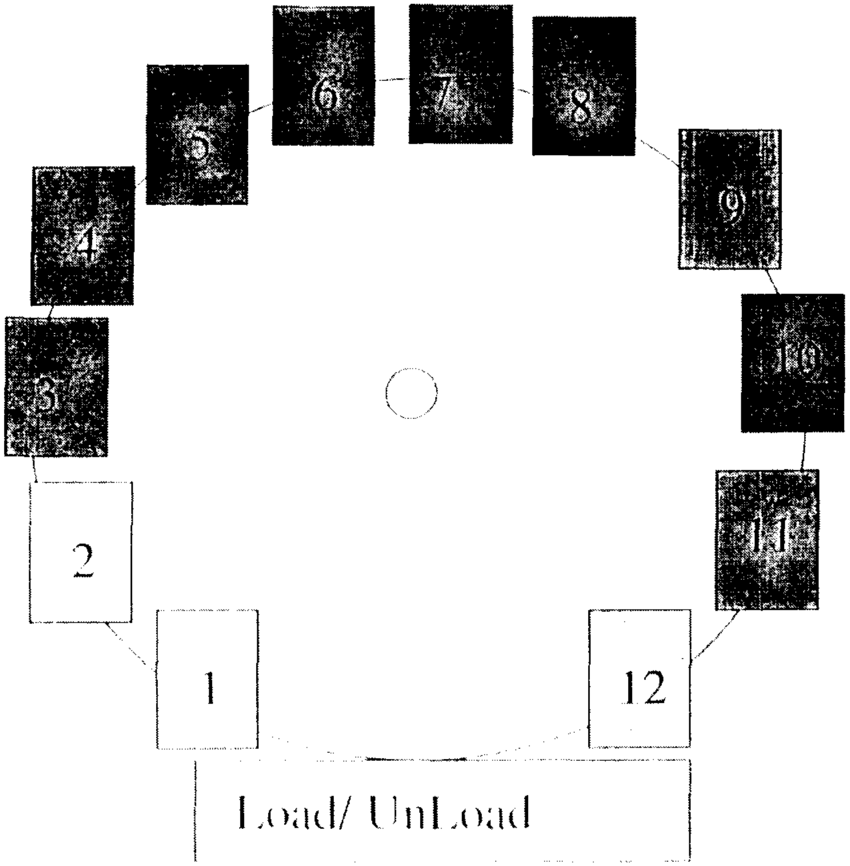

1. Heater
2. Heater
3. Cr
4. CrW
5. Coupling Mag
6. Ru
7. Mag 1
8. Spacer Layer
9. Mag 2
10. Cooling
11. Cr Cap
12. Carbon

Media Parametric Performance

- High signal amplitude and low noise power.
- Good writability.
- Good reliability of Signal to Noise (BER)

Where is the link?

Good materials scientists and engineers.

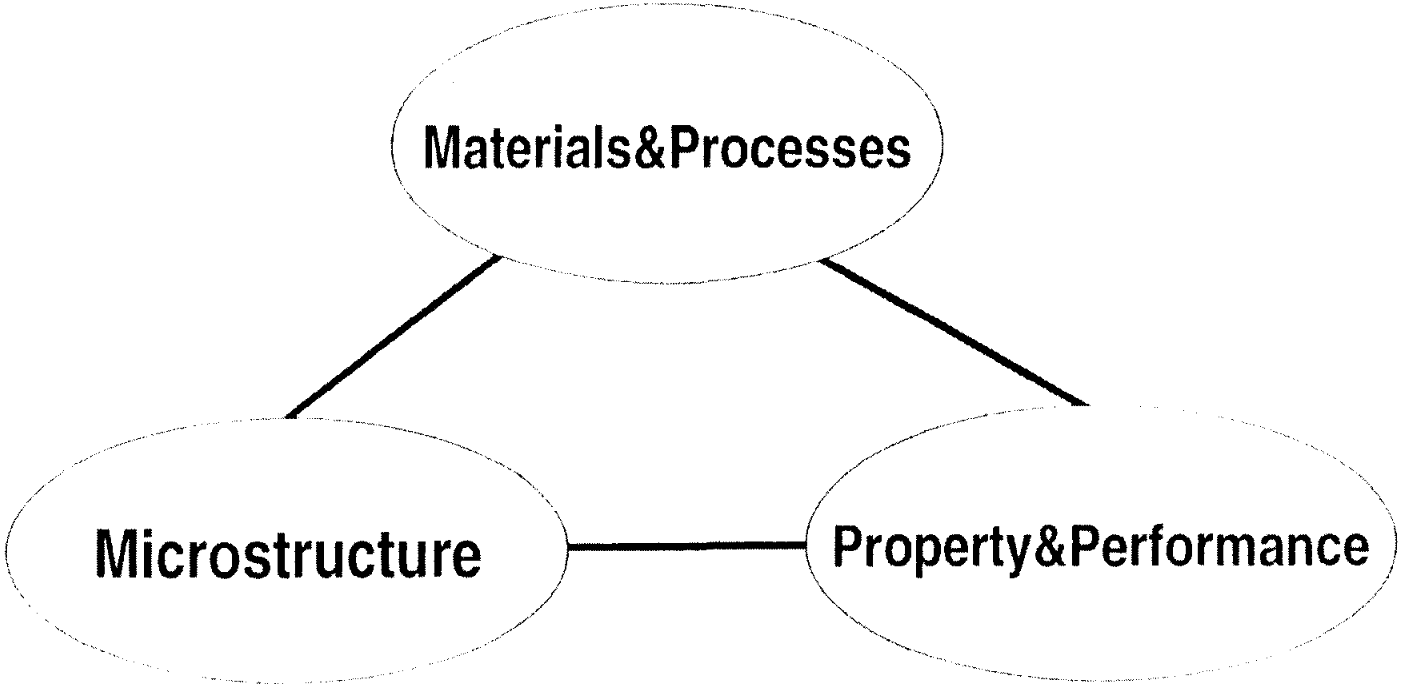

Materials&Processes

Microstructure

Property&Performance

Critical to Media Performance

- Processes (sputter) and materials selection determine thin film microstructure.
  - Engineering surface chemistry and lattice match between each adjacent layer to achieve fine grain size and preferred crystallographic orientation.
  - Properly alloying magnetic materials to achieve optimum grain boundary segregation.
- Thin film microstructures determine magnetic media performance.
  - Highly HCP c-axis in-plane film will provide highest signal amplitude.
  - Grain boundary segregation of non-magnetic materials will minimize intergranular exchange coupling for sharper transition and lower noise.

4. Challenge & Opportunity

1. Dimension:
   - Recording bit length is in sub-50 nanometer range.
2. Technology:
   - Complex states of magnetic reversal need
     - Modeling and characterization of magnetic behavior
     - Metrology tool to measure response
     - Thoroughly understand materials-structure-property.
3. Product Integration:
   - Reliability & process capability of ultra-thin magnetic film is a big challenge and requires novel process approach
   - Equipment, monitoring and testing tool for ultra-thin film processing is still in development

4. Challenge & Opportunity

As material engineers / scientists in recording media industry, our strength have always been knowing the interrelationship among materials(processes)-microstructure-property(performance). It's a great opportunity to extend our strength to overcome the future challenges and fulfill our dream.

Jim Jacobs

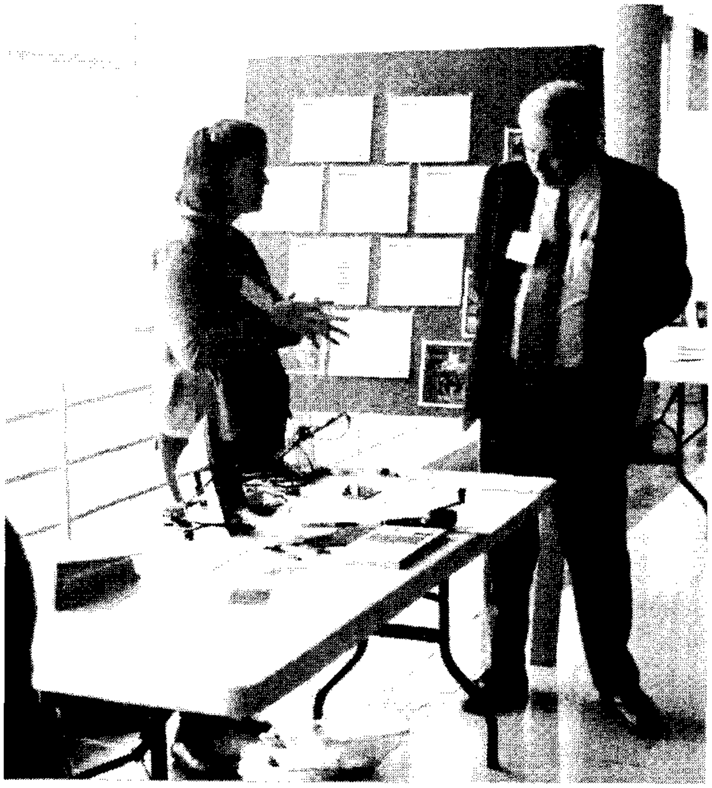

Janet K. Lumpp and Edwin J. Prior

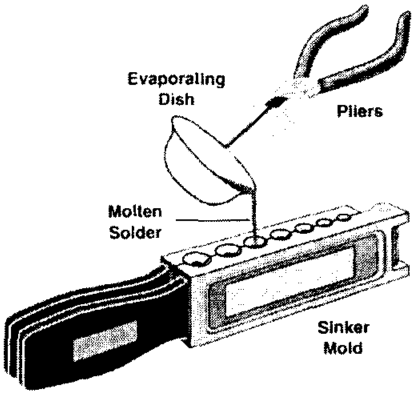
Evaporating Dish
Pliers
Molten Solder
Sinker Mold

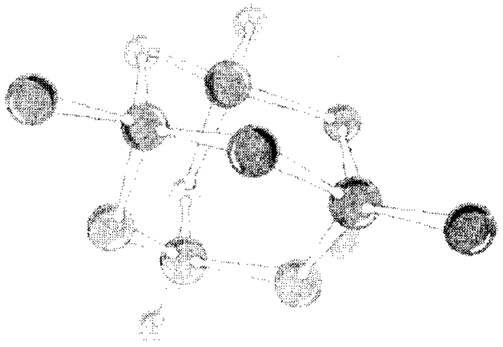

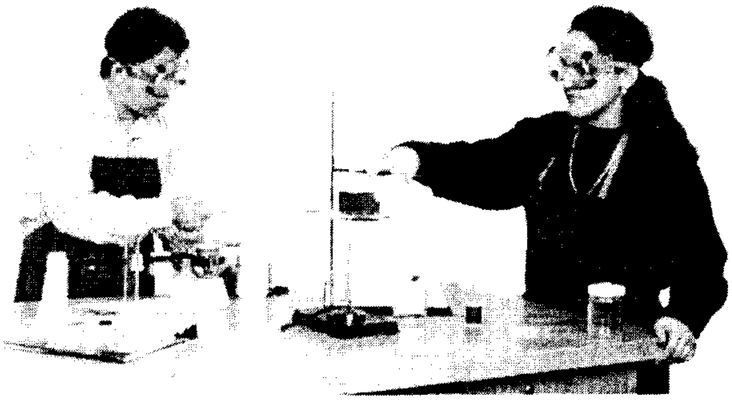

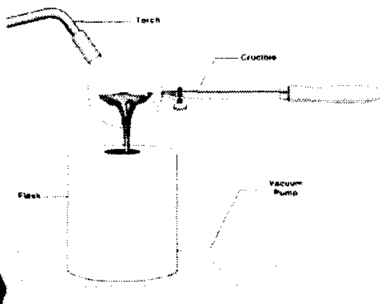
Torch
Crucible
Flask
Vacuum Pump

Merrill Rudes

Jim Jacobs, Nikki Harris, Diana LaClaire, Kyo Song, and Ransom Douglas

UltratechStepper

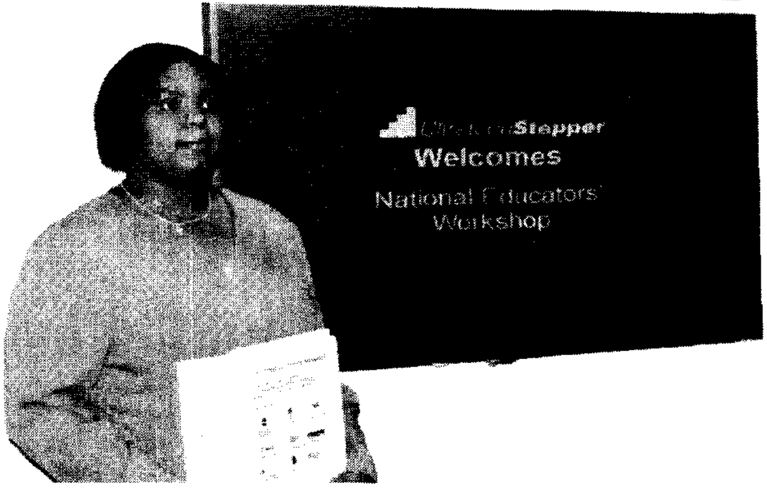

Nikki Harris

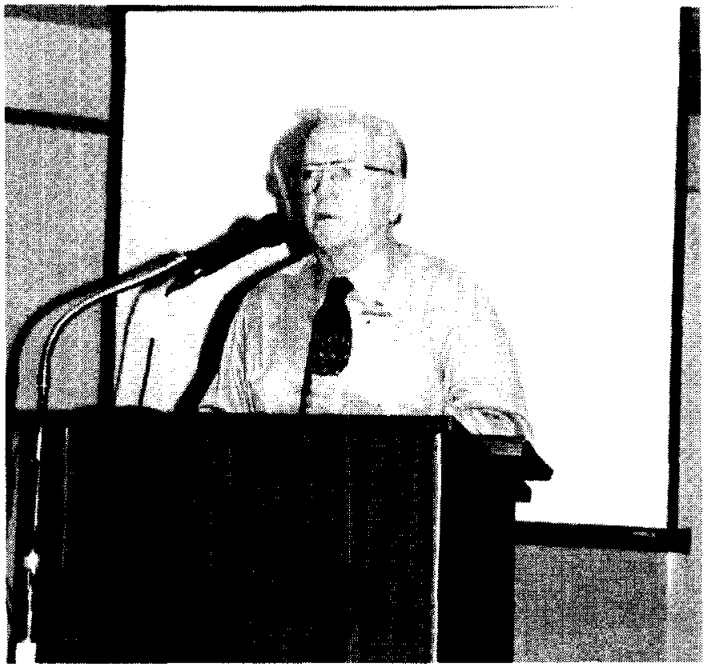

Dave Holmes

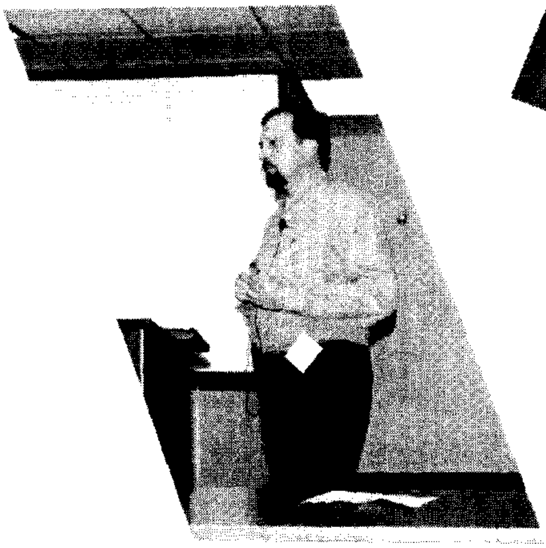


INFORMATION
about the
th Annual
TIONAL
CATORS'
KSHOP

Don Bethune

Hans Coufal

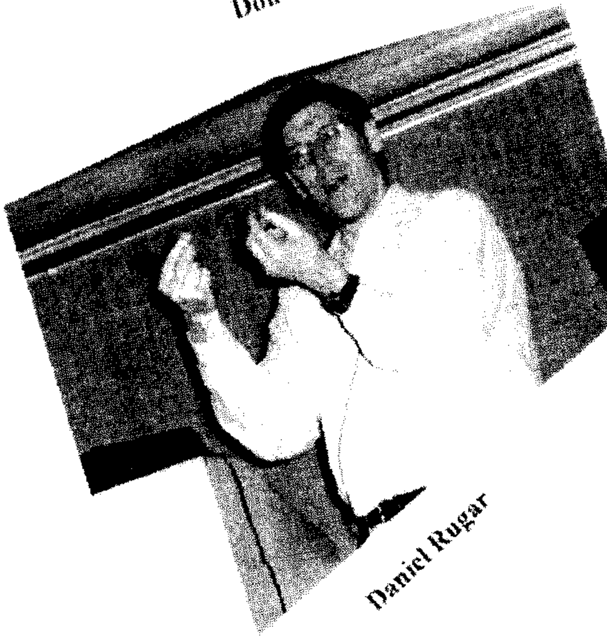

Daniel Rugar

Stuart Parkin

Campbell Scott

Craig Hawker

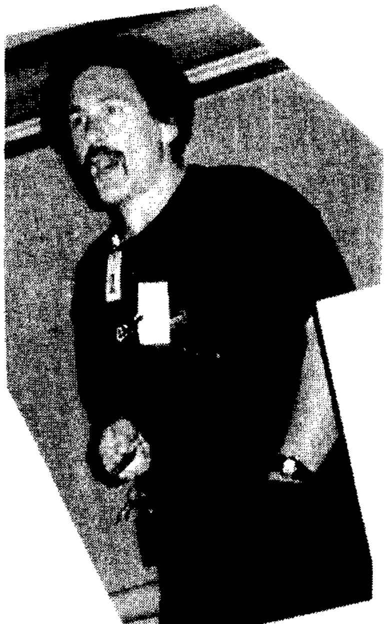

Charles Rettner

Don Eigler

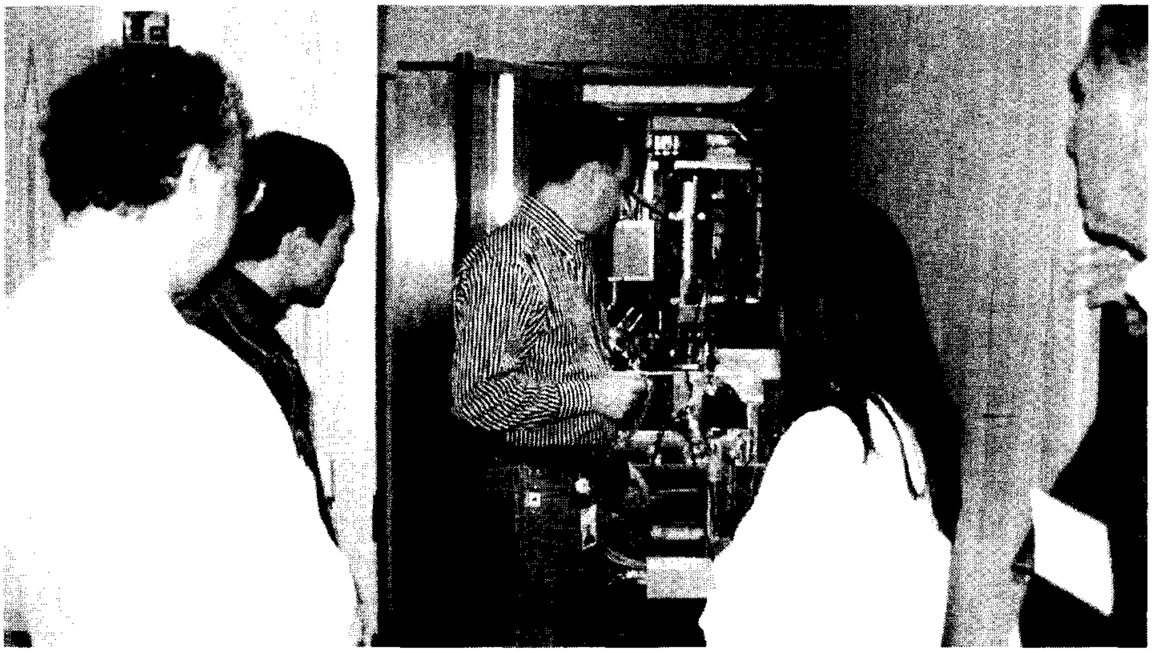

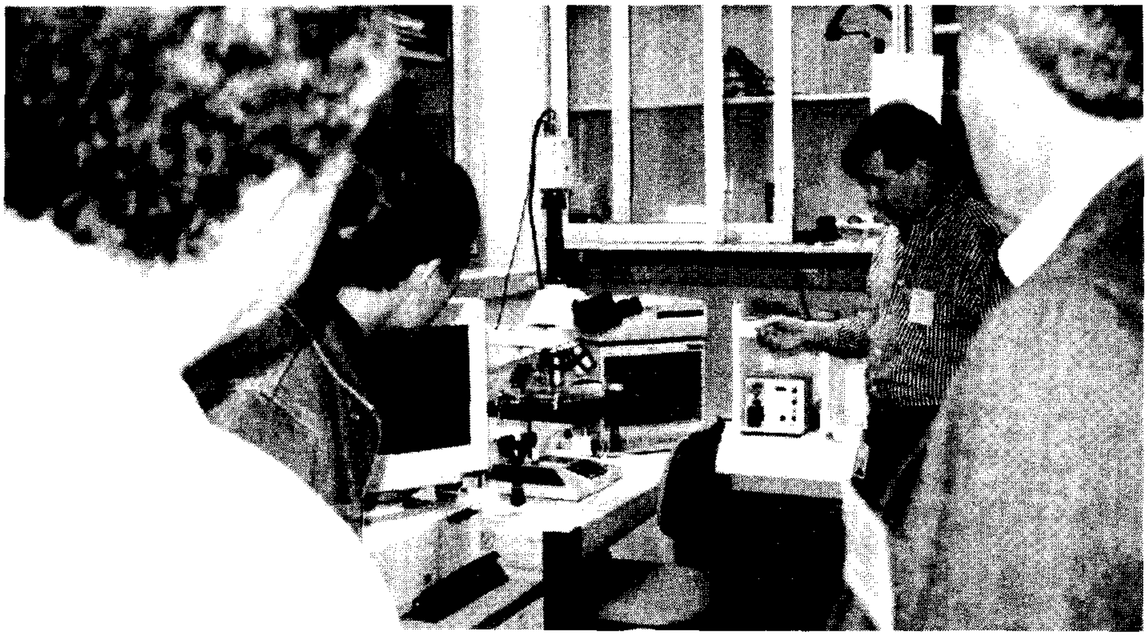

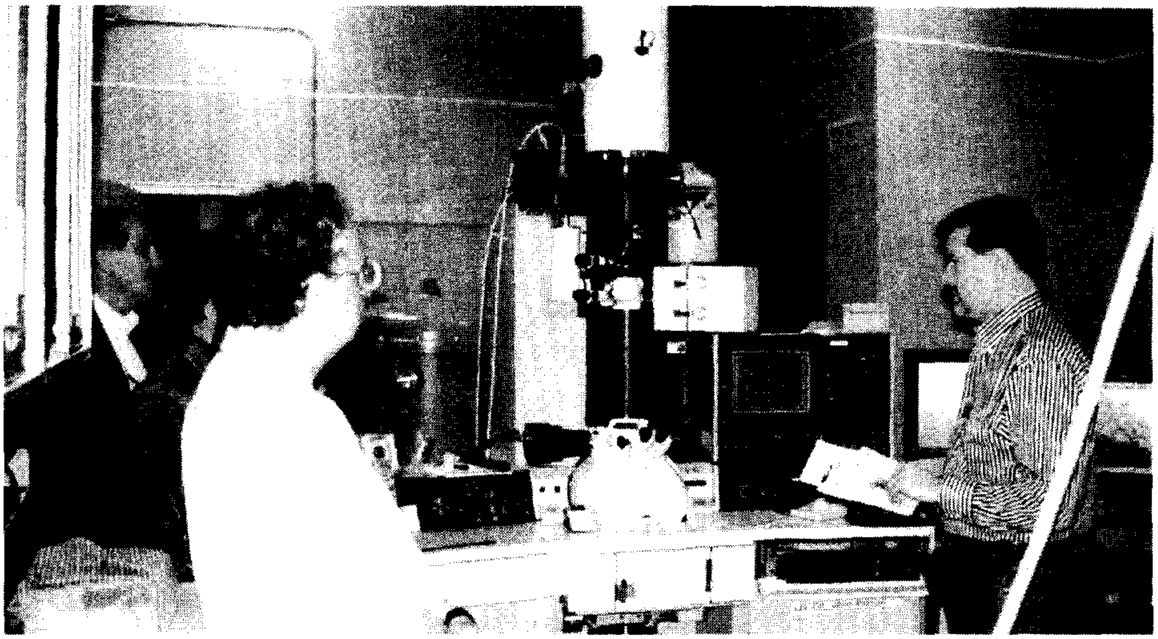

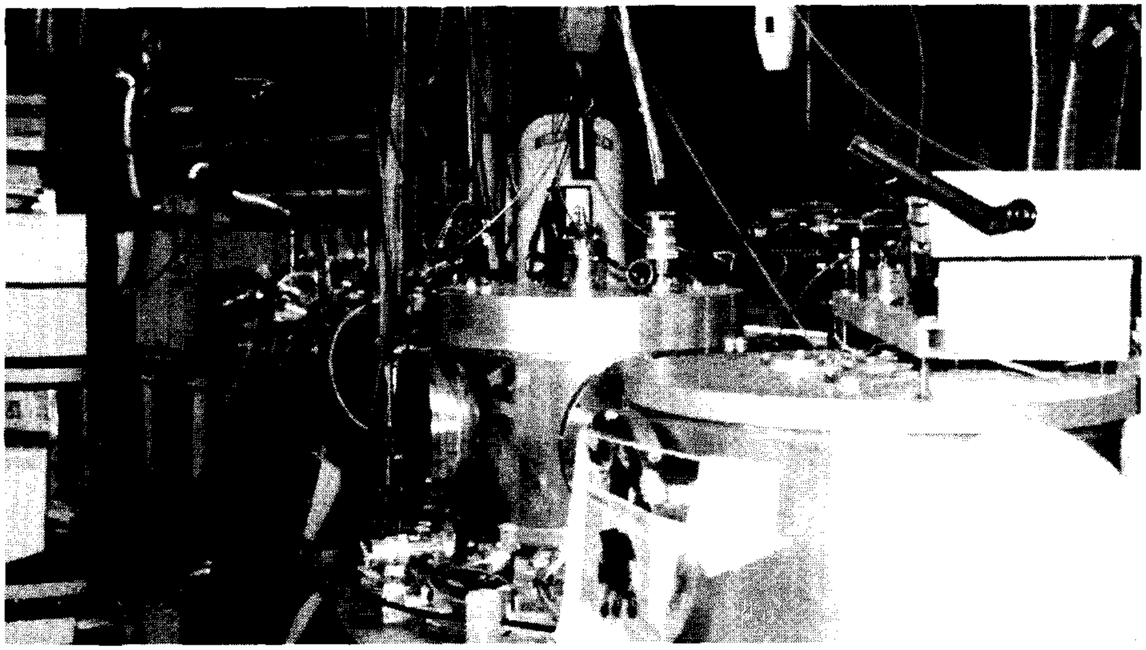

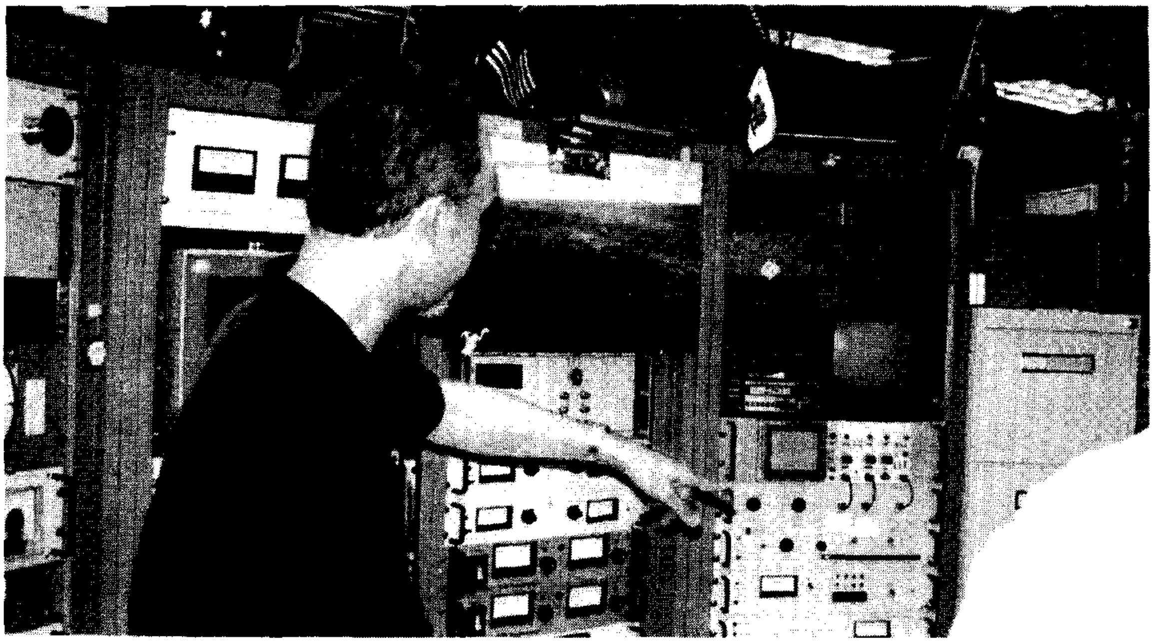

NANOTECHNOLOGY: OPPORTUNITIES AND CHALLENGES

Meyya Meyyappan

Director, Center for Nanotechnology
NASA Ames Research Center
MS 229-3
Moffett Field, California 94035

Telephone: 650-604-2616
e-mail Meyya@orbit.arc.nasa.gov

Meyya Meyyappan

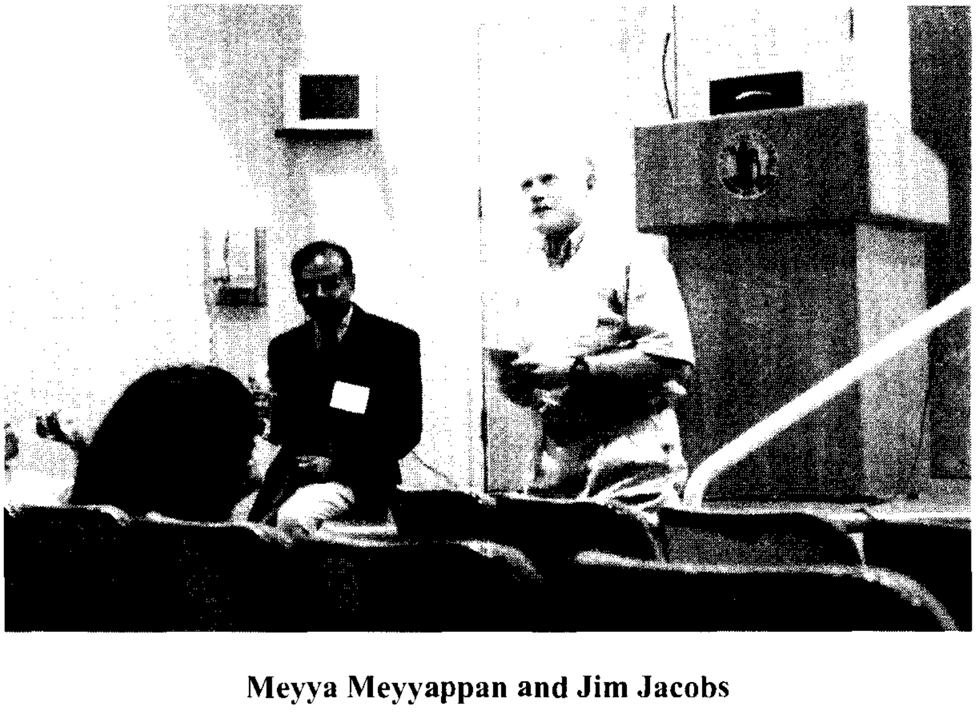

Meyya Meyyappan and Jim Jacobs

NANOTECHNOLOGY: OPPORTUNITIES AND CHALLENGES

Nanotechnology seeks to exploit novel physical, chemical, biological, mechanical, electrical, and other properties, which arise primarily due to the nanoscale nature of certain materials.

A key example is carbon nanotubes (CNTs) which exhibit unique electrical and extraordinary mechanical properties and offer remarkable potential for revolutionary applications in electronics devices, computing, and data storage technology, sensors, composites, nanoelectromechanical systems (NEMS), and as tip in scanning probe microscopy (SPM) for imaging and nanolithography.

Thus the CNT synthesis, characterization, and applications touch upon all disciplines of science and engineering.

This talk will provide an overview and progress report on this and other major research candidates in Nanotechnology and address opportunities and challenges ahead.

Ames Research Center

Nanotechnology: Opportunities and Challenges

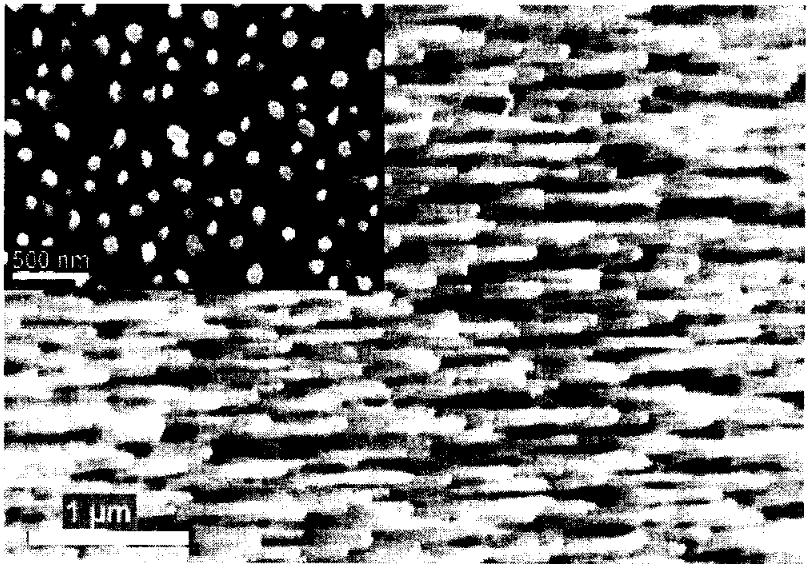

M. Meyyappan
Director, Center for Nanotechnology
NASA Ames Research Center
Moffett Field, CA 94035
meyya@orbit.arc.nasa.gov
web: http://www.ipt.arc.nasa.gov

Ames Research Center

Agenda

- Impact of Nanotechnology on various sectors
- National Nanotechnology Initiative
- Carbon Nanotubes
    - CNT - growth and characterization
    - CNT based microscopy
    - CNT based biosensors
- Some other Nano examples
- Educational Issues

Nanotechnology R & D

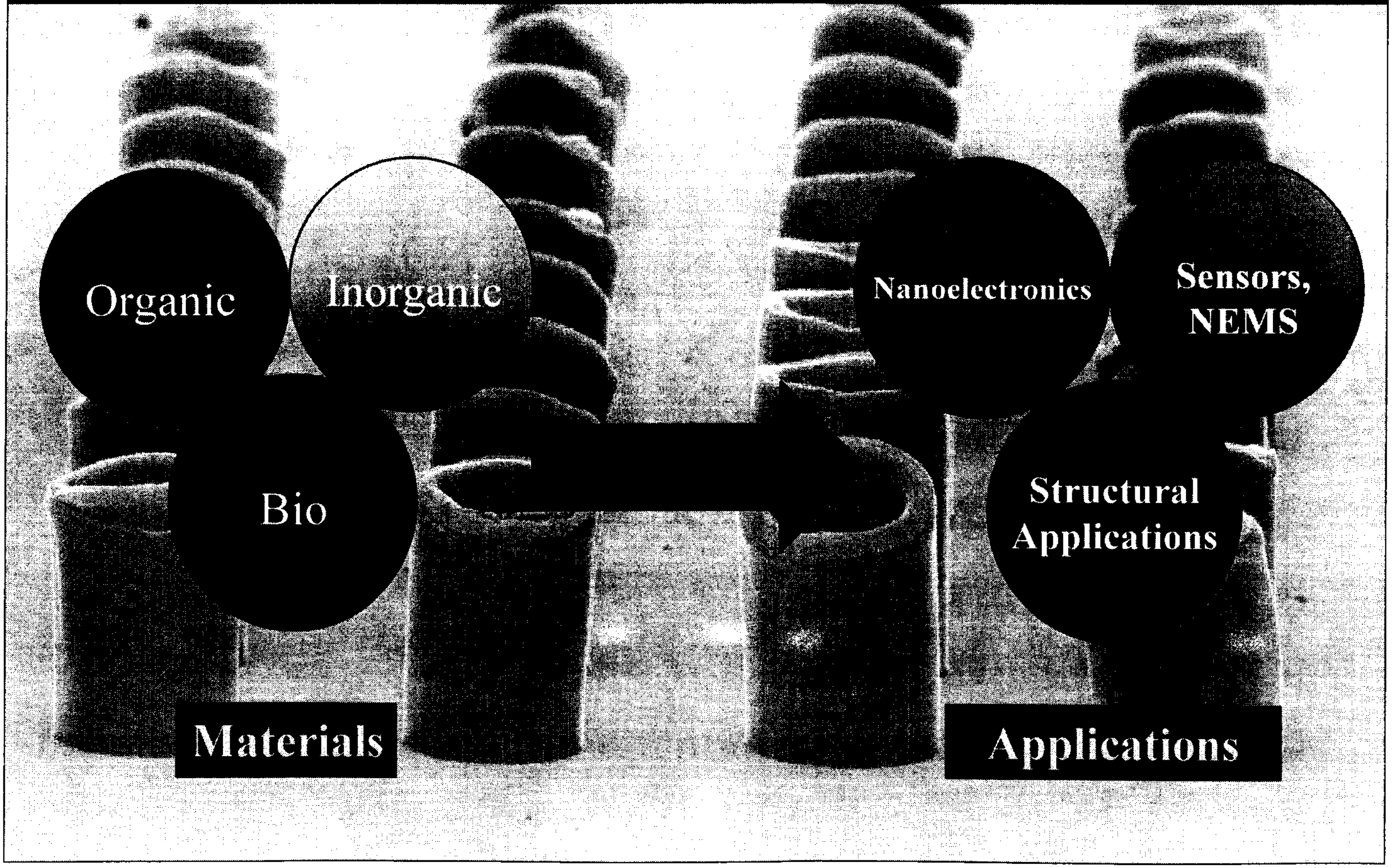

Organic

Inorganic

Bio

Materials

Nanoelectronics

Sensors, NEMS

Structural Applications

Applications

Some Fundamental Science Issues

1. What novel quantum properties will be enabled by nanostructures (at room temp.)?
2. How different from bulk behavior?
3. What are the surface reconstructions and rearrangements of atoms in nanocrystals?
4. Can carbon nanotubes of specified length and helicity be synthesized as pure species? Heterojunctions in 1-D?
5. What new insights can we gain about polymer, biological...systems from the capability to examine single-molecule properties?
6. How can one use parallel self-assembly techniques to control relative arrangements of nanoscale components according to predesigned sequence?
7. Are there processes leading to economic preparation of nanostructures with control of size, shape... for applications?

Impact of Nanotechnology

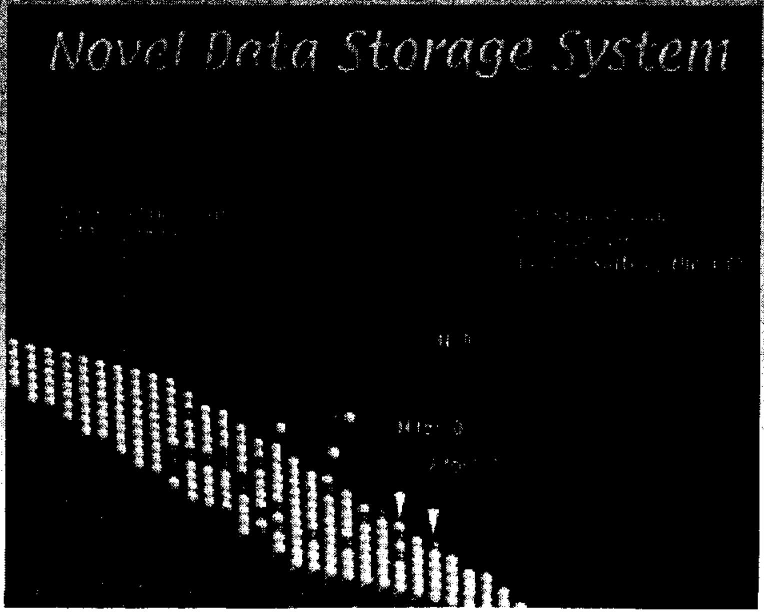

- Computing and Data Storage
- Materials and Manufacturing
- Health and Medicine
- Energy and Environment
- Transportation
- National Security
- Space exploration

Ames Research Center

Nanoelectronics and Computing

Past
Shared computing ➡ thousands of people sharing a mainframe computer

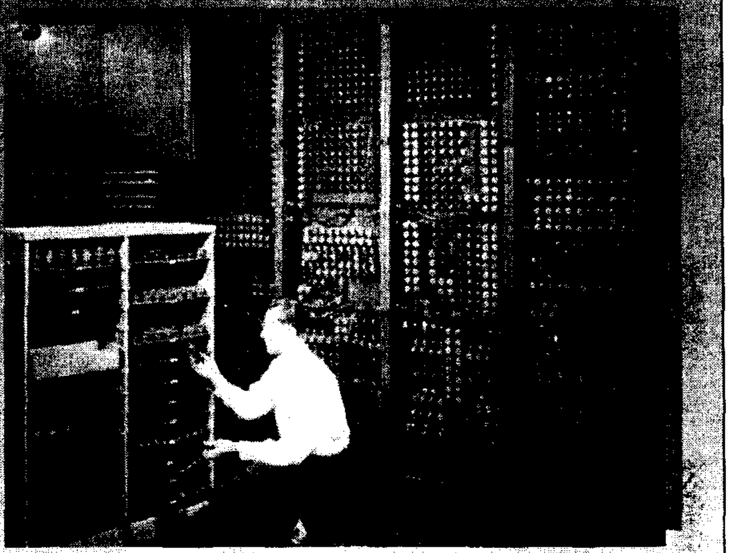

Present
Personal computing

Future
Ubiquitous computing ➡ thousands of computers sharing each and everyone of us; computers embedded in walls, chairs, clothing, light switches, cars….; characterized by the connection of things in the world with computation.

Ames Research Center

Sensors for the Automotive Industry

- Automotive electronics to grow to $30 Billion by 2005
- Pressure to keep cost of devices low is enormous
- Sensors in use now include monitoring wheel speed, pedal positions, oxygen sensors to check exhaust, accelerometers to detect sudden stops, pressure and temperature sensors
- Future systems
  - Collision avoidance
  - Break-by-wire, steer-by-wire systems (slowing the car and guiding electrically instead of manually)
  - Sensor systems when new fuel sources become common
- Challenges
  - High temperature survival of sensors
  - Withstanding mechanical shock, hostile environment
  - Conditions: sever swing in T; variable humidity; road salt; noxious gases; f ~ 10 g; ~ 10 year life-time
- MEMS made it in the airbag. But the car interior is a benign environment. Will MEMS work elsewhere in the car?

Ames Research Center

Nanoelectronics: What is Expected from Alternative Technologies?

- Must be easier and cheaper to manufacture than CMOS
- Need high current drive; should be able to drive capacitances of interconnects of any length
- High level of integration (>10^{10} transistors/circuit)
- High reproducibility (better than ± 5%)
- Reliability (operating time > 10 years)
- Very low cost (< 1 µcent/transistor)
- Everything about the new technology must be compelling and simultaneously further CMOS scaling must become difficult and not cost-effective. Until these two happen together, the enormous infrastructure built around silicon will keep the silicon engine humming….

Ames Research Center

Switching Energy of Electron Devices and Brain Cells

(E. Takeda, Microelectron. Rel., 1997)

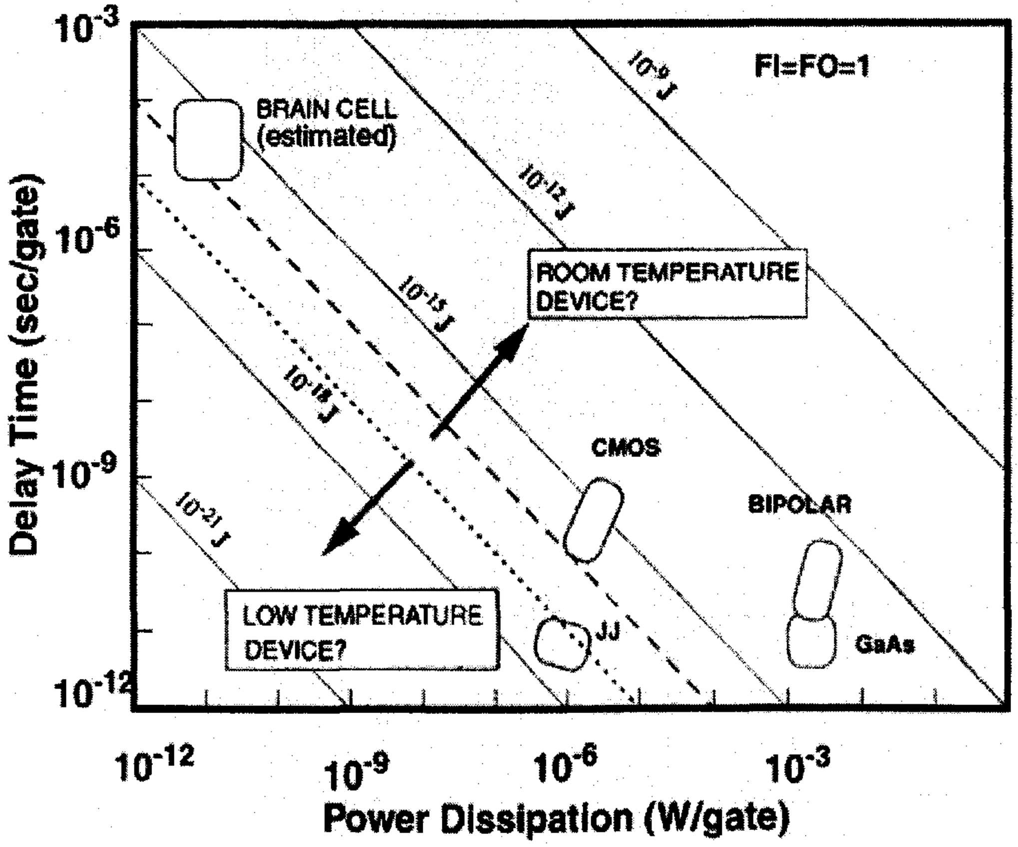

Ames Research Center

Materials and Manufacturing

- Ability to synthesize nanoscale building blocks with control on size, composition etc. ➡ further assembling into larger structures with designed properties will revolutionize materials manufacturing
  - Manufacturing metals, ceramics, polymers, etc. at exact shapes without machining
  - Lighter, stronger and programmable materials
  - Lower failure rates and reduced life-cycle costs
  - Bio-inspired materials
  - Multifunctional, adaptive materials
  - Self-healing materials

- Challenges ahead
  - Synthesis, large scale processing
  - Making useful, viable composites
  - Multiscale models with predictive capability
  - Analytical instrumentation

Ames Research Center

Materials and Manufacturing Some Recent Advances

- Carbon Nanotubes
- Nanostructured Polymers
- Optical fiber preforms through sol-gel processing of nanoparticles
- Nanoparticles in imaging systems
- Nanostructured coatings
- Ceramic nanoparticles for netshapes

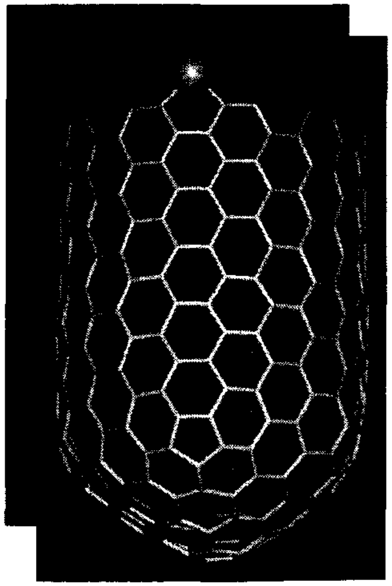

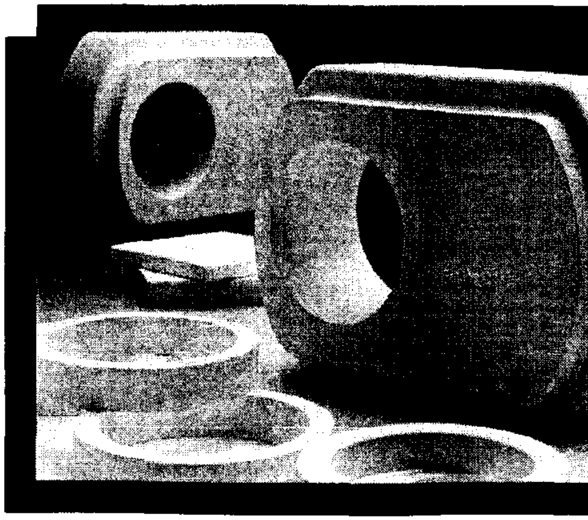

Source: IWGN Report

Ames Research Center

Health and Medicine

- Expanding ability to characterize genetic makeup will revolutionize the specificity of diagnostics and therapeutics
    - Nanodevices can make gene sequencing more efficient
- Effective and less expensive health care using remote and in-vivo devices

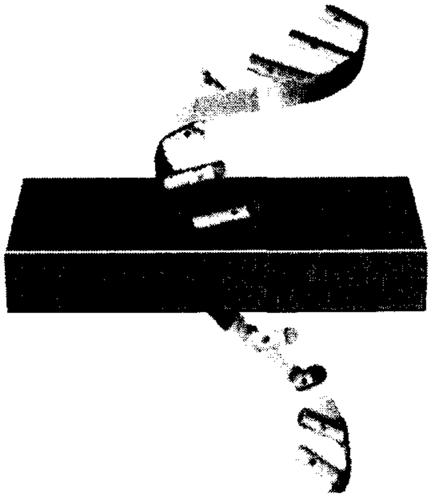

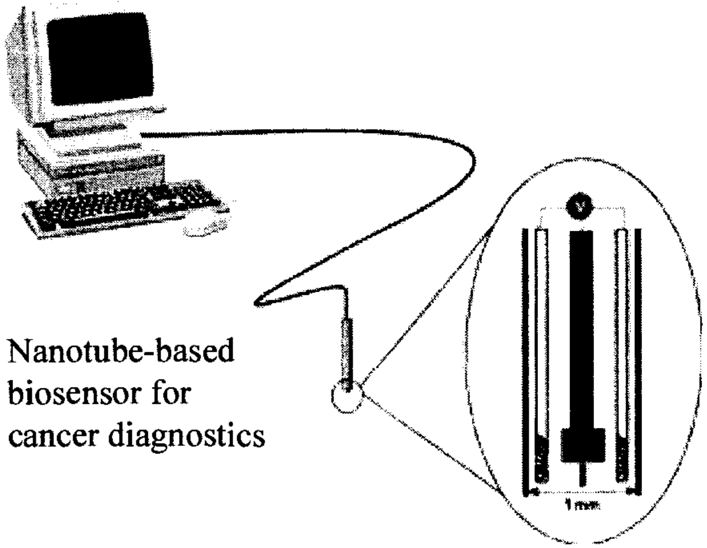

Nanotube-based biosensor for cancer diagnostics

- New formulations and routes for drug delivery, optimal drug usage
- More durable, rejection-resistant artificial tissues and organs
- Sensors for early detection and prevention

Ames Research Center

Energy and Environment

- Nanotechnology has the potential to impact energy efficiency, storage and production

- Materials of construction sensing changing conditions and in response altering their inner structure

- Monitoring and remediation of environmental problems; curbing emissions; development of environmental friendly processing technologies

- Some recent examples:
  - Crystalline materials as catalyst support, $300 b/year
  - Ordered mesoporous material by Mobil oil to remove ultrafine contaminants
  - Nano-particle reinforced polymers to replace metals in automobiles to reduce gasoline consumption

Ames Research Center

National Security

Some critical defense applications of nanotechnology include

- Continued information dominance: collection, transmission, and protection
- High performance, high strength, light weight military platforms while reducing failure rates and life cycle costs
- Chemical/biological/nuclear sensors; homeland protection
- Nano and micromechanical devices for control of nuclear and other defense systems
- Virtual reality systems based on nanoelectronics for effective training
- Increased use of automation and robotics

Ames Research Center

National Nanotechnology Initiative

- NNI has been effective since FY01. President's request for FY03 $679 M, representing 17% increase
- Proposal to introduce a Nanotechnology Bill in Congress is at early stages
- "Detection and Protection" gaining importance
- Biggest portion of the funding goes to NSF
  - Followed by DoD, NASA, DOE, NIH
  - All these agencies spend most of their nano funding on university programs
- Very strong activities in Japan, Europe, China, Singapore, fueled by Government Initiatives
- Nano activities in U.S. companies: IBM, Motorola, HP, Lucent, Hitachi USA, Corning, DOW, 3M...
  - In-house R & D
  - Funding ventures
- Nano Centers being established at Universities all across the world
- Emerging small companies
  - VC funding on the increase

Ames Research Center

Grand Coalition

- **Academia** will play key role in development of nanoscience and technology
  - Promote interdisciplinary work involving multiple departments
  - Develop new educational programs
  - Technology transfer to industry

- **Government Labs** will conduct mission oriented nanotechnology research
  - Provide large scale facilities and infrastructure for nanotechnology research
  - Technology transfer to industry

- **Government Funding Agencies** will provide research funding to academia, [illegible] industry through the NNI and other programs (SBIR, STIR, ATP…)

- **Industry** will invest only when products are within 3-5 years
  - Maintain in-house research, sponsor precompetitive research
  - Sponsor technology start-ups and spin-offs

- **Venture Capital Community** will identify ideas with market potential and help to launch start-ups

- **Professional societies** should establish interdisciplinary forum for exchange of information; reach out to international community; offer continuing education courses

Ames Research Center

NASA's Own Moore's Law

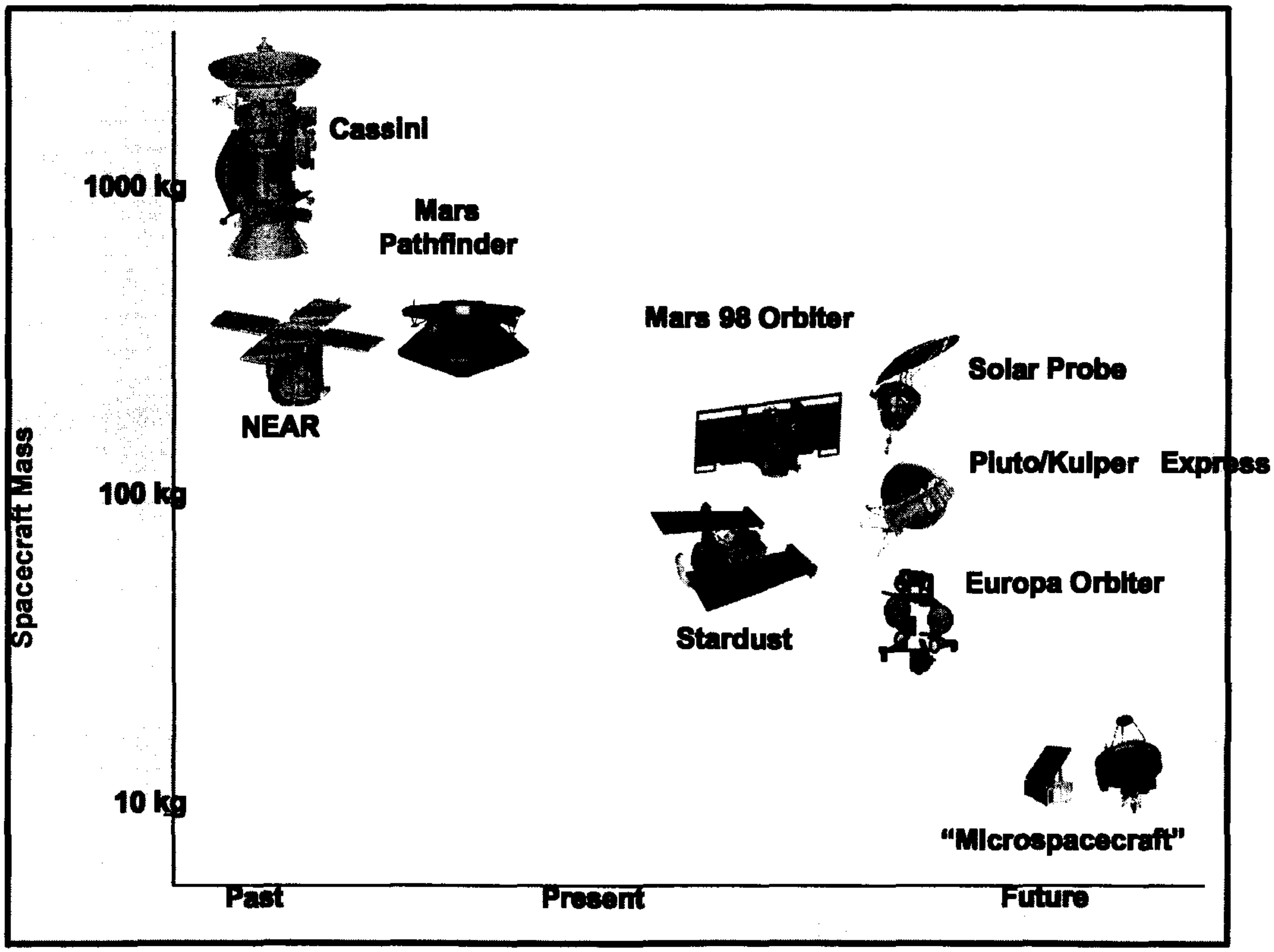

Ames Research Center

Why Nanotechnology at NASA?

- Advanced miniaturization, a key thrust area to enable new science and exploration missions
    - Ultrasmall sensors, power sources, communication, navigation, and propulsion systems with very low mass, volume and power consumption are needed
- Revolutions in electronics and computing will allow reconfigurable, autonomous, “thinking” spacecraft
- Nanotechnology presents a whole new spectrum of opportunities to build device components and systems for entirely new space architectures
    - Networks of ultrasmall probes on planetary surfaces
    - Micro-rovers that drive, hop, fly, and burrow
    - Collection of microspacecraft making a variety of measurements

Europa Submarine

Ames Research Center

Just one Material, so much Potential

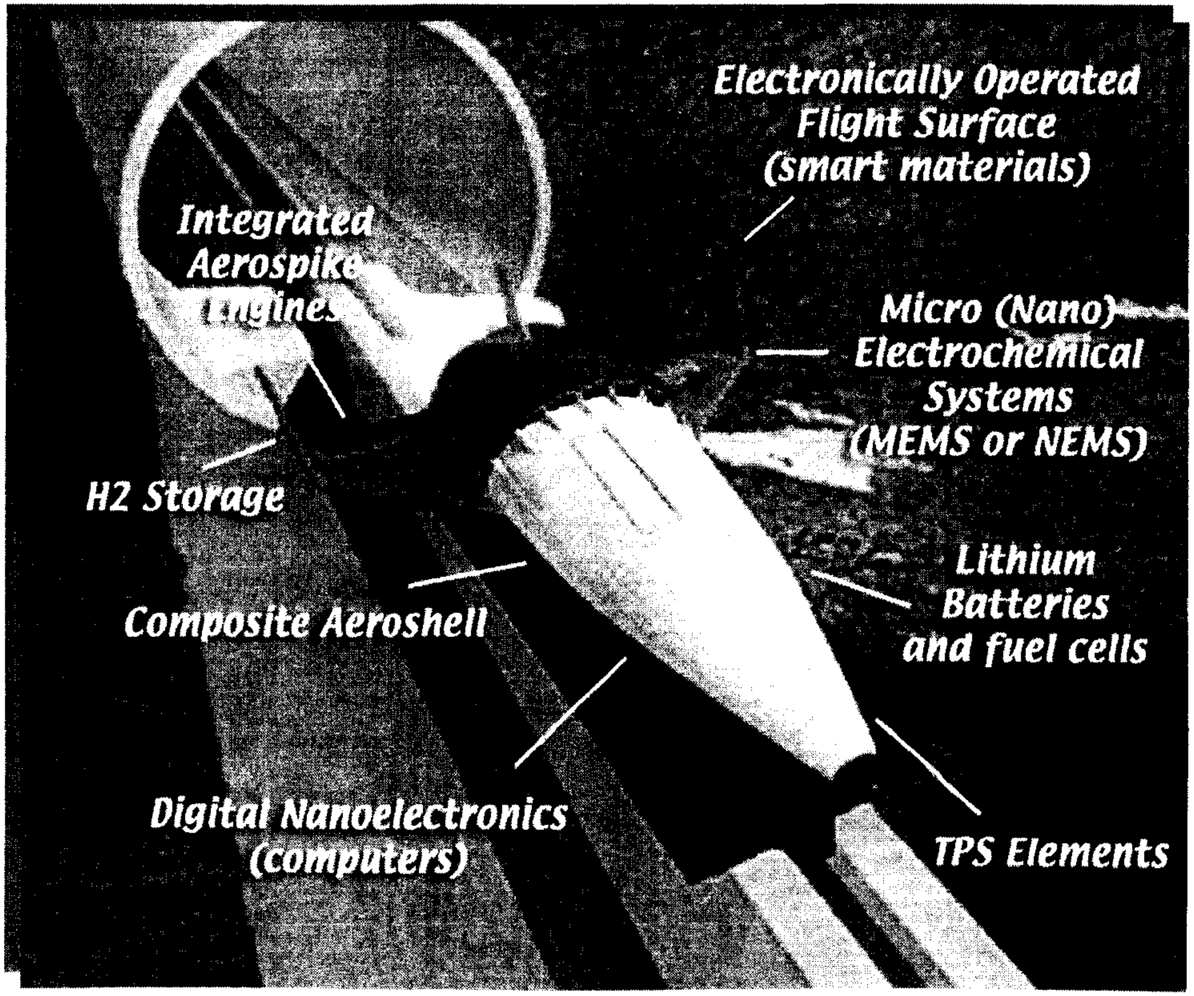

Ames Research Center

NASA's Investments in Nano

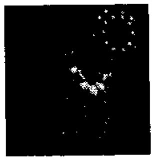

- NASA Ames Center for Nanotechnology, started in 1996, is the largest in-house R & D in Federal Government, consists of 50 scientists and engineers working on various aspects of experimental and computational nanotechnology fields.

- NASA Ames has strong collaboration with the academia
  - undergraduate student research program
  - high school student research program

- Smaller programs at JSC (CNT composites), Langley (Nano materials), Glenn (Energy storage), and JPL

- NASA's university-based Nano-Institutes
  - Three institutes, $3 M/year/institute for 5 + optional 3 years (Purdue, UCLA, Princeton/Texas A & M)

- Recent spin-off: Integrated Nanosystems, Inc.

Ames Research Center

NASA Ames Nanotechnology Research Focus

- * **Carbon Nanotubes**
  - Growth (CVD, PECVD)
  - Characterization
  - AFM tips
    - Metrology
    - Imaging of Mars Analog
    - Imaging Bio samples
  - Electrode development
  - Biosensor (cancer diagnostics)
  - Chemical sensor
  - Logic Circuits
  - Chemical functionalization
  - Gas Absorption
  - Device Fabrication
- * **Molecular Electronics**
  - Synthesis of organic molecules
  - Characterization
  - Device fabrication
- * **Inorganic Nanowires**
- * **Protein Nanotubes**
  - Synthesis
  - Purification
  - Application Development
- * **Genomics**
  - Nanopores in gene sequencing
  - Genechips development
- * **Computational Nanotechnology**
  - CNT - Mechanical, thermal properties
  - CNT - Electronic properties
  - CNT based devices: physics, design
  - CNT based composites, BN nanotubes
  - CNT based sensors
  - DNA transport
  - Transport in nanopores
  - Nanowires: transport, thermoelectric effect
  - Transport: molecular electronics
  - Protein nanotube chemistry
- * **Quantum Computing**
- * **Computational Quantum Electronics**
  - Noneq. Green's Function based Device Simulator
- * **Computational Optoelectronics**
- * **Computational Process Modeling**

Carbon Nanotube

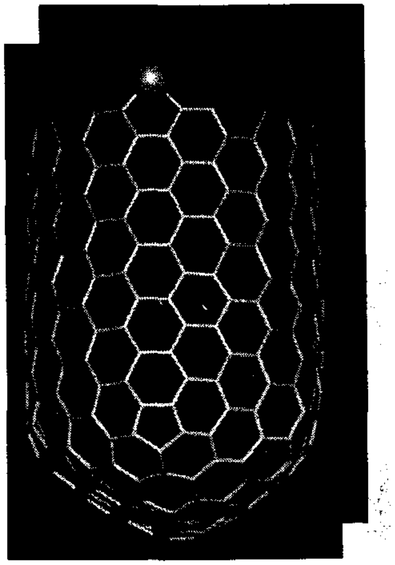

CNT is a tubular form of carbon with diameter as small as 1 nm. Length: few nm to microns.

CNT is configurationally equivalent to a two dimensional graphene sheet rolled into a tube.

- **STRIP OF A GRAPHENE SHEET ROLLED INTO A TUBE**

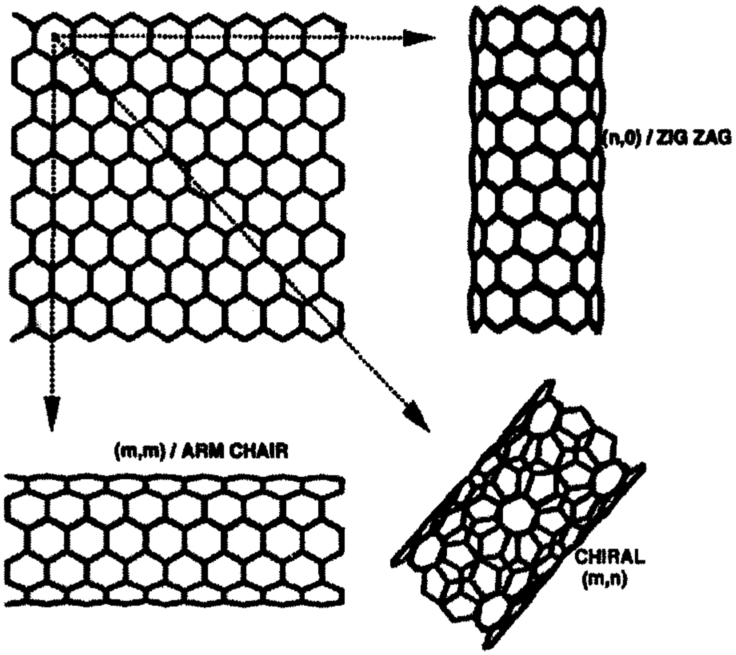

CNT exhibits extraordinary mechanical properties: Young's modulus over 1 Tera Pascal, as stiff as diamond, and tensile strength ~ 200 GPa.

CNT can be metallic or semiconducting, depending on chirality.

CNT Properties

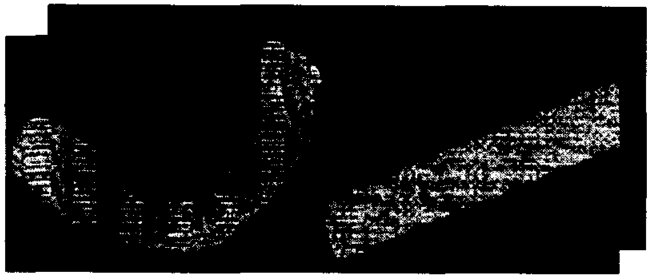

- The strongest and most flexible molecular material because of C-C covalent bonding and seamless hexagonal network architecture

- Young's modulus of over 1 TPa vs 70 GPa for Aluminum, 700 GPA for C-fiber
    - strength to weight ratio 500 time > for Al; similar improvements over steel and titanium; one order of magnitude improvement over graphite/epoxy

- Maximum strain ~10% much higher than any material

- Thermal conductivity ~ 3000 W/mK in the axial direction with small values in the radial direction

CNT Properties (cont.)

- Electrical conductivity six orders of magnitude higher than copper
- Can be metallic or semiconducting depending on chirality
    - 'tunable' bandgap
    - electronic properties can be tailored through application of external magnetic field, application of mechanical deformation…
- Very high current carrying capacity
- Excellent field emitter; high aspect ratio and small tip radius of curvature are ideal for field emission
- Can be functionalized

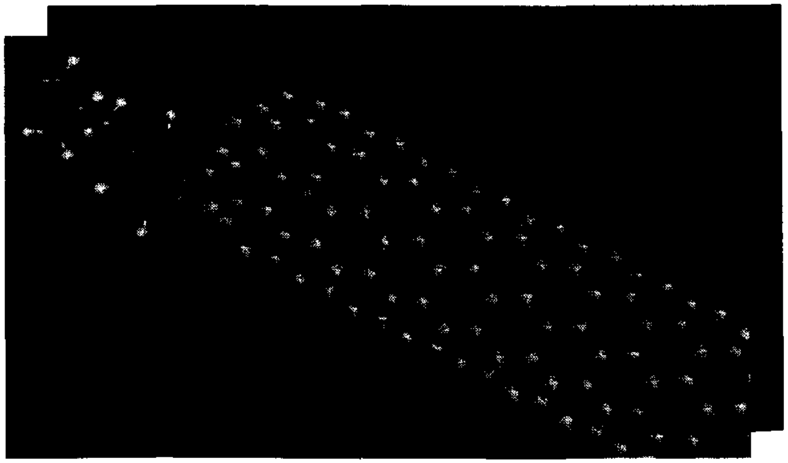

Ames Research Center

CNT Applications: Structural, Mechanical

- High strength composites
- Cables, tethers, beams
- Multifunctional materials
- Functionalize and use as polymer back bone
  - plastics with enhanced properties like “blow molded steel”
- Heat exchangers, radiators, thermal barriers, cryotanks
- Radiation shielding
- Filter membranes, supports
- Body armor, space suits

Challenges

- Control of properties, characterization
- Dispersion of CNT homogeneously in host materials
- Large scale production
- Application development

CNT Applications: Electronics

- CNT quantum wire interconnects
- Diodes and transistors for computing
- Capacitors
- Data Storage
- Field emitters for instrumentation
- Flat panel displays
- THz oscillators

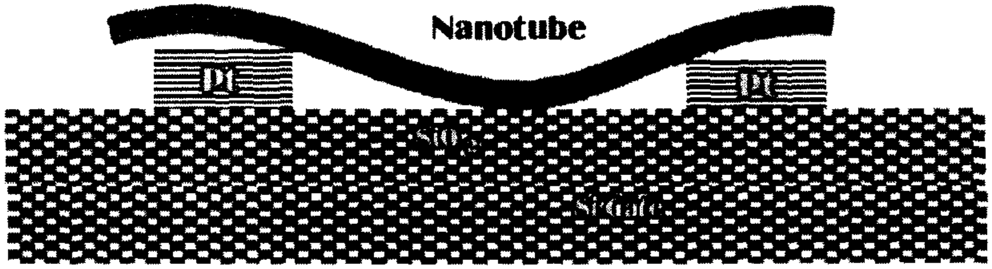

Challenges

- Control of diameter, chirality
- Doping, contacts
- Novel architectures (not CMOS based!)
- Development of inexpensive manufacturing processes

CNT Applications: Sensors, NEMS, Bio

- CNT based microscopy: AFM, STM…
- Nanotube sensors: force, pressure, chemical…
- Biosensors
- Molecular gears, motors, actuators
- Batteries, Fuel Cells: H_2, Li storage
- Nanoscale reactors, ion channels
- Biomedical
    - in vivo real time crew health monitoring
    - Lab on a chip
    - Drug delivery
    - DNA sequencing
    - Artificial muscles, bone replacement, bionic eye, ear...

Challenges

- Controlled growth
- Functionalization with probe molecules, robustness
- Integration, signal processing
- Fabrication techniques

CNT Synthesis

- CNT has been grown by laser ablation (pioneering at Rice) and carbon arc process (NEC, Japan) - early 90s.
  - SWNT, high purity, purification methods
- CVD is ideal for patterned growth (electronics, sensor applications)
  - Well known technique from microelectronics
  - Hydrocarbon feedstock
  - Growth needs catalyst (transition metal)
  - Multiwall tubes at 500-800° deg. C.
  - Numerous parameters influence CNT growth

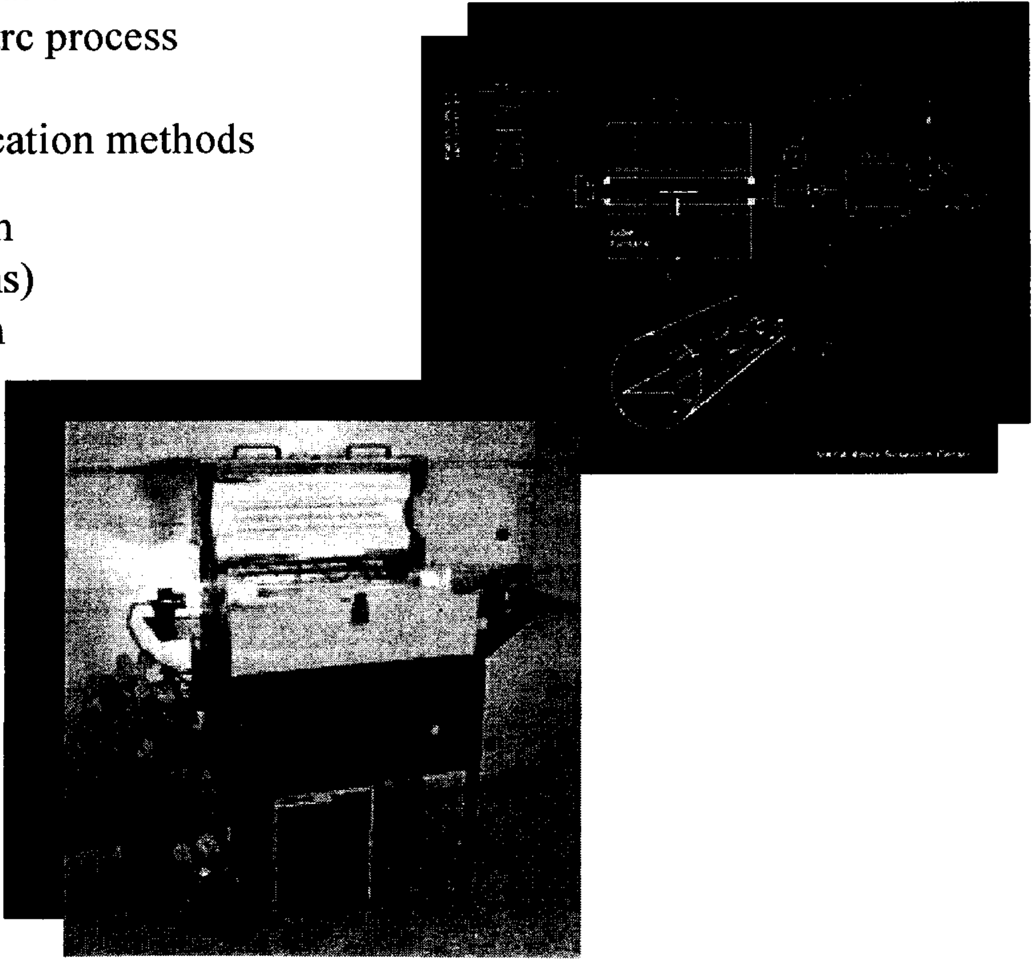

Ames Research Center

Catalyst Characterization

- Catalyst surface characterized by AFM (with SWNT tip) and STM.
- AFM image of as-sputtered 10 nm iron catalyst (area shown is 150 nm x 150 nm). Also, the same surface after heating to 750° C (and cooled) showing Fe particles rearranging into clusters.

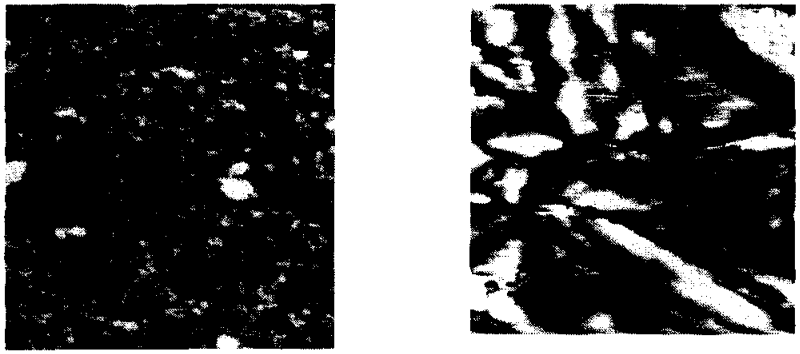

- STM image of a nickel catalyst showing nanoscale particles

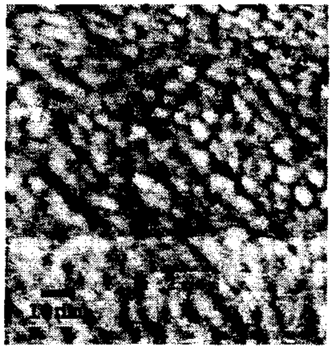

- These results are consistent with high resolution TEM showing particles as small as 2 nm.

Ames Research Center

CVD Growth Mechanisms For Carbon Nanotubes

- Adsorption and decomposition of feedstock on the surface of the catalyst particle
- Diffusion of carbon atoms into the particle from the supersaturated surface
- Carbon precipitates into a crystalline tubular form
- Particle remains on the surface and nanotube continues to lengthen - “base growth” mechanism
- Growth stops when graphitic overcoat occurs on the growth front - “catalytic poisoning”

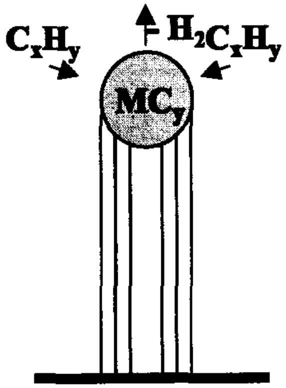

Tip Growth

Typically occurs when there are very weak metal-surface interactions

M = Fe, Ni, Co, Pt, Rh, Pd and others

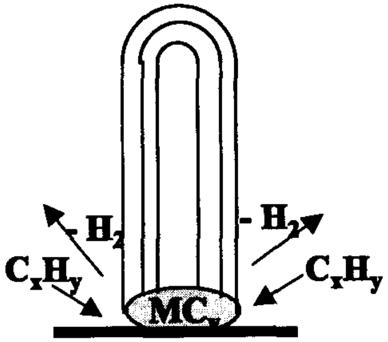

Base Growth

Occurs when the metal-surface interactions are strong

Ames Research Center

SWNTs on Patterned Substrates

- Surface masked by a 400 mesh TEM grid
- Methane, 900° C, 10 nm Al/1.0 nm Fe/0.2 nm Mo

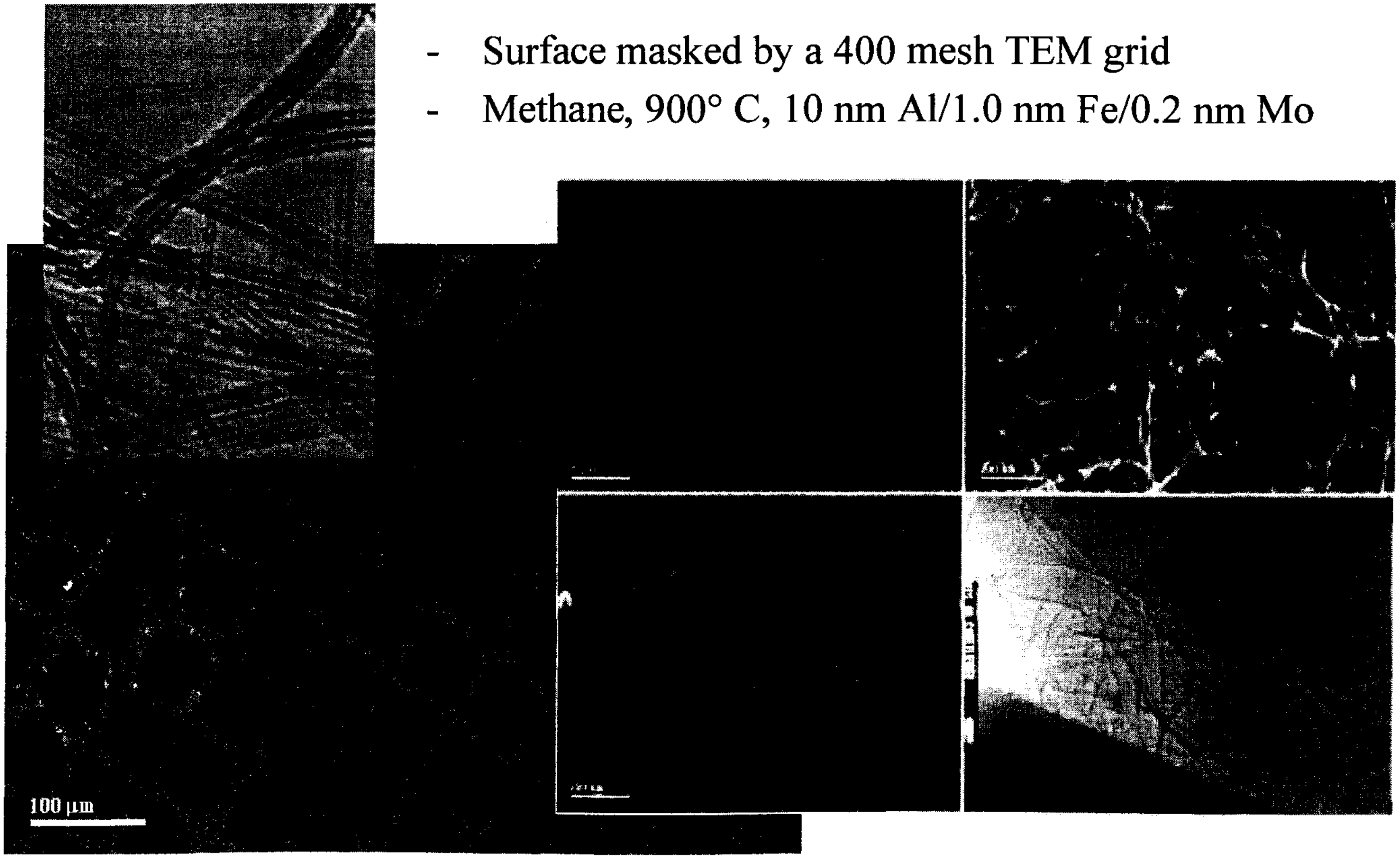

Raman Analysis of SWNTs

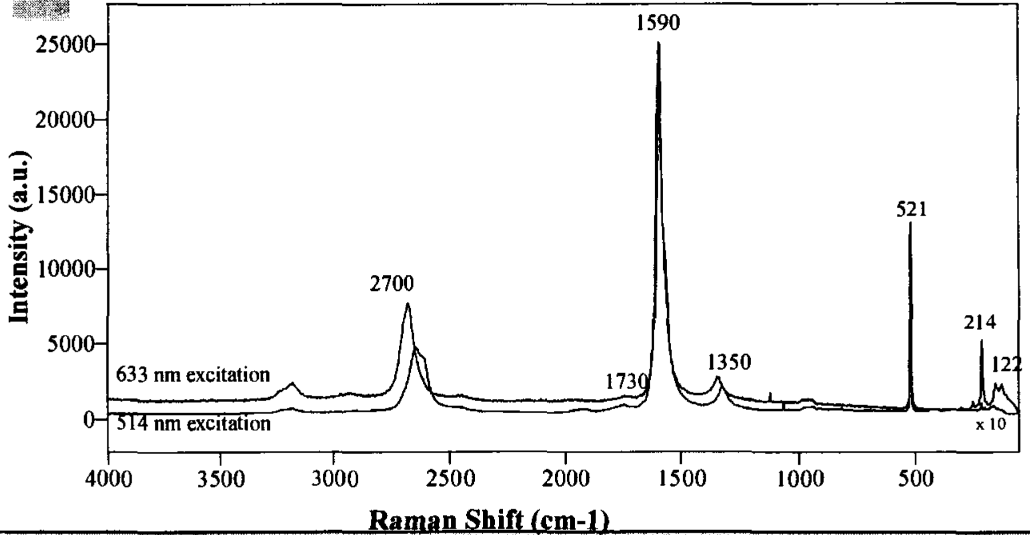

- 2 mw laser power, 1 µm focus spot
- Characteristic narrow band at 1590 cm^{-1}
- Signature band at 1730 cm^{-1} at SWNTs
- Diameter distribution 1.14 nm to 2 nm; consistent with TEM results
- High metallic % of NTs

Ames Research Center

Multiwall Nanotube Towers

- Surface masked by a 400 mesh TEM grid; 20 nm Al/ 10 nm Fe; nanotubes grown for 10 minutes

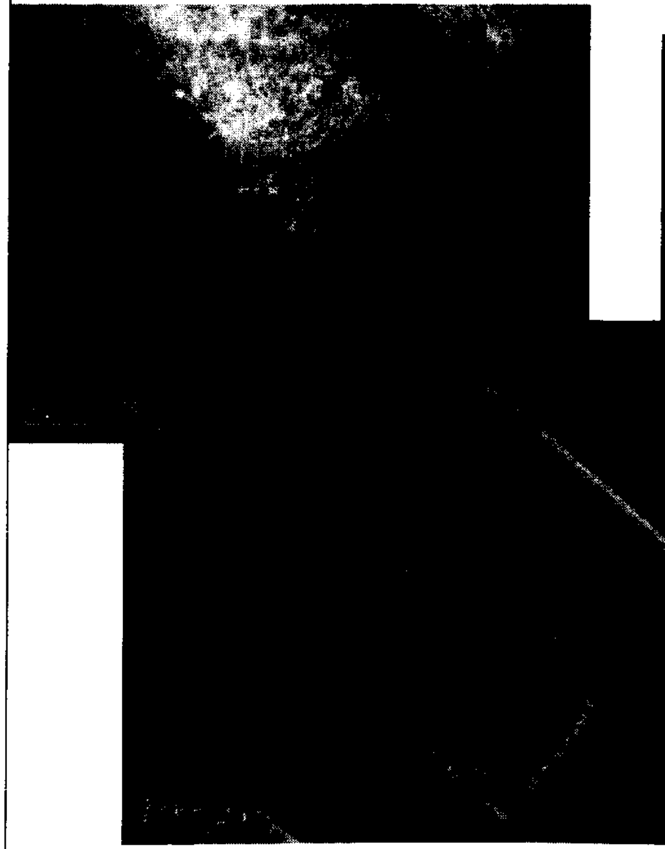

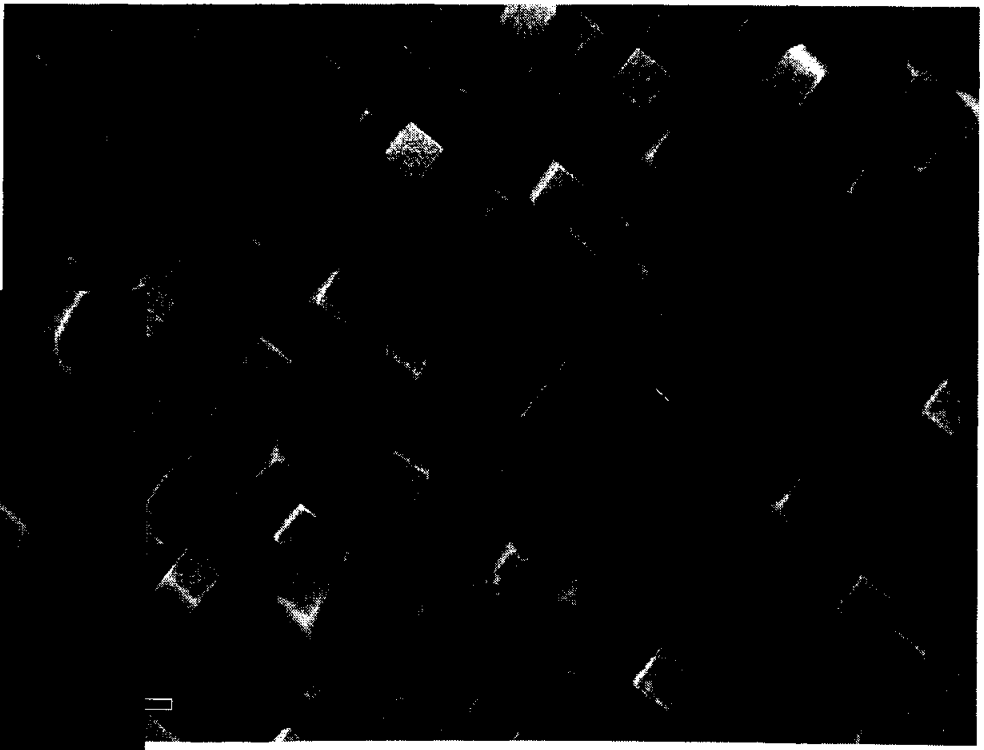

Grown using ethylene at 750° C

ICP Reactor for CNT Growth

- Inductively coupled plasmas are the simplest type of plasmas; very efficient in sustaining the plasma; reactor easy to build and simple to operate
- Quartz chamber 10 cm in diameter with a window for sample introduction
- Inductive coil on the upper electrode
- 13.56 MHz independent capacitive power on the bottom electrode
- Heating stage for the bottom electrode
- Operating conditions
  CH_4/H_2 : 5 - 20%
  Total flow : 100 sccm
  Pressure : 1 - 20 Torr
  Inductive power : 100-200 W
  Bottom electrode power : 0 - 100 W

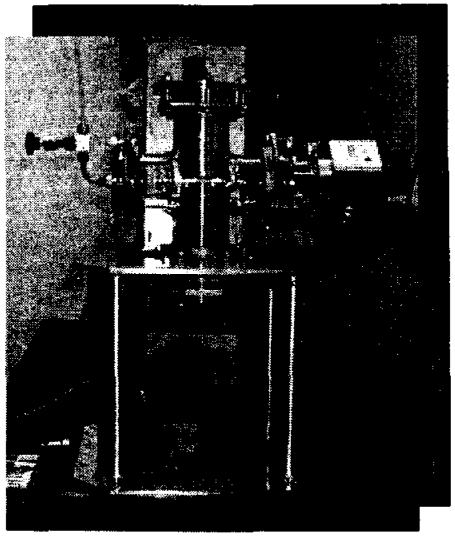

Ames Research Center

CNT in Microscopy

Atomic Force Microscopy is a powerful technique for imaging, nanomanipulation, as platform for sensor work, nanolithography...

Conventional silicon or tungsten tips wear out quickly. CNT tip is robust, offers amazing resolution.

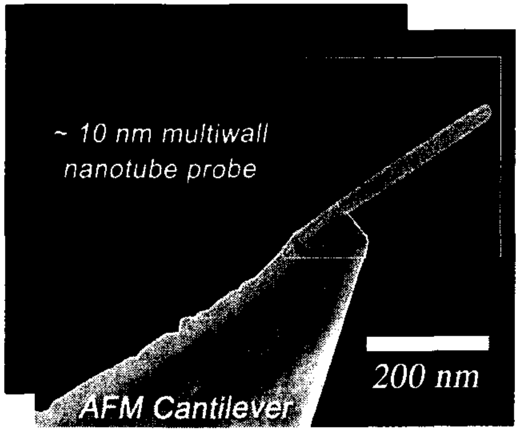

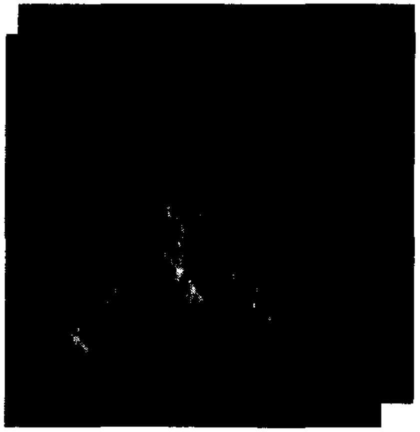

Simulated Mars dust

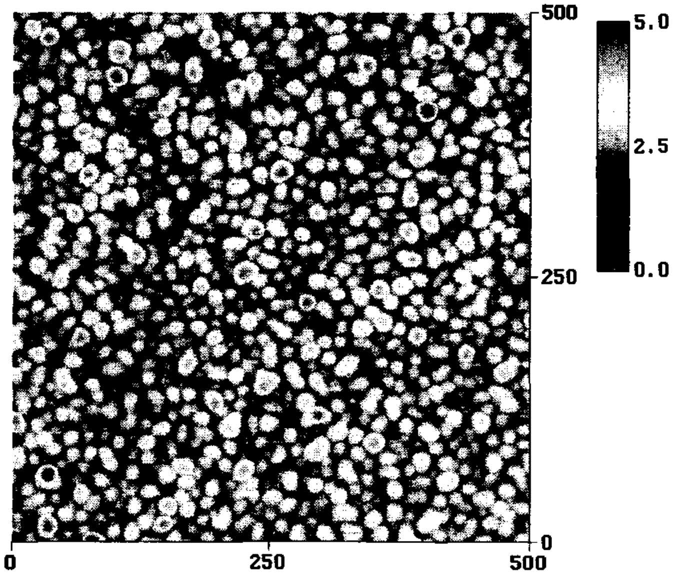

2 nm thick Au on Mica

WWW.NANO.GOV

NASA Ames Research Center
Ramsey Stevens, Lance Delzeit, Cattien Nguyen

Ames Research Center

Fabrication of CNT Probes

Transition metal catalyst is deposited from liquid phase or sputtered on the tip of the cantilever

Carbon nanotube is grown in thermal CVD or plasma reactor

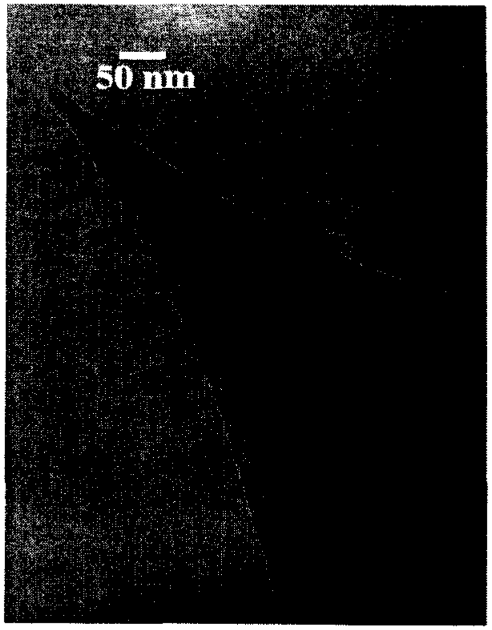

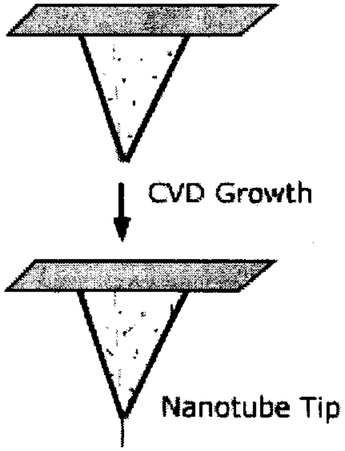

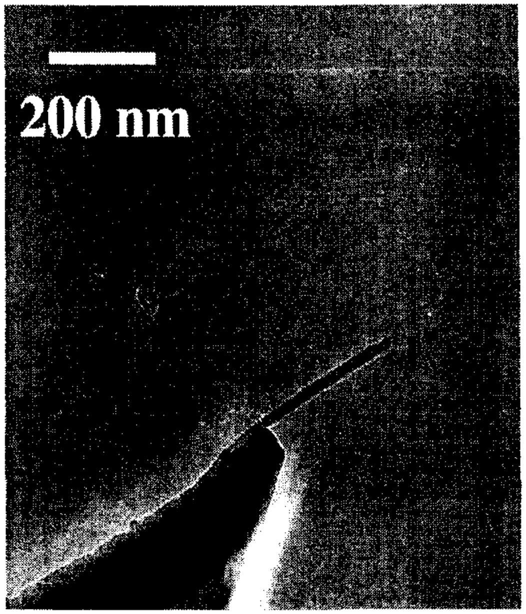

Ames Research Center

Profilometry in Integrated Circuit Manufacturing

280 nm line/space. Array of polymeric resist on a silicon substrate.

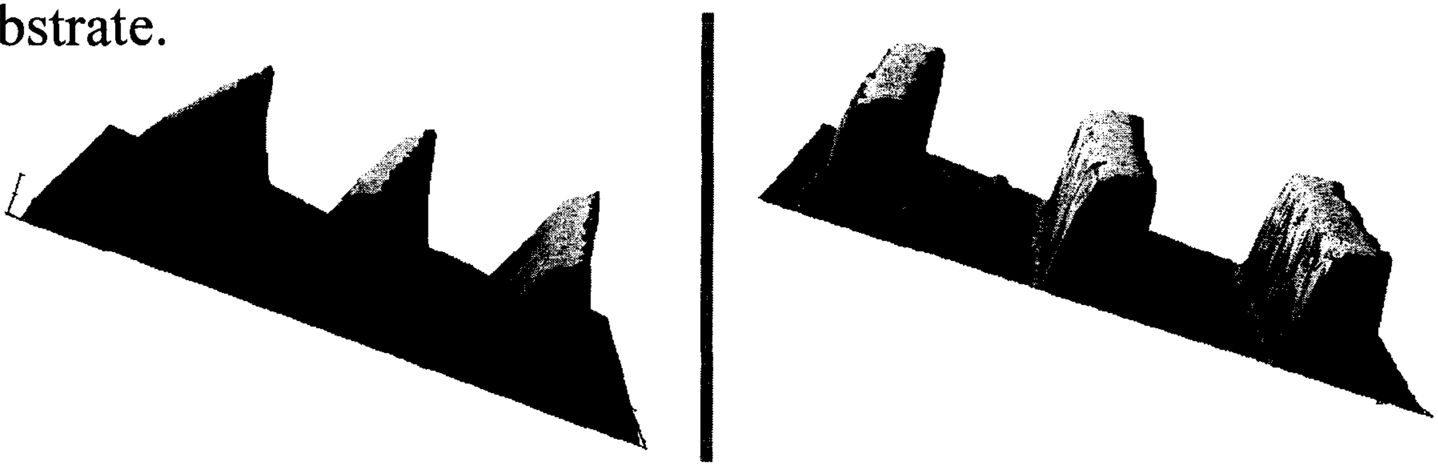

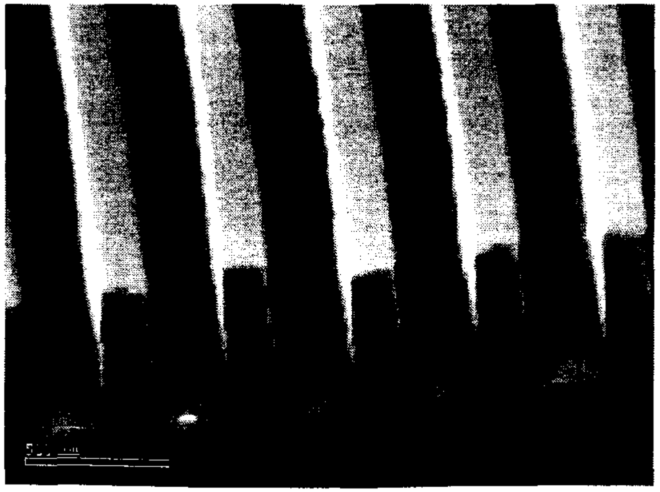

Ames Research Center

AFM Imaging with Single Wall Nanotube Tips

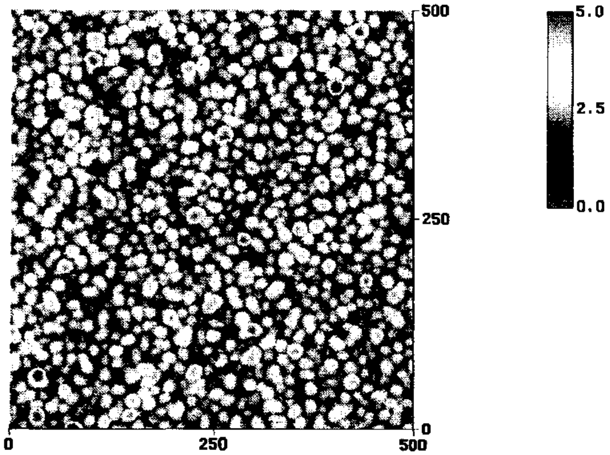

2 nm thick Au on Mica

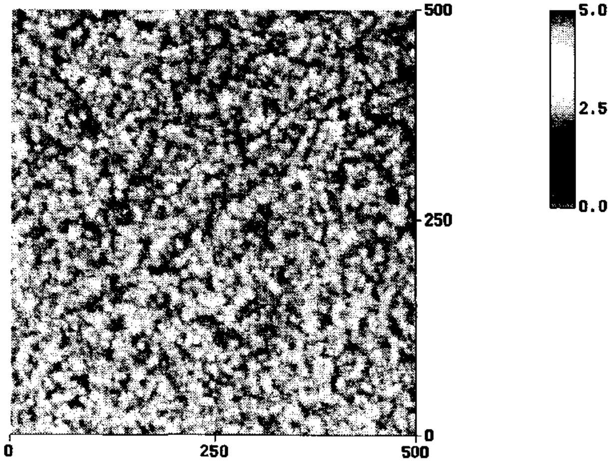

5 nm thick Ir on Mica

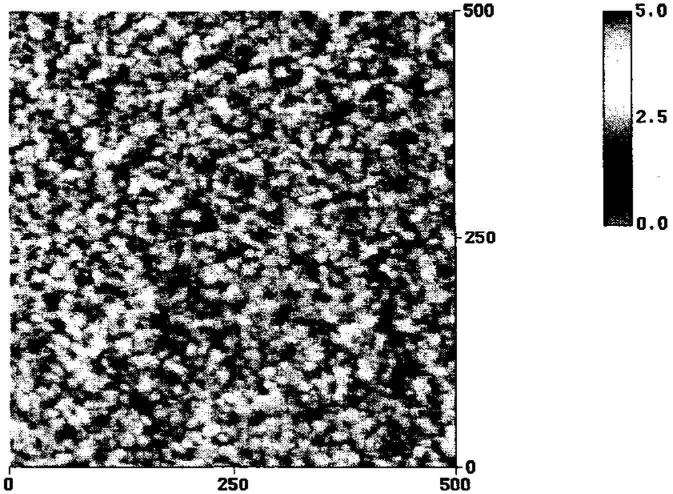

Si_3N_4 on Silicon substrate

Ames Research Center

Imaging of Mars Analogs

Optical image

Red Dune Sand (Mars Analog)

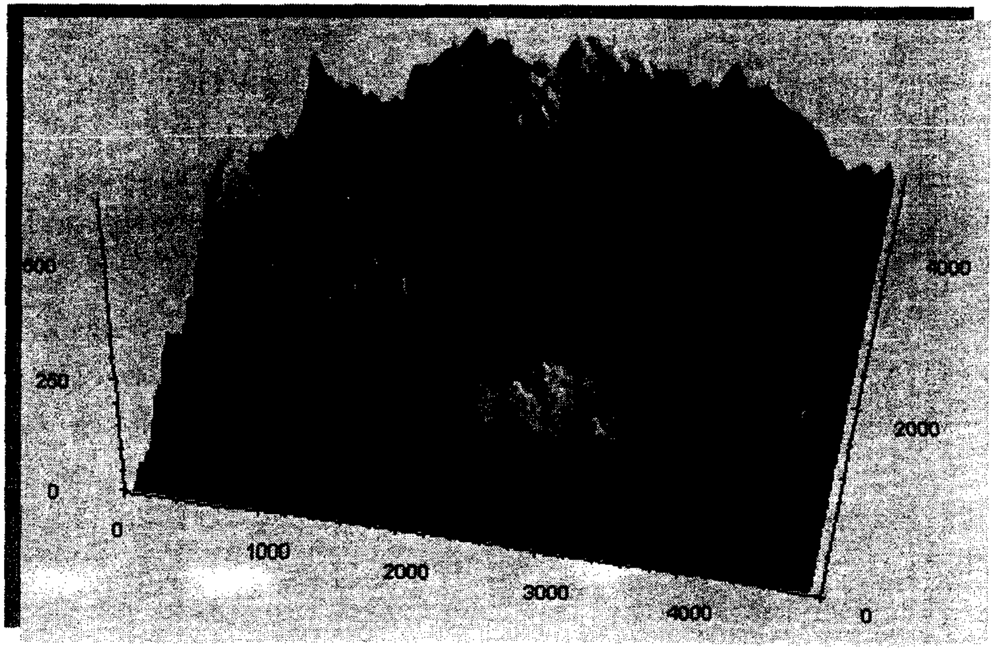

AFM image using
carbon nanotube tip

Ames Research Center

CNT Based Biosensors

- Our interest is to develop sensors for astrobiology to study origins of life. CNT, though inert, can be functionalized at the tip with a probe molecule. Current study uses AFM as an experimental platform.

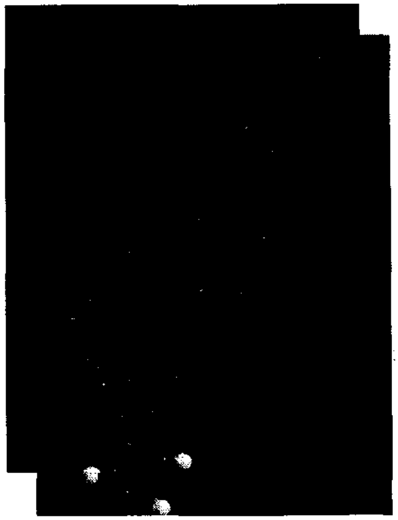

- The technology is also being used in collaboration with NCI to develop sensors for cancer diagnostics
  - Identified probe molecule that will serve as signature of leukemia cells, to be attached to CNT
  - Current flow due to hybridization will be through CNT electrode to an IC chip.
  - Prototype biosensors catheter development

- **High specificity**
- **Direct, fast response**
- **High sensitivity**
- **Single molecule and cell signal capture and detection**

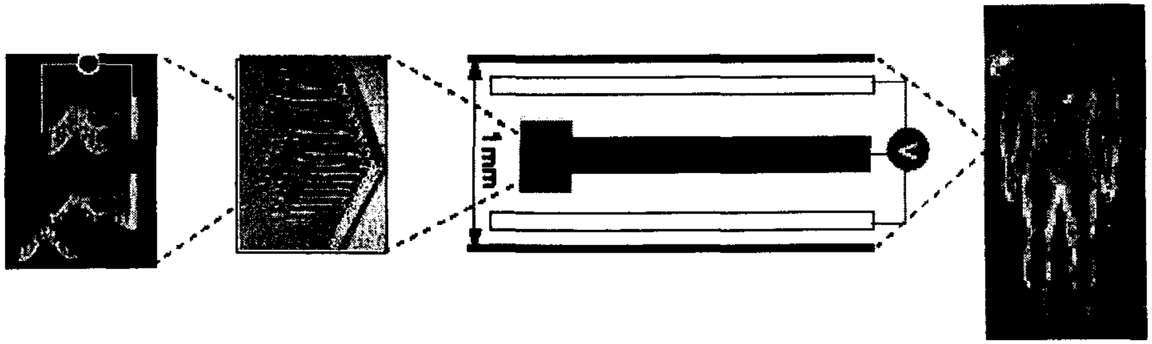

Ames Research Center

The Fabrication of CNT Nanoelectrode Array

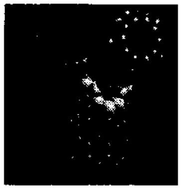

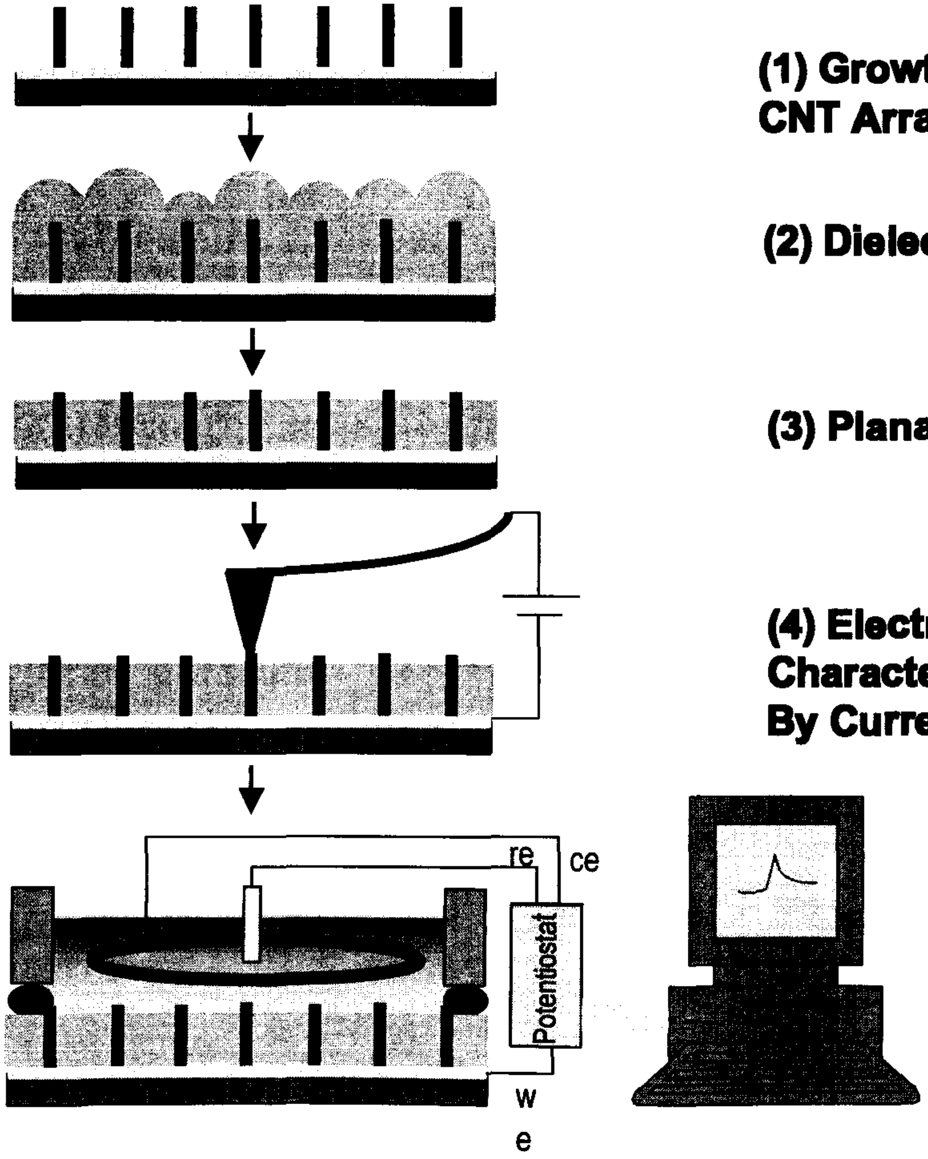

(1) Growth of Vertically Aligned CNT Array

(2) Dielectric Encapsulation

(3) Planarization

(4) Electrical Property Characterization By Current-sensing AFM

(5) Electrochemical Characterization

Ames Research Center

Electrical Properties of CNTs

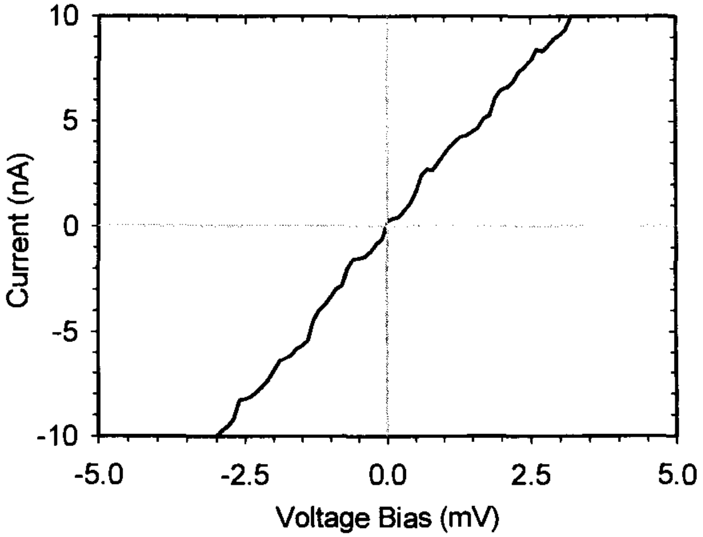

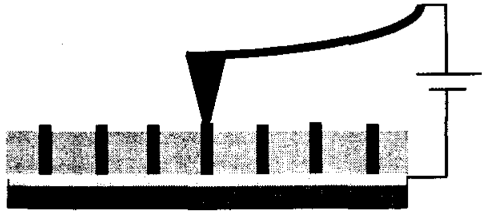

Current Sensing AFM

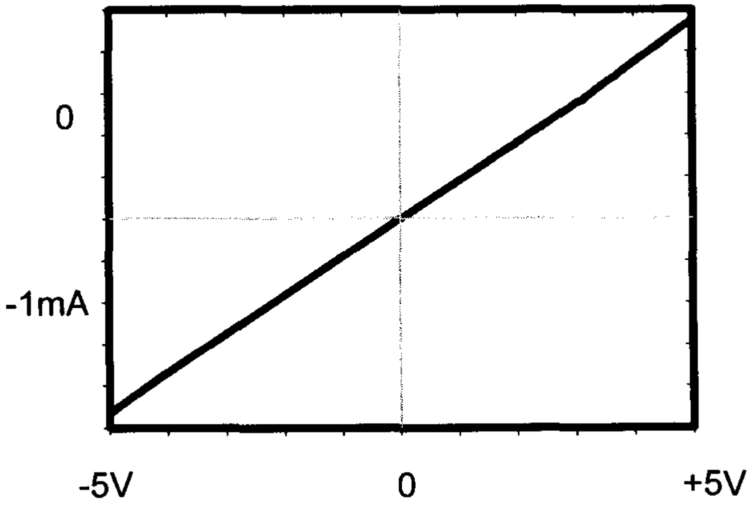

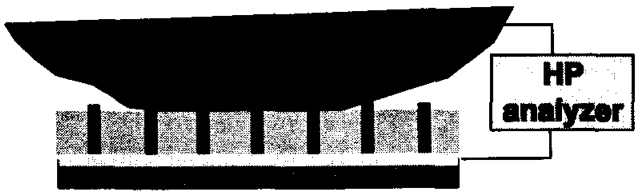

Four-probe station
And HP parameter analyzer

Chemical Functionalization

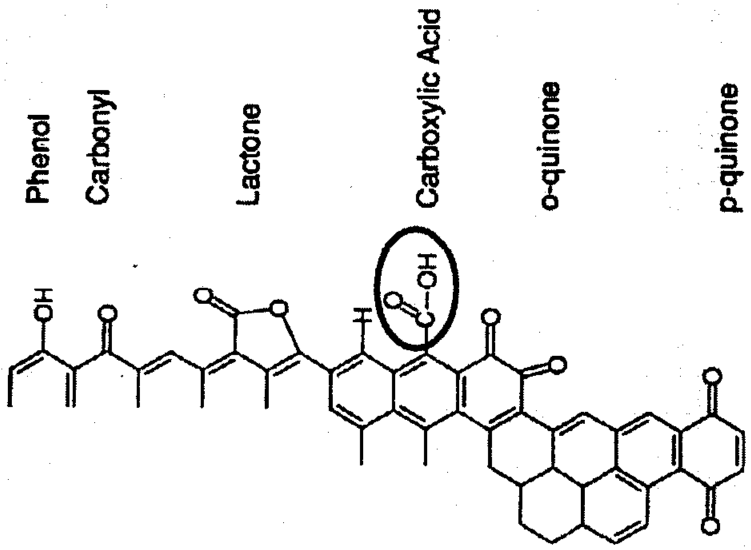

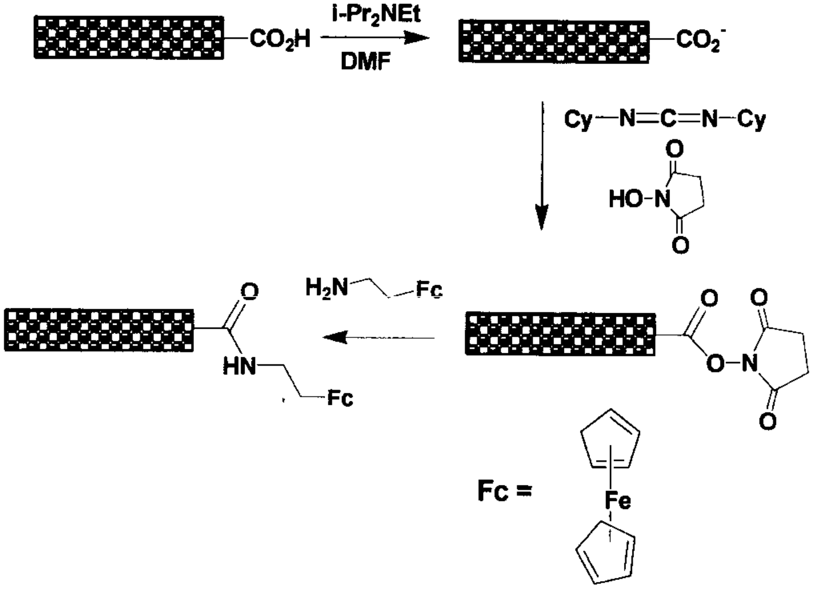

Highly selective reaction of primary amine with surface –COOH group

Ames Research Center

Functionalization of DNA

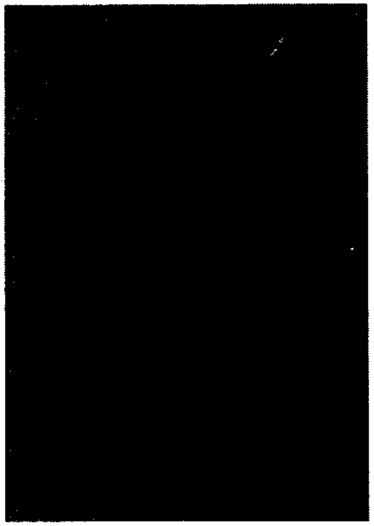

Cy3 image

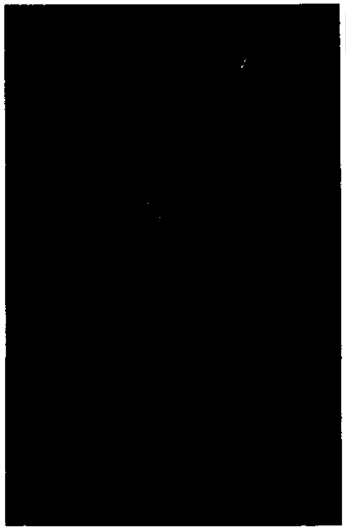

Cy5 image

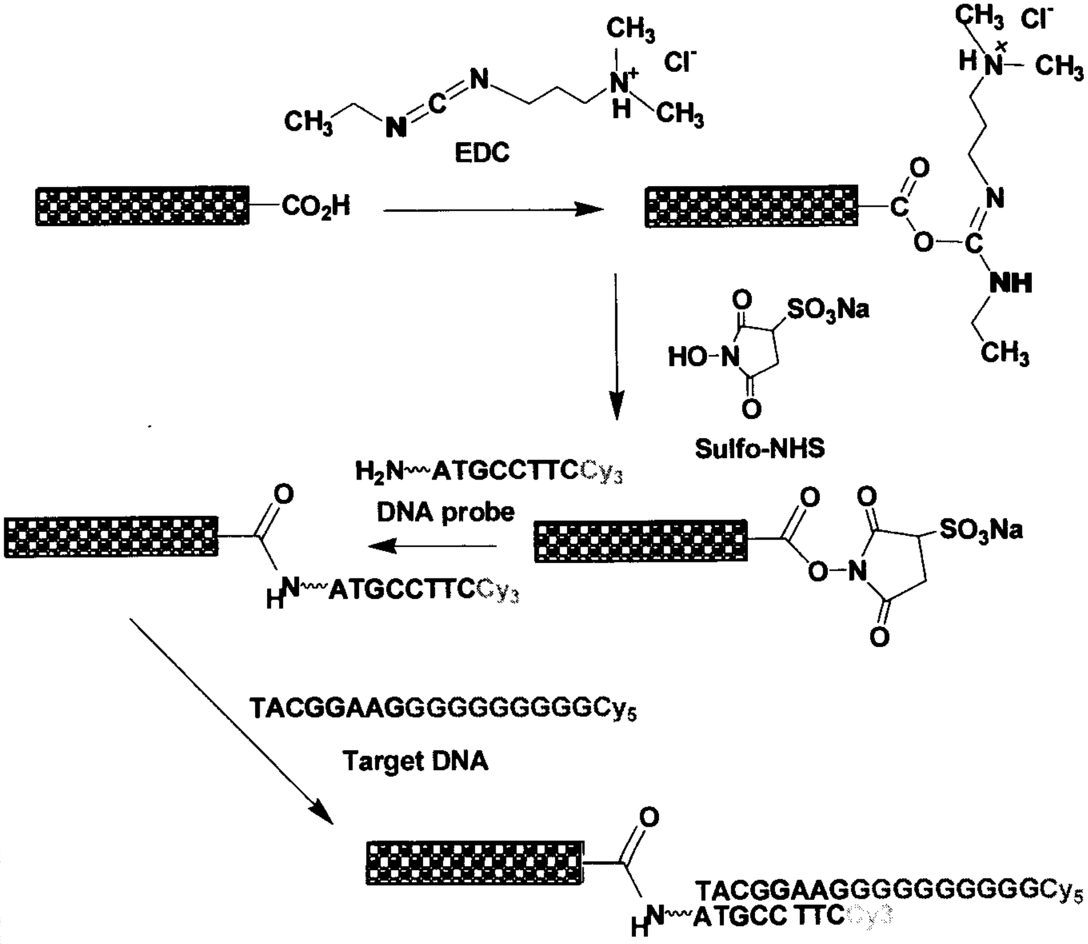

Ames Research Center

CNT DNA Sensor
Using Electrochemical Detection

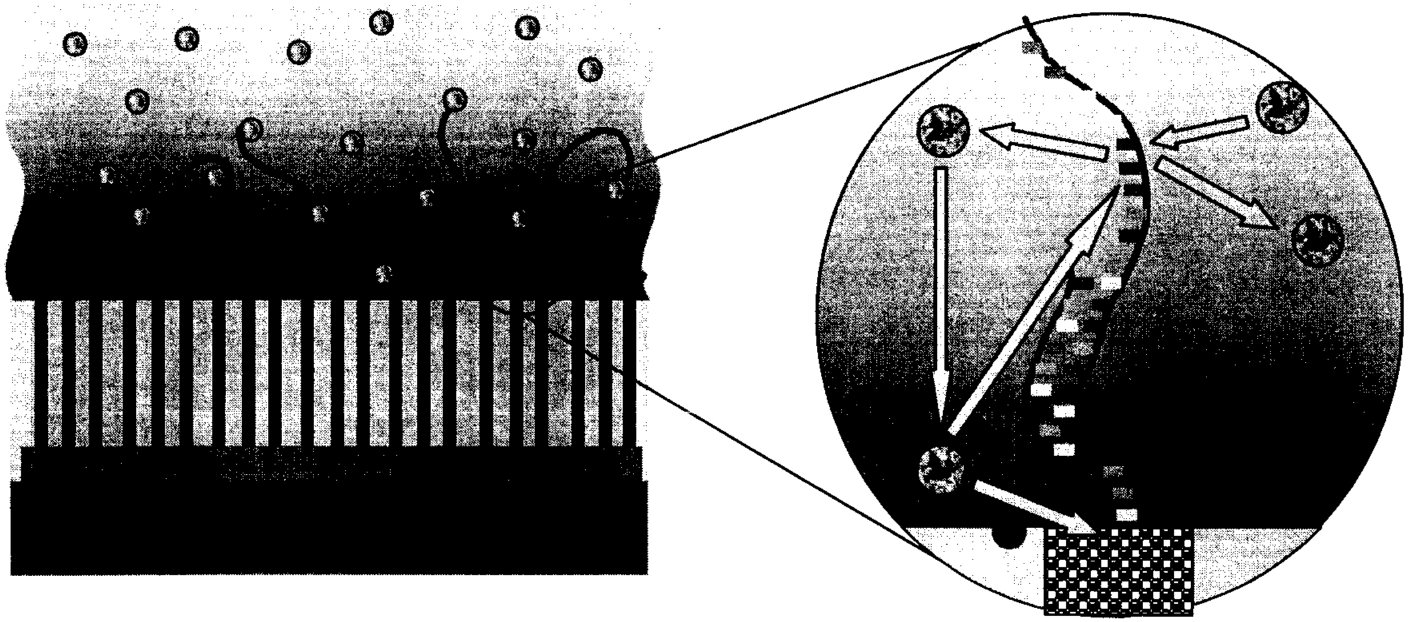

☐ **MWNT array electrode functionalized with DNA/PNA probe as an ultrasensitive sensor for detecting the hybridization of target DNA/RNA from the sample.**

- Signal from redox bases in the excess DNA single strands

☐ **The signal can be amplified with metal ion mediator** $\left[Ru(bPy)_3^{2+}\right]$ **oxidation catalyzed by Guanine.**

Ames Research Center

Electrochemical Detection of DNA Hybridization

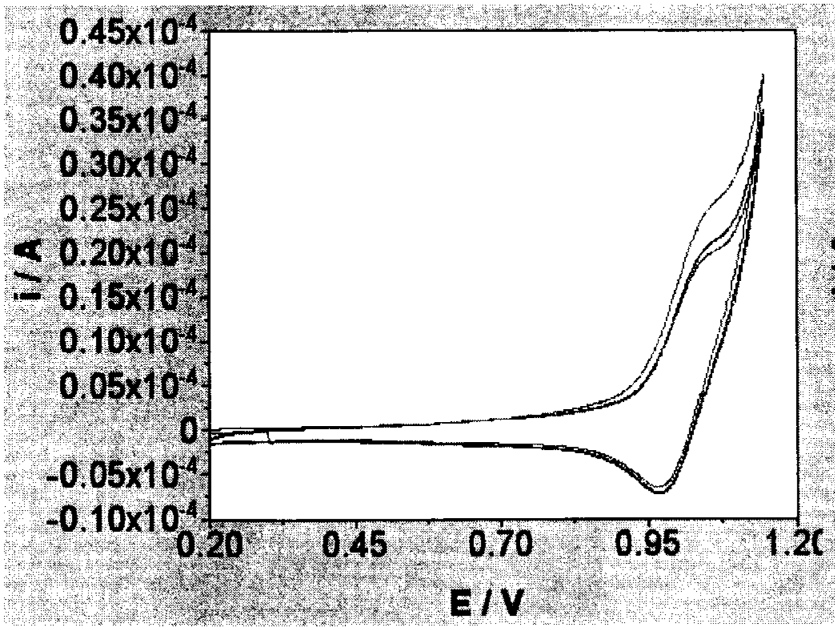

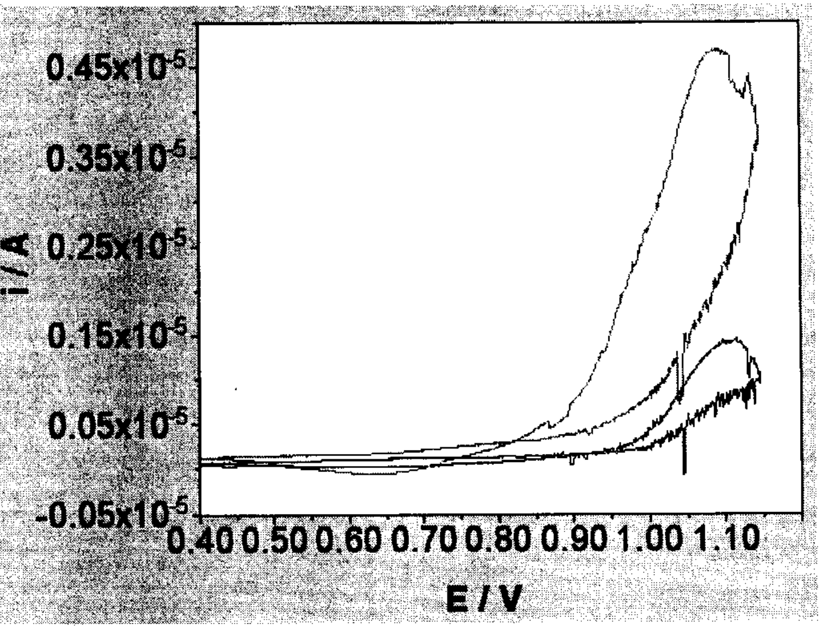

1st, 2nd, and 3rd cycle in cyclic voltammetry

1st – 2nd scan: mainly DNA signal

2nd – 3rd scan: Background

Ames Research Center

CNT - Field Emission Devices

- When subjected to high E field, electrons near the Fermi level can overcome the energy barrier to escape to the vacuum level
- Fowler - Nordheim equation: $I = aV^2 \exp(-b\phi^{1.5}/\beta V)$
- Critical: low threshold E field, high current density, high emission site density (for high resolution displays)
- Tips: Mo, Si, diamond
- Applications:
  - Cathode ray lighting elements
  - Flat panel displays
  - Gas discharge tubes in telecom networks

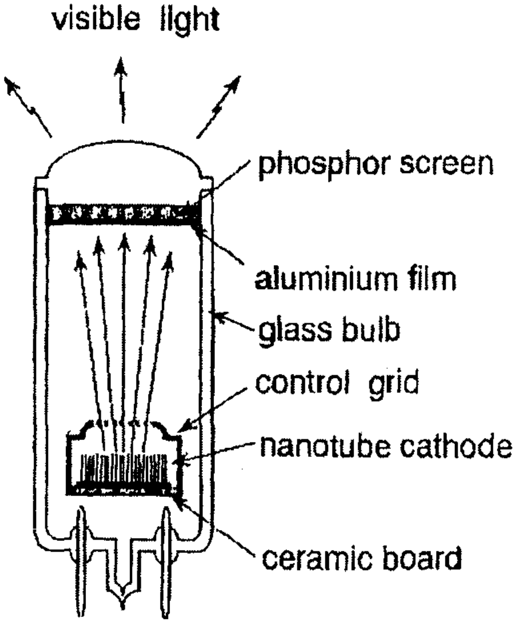

Ames Research Center

N_2 Adsorption Isotherm

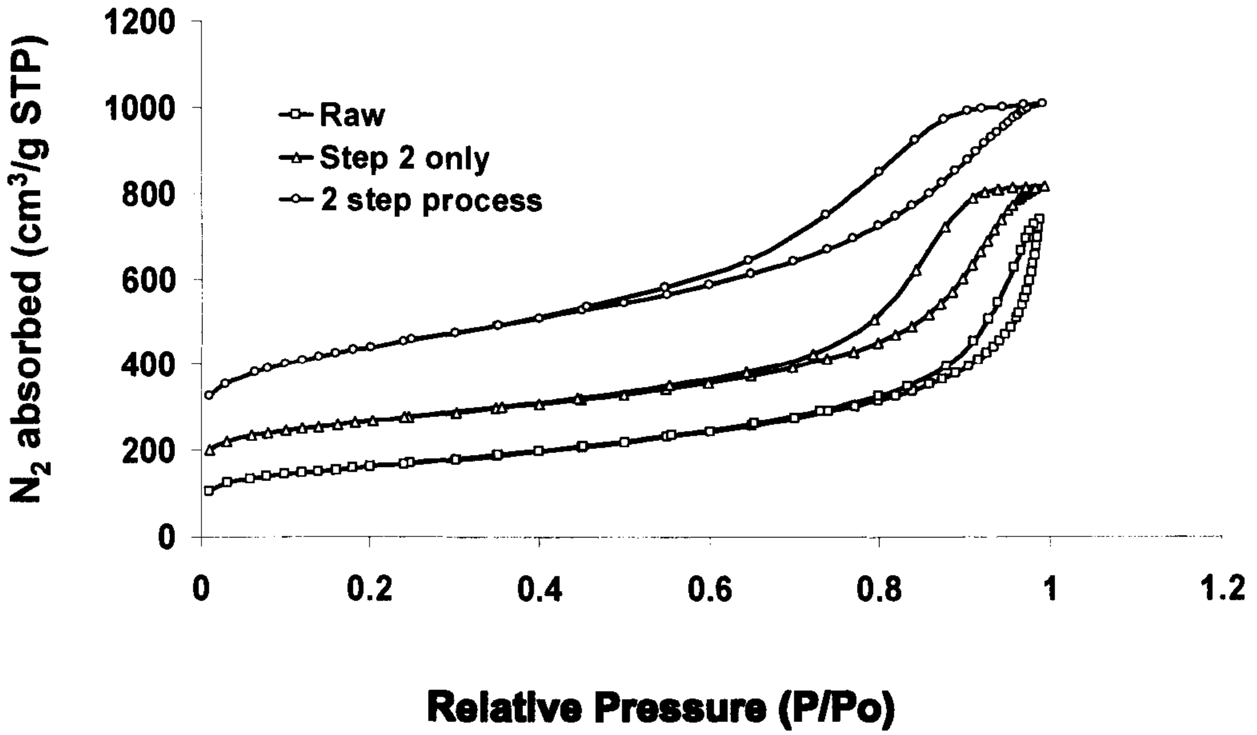

- Estimated surface area of purified HiPCo SWNTs is 1580 m^2/gm
- Applications in catalysis, gas absorption….

Ames Research Center

Zinc Oxide Nanowires

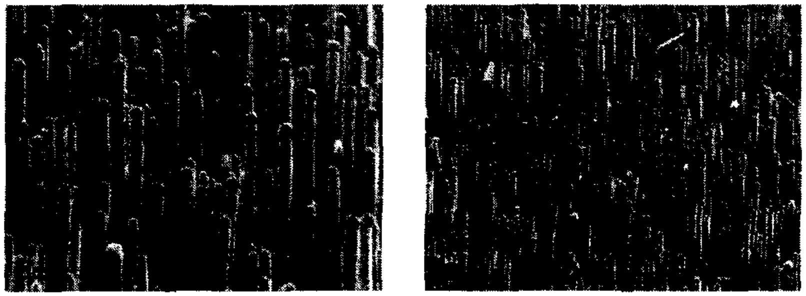

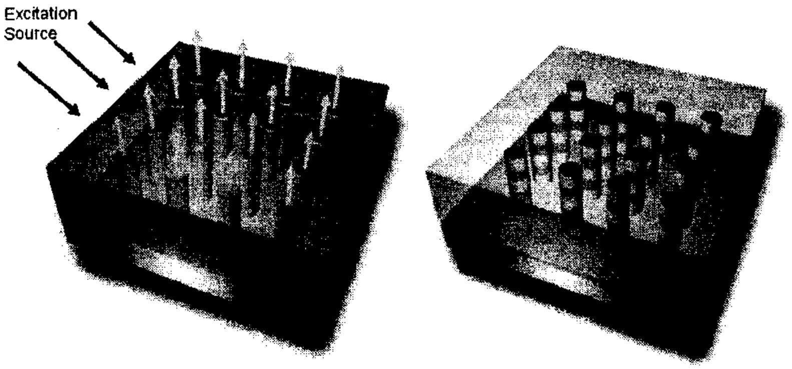

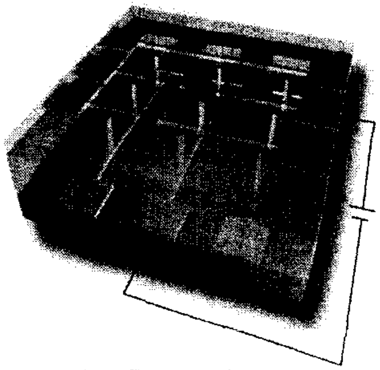

Field-Emitter Display

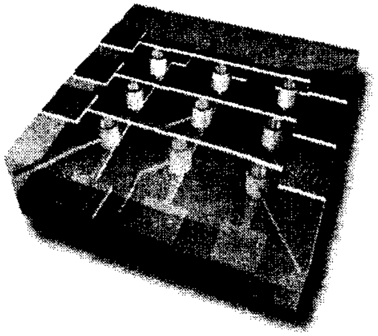

Vertical Transistor Arrays

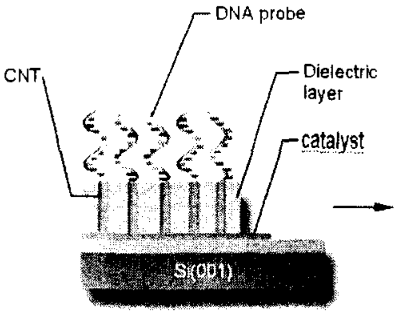

Functionalization

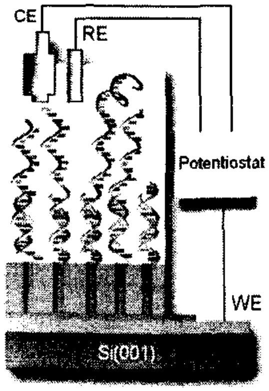

Detection

Protein Nanotubes

Ames Research Center

- Heat shock protein (HSP 60) in organisms living at high temperatures (“extremophiles”) is of interest in astrobiology
- HSP 60 can be purified from cells as a double-ring structure consisting of 16-18 subunits. The double rings can be induced to self-assemble into nanotubes.

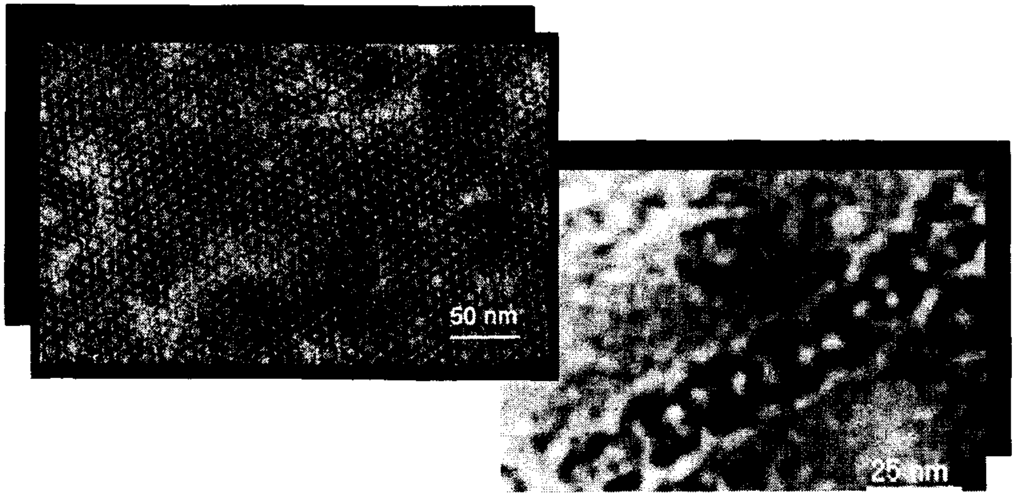

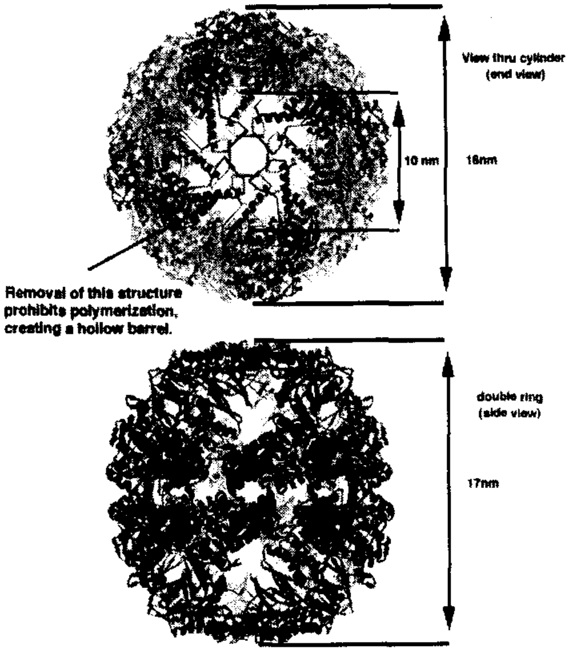

Model based on 2.3 angstrom crystallographic structure

Ames Research Center

Extremophile Proteins for Nano-scale Substrate Patterning

NASA

Nano-scale engineering for high resolution lithography

Future: Bio-based lithography
- •Batch self-assembly
- •Evolving
- •Inexpensive

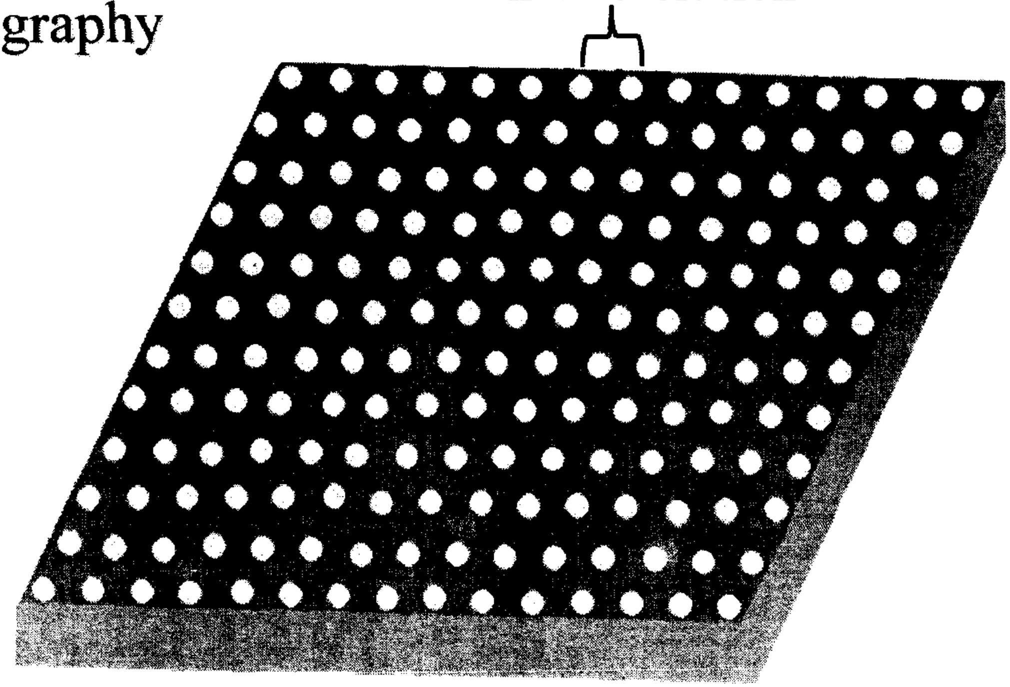

Ames Research Center

DNA Sequencing with Nanopores

The Concept

- Nanopore in membrane (~2nm diameter)
- DNA in buffer
- Voltage clamp
- Measure current

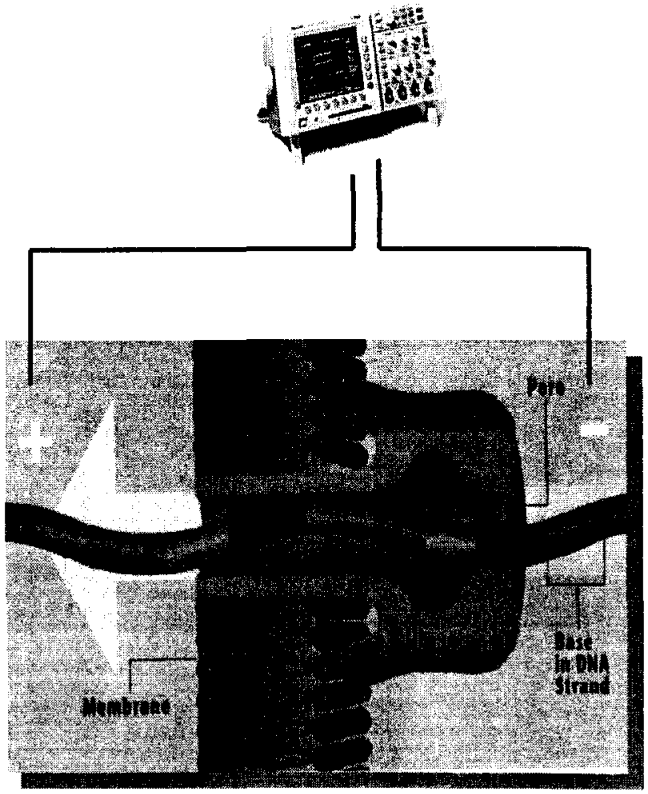

G. Church, D. Branton, J. Golovchenko, Harvard
D. Deamer, UC Santa Cruz

Ames Research Center

The Sequencing Concept

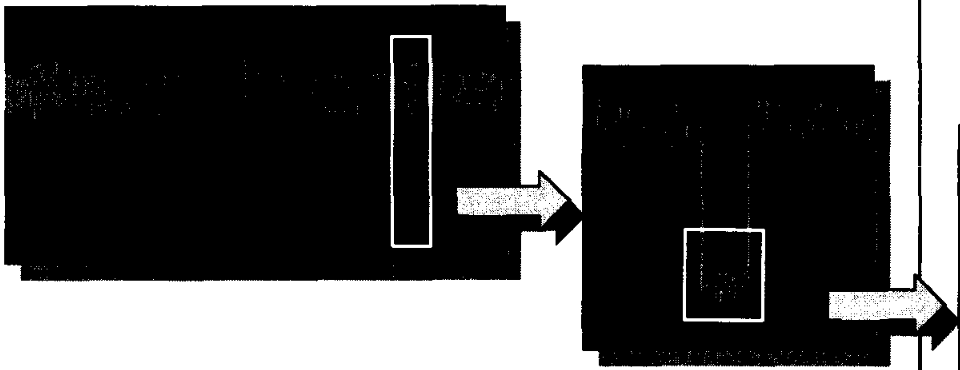

Present

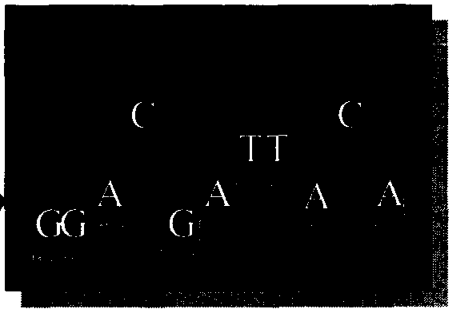

Future

Ames Research Center

Undergraduate Engineering Curriculum

Before taking the bread and butter courses, the undergraduate training begins with:

NOW

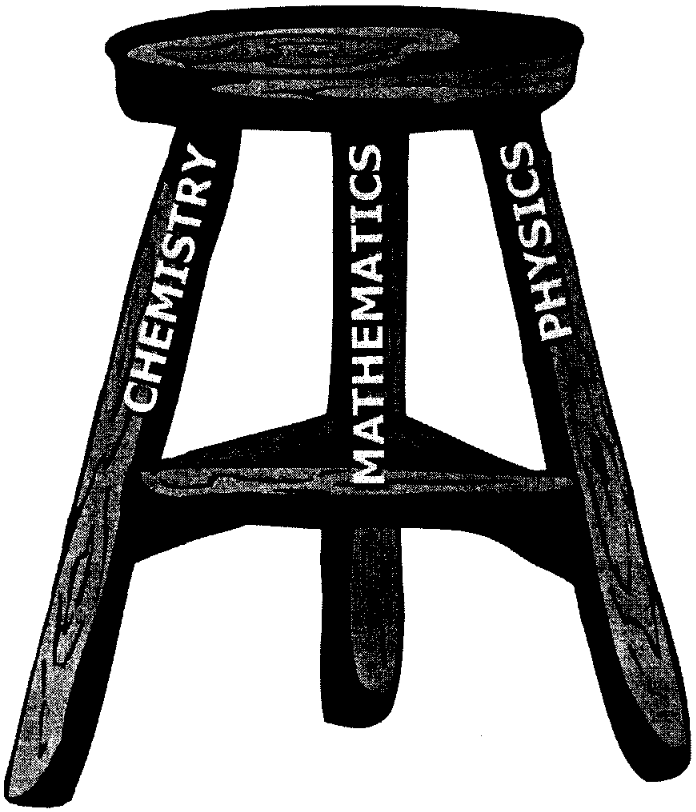

SHOULD WE CONSIDER?

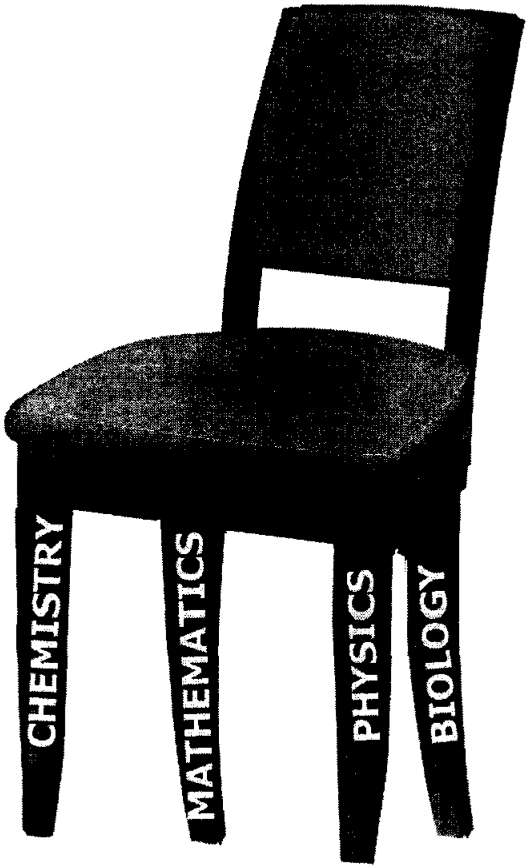

Undergraduate Curriculum

- Should elective courses on nanotechnology be considered (one or two)? If so, coverage includes, but not limited to:
    - Bulk vs. nano properties
    - Introduction to synthesis and characterization
    - Examples of nanomaterials: tubes, wires, particles…
    - Surface phenomena
    - Quantum phenomena
    - Focus on emerging applications
    - ?
- Summer internship and/or academic year co-op
    - National labs
    - Small and large companies with nano programs
    - University research
- Degree in Nanotechnology?
    - Flinders University and University of New South Wales in Australia now offer B. Sc. in Nanoscience and Technology
    - Leeds University and Crane University in U.K. offer M. Sc. in Nanoscience and Technology
    - This, of course, has to be a university-wide effort with courses taught by Physical and Biological Sciences and **Engineering** Departments

Ames Research Center

Summary

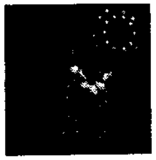

- Nanotechnology is an enabling technology that will impact electronics and computing, materials and manufacturing, energy, transportation….
- The field is interdisciplinary but everything starts with material science. Challenges include:
    - Novel synthesis techniques
    - Characterization of nanoscale properties
    - Large scale production of materials
    - Application development
- Opportunities and rewards are great and hence, tremendous worldwide interest
- Integration of this emerging field into engineering and science curriculum is important to prepare the future generation of scientists and engineers

NiTi-MAGIC OR PHASE TRANSFORMATIONS?

Katherine C. Chen

Materials Engineering Department
California Polytechnic State University
San Luis Obispo, California 93407

Telephone 805-756-6634
e-mail kcchen@calpoly.edu

Katherine C. Chen

NiTi – Magic or Phase Transformations?

Katherine C. Chen
Materials Engineering Department
California Polytechnic State University
San Luis Obispo, CA 93407
kcchen@calpoly.edu

Key Words: NiTi, Nitinol, martensite, austenite, phase transformations, phase diagrams, TTT diagrams, shape memory effect, superelasticity, annealing, precipitation, nucleation and growth, kinetics

Prerequisite Knowledge: crystal structure, intermetallics, annealing treatments, diffusion, TTT diagrams, phase diagrams, phase transformations, nucleation and growth, thermodynamics, kinetics, differential scanning calorimetry (DSC), tensile tests, stress-strain plots, twinning

Objectives: To demonstrate and investigate the phase transformations of NiTi due to stress and/or temperature.

- identify the different phases and crystal structures of NiTi
- identify the region (i.e., phase field) on the phase diagram (T, composition) where NiTi is thermodynamically stable
- demonstrate and differentiate between the *shape memory effect* and *superelasticity*
- explain why annealing can change the A_f (using the phase diagram and TTT diagram)
- design and perform the necessary heat treatment to achieve a specific transformation temperature or transformation stress (e.g., change from superelastic to shape memory) using a TTT diagram
- identify the start and end of the phase transformations (i.e., A_s, A_f, M_s, M_f) on a DSC scan
- discuss the effect of test temperature (i.e., below and above A_f) on the mechanical behavior of NiTi
- determine the stress needed to start the martensitic transformation (i.e., superelasticity) by tensile tests
- relate the plateau stress and A_f to the heat treatment (i.e., processing-structure-properties relationships) of the NiTi samples
- propose applications for the shape memory effect and for the superelastic effect of NiTi

Equipment and Materials:

1. NiTi wires in superelastic state (various sources, Nitinol Devices and Components)
2. wire cutters
3. furnaces
4. hot plates
5. large beakers
6. Differential Scanning Calorimeter (DSC) with liquid nitrogen capability
7. Tensile Tester

Introduction:

NiTi alloys possess exciting properties and are staples of materials demonstrations. The shape memory effect and superelasticity property of NiTi fascinate people, but actually require significant materials knowledge to fully understand the phenomena. A laboratory dealing with phase transformations was thus developed to capitalize on the allure of NiTi for a junior/senior level "Thermodynamics and Kinetics of Materials" course.

Students examine and characterize the *shape memory* and *superelastic* properties of NiTi wire, and then realize the difference is in the transformation temperature (i.e., A_f - the austenitic finish temperature). They then use the phase diagram and TTT diagram to develop appropriate annealing treatments to change a sample from superelastic into shape memory behavior. Concepts of precipitation, nucleation and growth, and kinetics are incorporated into the lab. The lab is somewhat open-ended and asks the students to formulate explanations for the observed trends.

The following background can be included in the laboratory handout, and/or explained in lecture.

BACKGROUND

NiTi Phase Transformations

The unique behavior of NiTi is based on a *thermoelastic* (i.e., thermal and mechanical) *phase* (or crystal structure) *transformation*. The high temperature (or *parent*) phase is known as "**austenite**" and has the ordered intermetallic crystal structure, B2 or CsCl ($Pm\bar{3}m$). At particular temperatures or strains, the austenite transforms into "**martensite**," which has a monoclinic crystal structure ($P2_1/m$).

If the parent phase is cooled below M_f (the martensite finish temperature), the austenite completely transforms to martensite, yet the bulk macroscopic shape is left intact! However, on the atomic scale, several different martensite variants have been created and are twinned to maintain the original bulk shape (Figure 1). There are a total of 24 possible crystallographically-equivalent habit planes of martensite. Once in the martensite form, the material is easily deformable through **twinning**. Particular variants grow at the expense of others to produce *plastic* deformation of shape change.

While most metals deform by **slip** or dislocation movement, NiTi responds to stress by simply changing the orientation of its crystal structure through the movement of twin boundaries. A NiTi specimen will deform until it consists only of the correspondence variant (crystallographic orientation) which produces maximum strain. However, deformation beyond this will result in classical plastic deformation by slip, which is irrecoverable and a "permanent set" will result.

The **shape memory effect** occurs when shape change occurs through martensitic twin reorientation and then the material is heated above A_f (the austenite finish temperature) to induce the phase transformation. Since there is only one possible parent phase (austenite) orientation, all martensitic configurations revert to that single defined structure and shape upon heating (Figure 2). This phenomenon causes the specimen to revert completely to the shape before deformation, and thus the material *"remembers"* its original shape. The thermoelastic martensitic transformation causing the shape recovery is a result of the need of the crystal lattice structure to accommodate to the minimum energy state for a given temperature and stress.

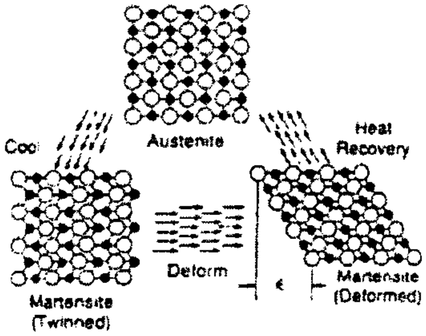

Reprinted with permission of Raychem Corp.

Figure 1. Phase changes associated with the shape memory effect [1].

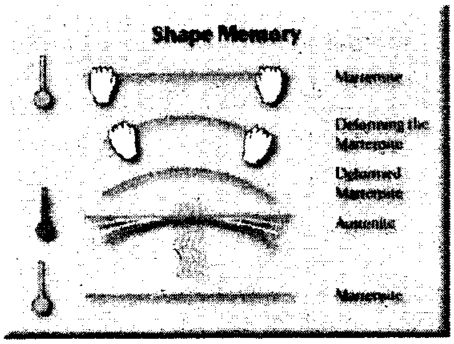

Figure 2. Demonstration of the shape memory effect [2].

Superelasticity (or pseudoelasticity) refers to the ability of NiTi to return to its original shape upon unloading after substantial deformation, similar to stretching a rubber band (Figure 3). This phenomenon is based on ***stress-induced*** martensite formation. The application of an applied stress causes martensite to form at temperatures higher than M_s (martensite start temperature). With stress-induced martensite, only 1 variant is formed that is parallel to the direction of the applied stress. When the stress is released, the martensite transforms back into austenite, and the specimen returns back to its original shape. Thus, stress rather than temperature causes the phase transformation.

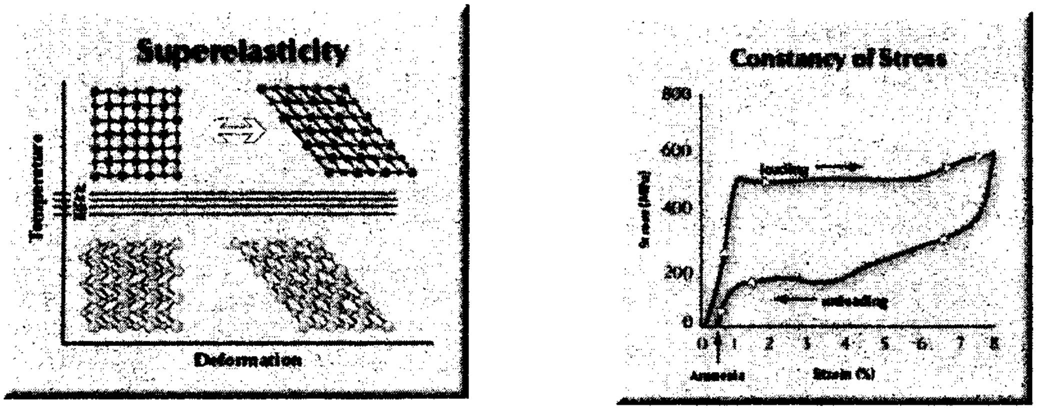

(a) (b)

Figure 3. a) Superelasticity involves the stress-induced phase transformation of austenite to martensite. b) The plateau stress is associated with the martensitic transformation [2].

Heat Treatments of NiTi

With knowledge of *processing-structure-properties* relationships, materials engineers can tailor materials to have the desired properties and performances. In order to harness the unique properties of NiTi, control of the transformation temperatures and/or stress is essential. The A_f temperature is determined primarily on the specific Ni-Ti alloy composition. In general, increasing the Ti content of the NiTi leads to an increase in the A_f. Examination of the equilibrium phase diagram of the Ni-Ti system (Figure 4) reveals that NiTi is stable only at temperatures above 630°C!

The phase diagram and TTT diagram (Figure 5) below will assist in determining the phase transformations with isothermal holds outside the NiTi single-phase field. The TTT diagram suggests that *metastable* precipitation will first result [4], and in turn, the A_f of the NiTi can change. Thus, manipulation of the transformation temperatures is possible!

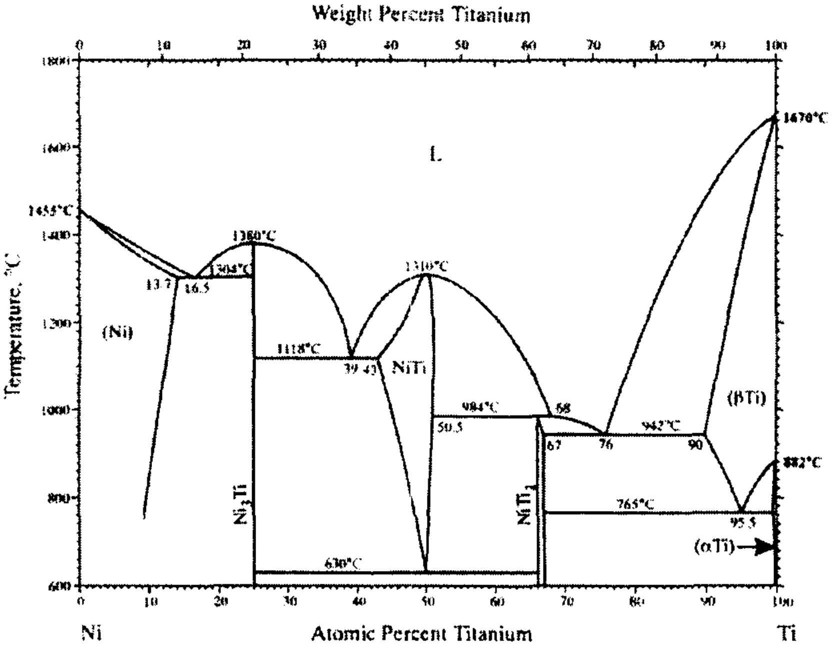

Figure 4. The Ni-Ti equilibrium phase diagram [3].

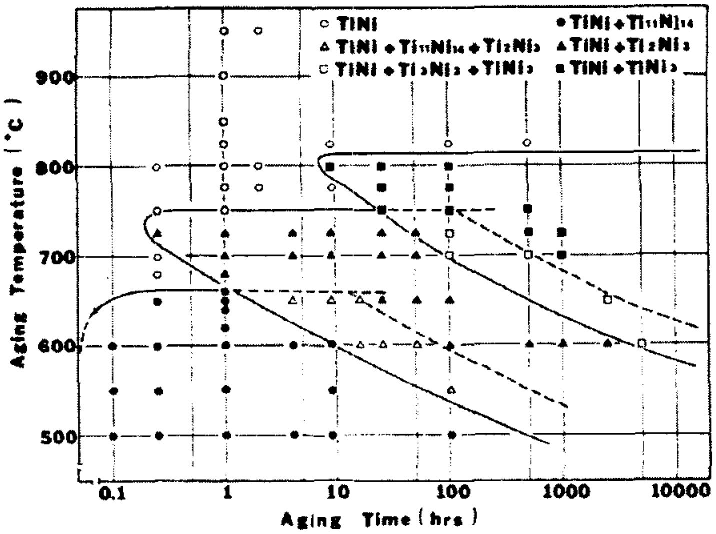

Figure 5. TTT diagram describing aging behavior for Ti-52Ni [4].

Procedure:

HEAT TREATMENTS

As a class, construct a heat treatment **test matrix** (grid of test times and temperatures) that will produce a range of A_f's, and thus, different mechanical properties. Each group will be responsible for one heat treatment **temperature**. Every group will conduct heat treatments for similar heat treatment **times**. Keep in mind that the goal of this experiment is to produce a range of A_f's. In the end, you will produce a TTT-like diagram that gives contours of A_f temperatures.

After heat treating, deform the NiTi wires and determine which phase (i.e., martensite or austenite) is present at room temperature. The temperature in which the deformed wire "remembers" its shape is the A_f. Use hot plates and beakers of water (or other means) to get "ballpark" numbers for the A_f's.

DIFFERENTIAL SCANNING CALORIMETRY (DSC)

Each group should cut off a small piece (no more than 3 mm) from the end of each heat-treated wire for DSC analysis. Make sure each DSC sample is properly labeled with the correct annealing time and temperature.

Perform DSC on each sample. Use your "ballpark" temperatures to assist your selection of temperature ranges to use for DSC. In order to scan temperature below room temperature, fill the liquid nitrogen dewer. Take note of the $\mathbf{A_s}$, $\mathbf{A_f}$, $\mathbf{M_s}$, $\mathbf{M_f}$ temperatures (Figure 6) for each sample. Integrating under the transformation curve will give the heat of transformation (ΔH). Discuss and explain the trends you find.

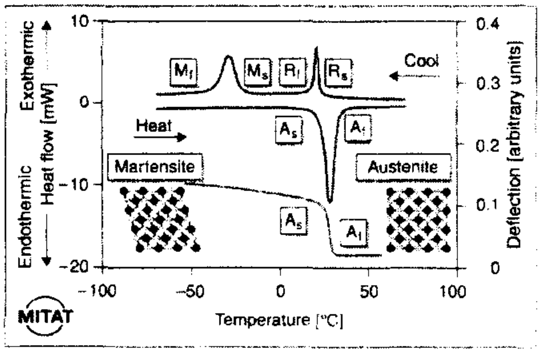

Figure 6. Differential scanning calorimetry and free recovery of the same processed wire. Note that upon cooling the wire transforms to R-phase prior to the martensitic transformation. Upon heating, both techniques provide similar A_s and A_f temperatures as the (monoclinic) martensite transforms to the (cubic) austenite. [5]

TENSILE TEST

Each group should pull an as-received wire and their heat-treated wires with a tensile tester to generate a stress-strain plot. The plateau stress indicates the stress required for the martensitic transformation or superelasticity (Figure 7). Determine the trends of the transformation stress with the annealing temperatures and times. In addition, relate the trends to the DSC data.

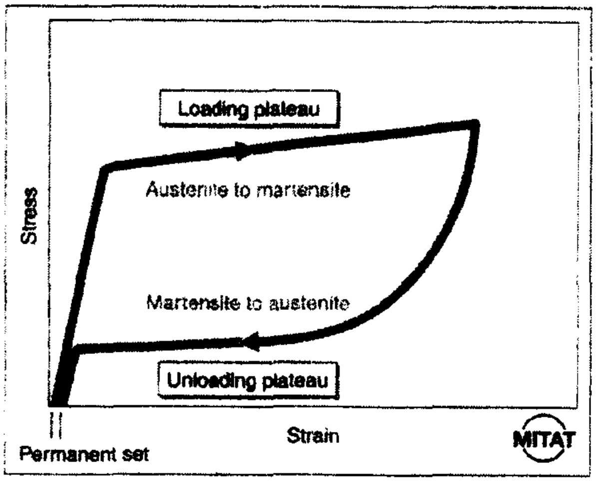

Figure 7. Schematic stress–strain curve of superelastic Nitinol. There is a transformation from austenite to martensite that begins at the apparent yield stress. The plateau stress remains nearly constant with increasing strain as the amount of martensite increases. Upon unloading, the martensite reverts to austenite along the unloading plateau. The 'permanent set' measures any residual strain. [5]

All groups in the class should share their DSC and tensile test data in order to observe the trends in properties due to the different processing treatments. Assemble a TTT-like diagram that plots contours of the A_f temperatures on a plot of temperature versus time. In addition, discuss the how and why's of the following:

- heat treatment effects the loading or stress plateau
- C-curves of the contour plots of the A_f temperatures
- correlation of the trends of the DSC and tensile test results
- heat treatment effects the A_f temperature

*Hint: Use the phase diagram, TTT diagram, and your knowledge about kinetic processes (e.g., diffusion, precipitation, phase transformations) in your analysis.

Comments:

The plot of A_f temperatures should resemble C-curves, as in Figure 8. Essentially, Ni-rich precipitates are formed during the annealing treatments (outside of the single-phase region), which results in a more Ti-rich NiTi matrix. The small change in NiTi composition results in the change in A_f, and can take the material from *superelastic* (A_f below room temperature) to *shape memory* (A_f above room temperature). Since the whole process of changing the A_f's is governed by the precipitation of Ni-rich phases, the kinetics follow nucleation and growth.

In addition, the plateau stress of the austenitic samples should increase with samples of decreasing A_f temperatures. A sample with a low A_f, relative to room temperature, can be considered to be far from the transition point, and thus a larger stress (or change in temperature) is needed to start the transformation. A sample plot of load vs. extension from the actual lab is shown in Figure 9. The plateau stress decreases as the heat treatment time increases, and the A_f gets closer to room temperature. If the samples are martensite at room temperature, a very low "plateau stress" will appear, since deformation by twinning occurs (as opposed to transforming).

References:

1. http://www.sma-inc.com/
2. http://www.nitinol.com/
3. Phase Diagrams for Binary Alloys, ASM International, 2000.
4. M. Nishida, C.M. Wayman, and T. Honma, *Met Trans* 17A, 1505, 1986.
5. A.R. Pelton, J. DiCello and S. Miyazaki, *Min Invas Ther & Allied Technol* 2000: 9(1) 107.
6. J. Sheriff, NDC, private communications.

Other useful sources:
http://mrsec.wisc.edu/EDETC/memmetal/index.html
http://www.raychem.com/products/nitinol/index.htm
http://www.memry.com/
http://discover.lib.calpoly.edu/servlet/edu.calpoly.lib.ecp.EcpServlet?catID=458

Bibliography:
Katherine C. Chen is an Associate Professor in the Materials Engineering Department at Cal Poly State University, San Luis Obispo, CA. She received her bachelor degrees (in Chemistry and Materials Science & Engineering) from Michigan State University, and Ph.D. from the Massachusetts Institute of Technology. She worked at Los Alamos National Laboratory for three years. At Cal Poly, she teaches the undergraduates Structures of Materials, Kinetics of Materials, and various other courses. She is a member of ASEE, MRS, ASM, and TMS.

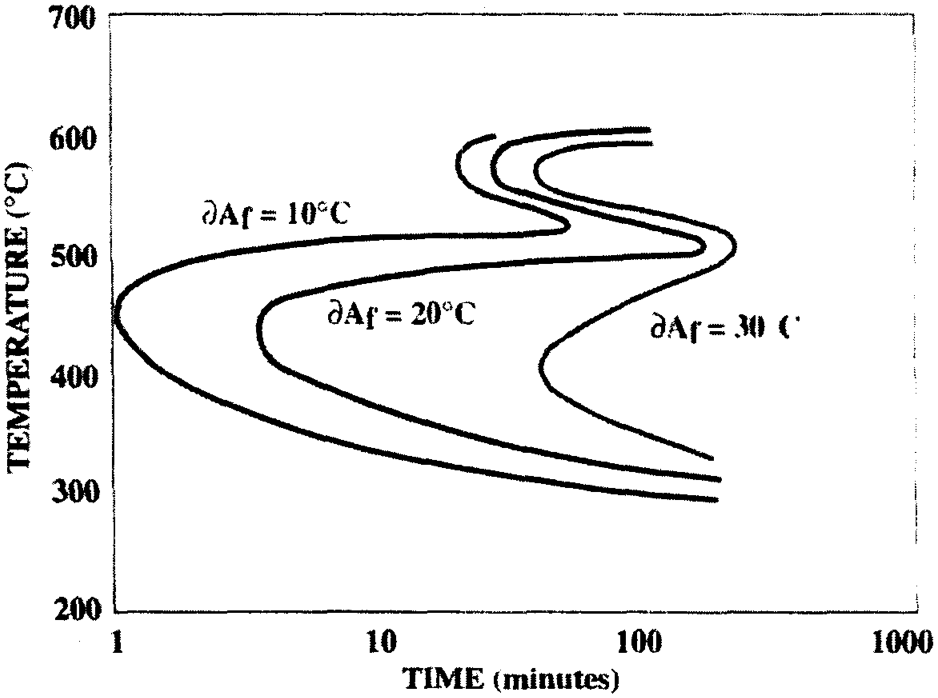

Figure 8. Contour curves of changes in the Af temperature of NiTi upon annealing at specific temperatures and times [6].

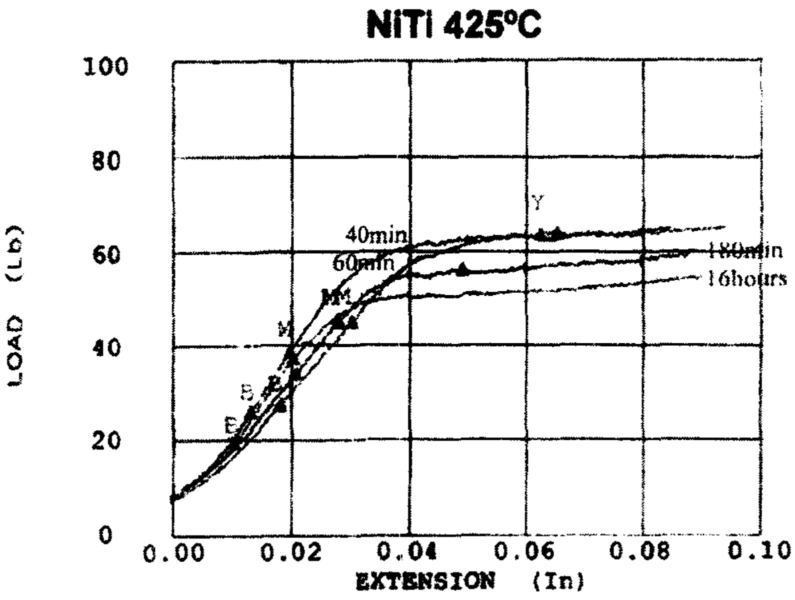

Figure 9. Tensile test results for NiTi heat-treated at 425°C for four different times. Longer anneal times produce lower plateau stresses for the martensitic transformation due to higher A_f temperatures (that are closer to room temperature).

SWING SET DESIGN
A PROJECT IN STRESS ANALYSIS

Nikhil K. Kundu

and

Sarah E. Leach

Mechanical Engineering Technology
Purdue University
School of Technology
Elkhart, Indiana 46634-7111

Telephone 574-237-4172
e-mail seleach@pusb.iusb.edu
nkkundu@pusb.iusb.edu

Sarah E. Leach

Swing Set Design
A Project in Stress Analysis

Nikhil K. Kundu
Sarah E. Leach
Purdue University, School of Technology
Mechanical Engineering Technology
Elkhart, Indiana

Key Words:
Force, Shear Stress, Bending Moment, Deflection

Prerequisite Knowledge:
Statics and dynamics and concurrent enrollment in strength of materials.

Objective(s):
To reinforce the students' understanding of materials, statics, dynamics, and strength of materials.

Equipment and Materials:
(Optional) Students may choose to construct a scale model of their swing set design.
Wood: dowel rod, small pieces of pine or balsa
glue
string
plastic sheet: heavyweight polypropylene or similar
hardware: small screw eyes, brads,

Introduction:
Using a backyard swing set is one of the most popular activities for children. This simple piece of equipment does require serious engineering considerations. Mechanical Engineering Technology at Purdue University requires among others a series of foundation courses in statics, dynamics, and strength of materials. This project was designed to reinforce students' knowledge in those courses and give them an opportunity for an overall learning experience involving different aspect of design, engineering, manufacturing, and assembly operations.

Procedure:
The project assignment began after the fourth week of a fifteen-week semester. The class was divided into groups of four students. They followed a weekly assignment schedule given by the instructor. The first half of the project required step-by-step procedures following the format given by the instructor. The teams were given an initial problem statement and were required to develop statements covering the topics of: design concept, preliminary layout, load assumptions, material selection, assembly, and safety. Once the preliminary definition of the project was complete, the team proceeded to define the details of the design and construction. The second part of the project was team-directed, and included engineering calculations, the development of

a manufacturing procedure, assembly considerations, and the development of a detailed bill of materials. The major thrust was given in stress analysis and calculations of bending and bearing stresses that involved shear stress diagrams and moment diagrams for every structural item. All of the information used to design and specify the swing set was included in a final written report which was submitted by the team. The team was also required to make an oral presentation of their project. Construction of a scale model of the swing set was optional, but many teams found scale models useful as aids for visualizing assembly techniques and as presentation tools for their final report. The initial project statement and a project schedule are given below.

Project Statement: Design a backyard swingset for residential use. The prime concern in the design process is safety of the children. A design factor of two (2) or higher is sufficient for this project. (based on static loading of ductile materials)[1] Consideration should be given to the construction materials, manufacturing processes, assembly, product life, and the cost. You will be competing with fellow students to develop a safe, cost effective design. Evaluation of the project is based on design concept, technical content, stress analysis, cleanliness and clarity of the report and presentation.

Table 1
Week by week assignment schedule and assessment values:

Timeframe	**Project Assignments**	**Percentage of Overall Project Assessment**
Weeks 1 and 2	Problem Statement	2
	Design Concept	2
	Preliminary Layout	
	Safety Considerations	2
	Assumptions Load Load Points Weather Conditions	2
Week 3	Foundation	2
	Basic Materials Selection	2
Week 4	Trial Calculations	
Weeks 5 and 6	Final Calculations Moment of Inertia Shear Force Bending Moment Stress	 2 15 15 15
Weeks 7 and 8	Final Material Selection	5
	Final Geometry Consideration	5
	Final Drawing (to scale)	10
Weeks 9 and 10	Manufacturing	2
	Assembly	2
	Bill of Materials	2
	Final Presentation	15

After the initial process of developing assumptions and a design concept, student teams were required to analyze the structures to ensure safe operation. They analyzed each component of the structure to the determine the forces and stresses present. The stress levels were compared with material properties to make sure that each component met or exceeded a design factor of two. Redesign continued until all components satisfied the safety requirement. Calculations were performed using standard formulas as follows:

Formulas and Nomenclature:

Direct Normal Stress, $\sigma = F/A$
Force, F
Cross-sectional Area, A
Bending stress, $\sigma = Mc/I$
Bending moment, M = the internal moment developed in the material of a beam to balance the tendency for external forces to cause rotation of any part of the beam
Centroid, I
Shear stress, $\tau = F/A$ or $\tau = V/A$
Internal Shear Force, V = the internal force developed in the material of a beam to balance externally applied forces in order to maintain static equilibrium for all parts of the beam

Figure 1 shows the concept drawing for a swing set project, designed by a student team. The following paragraphs are examples of project documentation from the team. In addition to designing and analyzing the swing set, the team was required to consider weather, costs and assembly methods. Figures 2, 3, and 4 show analysis of swing set components, and Figure 5 shows the assembly drawing for the finished design. Table 3 is the Bill of Materials List, coded to the Assembly Drawing. Table 4 lists the final material costs for the swing set design. Figures 6, 7 and 8 are swing set projects designed by other student teams.

Figure 1
Student Team Example: Initial Design Concept of Swing Set

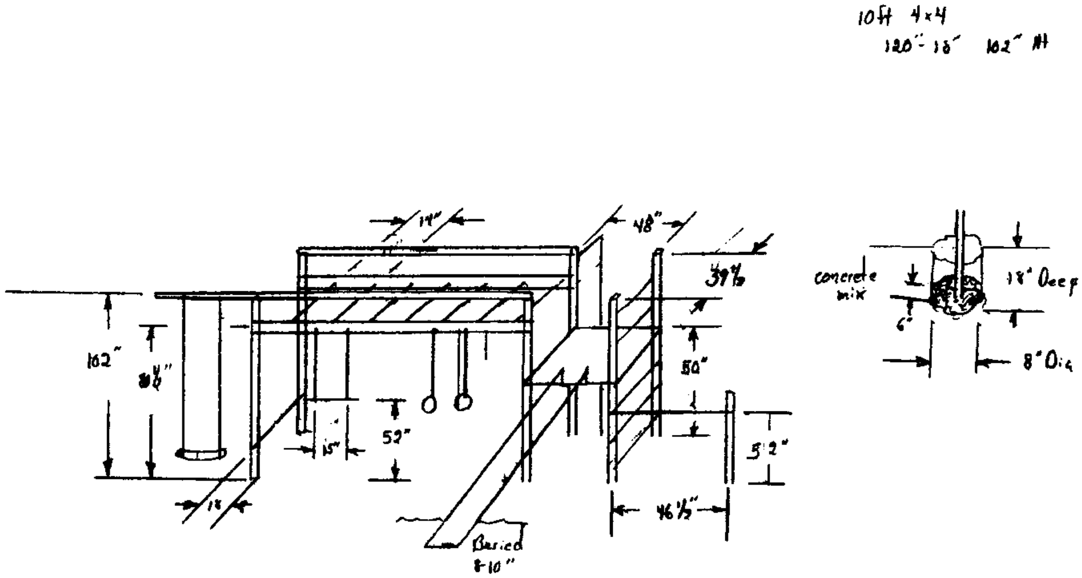

Design concept:
The swing set includes one swing, a trapeze and a set of rings for swinging and acrobatic activities. Monkey bars are included for upper body and arms, fireman's pole and banister slide for balancing and coordination, and a parallel bar for acrobatic type activities. This design allows for the involvement of several children with different types of activities that challenge them physically. Design considerations also included adults who like share the fun with their children.

Load assumptions (with each child 100 lb and each adult 250 lb)

Monkey Bars:	four children or two adults
Step Up Area For Monkey Bars:	two children or one adult
Swing and or Rings:	three children or one adult
Parallel Bar:	two children or one adult
Fireman's Pole:	one child or one adult
Platform:	five children or two adults
Bannister Slide:	one child or one adult

Weather:

No effect on wood (treated lumber)
No effect on galvanized pipe
Snow load on platform should be under the assumed use load of 500 lbs

Foundation
The foundation we plan to use is 8 inches in diameter and 16 inches deep. We will use part of a bag of concrete mix in each hole. This will give a surface area of 50.26 square inches. The worst case condition is 15 pounds/square inch for soft clay or loose sand. The load ability per post is then 754 pounds/post.

Basic Material List (preliminary):

- Treated lumber (8) 4' x 4' and (2) 2' x 8'
- 1 inch diameter galanized pipe or hardwood rod
- Chain for swings
- Eyebolts for swings
- Carriage bolts for joints
- Galvanized nails 16d to pin pipe or wood and floor
- Seat for swing
- Rings
- Bags of concrete mix

Comments:
Students learn statics, dynamics, and strength of materials as required courses at Purdue University. Homework problems and exams are the usual means for evaluating students' progress and understanding of the lecture materials. Exams are done within limited time frames whereas projects allow them sufficient time to explore reference materials and discuss various options with fellow students and the instructor. Students contact vendors and suppliers of

construction materials and work with a sense of teamwork and responsibility to create a product they may some day like to build for themselves.

Playground safety plays a major role in the design and material selection process. Load assumptions, environmental considerations, and budgetary restraints are used as guidelines for design and engineering. Engineering decisions are based on stress calculations using maximum static load assumptions at worst situations and locations.

Thanks and credit are due to the students who worked on swingset project examples used in this paper. Contributions were made by: Steve Beneker, Zoe Burns, George Jenkins, Jamie Miller, Marion Nisley, and Mechelle Radde.

References:

1. Robert L. Mott, Applied Strength of Materials, Fourth Edition, Prentice Hall, Upper Saddle River, New Jersey, 2002
2. F. F. Wangaard, Ed., Wood: Its Structure and Properties, Vol. 1, Educational Modules for Materials Science and Engineering Project, Pennsylvania State University, University Park, PA, 1981

Biography:

Mr. Nikhil Kundu has been an associate professor of Mechanical Engineering Technology at Purdue University Elkhart/South Bend since 1988. He has an undergraduate degree from the Technical University Berlin, Germany and a master's degree from the University of California at Berkely, both in mechanical engineering. He has more than ten years of industrial experience in the field of research and development. He was associated with Siemens Ltd. in Germany, Dow Chemical, Halliburton, and Western Company of North America in the United States. His industrial experience was in the field of heat transfer, fluid mechanics, hydraulics and pneumatics, and plastics. Previously he taught at Texas A&M University at College Station and University of North Texas in Denton. Mr. Kundu has published numerous technical papers. He is an active member of the American Society of Mechanical Engineers, Society of Manufacturing Engineers, and the American Society for Engineering Education.

Sarah Leach, P.E., is an assistant professor of Mechanical Engineering Technology at Purdue University Elkhart/South Bend. She has an undergraduate degree in Mechanical Engineering from Vanderbilt University, and a Master's Degree in Materials Science and Engineering from the University of Notre Dame. Her primary teaching responsibilities are in materials and applied mechanics. Sarah possesses over 15 years of industrial experience in manufacturing, research, and product development for electromechanical devices, multiplayer circuits, and sliding electric contacts. She remains an active member of the American Society of Mechanical Engineers and the American Society of Engineering Educators, and serves as the faculty advisor for the local student chapter of the American Society of Mechanical Engineers.

Figure 2
Student Team Example: Bannister Slide Analysis

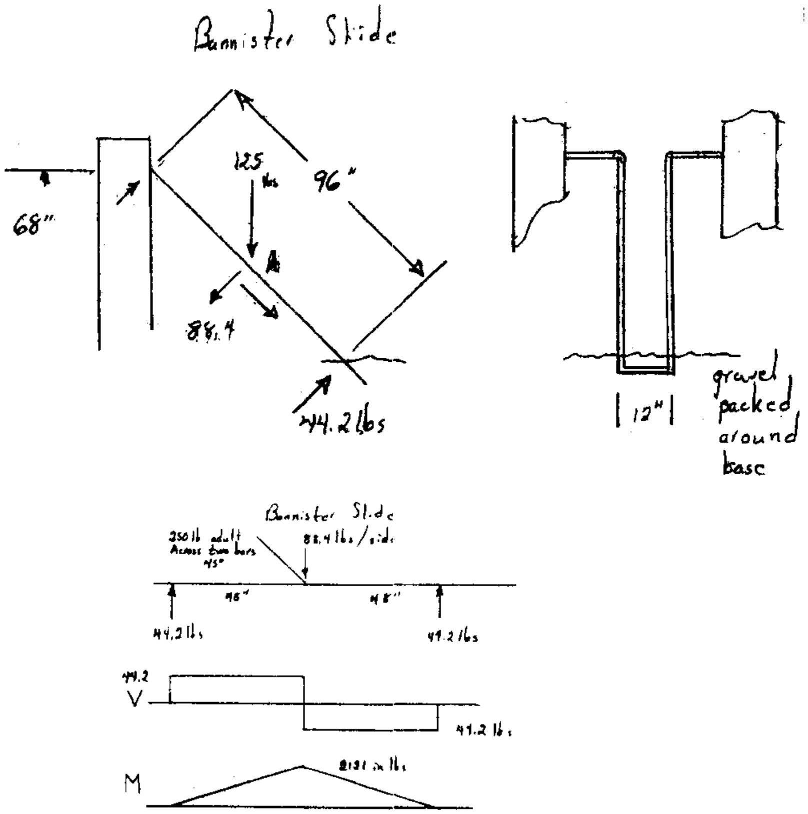

Figure 3
Student Team Example, Rings Analysis

Rings

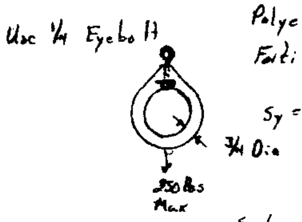

Polyethylene LLPDE
Fortiflex T35

$S_y = 2300 \text{ psi}$

Design Factor 2

$S_y/2 = 1150 \text{ psi} = \sigma_b$

$\sigma_b = F/A$

$1150 \text{ psi} = 250/A$

A = .217 = Washer Size Minimum for Design Factor 2

Washer .625 OD - .250 ID

Area = .3067 - .049

Area = .2577

Figure 4
Student Team Example, Monkey Bar Analysis

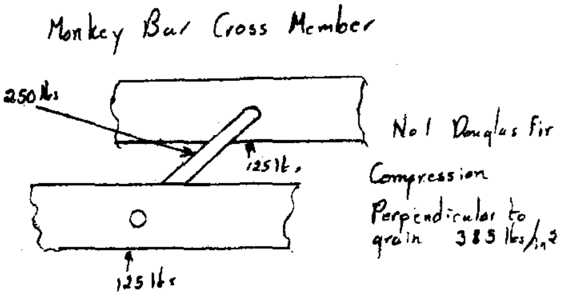

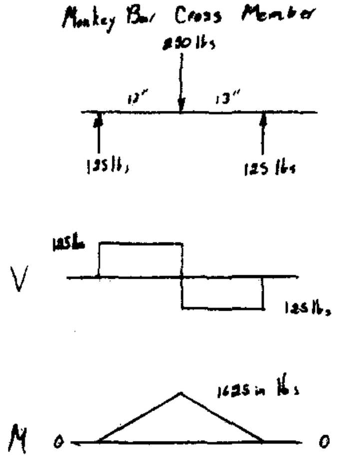

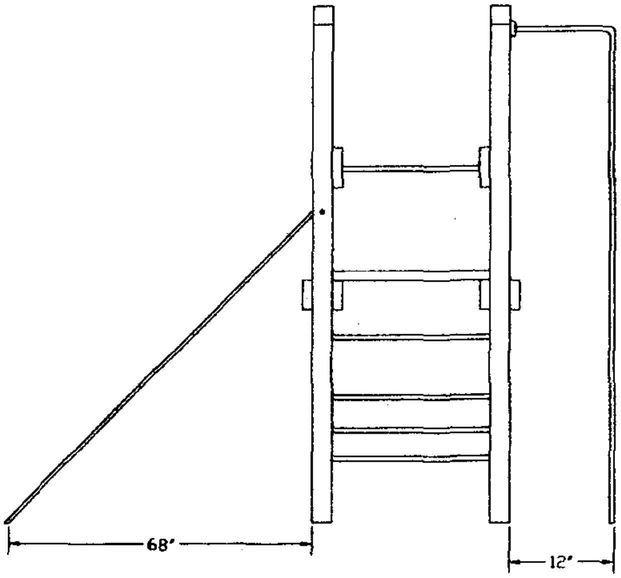

Swingset Side View
Basic Dimensions

Figure 5
Student Team Example, Assembly Drawing

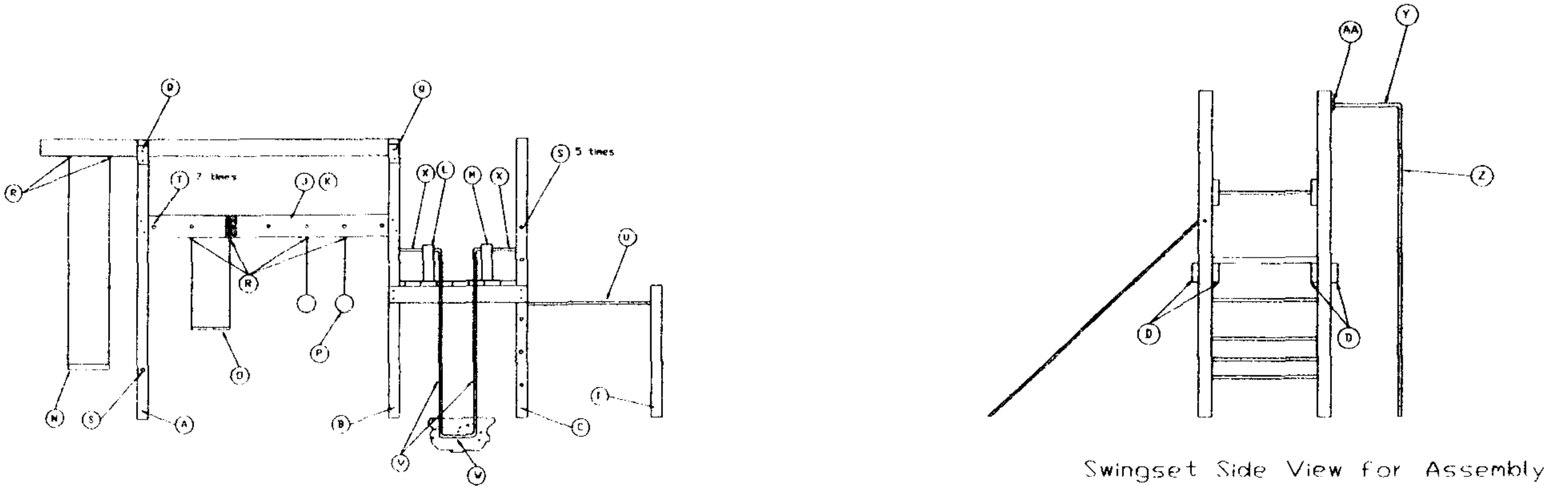

Swirgset Front View Assembly

Swingset Side View for Assembly

Table 2
Swing Set Bill of Materials

Letter	Description	Quantity	Usage
A	4' x 4' x 10' Douglas Fir	2	Upright
B	4' x 4' x 10' Douglas Fir	2	Upright
C	4' x 4' x 10' Douglas Fir	2	Upright
D	2' x 6' x 4' Douglas Fir	4	Platform
E	2' x 6' x 29" Douglas Fir	2	Platform
F	2' x 6' x 39" Douglas Fir	6	Platform
	½" x 6" Carriage Bolts	8	Platform
G	4' x 4' x 12' Douglas Fir	1	Swing Crossmember
H	4' x 4' x 9' Douglas Fir	1	Crossmember
I	4' x 4' x 6' Douglas Fir	1	Parallel Bar Upright
J&K	2' x 8' x 12' Douglas Fir	2	Monkey Bar Crossmember
L&M	4' x 4' x 2' Douglas Fir	2	Bannistger Slide Supports
N	Swing Assembly	1	
O	Trapeze Assembly	1	
P	Ring Assembly	2	
Q	062 x 3-1/2" x 7 Steel Plate	4	
R	Eyebolts	6	
S	¾" 36" Pipe	6	Steps
T	¾" 29" Pipe	7	
U	1" 48" Pipe	1	
V	1" 96" Pipe	2	Bannister Slide
W	1" 12" Pipe	1	Bannister Slide
X	1" 18" Pipe	2	Bannister Slide
	1" Elbows	4	Bannister Slide
Y	1-1/4" 12" Pipe	1	Fireman's Pole
Z	1-1/4" 108" Pipe	1	Fireman's Pole
AA	1-1/4" Flange	1	Fireman's Pole
	16D Galvanized Nails	½ #	
	½" x 3-1/2" Carriage Bolts	16	
	½" Washers	24	
	½" Nuts	24	
	Concrete Mix	2 Cu. Ft.	

Table 3
Student Team Example, Swing Set Material Costs

Quantity	Description	Cost (per unit)	Total
16	1/2 x 3-1/2 Carriage Bolts	0.29	4.64
8	½ x 6" Carriage Bolts	0.60	4.80
24	½ Washers	0.02	0.48
24	½ Nuts	0.06	1.44
6	Eyebolts	3.32	19.92
3	10 Ft 4/0 Zinc Twinloop Chain	6.99	20.97
2	2 x 8 x 12	9.43	18.86
6	4 x 4 x 10	10.69	64.14
1	4 x 4 x 6	7.99	7.99
1	4 x 4 x 12	12.69	12.99
1	4 x 4 x 9	10.69	10.69
4	2 x 6 x 4	4.20	16.80
2	2 x 6 x 29"	3.10	6.20
6	2 x 6 x 39"	4.20	25.20
4	.062 x 3-1/2" x 7" Steel Plate	3.60	14.40
40	(ft) 1" Structural Pipe	1.35	54.00
20	(ft) ¾" Structural Pipe	0.98	19.60
10	(ft) 1-1/4" Structural Pipe	1.75	17.50
4	1" Elbow	1.81	2.83
1	1-1/4" Elbow	2.83	2.83
.5	Galvanized Nails	7.17	3.59
1	1-1/4" Flange Threaded	9.42	9.42
1	Polyethylene Swing Seat	13.00	13.00
1	Polyethylene Rings	13.00	13.00

Total Swing Set Cost	$369.4

Figure 6, Student Team Example, Swing Set Design

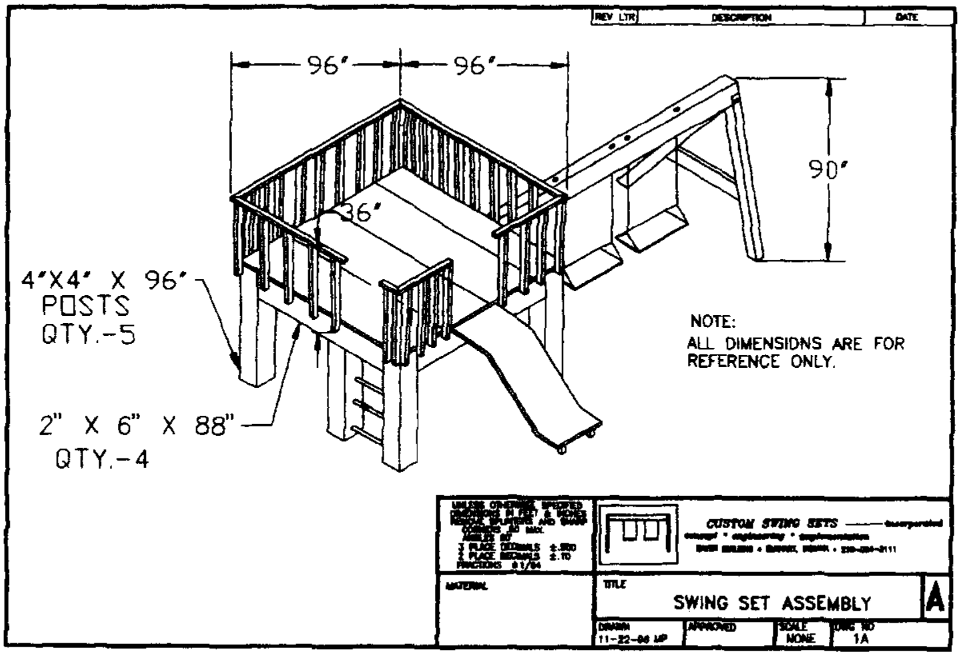

Figure 7, Student Team Example, Swing Set Design

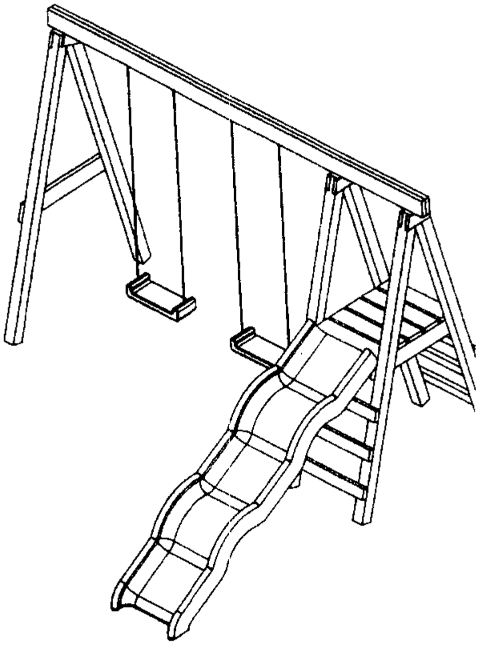

Figure 8, Student Team Example, Swing Set Design

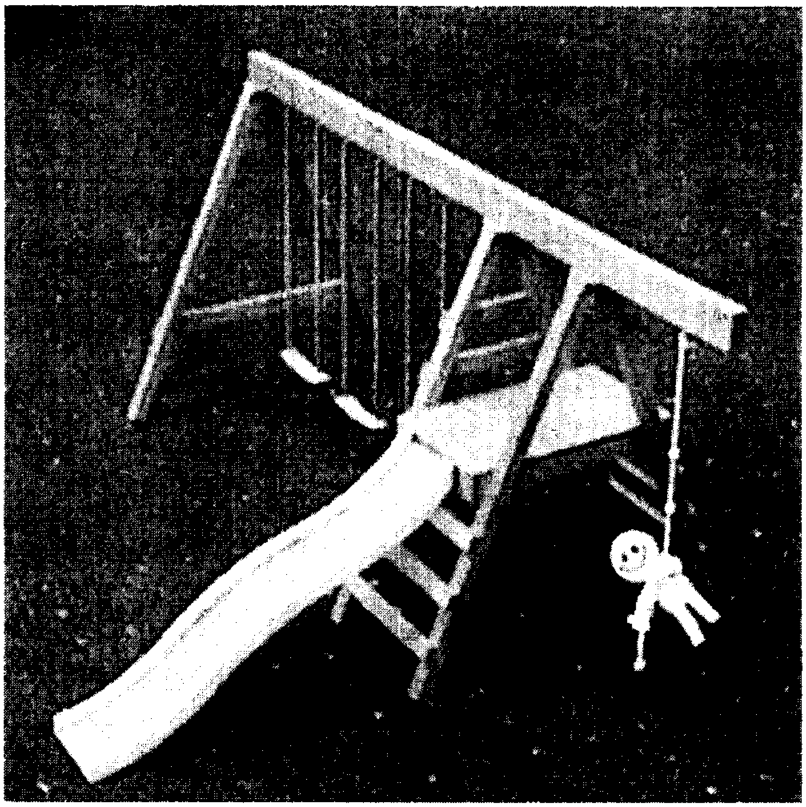

DISTRIBUTION OF ELECTROMAGNETIC ENERGY IN A MICROWAVE OVEN
PART II

J. N. Dahiya

and

Pankaj Choudhary

Physics Department
Southeast Missouri State University
One University Plaza
MS 6600
Cape Girardeau, Missouri 63701

Telephone: 573-651-2390
e-mail dahiya@physics.semo.edu

and

Aman Anand

Computer Science Department
Southeast Missouri State University
One University Plaza
Cape Girardeau, Missouri 63701

e-mail amanfromcs@hotmail.com

and

J. A. Roberts

University of North Texas
Denton, Texas 76203

e-mail Roberts@unt.edu

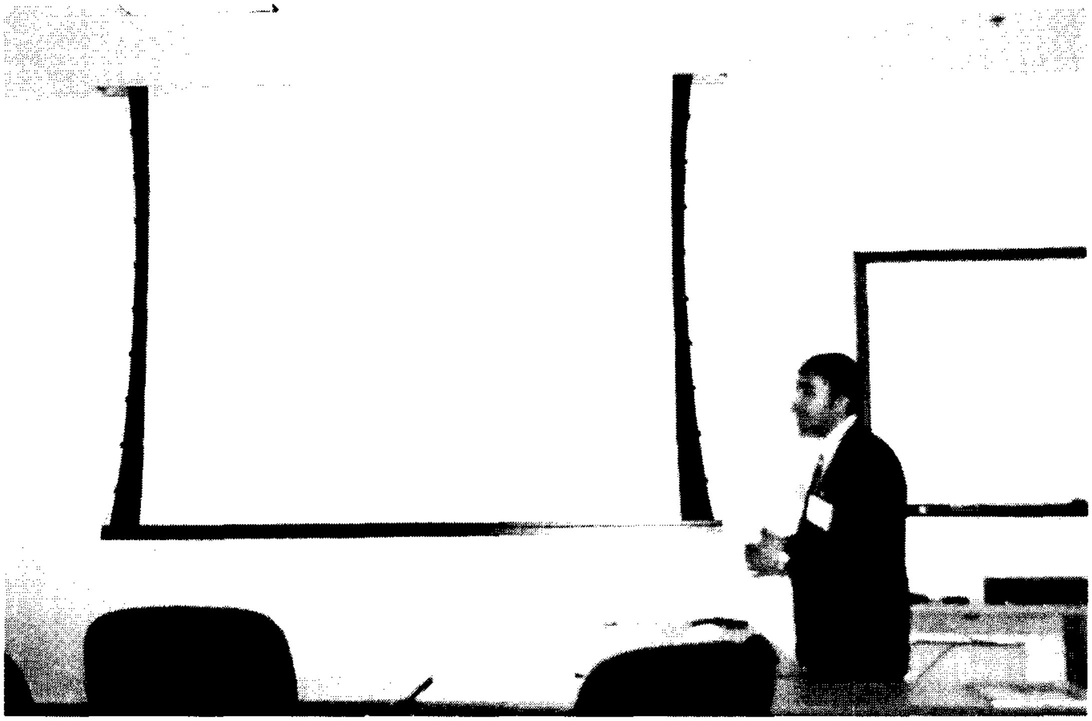

Aman Anand

Distribution of Electromagnetic Energy in a Microwave Oven Part II

J. N. Dahiya, Aman Anand and Pankaj Choudhary
Southeast Missouri State University
Cape Girardeau, MO 63701
dahiya@physics.semo.edu

and

J. A. Roberts
University of North Texas
Denton, Texas 76203
Roberts@unt.edu

Key Words: Microwave Oven, electromagnetic energy, histograms, frequency

Objectives: This is the second phase of an experiment that follows the first in which we studied the distribution of heat energy inside a microwave oven using some specific food samples like American Style Cheese Pie and Normal Wheat Dough. After performing several experiments and plotting the temperature and energy distribution histograms, it was found that the distribution of electromagnetic energy in the food samples used was not very uniform. As a result our quest for exploring the question of whether the heat energy gets distributed uniformly or not remained incomplete. To ensure the uniform behavior of the distribution of electromagnetic energy inside the microwave oven we used distilled water in different shaped containers placed strategically in the oven.

Introduction:

A few experiments have been conducted to try to model the microwave distribution inside a microwave oven using a variety of methods. In 1990, Alistair Steyn-Ross of the University of Waikato and Alister Riddell of the Hamilton Boys High School conducted an experiment to test for the existence of standing wave patterns inside a microwave oven. They used a paper towel dipped in a concentrated $CoCl_2$ solution, a common method used to test for water. When the compound is wet, a pink, hydrated $Co(H_2O)^{2+}$ complex is formed. When the compound is dry, the blue anhydrous $CoCl_2$ compound is present. The team heated the paper for 15 seconds at ten different heights and recorded the pattern of blue and pink areas. They discovered a series of blue dots evenly spaced on the pink towel. They also noticed that the placement of these wet and dry spots changed as the height was changed.

Nearly eight years later, Jouni Viiri of North Karelia Polytechnic performed a similar experiment using a sheet of acrylic. Viiri took a thermogram of the sheet after 35 seconds of heating at different heights. Viiri also noticed hot and cold spots, and the location of the spots changed as the height changed. Steyn-Ross and Riddell's experiment proved the existence of standing waves inside a microwave oven and characterized their distribution. Viiri's experiment measured the temperature difference between these hot and cold spots.

In 1999, M. F. Diprose of the University of Sheffield conducted a series of experiments to determine the parameters under which a microwave oven should be used in a laboratory. They used a variety of samples, including water and soil, in containers of different shapes and sizes. They used thermocouples to measure the temperatures at different locations within the sample. Their research resulted in an excellent reference as to what variables one should keep in mind when using a microwave oven in the laboratory. Our experiment intends to build upon these discoveries by measuring the effect, or lack thereof, of rotating a sample inside a microwave oven

Theory:

Before discussing the details of our experiment we would like to briefly discuss the theory of microwaves. Microwaves are electromagnetic waves of frequency that falls between 300 MHz to 300 GHz. This range of frequencies falls between the radio waves and the infra-red in the electromagnetic spectrum. The microwave oven is one of the great inventions of the 20th century: millions of homes in America have one. Microwave ovens are popular because they cook food very quickly. They are also extremely efficient in their use of electricity because a microwave oven heats only the food, nothing else. In the case of microwave ovens, the commonly used frequency is roughly 2,500 megahertz (2.5 gigahertz). The electromagnetic waves in this frequency range have an interesting property: water, fats and sugars absorb them. When they are absorbed they are converted directly into heat energy due to the rotation of the dipoles in that force field. Microwaves in this frequency range have another interesting property: most plastics, glass or ceramics do not absorb them. Metal reflects microwaves, which is why metal pans do not work well in a microwave oven.

Now inside the microwave oven the microwaves penetrate the food and excite water and fat molecules pretty much evenly throughout the food. There is no heat having to migrate toward the interior by conduction. There is heat distributed everywhere "at once" because the molecules are all excited together. There are limits of course. Microwaves penetrate unevenly in thick pieces of food (they don't make it all the way to the middle), and there are also "hot spots" caused by wave interference. The whole heating process is different because you are "exciting atoms" rather than "conducting heat".

The water dipoles attempt to continuously reorient in the electromagnetic radiation's oscillating electric field. Dependent on the frequency, the dipole may move in time to the field, lag behind it or remain apparently unaffected. When the dipole lags behind the field then interactions between the dipole and the field lead to an energy loss by heating, the extent of which is dependent on the phase difference of these fields. The ease of the movement depends on the viscosity and the mobility of the electron clouds. In water these, in turn, depend on the strength and extent of the hydrogen bonded network. The re-orientation process may be modeled using a 'wait-and-switch' process where the water molecule has to wait for a period of time until favorable orientation of neighboring molecules occurs and then the hydrogen bonds switch to the new molecule.
The applied field potential (E, volts) of electromagnetic radiation is given by $E = E_{max}.\cos(\omega t)$, where E_{max} is the maximum amplitude of the potential, ω is the angular frequency in radians/second and t is the time in seconds. It is because of to this behavior of water molecules inside a microwave field that we chose the heating water for studying the distribution of heat inside a microwave over. The experiment was performed slowly in various steps as explained later in this paper.

Apparatus Required:

1) A Microwave Oven with a turntable
2) Three different shaped bowls made of plastic to hold water
3) Styrofoam to cover the bowl and used as a perforated lid to hold thermometers
4) Nine Alcohol based thermometers well calibrated
5) Data logger to record data of temperature, microwave power, time of heating and status of the turntable while the experiment is performed

Procedure and Results

The experiment was carried out in different steps. Nine alcohol-based thermometers were aligned in different manner as mentioned in the histogram section of this paper. Three different shape bowls: rectangular, circular, and oval were used for carrying out these experiments. Every time the microwave oven was run, the initial and final temperatures were recorded as efficiently as possible. Then, using softwares like MS Excel and Origin the thermal distribution was found and plotted on a bind transpose matrix of this data. In the bind transpose matrix one can get the correlation between the temperature distribution as well as the nine plots of the thermometer. The pictures of the equipment in use were presented in part I of this experiment. The results of this experiment are presented in the graphs indicated in Figures 1-5. Before explaining the histograms, it is worth mentioning that the time of each run in this experiment is kept constant. The only dependent variables of this experiment were the

a) Power of the Microwave Oven
b) Turn Table Status Of the Oven **ON / OFF**
c) Shape of the Bowl In use

Now, with respect to each of these five different readings obtained from the experiment the temperature distribution is plotted on the Y-axis and the thermometer number on the X-axis. The temperature distribution means the difference in the final temperature and the initial temperature after carrying out the heating inside the microwave oven. By observing Figure 1, it can be seen that there are isotropic lines which have been correlated to the depth of the thermometer. There is a regression formula that the software Origin 7.0 uses to account for the 3 dimensional plotting. It relates the depth of three things: temperature, position on x-axis and the position on y-axis. Therefore, these isotropic lines show how the heat has been flowing from the top of the sample. On the other hand, the color and thickness shows the amount and the radial distribution of the heat across the sample. It is found that the thermometer numbers 6, 7, 8 receive maximum amount of heating, whereas, the rest of the thermometers are being heated, but slowly. This graph gives proof for an irregular distribution of heat in the microwave oven.

In Figure 2, the object shape is circular and the turntable is kept rotating, it can be seen that there is a difference in pattern of heating. It is found that the area of maximum absorption of heat shifts from thermometer number 6, 7, 8 to 5, 6, 7. The pattern for the flow of heat in this case is just the same as in the previous one. It is only the region of maximum probability that is being shifted from one experiment to another, which is due to the change in those controlled variables as mentioned above. It is found that in all the five runs shown and plotted in different figures (Figures 1-5) that the temperature distribution pattern when seen from top to bottom is the same, but the intra – layer distribution or the so called radial distribution of heat in the microwave oven is non uniform. In part I of this experiment the sample used was a cheese cake. In this part of the experiment the sample used is a perfect dielectric constant material that is water and it is the water inside the food that is assumed to be responsible for the heating. As water is a polar molecule and when subjected to 2.5 GHz frequency microwave field inside the oven the water molecule starts "spinning" and exhibits the resonance phenomenon. At resonance, its bonds break and this accounts for the release of energy, which is then absorbed by the food particles. Now, if the water molecule itself doesn't receive a uniformly distributed energy as seen in this experiment, how can one expect the food particles to be heated uniformly.

<u>References</u>:

1. Diprose, M. F. "Some Considerations when Using a Microwave Oven as a Laboratory Research Tool." <u>Plant and Soil</u>. 229, no 2, (2001): 271.

2. <u>http://www.gallawa.com/microtech/history.html</u>

3. http://www.princeton.edu/~ehs/laserguide/spectrum.jpg

4. Roddy, Dennis. Microwave Technology. Prentice-Hill, 1986.

5. Steyn-Ross Alistair and Alister Riddell. “Standing Waves in a Microwave Oven.” The Physics Teacher. 28, no. 7, (Oct 1990): 474.

6. Thuery, Jacques. Microwaves: Industrial, Scientific, and Medical Applications. Artech House, 1992.

7. Townes and Schawlow. Microwave Spectroscopy. McGraw-Hill, 1955.

8. Viiri, Jouni. “Temperature Distribution in a Microwave Oven.” The Physics Teacher. 36, no 1, (Jan 1998): 48.

THE DATA AND THE GRAPH

With the turntable on and the microwave power at 50%

(Rectangular Bowl)

SNO (X)	Initial Temp (°C)	Final Temp (°C)	Distribution (Y)
1	23.5	24	0.5
2	22.5	24	1.5
3	21	24	3
4	22.3	26	3.7
5	22.5	28	5.5
6	22.5	29	6.5
7	24	30	6
8	22.8	24	1.2
9	22	30	8

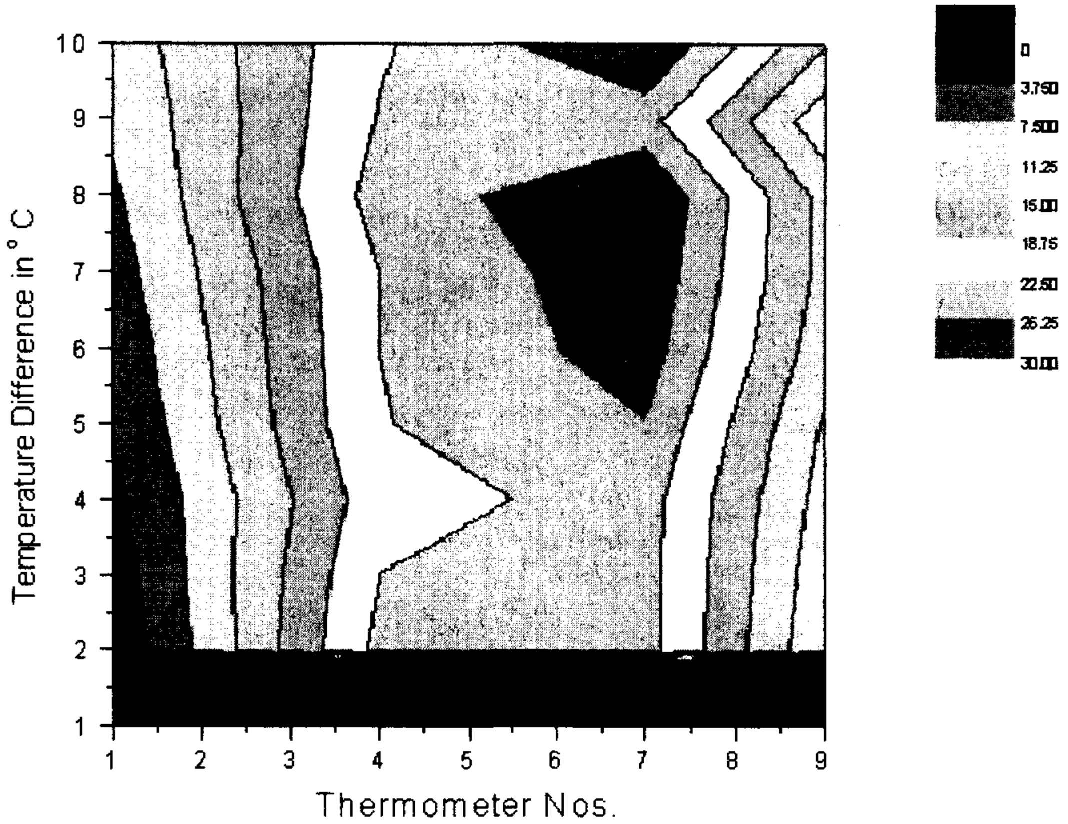

Fig. 1. Temperature in °C vs the number of thermometers for a rectangular Bowl

With the turntable on and the microwave power at 50%
(Circular Bowl)

SNO (X)	Initial Temp (°C)	Final Temp (°C)	Distribution (Y)
1	24	26	2
2	24	25	1
3	24.5	25.5	1
4	26	28	2
5	23	29	6
6	22.5	25.5	3
7	24	24	0
8	22.8	26	3.2
9	23	26	3

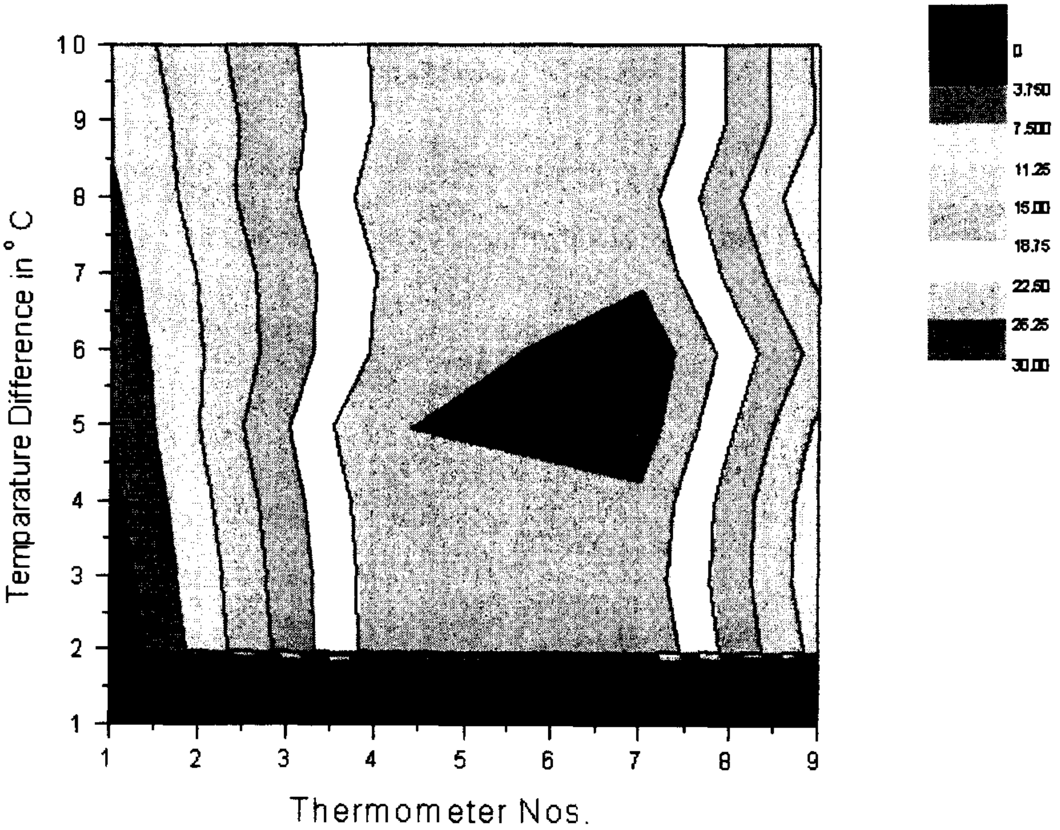

Fig. 2. Temperature in °C vs the number of thermometers for a Circular Bowl

With the turn table off and microwave power at 50%

(Rectangular Bowl)

SNO (X)	Initial Temp (°C)	Final Temp (°C)	Distribution (Y)
1	24	25	1
2	24	29	5
3	24.5	28	3.5
4	26	27	1
5	23	26	3
6	22.5	23	0.5
7	24	29	5
8	22.8	25	2.2
9	23	26	3

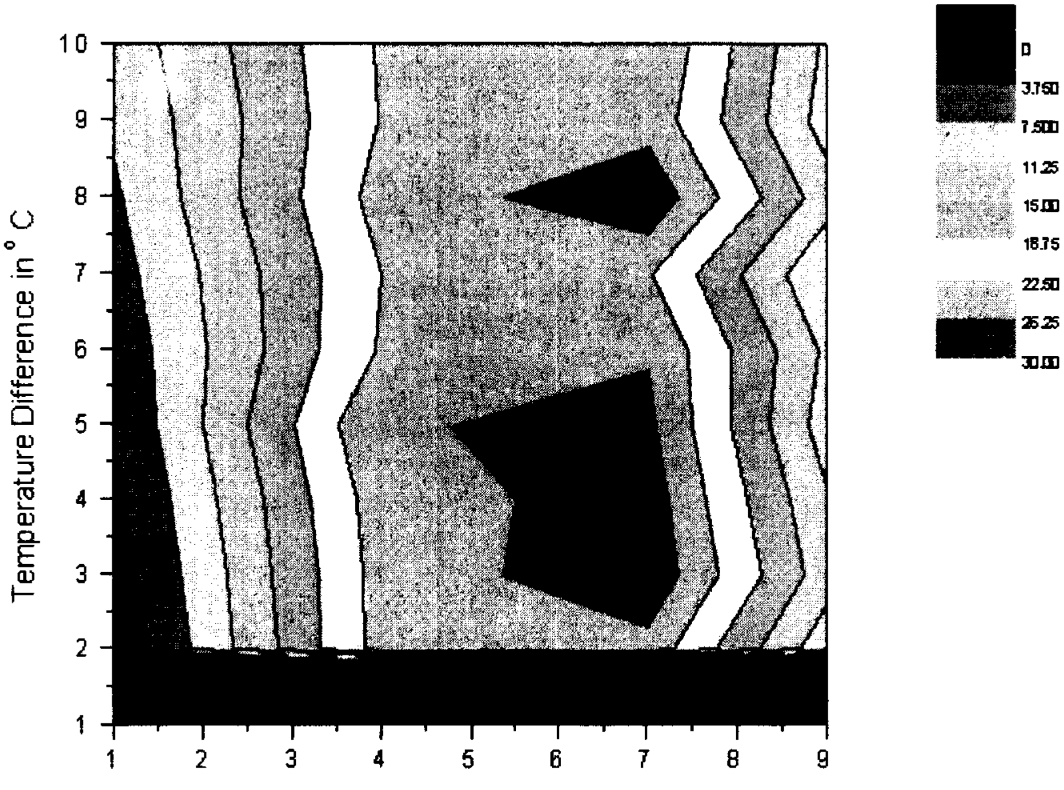

Fig. 3. Temperature in °C vs the number of thermometers for a rectangular Bowl

With the turntable off and microwave power at 100%

(Rectangular Bowl)

SNO (X)	Initial Temp (°C)	Final Temp (°C)	Distribution (Y)
1	20	30	10
2	25	32	7
3	26	33	7
4	22	35	13
5	23	36	13
6	24.5	35	10.5
7	24	33	9
8	26	33	7
9	25	32	7

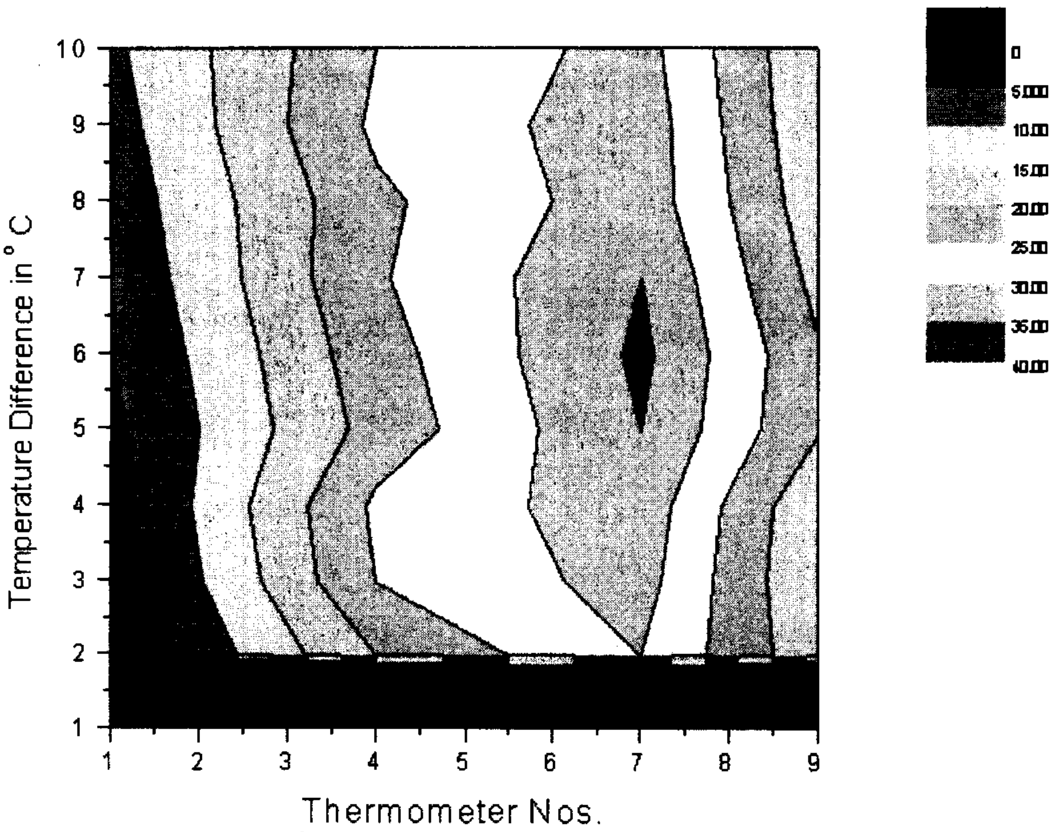

Fig. 4. Temperature in °C vs the number of thermometers for a rectangular Bowl

With the turntable off and the microwave power at 100%

(Oval-Shaped Bowl)

SNO (X)	Initial Temp (°C)	Final Temp (°C)	Distribution (Y)
1	26	33	7
2	28	33.2	5.2
3	26	31.2	5.2
4	25	31.5	6.5
5	28	33	5
6	28.5	33.5	5
7	26.3	34	7.7
8	25.5	35	9.5
9	25	32	7

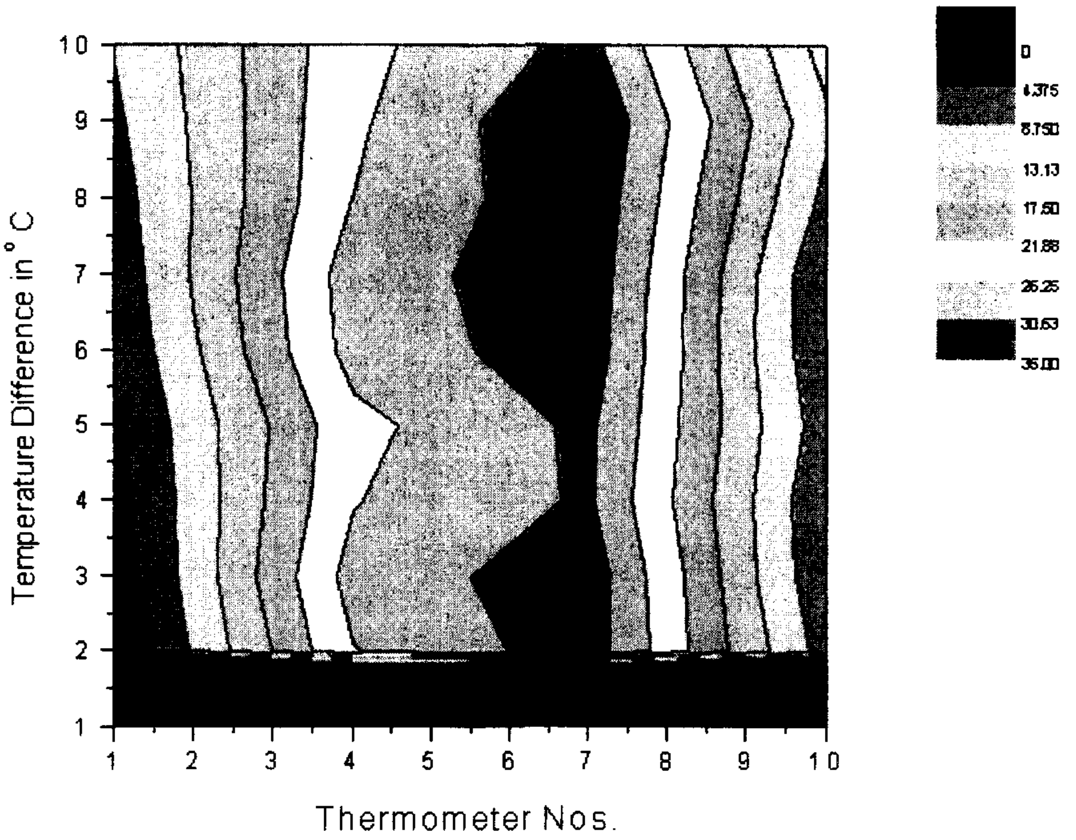

Fig. 5. Temperature in °C vs the number of thermometers for an oval shaped Bowl

EXPLORING SOLAR CELLS: A FRESHMAN ENGINEERING PROJECT

Emily L. Allen (1)

Huong Vu (1)

and

David Parent (2)

(1) Department of Chemical and Materials Engineering
(2) Department of Electrical Engineering
San Jose State University
One Washington Square
San Jose, California 95192-4010

Telephone 408-924-4010
e-mail elallen@email.sjsu.edu

Emily L. Allen

Exploring Solar Cells:
A Freshman Engineering Project

Emily L. Allen*, Huong D. Vu*, and David Parent**
*Department of Chemical and Materials Engineering
**Department of Electrical Engineering
San José State University

E10: Introduction to Engineering

- Introduction to Solar Cells
- One week module offered to E10 instructors
- Guest lecturer
- Student lab assistants
- Hands-on lab experience

E10 Project Goals

- Interest students in semiconductor technology
- Recruit for Microelectronics Process Engineering program & courses
- Photovoltaics: simple process, appeals to students, easy to test
- E10 objectives: spreadsheets, multimeter usage, design

Project Activities

- Pre-lab homework assignment
- Guest lecture on photovoltaic technology
- Measure solar cell IV curves in series & parallel
- Plot power output curves
- Design solar cell array for remote application
- Currently: test commercial cells
- Future: test Spartan Solar cells

Related Activities

- MatE 25/153: Fabricate solar cells
  - Pilot tested
  - Feasible activity for one lab period
  - Process needs improvement
- Spartan Solar City
  - Device/machine designs powered by photovoltaics
  - Replace E10 design problem
  - Energy conversion demo
  - Open House, CoE PR

E10 Lecture

- Varies by lecturer
  - Microelectronics Process Engr faculty
- Introduction to Photovoltaics
  - Applications, Device Physics
- Introduction to Processing
  - Process flow, materials science

Uses for Solar Energy

- Renewable power
- Power for remote locations
- It's free…(sort of)

What is a Solar Cell?

- *Semiconductor* device (diode)
- *Photovoltaics* convert solar energy to DC electrical energy.
  - Supplies a voltage and a current to a resistive load
  - Power = Current x Voltage
- *Like a battery*: it supplies DC power
- *Unlike a battery*: voltage supplied changes with the resistance of the load.

Basic Physics of Solar Cells

- Semiconductor material can be p-type or n-type

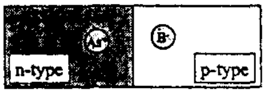

- *N-type* - impurities with an extra electron (phosphorus)
- *P-type* - impurities with one fewer electron (boron)
- Put them together: *p-n junction*
- A solar cell is a very large p-n junction (or *diode*)

Generating Charges From The Sun

- Light breaks silicon bonds and creates "free" electrons and holes "missing electrons"
- Holes are positive charges
- Built-in field separates electrons and holes

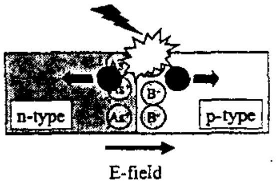

Generating Charges From The Sun

- Connect diode to a circuit
- Photocurrent goes through resistor
- Causes a voltage drop

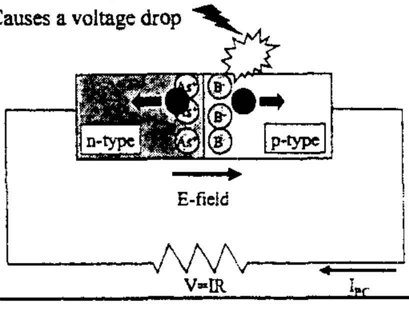

Generating Charges From The Sun

- Forward biases the diode
- Causes a current in opposite direction

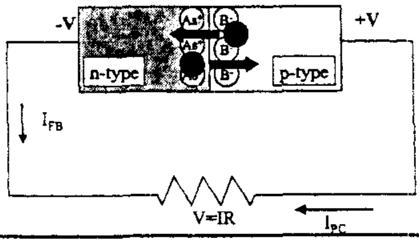

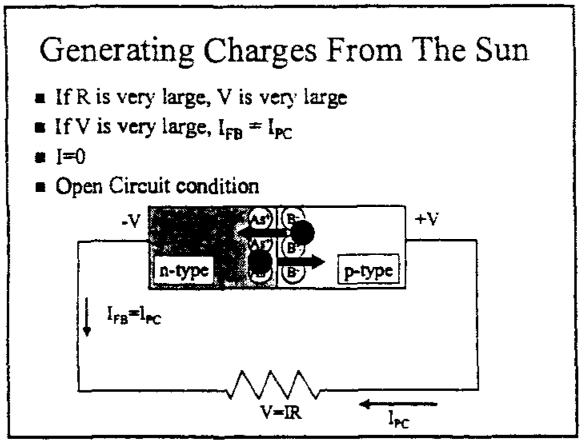

Generating Charges From The Sun

- If R is very large, V is very large
- If V is very large, $I_{FB} = I_{PC}$
- I=0
- Open Circuit condition

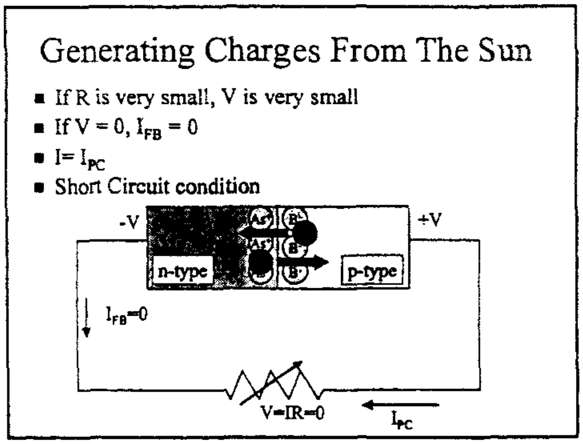

Generating Charges From The Sun

- If R is very small, V is very small
- If V = 0, $I_{FB} = 0$
- $I = I_{PC}$
- Short Circuit condition

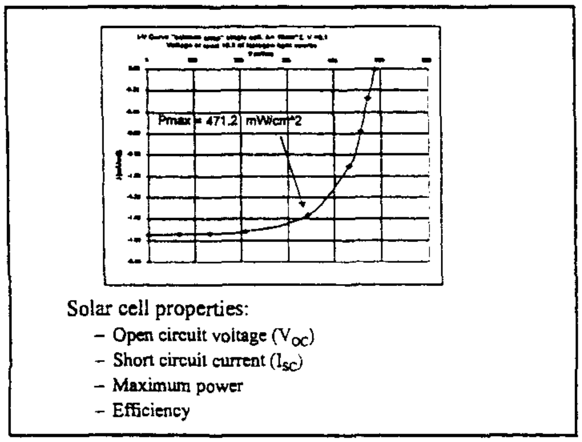

Solar cell properties:

- Open circuit voltage (V_{OC})
- Short circuit current (I_{SC})
- Maximum power
- Efficiency

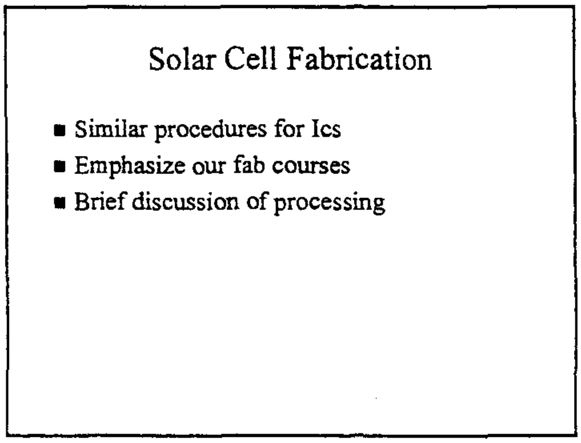

Solar Cell Fabrication

- Similar procedures for Ics
- Emphasize our fab courses
- Brief discussion of processing

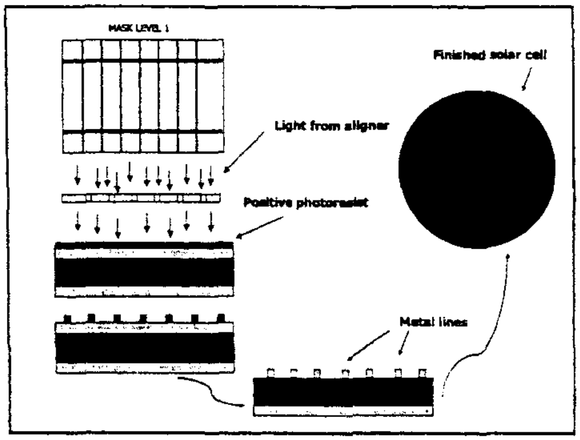

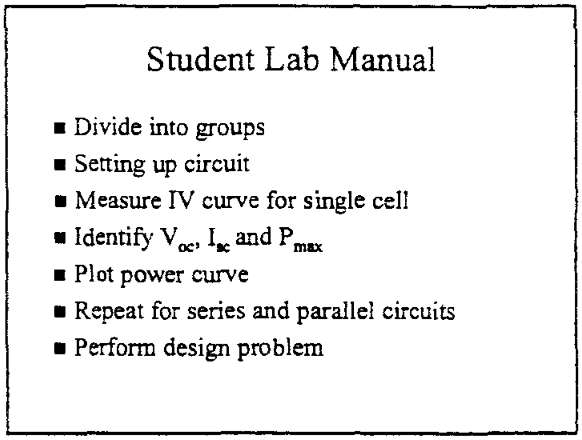

Student Lab Manual

- Divide into groups
- Setting up circuit
- Measure IV curve for single cell
- Identify V_{oc}, I_{sc} and P_{max}
- Plot power curve
- Repeat for series and parallel circuits
- Perform design problem

Student Lab Manual

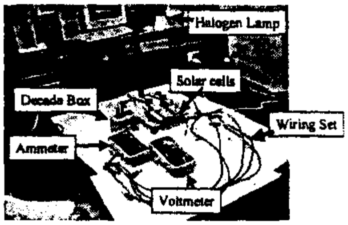

Design Problem

The figure below shows a photovoltaic system which powers a vaccine storage refrigerator. The system provides a means of storing vaccines and medical supplies in a region where reliable power is not available. Your Team's job is to design a photovoltaic array to power this system to its required specifications.

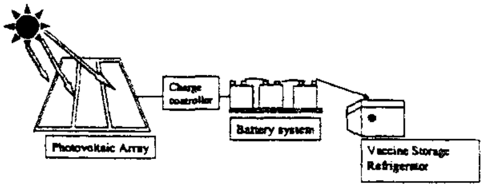

Design Questions

- What is the total number of solar cells you need in your photovoltaic array?
- Based on the cells that you measured in the lab, how big would this solar array need to be (in m^2)?
- If the cells cost $2 apiece, what would be the cost?
- What do you think would be an affordable price?
- What do you think is an appropriate size?
- What are some ways to reduce the size and cost of the array?

Project Results

- Grad student project
  - S01: 150 students; F01: 350 students
- AY 02-03
  - Two students hired to improve equipment
  - Team captains for student assistants
  - Recruited 18 new assistants for 24 labs
  - 480 students

Project Results

- Good questions from students
- Spr 01 - F01 results
  - 40-50% feel skills improved
  - 20% "very interested"
  - 78% interested or somewhat interested
- Instructors evaluations
  - Keep it in curriculum
  - Improve equipment access (more stations)
- New eval form this year

Solar Cell Workshop

- Monday 1 pm
- SJSU Microelectronics Process Engr lab
- Make and test your own solar cells!

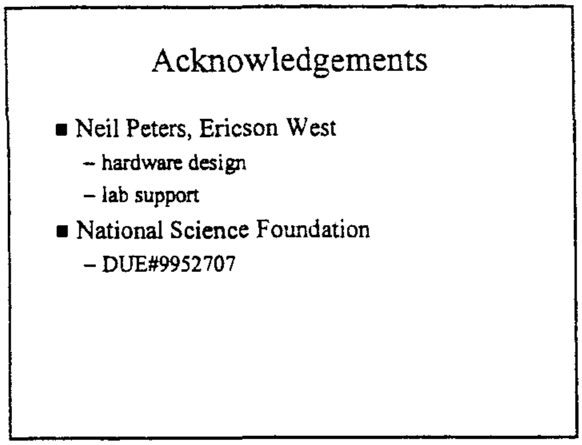

Acknowledgements

- Neil Peters, Ericson West
  - hardware design
  - lab support
- National Science Foundation
  - DUE#9952707

THE RAPID COLLECTION AND ANALYSIS OF BIOCATALYTIC DATA

H. Alan Rowe

Chemistry/Center for Materials Research
Norfolk State University
700 Park Avenue
Norfolk, Virginia 23504

Telephone: 757-823-2531
e-mail harowe@nsu.edu

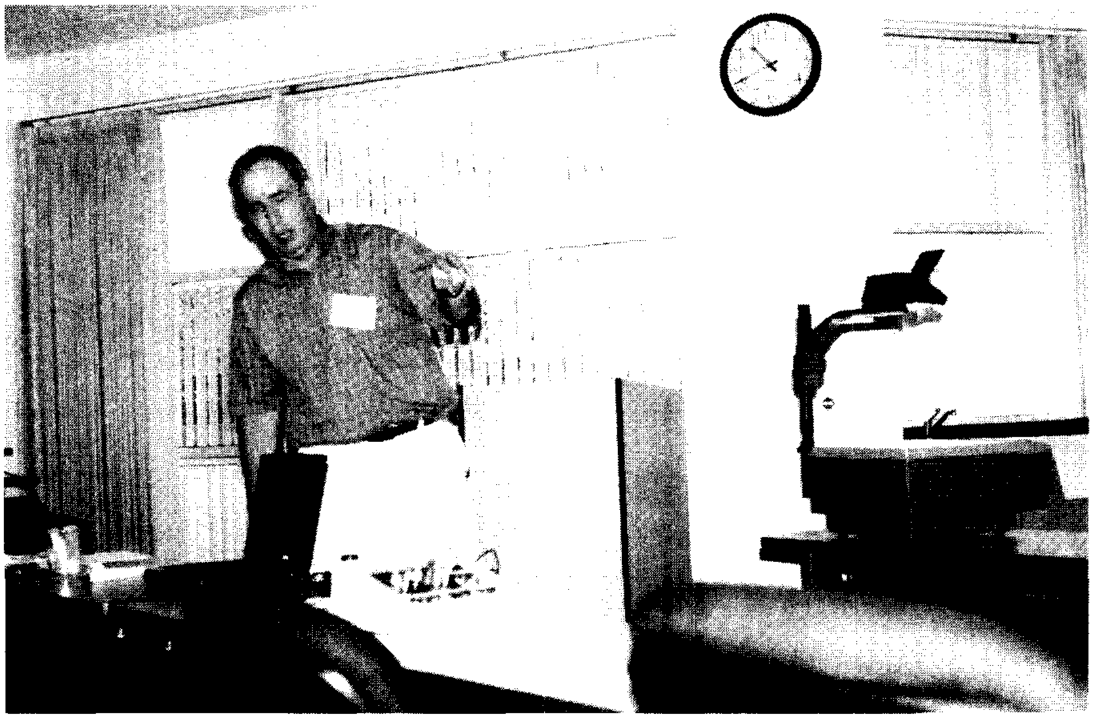

H. Alan Rowe

The Rapid Collection and Analysis of Biocatalytic Data

H. Alan Rowe
Professor of Chemistry
Norfolk State University
Norfolk, Virginia

Key Words: catalyst, reaction kinetics, reaction order, enzymes, inhibitors

Prerequisite Knowledge: Basic knowledge of chemical reactions, basic chemical kinetics, action of catalysts on chemical reactions

Objective: To use the interface to spend a small amount of time collecting data so much more time can be devoted to the understanding and analysis of catalytic data. In this manner, the concepts (basic chemical kinetics, the action of catalysts) the lab exercise is intended to demonstrate and reinforce can be more effectively presented.

Equipment: Labworks ™ (or similar) interface with spectrophotometer probe/software, computer, catechol, polyphenoloxidase, appropriate buffers, pipettors

Introduction:

The use of catalysts is an extremely important concept in chemical kinetics. However, it is often difficult to examine catalysis quantitatively in the laboratory setting . This exercise allows for the study of catalysts and kinetics in a setting that minimizes time spent on data collection and maximizes analysis and consideration of the data. A 2000 National Assessment of Educational Progress study in science has shown that science students improve their performance when using probes and computers to collect and analyze data (1). Reaction rates can be rapidly calculated and reaction orders inferred. Inhibitors of catalysts and catalytic response to variables of temperature, differing reactant concentration, etc. can be easily incorporated into the experiment.

Procedure:

The biological catalyst, polyphenoloxidase, reacts with ortho- ("side by side") diphenols and oxygen gas to produce a quinone and water. Specifically, nearly colorless catechol (an ortho diphenol) reacts with oxygen and the quinone formed is a brown color that absorbs light at a wavelength of 430 nanometers. Oxygen gas is always in excess in this reaction. The catalyst assay consists of the addition of: 1.0 ml of 0.1 M catechol, 1.5 ml of 0.20 M sodium phosphate buffer, pH 7.2, and 0.5 ml of the polyphenoloxidase catalyst. With the Labworks™ interface (SCI Technologies Inc.) the solution of catechol and buffer is used to zero the instrument and then the enzyme is added as the timer is started. The progress of the reaction is followed by the increase of the absorbance at 430 nm with time. The Labworks™ interface can measure 5 data points per second (and the newer version is much faster) allowing for the collection of very many more data points over the 3 minute reaction period than can be collected manually. To be done "by hand" only about one point every 15 seconds can be collected from rapidly changing spectrophotometer readings so frequently the reaction is stretched out over a very much longer time period and the concentrations of reactants and catalyst are appropriately adjusted.

The spreadsheet included with the software allows the student to convert the readings into absorbance values and then to plot them versus time. The slope of the curve can directly calculated for each series of measurements and this value directly related to the reaction rate.

Comments:

Since the collection of data is so rapid, very many determinations can be conducted in a short amount of time. This gives the students the opportunity to design their own investigations altering different variables in the assay. For example a series of measurements can be made changing: pH, temperature, reactant concentration, catalyst concentration, the amount of potential activators or inhibitors, etc. This is an "open ended" reaction where the student can take a meaningful part in the exploration of the kinetics of this reaction.

References:

1) http://nces.ed.gov/nationsreportcard

Bibliography:

H. Alan Rowe is a Professor and Head of the Chemistry Department at Norfolk State University. He has a bachelor's degree from the University of North Carolina at Chapel Hill and a Ph.D. in Biochemistry from North Carolina State University in Raleigh, NC. He conducted research as a Research Fellow at the Bowman Gray School of Medicine of Wake Forest University. He is a former Teacher of the Year at Norfolk State University and has been honored as a Senior Fulbright Scholar at the University of Kelaniya in Sri Lanka.

A SIMPLE BUT EFFECTIVE EXPERIMENT TO ILLUSTRATE SECOND ORDER DYNAMIC SYSTEMS

G. Song

M. Zeng

and

P. Lam

Department of Mechanical Engineering
The University of Akron
Akron, Ohio 44325-3903

Telephone 330-972-6715
e-mail gsong@uakron.edu
zengming168@yahoo.com

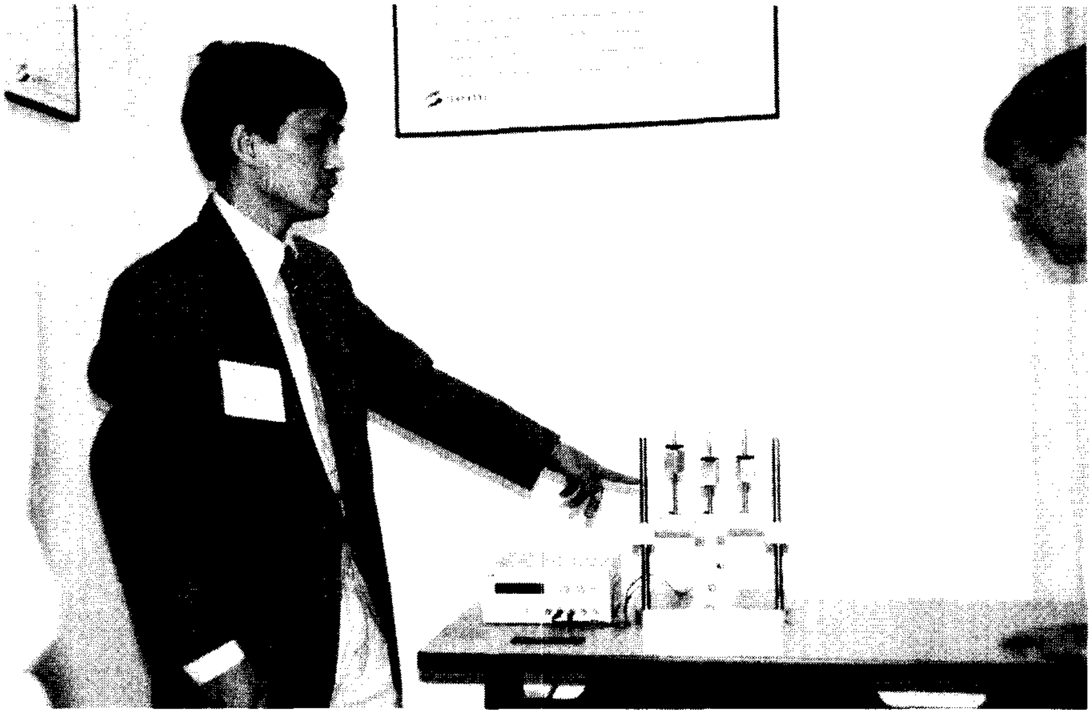

Ming Zeng

A Simple but Effective Experiment to Illustrate Second Order Dynamic Systems

G. Song*, M. Zeng, and P. Lam

Department of Mechanical Engineering
The University of Akron
Akron, OH 44325-3903

* Tel: (330) 972-6715; Fax: (330) 972-6027; Email: gsong@uakron.edu

Key Words: Spring-mass-damper dynamic system, resonant frequency, undamped natural frequency

Prerequisite Knowledge: Basic concepts of a dynamic system

Objective: To illustrate mechanical resonance and verify the relationship between its occurrence and the excitation frequency

Equipment and Materials:

1. A vibrating platform with 3 spring-mass-damper systems. The platform is driven by a DC motor (24V, 1.6A)
2. A Tachometer
3. A DC power supplier

Introduction:

1. Motivation and technical background:

A vibration experiment is built to demonstrate mechanical resonance of second order dynamic systems for mechanical engineering students who are taking System Dynamics and Responses. This vibration experiment employs a platform subjected to sinusoidal input force via a DC motor. By employing three underdamped spring-mass systems with different spring stiffness but same mass, this experiment can clearly demonstrate the relationship between the natural frequency and stiffness, the occurrence of resonance and its dependence on the input frequency.

2. Mechanical model and the equation of motion:

A typical second order mechanical system can be represented as shown Figure (1).

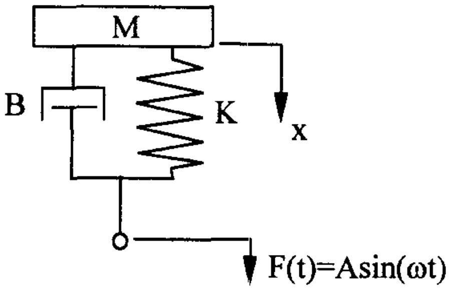

Figure (1) Spring-mass-damper system

M, B, and K represent the mass, the damping coefficient, and the spring constant of the system, respectively. x represents the system coordinate. F(t) is the external harmonic excitation. Since most mechanical systems are underdamped and resonance occurs in underdamped systems, we will only consider such systems in this paper.

There are two kinds of vibrations to be involved in this paper. One is a free vibration. In this case the response is caused by non-zero initial conditions, and the vibration will die out due to viscous damping. In this paper, this free response is used to determine the damping ratio of the system by utilizing the logarithmic decrement method. The other one is a forced vibration, which is induced by external harmonic force. The system will oscillate and its magnitude depends upon the frequency of the driving force. When the excitation frequency matches the resonant frequency of the system, the amplitude of the motion will be at its maximum and resonance will take place. The forced vibration is used to demonstrate the resonance of a mechanical system in this paper.

The free vibration of the spring-mass-damper system is governed by the following second ordinary differential equation:

$$M\ddot{x} + B\dot{x} + Kx = 0 \text{ or } \ddot{x} + 2\zeta\omega_n\dot{x} + \omega_n{}^2x = 0 \tag{1}$$

Where $\zeta = \frac{B}{2\sqrt{KM}}$ and $\omega_n = \sqrt{\frac{K}{M}}$ denote the damping ratio and undamped natural frequency of the system.

The forced vibration response is governed by equation (2):

$$M\ddot{x} + B\dot{x} + Kx = F(t) \tag{2}$$

The force can be a sinusoidal forcing function. Substituting $F(t)=A\sin\omega t$ into equation (2) yields:

$$M\ddot{x} + B\dot{x} + Kx = A\sin\omega t \tag{3}$$

Here A and ω represent the amplitude and frequency of the harmonic excitation force respectively.

The steady state solution to the second ordinary differential equation (3) is:

$$x(t) = X\sin(\omega t + \phi) \qquad (4)$$

The amplitude, X, can be written as $X = \frac{A/K}{\sqrt{(1-\mu^2)^2 + (2\zeta\mu)^2}}$ and the phase shift, ϕ, is given by $\phi = -\tan^{-1}\left[\frac{2\zeta\mu}{1-\mu^2}\right]$. μ is the ratio of the excitation forcing frequency to the natural frequency of the system. This ratio is defined as: $\mu = \frac{\omega}{\omega_n}$.

When $0 \le \zeta \le 0.707$, resonance may occur and the resonant frequency is $\omega_r = \omega_n\sqrt{1-2\zeta^2}$. The magnitude of the resonant peak is $M_r = \frac{1}{2\zeta\sqrt{1-\zeta^2}}$.

Procedure:

1. Experimental setup:

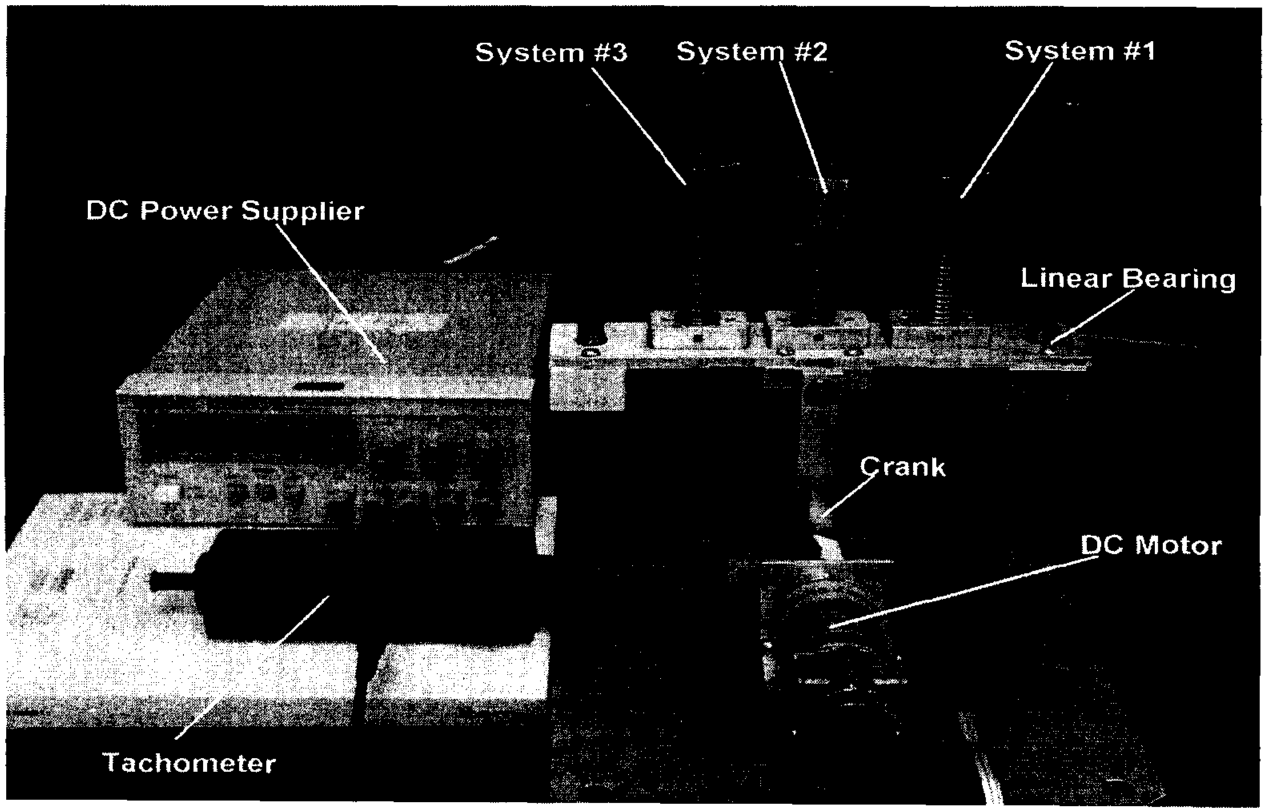

Figure (2) Experimental setup

The experimental setup, as shown in Figure (2), consists of a vibrating platform with three different underdamped spring-mass systems. These three spring-mass systems have identical mass but different springs. The platform can be excited by a DC motor via a crankshaft by adjusting the applied voltage. Each mass block can oscillate along the stainless steel guide with a linear bearing, which generates some damping to the system.

2. Experimental Demonstration:

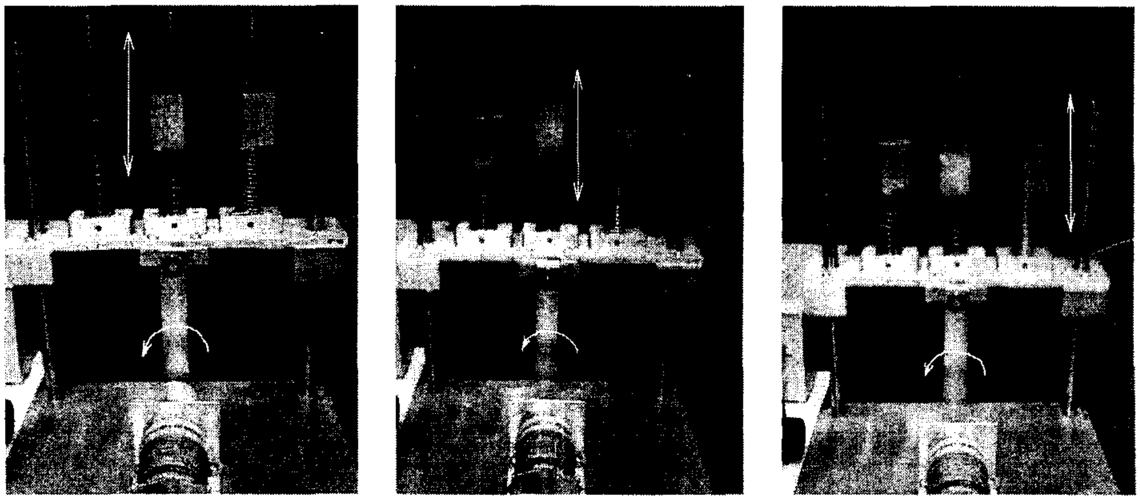

a). Motor speed at 370 rpm System #3 is in resonance
b). Motor speed at 610 rpm System #2 is in resonance
c). Motor speed at 710 rpm System #1 is in resonance

Figure (3) System #1, 2, and 3 in resonance

In the demonstration, the speed of the DC motor is increased by adjusting the DC power supply. The rotation of the motor can be measured by a tachometer. When the motor speed is about equal to 370 rpm, close to the resonant frequency of the system #3, only the block #3 oscillates with a large magnitude and the other two blocks do not vibrate too much. The so-called resonance occurs for system #3 as shown in Figure (3)a. When the DC motor speed increased, the vibration of the block #3 disappeared. At about 610 rpm, the block #2 is in resonance and vibrates dominantly as shown in Figure (3)b. When the block #1 is vibrating in resonant frequency as shown in Figure (3)c, the speed of the motor is about 710 rpm. Decreasing the DC motor speed slowly, the resonance occurs from system #1 to #2 then #3.

3. Experiment data and analysis:

The undamped natural frequencies of the system #1, #2, and #3 can be calculated from the equation $\omega_n = \sqrt{K/M}$ and shown in Table 1.

Table 1. Characteristic Parameters of the Systems.

System	Mass M (kg)	Stiffness K (N/m)	Natural frequency ω_n	
			(Hz)	(rpm)
#1	0.083	410	11.2	672
#2	0.083	368	10.6	636
#3	0.083	157	6.9	414

The free decaying oscillations of the systems are captured by a laser sensor. The logarithmic decrement method, as shown in equation (5), is used to determine the damping ratio of the system from the free vibration response [Ogata, 1998].

$$\zeta = \frac{\frac{1}{n-1}\left(\ln\frac{x_1}{x_n}\right)}{\sqrt{4\pi^2 + \left[\frac{1}{n-1}\left(\ln\frac{x_1}{x_n}\right)\right]^2}} \tag{5}$$

Where x_1 is the peak amplitude at the time t_1, x_n is the amplitude measured at time $t=t_1-(n-1)T$. T is the period of decaying oscillation. The damping ratios and the resonant frequencies of the systems are calculated and listed in Table 2.

Table 2. Comparison of Calculated Resonant Frequencies (ω_r) and Observed ω_r.

System	Damping ratio ζ	Calculated ω_r		Observed ω_r	
		(Hz)	(rpm)	(Hz)	(rpm)
#1	0.02	11.2	671.7	11.83	710
#2	0.036	10.59	635.2	10.17	610
#3	0.038	6.89	413.4	6.17	370

Comments

From the experimental data, it is clear that the observed resonant frequencies are very close to the calculated ones. The differences between the results are mainly due to the nonlinearity of the spring constants. The damping of each subsystem in this experiment is very small. The natural frequency is approximately equal to its resonant frequency. The dependence of the natural frequency and the resonant frequency on the system's stiffness constant is clearly illustrated through the experiments. The experiments also clearly demonstrate the occurrence of resonance and its dependence on the frequency of the external force.

Survey Results

The effectiveness of this demonstration was surveyed during the class of System Dynamics and Responses in the Spring semester of 2002. There are 12 students responded to the survey. The survey results are shown in Table 3, which clearly demonstrates the effectiveness of this resonance experiment.

Table 3: Demonstration Survey Results

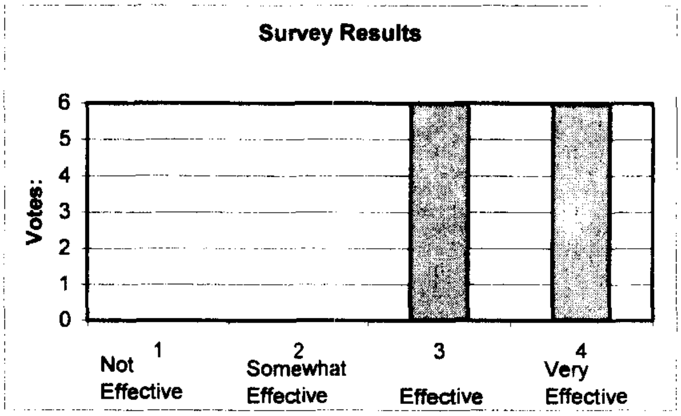

References:

1. K. Ogata, System Dynamics, 3rd edition. Upper Saddle River, NJ: Prentice Hall, 1998

Bibliography:

Dr. Gangbing Song is an Associate Professor and Director of the Smart Materials and Structures Laboratory in the Department of Mechanical Engineering at The University of Akron. Before joining The University of Akron in 1998, Dr. Song was an Assistant Research Professor in the Department of Aeronautics and Astronautics (AA) at US Naval Postgraduate School (NPS) for two years and a research associate in the Mechanical Engineering Department at NPS for one year. Dr. Song received his Ph.D. and MS degrees from the Department of Mechanical Engineering at Columbia University in the City of New York in 1995 and 1991, respectively. Dr. Song received his B.S. degree in 1989 from Zhejing University, P.R.China. Dr. Song is a member of ASME and ASEE. His research interests include smart structures, robust control, adaptive control, neural network and their applications in robotics, vibration, and position control.

Ming Zeng is a graduate student in the Department of Mechanical Engineering at the University of Akron. Ming Zeng received his B.S. degree in 1995 from Zhengzhou University, P.R. China and worked as a Mechanical Engineer for China Tianchen Chemical Engineering Corp. in Tianjin City, P.R. China from 1995 to 2000.

Dr. Paul C. Lam is Professor and Associate Dean of Undergraduate Studies, Co-op and Diversity Programs in the College of Engineering at the University of Akron. He received his BS degree in 1969 at Purdue University, MS degree in 1970 at University of Illinois, and PhD in 1978 at the University of Akron. Research interests include structural dynamics, fatigue and fracture evaluation of material behavior, pre-college math/science/technology programs, and pre-engineering minority and retention models of engineering education. Dr. Lam is an ASME Fellow and the recipient of numerous outstanding teacher and outstanding alumni awards at the University of Akron.

METALLIC GLASS: DRIVING FAR FROM EQUILIBRIUM AND RETURNING BACK

Katherine C. Chen

Materials Engineering Department
California Polytechnic State University
San Luis Obispo, California 93407

Telephone 805-756-6634
e-mail kcchen@calpoly.edu

Katherine C. Chen

Metallic Glass: Driving Far from Equilibrium and Returning Back

Katherine C. Chen
Materials Engineering Department
California Polytechnic State University
San Luis Obispo, CA 93407
kcchen@calpoly.edu

Key Words: Noncrystallinity, crystal structures, thermodynamics, kinetics, metallic glass, amorphous metals, x-ray diffraction, rapid solidification, diffusion, equilibrium, metastability

Prerequisite Knowledge: Crystal structures, noncrystallinity, diffusion, annealing treatments, x-ray diffraction, equilibrium

Objectives: Devise and perform experiments to monitor the change from the noncrystalline to crystalline state of metallic glass ("metglass").

- characterize noncrystalline material
- explain different processing methods to fabricate metallic glass
- predict and perform x-ray diffraction (XRD) on a noncrystalline material
- describe the interplay of thermodynamics and kinetics in context of annealing metglass
- devise annealing treatments (based on Temperature and time) to crystallize metglass
- monitor the changes from the noncrystalline state to the crystalline state
- explain the mechanism for the structural changes
- explain the structural changes (due to processing) and the effects on properties
- give examples of applications of metallic glass

Equipment and Materials:

1. Metallic glass (Honeywell, other sources)
2. X-Ray Diffractometer
3. Furnace

Introduction:

Incorporation of metallic glass (or "metglass") into a sophomore-level "Structures of Materials Laboratory" has allowed the illustration of several different concepts in Materials Science and Engineering. The structural differences between crystalline and noncrystalline materials are defined and observed experimentally through x-ray diffraction (XRD). Special fabrication techniques (e.g., rapid solidification by melt spinning, or lattice frustration) are first explored to explain how processing results in nonequilibrium or metastable structures.

Thermodynamics and kinetics are invoked to help frame the situation and also to help predict structural changes upon heating. Annealing treatments are then performed to confirm predictions. Further exploration of metallic glass or of processing treatments *far from equilibrium* can then be made.

Procedure:

X-ray diffraction is first performed upon the metallic glass. The differences in XRD scans with typical crystalline metals are investigated. Discussions on rapid solidification and non-equilibrium processing are employed. The return to equilibrium is usually correctly proposed by the students.

Students are then asked to devise their own annealing treatments to monitor the transformation that will occur during annealing of the metallic glass. After a discussion on diffusion, a grid of different temperatures and times are often generated. (A couple of temperatures and times are sufficient to observe the trend.) One treatment (at a particular temperature and time) can be assigned to a group or team, and the class shares all the data. Students then perform the annealing treatments and redo the XRD. Applications of metallic glass are also explored in order to make the full connections among processing, structure, properties, and performance.

1. Perform x-ray diffraction (XRD) on a piece of the metglass. (For contrast, also try a piece of aluminum foil.) What kind of XRD pattern do you get with the noncrystalline material? Why is the pattern different from most metals?

2. Devise some experiments to monitor the change from the noncrystalline state to the crystalline state. (What are your possible test parameters?)

3. Perform the experiments and discuss trends that you see with the processing/history and the structure of the samples.

Further Applications

4. What are some applications of metglass? (Cite sources.) What are some special properties that are derived from the amorphous structure?

5. What are some typical compositions of metglass? (Cite sources.) Why are these particular elements used?

Comments:

This laboratory can be easily adapted as a demonstration, or could be expanded to fit the needs of the course. With the right samples, magnetic properties can also be studied as a function of the processing treatments (to connect processing-structure-properties).

The as-received amorphous metal should produce a single, large XRD peak (Figure 1a). The lack of periodicity, or *translational symmetry*, results in noncrystallinity and, therefore, the absence of sharp XRD peaks. While thermodynamics dictates that metals are generally crystalline, rapid solidification can prevent the atoms from ordering onto a periodic lattice. In addition, a mixture of several different sized atoms can "frustrate the lattice" and assist in the ability to form a noncrystalline structure.

The actual annealing treatments will vary according to the metglass. A window of times and temperatures should be determined by the instructor before the lab. The students should realize the effects of temperature and of time, based on the diffusion equation,

$$x = \sqrt{Dt}$$

were x is the average diffusion distance, D is the diffusion coefficient (which is dependent on Temperature), and t is time.

With annealing, the metglass obtains enough energy to return to equilibrium (i.e., crystallinity) through diffusion of the atoms. The XRD scans should display a decrease in the large, broad peak and the appearance of well-defined peaks (Figure 1b and 1c).

The lab works well as an *inquiry-based exercise,* where the students are asked several questions and then discover answers through experimentation. Excitement and satisfaction are usually generated when discovering that predictions are verified by experiments.

Students are usually fascinated with the topic of metallic glass and their applications. Because the metglass is noncrystalline, there are no defects (in the usual sense) such as dislocations. Rather than plastically deforming, the metglass can be quite strong and have more of an elastic response. Several websites on golf clubs and coatings exist (see References section). A demonstration called "Atomic Trampoline" is also available for purchase (http://ice.chem.wisc.edu/order.html) and has proven to be very popular.

References: (websites on applications or demonstrations)

http://mrsec.wisc.edu/edetc/amorphous/
http://www.metglas.com/
http://www.liquidmetalgolf.com/
http://www.physics.helsinki.fi/~diamond/index.html
http://www.armacor.com/
http://science.nasa.gov/headlines/y2001/ast23apr_1.htm?list48859
http://www.msnbc.com/news/776076.asp

Bibliography:

Katherine C. Chen is an Associate Professor in the Materials Engineering Department at Cal Poly State University, San Luis Obispo, CA. She received her bachelor degrees (in Chemistry and Materials Science & Engineering) from Michigan State University, and Ph.D. from the Massachusetts Institute of Technology. She worked at Los Alamos National Laboratory for three years. At Cal Poly, she teaches the undergraduates Structures of Materials, Kinetics of Materials, and various other courses. She is a member of ASEE, MRS, ASM, and TMS.

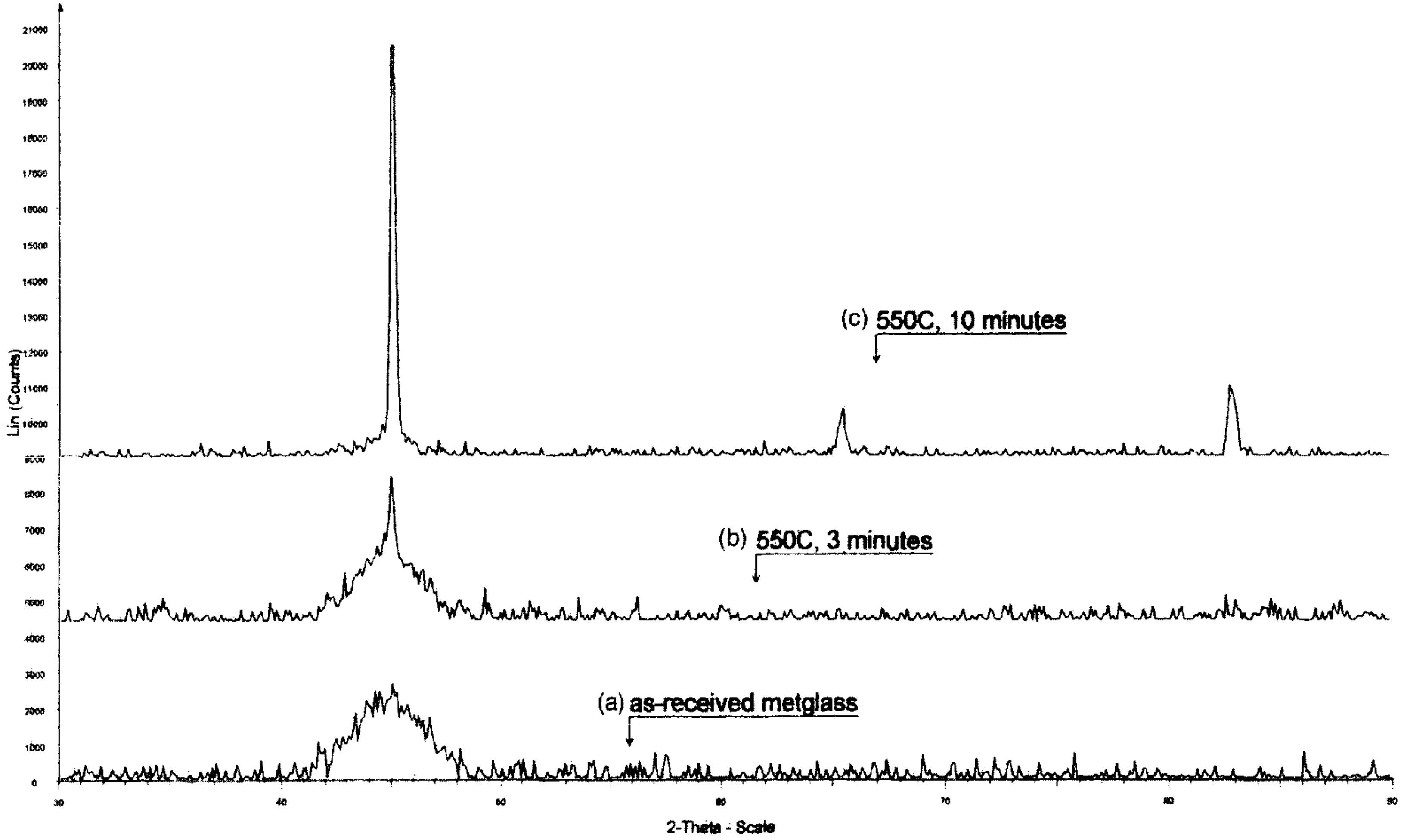

Figure 1. X-ray diffraction scans of the metglass in the a) as-received condition, b) annealed at 550°C, 3 minutes, and c) annealed at 550°C, 10 minutes. The metallic glass changes from an amorphous to crystalline structure upon annealing.

CASTING THERMOSET POLYMERS: PROCESS CONSIDERATIONS AND EVALUATING THE EFFECTS OF FILLERS ON FLEXURAL STRENGTH

Sarah E. Leach[1]

and

Patricia J. Olesak[2]

Mechanical Engineering Technology
Purdue University

[1] South Bend, Indiana
Telephone 574-237-4172
e-mail seleach@pusb.iusb.edu

[2] West Lafayette, Indiana
Telephone 765-494-7532
e-mail pjolesak@tech.purdue.edu

Sarah E. Leach

Casting Thermoset Polymers: Process Considerations and Evaluating the Effects of Fillers on Flexural Strength

Sarah E. Leach[1] and Patricia J. Olesak[2]
Mechanical Engineering Technology, Purdue University
[1]South Bend, IN (574) 237-4172 seleach@pusb.iusb.edu
[2]West Lafayette, IN (765) 494-7532 pjolesak@tech.purdue.edu

Key words: polymer, urethane, casting, silicone, polymerization, thermoset, thermoplastic, fiber reinforced composite, flexural strength

Prerequisite knowledge: Students should understand the basic concepts of polymerization, modulus of elasticity, and tensile strength. This experiment can also be used for illustrating the processing steps for casting, by including observations about mold design features (gating system, draft, mold cavity alignment, venting) and process considerations including; mixing and pouring requirements, removal of air bubbles, mold maintenance, and flash removal.

Objectives: Students gain hands-on experience creating and using single and multiple-use molds to cast thermoset polymer materials. Students create test bars of filled and unfilled materials which are tested as cantilever beams to determine the modulus of elasticity of the material.

Equipment and Materials:

Urethane casting compound (2-parts)
Silicone rubber casting compound (2-parts)
polymer fibers (e.g. acrylic, nylon)
talc (talcum powder)
silica sand
Synthetic clay
Plastic disposable plates
Mold release
Small disposable plastic cups
Stir sticks
Patterns (small non-porous objects)
scissors
aluminum foil
paper towels

Procedure:

The thermoplastic casting experiment is typically performed over at least two sessions, at least 24 hours apart, to allow the polymer materials to cure. During the first session, the instructor gives a short introductory lecture to explain the procedure and review appropriate material handling techniques. Each student is given a handout which details the procedures and equations to be used, and provides a worksheet for calculations. Students work in teams of two to four students, as assigned by the instructor. During the first laboratory period each team is given a kit of materials and allowed to choose their own pattern for the first casting exercise. Keys, coins, medallions and other small objects have been effectively used as patterns. The students make a mold cavity using clay, and cast an article using the urethane casting compound. The urethane resin and hardener are mixed at a ratio of 1:1, by volume. Small plastic cups are used to measure the components, which are mixed by stirring. After stirring, the mixture is poured into the mold cavity, then allowed to cure, which takes approximately 3 minutes. Aluminum foil or disposable plates are used under the clay to catch any overflow of the urethane and to provide a base for the clay. After the resin is cured, the part can be removed, cleaned, and trimmed, if necessary.

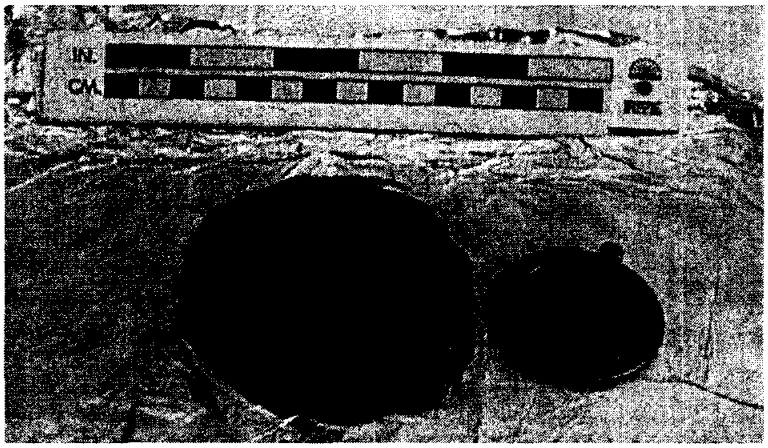

Figure 1
A single-use cavity formed from synthetic clay. Next to the clay is the pattern used to make the cavity.

Student teams then use a silicone rubber mold cavity (provided for them) to create test bars of urethane. Figure 2 shows the preparation of the mold cavity for the test bars. The pattern is shown in the bottom of the container, which is being filled with silicone rubber molding material. The mold material is poured slowly from one end to avoid trapping air bubbles.

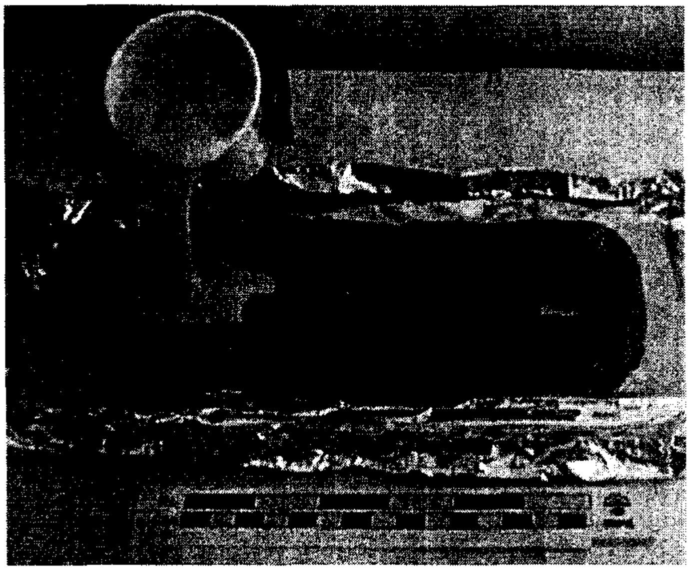

Figure 2
Making a multiple use mold cavity from silicone rubber, using a clay "moat" to contain the silicone rubber.

The students cast bars from unfilled urethane, urethane filled with 1.5 % fiber, and urethane filled with 3 %, 6% and 30% particulates, by weight. Fibers are prepared by cutting yarn into 1/8 inch long pieces.

Each cast bar is removed from the mold cavity after approximately 5 minutes, but is allowed to cure for at least an additional 24 hours before deflection testing. Figure 3 shows a test bar being cast in the silicone rubber mold cavity. Urethane resin has been poured into the mold and has begun to cross link. The color change from translucent to opaque can be observed at the center of the right side of the test bar. Figure 4 shows several samples of cast bars, ready for deflection testing.

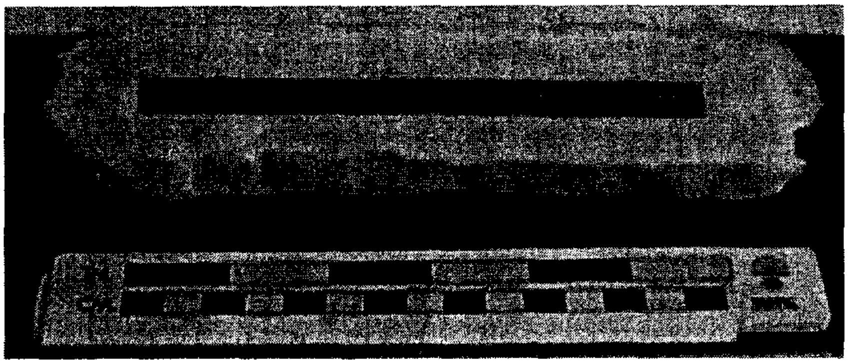

Figure 3
Silicone rubber mold for casting test bars.

Figure 4
Cast bar samples, shown with the silicone rubber mold cavity.

The final activity for the first laboratory period is to create the first half of a two-part silicone rubber mold. Students choose an object to use as a pattern, and create a container to hold the mold. The students must choose an orientation for the parting line and for a gating system through which the finished mold with be filled with casting material. Careful planning is required at this stage to create a useful mold cavity. Synthetic clay is used to fill the bottom half of the mold container, and the object is pressed into the clay, up to the desired location of the parting line. Figure 5 shows a mold container with the clay and a pattern in place. Additional clay has been used to create a sprue extending from the top of the screw. This sprue will be vertical when the completed mold cavity is used.

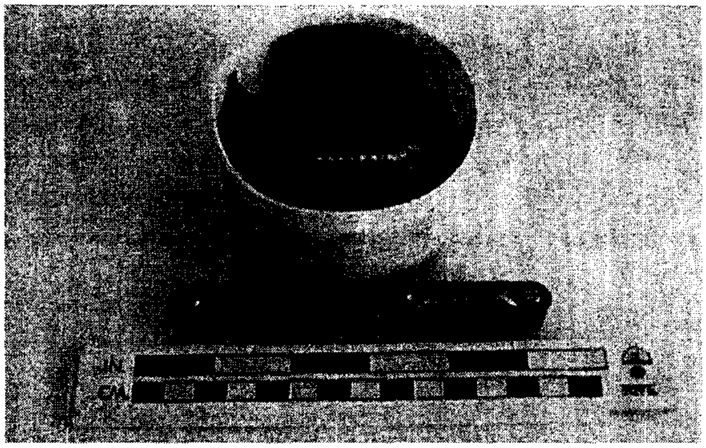

Figure 5
Mold container with clay and pattern.

After the pattern is inserted into the clay, the top part of the mold container is filled with silicone rubber mold compound. The silicone rubber is allowed to cure for at least 4 hours.

During the second laboratory session, the mold container is inverted, and the clay removed. Figure 6 shows the first half of the silicone rubber cavity now in the bottom of the mold container, with features cut into the silicone rubber on either side of the pattern to provide a means of aligning the two parts of the finished mold cavity.

Figure 6
Mold container with half of the silicone rubber mold cavity, inverted, ready for second part of mold cavity.

This mold container is now ready to be filled with silicone rubber mold material, to form the second part of the mold cavity. The pattern remains in the cast silicone rubber, and the surface of the exposed pattern and the silicone rubber are cleaned with isopropyl alcohol. After coating the silicone rubber surfaces with mold release, the remainder of the mold container is filled with silicone rubber, which is again allowed to cure for at least 4 hours. After the cure is complete, the mold container is removed, the two halves of the mold cavity are separated and the pattern is removed. A sprue, gate, and runners can now be cut into the mold cavity as required. The two-part mold can now be used to cast "copies" of the original pattern, using the two-part urethane casting compound. Figure 7 shows the finished two-part silicone rubber mold cavity, with the original pattern on the right, and two parts cast from urethane. The sprue can be seen on the cast parts, and mold "flash" is also visible on the cast part that has been removed from the mold.

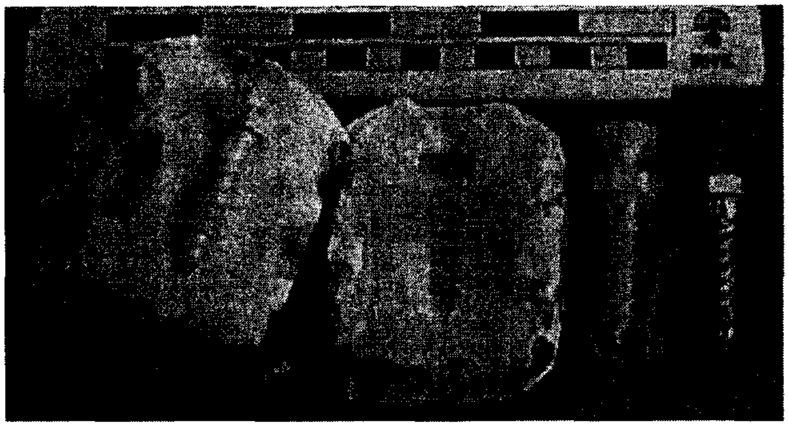

Figure 7
Silicone rubber two-part mold, with cast parts and pattern.

Also during the second laboratory session, the cast urethane test bars are analyzed to evaluate the effects of the additives on the modulus of elasticity. Data is collected for the thickness of each of the test bars, and the bars are tested for deflection under load. The bars are mounted as cantilever beams using a clamp to secure one end. A load is applied to the free end, and the deflection of the free end is measured. A load value should be chosen to allow for measurable deflection in the elastic range of the beam material. For this experiment, a load of 0.2 pounds was selected, and all of the beams were 0.5 inches wide, with a free length of 5 inches. The thickness and deflection data were used to compute the modulus of elasticity for the materials using the following formula:

$$E = PL^3/yI$$

Where E = modulus of elasticity in tension, in psi
P = load in pounds (0.2 pounds)
L = beam length, in inches (5 inches)
y = beam deflection, in inches
I = beam section modulus, $(\text{width}*\text{thickness}^3)/12$, in inches^4
(the test bars were 0.5 inches wide)

Table 1 lists average modulus values calculated from cast urethane test bars. The results indicate that adding small amounts of talc had no significant effect on the modulus value. Adding 30% by weight did increase the modulus, and the effect was larger for sand than for the very soft and finely divided talc. The addition of 1.5 % by weight of acrylic fibers may have raised the modulus slightly, but the effect was small and may not have been significant. Larger weight percentage additions of acrylic fibers were not practical for this gravity-casting method.

Table 1
Composition and Modulus for Cast Test Bars

Material	Average Calculated Modulus, ksi
Unfilled Polyurethane	151
Polyurethane with 3 wt. % talc	148
Polyurethane with 6 wt. % talc	147
Polyurethane with 30 wt. % talc	190
Polyurethane with 1.5 wt. % acrylic fibers	159
Polyurethane with 30 wt. % sand	225

Comments:
Casting samples and test bars with urethane requires some care in laboratory technique. The two components of the system must be measured carefully, and then quickly mixed thoroughly without stirring in additional air bubbles. Urethane materials are moisture sensitive, so measuring should be done just before use, and raw materials and additives must be kept dry. If excessive moisture is present in the materials, the cast parts will "foam" and contain excessive amounts of trapped gas bubbles. The weight percent of added fibers must be kept low, to allow for complete wetting of the fibers, and to allow the filled resin to flow into the mold cavity.

This exercise provides many opportunities for discussion of process parameters and considerations. Students can observe the ways in which mold design and material preparation influence successful casting. Allowing the students to cast an object that they would like to take home as a "souvenir" increases their desire to create defect-free castings. Using a resin with a short cure time allows the students to experiment with process variables and develop an understanding of the repeatability of the process.

Many variations on this experiment are possible. Other resin and additive choices are available and may provide good alternatives or additions to the materials used here.

Small quantities of casting resins and mold materials can be purchased from the following sources:

Alumilite Corporation, 315 East North Street, Kalamazoo, MI 49007 (800) 447-9344
www.alumilite.com

Eager Plastics, Inc., 3350 W. 48th Pl., Chicago, Il 60632-3000 (773) 927-3484
www.eagerplastics.com

References:

Alumilite's Casting Manual, Alumilite Corporation, Kalamazoo, MI

Kenneth G. and Michael K. Budinski, Engineering Materials: Properties and Selection, Seventh Edition, Prentice Hall, Upper Saddle River, New Jersey, 2002

Robert L. Mott, Applied Strength of Materials, Fourth Edition, Prentice Hall, Upper Saddle River, New Jersey, 2002

Biography:

Sarah Leach, P.E., is an assistant professor of Mechanical Engineering Technology at Purdue University Elkhart/South Bend. She has an undergraduate degree in Mechanical Engineering from Vanderbilt University, and a Master's Degree in Materials Science and Engineering from the University of Notre Dame. Her primary teaching responsibilities are in materials and applied mechanics. Sarah possesses over 15 years of industrial experience in manufacturing, research, and product development for electromechanical devices, multiplayer circuits, and sliding electric contacts. She remains an active member of the American Society of Mechanical Engineers and the American Society of Engineering Educators, and serves as the faculty advisor for the local student chapter of the American Society of Mechanical Engineers.

Patricia J. Olesak is an assistant professor of Mechanical Engineering Technology at Purdue University, where she has taught courses in quality and materials science. She received a B.S. in Metallurgical Engineering from Michigan Technological University and an M.S. in Material Science Engineering from Purdue University. She has twelve years of industrial experience in the metallurgical and quality areas. She is a CQE and belongs to ASQC, ASEE and TMS.

HEAT TREATMENT OF Cu-Be COMPONENTS FOR HIGH-FREQUENCY COAXIAL CONNECTOR ASSEMBLIES – A UNIVERSITY/INDUSTRY DESIGN PROJECT COLLABORATION

James F. Shackelford

Department of Chemical Engineering and
Materials Science
University of California
One Shields Avenue
Davis, California 95616

Telephone: 530-752-4030
e-mail jfshackelford@ucdavis.edu

and

Michael T. Powers

Agilent Technologies
1400 Fountaingrove Parkway
Santa Rosa, California 95403

e-mail mike_powers@agilent.com

James F. Shackelford

Heat Treatment of Cu-Be Components for High-Frequency Coaxial Connector Assemblies – A University/Industry Design Project Collaboration

James F. Shackelford
Department of Chemical Engineering and Materials Science, University of California, One Shields Avenue, Davis, CA 95616
and
Michael T. Powers
Agilent Technologies, 1400 Fountaingrove Parkway, Santa Rosa, CA 95403

Key Words:

Heat treatment, design, copper-beryllium alloys

Prerequisite Knowledge:

Senior standing in engineering, preferably with a major or double major in materials engineering.

Objectives:

In Spring 2002, an undergraduate process development team at the University of California, Davis investigated new processes for heat treating of copper-beryllium alloy in collaboration with a process design engineer at Agilent Technologies. Specific project objectives were:

1. *Dimension and tolerance (before and after heat treatment)*
   To ensure that the center conductor fits inside the connector and the connector achieves its intended electrical performance, the dimension and tolerance of the material before and after heat treatment must be precise. The ratios of tolerances compared to the dimensions are between one one-hundredth to one three-hundredth and the accuracy of the tolerance is within a thousandth of a millimeter.
2. *Hardness : 35 to 40 Rockwell Hardness C*
   After heat treatment, the material must be between 35 to 40 HRC to prevent the material from deforming during use.
3. *98% Overall Yield*
   A process yield of 98% or greater represents an optimum process.
4. *Decrease residence time*
   Decreased residence time of the process will increase the throughput of the product. Increasing throughput also decreases the engineering overhead and operating cost of the system.
5. *Decrease cost*
   Decreased cost will increase the revenues from the product.

Equipment and Materials:

Currently, Agilent Technologies employs two processes for the heat treatment of copper-beryllium center connector components involving the use of a) a batch furnace and b) a belt furnace.

The batch furnace is a closed heat treatment system. Control of the furnace's atmospheric pressure and temperature along with the application of an inert gas blanket precludes oxidation of the samples during heat treatment. Agilent uses pure nitrogen gas from a liquid source for oxidation prevention in their batch heat treatment process. Parts are held at a temperature of approximately 315°C for two to four hours. Cooling of the parts is enhanced by increasing the nitrogen flow rate inside the furnace muffle during temperature ramp down.

The belt furnace is an open and continuous heat treatment system. Samples placed on a belt move at constant speed through three heating chambers and one cooling chamber. The two ends of the furnace muffle are exposed to the ambient atmosphere, which leads to a greater possibility of oxidation as compared with the batch furnace process. However, high flow rate nitrogen "curtains" are used to minimize the amount of air that can enter the furnace at the ends of the muffle. Agilent's belt furnace process involves heating parts to approximately 370°C with a total furnace residence time of approximately 17 minutes. In the heating zone, forming gas (nitrogen with about 4 volume percent hydrogen) is injected into the muffle to preclude oxidation. Then, pure nitrogen is injected into the cooling zone to accelerate the temperature ramp down process.

Testing was performed on one-centimeter diameter by one-centimeter long copper-beryllium test blanks. The material for the test samples was Brush-Wellman Alloy 25 UNS C17200 received as half-hard wrought rod. The composition was 1.8 %(wt.) Beryllium, 0.2 %(wt.) Cobalt, with 0.6 %(wt.) maximum allowable Nickel and 0.2% (wt.) maximum allowable Lead. The material used for the actual center conductors at Agilent is Brush Wellman Alloy M25 UNS C17300. This alloy has an addition of 0.2 to 0.6 %(wt.) Lead to improve the machinability of the material. It is assumed that the difference in lead content between the two alloys is inconsequential with regard to the results of the Rockwell hardness testing.

Introduction:

Accreditation criteria and employer expectations increasingly require that students obtain "real world" design experience before graduation. To enhance this experience for Materials Science and Engineering majors at the University of California, Davis, the Department of Chemical Engineering and Materials Science revised its senior design course. In the Spring of 2002, a new course EMS 188 (Materials Design Project) was taught jointly by the two authors. The format of the course was one in which the students worked together as a team to define, justify and develop a cost effective process for heat treating Cu-Be components used in high frequency coaxial connector assemblies (a project of ongoing interest to Agilent Technologies). To define and develop this process, the students needed to consider the desired material properties, as dictated by the component design, and how the heat treat process affects the properties. They also needed to consider pre- and post-heat treat process sequences, such as machining operations and electroplating, to ascertain what ancillary process steps may be impacted (e.g. cleaning processes). The team was expected to address economic, regulatory and environmental/safety issues associated with the proposed process design and its development. The team was responsible for designing and conducting any experiments necessary to evaluate the process design and the resulting material properties of the components. The team reviewed both batch furnace and belt furnace methods. Experimental tests on both processes were conducted to investigate resolutions to existing issues. Tests were performed to investigate a shorter residence time at a higher temperature. Experiments were run in an attempt to increase the throughput of the process. Final team recommendations focused on the belt furnace process and modifications to increase product throughput.

There is an ongoing interest in improving the residence time, cost and periodic yield (lot to lot) for both the batch and belt furnace processes. This proved to be an excellent, "real world" problem for the student team.

For the batch furnace process, the mean residence time of six to eight hours (depending on the application) results in a relatively low throughput that in turn dictates a higher than desired operating cost. Unfortunately, increasing the set point temperature of this process is not practical because the parts can undergo overaging as a result of the slow heating and cooling rates of the batch furnace. Although the overall yield of the batch furnace is maintained at or above the 98% target for an optimal process, the periodic yield can occasionally fall below this value with a detrimental impact on cost variance for the process center.

The belt furnace process with residence time of only 17 minutes has a higher relative throughput than the batch process, but the parts are more susceptible to the risk of oxidation because the furnace is an inherently open system. This can occasionally result in a lower periodic yield for the continuous heat treat process. The student team estimated cost of the belt furnace process to be about 30% of the cost for the batch furnace process, as compared on a per boat basis.

Procedure:

The background knowledge on copper-beryllium material properties, safety precautions, the Brush-Wellman Cu-Be aging curve, and the key objectives of this project were all factored into the experimental design for determining an improved heat treatment process. Although both the batch and belt furnaces were studied, process economics and time limitations led the team to concentrate on the belt furnace process.

The Cu-Be samples were first cleaned of any organic contamination using an industrial detergent obtained from Agilent Technologies called Formula 815GD by Brulin and Company, Inc. The concentrated detergent was diluted using distilled water at a ratio of 1:20. The cleaning solution was heated to a temperature of 60-80°C, and the Cu-Be samples were then placed in it for approximately ten minutes. The samples were removed from the cleaning solution, rinsed with de-ionized water, and carefully dried with pressurized air.

The design objective of the belt furnace experiment involved attempting to achieve the appropriate material hardness by employing a higher temperature than the 370°C process used at Agilent. In this way, the team hoped to shorten the process residence time and ultimately improve overall yields. The belt furnace experiment involved four iterative trials using a Lindberg Model 814 continuous belt furnace at the Agilent Technologies plant in Santa Rosa, California. For each trial, five cylindrical Cu-Be samples were placed into a boat and then run through the belt furnace. The trials used the temperature set points and belt speeds indicated in Table 1.

The furnace cooling rate using only nitrogen gas in the cooling zone was determined from initial temperature profiles to be approximately 54°C/min. With the addition of an equivalent flow rate of hydrogen to the cooling zone gas flow (which effectively doubled the cooling zone flow rate), the cooling rate increased by over 50%.

Two Cu-Be samples were tested at least four times each using a Rockwell hardness tester in the mechanical metrology laboratory at the Agilent site. The hardness results corresponding with belt speed and temperatures are listed in Table 1.

Table 1. Belt Furnace Parameters and Resulting Sample Hardness

Trial	Belt Speed (in/min)	Temperature (°C)	Hardness (HRC)
1	10.4	450	32.7
2	11.25	450	33.6
3	11.25	430	35.2
4	11.25	410	36.2

Some of the Cu-Be samples that were heat treated in the belt furnace were cut axially with a diamond blade saw. Half of the sample was then mounted in Epomet mounting powder. The mounted samples were machine polished using 240, 300, 420, and 600-grit sandpaper. Next, the samples were further polished using 6-micron diamond polishing compound. Colloidal silica polishing suspension with a pH of 9.8 was used to fine polish the samples and complete the polishing process. The solution used for general purpose etching of these copper alloys is: 3 grams ammonium persulfate, 1-mL NH_4OH, and 100-mL water. To achieve better grain boundary contrast, the design team also used an etchant comprised of: 2 grams $K_2Cr_2O_7$, 4-mL saturated aqueous NaCl, 8-mL H_2SO_4, and 100-mL water. Optical micrographs taken by members of the student design team (Figures 1 and 2) indicate that samples with higher hardness values display finer grain sizes due to being heat treated for shorter times and at lower temperatures.

Comments:

Hardness values were used as the measure of success for the trials conducted at the Agilent plant. Hardness from 35- to 40-HRC was considered an acceptable value for the Cu-Be samples. As indicated in Table 1, the requisite hardness range was achieved for trials 3 and 4 where the effective peak temperatures were decreased relative to those in trials 1 and 2, while the belt speed was held constant at 11.25 inches per minute. Of the trials that were conducted by the student design team at Agilent, the best results were obtained for trial 4. If the conditions of trial 4 were implemented, the residence time would decrease by approximately 8%, with a concurrent increase in the overall throughput.

The student design team identified several potential risks associated with the implementation of the procedure developed in trial 4 including the increased use of hydrogen gas in the cooling process, the effect of higher temperature on the parts, and increased wear on the furnace. The safety issue associated with an increased flow rate of hydrogen in the furnace cooling atmosphere is always a concern due to the combustible nature of hydrogen. The team suggested that this concern could be mitigated by dilution of the cooling zone gas mixture with inert gases such as nitrogen or argon. The higher temperature used in trial 4 could result in over-aging of the material if the time at temperature is not closely controlled. The higher temperature and belt speed can also accelerate mechanical wear in the furnace. In light of this fact, the team suggested that inspections of the furnace should occur more frequently. It was the consensus of the design team that their trials could have benefited from more on-site testing at Agilent Technologies. They felt that further testing would be needed before final recommendations on optimum furnace set point temperatures and belt speed could be made.

During the early part of the course, the students were required to make an oral presentation in which they outlined and justified their project investigation. This included a return-on-investment (ROI) for their expected results. The project final review was also conducted as an oral presentation, but one presented to a "management review panel" comprised of an engineering manager and two engineers from Agilent Technologies, along with the authors. For both oral presentations, each of the students was required to participate. In addition, the students were required to provide a final project report to the course instructors. It should be noted that the panel members from Agilent were very impressed with the thoroughness and professionalism displayed by the student design team in the final project review and report.

Both the students and faculty assessed the design project class as part of a Total Quality Management process to improve future offerings of the course. It was agreed that equipment and safety training should be set up during the first few weeks of class to minimize the impact on the time available for actual experimentation. This would include distribution of laboratory door access codes. Lists of all equipment available at UC Davis facilities would be given to the students, including equipment outside of Central Facilities, during the first week of class. It was also recommended that on-site experiments at the facility of the industrial partner should occur in several visits. This would allow the students to plan their follow-up experiments based on the findings of the initial visit. It was suggested that the design project could be more effective if extended to two quarters instead of one. In the interim, a one-unit orientation course is planned prior to the quarter of offering to allow the student team to be more fully prepared at the beginning of the design project quarter.

Figure 1. Optical micrograph of Cu-Be alloy heated at 450° C and 10.4 in/min belt speed at Agilent Technologies, with some polarized light and color-enhancement.

Figure 2. Optical micrograph of Cu-Be alloy heated at 410° C with a belt speed of 11.25 in/min at Agilent Technologies, with some polarized light and color enhancement.

Although this experiment is clearly specific to this particular industrial collaboration, we present it as a general example of the unique opportunities that are available to students in such a partnership.

We thank Professors Jeffrey Gibeling and Joanna Groza of the Department of Chemical Engineering and Materials Science at UC Davis for their substantial involvement in the design of EMS 188 and to Professor Groza for participating in this inaugural offering. The authors gratefully acknowledge Jerry Stiles of Agilent Technologies for assisting the process design team with temperature profiling and operation of the belt furnace. We would also like to thank Paul Lomeli, Matt Condron, and Nelson Settles of Agilent Technolgies for attending the final review presentation and for their generous comments and input to the design team. Most of all, we gratefully acknowledge the participation of the students: Karen Chan, Ivy Chow, Daniela Fredrick, Ivan Hung, Dena Joseph, Nancy Maa, and Air Sritiraj (shown in Figure 3 at Agilent Technologies with M. Powers).

Figure 3. UC Davis - Agilent Technologies design team.

Bibliography:

1. Shackelford, J.F., *Introduction to Material Science for Engineers*, 5th Edition, Prentice-Hall, Upper Saddle River, NJ (2000) pp. 355 – 389.
2. Fee, Andrew R., Segabache, Robert, and Tobolski, Edward L., "Rockwell Hardness Testing," *Mechanical Testing, Metals Handbook*, 9th Edition, Volume 8, American Society for Metals Metals Park, OH (1985) pp. 74 – 78.
3. Byrnes, Ed R. Jr, Anderson, Roger C., "Heat Treating in Vacuum Furnaces and Auxiliary Equipment," *Heating Treating, Metals Handbook*, 9th Edition, Volume 4, American Society for Metals, Metals Park, OH (1981) pp. 307 – 324.
4. "Heating Treating of Copper Alloys," *Properties and Selection: Nonferrous Alloys and Pure Metals, Metals Handbook*, 9th Edition, Volume 2, American Society for Metals, Metals Park, OH (1979) pp. 719 – 739.
5. Courtney, Thomas H., *Mechanical Behavior of Materials*, 2nd Edition, McGraw-Hill,NY (2000) p 207 – 233,
6. Porter, D. A. and Easterling, K E., *Phase Transformations in Metals and Alloys*, 2nd Edition, Chapman & Hall, London (1992) pp. 110 – 180 and 291 – 349.
7. Harkness, John C. and Guha, Amitava, "Beryllium-Copper and Beryllium-Nickel Alloys," *Properties and Selections: Nonferrous Alloys and Pure Metals*, 9th Edition, Volume 2, American Society for Metals, Metals Park, OH (1979) pp. 393 – 398.
8. "Properties of Wrought Copper, C17200, C17300," *Properties and Selections: Nonferrous Alloys and Pure Metals*, 9th Edition, Volume 2, American Society for Metals, Metals Park, OH (1979) pp. 303 – 305.
9. *Guide to Beryllium Copper*, Brush Wellman Inc., Cleveland, OH (1993)
10. Powers, M.T., "Precision Glass-To-Metal Seals for High Frequency Microwave Applications," in *Joining of Advanced and Specialty Materials III*, Singh, M., Indacochea, J.E., and DuPont, J.N., Eds., ASM International, Materials Park, OH (2001) pp. 31-35.
11. Material Hardness, http://www.calce.umd.edu/general/Facilities/Hardness_ad_.html
12. Beryllium Copper, Copper & Copper Alloy Microstructures, http://www.microstructure.copper.org/be_cu.htm
13. Copper Beryllium, http://microstructure.copper.org/overview/be_cu.htm
14. Brush Wellman Engineered Materials http://www.brushwellman.com/www/homepage.html
15. White, Frank M,. *Fluid Mechanics*,WBC McGraw-Hill, Boston (1999).

MOLECULAR DYNAMICS SIMULATIONS OF THE MECHANICAL BEHAVIOR OF TWO-PHASE POLYMERS

Wieslaw K. Binienda

(1) Department of Civil Engineering
University of Akron
Akron, Ohio 44325-3905

Witold Brostow

and

J. Adam Hinze

(2)Laboratory of Advanced Polymers
and Optimized Materials
Department of Materials Science
University of North Texas
Denton, Texas 76203-5310

e-mail brostow@unt.edu
e-mail rsimoes@unt.edu

Lucas Kinzel (2 and 3)

and

Ricardo Simões(2)

(3)Department of Mechanical Engineering
University of Akron
Akron, Ohio 44325

Ricardo Simões

Molecular Dynamics Simulations of the Mechanical Behavior of Two-Phase Polymers

Wieslaw K. Binienda [1], Witold Brostow [2], J. Adam Hinze [2], Lucas Kinzel [2, 3],
and Ricardo Simões [2]
(1) Department of Civil Engineering, University of Akron, OH 44325-3905, USA;
(2) Laboratory of Advanced Polymers and Optimized Materials (LAPOM), Department of Materials Science, University of North Texas, Denton, TX 76203-5310, USA; brostow@unt.edu;
(3) Department of Mechanical Engineering, University of Akron, OH 44325, USA

Abstract

In order to predict the mechanical behavior of polymers such as polymer liquid crystals (PLCs) we create one and two-phase materials on a computer and subject them to tensile or compressive stress. These materials are composed of flexible and rigid segments, the later spatially arranged in the form of islands amidst the flexible matrix.

A method to create *realistic* computer generated materials has been developed, as well as procedures to visualize in three-dimensions the materials and the simulations performed on them.

We conduct molecular dynamics simulations on these materials to obtain information on crack formation and propagation as well as scratch resistance and recovery as a function of time.

The results so obtained can be used to develop new real materials with improved performance and better scratch resistance. The methods used for graphical visualization can be used as a tool both in teaching and in research.

Keywords: Computer simulation, OpenGL, Molecular Dynamics, Fracture Analysis

Prerequisite Knowledge: Basic understanding of the structure of polymeric materials

Objective: To learn about the structure of polymers, deformation processes, failure mechanisms and scratch resistance and recovery

Equipment: PC running Windows 98/2000/ME/XP

1. Introduction

The mechanical behavior of materials has been an important field of activity for engineers along time. Understanding and predicting the response of a part under service is not only important for the manufacturers but has implications for the consumer as well. Thus, reliability of materials is of great interest to all of us [1, 2].

Although metals have been used for centuries and many of their properties are well characterized, much still needs to be researched. Comparatively, polymers have only recently been used on a global scale and the knowledge of their properties is very limited. Most plastic parts continue to be manufactured with little use of Materials Science and Engineering (MSE) knowledge but instead relying on empirical experience.

Computer simulations have been evolving in the past years and have reached a degree that makes their use as a predictive tool viable, allowing us to study a variety of phenomena that cannot be studied experimentally. Simulating the mechanical behavior of polymers requires a high degree of complexity though, due to the large number of variables involved. Another problem presented by simulations is that the material being simulated on the computer must adequately mimic the characteristics and behavior or real materials [3]. Although our earlier simulations [4-6] have been performed using two-dimensional materials, these lacked several features that can only exist in three dimensions.

We have developed reliable simulations based on molecular dynamics (MD) using realistic computer-generated polymers. To this end our computer-generated materials are created using a polymerization process on a triangular lattice of individual monomers, resulting in an agglomerate of chains with controllable degree of orientation, molecular weight and composition. These computer-generated polymers have shown to mimic several features of real polymers [3].

A different approach to the generation of polymeric chains was developed by Theodorou and Suter [7, 8] for the structures of glassy polymers. They have proposed a method for the generation of a material on the computer based on the rotational isomeric state (RIS) theory as espoused by Flory [9]. After an initial guess of the chain conformation, the system is brought to a low energy state at or near the minimal potential energy.

Fossey and Tripathy [10] have provided an improved way of modeling spider silk elasticity. They have combined the method of Theorodou and Suter to form a polypeptide glass and Termonia's three-phase system model of the spider silk elasticity [11].

Non-atomistic methods also exist, such as the use of fracture mechanics for the study of crack formation and propagation phenomena as well as calculation of stress intensity factors in materials. Binienda and coworkers [12-14] have been using this method for the analysis of interfacial and interactive cracks.

Computer simulation and animation can also play an important role in teaching students about the structure of polymers as well as their mechanical behavior. The animations resulting from our simulations clearly show a variety of physical phenomena which may not be easily understood from static two-dimensional pictures. These animations are available from our website at *http://www.unt.edu/LAPOM/resources.html* [15].

We have also been developing a code for the simulation of scratch resistance and recovery of two-phase polymers. Early results of our simulations can be seen in Figure 1. In this figure we represent the depth of each segment on the surface of the material along time. The force is applied perpendicular to the surface and moves along the surface from one segment to the next. As the force moves to a segment, it is pushed deeper into the material and then recovers along time after the force moves to another segment. Since our group conducts scratching experiments on polymers [16, 17], comparing the result from simulations and experiments should prove valuable. The animations resulting from our simulations enable students to understand on a molecular level why and how materials recover from scratching.

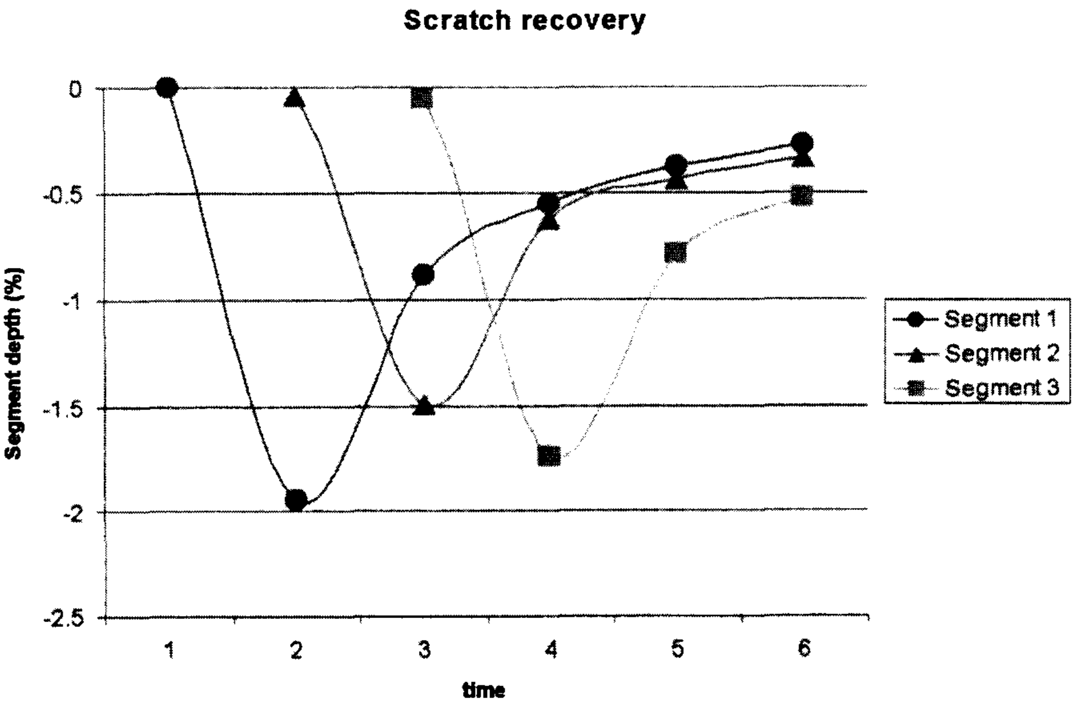

Figure 1 – Scratch resistance and recovery as a function of time

2. Procedure

The creation of our computer-generated materials is based on a polymerization process [3]. Initially we have a large number of individual monomers arranged in a triangular lattice. Each of these individual monomers can react with a neighboring monomer and form a polymer chain. Therefore, we rapidly will have many small chains formed from the monomers. Each of those chains will keep growing by addition of more monomers until there are no neighboring reactive ends of chains. At this stage, the material will contain chains with a distribution of molecular weights, ranging from very small to very large chains; see Figure 2. The distribution obviously depends on the random nature of the polymerization process. However, it can also be somewhat controlled. If the process is stopped before full polymerization was achieved, the average molecular weight will be lower. On the other hand, promoting further growth of chains after complete polymerization by creation of new reactive centers will increase the average molecular weight. Students can learn about these details of polymerization by watching the chain growth process in real-time and stopping it at several stages.

Another feature of our polymers that mimics real materials is the presence of entanglements between chains [3]. As shown by Goldman [18], entanglements can largely define the mechanical behavior of polymers. The random nature of chain growth and their coiled shape allows for this phenomenon. A higher average molecular weight of the chains indicates longer chains and as a consequence, a higher probability of entanglements between different chains or different parts of a chain. The influence of the molecular weight on mechanical properties such as the elastic modulus of the material can also be studied by simulating materials with varying average molecular weight of the chains.

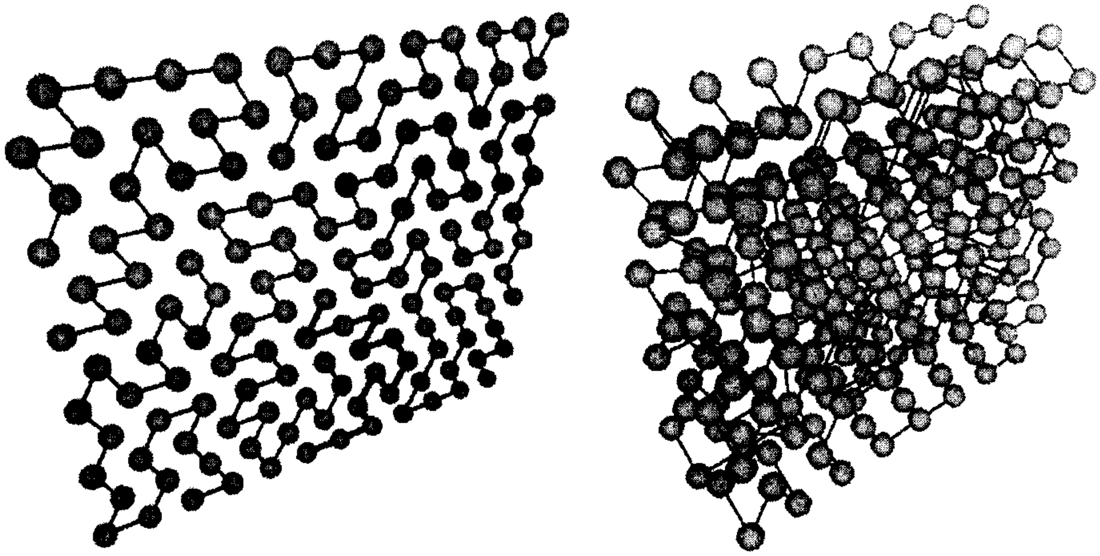

Figure 2 – Polymeric structures created in three-dimensions on the computer show several important features of real materials

Both single and two-phase materials can be created using this method. We have devoted more attention to two-phase materials since these have been less studied and usually present more complex behavior. Such is the case of polymer liquid crystals (PLCs) which consist of a rigid phase dispersed in the midst of a flexible matrix. The rigid segments tend to agglomerate in the form of quasi-spherical islands [19]. When creating our computer-generated materials we can specify the concentration of rigid phase that we want and that will determine how many islands will be distributed in the material. Due to random chain growth and the fact that islands are placed in random positions but are not allowed to touch, there will be a physical limit to how many islands we can place on the matrix. We have found that concentrations above 50 % become increasingly difficult to achieve. However, this limit will depend on the size of the islands, which can be chosen [6]. Also, due to the discrete nature of the segments we cannot achieve any concentration; the total number of rigid segments has to be a multiple of the number of segments in a single island. We cannot place only part of an island or even part of a segment in the material.

Using this procedure we can create a variety of two-phase structures, with varying concentration, island size and island distribution. Thus, the structure of two-phase polymeric systems can also be graphically represented.

Our computer simulations are based on the MD method [4]. In this method, originally developed by Berni J. Alder and collaborators [20], all particles in the system are moved simultaneously. Each of these particles is defined by a set of three cartesian coordinates and three momentum components along the cartesian axes.

When external forces are applied to particles, their effect on the system can be observed. A sufficiently high tensile force applied along one of the Cartesian axes will cause the material to elongate along that axis and contract along the other two axes. The ratio of the elongation along the force axis to the perpendicular contraction is defined as the Poisson ratio. In our simulations, a uniaxial tensile force increasing linearly with time is applied to the extreme segments of the material on that axis. This is the same procedure followed in real-life tensile testing with a sample between two grips of the machine. Again, the behavior of the material can be emulated in computer simulations, and the resulting animations used to teach about the viscoelastic properties of polymers.

An important aspect of reliability of polymers consists on the analysis of failure mechanisms, including crack initiation and crack growth patterns. Previously [6] we have reported on the use of computer simulations to predict crack initiation loci and crack growth. We found that paths of high local concentration in the material create favorable conditions for cracks to grow along. The animations that resulted from these simulations can also be used for teaching on the cracking phenomena in polymers [21]; these are available on our website [15]. We have since devoted our attention to the different deformation mechanisms that the material can exhibit before fracture occurs.

Several concurrent deformation mechanisms occur in real materials during deformation; the most common being chain slippage, chain scission and conformation changes. Chain slippage allows for deformation without rupture of chemical bonds inside the chains. This can occur at relatively low values of applied force, since it must only overcome the weak van der Waals (dispersive) forces between chains; see Figure 3. Chain scission occurs for higher values of force, since chemical bonds inside the polymeric chain have to be ruptured. Usually before chain scission occurs we observe a change in conformation of the bonds, from cis to trans. That allows for deformation without any rupture of bonds.

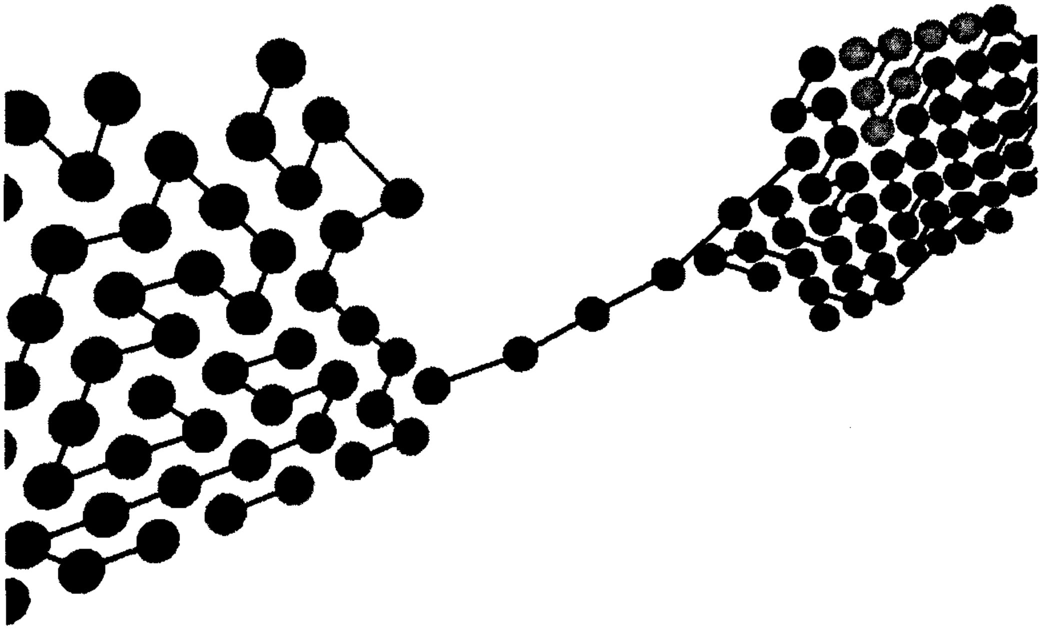

Figure 3 – Chain slippage allowing for failure of the material without any rupture of chemical bonds between segments

Entanglements also play an important role in deformation since these constitute additional linkage between chains; see Figure 4. Thus, two entangled chains will reach a deformation limit when one of them will have to break so that further elongation is possible. The influence of entanglements on the mechanical properties of materials has hardly been characterized, since one cannot measure experimentally how many chain entanglements exist in a material. However, simple logic would indicate that a higher degree of entanglements would result in higher rigidity of the material. We are now trying to confirm that statement with our simulations.

Ultimate material failure may result from several or mainly one of the possible mechanisms. Our simulations have shown in different cases all these molecular phenomena. The graphical animations created and made available on our website [15] can be used to teach them interactively.

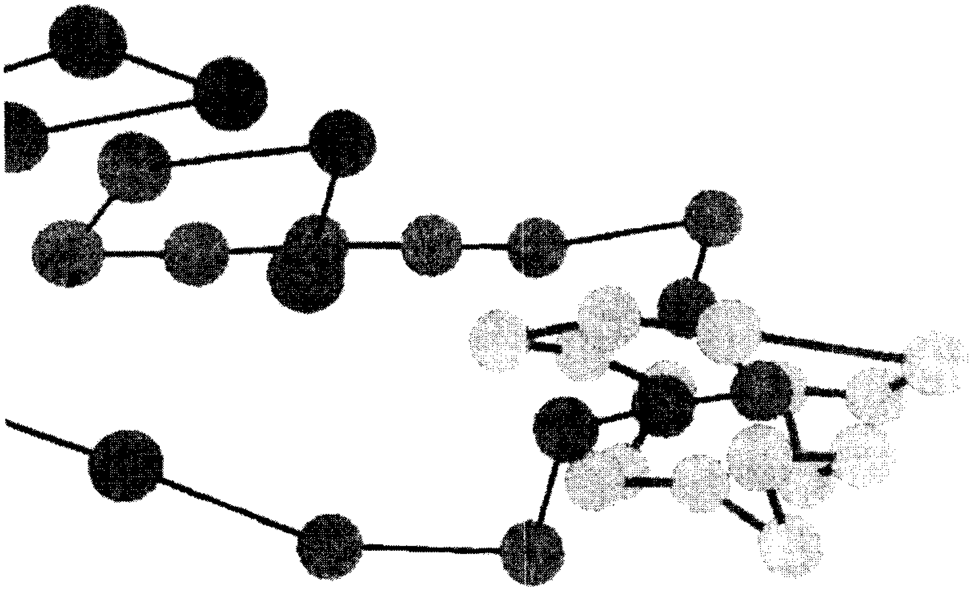

Figure 4 – The presence of entanglements between chains on computer generated materials

In order to graphically visualize the structure of our computer-generated materials as well as the results from the simulations, a program was developed using the OpenGL rendering engine [22]. This program was written in Visual C++ and runs under Microsoft Windows environment. The program takes text-based information files resulting from the creation of the material or the mechanical simulation and displays it in a three-dimensional (3D) environment. Thus, each segment in the material can be represented as a sphere, and their motion along time can be visually followed. Animations can then be created to exemplify a specific phenomenon. This type of graphical representation has only recently started to be used for educational purposes; however, its advantages are obvious. Students respond well to visual stimuli and complex phenomena such as fracture in polymers can be more easily understood with 3D graphical representation.

3. Concluding remarks

Computer simulations present several interesting features; results can be obtained fairly fast once the program exists and runs adequately. We can avoid costly materials as well as human inaccuracies during experimentation. But the most important aspect is that simulations can provide us information which is not accessible experimentally [23]. Experimentally observing physical phenomena such as deformation and fracture at a molecular level is still not possible, although progress is continuously being made in this area.

However, simulations also present several problems, including the need to validate data with experimental results, the limited capability of fully representing physical systems on a computer, and limitations in computational power which determines the maximum level of complexity of the simulated systems.

We have devoted a significant effort to ensure the materials we create on the computer mimic the important features of real materials. We found that features such as molecular weight distribution, varying chain orientation and chain entanglements are all present in our materials [3]. We have also observed realistic deformation mechanisms in our simulations.

The animations created from our simulations results can be used as a visual teaching tool. Three-dimensional graphical representation in real-time allow a student to observe and understand complex physical phenomena at a molecular level interactively. The same methods we use for the representation of polymeric materials, mainly PLCs, can be used for the representation of any material. Computer animation has been increasingly used for educational purposes and this trend will surely continue in the future. An important advantage of animations is that they can be seen in any home computer, allowing students to dedicate variable amounts of time to each subject, depending on its complexity and the student's interest on that particular topic.

Acknowledgements

Parts of this project have been supported by the Robert A. Welch Foundation, Houston, TX (Grant #B-1203), by the Fundação para a Ciência e a Tecnologia, 3° Quadro Comunitário de Apoio, Lisbon, and by the National Science Foundation (to LK).

References

1. W. Brostow and R.D. Corneliussen, editors, Failure of Plastics, Hanser, München – Wien – New York 1986, 1989, 1992
2. W. Brostow, editor, Performance of Plastics, Hanser, Munich – Cincinnati, 2000
3. W. Brostow, A.M. Cunha, R. Simoes, J. Mater. Ed., to be published (2002)
4. W. Brostow, M. Donahue III, C.E. Karashin, R. Simoes, Mater. Res. Innovat. 4, 75 (2001)
5. W. Brostow, R. Simoes, Rev. Plasticos Modernos 83, 177 (2002)
6. W. Brostow, A.M. Cunha, J. Quintanilla, R. Simoes, Macromol. Theory & Simul. 11, 308 (2002)
7. D. Theodorou, U. Suter, Macromolecules 18, 1467 (1985)

8. D. Theodorou, U. Suter, Macromolecules 82, 955 (1985)
9. P.J. Flory, Statistical Mechanics of Chain Molecules, Wiley-Interscience, New York, 1969
10. S. Fossey, S. Tripathy, Internat. J. Biol. Macromol. 24, 119 (1999)
11. Y. Termonia, P. Smith, Macromolecules 20, 835 (1987)
12. Y. Li, H. Ann, W.K. Binienda, Internat. J. Solids Structures 11, 981 (1998)
13. N.I. Shbeeb, W.K. Binienda, K.L. Kreider, J. Appl. Mech. 66, 493 (1999)
14. N. Shbeeb, W.K. Binienda, K. Kreider, Internat. J. Fracture 104, 23 (2000)
15. http://www.unt.edu/LAPOM
16. W. Brostow, P.E. Cassidy, H.E. Hagg, M. Jaklewicz, P.E. Montemartini, Polymer 42, 7971 (2001)
17. W. Brostow, B. Bujard, P.E. Cassidy, H.E. Hagg, P.E. Montemartini, Mater. Res. Innovat. 6, 7 (2002)
18. A.Y. Goldman, K. Venkatashan, Proc. Ann. Tech. Conf. Soc. Plastics Engrs. 60, 1363 (2002)
19. W. Brostow, T.S. Dziemianowicz, R. Romanski, W. Werber, Polymer Eng & Sci 28, 785 (1988)
20. B.J. Alder, T.E. Wainwright, J. Chem. Phys. 27, 1208 (1957)
21. W. Brostow, A.M. Cunha, R. Simoes, Proc. NEW:UPDATE 2001, Gaithersburg, Maryland, USA (2001)
22. M. Woo, J. Neider, T. Davis, D. Shreiner, OpenGL Programming Guide, 3rd Ed., Addison-Wesley, Reading, Massachusetts, 1999
23. S. Fossey, Ch. 4 in: Performance of Plastics, W. Brostow, editor, Hanser, Munich – Cincinnati, 2000

APPARENT EFFECTS OF GEOMETRY ON FATIGUE AND STRENGTH BEHAVIOR OF ALUMINUM AND STEEL

Aaron S. Blicblau

School of Engineering and Science
Swinburne University of Technology
P. O. Box 218
Hawthorn, Victoria
Australia 3122

Telephone +61 3 9214 8531 or 8372
e-mail ablicblau@swin.edu.au

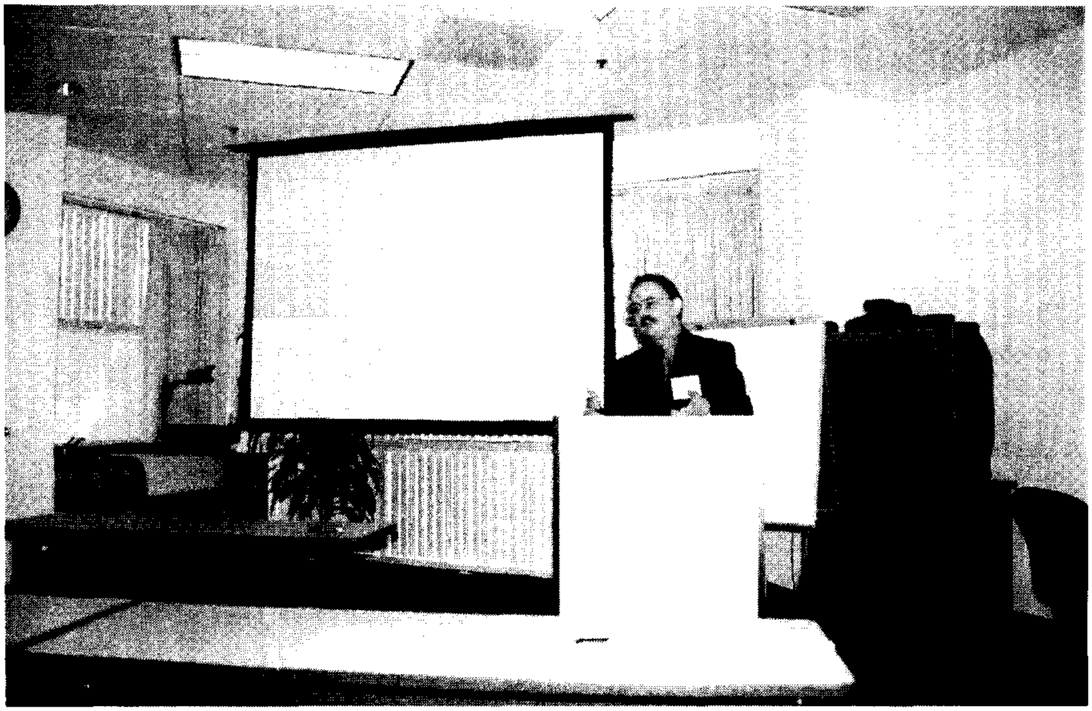

Aaron S. Blicblau

Apparent Effects of Geometry on Fatigue and Strength Behavior of Aluminum and Steel

Aaron. S. Blicblau

School of Engineering and Science, Swinburne University of Technology
P.O. Box 218 Hawthorn, Victoria Australia 3122
E-mail: ablicblau@swin.edu.au

Key Words: notch effects, stress concentration factor, fatigue, fracture, strength, fatigue life, life prediction.

Prerequisite Knowledge: basic knowledge on strength of materials, stress analysis, deflection of cantilever beams.

Objective: to understand that the strength and fatigue behaviour of metallic components is influenced by their geometry. To determine the differences in fatigue behavior of components with geometric discontinuities.

Equipment and Materials:

Equipment

1. A universal tensile testing machine, Instron.
2. A rotating-bending fatigue machine powered by an AC motor*.
3. Separate sets of sets of metal fatigue samples with a 90 mm radius, a semi-angle 36°notch, and a set of parallel-sided tensile samples.
4. A measuring device to determine the number of cycles to failure of the metal samples.

*The fatigue machine design is based on that developed by R R Moore and uses the cantilever bending rotating beam principle(Collins 1993; Instron 2002). The specimen functions as simple cantilever beam loaded at one end. When the specimen is rotated one half cycle, the stresses in the metal just below the neutral axis ate reversed from tension to compression and vice versa. At the end of one revolution the stresses are once more reversed so that during one revolution the test specimen goes through a complete cycle of flexural stresses. The machine accepts parallel circular shaped specimens which are locked into a jaw chuck within a set of collets, the spacing between clamped ends is 62mm. Stress is applied to the specimen at *free* end by applying a deflection to the end of the beam not attached to the motor. The machine operates at a speed of 1380rpm. At the nominal rate of 1380rpm the machine is capable of 82,800 cycles per hour. . A pulley is attached to the end of the specimen which is then attached by a belt to the counter. The mechanical digital counter provides an accurate indication of the number of cycles attained by each specimen. When the sample fails, the counter stops. At no stage are stress calculations required. Observation of the effect of end deflection is an indicator of the relative stress loading.

Materials:

There are 3 samples of either aluminum or steel, with one of the geometries given in Table 1. A total of 6 samples for fatigue testing. A further 3 samples of parallel-sided tensile samples of aluminum or steel are also provided [Figure 3]. Due to time restrictions, only one type of metal is tested. Results for the other type of metal are collected from other experiments and distributed to the student groups. At the end of the semester all the results for all the test samples are collected and a statistical analysis of the data is performed.

Table 1. Typical geometries of fatigue and tensile test specimens.

	Aluminum	**Steel**
(a)	36 semi-angle° notch	36 semi-angle° notch
(b)	90 mm radius	90 mm radius
(c)	Parallel sided	Parallel sided

Introduction:

By far, the majority of mechanical failures happen from fatigue. According to independent studies by Battelle in 1982, between 80-90% of all structural failures occur through a fatigue mechanism (Halfpenny). Fatigue may be defined as *failure under a repeated or otherwise varying load which never reaches a level sufficient to cause failure in a single application.* An understanding of the effects of fatigue is critical to the design of devices and structures subjected to cyclic loading. Failure can result in fracture, customer dissatisfaction, financial losses, or endangerment.

A stress concentration is a physical or metallurgical condition that increases the local stress in the part by some factor. Geometric discontinuities which are unavoidable in design, such as holes, fillets, groove and keyways, cause the stress to be locally elevated and so are called stress raisers or notches (Dowling 1999). Their presence may reduce the resistance of a metal component to fatigue failure. A good example is the shaft with a keyway. The stress in the area of the corner of the keyway varies depending on the size of the corner radius. A small radius can increase the stress dramatically. This may simply be a consequence of the locally higher stresses, causing fatigue failure cracks to initiate and propagate at such locations. Stress concentrations, indicated by the symbol Kt, can be caused by changes in metallurgy, internal defects, or changes in shape. The resultant values depends on both the type of stress, i.e., bending, torsion, etc., and the general shape of the part. Stress concentrations have a great effect on crack initiation because of their effect on increasing the local stress. The crack can start solely as the effect of the operating loads or it can be multiplied by the stress concentration factor (Hyler, Lewis and Grover 1954).

In many engineering applications a shaft is a metal bar usually cylindrical in shape and solid, but sometimes hollow, that is used to support rotating components or to transmit power or motion by rotary or axial movement. Shafts may be subjected to a variety of loads in general, tension, torsion, compression, bending or a combination of these.

When smooth specimens of metal shafts are fatigue tested at a range of stress levels a variation in fatigue life (stress at failure) is found (Dowling 1999; Callister 2001),resulting in the common S-N curves. When tested in tension the result is one value which is indicative of the material strength. Aluminum and steel display such a range of fatigue lives and tensile strengths. Moreover, due to the effect of different stress concentrators, there may also be a distinct difference in fatigue life and tensile strength of these metals. In applications involving relatively low stresses applied for large numbers of cycles design against fatigue may require only that the fatigue strength at long lives of the order 10^6 to 10^8 cycles be known. Rotating-bending fatigue tests are often used for these calculations .

Many modification factors may be incorporated into the analysis of fatigue life (Callister 2001). A quantifiable effect is that of the presence of a notch. If a notch is present, the fatigue life is reduced by a fatigue notch factor k_f which may be simply defined by the ratio of fatigue strength of the metal component with the notch, divided by the fatigue strength of the metal component without the notch (Dieter 2000). The S-N type fatigue behaviour may often not be seen for these samples with a notch, or the fatigue life may be dramatically reduced (Hyler, Lewis and Grover 1954) The mathematical applications of the effect of stress concentration factors can become quite complex and has been detailed in a number of extensive publications (Neuber 1946). .These applications and approaches are not investigated in this exercise. They are left as a major exercise in the junior year of the course for mechanical engineers.

Normally, long life fatigue testing is performed in rotating bending or cantilever bending where a stress gradient is imposed on the material (Collins 1993) (Instron 2002). However, the effect of notches and geometrical changes on the tensile and fatigue strength and life of metal components can be illustrated by simple experiments which do not require an understanding of the mathematics of notches. The experiments are phenomenological in that the results illustrate the outcome of rotating bending fatigue conditions on metal samples with varying loading and geometric conditions.

In these experiments a selection of either steel or aluminum test pieces which contain either a severe stress concentrator, semi-angle semi-angle 36° notch, or a mild stress concentrator in the form of a 90 mm radius groove(essentially a specimen without a notch) are tested in both a rotating-bending fatigue mode, and tensile mode. In addition, all the sample geometries together with standard test pieces are tested in a Universal tensile testing machine, to illustrate the effect of stress concentrators on the tensile strength of metals .

The fatigue equipment used in this experiment is a typical bending-fatigue rig that is applying a constant load to one end of a rotating shaft causing a cyclic tensile and compressive stress to operate [Figures 1a,1b and 1c] . An indication of the loads applied as the deflection is increased is given in Figures 2a,2b,2c, and 2d. This data was obtained from simulation modeling using Mathematica©.

Procedure:

Tensile testing (Figure 4)

1. Measure the minimum diameter of each sample
2. Use the Instron Universal tensile testing machine on the 20 kN range. Run the chart at 2 cm per minute to obtain graphs for each test.
3. .Tensile test <u>THREE</u> samples of each of test specimens [Figure 4].
4. **Record and calculate** the tensile strength, and the fracture strength, including the mean value and standard deviation.
   in either **Table 2 or 3** as appropriate for your specimens

Fatigue Testing (Figure 1a,1b, and 1c)

1. Conduct fatigue test at four **deflections,**
   i.e.: 1, 1.25 and 1.54 and 175 mm
   each representing a different loading condition.
   The value of the loading condition is not required.
   An indication of the load applied to the specimens is shown in the graphs of Figure 1a, 1b, 1c, and 1d.
2. Fatigue test **THREE** samples at each deflection.
3. Refer to Figure 4 for a view of the experimental equipment.
4. Raise the bearing moulding until the dial gauge just stops turning Place the test piece in the chuck and tighten the chuck with the tools provided. It is absolutely vital at this point that the bearing centre and the chuck are at the same height and collinear otherwise the act of tightening the chuck will bend the specimen before the test load is applied.
5. Simultaneously turn the chuck by hand and lower the bearing housing. Continue until the bearings just begin to rotate and have just touched the test piece.
6. Set zero on the dial gauge.
7. Continue lowering the bearing housing until the pre-determined deflection is shown on the dial gauge.
8. Fasten a pulley onto the test piece. Make sure that the groove of the pulley is in the same vertical plane as the groove of the pulley on the counter.
9. Set the counter to read zero.
10. Install a rubber band as a belt between the pulleys.
11. Switch the motor on.
12. **Record** in the table provided, the number of revolutions to failure at each deflection in *either* Table 2 or 3 below. The loads at each deflection have been previously measured and are inserted in the tables. If a fatigue specimen remains unbroken after 25000 cycles, remove it and record the number of cycles as >25000

Comments:

The overall fatigue results should show a decrease in the number of cycles to failure as the applied load (deformation) is increased. Since only four deflections are used, a curve of 'best fit' is drawn through the data. The curve indeed does show that there is a decrease in fatigue life as the applied stress increases. This situation occurs for both the 90 mm radius samples and the semi-angle 36° notch samples. When the effect of severity of notch is compared, the semi-angle 36° notch samples have a marked decrease in fatigue life when compared with the 90 mm radius samples.

Shown in Figure 5 are the failed steel tensile samples. All samples appeared to fail in a ductile manner. A similar result occurred for the aluminumtensile samples. When comparing results from the tensile test, it is again seen that the semi-angle 36° notch samples fail at a higher stress than the other samples. The local stress at the root of the notch is higher than the 'far field' stress for either the 90 mm radius samples or the standard parallel-sided samples.

This phenomenological approach is implemented for the conduct of these experiments for freshman students of engineering. Over half the cohort is comprised of electrical engineering/computer science students and only require a basic knowledge of fatigue behavior. The remainder of the cohort is comprised of civil and mechanical and biotechnology engineering students – they will have the principles of fatigue behavior elaborated upon in later years. At this stage it is sufficient that they also have a basic understanding of the effect of various stress concentrators on the fatigue behavior of metals.

Typical Results:

A set of typical results for the tensile testing of specimens is given in the last row of results from Tables 2 and 3. Here it is seen that the effect of stress concentrators is to modify the load at which the various specimens fail. Before the fatigue tests take place, a class discussion ensues as to the effect of the stress concentrators and various loads on the final life of the specimens. The students then undertake the experiment.

Bibliography

Callister, W. D. (2001). Materials Science and Engineering. N.Y., Wiley.

Collins, J. A. (1993). Failure of Materials in Mechanical Design. New York, Wiley-Interscience.

Dieter, G. E. (2000). Engineering Design. New York, McGraw-Hill.

Dowling, N. E. (1999). Mechanical Behavior of Materials. Upper Saddle, Prentice-Hall.

Halfpenny, A. (2002). A Practical Discussion on Fatigue TP-0123. nCode internationalSheffield S9 3LQ, UK.

Hyler, H. J., W. S. Lewis and R. A. Grover (1954). Experimental Investigation of Notch Size Effects on Rotating-Beam Fatigue Behavior of 75S-T6 Aluminum Alloy. Washington, National Advisory Committee for Aeronautics.

Instron, S. S. (2002). http://www.satec.com/Literature/RRMoore.PDF.

Neuber, H. (1946). Theory of Notch Stresses: Principles for Exact Stress Calculation. Ann Arbor, J.W.Edwards.

Table 2: 90 mm radius test pieces of Aluminum and Steel(average of 30 tests) *

DEFLECTION	**STEEL**		**ALUMINUM**	
	Force (newton)	**Number of Cycles**	**Force (newton)**	**Number of Cycles**
1.00 mm	32	>25000	12	5679
1.25 mm	38	10454	14	1100
1.50 mm	48	3763	16	616
1.75 mm	55	770	18	25
Stress at offset yield of 90 mm radius test pieces	659 MPa		212 MPa	
Stress at offset yield of parallel sided tensile samples	523 MPa		332 MPa	

Table 3: semi-angle 36° notch test pieces of Aluminum and Steel(average of 30 tests) *.

	STEEL		**ALUMINUM**	
DEFLECTION	**Force (newton)**	**Number of Cycles**	**Force (newton)**	**Number of Cycles**
1.00 mm	248	1002	95	52
1.25 mm	310	535	130	18
1.50 mm	420	238	145	6
1.75 mm	490	46	170	2
Stress at offset yield of semi-angle 36° notch samples	1178MPa		422 MPa	
Stress at offset yield of parallel sided tensile samples	523 MPa		332 MPa	

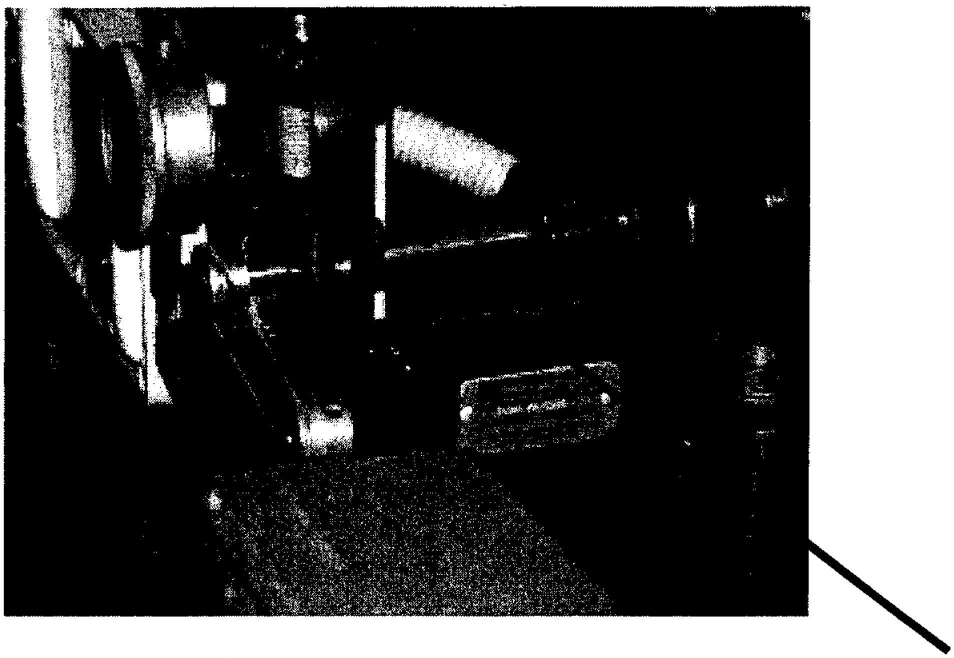

Fig. 1a. Typical arrangement of the bend rotating fatigue rig with a fatigue sample eg with semi-angle 36° notch test pieces of Steel

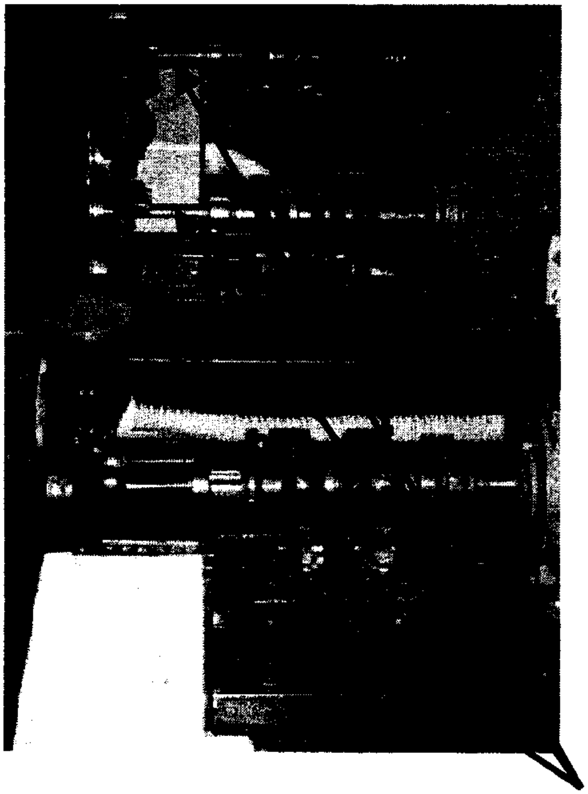

Fig. 1b. Typical arrangement of the bend rotating fatigue rig with three fatigue samples running at once.

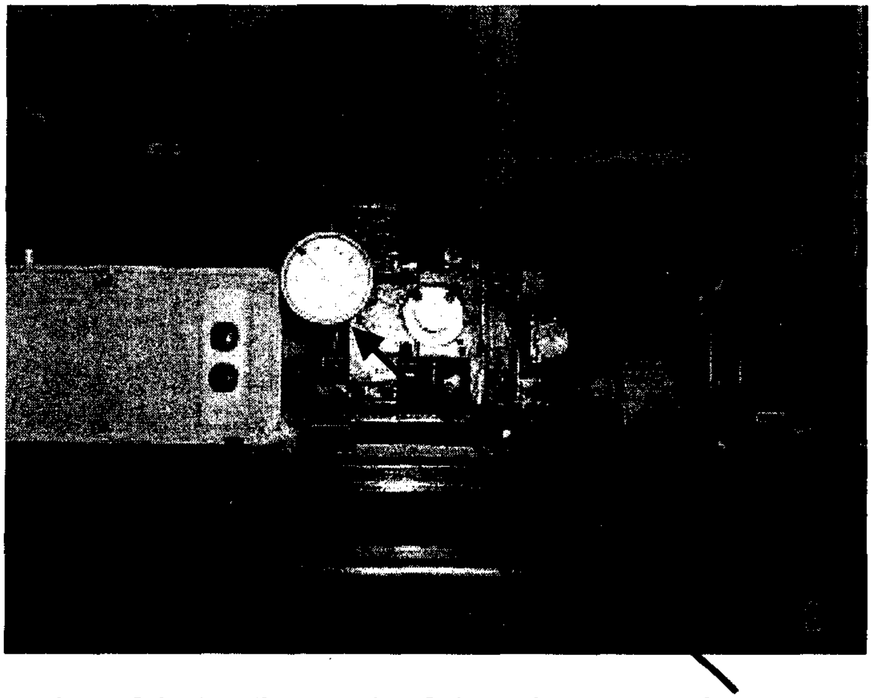

Fig. 1c. Front view of the bending-rotating fatigue showing the dial indicator employed to establish a deflection of the cantilever beam.

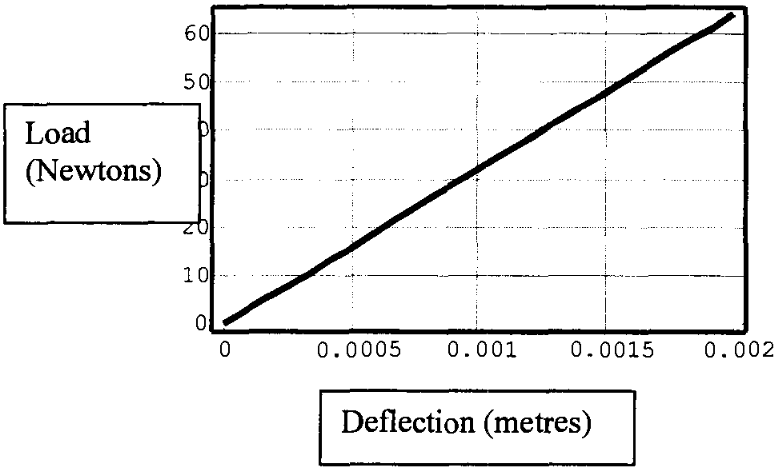

Figure 2a. Deflection Force (Newton) Vs Deflection (metre) for Steel: 90 mm radius test pieces. (data obtained from simulation modeling using Mathematica©

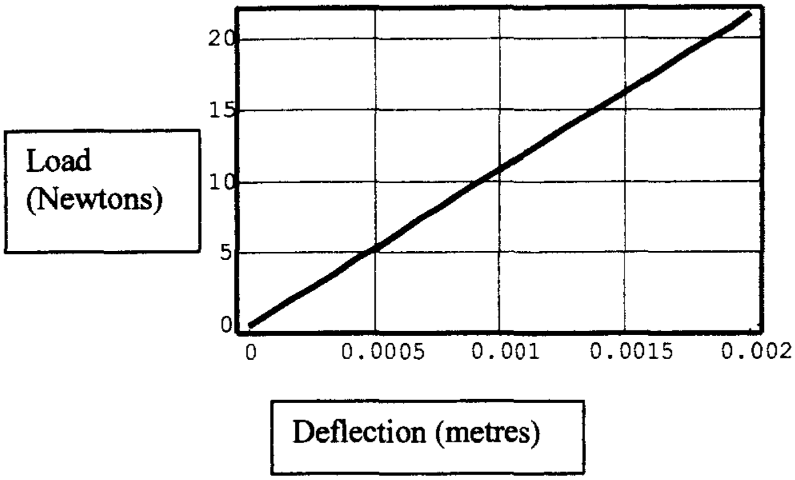

Figure 2b. Deflection Force (Newton) Vs Deflection (metre) for Aluminum: 90 mm radius test pieces. (data obtained from simulation modeling using Mathematica©

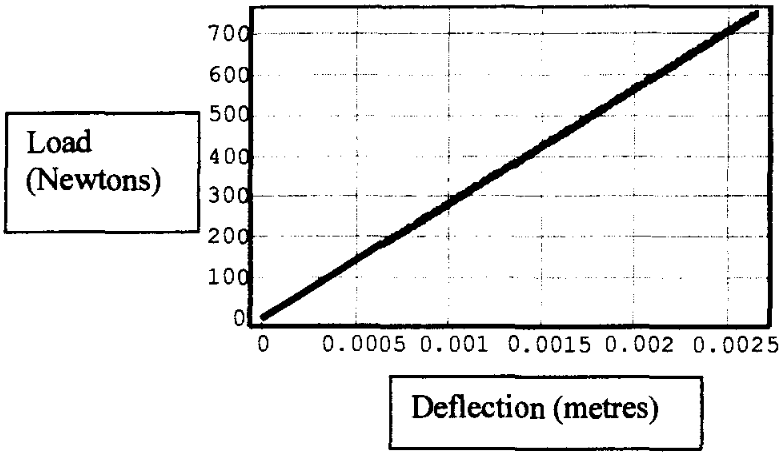

Figure 2c. Deflection Force (Newton) Vs Deflection (metre) for Steel: semi-angle 36° notch test pieces. (data obtained from simulation modeling using Mathematica©)

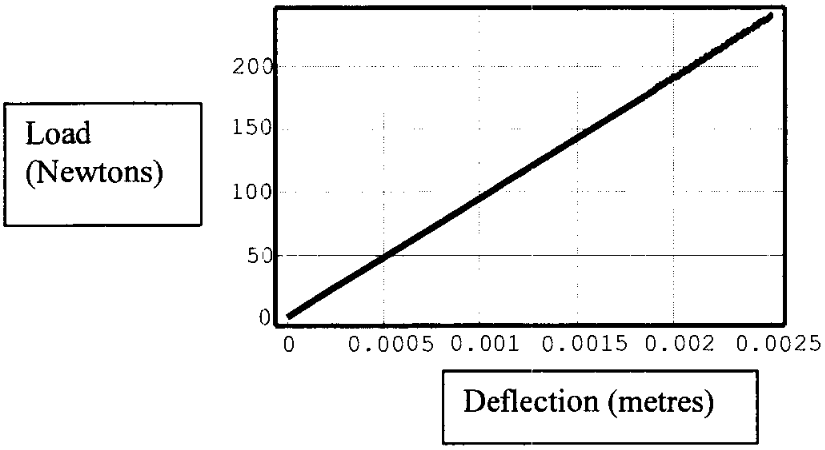

Figure 2d. Deflection Force (Newton) Vs Deflection (metre) for Aluminum: semi-angle 36° notch test pieces. (data obtained from simulation modeling using Mathematica©

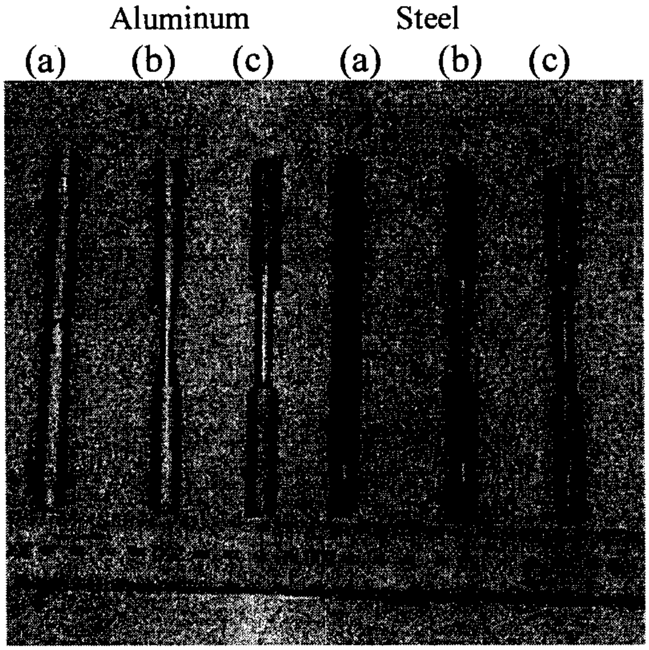

Fig. 3. Layout of the fatigue and tensile sample (refer to Table 1)

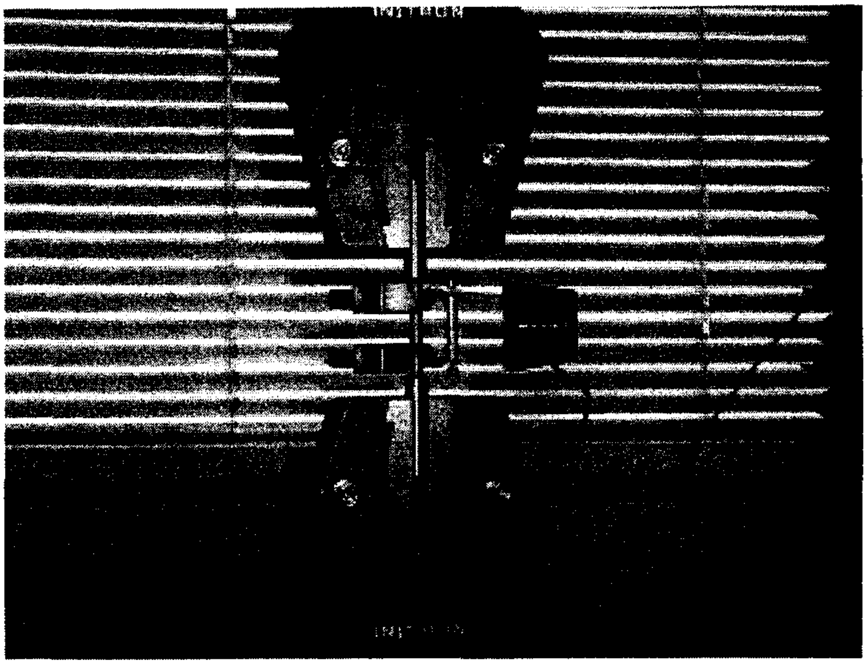

Figure 4. Sample in the tensile testing machine [Instron]

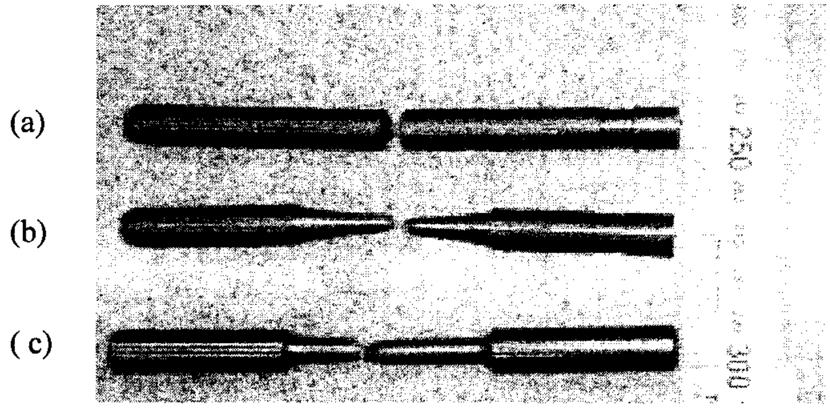

Figure 5. Example of failed specimens; (a) semi-angle 36° notch, (b) 90 mm radius, and (c) parallel sided tensile sample.

FATIGUE TESTING METHODS

Yulian Kin

and

Bernard Parsons

Purdue University Calumet
Hammond, Indiana 46323

Telephone: 219-989-2684
e-mail kin@hwi.calumet.purdue.edu
parsons@calumet.purdue.edu

Yulian Kin

Fatigue Testing Methods

Yulian Kin
Bernard W. Parsons
Purdue University Calumet
Hammond, Indiana

Key Words: High-cycle fatigue, statistical treatment of fatigue test results, probability paper, material fatigue properties, fatigue diagrams, family of fatigue curves.

Prerequisite Knowledge: Basic knowledge of fatigue strength of materials, fatigue failures, the relation between fatigue strength and number of test cycles, and statistical treatment of test results.

Objectives: Determine fatigue properties of steel or polycarbonate specimens using:

1. Conventional method,
2. Constant stress level,
3. Response or survival method, and
4. Step test procedure.

Compare test results collected from the different testing methods and make appropriate conclusions.

Equipment:

1. Three cantilever type rotating-bending fatigue machines.
2. 100 standard round fatigue specimens of 1018 cold rolled steel or an equivalent material.
3. A computer with MS Excel© or equivalent software for construction of S-N plots.
4. Probability graph paper (normal and log-normal) for performing statistical treatment of test results.

Introduction: The fatigue testing methods were incorporated into laboratory sections of the Mechanical Engineering Design Course at Purdue University Calumet. These experiments and fracture mechanics tests (observation and analysis of crack growth, determination of stress intensity factor and J-integral, accelerated fatigue testing) discussed in [1,2,3] give our students a comprehensive knowledge of various fatigue testing techniques and the interpretation of their results. Through experimentation, students receive the necessary background in fatigue testing and statistical treatment of test results, to permit evaluation of accumulated damage and prevention of fatigue failures.

The students work in teams of three or four and conduct tests at assigned load levels. These teams then share their test results, and in order to perform a reliable statistical treatment, results from previous years are included in the analysis. All accumulated data and procedures are available on our web page as well as on Blackboard,© our e-Education provider.

Formal reports are required. The reports include an introduction, all collected data from these tests as well as other sources, which are used in statistical analyses, presentation of data in the form of plots (constructed on probability graph paper), discussion of results, and conclusions. Use of appropriate software for the generation of plots (instead of the attached probability paper) is encouraged.

Procedures: We used recommendations given in reference 4 sections 10.2 through 10.5 to develop procedures for the four different tests described below. The Conventional Test results in a load vs. life (S-N) graph. A best-fit straight line is drawn through the data points. This is the inclined region (where most samples fail at a lifetime less than 10^6 cycles and can be considered a 50% probability of failure due to fatigue. The shortcoming of this method is the large scatter that can result from the probability nature of fatigue, using only a few specimens at each loading level (and the resulting uncertainty) and the number of load levels tested to accurately reach the bottom of the inclined region. The Constant Stress Test assumes the fatigue limit is roughly known. Four equally spaced load levels starting at 80% of the tested material's yield strength to this fatigue limit are tested. S-N results replotted on log-normal probability paper (of life time vs. probability of survival by loading levels) permit determination of the 95 – 50 – 5% probability of survival along the inclined portion of the S-N curve. Up to this point, the fatigue endurance limit has not been found in a statistically sound manner. The Response or Survival Method is designed to overcome this inadequacy by testing several specimens each at closely spaced stress levels near this limit. A statistical treatment is performed to determine the fatigue limit. A major drawback of this method is the many samples that are required to perform the test. The Step Method requires a prior estimate of the approximate fatigue limit. This test is a quicker method that can be used to verify material properties, e.g. during a manufacturing process.

1. Conventional Test

Twelve to fifteen specimens are tested on six load levels, two or three on each level. (We typically run three groups of three per lab on separate fatigue machines.) The test begins at the load level corresponding to 90% of the yield strength of the selected material. The results are recorded on a standard S-N (Stress Amplitude versus number of cycles) plot, semi-log paper, as shown on Figure 1. A best fit or mean curve is constructed through the results. The horizontal portion or endurance limit of the curve, the stress level below which failure by fatigue is not expected, is difficult to construct from this test. Two or three specimens can be tested below this estimated fatigue limit for validation. Additionally, a "conservative" fatigue curve can be constructed by "eyeing a curve, inclined and horizontal portions, that is just below all test data points and the corresponding endurance limit is recorded.

2. Constant Stress Level Test

Sixty or more specimens are tested on four different, equally spaced, amplitude stress levels. At least fifteen specimens are tested on each selected level, beginning with a maximum stress level that is 80% of the yield strength of the selected material. For each test, the following procedure is carried out:

a. Record the failure life.

b. Plot the data on a standard S-N plot (use semi-log paper). The test results are used to plot probability of survival versus cycles to failure for the different stress levels, and then to draw incline portions of 5%, 50%, and 95% probability fatigue curves on S-N plots (stress amplitude versus number of cycles).

c. Plot stress amplitude versus cycles to failure on log-normal probability paper for each stress level and verify the actual statistical distribution (Figure 2.).

d. From this plot, determine the mean and variance for log-life at the particular stress level.

e. From this plot, determine mean and variance for log-life at the particular stress level.

f. Determine the fatigue endurance limit for the 50% probability of survival.

3. Response or Survival Test (Probit Method).

The following procedure is utilized for this test method.

a. Determine or estimate a fatigue limit for the specimen material. For ferrous materials with an ultimate strength, σ_u, less than approximately 180,000 psi, the fatigue or endurance limit can be estimated as $\sigma_u/2$ at a lifetime of 10^6 cycles.

b. Based on the estimated fatigue limit, four additional stress levels are selected for testing. Two levels are greater than and two levels are less than the estimated fatigue limit. These levels should span approximately two standard deviations above and below the mean for the estimated fatigue limit. Standard deviations can be determined from the results of Constant Stress Level testing (described above). One standard deviation is the change in stress from 50% to 84.4% probability of failure. (Figure 3.).

c. Test fifteen specimens at each load level (there are a total of five levels).

d. Record the results on a standard S-N plot. The numbers of surviving specimens or run-outs (survival test) at each load level are noted on the plot.

e. Calculate the probability of survival at each load level, e.g. 5 survive of 15 at given load level equates to 33% probability of survival.

f. Plot the probability of survival versus amplitude stress level (at a specified number of cycles) on normal probability paper. A best fit or mean curve can be constructed through the results. If a least squares analysis is performed to draw an optimum line through the points then the Probit method was utilized. Record directly from the plot the mean fatigue limit and the standard deviation of the stress (Figure 3.).

g. Plot S-N-P curves (family fatigue curves) determined by using the constant stress level method in the finite life range ,inclined portion as in Figure 2., and survival method in the infinite life range , horizontal portion as in Figure 3. Plot is shown in Figure 4.

4. **Step Test Method**

Start the test at an amplitude stress level that is about 70% of the estimated mean fatigue limit, or the mean fatigue limit determined from the results of the Probit test.

a. Test one specimen at this stress level until either failure occurs or the run-out life is registered at one million cycles. If failure occurs, the stress level and failure life are recorded, and a second test is to be conducted at a lower stress level, approximately one estimated standard deviation of the estimated fatigue limit, which can be determined from the S-N-P plot of the Probit test.

b. If run-out occurs, increase the stress level approximately one standard deviation of stress. Run the test at this new stress level until failure occurs or run-out is registered at one million cycles.

c. Repeat this procedure until the specimen fails. It is recommended to have at least five progressive survival steps to obtain reliable results.

d. Test 10 additional specimens using the same procedure.

e. Plot progressive testing results (number of cycles versus stress on semi-log paper) for each specimen tested (Figure 5.).

f. Using the results from all of the progressive tests, construct a plot of stress amplitude versus probability of surviving at one million cycles. From the probability plot, the 50% probability (mean) fatigue limit and standard deviation can be recorded.

The test results are presented in Figures 1-6. As we can see from Figures 3 and 6, the difference in endurance limits determined from the survival test and the step test is negligible for a life-time of 10^6 cycles and 50% probability of failure.

References:

1. Y. Kin, H. Abramovitz, T. Hentea, Jim Higley, and J. Richards, **Laboratory Measurements of J-Integral**, Proceedings of National Educators Workshop, pp. 143-153. Update 98, Standard Experiments in Engineering and Material Science, Brookhaven National Laboratory, Upton, New York
2. Y. Kin, H. Abramovitz, T. Hentea, and Ying Xu, **Life Estimate Based on Fatigue Crack Propagation**, Proceedings of National Educators Workshop, pp.369-381. Update 97, Standard Experiments in Engineering and Material Science, Boeing Commercial Airplane Company, Seattle Washington.
3. Y. Kin and D. Holler, **Accelerated Fatigue Test,** Proceedings of National Educators Workshop, pp.187-197. Update 99, Standard Experiments in Engineering and Material Science, Daimler Chrysler Corporation, Auburn Mills, Michigan.
4. J. A. Collins, **Failure of Materials in Mechanical Design**, John Wiley & Sons, Inc., New York, 1993.

Dr. Kin worked more then 20 years in industry and his current research interests are in fatigue life estimate based on crack propagation, non-linear acoustic applications for flow detection, and failure mechanisms of aging components. He is working as a consultant and was awarded grants from industry, United States Air Force, and the National Science Foundation.

Yulian B. Kin is Professor of Mechanical Engineering at Purdue University Calumet where he teaches Machine Design, Fatigue Analysis, Reliability Engineering, and Mechanics. He joined the Faculty at Purdue Calumet in 1983. He received his Ph.D. in Mechanical Engineering from Petrochemical and Gas Industry Institute, Moscow, Russia, 1971.

Mr. Bernard W. Parsons is Technical Supervisor of the Mechanical Engineering Laboratories. He conducts laboratories in the areas of machine design, mechanical engineering experimentation, heat transmission, fluid mechanics, and kinematic analysis and design. He has an extensive background in equipment operation, testing, calibration, and repair. He received a B.S.E. from Purdue University, 1998.

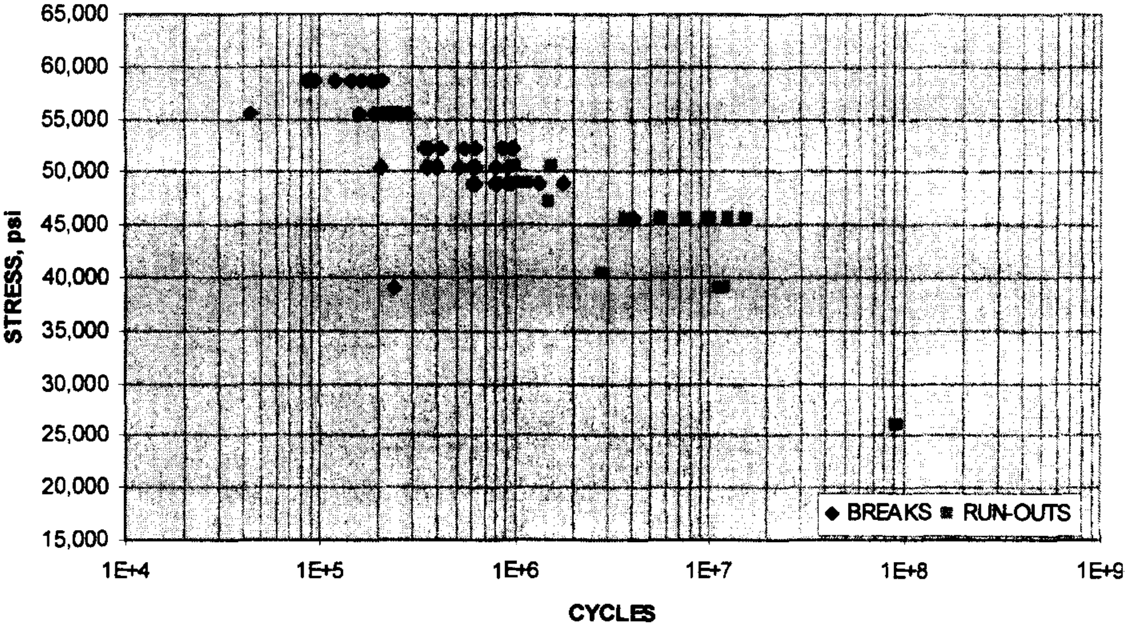

Figure 1. Convential test. S-N Data

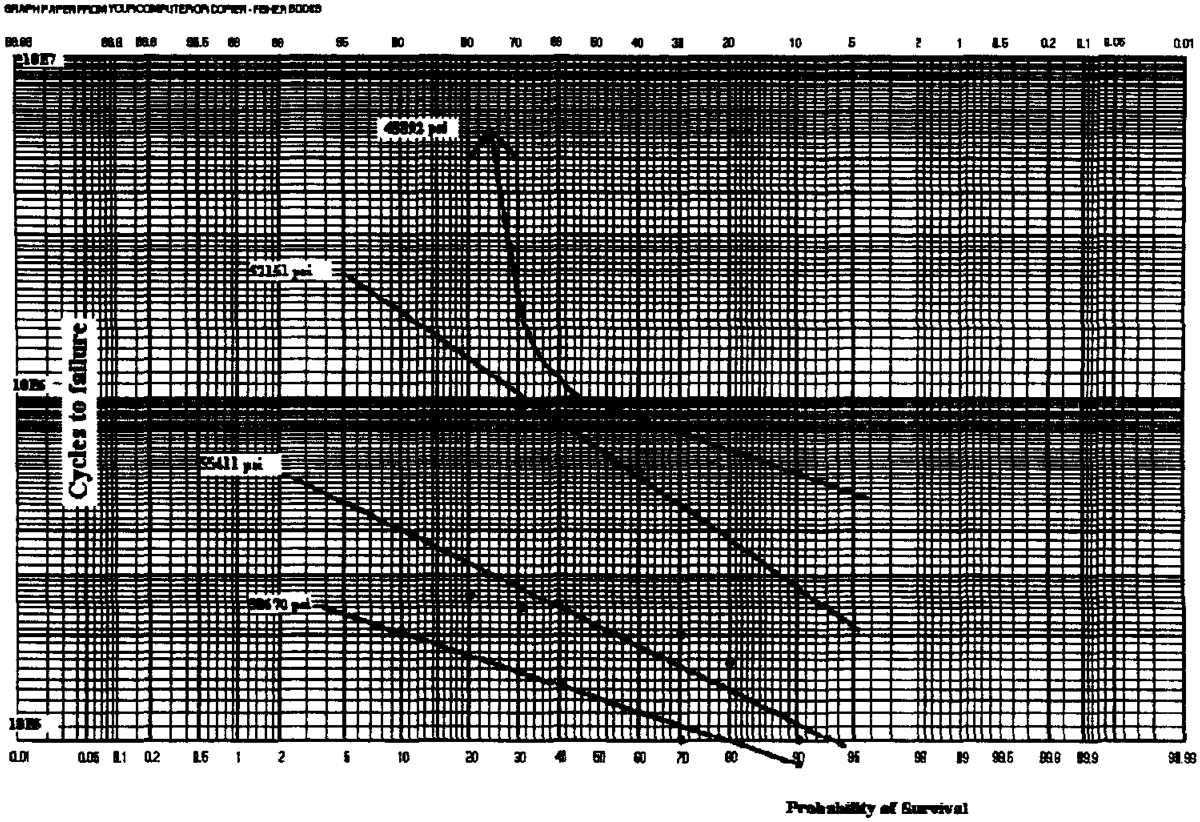

Figure 2. Fatigue data from constant stress level test

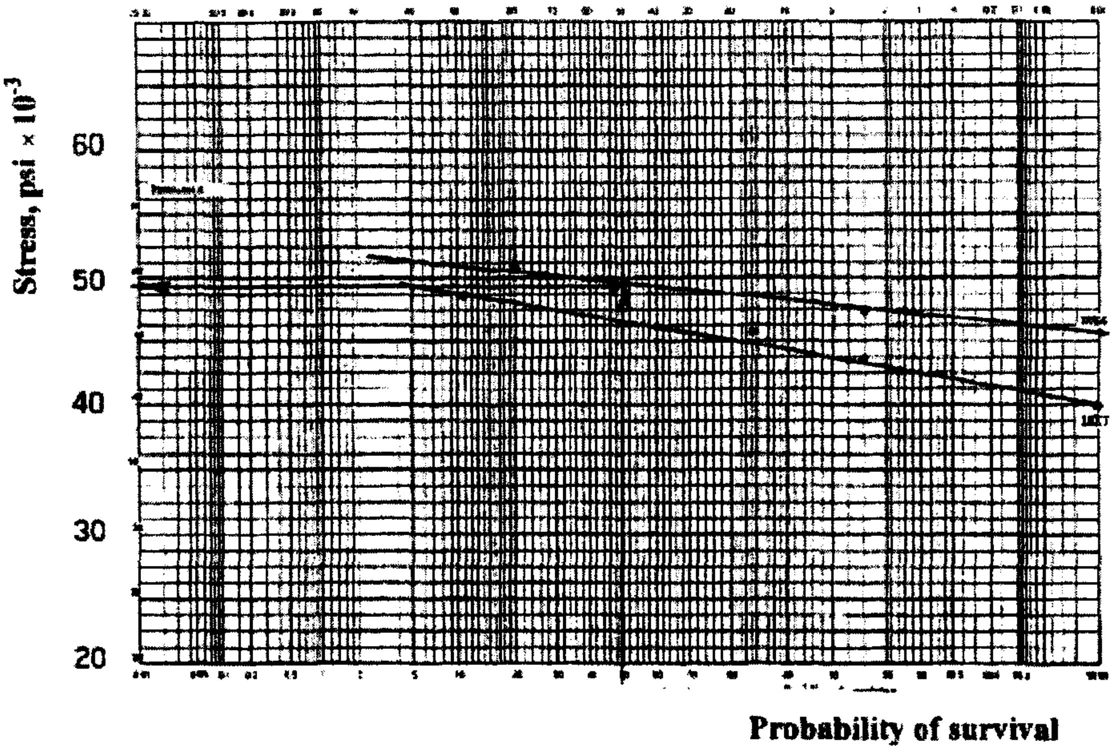

Figure 3. Survival test data for 10^6 and 10^7 cycles

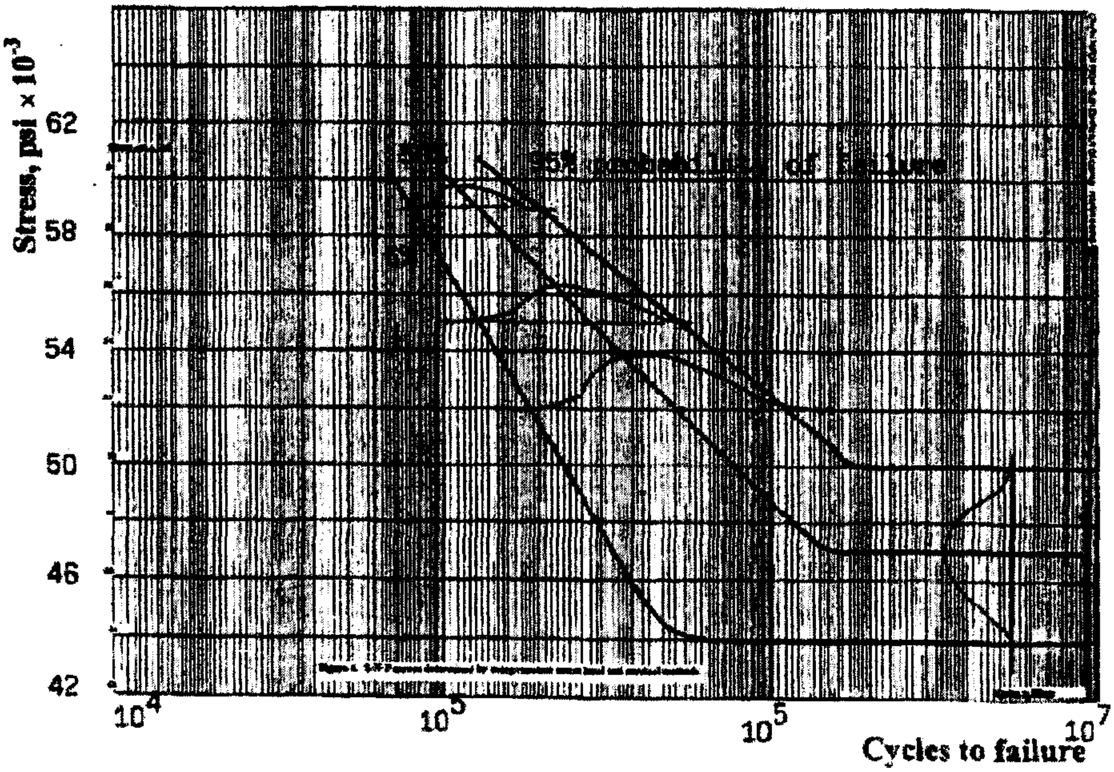

Figure 4. S-N-P curves determined from constant stress level and survival tests

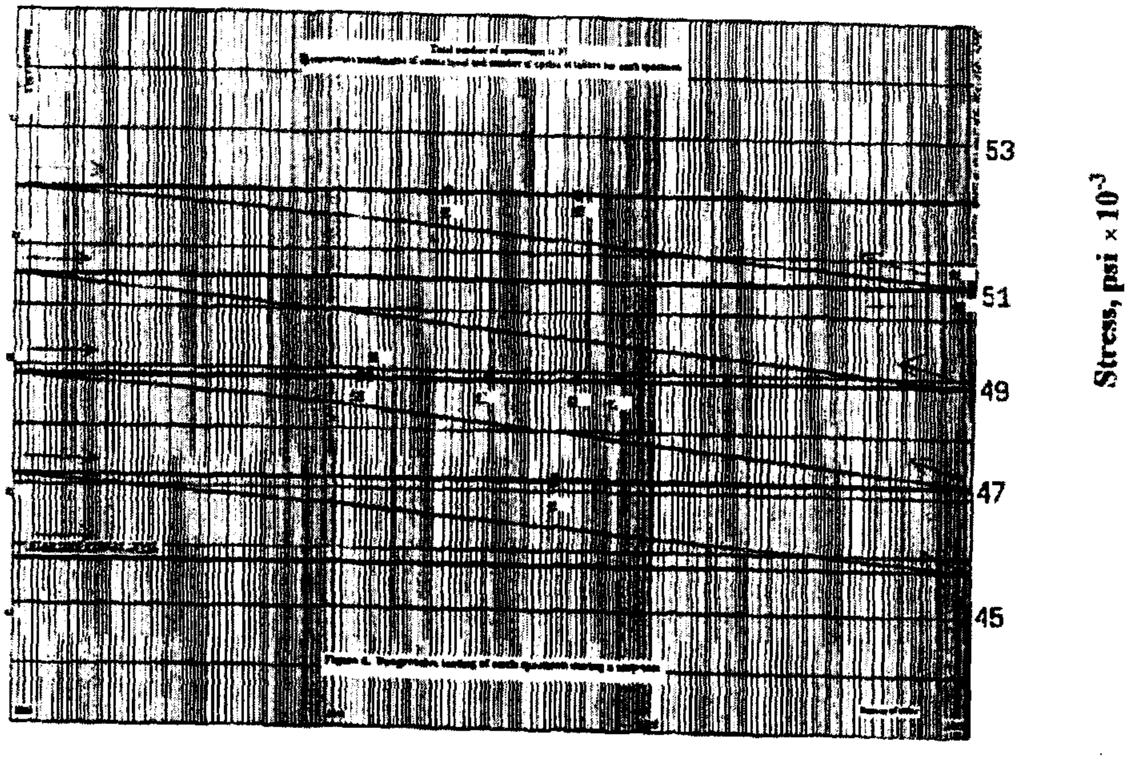

Figure 5. Progressive testing of each specimen during a step test

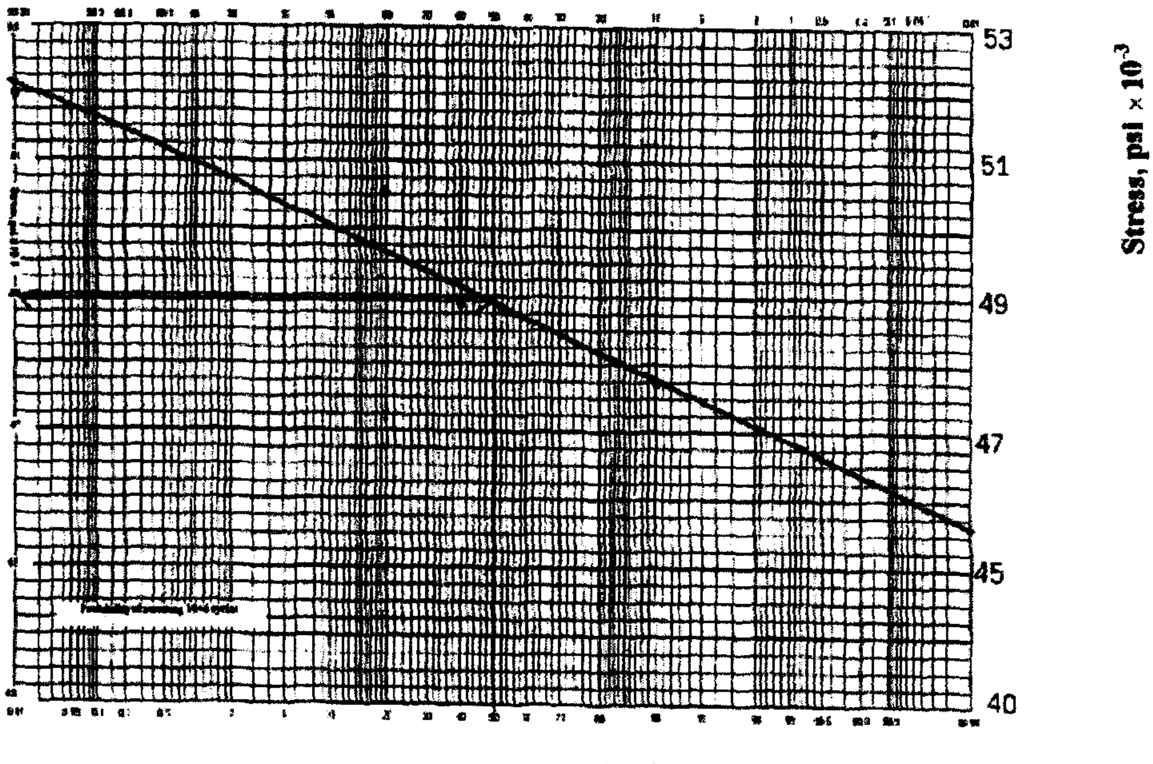

Figure 6. Step test results

THE CAM SHELL: AN INNOVATIVE DESIGN WITH MATERIALS AND MANUFACTURING

W. Richard Chung

Department of Chemical & Materials Engineering
San Jose State University
San Jose, California 95192-0082

Telephone 408-924-3927
e-mail wrchung@email.sjsu.edu

and

Frank M. Larsen

and

Rob Kornienko

NASA-Ames Research Center
Moffett Field
California 94035-1000

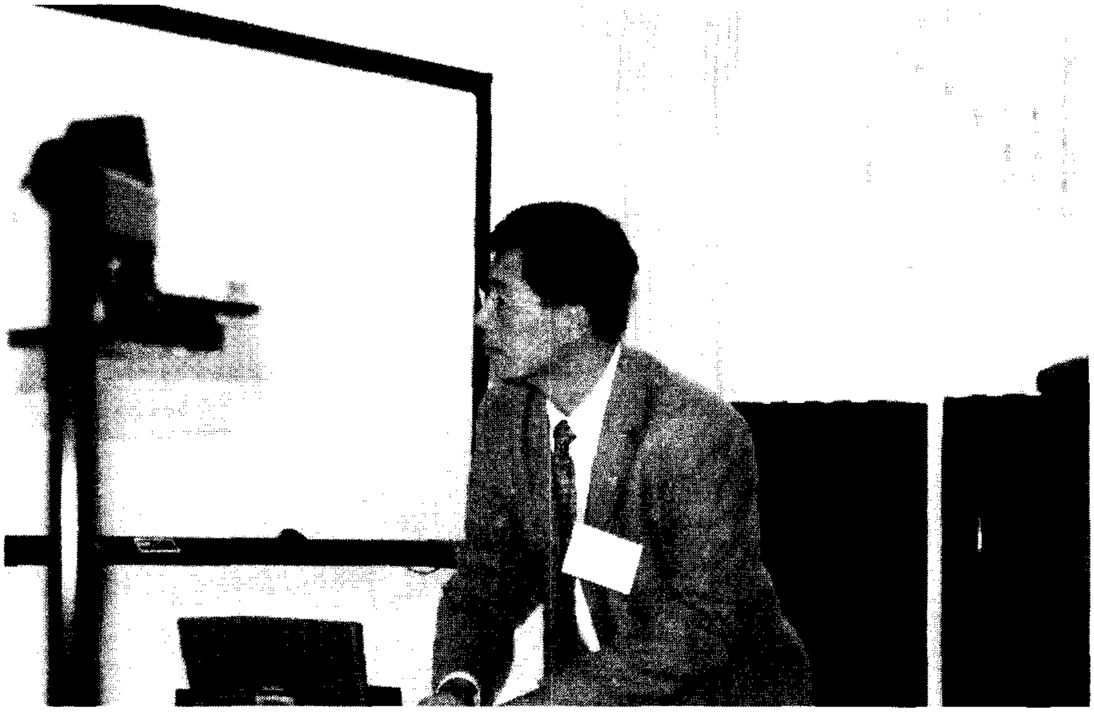

W. Richard Chung

The Cam Shell: An Innovative Design with Materials and Manufacturing

W. Richard Chung, Department of Chemical and Materials Engineering, San Jose State University, San Jose, CA 95192-0082

and

Frank M. Larsen and Rob Kornienko, NASA-Ames Research Center, Moffett, Field, CA 94035-1000

Abstract

Most of the personal audio and video recording devices currently sold on the open market all require hands to operate. Little consideration was given to designing a hands-free unit. Such a system once designed and made available to the public could greatly benefit mobile police officers, bicyclists, adventurers, street and dirt motorcyclists, horseback riders and many others. With a few design changes water sports and skiing activities could be another large area of application. The cam shell is an innovative design in which an audio and video recording device (such as palm camcorder) is housed in a body-mounted protection system. This system is based on the concept of viewing and recording at the same time. A view cam is attached to a helmet wired to a recording unit encased in a transparent body-mounted protection system. The helmet can also be controlled by remote. The operator will have full control in recording everything. However, the recording unit will be operated completely hands-free. This project will address the design considerations and their effects on material selection and manufacturing. It will enhance the understanding of the structure of materials, and how the structure affects the behavior of the material, and the role that processing play in linking the relationship between structure and properties. A systematic approach to design feasibility study, cost analysis and problem solving will also be discussed.

Key Words: Polymers, Acrylics, Polycarbonates, Thermoforming Process, Computer-Aided Design (CAD), Design for Manufacturability (DFM), Design for Assembly (DFA), Rapid Prototyping (RP), Concurrent Engineering, Quality Function Deployment (QFD), Ashby Diagrams

Objective: To provide an environment with a realistic understanding of the design process.
To apply the structure-property-processing relationship to a real product design.

Equipment and Materials:

1. Acrylic sheet (3.175 mm thick, 609.6 mm x 609.6 mm)
2. Polycarbonate (4.76 mm thick, 609.6 mm x 609.6 mm)
3. Thermoforming machine
4. Strip heater
5. Double stick adhesive tape
6. Scissors
7. Exactor knife
8. Super glue
9. Velcro (50.8 mm wide and 914.4 mm long, 2 pieces)
10. Allen head screws (31.75 mm long, 6.35 mm in diameter, 2 pieces)
11. Acrylic plastic hinges (2 pieces)
12. Poyurethane foam (12.7 mm thick)

Introduction

In our technological society, engineering design plays an important role in creating innovative products and services, improving existing commercial machine performance, promoting new product development, encouraging business entrepreneurship, and enhancing the quality of life for our society. To teach the design process and to enhance the learning opportunity and experience in product/process design for our students, a product design laboratory project in conjunction with thermoforming process was developed. Students were guided through the entire design process beginning with the design concept, material selection to a fabricated product using a correct manufacturing process. The structure-property-processing relationship was then evaluated upon the completion of the project.

Product design process can be broadly categorized into three major areas: computer-aided engineering design (CAD), design for manufacturability and assembly (DFM/A), and rapid prototyping fabrication (RP). Each area requires computer hardware, unique software, and certain equipment to perform specific functions for developing a new product. Before the product design process initiates, the problem statement must be identified first. Then, a product development plan will be generated. Engineering specifications and initial concepts for the design will be developed, concept feasibility evaluation will be performed, and final concept selection will be refined. Based on the selected design concept, a product design development and evaluation will then be performed. These may include material and geometric configuration selections for the design (Ashby diagrams), relevant engineering analyses, and design optimization tasks. Rapid prototype fabrication will be implemented to expedite and enhance the design process. (Due to time constraints, this step was not performed in this project.) Tests will be performed on the design prototype. An iterative process will be used to finalize the product design. Cost evaluation and manufacturing specifications will also be considered. Final as-built documentation will be made for the product.

Product Design

- **Establish a Design Procedure with Key Elements**

At this stage, a basic design concept and product cycle for a product design process will have to be developed in class. This includes needs assessments, product specifications (employing concurrent engineering and quality function deployment practices), functional requirements, concept evaluations and decision-making. Tasks associated with the product and process design will be identified and grouped so that they can be planned, scheduled, and processed easily. Students will be asked to use computer software such as Auto CAD and Microsoft Project 2000 to aid in their design. Besides the Thomas Register database and Internet access, supplementary design handbooks (Dieter's engineering design book and ASM handbooks) will be provided for this lab project.

- **Learn how to do Process Planning**

Lab instruction materials related to process planning will be provided. In this lab activity, students will learn how to use computer software to help manage multiple tasks. First, students will learn the functions and requirements for Microsoft Project 2000. Then they will design and list all possible manufacturing processes related to the product they have just created. All variables affecting the production process will be implemented in the planning. They include cost factors, human resources, time management, priority scheduling, equipment allocation, etc. Finally, a network logic diagram will have to be constructed using the same software.

Students will have to apply the concepts of the critical-path method (CPM) and program evaluation review technique (PERT) to determine the most feasible and efficient way to conduct manufacturing processes. Priorities will be assigned according to the critical paths.

- **Develop a Laboratory Procedure for Manufacturing and Assembly**

In order to effectively design a product for manufacturability, one must clearly understand the principles and methodologies involved in manufacturing. Among conventional manufacturing practice in a manufacturing plant, process engineering is the utmost important. In the process engineering area, designers have to realize the advantages and disadvantages of each process chosen for a designed product. In general, there are eight major categories associated with processes: (1) casting processes, (2) deformation processes, (3) machining processes, (4) polymer processing, (5) powder processing, (6) joining processing, (7) surface treatment processes, and (8) assembly processes.

The factors that influence the selection of a process for a design involve the manufacturing cost and the cost associated with product life cycle, the quantity of parts to be made, the complexity of the product and material, quality of the part, and availability of material, manufacturing lead-time, and delivery schedule. The designers have to go through a systematic approximation for each factor. The total weighted number will help the designer find the most feasible way for a process. Using this approach, an algorithm embedded with the thoughts for manufacturability and assembly will be established in the software. Once a design is created, a designer can enter the dimensions of the product and any necessary requirements for a final product (such as packaging, vibration, and surface conditions). A systematic approach can be executed, and an optimal condition for manufacturing and assembly can be established.

At this stage, a polymer thermoforming process will be introduced to the class. The viscoelastic behavior of a polymer along with the material orientation will be analyzed in order to expedite the experiment. Temperature and time factors will be studied against each selected plastic material. Some statistical functions and defect controls and reporting can also be implemented in the various lab activities. Specific manufacturing and assembly processes will be recommended for optimal design consideration. In addition, students will also be able to analyze the operational planning procedure for production of the product design to determine the most feasible and efficient way to conduct manufacturing processes. Priorities will be assigned according to the critical paths.

Material Selection

Professor Ashby of University of Cambridge, UK, has generated many useful materials selection charts that can compare a large number of materials at the concept design phase. A common practice in a design phase is to minimize weight or cost. Lines of constant slope are drawn on the diagrams. Depending on the product requirements (geometry and loading conditions) lines of different slope will apply. In this project the product requirements such as lightweight, impact strength, damping resistance, optical clarity, and cost factors are determined to be the key factors for material selection. Polycarbonate is chosen due to its high impact resistance and acceptable cost. Two sample charts are selected and are shown below. Figure 2 is a chart comparing specific modulus to specific strength. Figure 3is a chart comparing strength with cost per volume.

Experimental Procedure

A pattern, as shown in Figure 1, was drawn based on the original design. A polycarbonate sheet (4.76 mm thick) was cut to size (355.6 mm x 558.8 mm). Edges were filed to provide a smooth surface. Four corners of the plastic sheet were drilled and milled to secure the attachment of the Velcro straps. A strip heater was utilized to form a bend in order to fit the body curvature.

A thermoformer was turned on, and the temperature was set to 200°C. The polycarbonate sheet was placed under a radiant heater. The heater was quickly removed once the plastic sheet was in a pliable state. The plastic sheet was then sandwiched between a pre-designed square shaped yoke and a platen. Air pressure was turned on slowly until movements of the plastic sheet began. Only one atmospheric pressure (14.7 psi) was needed to blow form a spherical (dome) shape of the polycarbonate sheet. Too much pressure would force the plastic into a bubble shape that, if too rapid, the plastic would burst. The air pressure was held until the polycarbonate sheet was cooled. A free air blown part was then created. A back sheet (acrylic) combined with the molded part was joined together using double-stick tape. Velcro straps were sewn to the four attachment points. The plastic hinges were bonded to the surface of the back plate using the super glue. The fabrication of the cam shell was then completed. The final integration part of this cam shell design was to add a camera to a recorder (kept in the cam shell). The cost analysis, shown in Table 1, was performed based on the total cost for one part (prototype) and for 300 parts (a mass-produced environment). Cost reduction was listed for future manufacturing consideration.

Table 1. Cost Analysis

Item	Prototype Cost (1 unit)	Production Cost (300 units)
Blow Mold	$300.00	$300.00
Foam	$8.00 ea.	$4.35/ea. x 300 = $1,305.00
Hinges	$3.00 ea. x 2 = $6.00	$1.25 ea. x 300 = $375.00
Hardware	$0.28 ea.	$21.00 lot
Adhesives	$19.25	$38.50 lot
Labor	6 hrs @$75.00 = $450.00/ person	40 hrs@$75.00 = $3,000/person
Polycarbonate sheet	$24.00 ea.	N/A
Polycarbonate sheet 4 x 8 enough for 10 pcs.	N/A	$117.00/sheet x 30 = $3,510 for 300 units
Acrylic sheet	$8.00 ea.	N/A
Acrylic sheet 4 x 8 enough for 15 pcs.	N/A	$42.00/sheet x 20 = $840 for 300 units
Total costs	$815.53	$9389.00 for 300 units or $31.29 per unit

Conclusions

The prototype development of the cam shell from the design concept to product completion was found to be educational and enjoyable. The product was completed with some satisfaction. Students learned the concept of design process by employing a system approach. The relationships among structure, property, and processing were studied using the Ashby diagrams. By evaluating the finished prototype, students can relate their design to future product improvement. During the design process the cost analysis and the material performance were evaluated at the same time. Although physically working the product development was a beneficial experience in understanding development processes. However. the real benefit would be to automate production providing consistent quality while maximizing profits and material performance.

References

1. Dieter, G. E.: "Engineering Design – A Materials and Processing Approach," McGraw Hill, New York, 2000.
2. Ashby, M.F.: "Materials Selection in Mechanical Design," Pergamon Press, New York, 1992.
3. ASMI (editors) "ASM Handbook," Vol. 20, Materials Selection and Design," ASM International, Materials Park, Ohio, 1997.
4. Budinski, K.G. and Budenski, M. K.: "Selection of Plastic/Polymeric Materials," Engineering Materials-Properties and Selection, Prentice Hall, New Jersey, 2002, pp. 213-273.

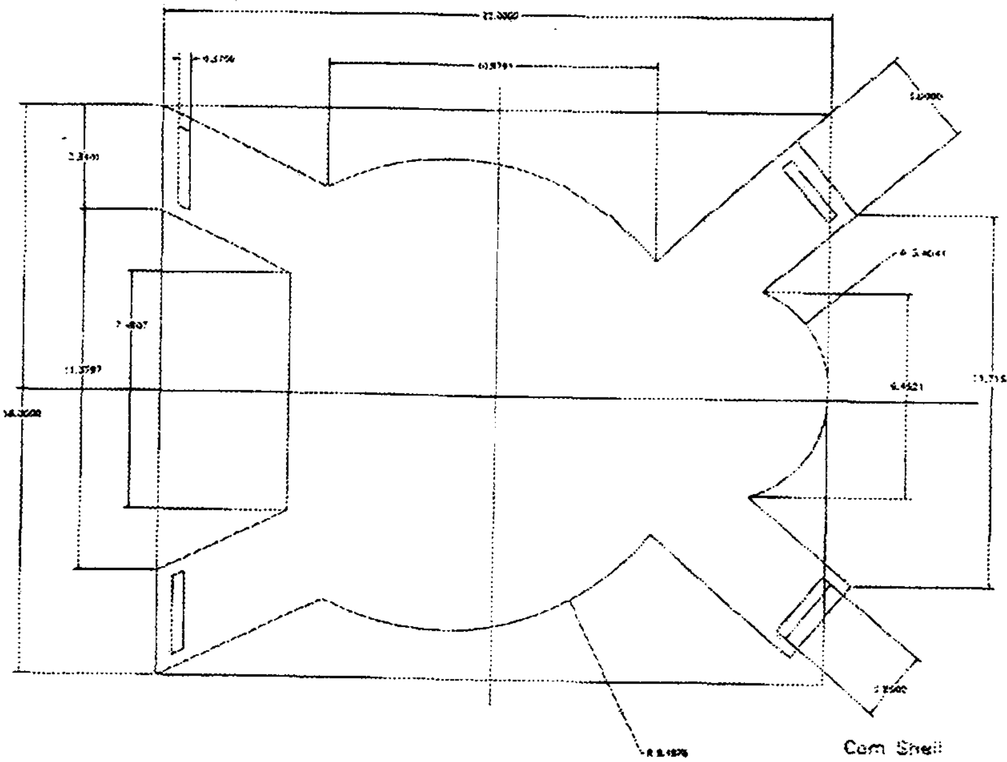

Cam Shell
Material: .187 Polycarbonate
All dimensions in inches

Figure 1. The Dimensions of the Cam Shell Design

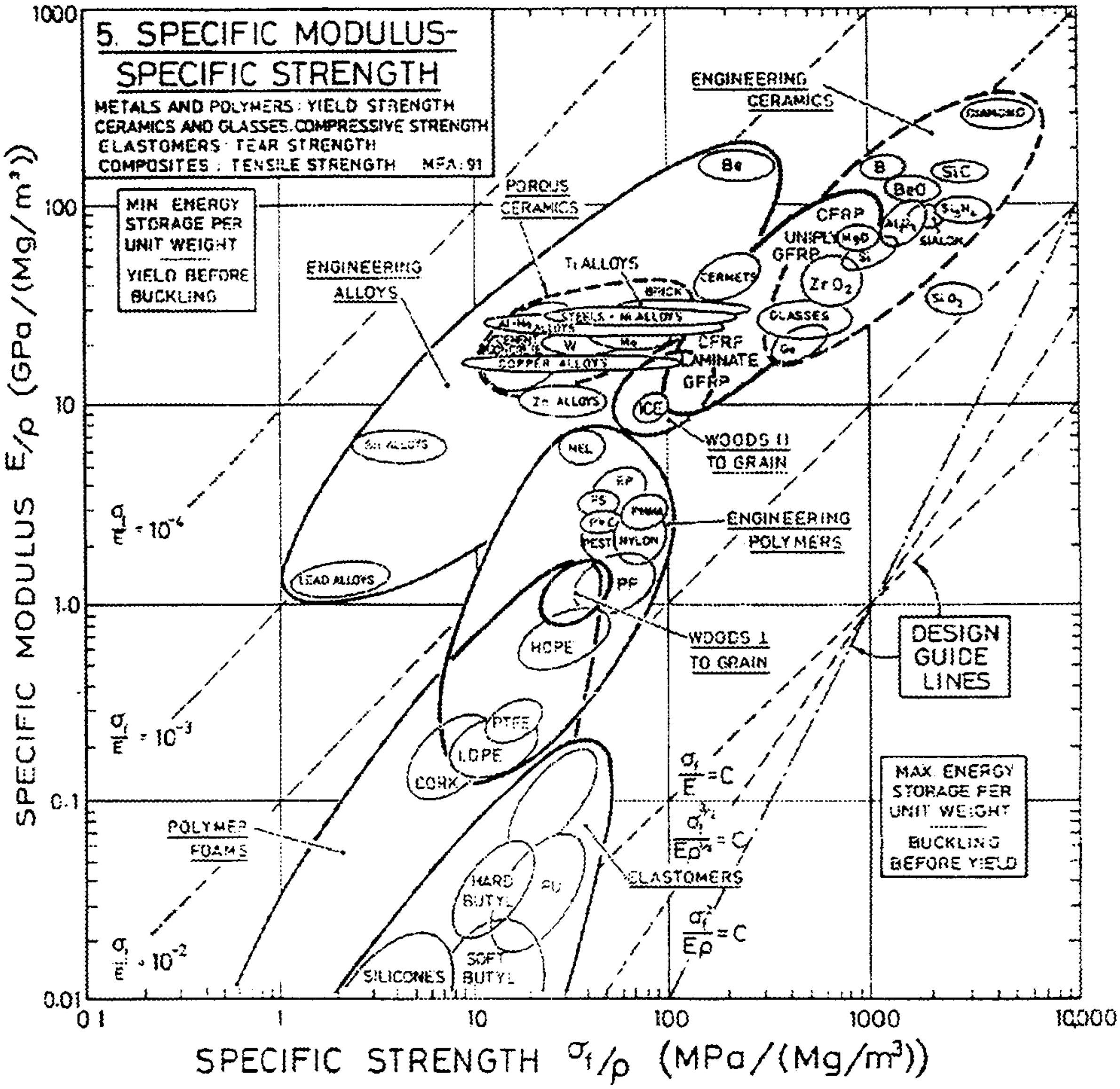

Figure 2. Ashby Diagram: Specific Modulus versus Specific Strength

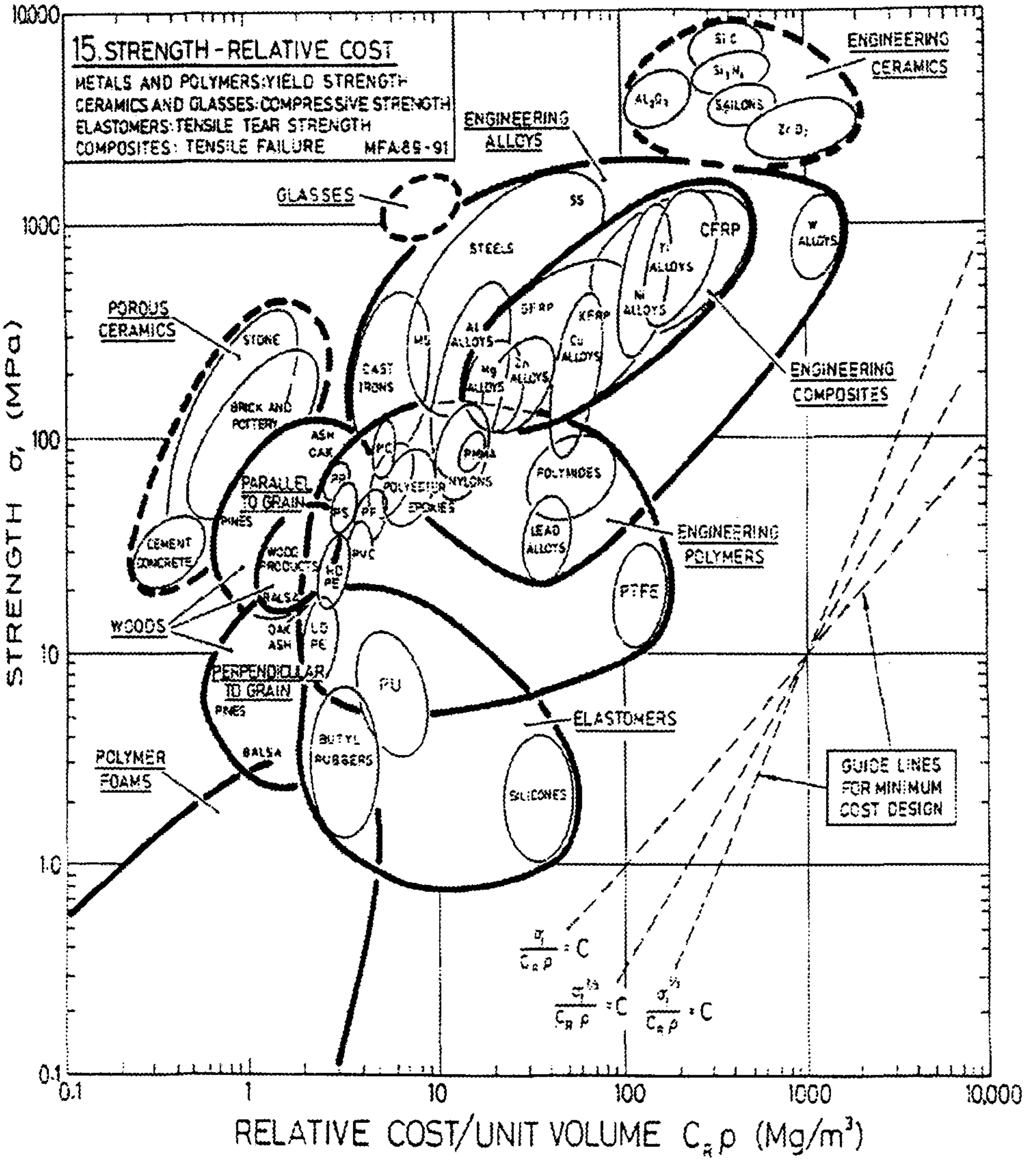

Figure 3. Ashby Diagram: Strength versus Relative Cost per Unit Volume

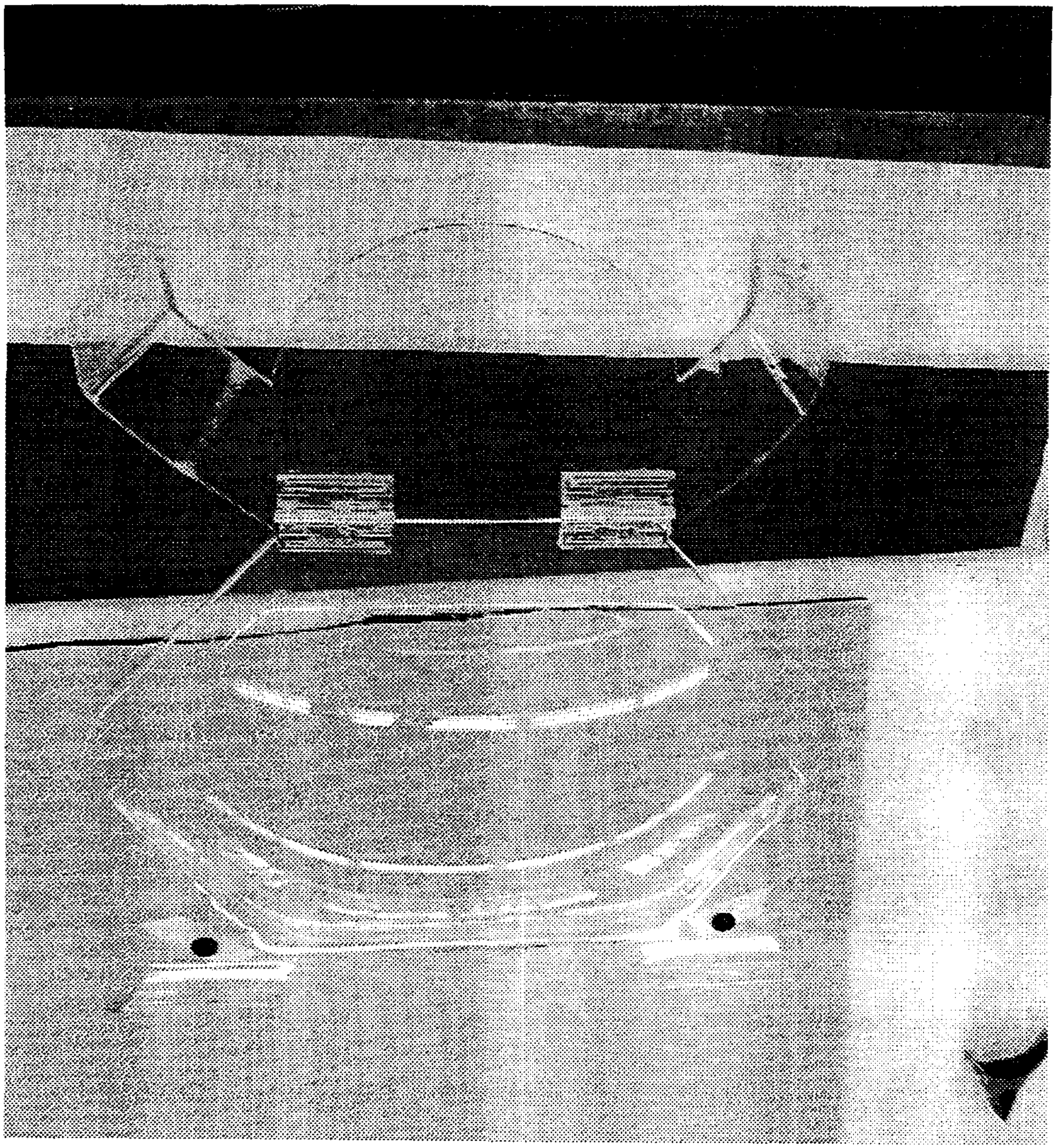

Figure 4. Semi-finished Product

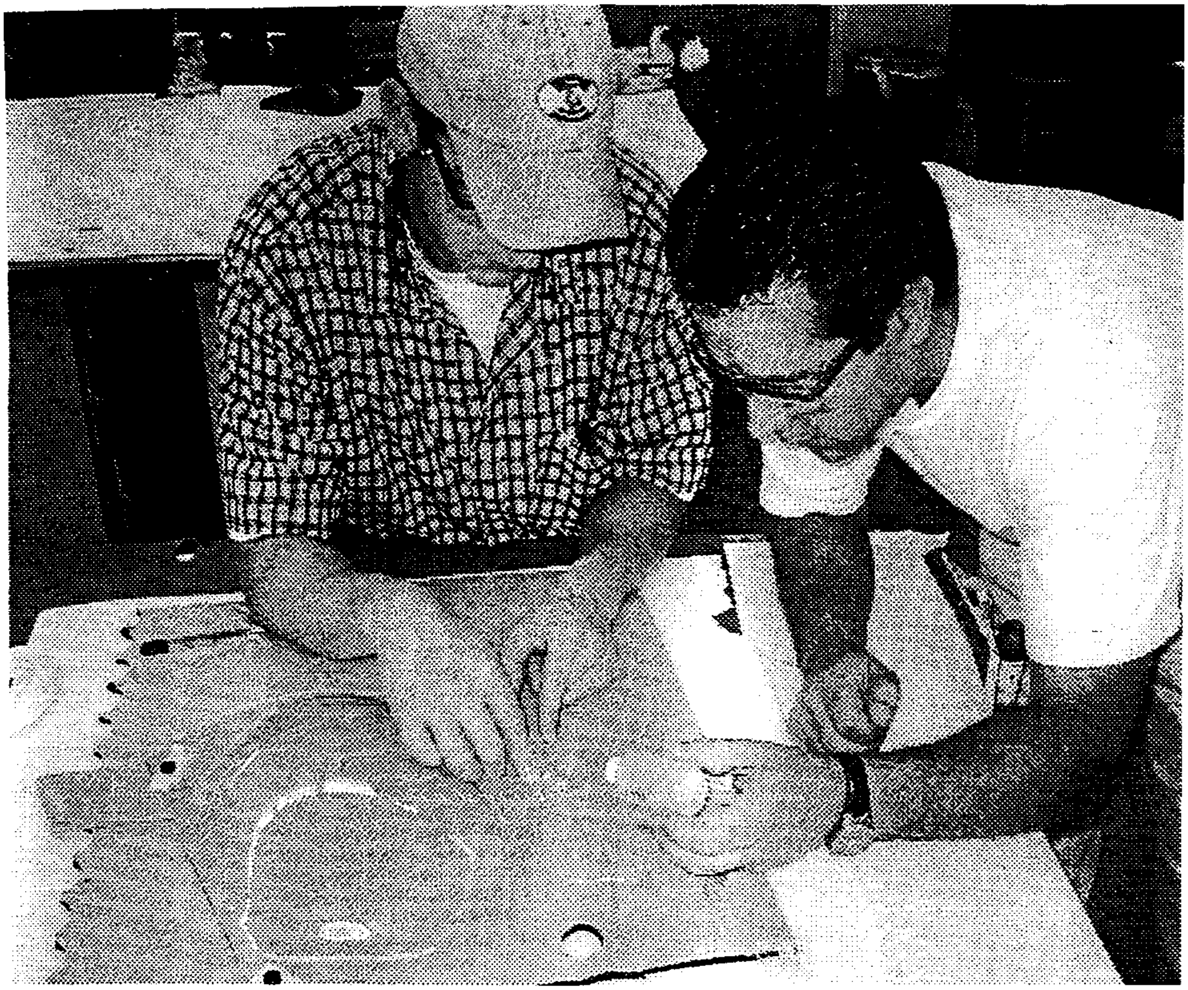

Figure 5. Acrylic Hinges Were Chemically Adhered to the Molded Part

Figure 6. Stand Back View

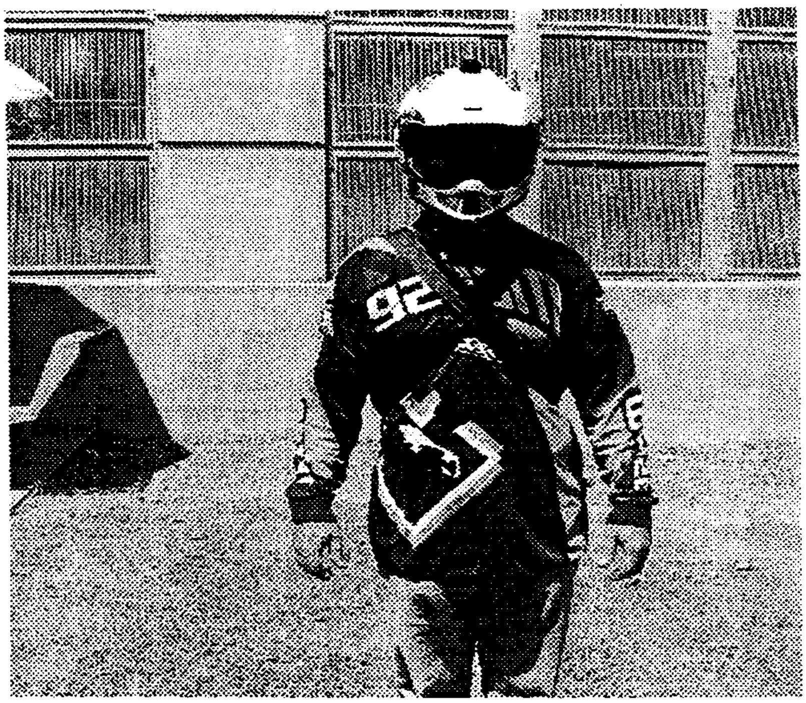

Figure 7. Stand Front View

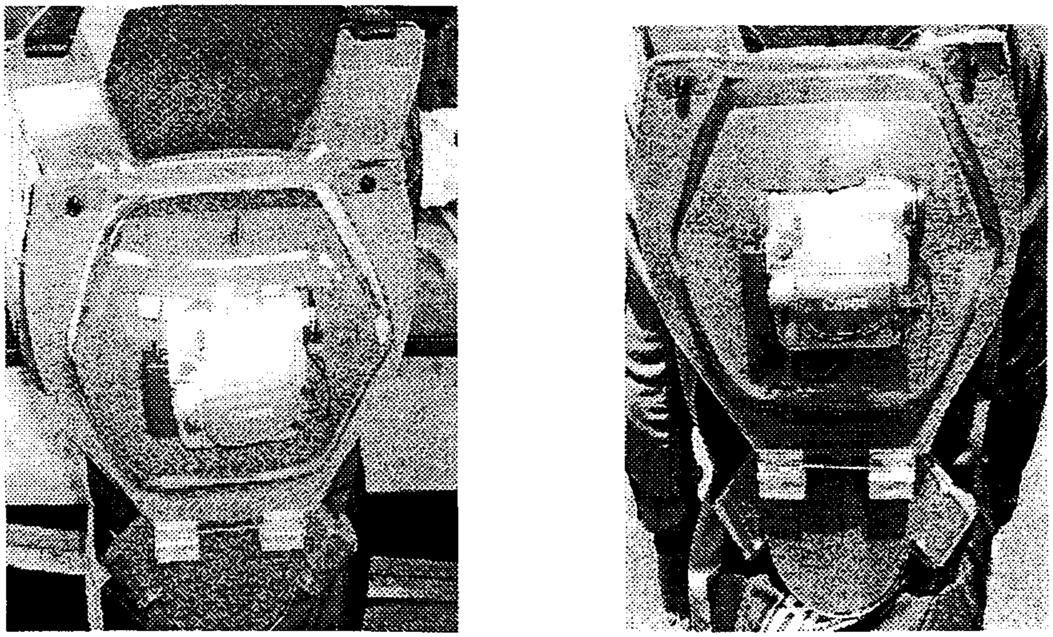

(a)

(b)

Figure 8. Rear Close Up Views (a) and (b)

VISCOELASTIC BEHAVIOR OF FOAMED POLYSTYRENE/PAPER COMPOSITES

Robert A. McCoy

Professor of Mechanical Engineering
Youngstown State Universitye
Youngstown, Ohio 44555

Telephone 330-742-1736
e-mail ramccoy@cc.ysu.edu

Robert A. McCoy

Viscoelastic Behavior of Foamed Polystyrene/Paper Composites

Robert A. McCoy
Professor of Mechanical Engineering
Youngstown State University
Youngstown, Ohio

Key Words: Sandwich composite, cantilever beam, elastic modulus, viscoelastic behavior.

Prerequisite Knowledge: Basic knowledge of stress, strain, Hooke's law, and creep.

Objective: To understand the principle behind why sandwich composites are so stiff as well as light-weight and therefore are in common use in structural applications where stiffness and low weight are important.

Equipment:
1. A sheet of Styrofoam (foamed polystyrene) approximately 122 cm (4 ft) long, 35.5 cm (14 in) wide, and 1.83 cm (0.72 in) thick.
2. A metal frame with a clamp to hold one end of the Styrofoam beam.
3. Six metal washers, about 3.8 cm (1.5 in) diameter.
4. One jumbo paperclip.
5. One large paper grocery bag.
6. Scissors, cutting knife, and paper glue.
7. A ruler or meter stick.
8. A weighing scale or balance.
9. A computer with MS Excel

Introduction:

A sandwich composite consists of a very lightweight core (such as a foamed polymer or honeycomb structure) with sheets of another material (such as paper, plastic, fiberglass, or aluminum) on the top and bottom surfaces. Applications for sandwich composites requiring both high-stiffness and lightweight include aircraft panels, boat hulls, jet skis, snow skis, partitions, and garage doors. In this experiment, the students clearly see the increase in stiffness when the top and bottom skins are added to the Styrofoam beam to form the sandwich composite. Also this experiment includes a creep test on the Styrofoam beam to illustrate the viscoelastic behavior of the polymer.

Procedure:

For each group of students performing this experiment, at least four rectangular bars approximately 2.5 cm (1 in) wide and 35.5 cm (14 in) long were cut from the Styrofoam sheet. Moreover, at least four paper strips, also approximately 2.5 cm (1 in) wide and 35.5 cm (14 in) long were cut from the grocery bag. The students then constructed the following four Styrofoam beam configurations:

A. Styrofoam bar with no paper.
B. Styrofoam bar with paper strip glued to the top surface.
C. Styrofoam bar with paper strip glued to the bottom surface.
D. Styrofoam bar with paper strips glued to the top and bottom surfaces.

The glue was allowed to dry thoroughly before testing the beams. The six metal washers were each weighed and their weights written on their sides. Starting with beam A, one end was clamped as shown in the photo in Figure 1. A jumbo paperclip was bent into a shape such that it penetrated the free end of the beam and looped to allow the hanging of six washers. The other end of the paperclip was bent horizontally to act as a pointer to read the vertical height of the beam end above the countertop using a ruler or meter stick. Before adding any weights (washers) onto the paperclip, the beam dimensions of b, d, L (defined below), and the initial height above the countertop were measured and recorded. Then the washers were added one at a time with height measurements taken after 10 seconds of adding each weight. This procedure continued until either the beam broke or all six washers had been added. All four beam configurations were tested in this same manner. On the data sheet seen in Table 1, the free-end deflection δ was found by subtracting the initial unloaded height from the loaded height. The cumulative weight on the beam was found by adding the weights of all the washers that were currently attached. Using the weight and deflection data shown in Table 1, four weight-versus-deflection curves, one for each beam configuration, were constructed as shown in Figure 2.

Finally a creep test was conducted on the beam A while a constant load of two washers was maintained for 20 minutes, whereupon the load was removed. Deflection measurements were taken at various time intervals (generally every 5 minutes). After the load was removed at the 20-minute time period, deflection measurements were acquired for an addition 10 minutes to test for recovery of the deflection. Data from this creep test is shown in Table 2 and plotted in Figure 3.

Comments:

By drawing a straight line through the first several data points on each weight-versus-deflection curve seen in Figure 2, the slope W/δ value for each beam was found graphically. Then by substituting this W/δ value into the following equation,[1] the elastic modulus E of each beam was calculated:

$$E = \frac{4L^3 W}{bd^3 \delta}$$

where L = unsupported beam length (from clamp to free end)
W = weight of attached washers
b = beam width
d = beam thickness
δ = free end deflection = unloaded height – loaded height

For beam A: $W/\delta = 8.7$ g/cm and $E = 55$ kg/cm^2
For beam B: $W/\delta = 24$ g/cm and $E = 152$ kg/cm^2
For beam C: $W/\delta = 28$ g/cm and $E = 174$ kg/cm^2
For beam D: $W/\delta = 105$ g/cm and $E = 651$ kg/cm^2

Note that the stiffness of beam D is 12 times that of beam A. This is a remarkable increase in stiffness due only to the presence of the paper skins.

The creep curve as seen in Figure 3 demonstrates the viscoelastic nature of the polystyrene. The instantaneous deflection of 4 cm upon the applying of the load and unloading at 20 minutes is the result of the elastic strain. The slowly increasing deflection during the first 20 minutes is due to viscous flow of the polystyrene. Part of this deflection is recovered over time after the load is removed as seen on the curve between 20 and 30 minutes. This type of viscoelastic behavior must be considered when a plastic or elastomeric part is to support a constant load over a long period of time.

References:

1. W. Callister, Materials Science & Engineering: An Introduction, John Wiley & Sons (2000).

Biography:

Robert A. McCoy is a Professor of Mechanical Engineering at Youngstown State University, Youngstown, Ohio. He has bachelor's and master's degrees from Ohio State University and a Doctor of Engineering degree from University of California at Berkeley. At YSU, he teaches freshmen engineering, mechanical engineering, manufacturing processes, and materials engineering courses. He is also a failure analysis consultant and a member of ASM and ASEE.

Table 1. Cantilever Beam Data

Beam A L = 26.8 cm

W (g)	Ht (cm)	δ (cm)
0.0	30.4	0.0
17.09	28.5	1.9
34.59	26.4	4.0
51.80	23.8	6.6
69.42	20.3	10.1
86.96	excessive deflection	

Beam B L = 26.9 cm

0.0	32.6	0.0
17.09	32.0	0.6
34.59	31.2	1.4
51.80	30.1	2.5
69.42	28.9	3.7
86.96	26.8	5.8
104.78	23.5	9.1

Beam C L = 26.7 cm

0.0	28.4	0.0
17.09	27.7	0.7
34.59	27.1	1.3
51.80	26.6	1.8
69.42	26.0	2.4
86.96	25.3	3.1
104.78	24.7	3.7

Beam D L = 26.7 cm

0.0	30.4	0.0
17.09	30.3	0.1
34.59	30.1	0.3
51.80	30.0	0.4
69.42	29.8	0.6
86.96	29.6	0.8
104.78	29.4	1.0

Table 2. Creep Data for Beam A

Loaded with 34.59 g

Time (min)		Ht (cm)	δ (cm)
0	Unloaded	29.8	0
0.1	Loaded	25.8	4.0
1	Loaded	25.7	4.1
3	Loaded	25.6	4.2
5	Loaded	25.55	4.25
10	Loaded	25.45	4.35
15	Loaded	25.4	4.4
20	Loaded	25.35	4.45
20.1	Unloaded	29.4	0.4
22	Unloaded	29.5	0.3
25	Unloaded	29.55	0.25
30	Unloaded	29.6	0.2

Figure 1. Cantilever Beam Fixture

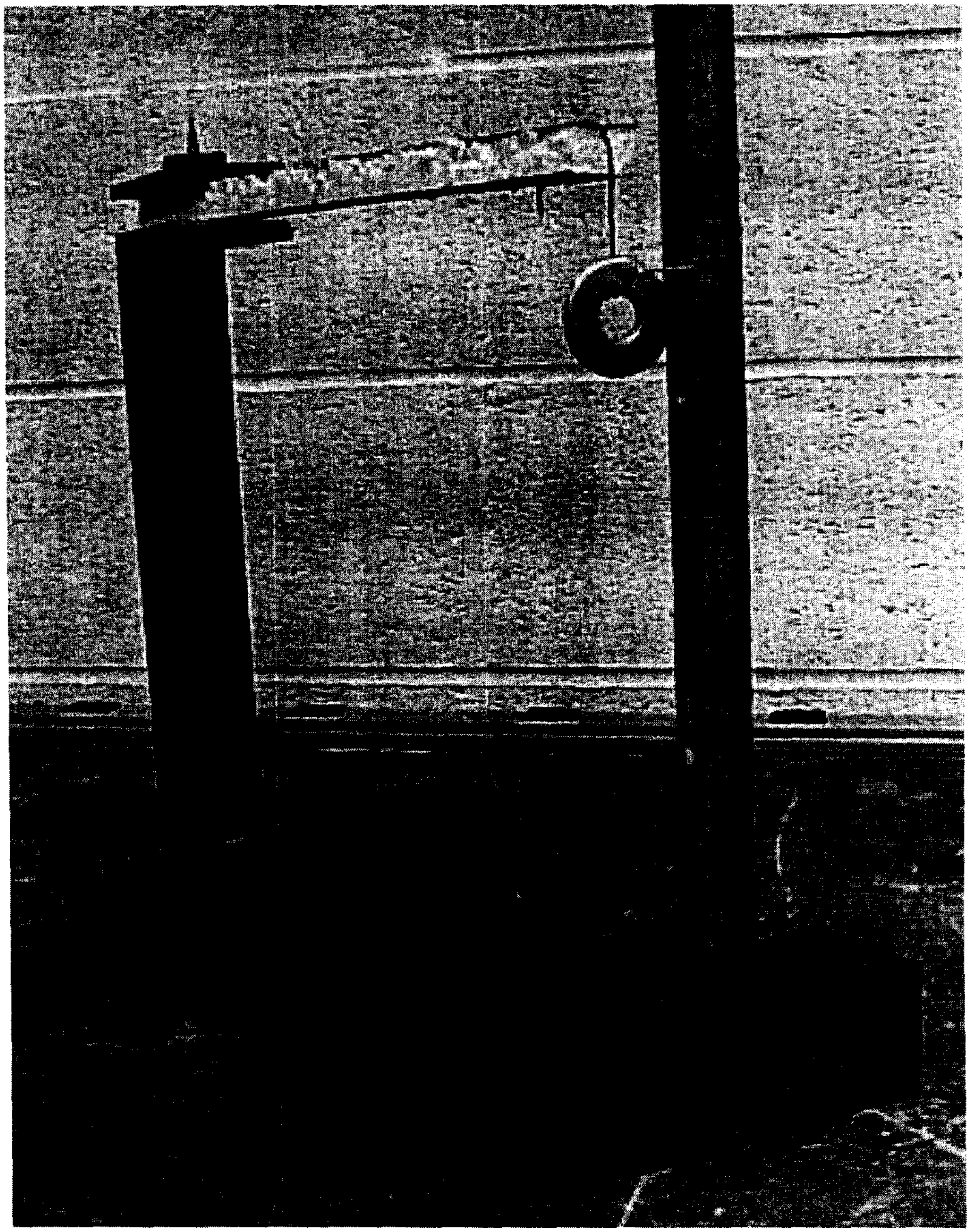

Figure 2. Weight vs. Deflection Curves

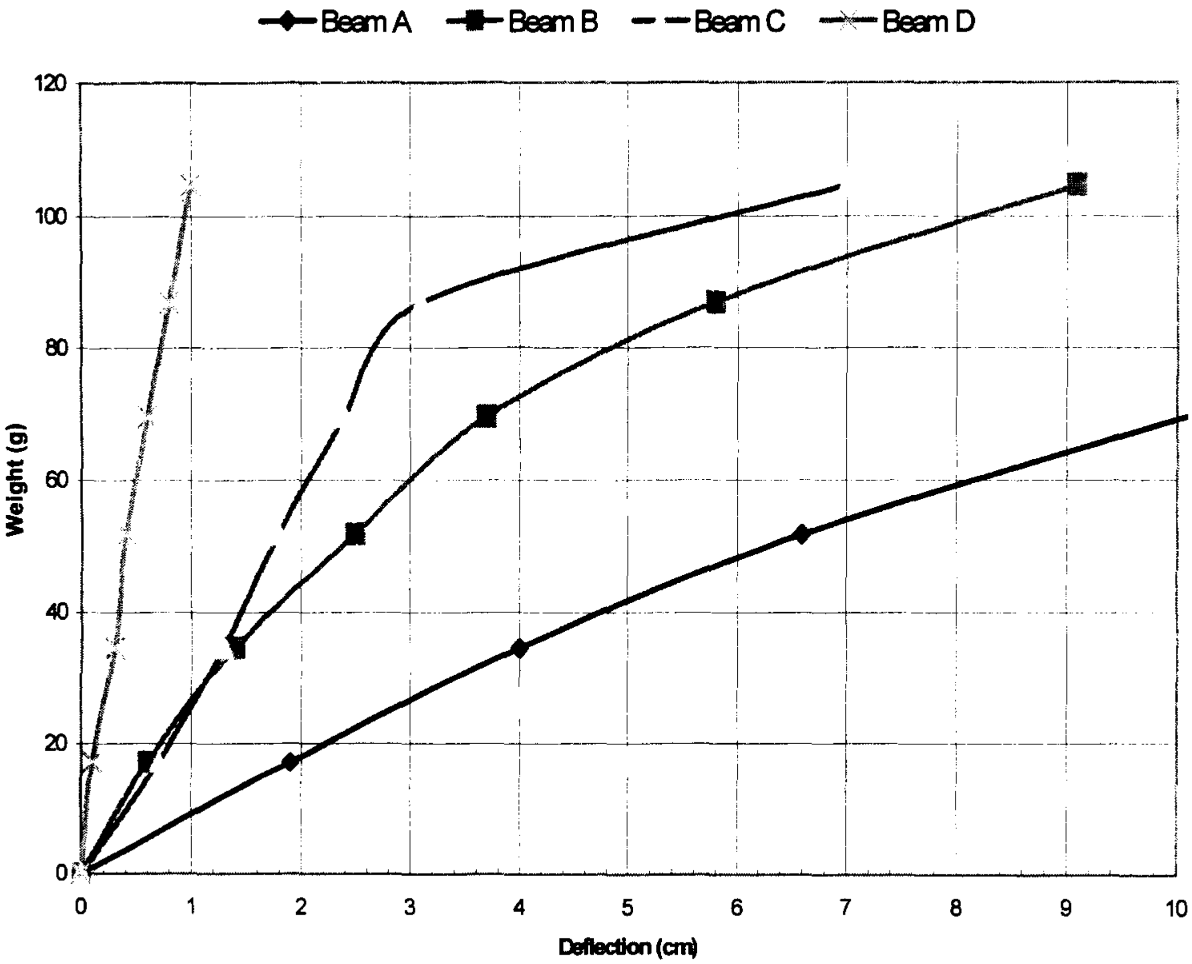

Figure 3. Creep Curve for Beam A

Loaded with 34.59 g at t = 0 and unloaded at t = 20 min

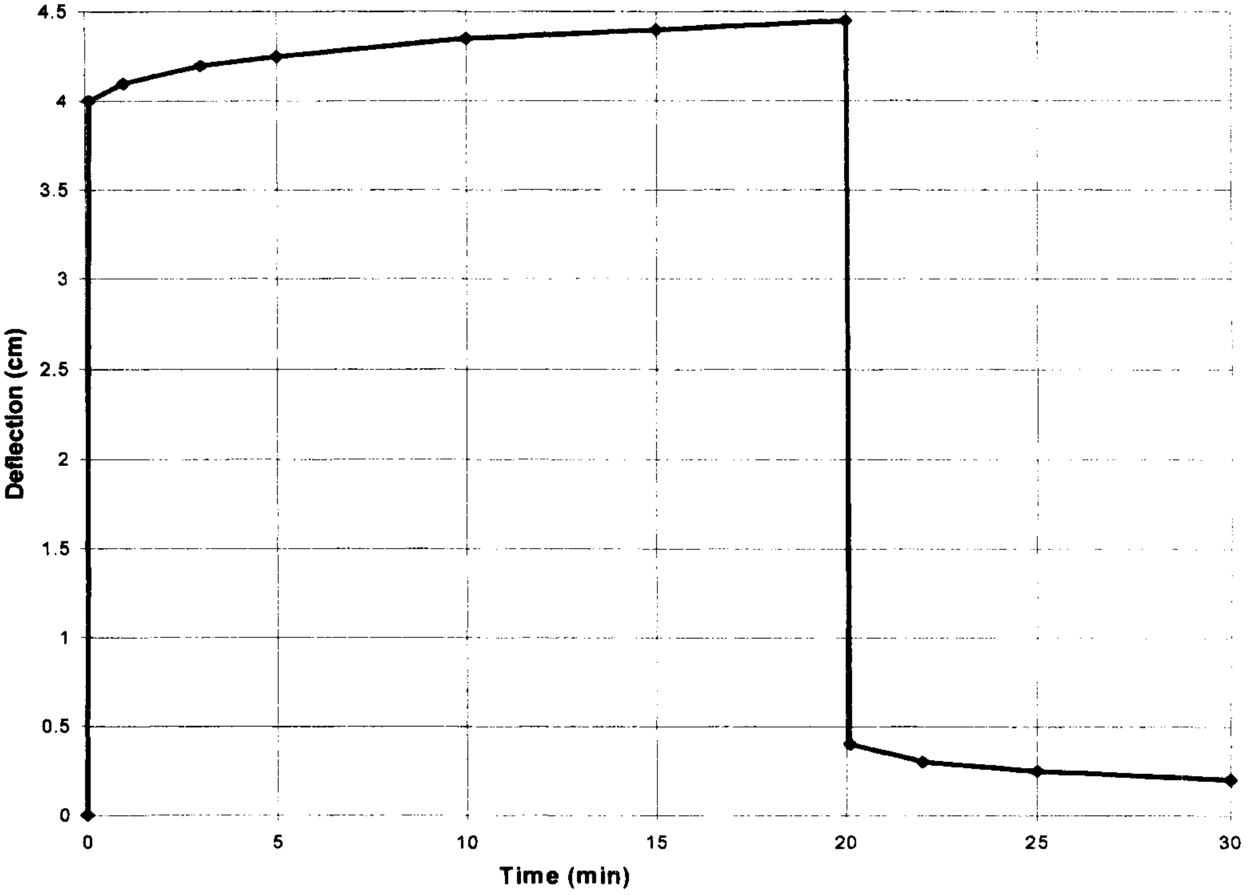

MST-ONLINE: THE UPDATING OF AN EDUCATIONAL INTERNET RESOURCE IN MATERIALS SCIENCE AND TECHNOLOGY

Nikki Harris
Student

Curtiss E. Wall

James A. Jacobs

School of Science and Technology
Norfolk State University
700 Park Avenue
Norfolk, Virginia 23504

Telephone 757-823-9421
e-mail cewall@nsu.edu
jajacobs@nsu.edu

Nikki Harris

MST-Online: the Updating of an Educational Internet Resource in Materials Science and Technology

N. Harris

Norfolk State University, 700 Park Avenue, Norfolk, VA 23504

Key Words: swap image, layers, library, template, and tweening.

Prerequisite Knowledge: basic knowledge of HTML

Objective: to add sound, animation, and newness to a commonly visited website.

Equipment:

1. Macromedia Flash MX
2. Macromedia Dreamweaver
3. Internet

Introduction:

MST-Online continues to provide students and educators with opportunities to learn more about materials technology and provide useful links, vibrant images, and informative resources. In order to better meet the needs of educators and students MST-Online is continuously being updated. We are adding animation created through Macromedia Flash MX and images provided by NASA Langley Research Center. Animations will be influenced by the *Centennial of Flight*, profile various airplanes, and other activities that occur at NASA Langley Research Center. By using animation, MST-Online hopes to provide students and others with an understanding of the activities and tasks that are involved with materials technology.

Procedure:

a) Develop a template for each web page.
b) Collect all of your resources needed for example sound, background colors, and images. Make sure to keep a record of the addresses at which you found your resources.
c) Place your items on the web page from back to front meaning choose your background first then your text and so forth. Think of everything as a layer i.e. an image layer, picture layer, text layer, etc.
d) Add or attach links to all necessary text and check to make sure the addresses connect.
e) Add images. Make sure that all images are visible and all the appropriate size.
f) Animation and or action can be created in various ways. For the welcome page animation called tweening was used in Macromedia Flash MX. To tween:

    1. Place your image in the beginning spot or frame at which you want your animation to begin.
    2. Select Insert then Create Motion Tweening.
    3. Move the image to the ending location or frame at which you would like your animation or tweening to stop.
    4. Select Control then Test movie to make sure that your image moves smoothly and correctly.

g) For the home page an action called swap image was used in Macromedia Dreamweaver. To swap an image:
    1. First name the image in which you want to swap. To name an image go to the upper left most text entry box and type in a name.
    2. While your image is highlighted or selected choose Windows then Behaviors.
    3. Select the plus button and choose the swap image action from the pop-up menu.
    4. Select the image whose source you want to change from the image list.
    5. Enter the path and file of the new image in the Set Source to field or click Browse to select an image file.
    6. Click OK.

Comments:

The results of the Macromedia Flash MX program should be an image that moves from on place to another. The results of the Macromedia Dreamweaver program should be an image that when the pointer or mouse selector is moved over the image it swaps or turns into another image.

COMPUTER GRAPHICS SOFTWARE FOR TEACHING CRYSTALLOGRAPHY

Ricardo Simões

Laboratory of Advanced Polymers
and Optimized Materials
Department of Materials Science
University of North Texas
Denton, Texas 76203-5310

Telephone: 940-565-3262
e-mail rsimoes@unt.edu

Ricardo Simões

Computer Graphics Software For Teaching Crystallography

Ricardo Simões
Laboratory of Advanced Polymers and Optimized Materials (LAPOM), Department of Materials Science, University of North Texas, Denton, TX 76203-5310, USA; rsimoes@unt.edu

Abstract

Continuous advances in computer hardware as well as graphical programming interfaces have made possible the development of graphical software tools for educational purposes. One of the many possible applications of using three-dimensional modeling and rendering software is in teaching crystallography. While it is sometimes confusing to learn the various structures of crystals from two-dimensional static pictures, this task becomes much easier when one can visualize, move, rotate and apply a variety of effects to a structure in three-dimensions.

Inexpensive software such as *Matvis* and the world-wide availability of computers allow students to have this software installed in their own computers or available in computer rooms at their university. In this way in-class learning can be complemented outside the classroom at a time convenient for the student. Educational software that students can run on their own can also be used in distance learning courses.

Keywords: Crystallography, Materials Science & Engineering, Computer Software, OpenGL

Prerequisite Knowledge: None

Objective: To learn crystallography

Equipment: PC running Windows 98/2000/ME/XP

1. Introduction

Materials Science and Engineering (MSE) can be a difficult subject both for teaching and learning [1]. This is due to its interdisciplinary nature, including elements of physics, chemical engineering, mechanics and others. Also, unlike some other areas, MSE often deals with phenomena that can be hard to visualize. Multimedia techniques were presented some time ago as a tool to solve this problem [2]. The worldwide availability and use of computers provides students access to graphical tools which can be helpful in understanding physical phenomena. Multimedia software does not intend to be a replacement for instructors, but can provide them with additional means to explain a subject [3].

However, the use of multimedia techniques is not yet being used to the extent of its capabilities. Three-dimensional (3D) computer graphics and animations are widely employed for game programming and have also been used for research purposes [4, 5]. However, their capabilities in terms of educational applications have been somewhat disregarded. Many classrooms still do not possess computer equipment to allow all students to use computer software during the class; however, the instructor can use the software for a multimedia presentation while covering the subject. Software that the students can run in their own computers outside the classroom environment provides an important complement to the lectures.

When teaching a crystallography course, it can be a difficult task to explain the non-basic crystal structures, particularly at the undergraduate level. Relying on stereographic projections or even static images presents several problems. This is further complicated when dealing with complex structures based on lattices containing many atoms. However, crystallography is a very important area of MSE, not only for basic understanding of metals and ceramics and their properties, but also for diffraction and a wide variety of phenomena. Performing mental operations to understand a 3D structure from a 2D image demands a cognitive effort from the brain in converting the representation. Not everyone can perform this operation easily. However, if the information is already presented in 3D, the effort of the brain is now perceptive, which is a much simpler operation [1].

2. The program

MATVIS [6] employs this principle and renders 3D structures in a virtual world, allowing the user to manipulate them at will; see Figure 1. The structure can be moved and rotated in any direction in space and several of its properties can be changed. For this, we have used the OpenGL graphics interface [7] with Visual C++ programming on the Microsoft Windows operating system. OpenGL is a software interface to graphics hardware. The key advantage of using OpenGL is that high quality rendering is easily achieved and the program can be made fully interactive. The advantage over using simple animation files as tutorials is that interactive learning can increase student interest and allow him to control the visualization to answer particular questions. Other software for interactive learning of crystallography has existed for some time [8], but advances in computer technology now allows us to use 3D real time graphics for this purpose.

This program currently runs under Windows 98/2000/ME/XP and does not require advanced resources. A Pentium II or an equivalent processor running at 400 MHz with 64 Mb of memory is the minimum recommended system. However, having a Pentium III or better processor and a 3D accelerator video board highly enhances the performance of the program and should be used for the manipulation of complex structures. Any of these systems is nowadays available on a common household and the majority of students in educational institutions at the undergraduate level should have access to one.

3. Procedure

There are two main components of the MATVIS program. One allows the students to visualize a diversity of pre-defined structures and the other allows the creation of new structures. By choosing a pre-defined structure, the student can learn from the most basic to moderately complex lattices. These include the most common lattices of metals and ceramics including so-called high technology materials:

- Simple cubic (SC);
- Body centered cubic (BCC);
- Face centered cubic (FCC);
- Hexagonal closed packed (HCP);
- Rock-salt (e.g. NaCl);

- Diamond / Zinc blend (e.g. ZnS);
- Perovskite (e.g. $CaTiO_3$);
- Spinel (e.g. Al_2MgO_4);
- Inverse spinel (e.g. $MgTiMgO_4$);
- Fluorite (e.g. CaF_2).

The student can load one of these lattices and change its properties, such as the radius of each type of atom. For visualization purposes, the spacing between the atoms in the lattice can also be changed. For each of these systems, some elements can be readily hidden or shown. As an example, when visualizing the diamond structure, one can choose to show only the atoms in the FCC sites or the atoms in the tetragonal sites; see again Figure 1. The lattice cell and the bonds on these structures can also be hidden or shown.

Along with these basic lattices, more complex structures of each type are also pre-defined:

- Triclinic;
- Monoclinic;
- Orthorhombic;
- Tetragonal;
- Trigonal;
- Hexagonal;
- Cubic.

A total of over 80 structures in over 40 different space groups have been included.
An example of a complex structure is shown in Figure 2.

The second main component of the program is a module to define new structures, which we call *custom structures*. The student can define any structure based on the positions of its atoms. These positions can be obtained for instance from diffraction of an unknown sample and its structure can then be visualized on the program. The program allows recording the information about the structure to a file for future use. In this way, any number of structures can be easily added to the program.

The structure construction procedure is very intuitive. The user adds atoms to the structure and inputs data about each atom. The required data are the coordinates of the atom in space, the radius of the atom and the type of atom (a structure can contain up to four different types of atoms). Each atom in the structure can be modified at any time and it can also be temporarily disabled, which removes it from the visualization of the structure. In this way, an atom or series of atoms can be hidden either to show some detail of the structure or to display only atoms in a determined lattice position. Along with defining atoms, one can also add bonds between atoms in a similar way. The information required for the bond is simply the definition of which two atoms are connected by that bond. Bonds can be disabled in the same way atoms can.

This module can also analyze the structure created and report on the total number of atoms and bonds, number of atoms of each type, statistics about atom radius and bond lengths, and the space occupied by the lattice.

Another important feature of the program is the representation of crystallographic planes; see Figure 3. Planes can be shown in any pre-defined or custom structure. Several of the most commonly used planes are pre-defined and can be readily shown or hidden with a simple click. A distinction is made between planes in hexagonal and non-hexagonal lattices. This is due to the fact that hexagonal lattices are defined by four indices instead of three indices in the non-hexagonal lattices case.

In addition to these pre-defined planes, any custom plane can be defined by three Miller indices (for non-hexagonal lattices) or by the coordinates of the three or four vertices of the plane (for any lattice). A total of up to 10 custom planes can be represented. Any custom plane can be deleted if it is no longer needed.

Representation of planes can be used not only for teaching about crystallographic directions and planes but also for the measurement of atomic density along a plane. Thus, the program can also be used in research. Since students can run this program in their own computers or any computer lab, homework can be assigned based on the representation of planes on a structure.

4. Special features of the program

Other features of MATVIS that enhance visualization include:

- Selection of the rendering quality. Since the program can be slow on some systems, the quality can be reduced while moving and changing the structure and then increased when the user wishes to capture the image to a file;
- The colors of each atom type, background, cell, bonds, axes, and on-screen information can be changed;
- Several textures for the atoms are pre-defined and their quality can be selected;
- Both the mouse and the keyboard can be used to move or rotate the structure and to control several features of the program;
- Other rendering settings include choice of light sources and transparency blending;
- The structure can be animated about one or more axes.

A toolbox window can be used to control most of the program functions in a simple manner.

The program also allows the capture of a current structure either to the clipboard, from where it can be pasted into other programs, or to a file, in the standard Windows Bitmap (.bmp) format. The image file in this format can be used in most Windows applications. In this way a student can easily prepare a report or a presentation based on images of structures obtained from the program.

5. Concluding remarks

The use of computer graphics for educational purposes is not a recent event. However, the use of computers in a classroom environment in the field of Materials Science and Engineering is still not very common so far. 3D graphical rendering through OpenGL has not been sufficiently explored for education. The program under discussion is also a step in this direction.

The advantages presented by multimedia teaching tools cannot be ignored: most crystallographic structures are very hard to explain in terms of their 2D images. Software that students can run at home allows them to spend as much time as they want or need to learn details of a structure. Therefore, programs such as this one can have a high impact inside and outside of the classroom. They can also be used for distance-learning courses.

Inexpensive group licenses of this program allow all students in a course to have access to it, which is an important aspect. More complex programs for creation and visualization of structures are commercially available [9, 10], offering complex structure manipulation and rendering options. However, their high prices limit their use. Possibly then can be more appropriate for research where a much higher level of detail may be required.

The second version of MATVIS is scheduled to be released in August 2002. For more detailed information about the program please visit our webpage at *http://matvis.htmlplanet.com/* where you can also download a free trial version.

6. Future development

New features are planned for inclusion in the program. Along with those, the library of pre-defined structures will be increased to accommodate for samples from additional space groups. However, it was found that some structures are either too complex for this type of representation or have little educational purposes, their usefulness limited to specific research topics. Future versions of the program will also contain amorphous and semi-crystalline structures, including polymers.

In development are new modules for representation of crystal defects, such as interstitials and dislocations, and ductility through movement of dislocations. The representation of diffusion mechanisms is also planned. These new features will be interactive but mostly prepared as tutorials, with text accompanying the visual representation.

Acknowledgements

Useful suggestions on this manuscript by Prof. Witold Brostow, University of North Texas, Denton, are appreciated.

Comments about the program and suggestions for its future enhancement will be appreciated.

References

1. M. Graef, J. Mater. Ed. 20, 31 (1998)
2. K.P. Constant, J. Mater. Ed. 19, 1 (1997)
3. B.N. Kodess, R.P. Krentzis, D.V. Krotov, F.A. Sidorenko, J. Mater. Ed. 21, 63 (1999)
4. W. Brostow, A.M. Cunha, J. Quintanilla, R. Simoes, Macromol. Theory & Simul. 11, 308 (2002)
5. W. Brostow, M. Donahue III, C.E. Karashin and R. Simoes, Mater. Res. Innovat. 4, 75 (2001)
6. The MATVIS website at http://matvis.htmlplanet.com/
7. M. Woo, J. Neider, T. Davis, D. Shreiner, OpenGL Programming Guide, 3rd Ed., Addison-Wesley, Reading, Massachusetts, 1999
8. P. Goodhew, T. Fretwell, J. Mater. Ed. 20 (1&2), 67 (1998)
9. Crystal Studio website at http://www.crystalsoftcorp.com/CrystalStudio/index.html
10. CrystalDesigner website at http://www.crystaldesigner.no/

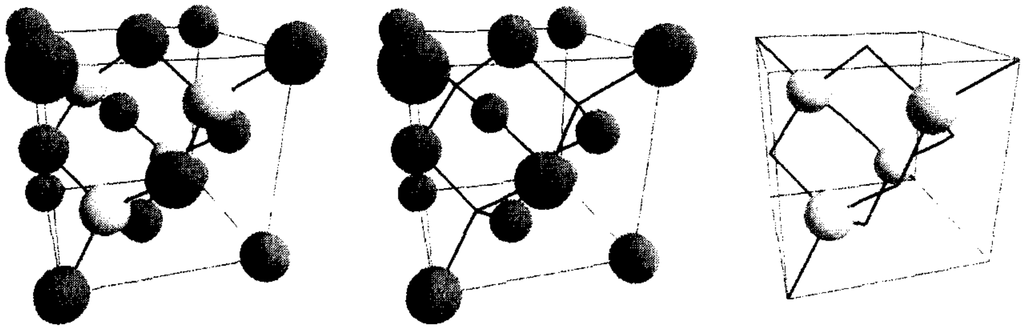

Figure 1 – Different representations of the Diamond structure. Atoms in the FCC and tetrahedral positions are shown in different colors.

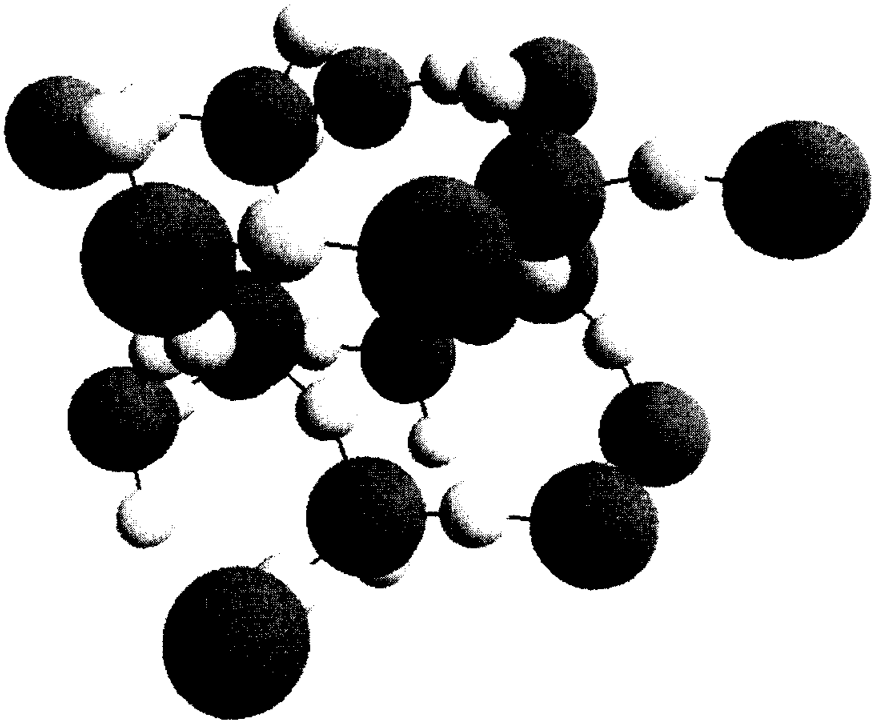

Figure 2 – The trigonal structure of SiO_2 alpha - quartz

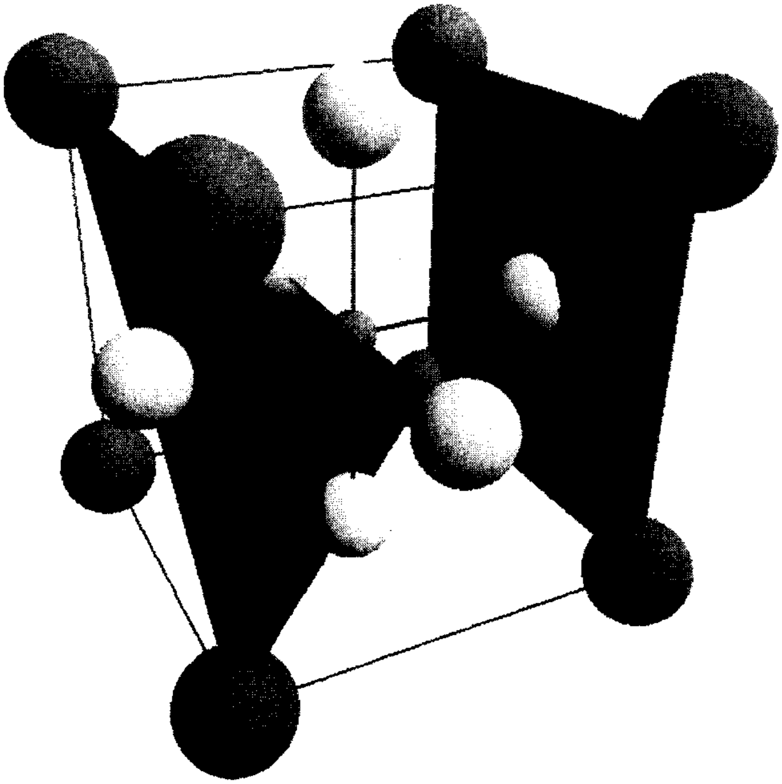

Figure 3 – Representation of the (111) and (100) planes in the Perovskite structure

THE USE OF PIEZOELECTRIC MATERIALS IN SMART STRUCTURES

D. M. Pai[1]

N. R. Sundaresan[2]

and

N. Cadenhead[3]

Associate Professor
[1]NSF Center for Advanced Materials and Smart Structures
[2]Summer Research Student
NASA Center for Aerospace Research
[3]Sophomore Shadow
NASA PAIR Program
Department of Mechanical Engineering
North Carolina A&T State University
Greensboro, North Carolina 27411

Telephone: 336-334-7620 ext. 316
e-mail pai@ncat.edu
mannur@ncat.edu

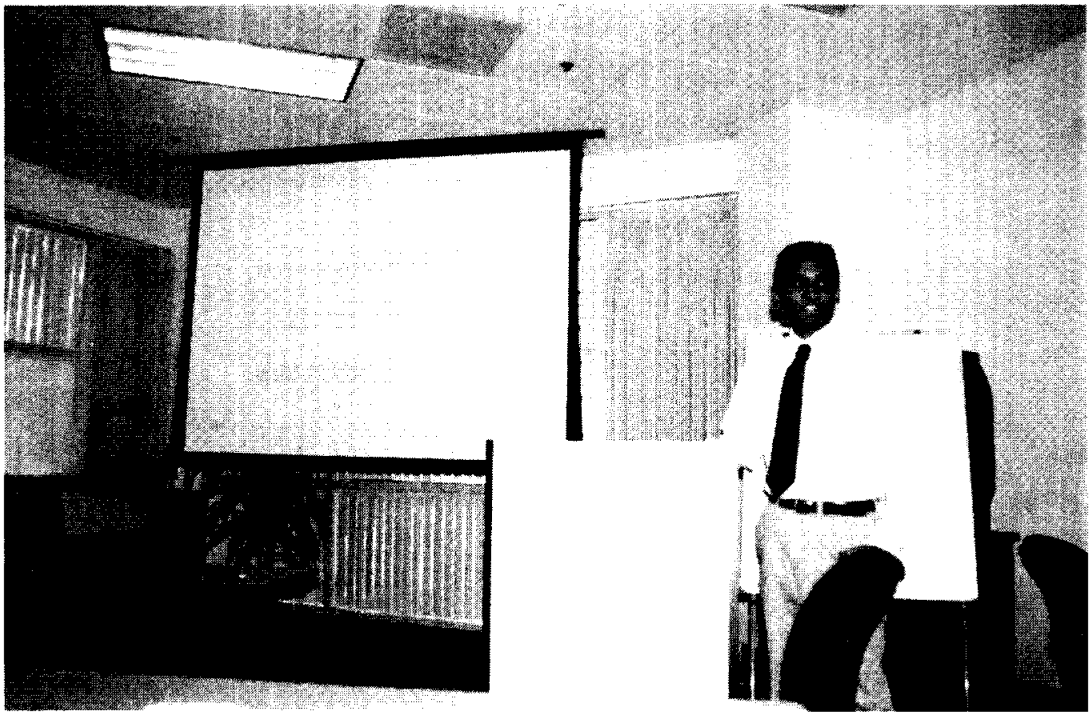

N. R. Sundaresan

The Use of Piezoelectric Materials in Smart Structures

D. M. Pai[1], N. R. Sundaresan[2] and N. Cadenhead[3]
[1]Associate Professor, NSF Center for Advanced Materials and Smart Structures
[2]Summer Research Student, NASA Center for Aerospace Research
[3]Sophomore Shadow, NASA PAIR Program
Dept of Mechanical Engineering
North Carolina A&T State University
Greensboro, NC 27411

Keywords: Smart material, piezoelectric, structural health monitoring, ultrasonic waves.

Prerequisite Knowledge: Introductory physics

Introduction

A piezoelectric material is basically a ceramic that outputs a voltage upon being mechanically strained. Sensors made of this material are sensitive enough to generate signals when subjected to low-amplitude mechanical waves such as sound waves traveling through solids. This makes them candidate materials for all kinds of exciting applications. For example, sensors mounted on a wing surface could detect ice formation on the wing using surface active waves. Since the velocity of sound in a given medium is a function of temperature, such sensors are also being used to actually measure temperature. It is important for students to be aware of this new generation of materials and to be familiar with the use of these materials for measuring fundamental quantities such as the velocity of sound. This experiment has been designed for use in an introductory mechanical or materials engineering instrumentation lab. Initial setup (after procuring all the materials) should take the lab instructor about 2 hours. A single measurement can be initiated and saved to disk in less than 3 minutes, allowing for all the students in a typical lab section to take their own data rather than share a single set of data for the entire class.

Approach

Our experiment utilizes long single strand wire of different materials coiled on a cylindrical spool with the coils widely spaced to avoid interference. A piezosensor is connected to each coil at the same polar location and the electric signal is fed through an amplifier to an oscilloscope. A sound wavetrain is generated by a pencil lead break at one end of the wire and progresses through the length of the wire. The time lag between the wavetrain's arrival at successive coils, and the reduction of the signal's amplitude are a measure of fundamental material properties such as the velocity of sound and the attenuation factor for that material. The experiment enables students to interface concepts of physics, materials science and materials engineering and encourage them to develop scenarios for the practical application of novel materials.

Equipment and supplies

General supplies and measuring equipment commonly found in most physics/instrumentation labs are listed in Table 1. Materials/supplies that will need to be purchased specially for this experiment are listed in Table 2.

General Purpose	
X-Acto Knife	240 Grit Sand Paper
6in. Metal Ruler	Soldering Iron and Supplies
Aluminum Backing Plate	Copper Foil
Pipe	Thread
Digital Oscilloscope (2 ch.) with necessary leads	Mechanical Pencil
Electric Insulating Tape	

Table 1. Generally available supplies and equipment

	Supplier	Part #	Qty.	Cost
Piezo Electric Material 2 in. X 2 in. (enough for at least 10 sensors)	Piezo Systems Inc. 186 Massachusetts Avenue Cambridge, Massachusetts 02139 (617) 547-1777 www.piezo.com	T110-A4E-602	1	$150
Galvanized Wire (a 10 lb coil)	Master Halco PO Box 365 La Habra, Ca 90631 (562) 694-6787 www.fenceonline.com	5570	1	$10
BNC Jack	Radio Shack 300 West Third Street Suite 1400 Fort Worth, Texas 76102 (817) 415-3200 www.radioshack.com	UG-1094	2	$4.00
Wood Supports	Home Depot 2455 Paces Ferry Rd. Atlanta, GA 30339 (770) 433-8211 www.homedepot.com	2 X 4 wood	1	$3

Table 2. Special supplies required for this experiment (piezoelectric material cost can be spread out over 5 sets of 2 sensors each)

Experimental Procedure

Initial Setup

1. Insert the pipe through the galvanized wire and arrange the wire so that none of the coils are touching. Tie the coils to the pipe with string
2. Arrange the pipe with the coils on two wood supports so that the coils are suspended.
3. Create two sensors by cutting a 1/2in. x 1/4in. piece of piezoelectric material into several thin strands. Attach the ends of the piezoelectric material to two pieces of electrical tape so that the middle of the piezoelectric material is exposed. Attach a thin piece of copper foil to the exposed area of the piezoelectric material and tape them together.
4. The coil of wire specified in Table 2 has about 23 ½ coils. For this coil, clean two sections of the wire 8 coils from one end and 1 coil from the other end with sand paper. Number of coils will vary if you use other materials, and the suggested numbers should be adjusted appropriately.

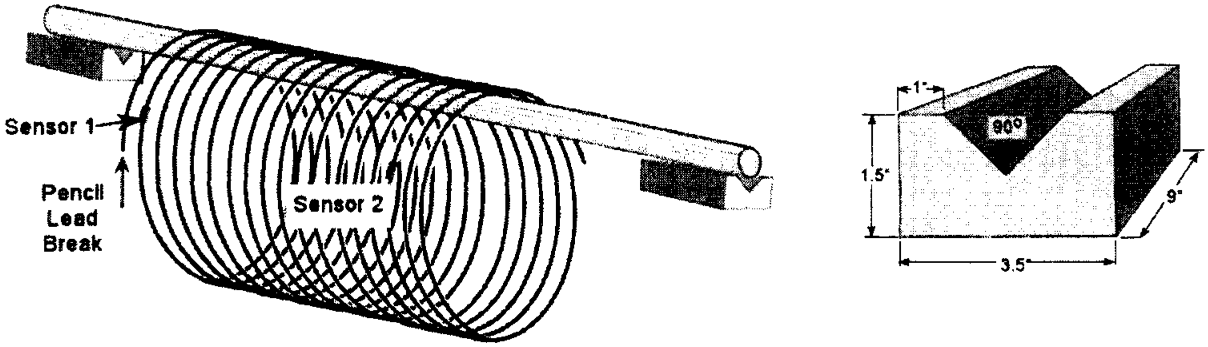

Figure 1 Coil setup & detail of wood support for pipe ends

5. Attach the sensors without cracking the piezoelectric material to the two cleaned areas. Make sure the copper is not touching the wire. Wrap the sensor tightly to the wire using electrical tape.
6. Attach a ground to the wire using copper foil. Wrap it tightly using electrical tape.
7. Solder a wire to the sensor, and then solder the wire to the inside of a BNC jack.
8. Solder a wire to the ground, and then solder the wire to the outside of a BNC jack.
9. Attach the BNC jacks to coaxial cables and attach them to an oscilloscope.
10. Cover the sensor and ground areas with aluminum foil.
11. Check the continuity of the circuit with a multimeter.

Experiment

1. Measure/count and record the following data regarding the coil: total number of turns in the coil, number of turns between left sensor (Sensor 1) and right sensor (Sensor 2), mean coil diameter, wire diameter.
2. Set the oscilloscope to trigger and collect left sensor (Sensor 1) and right sensor (Sensor 2) data to disk (implementing an easy-to-understand file naming system is crucial!)
3. Using a mechanical pencil, break about a 1/16 in. piece of lead on the tip of the galvanized wire.
4. Observe the results on the oscilloscope and store the voltage-time data to disk.
5. Repeat steps 2 and 3, except break the pencil on the other tip of the galvanized wire.
6. Steps 3-5 can be repeated to replicate the data, if desired.

Data Analysis

1. Plot side-by-side the voltage – time curves for left and right sensors for the left pencil break event. You should see one distinct peak for the left sensor plot and two distinct peaks for the right sensor plot. The second peak for the right sensor plot is the reflection of the wavetrain from the right end of the coil.
2. Determine the time elapsed between the left sensor peak and the first right sensor peak. Call this t_L.
3. Plot side-by-side the voltage – time curves for left and right sensors for the right pencil break event. You should see one distinct peak for the right sensor plot and two distinct peaks for the left sensor plot. The second peak for the left sensor plot is the reflection of the wavetrain from the left end of the coil.
4. Determine the time elapsed between the left sensor peak and the first right sensor peak. Call this t_R.

5. From your coil dimensional data, calculate the circumference of one coil turn and therefore the distance L_{1-2} along the coil between left and right sensors.
6. The velocity of sound for left pencil break will be L_{1-2} / dt_L and that for right pencil break will be L_{1-2} / dt_R.
7. Check that the two numbers match closely.
8. Also check how closely the numbers match with the theoretical velocity of a longitudinal sound wave propagating in a solid medium, given by the equation $v = (E/\rho)^{1/2}$.
9. Collect the velocity data from other class members and perform statistical analysis to determine the mean value and standard deviation of the data.
10. Present your results, graphs, calculations, discussions and conclusions in a report.

Typical Results

The results presented in Table 3 were obtained consistently by the student workers at NC A&T State University and are presented for the instructor's reference only. The authors found the data to be extremely repeatable and consistent. The result matched the theoretical calculation of longitudinal wave

Dimensional calculations					
Wire diameter	0.125	in.			
Coil diameter	28	in.			
Coil circumference	87.96	in.			
Left sensor location	7.5	th turn	=	659.73	in.
Right sensor location	22.5	th turn	=	1979.20	in.
Right end of coil	23.5	turns	=	2067.17	in.
(all distances measured from left end of coil)					
Distance between					
Left end and left sensor			=	659.73	in
Left sensor and right sensor			=	1319.47	in.
Right sensor and right end			=	87.96	in.

Location of pencil break	**Trial #**	**t_L (s)**	**t_R (s)**	**dt (s)**	**v (ft/s)**
Left	1	0	0.0065613	0.0065613	16,758
Right	1	0.0065145	0	0.0065145	16,879

Specific weight of steel	0.283	lb/in^3
Acceleration due to gravity	386.4	in/s^2
Density of steel (rho)	0.0007324	$lb.s^2/in^4$
Elastic modulus of steel E	3.00E+07	lb/in^2
Velocity of longitudinal wave in steel $v = (E/rho)^{1/2}$	202,389	in/s
=	16,866	ft/s
=	5,140	m/s

Table 3. Typical results of experiment

Figures 2 & 3 show the typical plots for left pencil break.

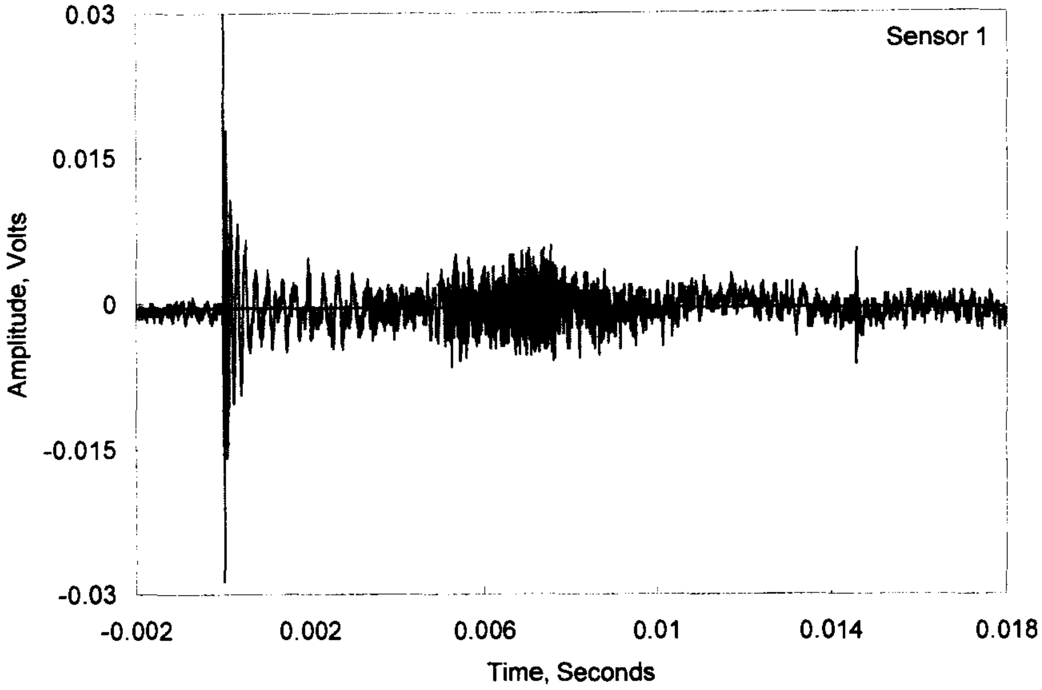

Figure 2 Left piezoelectric sensor signal for pencil break at left end of coil (peak location at 0 s and is the oscilloscope triggering event)

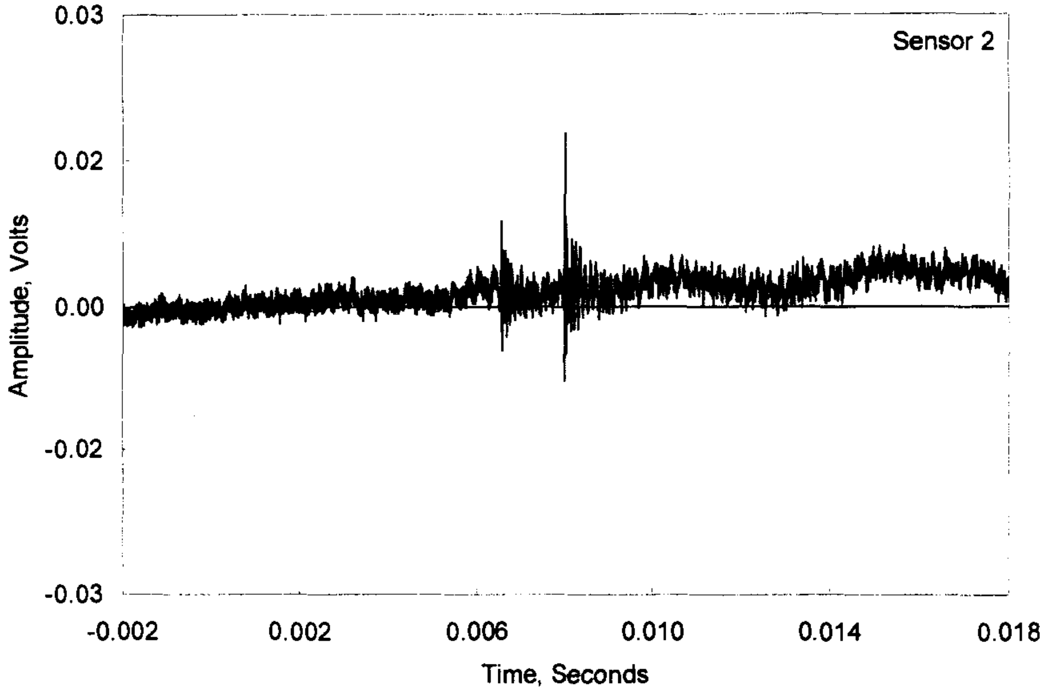

Figure 3 Right piezoelectric sensor signal for pencil break at left end of coil (notice initial peak at about 0.007 s and a second peak at about 0.008 s, a result of reflection of the wavetrain at the right end of the coil)

Conclusions

This paper reports on a fairly inexpensive test setup to expose students to a very sophisticated new generation of smart materials. Students are able to measure micro-timescale physical events and calculate meaningful values for physical properties and relate them to analytical quantities. Further, the nature of the experiment allows for generation of data by individual students and further statistical analysis of class data.

Acknowledgment

The authors wish to gratefully acknowledge financial, equipment and computing support for this project from the NSF Center for Advanced Materials and Smart Structures, the NASA Center for Aerospace Research and the NASA PAIR program at NC A&T State University.

Biographies

Devdas M. Pai is Associate Professor of Mechanical Engineering at NC A&T State University. He received his M.S. and Ph.D. from Arizona State University. He teaches manufacturing processes and machine design. A registered Professional Engineer in North Carolina, he serves on the Mechanical PE Exam Committee of the National Council of Examiners for Engineers and Surveyors and is active in the Manufacturing Division of ASEE.

Naresh R. Sundaresan was a Summer Research Student in 2002 at NC A&T State University. With support from the NASA Center for Aerospace Research, he worked with Dr. Pai on developing this experiment in the Intelligent Structures and Mechanisms Lab. A senior at Northwest High School in Greensboro, NC, he will graduate in 2003.

Natasha Cadenhead was a Sophomore Shadow student supported by the NASA-PAIR Program at NC A&T State University. A native of Kansas City, MO, Natasha is currently in her junior year in the Department of Mechanical Engineering and intends to pursue graduate school upon graduation.

SCIENCE FAIRS AS A VEHICLE TO INSPIRE THE NEXT GENERATION OF SCIENTISTS AND ENGINEERS

Roy K. Okuda

Department of Chemistry
San Jose State University

e-mail okuda@sjsu.edu

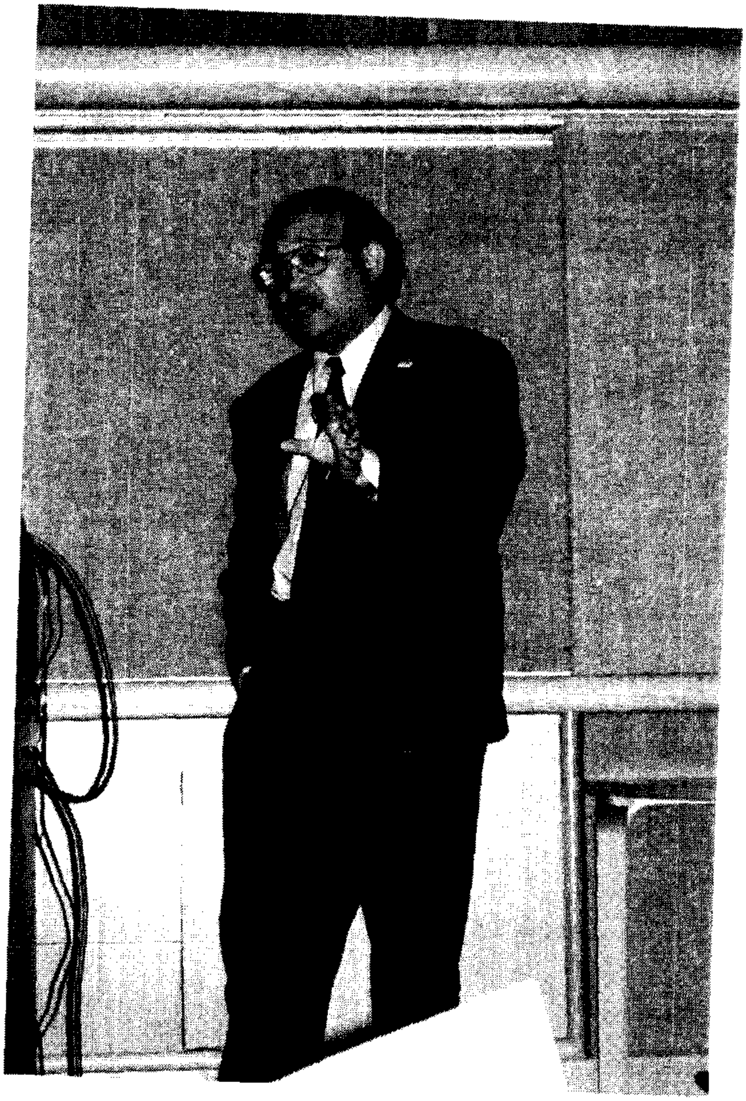

Roy K. Okuda

Science Fairs as a Vehicle to Inspire the Next Generation of Scientists and Engineers

Roy K. Okuda, Ph.D.
Department of Chemistry
San José State University

Why Science Fairs?

- Most communities in the US have existing science fairs, ranging from elementary to high school level
- The experience gives K-12 students an early introduction into performing hands-on experiments and critical thinking skills
- Can inspire students to continue to science and engineering majors in college

Levels of Science Fairs in the U.S.

- School Fair ("feeder fair")
- District or State Fair
- International Fair (e.g. Intel ISEF)

- Most fairs are held in the early spring

One community's approach: Science Fairs in Silicon Valley

- In 1999, Synopsys, Inc. provided $3M to establish a non-profit foundation to promote and sponsor activities related to science and engineering fair in the Santa Clara Valley.
- The mission of the Synopsys Outreach Foundation is to increase student interest in S&E, leading to increased numbers choosing these fields in college, and ultimately as careers
- Other area companies have joined to support the goals of the Outreach Foundation
- www.outreach-foundation.org

Science Fairs in Silicon Valley:

- The Synopsys Outreach Foundation oversees:
  - A program which provided stipends to high school *teachers* who *mentor students* in science fair projects, and material support for the projects
  - Research classes during the summer
  - The "Mad Science Laboratory" (opening Oct 30)
  - Two main events:
    - sciencepalooza! (middle school fairs)
    - The Synopsys Championship (the Intel ISEF affiliated Fair), in cooperation with the existing local science fair board

sciencepalooza!

- Mostly for junior high students
- An "introductory" science fair experience
- Projects are relatively simple
- Poster displays are judged
- Students, schools and teachers receive awards
- The experience has motivated many students to pursue more sophisticated projects for the Championship

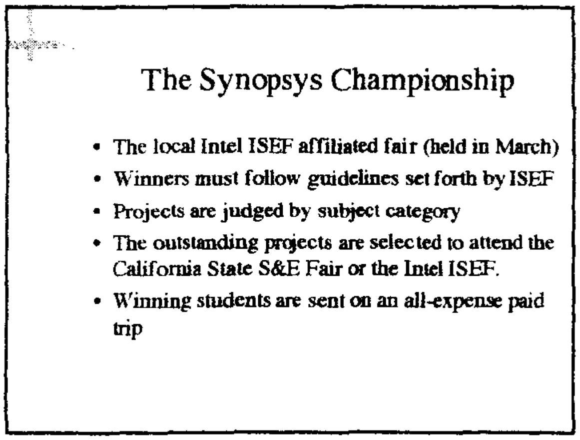

The Synopsys Championship

- The local Intel ISEF affiliated fair (held in March)
- Winners must follow guidelines set forth by ISEF
- Projects are judged by subject category
- The outstanding projects are selected to attend the California State S&E Fair or the Intel ISEF.
- Winning students are sent on an all-expense paid trip

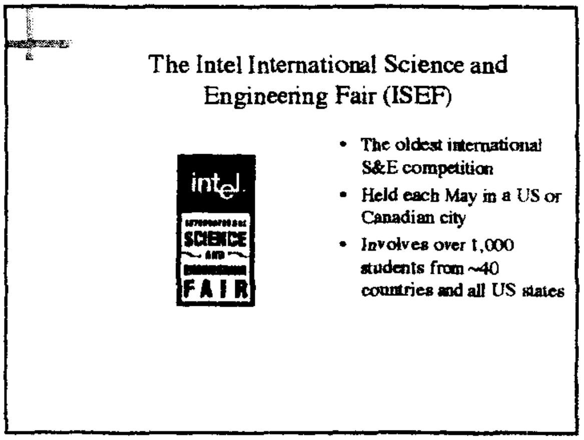

The Intel International Science and Engineering Fair (ISEF)

- The oldest international S&E competition
- Held each May in a US or Canadian city
- Involves over 1,000 students from ~40 countries and all US states

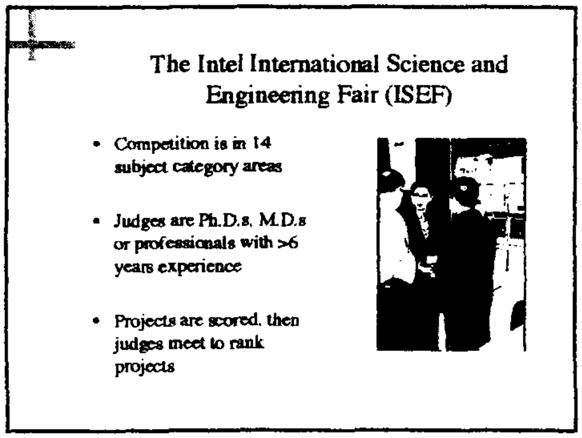

The Intel International Science and Engineering Fair (ISEF)

- Competition is in 14 subject category areas
- Judges are Ph.D.s, M.D.s or professionals with >6 years experience
- Projects are scored, then judges meet to rank projects

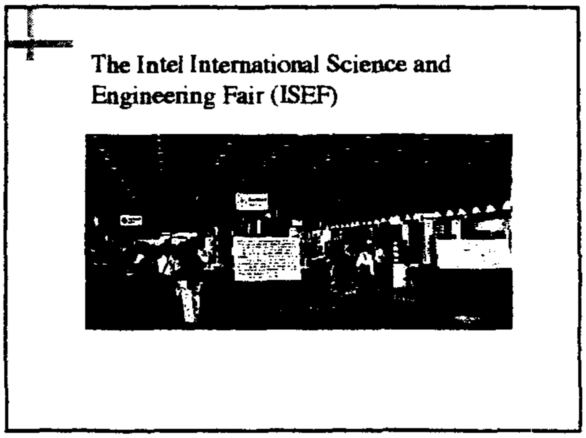

The Intel International Science and Engineering Fair (ISEF)

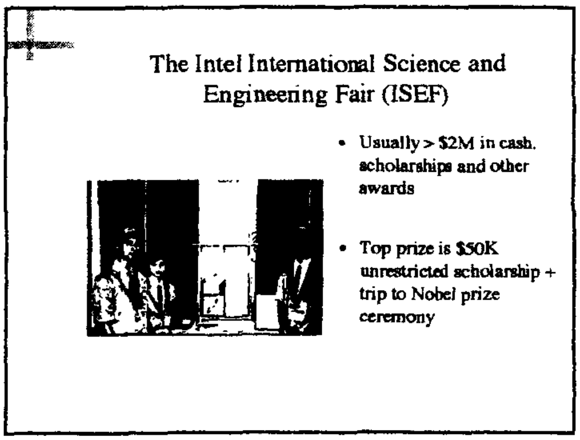

The Intel International Science and Engineering Fair (ISEF)

- Usually > $2M in cash, scholarships and other awards
- Top prize is $50K unrestricted scholarship + trip to Nobel prize ceremony

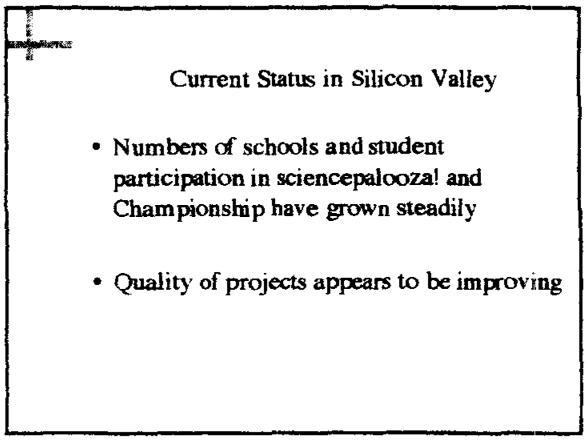

Current Status in Silicon Valley

- Numbers of schools and student participation in sciencepalooza! and Championship have grown steadily
- Quality of projects appears to be improving

The Challenges:

- For students
  - Time
  - Mentoring
  - Access to workspace, equipment
  - Family and/or peer perception
- For the science fair organization
  - Expense
  - Volunteer help
  - judges

Educators and Professionals: how you can support student involvement in science fairs

- At the local level:
  - Assist the local science fair organization
  - Offer mentoring help
    - One on one with a project
    - On specific aspects of conducting research
  - Financial or in-kind support
  - Promote among your company or professional societies

Educators and Professionals: how you can support student involvement in science fairs

- At the International level:
  - Volunteer to be a judge at Intel ISEF
    - Your help is needed for 2 days (Tues and Wed)
    - Cleveland (May 2003)
    - Portland, OR (tentative, May 2004)
  - www.sciserv.org

Summary

- Science and Engineering fairs need greater involvement by educators and professionals!
- This is one "cog in the wheel" to increase student interest in science and engineering

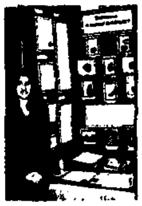

Acknowledgements

- Ms. Heidi Black (East Side Union HS District)
- Mr. Gary Robinson (President, Synopsys Outreach Foundation)
- Synopsys Outreach Foundation and Synopsys Championship Board

STATUS OF MATERIALS SCIENCE AND TECHNOLOGY (MST) CURRICULUM

John M. Rusin

Engineering Instructor
Edmonds Community College
20000 68th Avenue West
Lynnwood, Washington 98036-5999

Telephone: 425-640-1376
e-mail jrusin@edcc.edu

and

Thomas G. Stoebe

Professor Emeritus
Materials Science & Engineering
University of Washington
Box 352120
Seattle, Washington 98195-2120

Telephone: 206-543-7090
e-mail stoebe@u.washington.edu

John M. Rusin

Status of Materials Science & Technology (MST) Curriculum

John M. Rusin, Edmonds Community College,
20000 68th Avenue West, Lynnwood, WA 98036-5999, (425) 640-1376
jrusin@edcc.edu

Thomas G. Stoebe, Professor Emeritus, Materials Science & Engineering,
University of Washington, Box 352120, Seattle, WA 98195-2120, (206) 543-7090
stoebe@u.washington.edu

Materials Science and Technology (MST) are topics that excite students' interest because the student has everyday, hands-on experience with materials. Thus materials topics are great motivators in any engineering, technology or science course. Materials Science activities can also be used in both academic and vocational courses and thus assist in the transition for technology students across the high school-community college boundary.

Several institutions have developed MST activities and curriculum with support from the Department of Energy, the National Science Foundation, and other agencies. MST classes are currently being offered in several high schools throughout the U.S. Students obtain either science or technology credit for the class. MST curriculum has been aligned with National Science, Math, and Technology Standards and some state standards such as the Washington (State) Essential Academic Learning Requirements.

MST teacher training is currently offered by the NSF DUE/ATE Enhancement of Materials Technology for Manufacturing (EMTECH) program located at Edmonds Community College in Lynnwood, WA. EMTECH conducts workshops and institutes at several sites located throughout the U.S.

References & Resources

1. *Materials Science and Technology Teachers Handbook*, Battelle, Pacific Northwest National Laboratory, Karen J Wieda, Science Education Specialist / Science Education Programs, kj.wieda@pnl.gov , 509-375-3811, Battelle, Pacific Northwest National Lab, P.O. Box 999 / MS K1-12, Richland, WA 99352. See also http://www.pnl.gov/educationk20/mst.stm. The MST Handbook produced by PNL is used in our workshops and institutes. These web pages contain parts of the Handbook and other information and links relating to materials science curriculum.
2. *Materials Science Technology Curriculum Modules*, Energy Concepts Inc. - 404 Washington Blvd., Mundelein, IL 60060, Phone 847-837-8191 Fax 847-837-8171 info@energy-concepts-inc.com, http://www.energy-concepts-inc.com/

3. *Engineering Materials Technology: Structures, Processing, Properties and Selection*, 4/e, James A. Jacobs, Norfolk State University, Thomas F. Kilduff, (Emeritus) Thomas Nelson Community College, Copyright 2001, 767 pp., Cloth Bound with Disk format, ISBN 0-13-014280-8, Prentice-Hall, Inc., Upper Saddle River, NJ 07458, http://vig.prenhall.com/academic/product/1,3411,0130142808,00.html
4. *Introduction to Materials and Processes*, 1/e, John R. Wright, School of Technology, Central Connecticut State University, New Britain, CT, Larry D. Helsel, School of Technology, Eastern Illinois University, Charleston, IL, Delmar Publishers, 1996 ISBN/ISSN: 0-8273-5020-1, http://www.delmar.com/
5. *Materials World Modules*, Northwestern University, 2115 North Campus Drive, Evanston, IL 60208-2610. Modules in this series include: Biodegradable Materials, Biosensors, Ceramics, Composites, Designing Efficient Experiments, Infrastructure Materials, Materials and the Environment, Materials Design, Polymers, and Smart Sensors. http://www.materialsworldmodules.org/
6. MAST– Materials Science and Technology Teacher's Workshop, prepared by the Materials Science and Engineering department at the University of Illinois, Urbana/Champaign, Judy Brewer c/o MAST Modules, Department of Materials Science and Engineering, University of Illinois (UIUC), 1304 W. Green Street Urbana, IL 61801 (217) 333-1441, http://matse1.mse.uiuc.edu/~tw/
7. National Plastics Center & Museum, Valerie A. Wilcox, Executive Director, 210 Lancaster Street Route PO Box 639, Leominster, Massachusetts, USA Tel. (978) 537-9529, http://npcm.plastics.com
8. MTI – Materials Aspects of Manufacturing Technology, Dr. Thomas G. Stoebe, Materials Science and Engineering Department, University of Washington, http://depts.washington.edu/mti/. This is the web site for previous NSF materials science teacher-training grant at the University of Washington. Information and pictures from previous workshops and institutes can be found on this web site along with an extension list of web resource links.
9. EMTECH – Enhancement of Materials Technology of Manufacturing, http://emtech.edcc.edu. This is the web site for the current NSF materials science teacher-training grant at Edmonds Community College.
10. Materials Science and Technology: What do the Students Say? http://scholar.lib.vt.edu/ejournals/JTE/v5n2/whittaker.jte-v5n2.html. This article is by Guy Whittaker, one of our master teachers and a teacher of MST at Coupeville High School, Coupeville, WA. It is an excellent overview of the program.
11. National Science Education Standards – http://www.nap.edu/readingroom/books/nses/html/
12. Materials Education Library – a resource for Materials Educators and Students, www.materialseducation.org The site is under construction.
13. Chemistry and Materials Workshop – Sponsored by the Institute for Chemical Education (ICE) and the National Science Foundation (NSF), http://ice.chem.wisc.edu/materials/teachersusing.html

14. Institute for Chemical Education (ICE), Kathleen M. Shanks, Outreach Program Manager, Department of Chemistry, 1101 University Avenue, Madison, WI 53706-1396, 608-262-2940, 800-991-5534 FAX: 608-265-8094, shanks@chem.wisc.edu, http://ice.chem.wisc.edu/ice
15. American Plastics Council, Catherine Norris, Associate Director, Education, 1300 Wilson Boulevard, Suite 8000, Arlington, VA 22209, 703-253-0619 FAX: 703-253-0701, Cathy_Norris@plastics.org, www.plastics.org.
16. University of Wisconsin Materials Research Science and Engineering Center on Nanostructured Materials and Interfaces, http://mrsec.wisc.edu/edetc/
17. CORD – Center for Occupational Research and Development, Dan Hall, President and Chief Executive Officer, 800-972-2766, hull@cord.org, http://www.cord.org/index.cfm
18. Pitsco Inc., 800-835-0686, http://www.pitsco.com, orders@pitsco.com, source of laboratory supplies
19. Education Innovations Inc., 888-912-7474, http://www.teachersource.com, info@teachersource.com, source of laboratory supplies
20. Flinn Scientific Inc., P.O. Box 219, Batavia, IL 60510, 800-452-1261, http://www.flinnsci.com, source of laboratory supplies including "happy/sad balls."
21. Rio Grande, 7500 Bluewater Road NW, Albuquerque, NM 87121-1962, 1-800-545-6566, 1-505-839-3300 FAX 1-505-839-3310, http://www.riogrande.com,
22. IASCO – Industrial Arts Supply Co., 5724 West 36th Street, Minneapolis, MN 55416-2494, 1-888-919-0899, 952-920-7393, FAX 952-920-2947 http://www.iasco-tesco.com
23. KEVIN Technology, 280 Adams Blvd, Farmingdale, NY 11735, 1-800-535-8469, 1-631-756-1750, FAX 1-800-756-1025, 1-631-756-1763, http://www.kelvin.com
24. Otto Frey and Jules Borel, P.O. Box 796, 126 Second Street, Oakland, CA 94604, 800-772-3456, 510-832-0355 FAX: 800-900-3734, 510-834-6217
25. Seattle Pottery Supply, 35 South Hanford, Seattle, WA 98134, 1-800-522-1975, 206-587-0570, FAX: 888-587-0373, 206-587-0373, http://www.seattlepottery.com
26. Northwest Art Glass, 9003 151st Avenue NE, Redmond, WA 98052, 800-888-9444, 206-861-9600, FAX 206-861-9300
27. Fiberlay Inc., 2425 NW Market St, Seattle, WA 98107, 1-800-942-0660, fiberlay@fiberlay.com, http://www.fiberlay.com, source of resins, cloth, and supplies for making composite beams. Educational discount available.

ATTENTION-GETTING MATERIALS SCIENCE DEMONSTRATIONS

John M. Rusin

Engineering Instructor
Edmonds Community College
20000 68th Avenue West
Lynnwood, Washington 98036-5999

Telephone: 425-640-1376
e-mail jrusin@edcc.edu

Attention-Getting Materials Science Demonstrations

John M. Rusin, Edmonds Community College, 20000 68th Avenue West, Lynnwood, WA 98036-5999, (425) 640-1376, jrusin@edcc.edu

In the Materials Science & Technology (MST) teacher training workshops and institutes conducted by the NSF Enhancement of Materials Technology for Manufacturing (EMTECH) program at Edmonds Community College we use several quick, attention-getting demonstrations that teachers can use to "hook" their students. Most of the activities have been picked up from other sources including the MST master teachers in our program.

Happy/Sad or Decision Balls

Two balls that look identical are dropped from the same height onto a hard surface. One bounces to almost the same eight while the other does not bounce. Although the two balls have some similar physical properties, such as size, color, and density, they differ greatly in elasticity. Happy Balls contain highly cross-linked neoprene rubber or polybutadiene resulting in the high resiliency. If cooled, Happy Balls will not bounce as well. Sad Balls are composed of several different materials including butyl rubber and a block co-polymer of poly(styrene-butadiene) or a block co-polymer of poly(vinyl-butadiene); or polynorbornene rubber. Molecules in Sad Balls absorb most of the energy of the fall and thus do not bounce. If heated in boiling water, Sad Balls will bounce [1,2]. You can make your own Happy/Sad Balls from Dow Corning Slygard 184 elastomer [3]

Sources: Educational Innovations, Flinn Scientific

NiTinol Memory Metal

NiTinol memory metal has two crystalline phase forms with a transition temperature between 30° and 50°C. At high temperature the NiTinol alloy prefers the Austenite phase while at low temperature, the alloy prefers the Martensite phase. Because the Martensite phase crystal structure consists of a series of planes that may be displaced, it can be deformed. The Martensite structure has 24 different variants to carry out this transformation and, as a result, can be deformed in nearly any direction. When the alloy is heated to the Austenite phase, the planes are slid back into place and the structure reverts to its original form.

A sample of NiTinol wire can be "set" into a shape by heating to 500°C. Typical sample shapes include a straight wire, a four-leaf clover, and a paper clip. The wires can be deformed at room temperature and when heated to the transition temperature of 50°C (hot water or a hair dryer), they will return to their original "set" shape [1].

Source: Educational Innovations

Water Loc (Sodium Polyacrylate)

Sodium polyacrylate ($(CH_2\text{-}CH)_nCOONa$) is the sodium salt of polyacrylic acid ($(CH_2\text{-}CH)_nCOOH$). Like all polymers, this is a long-chain molecule, but in this case is also a "salt" with Sodium. The entire molecular array functions as a semi permeable membrane. This means that, on either side of the membrane [in this case, inside and outside the molecular array] the solutions strive for equal sodium concentration. Thus, very pure water will be absorbed very well, diluting the sodium solution within the array. The more salt you have in the water, the less water will be absorbed [4].

Take three paper cups and put a small amount of soldium polyacrylate into each of them. You can slightly moisten the powder to allow the cup to be turned upside down. Arrange the cups for the classic shell game. Pour some water into one of them. Shuffle the cups and ask a student to select which one has the water in it. Turn the cup upside down to show that there is no water in the cup. For greater effect, turn the cup over the student's head! At the end of the activity, add salt to the water absorbed sodium polycrylate to reverse the process.

Sources: Educational Innovations, Flinn Scientific

Heat Treating a Bobby Pin

Heat the "U-shaped" end of a bobby pin in the flame of a propane torch or Bunsen burner. Slow cool one of the heated bobby pins in air and quench another heated bobby pin in water. Hand out to students and have them pull the pins apart. The slow cooled pin should still bend but the water quench pin should break. Water quench another bobby pin and then gently reheat in the flame and slow cool. The reheated and slow cooled pin should no longer be brittle.

Steels (alloys of iron with up to 1% carbon) can also be hardened by heating and quenching. At high temperatures (red hot), iron has a face-centered cubic (FCC) structure, which can dissolve carbon. At low temperature, the iron changes to body-centered cubic (BCC), which cannot dissolve carbon, so it precipitates as an iron-carbon compound. If quenched, this compound does not have time to form; the carbon is trapped and distorts the BCC crystal structure to create a new, hard and brittle structure called Martensite. If Martensite is gently heated, the carbon can precipitate giving a strong, tough structure [5].

Cold Working or Work Hardening of Copper

Hammer pieces of 16 or 18-gauge solid copper wire of copper wire until it is about half its original thickness. Bend the flattened wire back and forth several times. Observe. Heat the flattened (work hardened) piece of copper in the flame of a Bunsen burner or propane torch until red-hot. Quickly quench the wire in a beaker of water to prevent it from oxidizing rapidly in the air. (Note: the wire may also be slow cooled without quenching). Bend the heat-treated wire back and forth several times. Observe.
Because plastic deformation results from the movement of dislocations, preventing this motion can strengthen metals. When a metal is deformed, new dislocations are produced. As dislocations are generated and move, the metal can be bent or shaped without

cracking. As the number of dislocations in the crystal increases, they will get tangled or pinned and will not be able to move. This will strengthen the metal, making it harder to deform. When this is done at or near room temperature, the process is known as cold working. When cold-worked metals are annealed (heated gently), new grains form from the cold worked structure and grow until they replace it with new, soft crystals [5, 6].

"GAK"

Polymer cross-linking can be easily demonstrated by making "GAK" (Elmer's Glue™ and Borax) or Slime (4% Polyvinyl Alcohol solution and 4% sodium borate or borax solution) [7]. I prefer to make GAK as the materials are readily obtained from a grocery store. Dilute 10 ml of Elmer's Glue with 10 ml of water. Prepare a 4% borax solution by supersaturating borax in water. Pour 20 ml of the Elmer's glue solution into a cup. Add 10 ml of the cross linker (borax solution) to each cup. Immediately begin stirring the solutions together using the wooden stick. Another source of sodium borate is liquid laundry starch such as Sta Flo™. Use equal portions of Elmer's Glue and liquid starch.

Elmer's glue is copolymer polyvinyl alcohol, PVA, a plastic made from oil. Borax is a natural mineral mined from the earth made of boron, sodium, oxygen and water. When you add water to Elmer's glue the PVA, being unstable, starts to dissolve in the water. When you add the wet borax, it is slightly acidic, and it reacts with the PVA to cross-link. This cross-linking causes the mixture to undergo an irreversible gelation [8].

References & Resources

1. Education Innovations Inc., 362 Main Avenue, Norwalk, CT 06851, 888-912-7474, 203-229-0730, FAX: 203-229-0740, http://www.teachersource.com, info@teachersource.com,
2. Flinn Scientific Inc., P.O. Box 219, Batavia, IL 60510, 800-452-1261, http://www.flinnsci.com
3. Elastomers, Materials Science Workshop, ICE and NSF 1998, http://ice.chem.wisc.edu/materials/elastomers.html Institute for Chemical Education (ICE), Kathleen M. Shanks, Outreach Program Manager, Department of Chemistry, 1101 University Avenue, Madison, WI 53706-1396, 608-262-2940, 800-991-5534 FAX: 608-265-8094, shanks@chem.wisc.edu
4. Experiment of the Month May 1997 A Plastic that "Grows", National Plastics Center & Museum, 210 Lancaster Street Route PO Box 639, Leominster, MA, (978) 537-9529, http://npcm.plastics.com/slimystuff4.html
5. MAST Metals Experiment 3 – Cold-working & Annealing, Materials Science and Engineering department at the University of Illinois, Urbana/Champaign, 1304 W. Green Street Urbana, IL 61801 (217) 333-1441 http://matse1.mse.uiuc.edu/~tw/
6. ECI – Annealing Copper, *Materials Science Technology Curriculum Modules*, Energy Concepts Inc. - 404 Washington Blvd., Mundelein, IL 60060, Phone 847-837-8191 Fax 847-837-8171 eciconcepts@energy-concepts-inc.com, http://www.energy-concepts-inc.com/

7. MAST Polymer Experiment 2 – Slime Away, Materials Science and Engineering Department at the University of Illinois, Urbana/Champaign, 1304 W. Green Street, Urbana, IL 61801 (217) 333-1441 http://matse1.mse.uiuc.edu/~tw/
8. MAST Polymer Experiment 3 – A Silly Polymer Cross-Linking a Polymer to Create Everyone's Favorite Childhood Toy, Silly Putty, Materials Science and Engineering department at the University of Illinois, Urbana/Champaign, 1304 W. Green Street, Urbana, IL 61801 (217) 333-1441 http://matse1.mse.uiuc.edu/~tw/

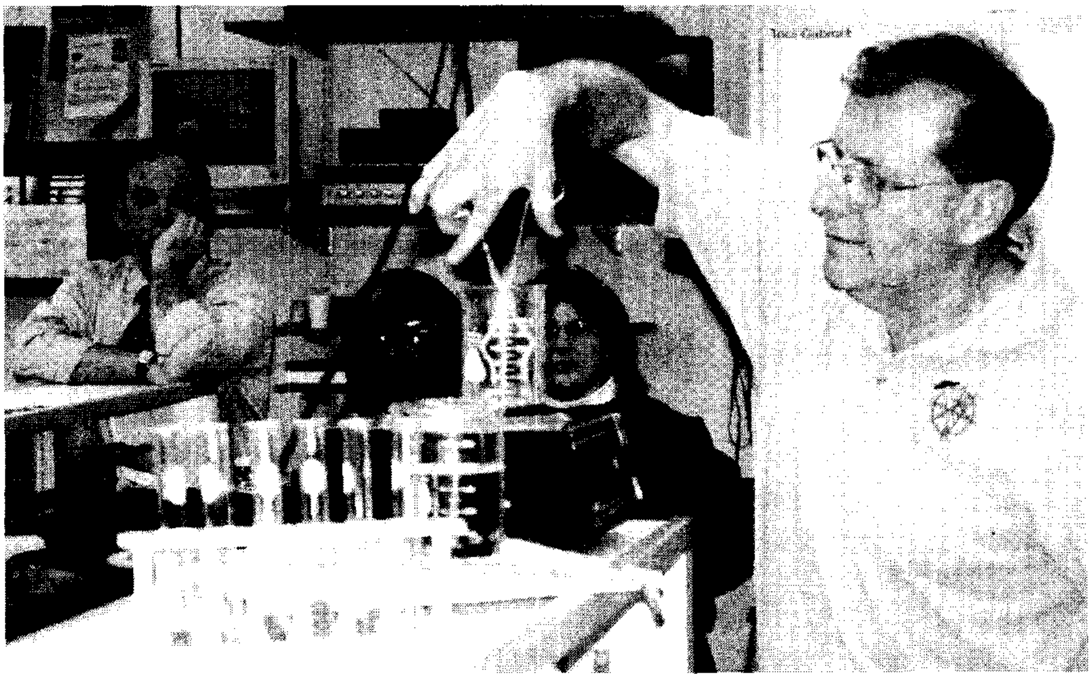

Materials Science and Technology Workshop

COMPOSITES APPROACHING NEUTRAL DENSITY IN WATER

L. Roy Bunnell

Teacher, Materials Science Technology
Southridge High School
Kennewick, Washington 99338

Telephone 509-734-3800
e-mail Bunnro@ksd.org

L. Roy Bunnell

COMPOSITES APPROACHING NEUTRAL DENSITY IN WATER

L. Roy Bunnell
Teacher, Materials Science Technology
Southridge High School
Kennewick, WA 99338

KEY WORDS: Composites, Neutral Density, Epoxy, Microballoons

PREREQUISITE KNOWLEDGE: Students should have a general understanding of the concept of density, and some experience mixing and casting epoxy resins.

REQUIRED MATERIALS:
Pumpoxy-UV epoxy, in containers with metering pumps, Industrial Arts Supply Co.
3M Glass Microballoons, Industrial Arts Supply Co., Minneapolis, MN
Paper Mixing cups and Popsicle sticks for stirring, same supplier as above
CAUTION: THE VERY SMALL SIZE AND LOW DENSITY OF MICROBALLOONS MAKE THEM HIGHLY RESPIRABLE. THE MICROBALLOONS SHOULD BE HANDLED ONLY WITH SUITABLE VENTILATION, SUCH AS AN OPEN-FACED HOOD.

INTRODUCTION

According to Archimedes, a solid object that displaces a volume of fluid with a weight exactly equal to the object's own weight is said to be neutrally buoyant in that fluid. Absolute neutral buoyancy is rarely if ever achieved, but the concept provides an interesting problem to be solved by the proper application of composite concepts. Loosely defined, a composite material is composed of at least two separate materials, combined to provide (generally mechanical) properties that are superior to those of the separate ingredients. By using two materials with appropriate densities, it should be possible to make a material with a bulk density approaching that of water. The lab described below provides some simple methods to produce such composites, and to measure how close their density is, at least in relative terms, to that of water.

EXPERIMENTAL

In principle, achieving neutral buoyancy in water requires only that two materials --one denser than water and one less dense—be combined in the proper ratio. For the two materials, I chose an epoxy resin and glass microballoons. These microballoons are hollow glass spheres, produced as a filler for polymers such as epoxies, where they perform as thickeners or density reducers and enable the cured epoxy to be sanded to a very fine finish. Figure 1 is a scanning electron micrograph of some of these microballoons, and shows that they are very spherical and quite variable in size.

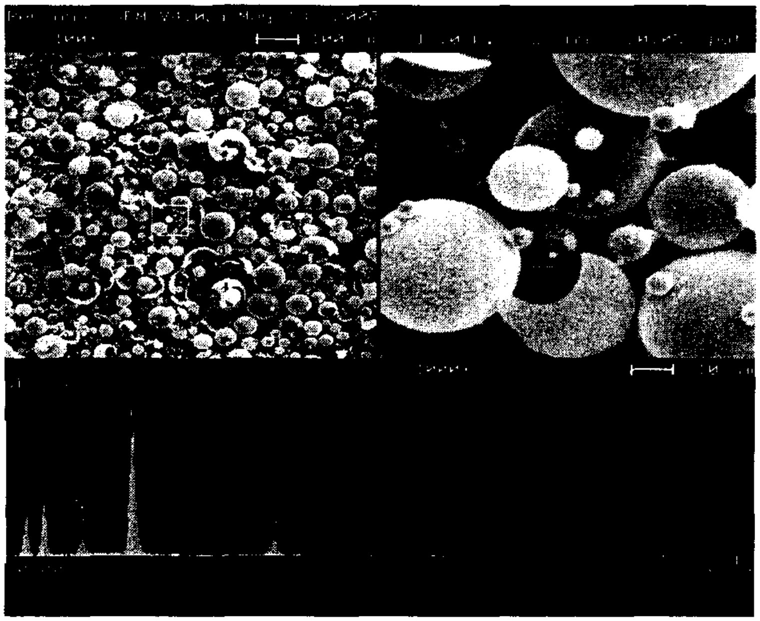

Fig. 1. SEM Micrograph of Glass Microballoons, at Low Magnification.

At a higher magnification, see Fig. 2, it can be seen that the balloons have very thin walls. Their density is extremely low; the bulk density is approximately 0.07 grams/cc.

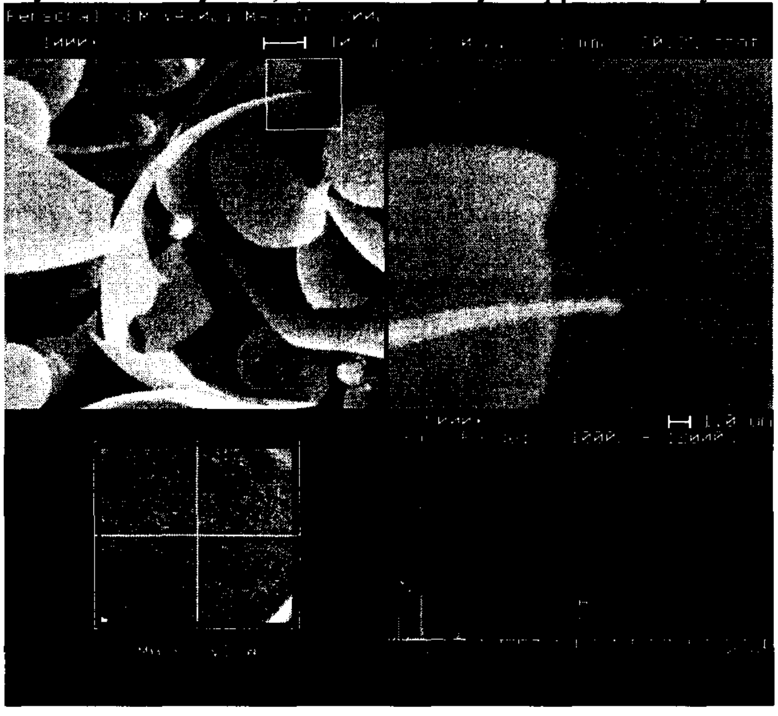

Fig. 2. Glass Microballoons, at Higher Magnification, Showing very thin walls. Spectrum indicates that the Glass Composition is Similar to Common Window Glass.

In principle, if the density of the epoxy and the lower-density material are both known, the proportion of each needed to produce a given density can be calculated by simple algebra. However, the true density of these tiny microballoons is not simple to measure, and they are so light that very precise weight measurements would be required to add the proper amount. So I decided that measuring the microballoons by volume would be more reproducible, especially for my high school students. A cooking measure (1/4 tsp) appeared to work very well, since the surface could be struck off flat using a straightedge to produce a reproducible volume.

Since the only certainty was that the epoxy was denser than water (it sinks in water) and the microballoons are less dense (they float), an iterative approach appeared to be the most reasonable way to approach the problem. Using values from the previous school year for some initial guidance, students were instructed to weigh out between 7 and 10 grams of premixed epoxy and hardener, and add a carefully-measured ¼ tsp of microballoons, stirring minimally to blend the materials while not introducing many air bubbles. The batches of epoxy/microballons were then placed in a vacuum chamber to eliminate air bubbles, then cast into a plastic ice-cube tray, see Fig. 3.

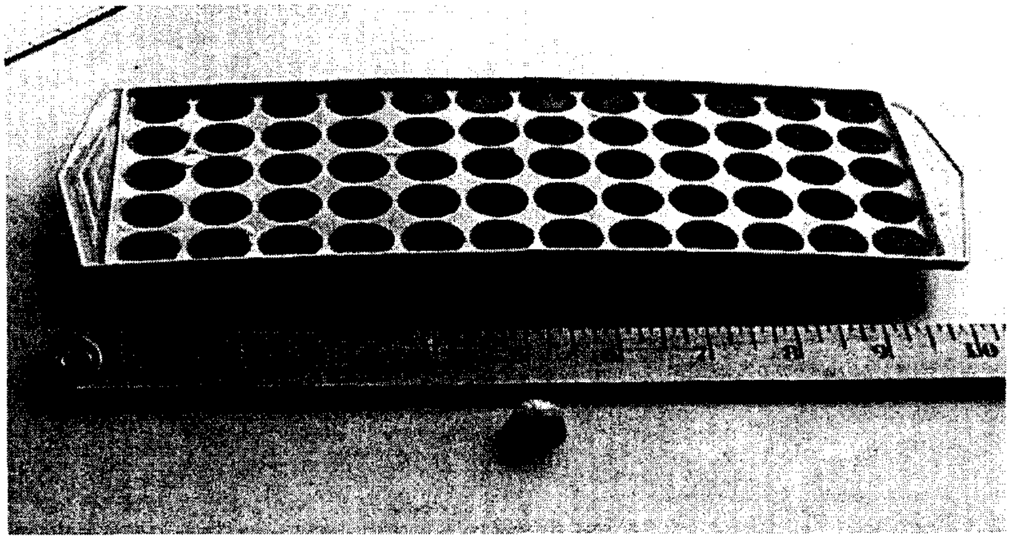

Fig. 3. Ice-cube Tray Used as a Mold for Composite Specimens; Tray makes up to 60 Specimens at a time.

Each student floated a tiny piece of paper, with their initials and period number, on the surface of the epoxy, so they could identify their specimens later. The epoxy was then cured for 1 h at a temperature of 60 degrees Celsius.

RESULTS:

The density of the specimens could have been measured by Archimedes' Method, but a simpler method was used which was easier and more interesting for students. This method was simply to release the specimens at mid-height in a 1000-cc graduated cylinder, then to use a stopwatch to time how long the specimen took to rise to the surface or sink to the bottom of the cylinder. The specimens are all similar in size and shape, so a graphical comparison of the sink/float times should be able to detect the proper amount of epoxy to approach neutral density. Note that, at this stage, we do not care whether specimens floated or sank, just how much time they took to do either. A peak should appear on a plot of sink/float times as a function of epoxy/microballoon ratio. Figure 4 shows a plot from this year's work, and a somewhat poorly defined peak can be seen between 2 and 6 grams of epoxy per ¼ tsp of microballoons.

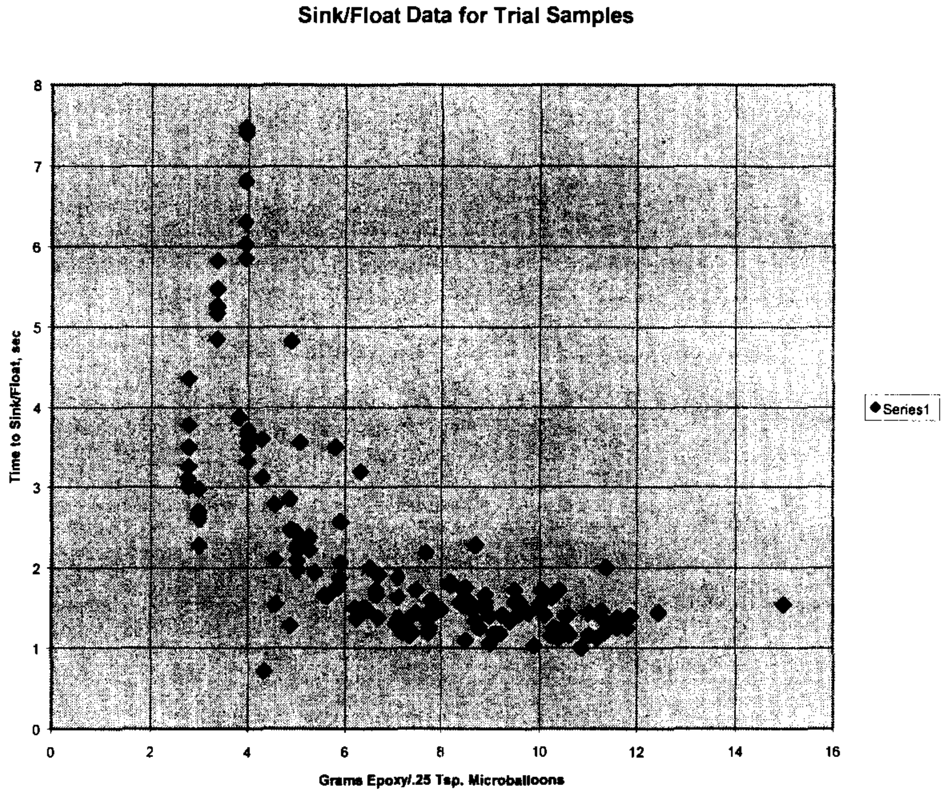

Fig. 4. Sink/Float times for First Round of Neutral-Buoyancy Composites

The peak did not appear at the location expected from the previous year's work; this was apparently caused by the fact that the current year used a different brand of epoxy. The bulk density of the epoxies, measured by Archimedes' Method, are 1.09 and 1.17 grams/cc, respectively, for last year's and this year's epoxies. Since the volume of microballoons is constant, a greater weight of the less-dense epoxy would be required to approach neutral buoyancy.

Once the peak was defined by the scouting experiments, a second round of specimens was prepared by the students, who were directed to examine the plot and prepare their "official" specimen to have the epoxy/microballoon ratio which would produce the longest time to sink or float. Students took extra care in their measurements this time, having benefited from the experience of the scouting experiment. Once again, students identified their specimens using the small pieces of paper.

Testing the specimens, done the following day, took the form of a "race" in which the slowest competitor was the winner. Students were fairly excited about the competition, and were surprised to see that specimens closest to neutral density would appear to "hover", if only for a period of a few minutes; see Fig. 5. this year's winning racer required about 3 minutes to surface. With more refinements, this time is expected to increase further.

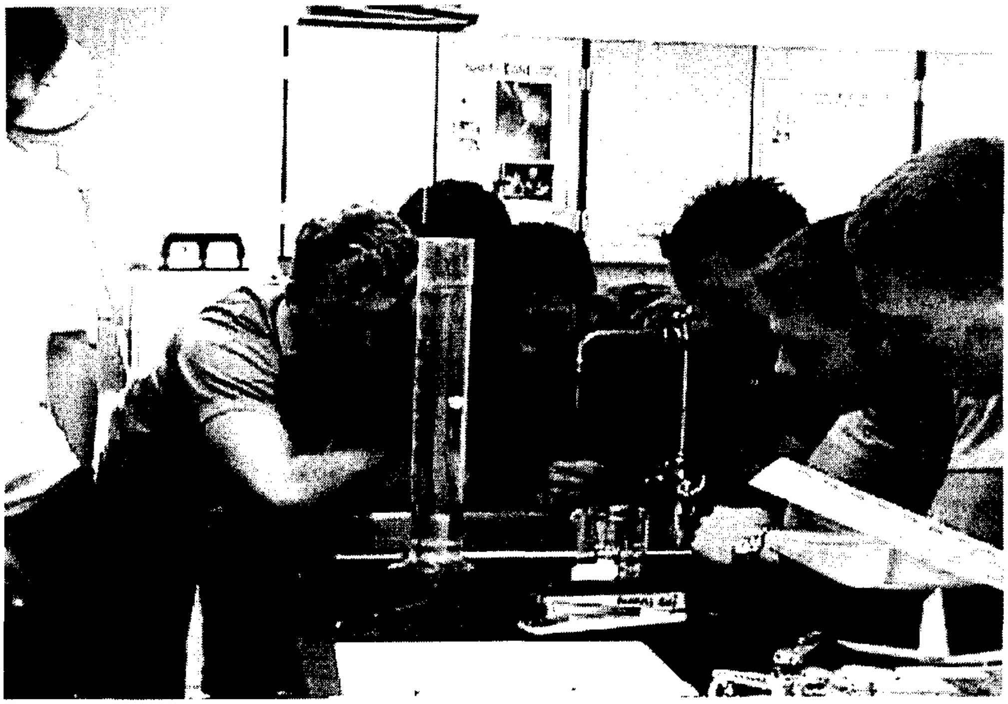

Fig. 5. Students Racing Neutral-Density Composites.

Since the microballoons tended to float to the surface, there was an additional opportunity for "tuning" on race day. Students could sand the top surface if racers were too buoyant, or sand the bottom if they were too dense. Figure 6 shows a plot from the actual race, and shows that performance generally increased as a result of students having a target as a result of the scouting experiment. This process of iteration could be repeated if time permitted, but the point of this iterative experiment appeared to have been made in two cycles. In summary, this lab activity appeared to be of high interest for students, and demonstrates both that composites can be made for various purposes and that iteration can sometimes be substituted for more precise data.

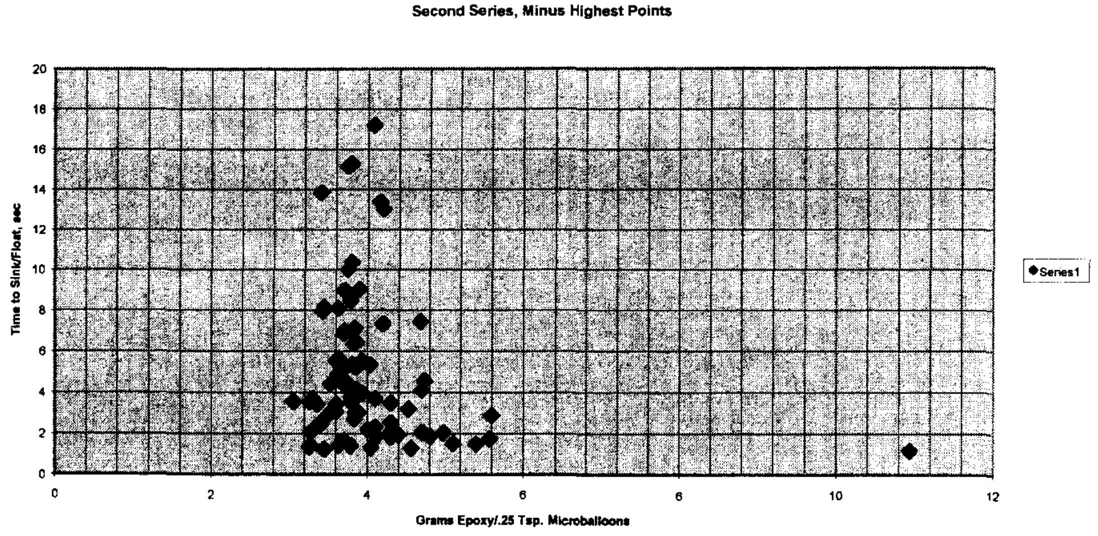

Fig. 6. Sink/Float Times for Second Series of Composites, with longest times omitted. The longest times were on the order of 3 minutes.

SCIENCE EXPLORATIONS WITH SIMPLE MATERIALS FROM THE EXPLORATORIUM

Paul Doherty

Senior Staff Scientist
The Exploratorium
3601 Lyon Street
San Francisco, California 94123

e-mail Pauld@exploratorium.edu

Paul Doherty

Science Explorations with Simple Materials
From The Exploratorium

By Paul Doherty
Senior Staff Scientist
Pauld@exploratorium.edu
The Exploratorium
3601 Lyon St.
San Francisco, CA 94123

The Exploratorium

The Exploratorium Website: www.exploratorium.edu
Online Explorations: www.exploratorium.edu/explore/online.html
Hands-on Activities: www.exploratorium.edu/explore/handson.html
Exploratorium Books: www.exploratoriumstore.com/clasres.html

Many new science explorations can be found in the book *Square Wheels*, from the Exploratorium.

Paul Doherty's website

Paul's Website: http://www.exo.net/~pauld
This website contains over a hundred explorations for science teachers and students.

A written version of this lecture

Written versions of the explorations demonstrated during this lecture are posted on Paul's website.

The Exploratorium Teacher Institute Workshops for science teachers.

The Exploratorium Teacher Institute offers 4 week summer institutes for high school physics, and biology teachers, and for middle school mathematics, life sciences, and physical science teachers. Teachers attending these institutes receive a stipend. For information, go to: http://www.exploratorium.edu/ti


Square Wheels
AND OTHER EASY-TO-BUILD, HANDS-ON SCIENCE ACTIVITIES
Don Rathjen
Paul Doherty
and the Exploratorium Teacher Institute
AN EXPLORATORIUM
exploratorium
SAMPLE ACTIVITY INSIDE!
TABLE OF CONTENTS ON BACK

ELECTRICITY • MAGNETISM • SOUND

Modulated Coil

Hear the magnet!

Using a simple electromagnet, you can wirelessly transfer the sound from a radio to the speaker of a tape player.

Materials

- wire stripper or knife
- about 3 ft (1 m) of insulated wire (e.g., RadioShack #20 or #22 solid copper wire with plastic insulation)
- steel bolt, about $\frac{1}{4}$-in diameter and 2 in long (nut optional); exact size of bolt is not critical
- audio cable, 6 ft (2 m), $\frac{1}{8}$-in phone plug on one end and two alligator clips on the other (e.g., RadioShack #42-2421; a phone plug is sometimes called a mini plug)
- small radio with headphone jack (e.g., RadioShack #12-799)
- portable tape cassette player with speaker (if the player doesn't have its own speaker, you'll have to have the headphones on)

TABLE OF CONTENTS

exploratorium
teacher institute

teacher induction program

The Exploratorium Teacher Institute (TI) has been offering workshops in content and pedagogy to middle and high school science teachers since 1984. Our mission is to help these teachers infuse their classes with hands-on activities, scientific inquiry, and strong content. Teachers who participate in the four-week introductory Summer Institute return to the museum as Teacher Institute alumni for ongoing professional development throughout their careers. The Teacher Institute is now a professional home to well over two thousand alumni—many have been active participants for over ten years.

In 1998, the Teacher Institute noticed a sharp increase in the number of beginning science teachers applying to our Summer Institute. We also found that many of our most experienced alumni were retiring from classroom teaching, yet were eager to help other teachers and continue their association with the Exploratorium.

We took the opportunity presented by this "changing of the guard" to create a two-year program for novice science teachers (TI Beginning Teacher Program) and another two-year program designed to train and support a group of experienced TI alumni who would serve as their mentors (TI Leadership Program). The programs make up the Exploratorium Teacher Induction Program. The primary goal of the program is to support, retain, and develop the next generation of science teachers, while also inducting them into the larger community of exemplary teachers who make the Exploratorium Teacher Institute their professional home.

The Exploratorium Teacher Institute is generously funded by The National Science Foundation, The Noyce Foundation, The William and Flora Hewlett Foundation, Carnegie Corporation of New York, Clarence E. Heller Charitable Foundation, Pacific Bell Foundation, The Mary A. Crocker Trust, California Department of Education, William Randolph Hearst Endowment, Phyllis Wattis Endowment, and Hambrecht Fellowship Endowment. The Exploratorium is designated as The California Regional Science Resource Center.

Beginning Teacher Program

Beginning science teachers at the middle and high school level are a diverse group with varying needs. Some are recent graduates of teacher-education programs, while others are still working on their credentials. Some have strong science backgrounds, whereas others have a more limited understanding of content. Because beginning science teachers differ so greatly in background and need, the TI Beginning Teacher Program offers participants a wide variety of content workshops, support-group meetings, teaching seminars, and in-class coaching sessions from which to choose. With the guidance of Exploratorium staff and experienced science teachers (who are also active participants in Teacher Institute programs) serving as their mentors, beginning teachers tailor the program to meet their unique needs.

Each fall, thirty beginning science instructors who teach in the San Francisco Bay Area start the two-year support program. Novices are required to attend four science-content workshops, a minimum of four teaching seminars, and a minimum of four support-group meetings each year. New teachers also receive classroom visits by experienced science teachers (either on sabbatical or retired from teaching), who coach them as they lead hands-on, inquiry-based activities.

After the first academic year, all novices attend the Summer Institute led by staff scientists, staff science educators, and Teachers in Residence. Beginning teachers attend the Summer Institute alongside experienced teachers from all around the country. During the second academic year, participants continue to attend workshops, teaching seminars, and support-group meetings—and continue to receive coaching from experienced teachers. At the end of the two years, the novices join the ranks of over two thousand alumni of the Teacher Institute and are eligible to return for advanced institutes, to attend Saturday workshops, and to take advantage of the vast selection of educational materials and resources available at the Exploratorium.

Leadership Program

The Exploratorium Teacher Induction Program also trains and supports experienced science teachers who then serve as mentors and in-class coaches for our beginning teachers. Each year, fifteen alumni of the Teacher Institute are selected to begin a two-year commitment as mentors.

Training begins with a four-week summer Leadership Institute where the Exploratorium staff prepares these alumni for their new roles. During the school year, the Exploratorium staff continues to work closely with the mentors on an individual basis, helping experienced teachers sharpen their mentoring and coaching skills. The most successful mentors are then asked to join the Leadership Training Institute the following summer, where they share their insights and expertise with a new group of exemplary teachers about to start their two-year service to beginning science teachers in the Teacher Induction Program.

For More Information

If you know a beginning middle or high school science teacher in the Bay Area who needs support, or if you would like more information about our Teacher Induction Program, please see our Web site at www.exploratorium.edu/ti. You may also contact Linda Shore, Director of the Teacher Institute (lindas@exploratorium.edu); Karen Mendelow Nelson, Program Manager of the Exploratorium Teacher Institute (teacher_institute@exploratorium.edu); or the Exploratorium Teacher Institute by phone at (415) 561-0313.

Exploratorium Teacher Institute   3601 Lyon Street   San Francisco, CA 94123
(415) 561-0313   FAX (415) 561-0307

Exploratorium Teaching Resources

Teacher Institute Publications

The Teacher Institute staff has produced several science and mathematics publications that are excellent classroom resources. The Exploratorium Science Snackbook Series provides "recipes" for creating small, inexpensive versions of the Exploratorium's most popular exhibits. The latest book in this series, *Square Wheels and Other Easy-to-Build. Hands-On Science Activities*, contains thirty-one of these projects. Other books include *Math and Science Across Cultures*, with creative experiments featuring games, art, music, and everyday activities from around the world. *Human Body Explorations: Hands-On Investigations of What Makes Us Tick*, contains twenty-eight activities enabling learners to discover how their bodies function on microscopic and macroscopic levels. *Math Explorer* provides a variety of engaging, hands-on activities for middle school students, and the *Science Explorer* series presents enriching projects for parents and children, ages 6–10, to do at home. *Traces of Time: The Beauty of Change in Nature* and *The Color of Nature* both contain stunning color photographs and lively text that encourage readers to observe and discuss nature in a completely different way. Available from the Exploratorium Store: www.exploratoriumstore.com.

Exploratorium Learning Studio

The Exploratorium Learning Studio offers further support for science and mathematics teaching by maintaining an extensive collection of books, journals, and videos. Alumni of the Teacher Institute may borrow materials at any time. Browse the Learning Studio catalog online at www.exploratorium.edu/ls. Other educators may borrow materials by purchasing an "Educator Membership" from the Exploratorium at www.exploratorium.edu/membership.

Web Sites

The Teacher Institute's Web site at www.exploratorium.edu/ti contains information about our program as well as classroom-tested activities we have developed. Alumni of the Teacher Institute can engage in online conversation on the Teacher Institute's listserv, Pinhole. Teachers provide resource information, present questions students have asked, discuss science in current events, and suggest activities. Access to Pinhole is given to all Teacher Institute participants.

www.exploratorium.edu/ti

Teacher Institute Staff

Tory Brady, Teacher in Residence, Beginning Teacher Program
Paul Doherty, Co-Director, Senior Scientist, Teacher Institute
Lori Lambertson, Coordinator Beginning Teacher Program, Staff Teacher
Karen Kalumuck, Staff Biologist
Eric Muller, Staff Teacher
Karen Mendelow Nelson, Program Manager/Educator
Don Rathjen, Staff Teacher
Linda Shore, Director, Staff Physicist, Teacher Institute
Modesto Tamez, Coordinator Mentor Program, Staff Teacher

The Exploratorium maintains an extensive collection of online educational resources for science and mathematics at www.exploratorium.edu. You'll find articles on science content, descriptions of hands-on activities developed by the Exploratorium, live Webcasts from science laboratories around the world, online exhibits, and links to other exemplary science education Web sites. The Web site's digital library allows you to search through archives of thousands of Exploratorium Web pages. Log on to www.exploratorium.edu/educate and find further "Tools for Teachers," including links to the Teacher Institute and the Learning Studio, and information about programs for students.

Webcasts and The Iron Science Teacher

The Exploratorium periodically conducts live Webcasts, including the very popular "Iron Science Teacher." A take-off of the Japanese TV program "Iron Chef," "Iron Science Teacher" participants build science activities based on a secret ingredient, using simple materials, and present these activities to both a live audience and a virtual audience over the Internet. See the archives: www.exploratorium.edu/ironscienceteacher.

Field Trips

A field trip to the Exploratorium can be an integral part of a science curriculum and a valuable addition to classroom work in many subjects. Field trips are by reservation only, 10 a.m. to 4 p.m. Plan your field trip early: Spring slots fill up fast. For reservations, call (415) 561-0317.

Exploratorium Store

The Exploratorium Store stocks a wide range of science and activity books, posters, and educational toys: www.exploratoriumstore.com.

The Exploratorium Teacher Institute is generously funded by The National Science Foundation, The Noyce Foundation, The William and Flora Hewlett Foundation, Carnegie Corporation of New York, Clarence E. Heller Charitable Foundation, Pacific Bell Foundation, The Mary A. Crocker Trust, California Department of Education, William Randolph Hearst Endowment, Phyllis Wattis Endowment, and Hambrecht Fellowship Endowment.

---

exploratorium

Exploratorium Teacher Institute
3601 Lyon Street
San Francisco, CA 94123

Teacher Institute: (415) 561-0313
Exploratorium: (415) 563-7337 FAX (415) 561-0307
e-mail: teacher_institute@exploratorium.edu
lindas@exploratorium.edu, Director TI

A CHEMICAL PERSPECTIVE TO STRATEGY AND DESIGN OF NANOSCALE MATERIALS: THE SCIENCE BEHIND NANOTECHNOLOGY

Stephen P. O'Brien

Materials Science and Engineering
Department of Applied Physics and Applied Mathematics
Columbia University
200 S. W. Mudd, 500 West 120th Street
New York, New York 10027

Telephone 212-854-9478
e-mail so188@columbia.edu

Stephen P. O'Brien

A Chemical Perspective to Strategy and Design of Nanoscale Materials: The Science behind Nanotechnology

Stephen O'Brien

Assistant Professor of Materials Science and Engineering

Department of Applied Physics and Applied Mathematics

17th Annual National Educators Workshop, Oct. 2002

Acknowledgement

olumbia University:

en Fine, Louis Brus, Irving Herman, Siu-Wai Chan, Colin ucholls, Jim Yardley, Franz Redl, Limin Huang, Jon panier, Feng Zhang, Ebru Apak, Todd Krauss, Stephanie rancharov, Ming Yin, Vincent Chiang.

’Brien, Brus, Chan and Herman groups.

BM Corp. T. J. Watson Research enter:

hris Murray*, Shouheng Sun, Shalom Wind, Hugh Doyle, olfgang Gaschler, Nanoscience group.

Mann and co-workers; Stucky, Belcher and co-workers

Biomaterials and Self Assembly

showing
ains of
aCrO4
es

graph of
surface
ing
Haliotis
at pearl

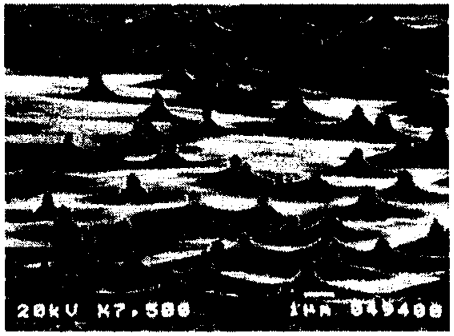

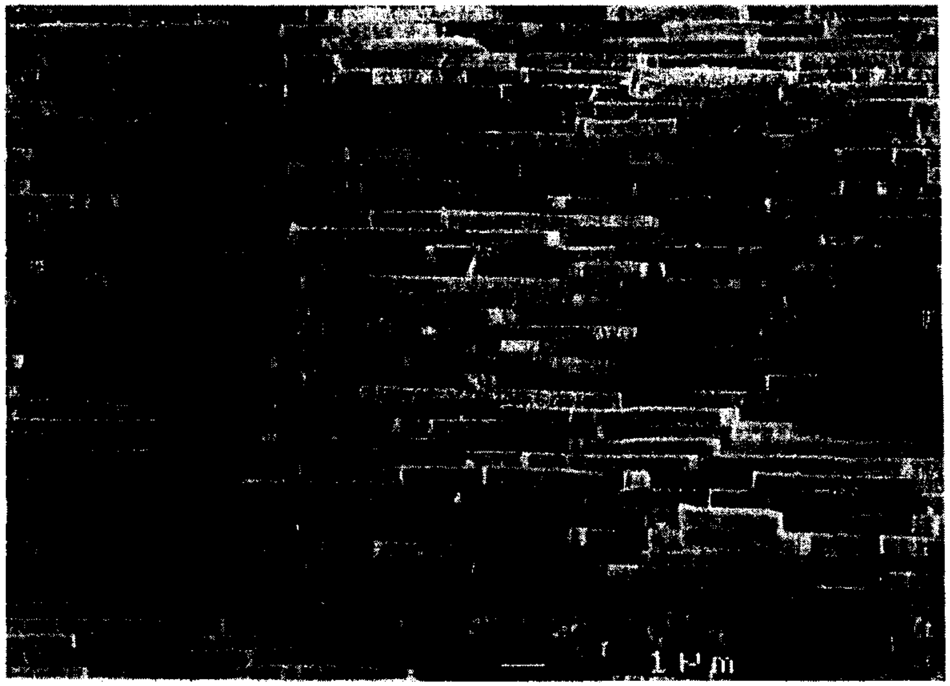

SEM image of a cross section of native gastropod (red abalone) nacre

From www.pubs.acs.org

X-ray diffraction Studies of CeO_2 Nanoparticles

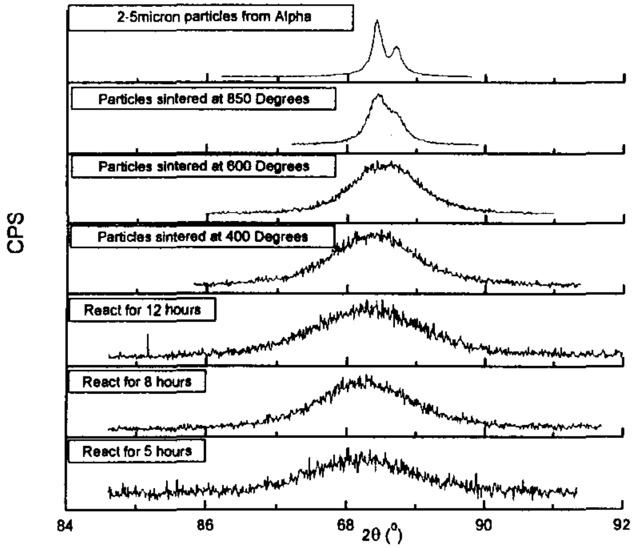

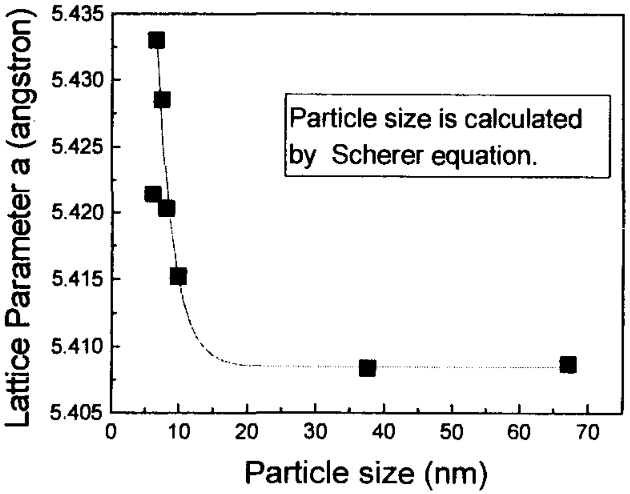

Particle size is calculated by Scherer equation.

- Aqueous $Ce(NO_3)_3$ synthesis. By controlling the reaction time - uniform CeO_2 nanoparticles with different sizes.
- Size of nanoparticles proportional to reaction time and sintering procedure
- Lattice strain observed for decreasing particle sizes

Chan, Zhang, Apak

Nanostructured Porous Silica

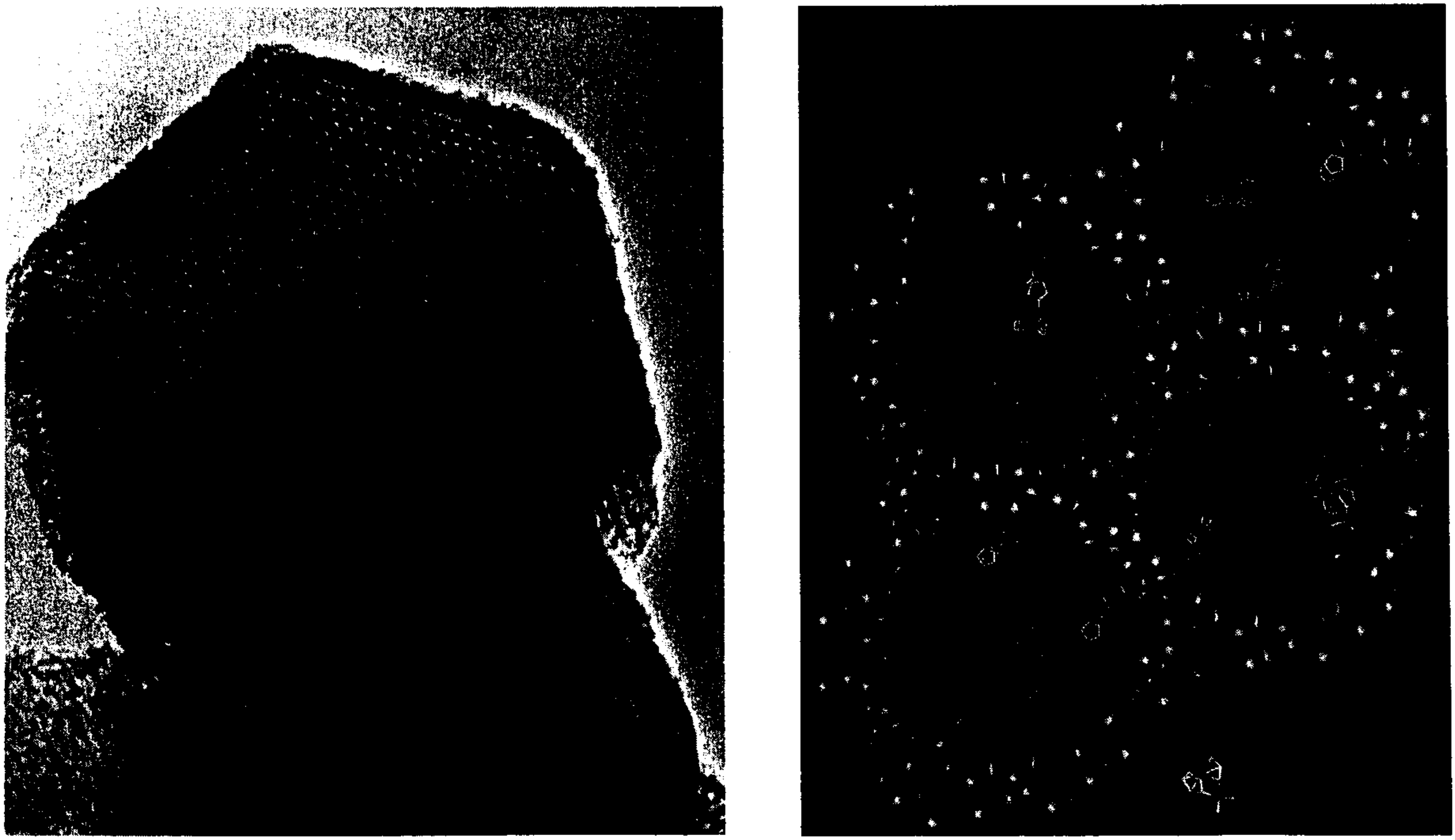

Nanoporous Silica from Block Co-Polymer Templates

M

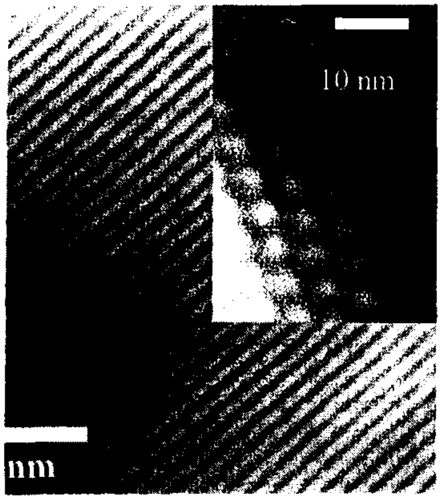

Self Assembled Structures as Templates - introduction of Molecular Precursors into Solutions containing liquid crystal arrays. The precursor crystallizes around the liquid crystal, using it as a template.

Developing ordered thin films.
Growing nanowires within the channels.
Using them as catalysts for SWNT growth.

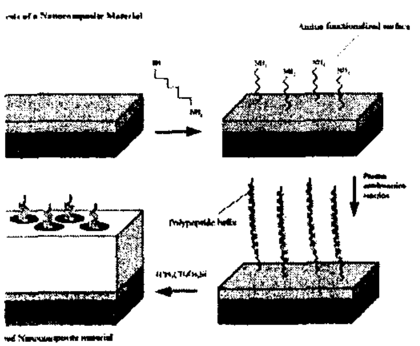

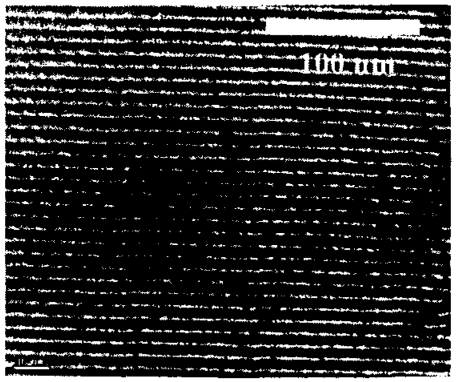

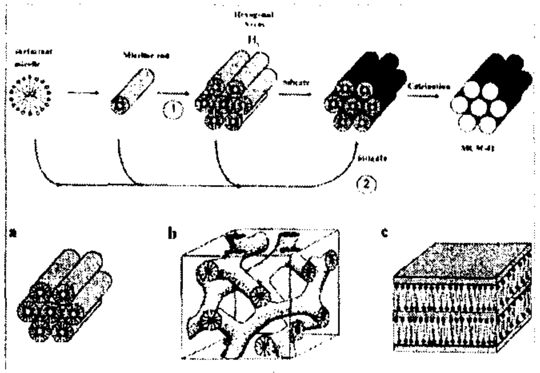

O'Brien, Huang, Grancharov

Synthesis of Iron and Iron Oxide Magnetic Nanoparticles

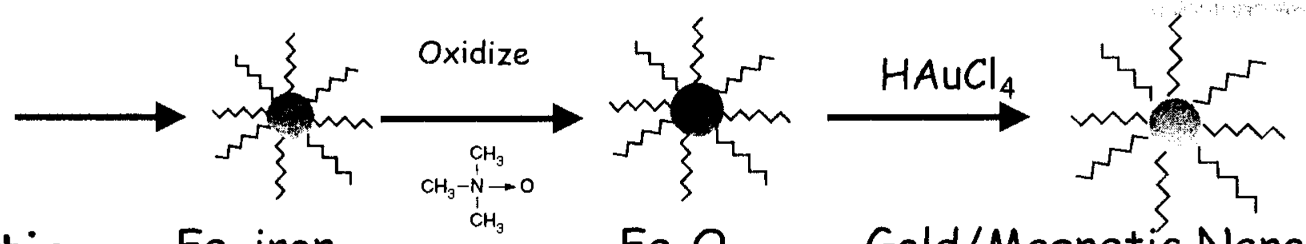

$(CO)_5$ → Fe, iron. $\xrightarrow{\text{Oxidize}}$ ($(CH_3)_3N \rightarrow O$) Fe$_2$O$_3$ $\xrightarrow{HAuCl_4}$ Gold/Magnetic Nanoparticle

rlattice

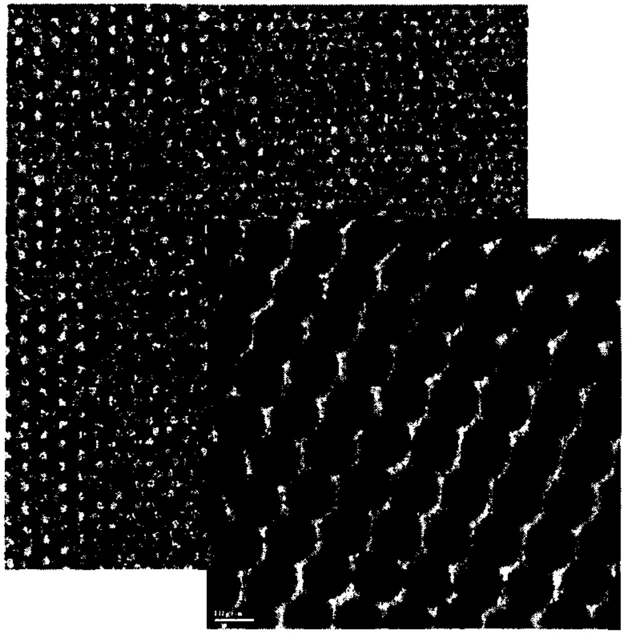

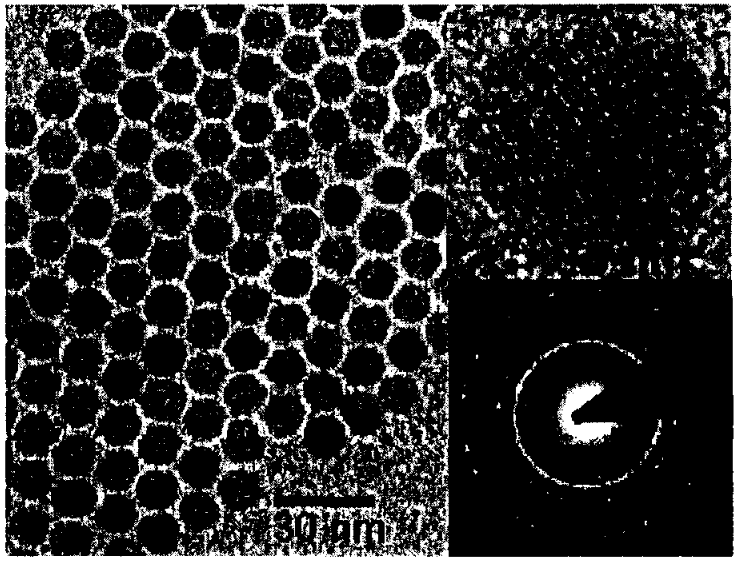

Hyeon, Murray, O'Brien, Redl, Grancharov, Yin

Iron Oxide Nanoparticle Synthesis

$$CO)_5 \xrightarrow[\text{100-290 C}]{\text{octyl ether or trioctyl amine oleic acid}} \text{Fe-NC} \xrightarrow[\text{or 200 C under air}]{(CH_3)_3N\text{-}O} \gamma\text{-}Fe_2O_3\text{-NC}$$

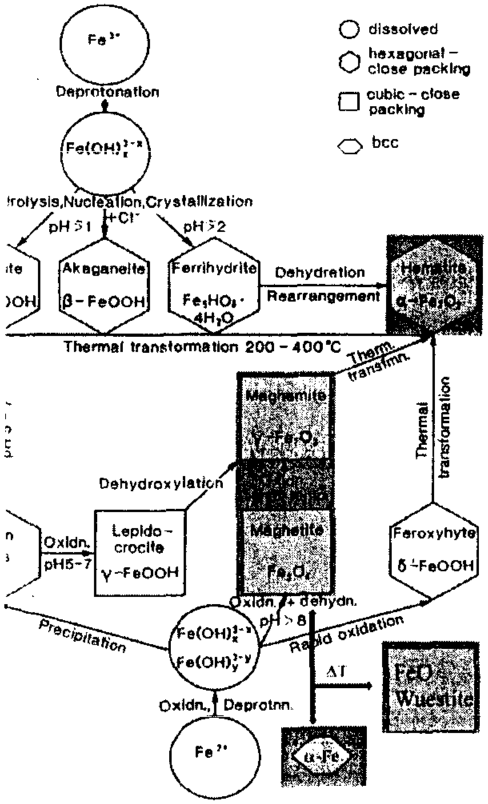

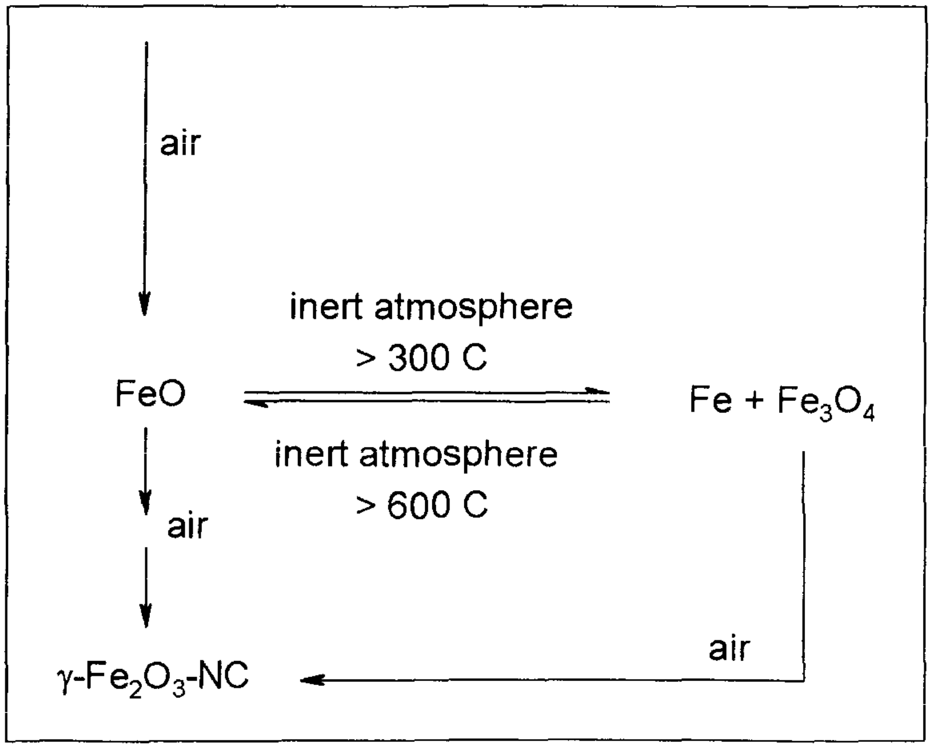

$$\begin{tikzcd}
\arrow[d, "\text{air}"] & \\
\text{FeO} \arrow[r, shift left, "\text{inert atmosphere} > 300\text{ C}"] \arrow[d, "\text{air}"] & Fe + Fe_3O_4 \arrow[l, shift left, "\text{inert atmosphere} > 600\text{ C}"] \arrow[dl, "\text{air}"] \\
\gamma\text{-}Fe_2O_3\text{-NC} &
\end{tikzcd}$$

Polarization Charateristics of Ferroelectric Materials

aelectric Phase Transition

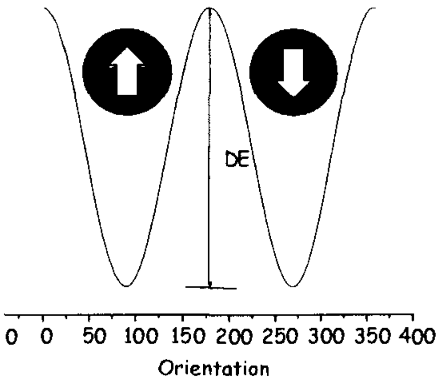

tulate single ferroelectric domain oparticles: orientation determined anisotropy energy, K. Energy rier to domain flipping,

$$\Delta E = KV / k_B T$$

Applied Electric Field

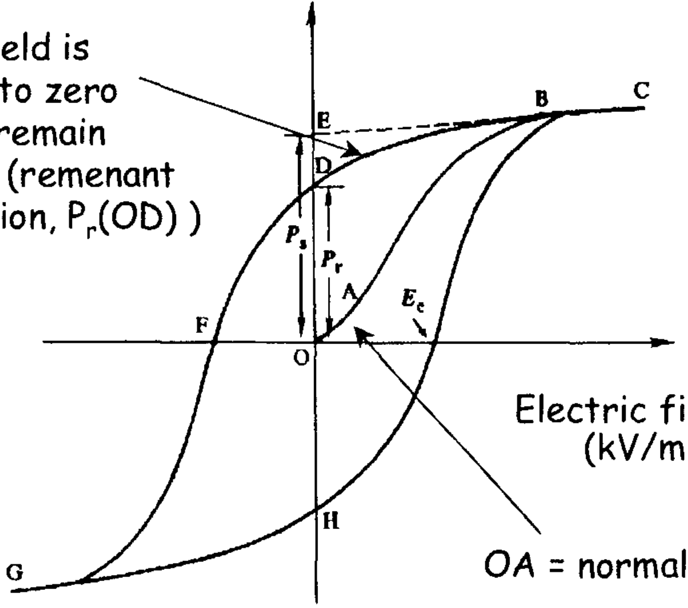

As the field is reduced to zero domains remain aligned = (remenant polarization, P_r(OD))

Electric field, E (kV/mm)

OA = normal dielectric

anoscale Ferroelectric Oxides: $BaTiO_3$

Ferroelectricity in bulk/films = spontaneous polarization in Applied Field, E.
Question: Can nanoparticles be ferroelectric?

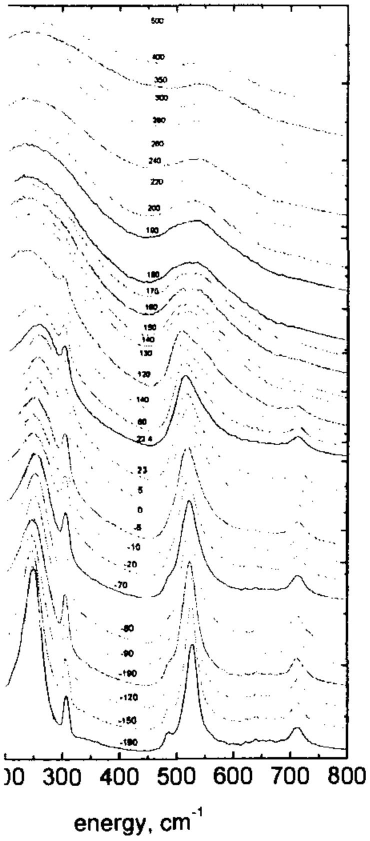

an

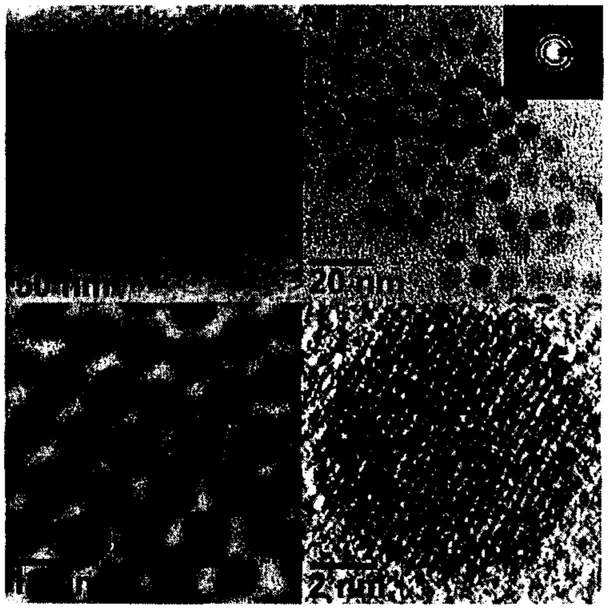

TEM

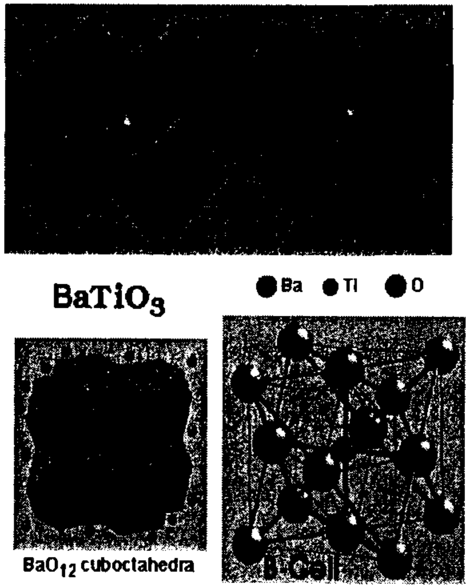

$BaTiO_3$

Brus, O'Brien, Herman, Murray, Chinag, Spanier, Robinson

Applications of Ferroelectrics - Non-volatile Memory (J. F. Scott, 2000)

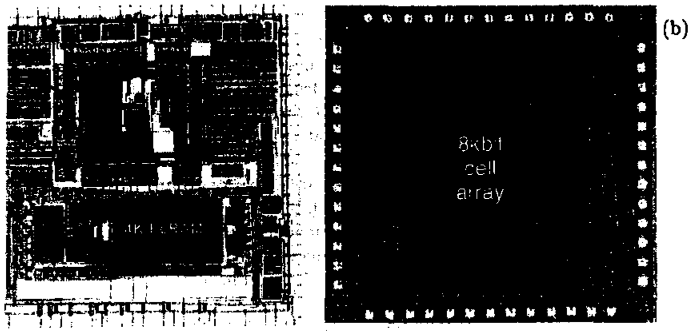

2.38. 4K (a) and 8K (b) embedded FeRAMs

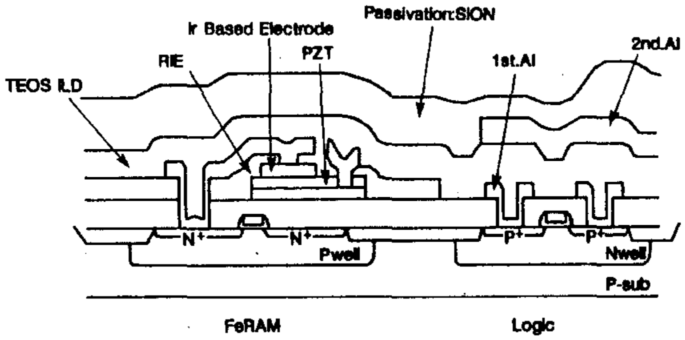

Fig. 2.27. Cross-section for NEC PZT memory

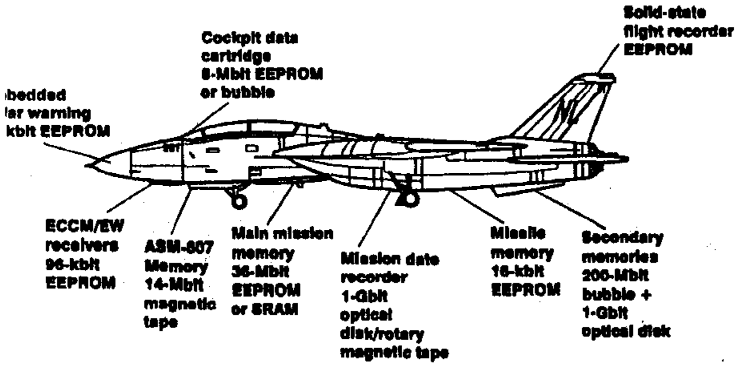

g. 2.2. Nonvolatile memories in a US military aircraft (1988); the original figure from the North American Defence Center (NADC), and its reproduction in [53] is through the private communication of R. Fedorak

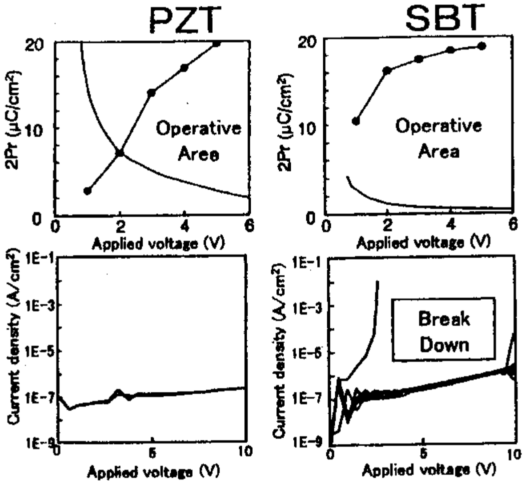

Fig. 2.28. Remanent polarisation and leakage current versus voltage

Optical and Electronic Properties of CdSe Quantum Dots

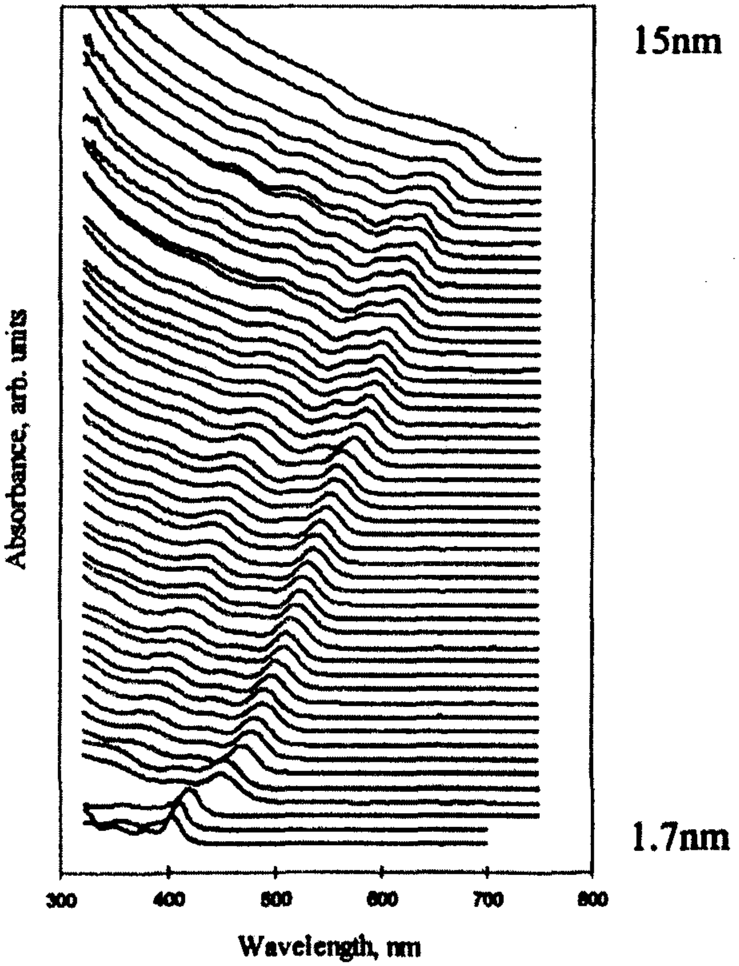

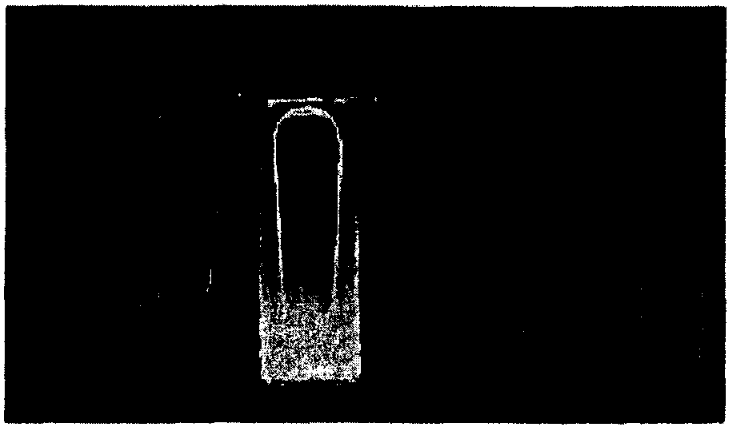

$$E^{*} = E_{bg} + \frac{\eta^{2}\pi^{2}}{2R^{2}}\left[\frac{1}{m_e} + \frac{1}{m_h}\right] - \frac{1.8e^{2}}{\varepsilon R}$$

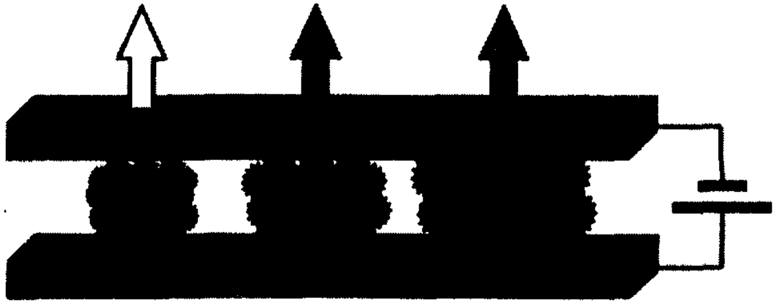

Murray, Brus, Prof. Bawendi and Researchers at MIT

Nanoparticles: generalized synthesis and self-assembly into thin-films

niconductors:
ℨe, PbSe
tals: Co, PtFe
ides: TiO_2, $BaTiO_3$

ƨ selective precipitation:
: particles are precipitated with the trolled addition of a flocculent and n centrifuged. The process can be ƨated to focus the size distribution to iations of +/- 10% of the diameter (+/- n or in some cases down to a +/- one ıolayer of atoms)

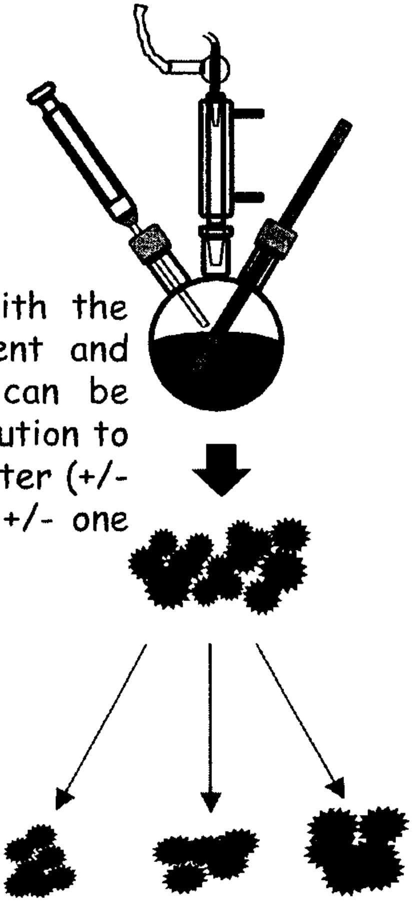

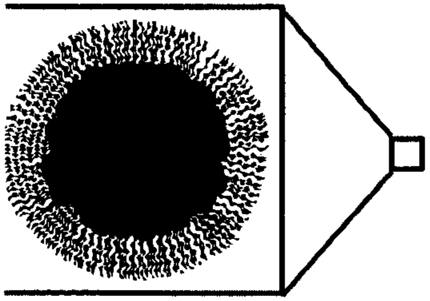

Film Growth :Self-Assembly

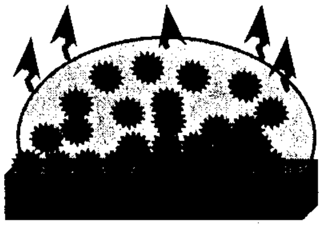

Nanoparticle Superlattice

Annealed Superlattice

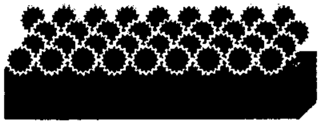

Columbia MRSEC Interdisciplinary Research Group

O'Brien, Murray, Chan, Adams, Akins

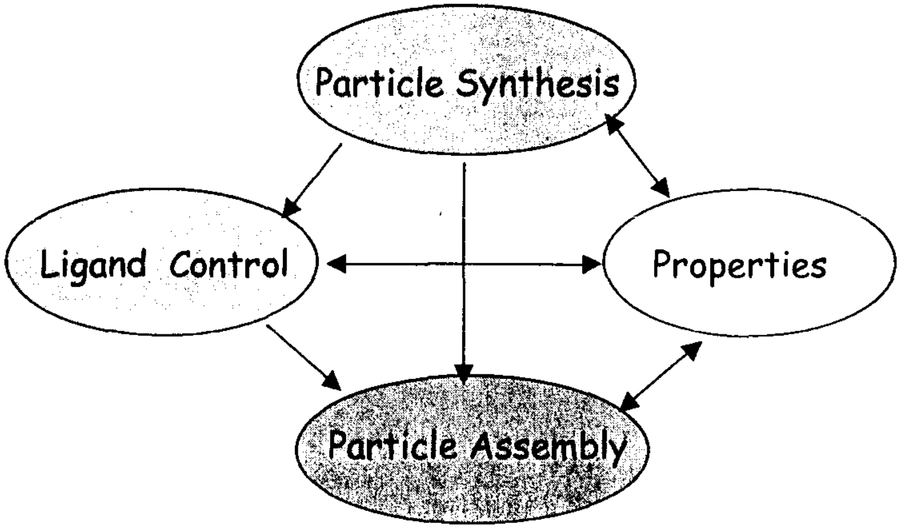

Particle Synthesis

kolls, O'Brien,
Koberstein

Ligand Control

Properties

Brus, Herman, Friesner,
Akins, Chan, Adams
(Flynn, Heinz)

Particle Assembly

Turro, Brus, Koberstein, Levicky,
O'Shaughnessy, Adams, Herman

The guiding principle is combining creative chemical synthesis with rigorous physical understanding in an environment of collaboration and industrial awareness.

Columbia Shared Materials Facilities

tag XRD: NSF/Columbia

Biorad FTIR: NSF/Columbia

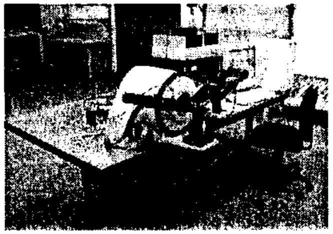

Beaglehole Ellipsometer:
NSF/Columbia

PHI XPS:
Champion/Int'l. Paper

"Yellow" Photolithography Room

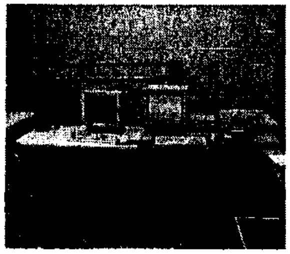

JSM-5600LV: MSE/MRSEC/Civil. Eng

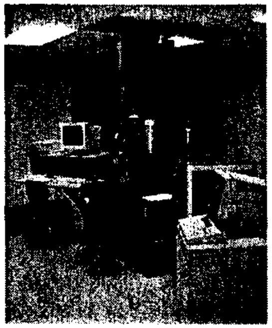

Philips 430 TEM: MSE/MRSEC

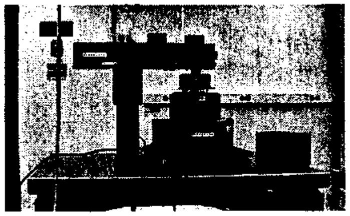

Thermomicroscopes AFM:
NSF/Columbia

Synthesis Objectives Within Columbia University MRSEC

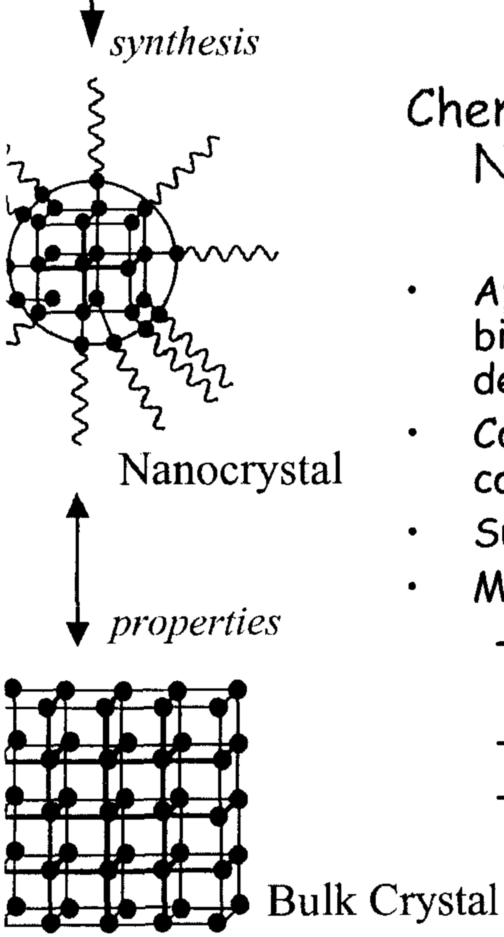

Chemical Preparation of Nanocrystals and Nanostructures

- Apply synthesis strategy to the synthesis of nanoscale binary or complex oxides with interesting or size dependent properties.
- Combine magnetic oxides and semiconducting to make composite materials
- Surface characterization and SPM studies of
- Materials and Properties with significant applications:
  - Ferroelectric and high k dielectric materials (e.g. $BaTiO_3$)
  - Catalytic, gas sensing, solid oxide fuel cells (e.g. CeO_2)
  - Semicondcutor systems

Methodology

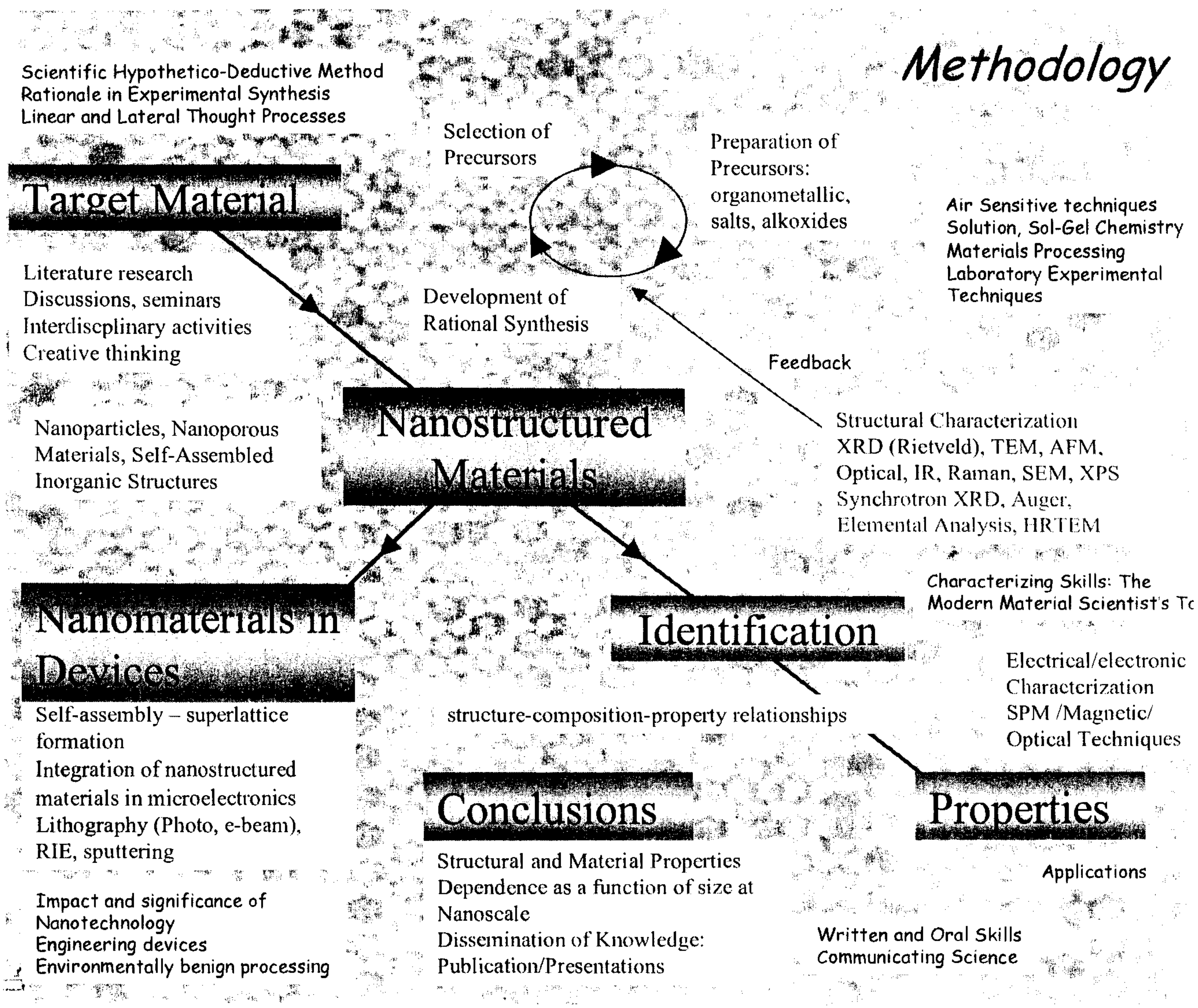

Scientific Hypothetico-Deductive Method
Rationale in Experimental Synthesis
Linear and Lateral Thought Processes

Target Material

Literature research
Discussions, seminars
Interdisciplinary activities
Creative thinking

Selection of Precursors

Preparation of Precursors: organometallic, salts, alkoxides

Air Sensitive techniques
Solution, Sol-Gel Chemistry
Materials Processing
Laboratory Experimental Techniques

Development of Rational Synthesis

Feedback

Nanostructured Materials

Nanoparticles, Nanoporous Materials, Self-Assembled Inorganic Structures

Structural Characterization
XRD (Rietveld), TEM, AFM, Optical, IR, Raman, SEM, XPS
Synchrotron XRD, Auger, Elemental Analysis, HRTEM

Nanomaterials in Devices

Self-assembly – superlattice formation
Integration of nanostructured materials in microelectronics
Lithography (Photo, e-beam), RIE, sputtering

Impact and significance of Nanotechnology
Engineering devices
Environmentally benign processing

Identification

Characterizing Skills: The Modern Material Scientist's Tc

structure-composition-property relationships

Electrical/electronic Characterization
SPM /Magnetic/ Optical Techniques

Conclusions

Structural and Material Properties Dependence as a function of size at Nanoscale
Dissemination of Knowledge: Publication/Presentations

Properties

Applications

Written and Oral Skills
Communicating Science

emical Approach to the Hierarchical Construction of Matter

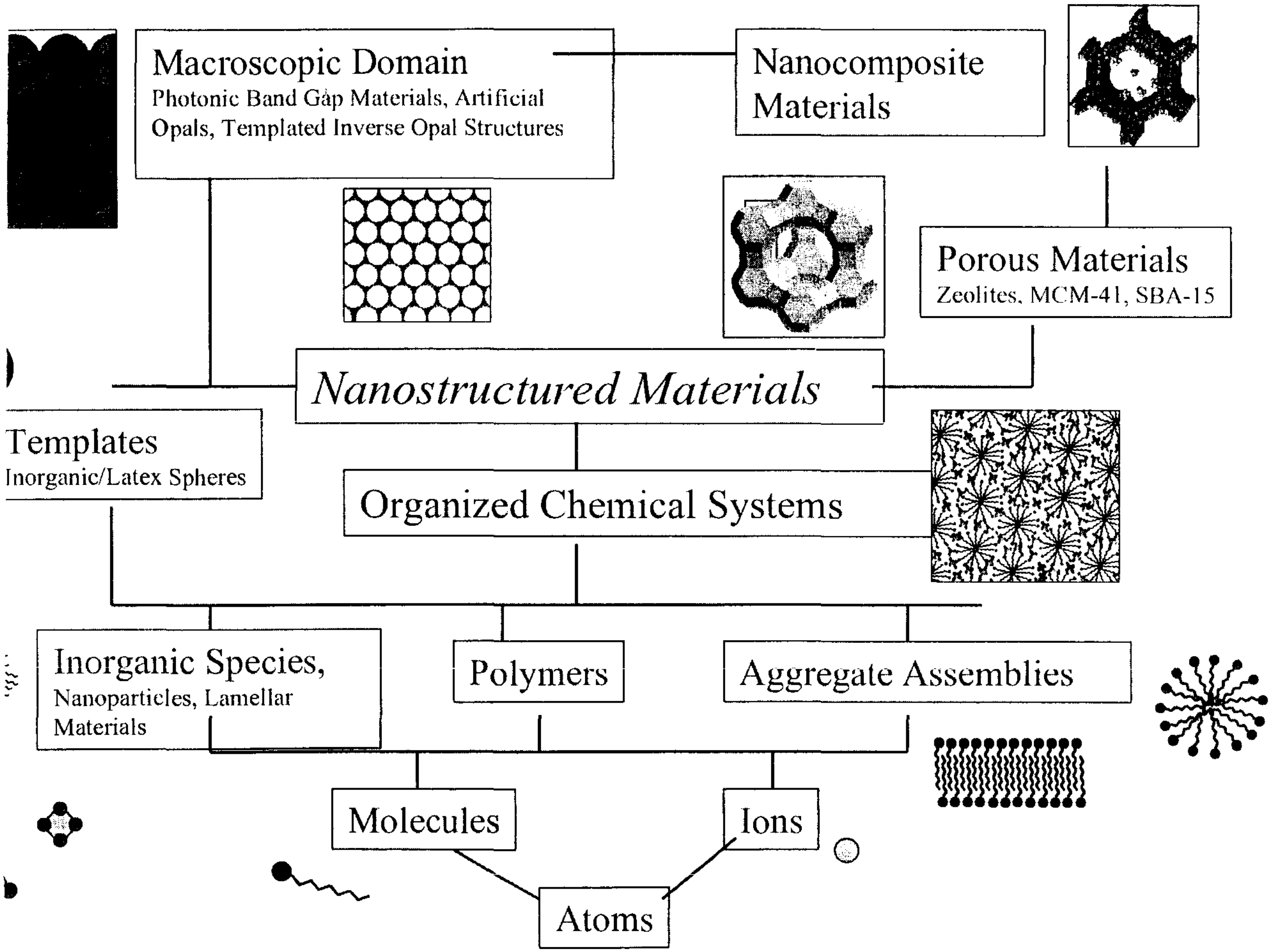

Macroscopic Domain
Photonic Band Gap Materials, Artificial Opals, Templated Inverse Opal Structures

Nanocomposite Materials

Porous Materials
Zeolites, MCM-41, SBA-15

Nanostructured Materials

Templates
Inorganic/Latex Spheres

Organized Chemical Systems

Inorganic Species,
Nanoparticles, Lamellar Materials

Polymers

Aggregate Assemblies

Molecules

Ions

Atoms

Iron Oxide Nanoparticle Synthesis

$$(CO)_5 \xrightarrow[\text{100-290 C}]{\text{octyl ether or trioctyl amine oleic acid}} \text{Fe-NC} \xrightarrow[\text{or 200 C under air}]{(CH_3)_3N\text{-}O} \gamma\text{-}Fe_2O_3\text{-NC}$$

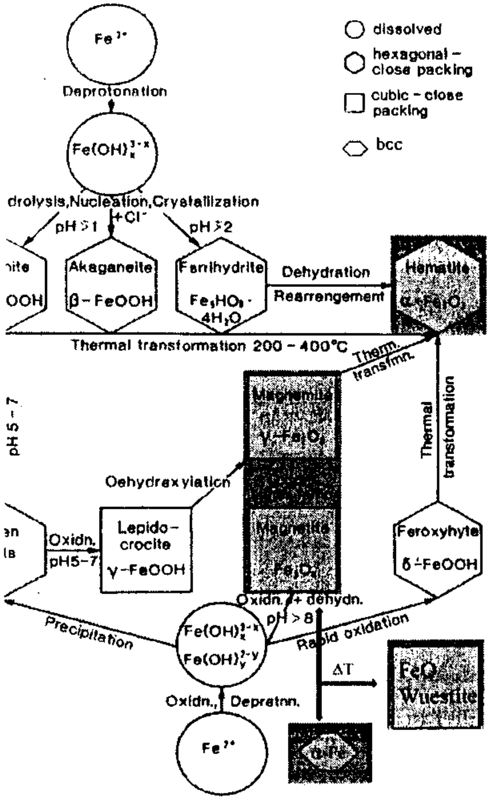

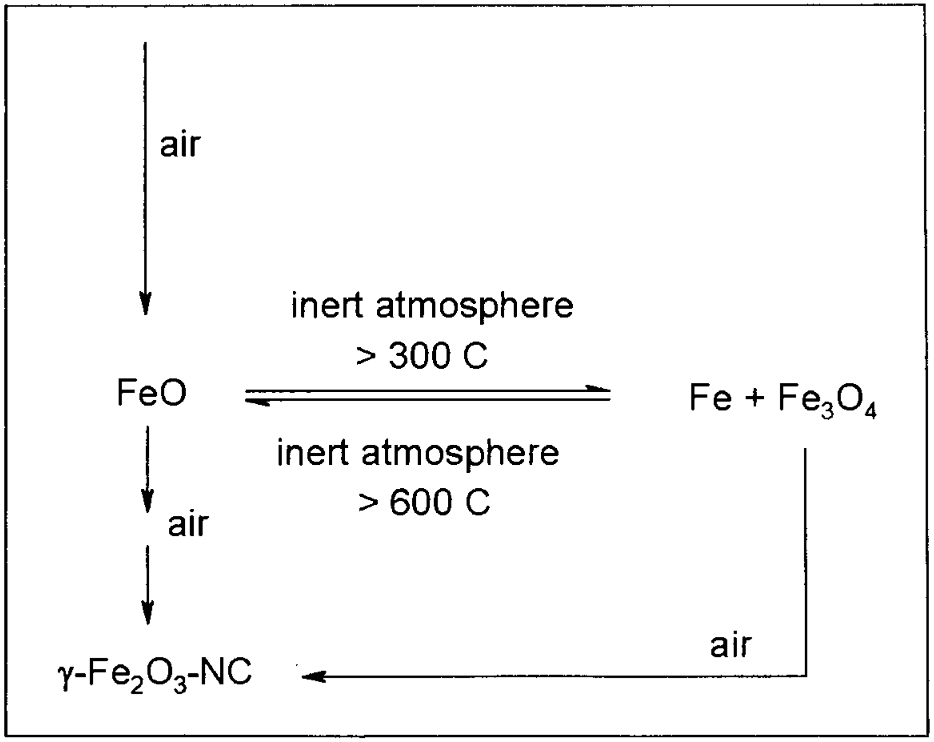

air

inert atmosphere > 300 C

FeO

Fe + Fe_3O_4

inert atmosphere > 600 C

air

air

γ-Fe_2O_3-NC

Polarization Charateristics of Ferroelectric Materials

Paraelectric Phase Transition

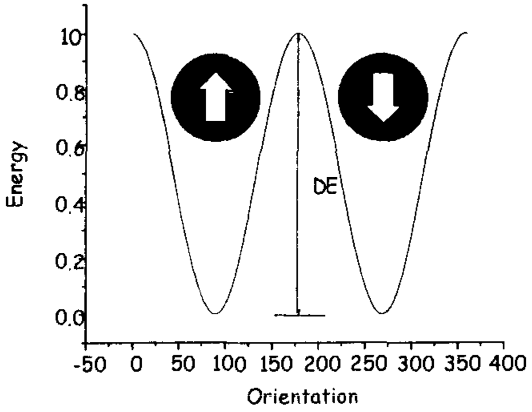

Postulate single ferroelectric domain nanoparticles: orientation determined by anisotropy energy, K. Energy barrier to domain flipping,

$$\Delta E = KV / k_B T$$

Applied Electric Field

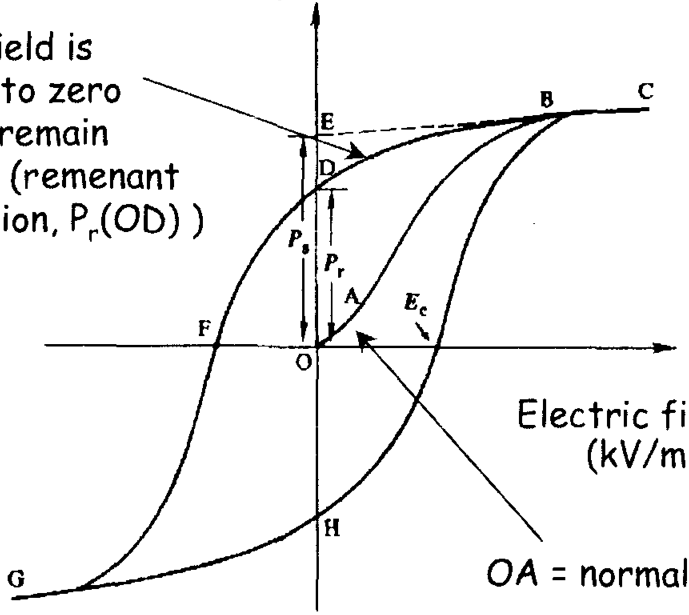

As the field is reduced to zero domains remain aligned = (remenant polarization, P_r(OD))

Electric field, E (kV/mm)

OA = normal dielectric

Nanoscale Ferroelectric Oxides: $BaTiO_3$

Ferroelectricity in bulk/films = spontaneous polarization in Applied Field, E.
Question: Can nanoparticles be ferroelectric?

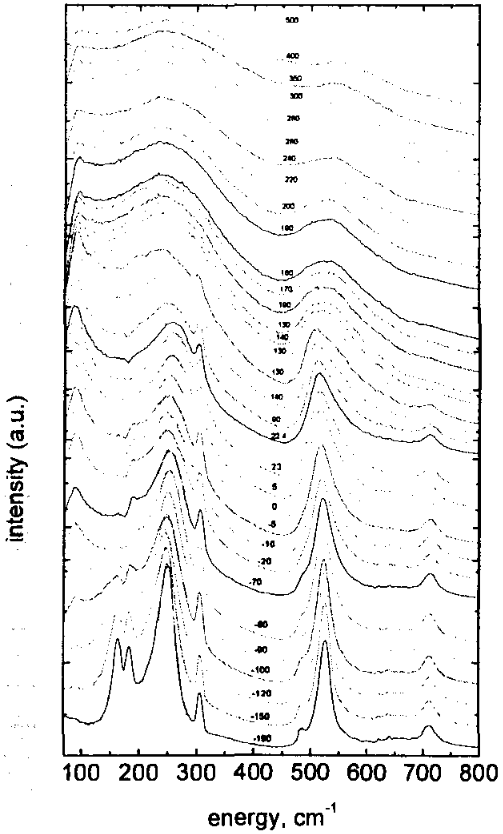

Raman

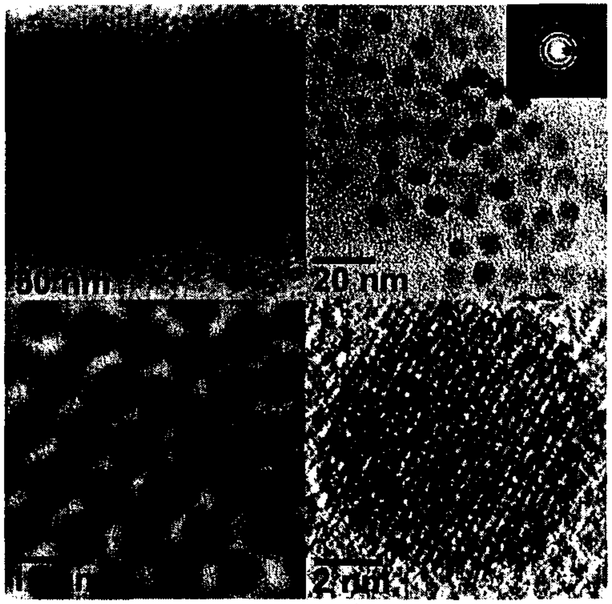

TEM

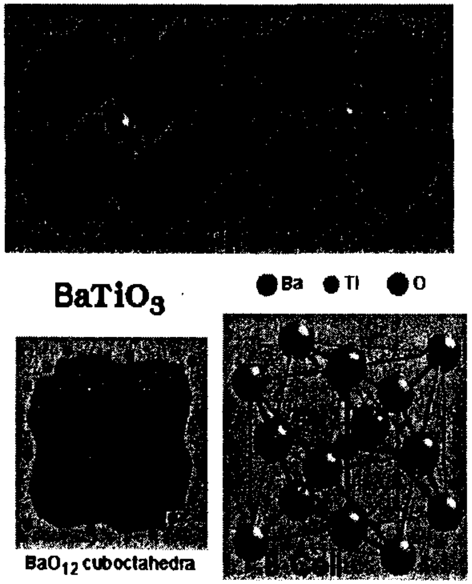

$BaTiO_3$

Brus, O'Brien, Herman, Murray, Chinag, Spanier, Robinson

Applications of Ferroelectrics - Non-volatile Memory (J. F. Scott, 2000)

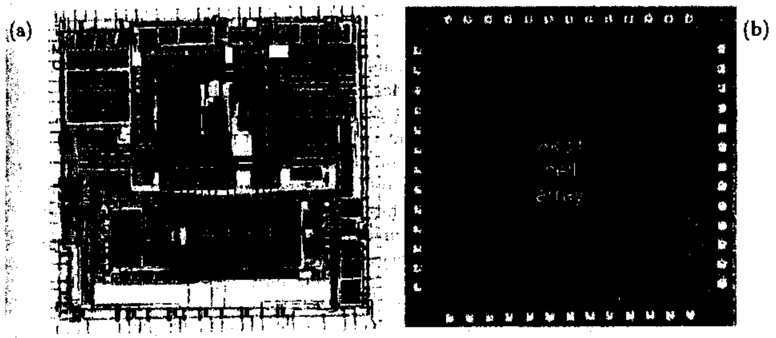

Fig. 2.38. 4K (a) and 8K (b) embedded FeRAMs

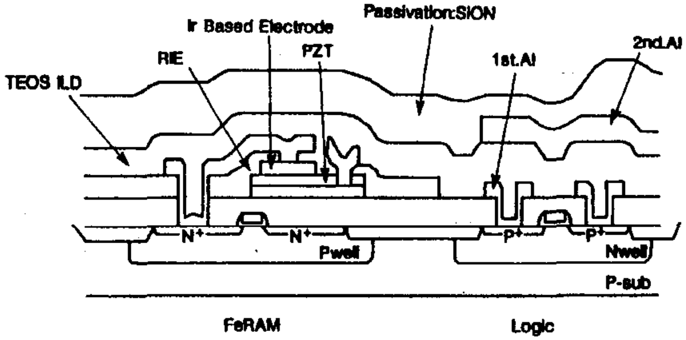

Fig. 2.27. Cross-section for NEC PZT memory

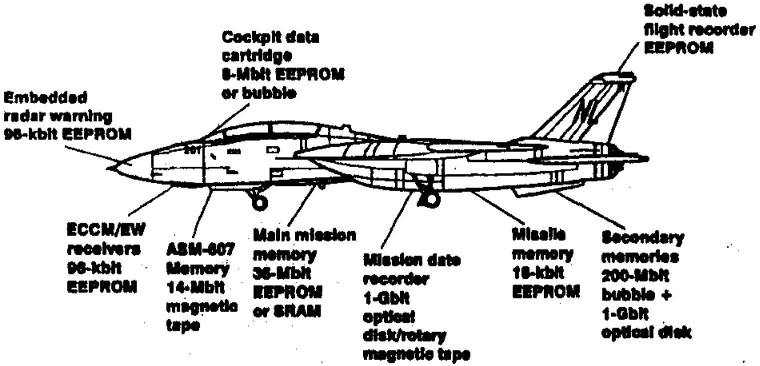

Fig. 2.2. Nonvolatile memories in a US military aircraft (1988); the original figure is from the North American Defence Center (NADC), and its reproduction in [53] was through the private communication of R. Fedorak

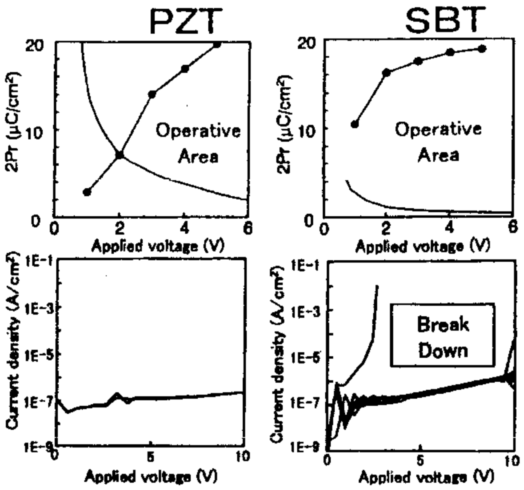

Fig. 2.28. Remanent polarisation and leakage current versus voltage

Nanoparticles and Nanostructures

Research

The key element in the synthesis of colloidal nanocrystalline particles is monodispersity. The proper choice of reagents and reaction conditions and size selected processing are essential for the synthesis of semiconductor or oxide nanocrystals. If the the size distribution is sufficently narrow the particles will self-organize to form a superlattice upon evaporation of the solvent.

Challenge

The synthesis of new nanoscale materials with optical, magnetic or dielectric properties of potential value for pure scientific research that underpin technological applications in optics and microelectronics.

Focus

- Oxides with applications in ferroelectrics, catalysis and magnetics.
- Oxide/Gold core/shell nanoparticles for biological applications.
- Synthesis and properties of novel selenide nanocrystal systems.
- Nanostructured materials based on supramolecular assembly

Nanoscale Materials Synthesis at Columbia

Columbia Nanoscale Materials: NSEC, MRSEC, Departments of Chemistry, Physics and Applied Physics

NSEC

Louis Brus, Irving Herman, Siu-Wai Chan, Stephen O'Brien, Nicholas Turro and co-workers

Collaboration with IBM Corp. T. J. Watson Research Center:

Christopher B. Murray and the Nanoscience group.

IBM Research

NATIONAL SCIENCE FOUNDATION
Columbia University
Materials Research
Science and Engineering Center

Nanotechnology

School of Engineering and Applied Science MSAE E6090x / APPH E6090x
Tues. & Thurs. 10:35-11:50 a.m.
Room: 214 Mudd
Instructor: Professor Stephen O'Brien

The science and engineering of creating materials, functional structures and devices on the nanometer scale. Carbon nantotubes, nanocrystals, quantum dots, properties of materials as a function of size, self-assembly, nanostructured materials. Nanoscale films and composites. Devices and applications. The "top down" manufacturing paradigm; prospects for the future. Molecular engineering, molecular electronics, nanofabrication, bionanotechnology. Imaging and manipulating at the atomic scale. Nanotechnology in industry.

Contact Professor O'Brien for information regarding prerequisites.
854-9478 or so188@columbia.edu

Nanotechnology

The domain of nanoscale structures, typically sized below 100 nm, lies dimensionally between that of ordinary, macroscopic or microdevices and single atoms or molecules. Traditional manufacturing techniques have been miniaturized for fabrication of microstructures as in microelectronics, in a top-down approach. Now that these reach the nanoscale, these devices are considered an evolution into nanotechnology. On the other hand, atomic or molecular units, with well-known subatomic structure in isolation, offer the ultimate building blocks for a bottom-up, atom-by atom manufacturing synthesis with applications in many industries. Nanotechnology as a discipline incorporates the fundamental science of current nanoscale materials and devices, and teaches an exciting conceptual approach (theory and modeling) for the integration of the appropriate scientific, engineering,and mathematical tools within a systems framework where the desired outcome is a viable product or service to society. Source: nsf.gov

ABCs OF NANOTECHNOLOGY: ATOMS, BITS, AND CIVILIZATION

George Lisensky

Chemistry Department
Beloit College
700 College Street
Beloit, Wisconsin 53511

Telephone: 608-363-2225
e-mail Lisensky@beloit.edu

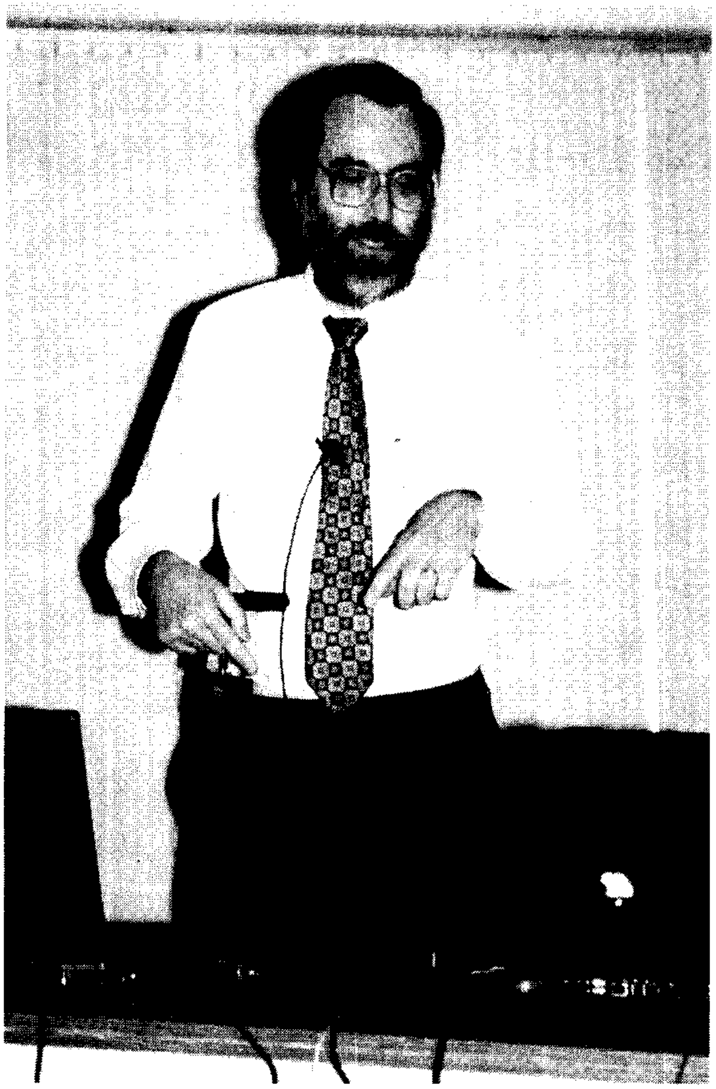

George Lisensky

ABCs of Nanotechnology: Atoms, Bits, and Civilization

George Lisensky, Beloit College, Beloit, WI 53511

Nanotechnology has provided tools for imaging individual atoms and positioning them to create desired architectures. Developments resulting from nanotechnology have the potential to change our society on a scale similar to that of the transistor-based computer.

How can the tools that scientists use to see atoms and to arrange them to create new materials be simulated in ways that make nanotechnology accessible to students?

This talk uses hands-on demonstrations to illustrate some ways that high-tech materials, advanced devices, and cutting edge research can be brought into introductory classrooms and laboratories. For examples of such demonstrations from the Materials Research Science and Engineering Center on Nanostructured Materials and Interfaces at the University of Wisconsin-Madison,

see `http://mrsec.wisc.edu/nano`

PREVIEW OF NEW:UPDATE WORKSHOP 2003

Edwin J. Prior

Office of Education
NASA Langley Research Center
Mail Stop 400
Building 1216, Room 103
17 Langley Boulevard
Hampton, Virginia 23681-0001

Telephone: 757-864-5800
e-mail e.j.prior@larc.nasa.gov

Edwin J. Prior

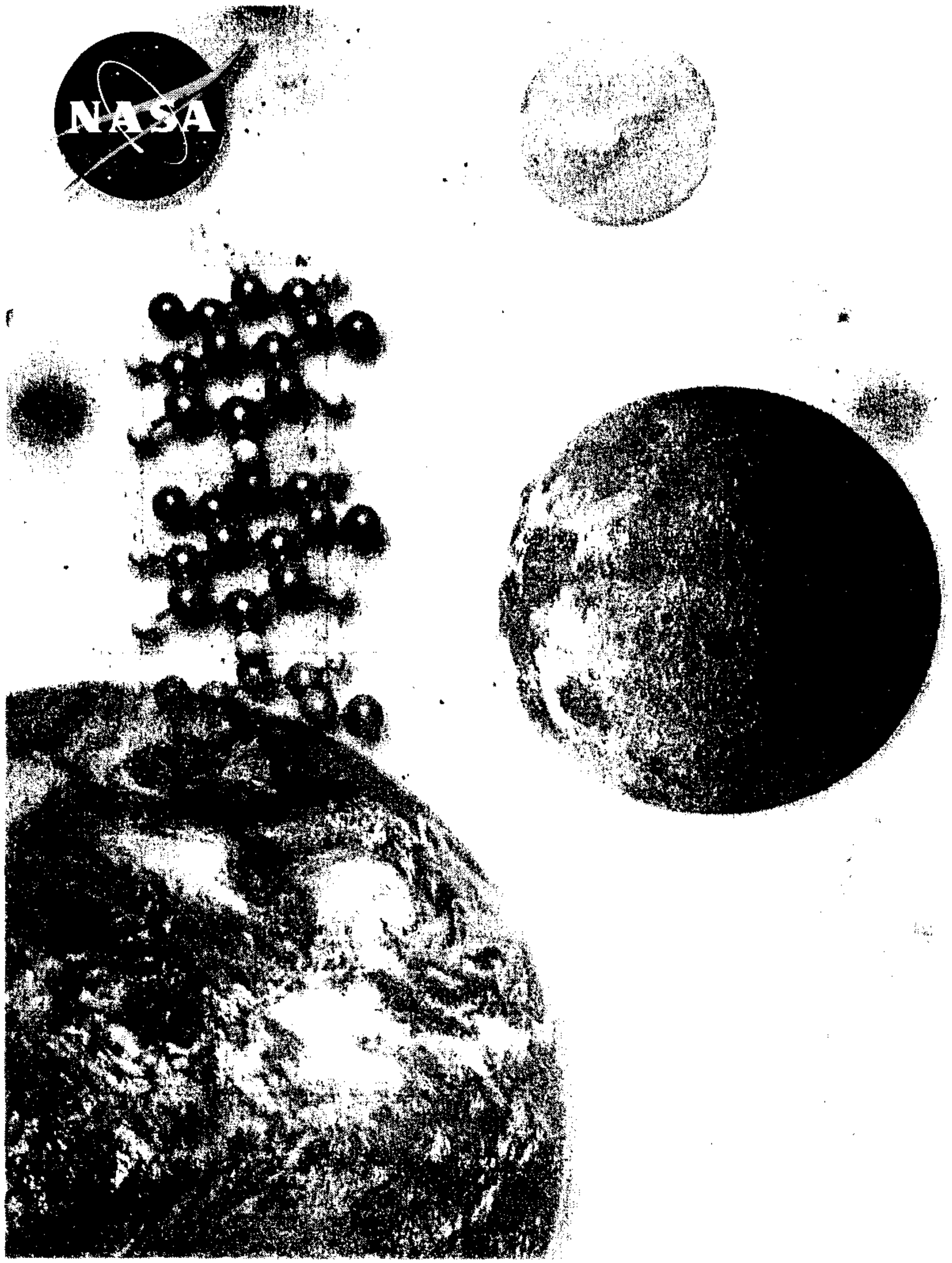

NASA Vision

April 2002

The World has Changed

- The Nation faces extraordinary challenges; the Agency has tremendous opportunities
- International terrorism has crossed our borders
- Global climate change may threaten our way of life
- Shortages in U.S. scientists and engineers threaten our economy
- Rapid advances in technology is profoundly affecting business conduct and survival
- Life is pervasive; we believe it must exist beyond our planet

To continue to serve the Nation well, *NASA must change.*

When the History of the First Quarter of the 21st Century is Written…

- **We have sought life's abodes:** NASA missions have mapped continents on dozens of planets circling nearby stars, some of which show signs of life-supporting atmospheres. Evidence continues to mount for the existence of life on planets within our own Solar System, as revealed by advanced generations of robotic explorers. Humans and their robotic partners assembled complex science facilities in space to unveil even more challenging cosmic questions.
- **We understand our home:** NASA's missions revealed the complex interactions among the Earth's major systems, vastly improving weather, climate, earthquake, and volcanic eruption forecasting – and the impact that our Sun has on our living world.
- **We have connected the world's citizens:** NASA's technologies have resulted in dramatic improvements in air transportation via "green" aircraft, higher-speed international travel, and innovative capabilities to reduce aircraft accidents and delays.
- **We have enabled new commerce:** Low Earth Orbit has become a rapid-growth economic zone, with commercial industries taking advantage of low-gravity, abundant solar energy, low-cost access from the Earth's surface, and a vista that encompasses the entire planet.
- **We share the vision and the experience:** Throughout the world, students in earthbound classrooms are learning the fundamentals of physics, math, and technology as they actively participate with space travelers via "telepresence technology."

And we continue to prepare the way for humanity's greatest adventures.

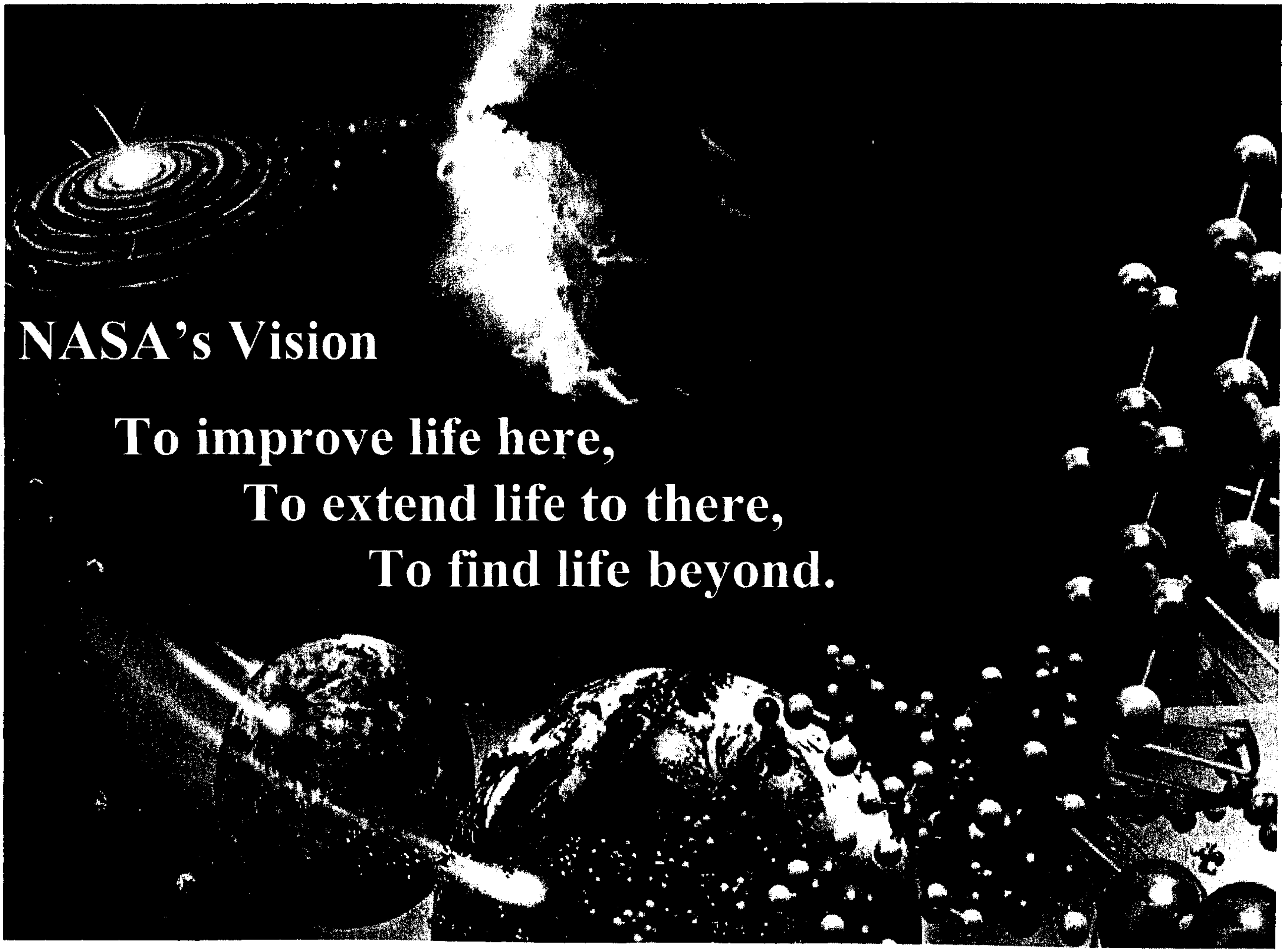

NASA's Vision

To improve life here,
To extend life to there,
To find life beyond.

The NASA Mission

To understand and protect our home planet
To explore the Universe and search for life
To inspire the next generation of explorers

...as only NASA can.

To Understand and Protect Our Home Planet

- Understanding the Earth's system and its response to natural and human-induced changes

- Enabling a safe, secure, efficient, and environmentally friendly air transportation system

- Investing in technologies and collaborating with others to improve the quality of life and to create a more secure world

To Explore the Universe and Search for Life

- Exploring the Universe and the life within it… enabled by technology, first with robotic trailblazers, and eventually humans… as driven by these compelling scientific questions:
    - How did we get here?
    - Where are we going?
    - Are we alone?

To Inspire the Next Generation of Explorers

- Motivating students to pursue careers in science, math, and engineering

- Providing educators with unique teaching tools and compelling teaching experiences

- Improving our Nation's scientific literacy

- Engaging the public in shaping and sharing the experience of exploration and discovery

Implications for NASA: What is Different?

To Understand and Protect our Home Planet

- Greater emphasis on providing policy-makers and others with timely information, technology, and useful tools that address priority issues of international importance
- A new spirit of cooperation with the national security community
- Greater emphasis on transferring technologies to others

To Explore the Universe and Search for Life

- Decisions are science-driven; not destination-driven
- Human presence beyond low Earth orbit will be enabled – as a means to scientific exploration, not an end in itself
- Investments are justified by their contribution to the long-range vision

To Inspire the Next Generation of Explorers

- Education is part of our core mission
- Education becomes an integral part of our programs
- More citizens and students will participate in our programs

As Only NASA Can

- We will pursue activities unique to our mission in air and space: if NASA did not do them, they would not get done
- Activities will be integrated across the Agency
- Programmatic and budget decisions will be aligned with our mission statement
- We will carry out our mission as a diverse, unified team
- We will use new technologies to move our physical infrastructure beyond brick and mortar, and to leverage the Nation's industrial and intellectual capital

What Does America Gain from NASA?

- A new generation of leaders and explorers ready to expand the frontiers of air and space
- Pioneering technological and scientific research that enables new industries
- A Nation reaching across borders to unite people
- A deeper understanding of life, ourselves, and the universe

NASA Langley Research Center

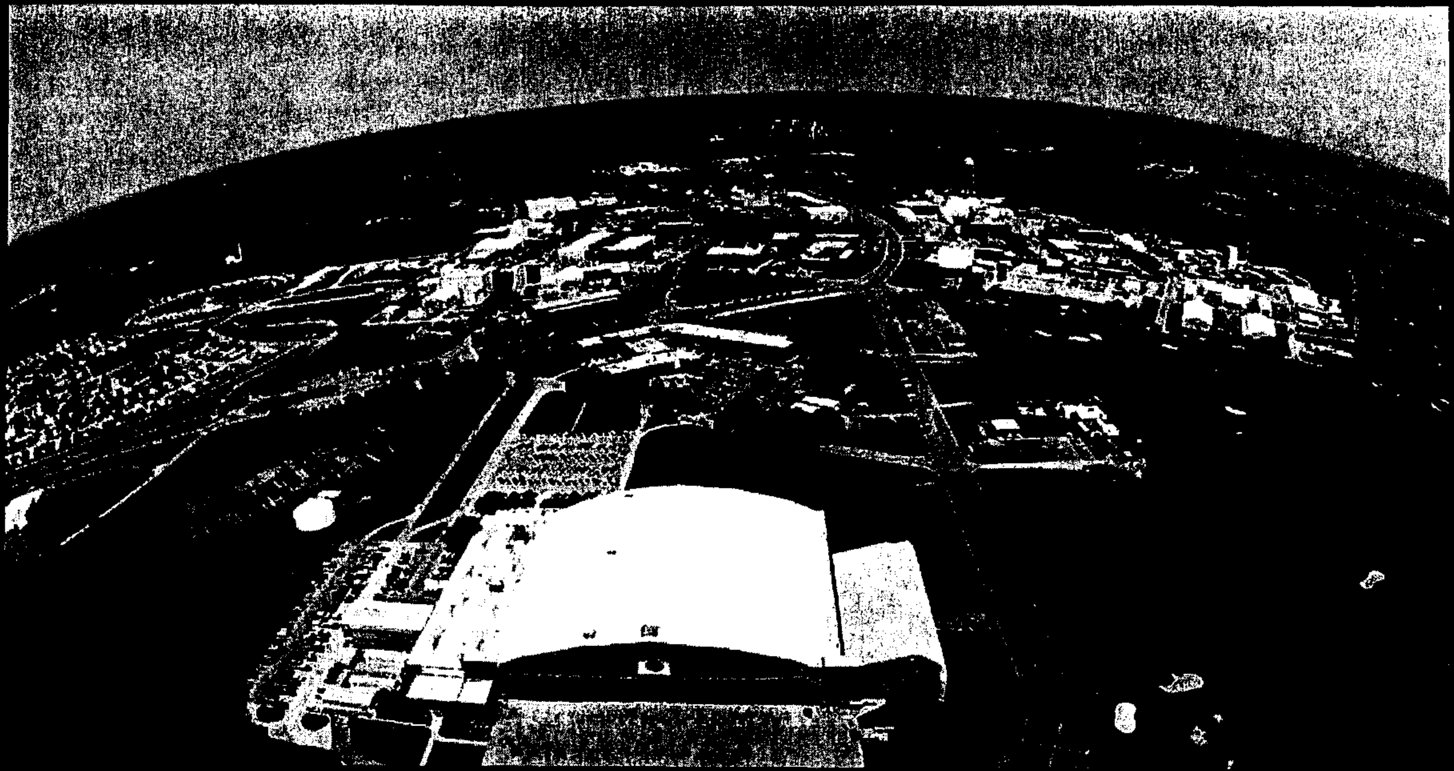

Founded in 1917
- First civil aeronautical research laboratory

Facilities
- $4 billion replacement value

Programs
- $689M total FY 01 budget

People
- 2374 Civil Servants
- 1420 Contractors

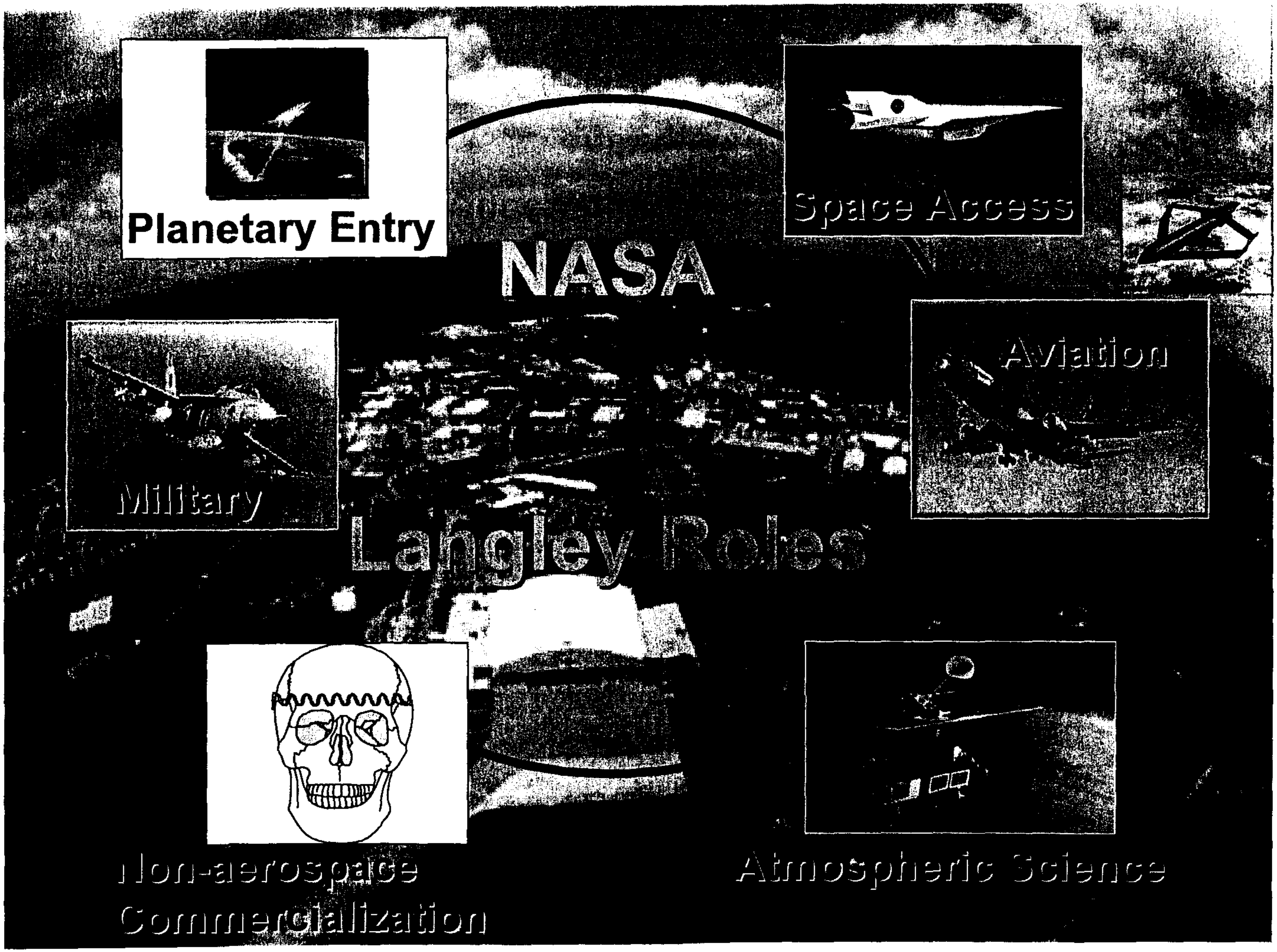

NASA Langley Roles

Planetary Entry

Space Access

Military

Aviation

Non-aerospace Commercialization

Atmospheric Science

LaRC's Contributions to Improve Quality of Life

- Improving the air transportation system - a critical element of the country's infrastructure
- Assuring the pre-eminence of U.S. military aircraft
- Reducing the cost of access to space
- Understanding the composition and evolution of the Earth's atmosphere as an aid to policymakers
- Providing atmospheric flight technologies for planetary exploration missions to extend the space frontier
- Developing innovative technologies for revolutionary aerospace systems
- Providing the benefits of aerospace technology breakthroughs to non-aerospace organizations

NASA Langley Major Aerodynamic Test Facilities Complex

Aero- and Gas-Dynamics Division
Langley Research Center

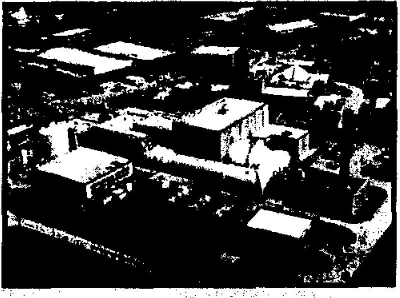

National Transonic Facility

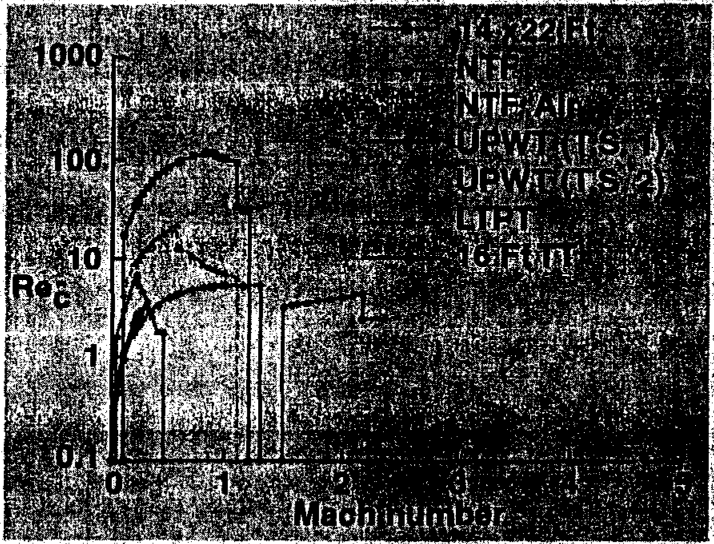

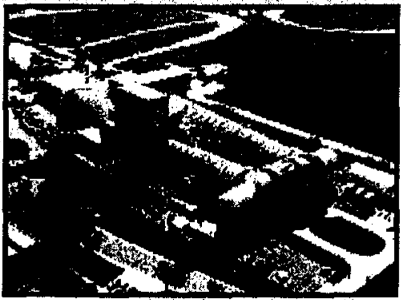

16-Foot Transonic Tunnel

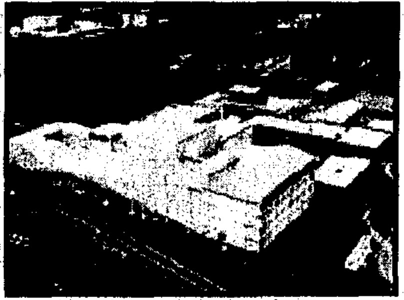

14-by 22-Foot Subsonic Tunnel

Low Turbulence Pressure Tunnel

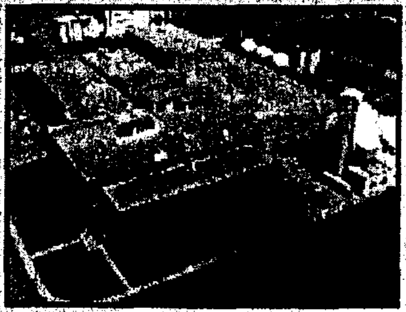

Unitary Plan Wind Tunnel

NASA Langley Aerothermodynamic Facilities Complex (AFC)

Aero- and Gas-Dynamics Division Langley Research Center

15-Inch Mach 6
Hi Temp. Air

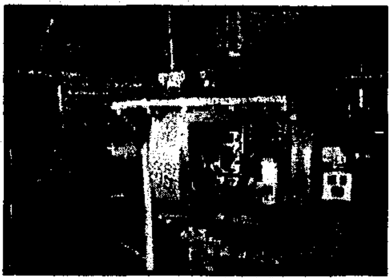

- 2/3 of Nation's conventional - type (as opposed to impulse) hypersonic wind tunnels
- Unique heavy and light gas test capability
- Provides wide envelope of flight simulation parameters
  - Mach number (6 to 20)
  - Reynolds number (0.05 to 20 million per foot)
  - Density Ratio (5 to 12); specific heat ratio (1.1 to 1.7)

20-Inch Mach 6
Air

20-Inch Mach 6
CF_4

31-Inch Mach 10
Air

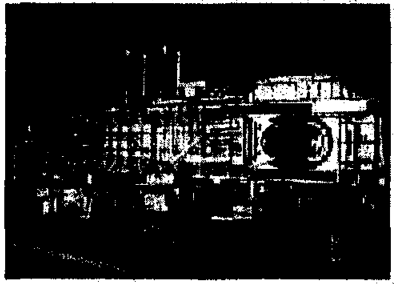

22-Inch Mach 15/20
Helium

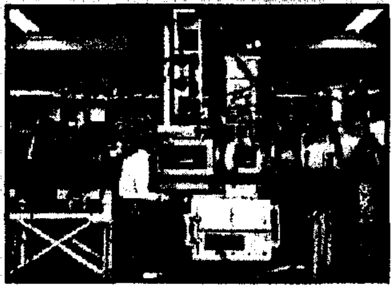

Plus complementary Langley subsonic to supersonic facilities

NASA Langley Scramjet Test Complex

Aero- and Gas-Dynamics Division
Langley Research Center

Combustion Heated STF

$M_\infty = 3.5 - 6$, $T_{t,\,max} = 1700K$

- ***Flight Mach simulation from 3.5 - 8 (near orbital w/HYPULSE upgrade)***
- ***Engine test facilities (STF):***
  - ***Active since mid 70's***
  - ***>3200 tests of 18 scramjet designs***
- ***Engine flowpath and components tests, inlets, nozzles, fuel injection, mixing and combustion***
- ***Established and confirmed design, and analysis methods***

Direct-Connect Supersonic Combustion Test Facility

$M_\infty = 4 - 7.5$, $T_{t,\,max} = 2100K$

Arc Heated STF

$M_\infty = 4.7 - 8$, $T_{t,\,max} = 2850K$

8 -Ft High Temperature Tunnel

$M_\infty = 4 - 7$, $T_{t,\,max} = 2000K$

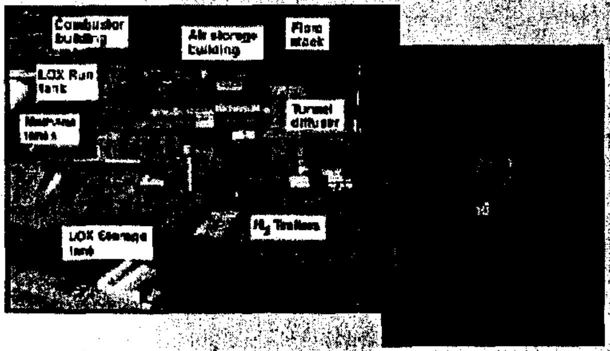

Hypersonic Pulse Facility

$M_\infty = 12 - 19$ (SET), $T_{t,\,max} = 9000K$

$M_\infty = 7 - 10$ (RST), $T_{t,\,max} = 4200K$

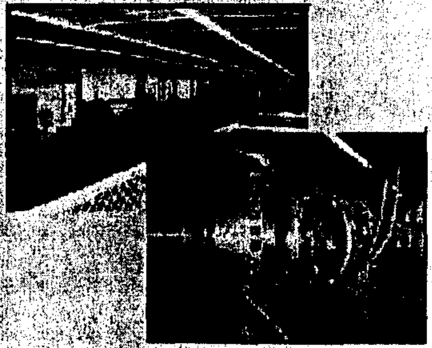

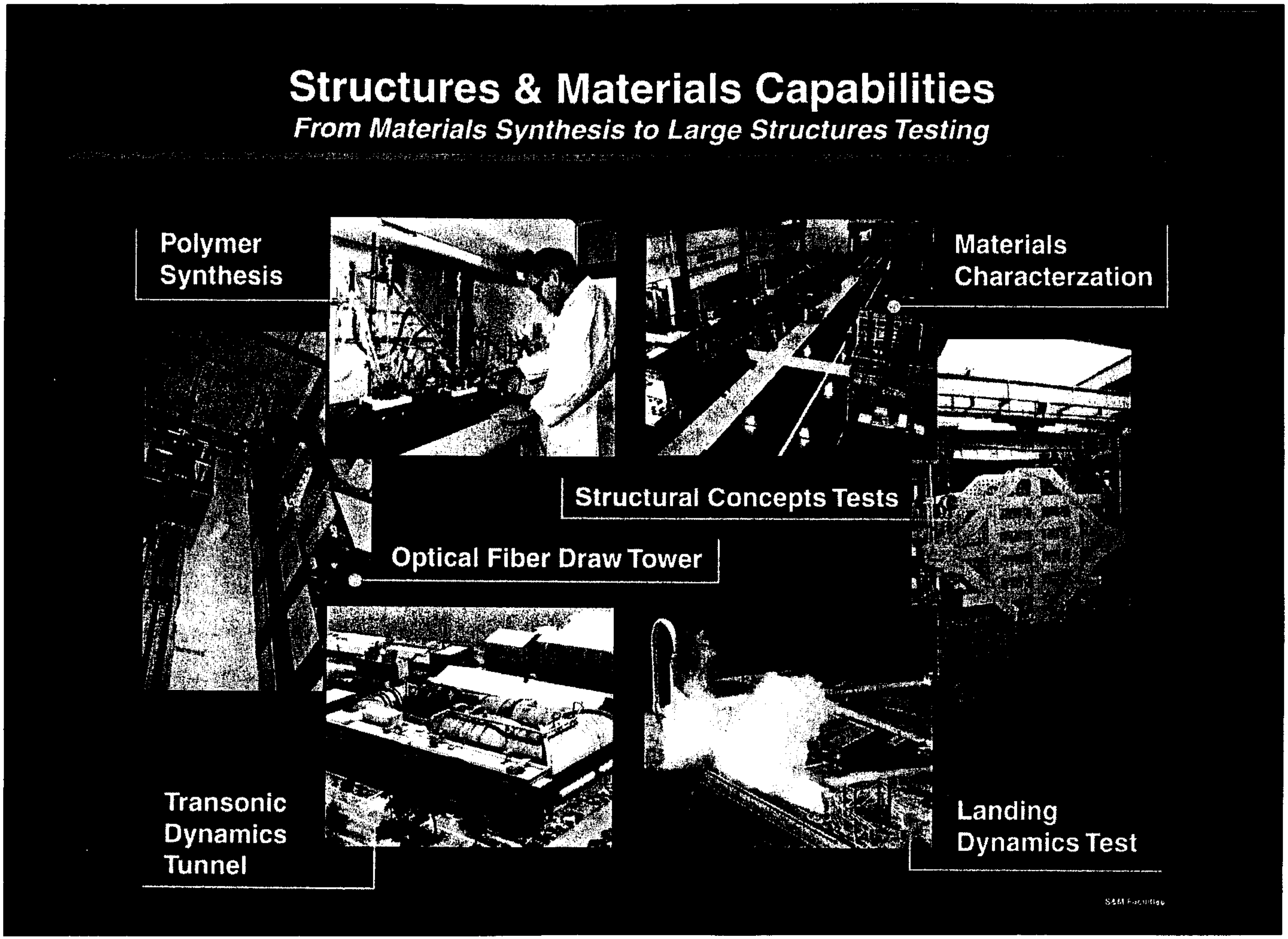

Structures & Materials Capabilities

From Materials Synthesis to Large Structures Testing

Polymer Synthesis

Materials Characterzation

Structural Concepts Tests

Optical Fiber Draw Tower

Transonic Dynamics Tunnel

Landing Dynamics Test

Research Aircraft and Research Simulators

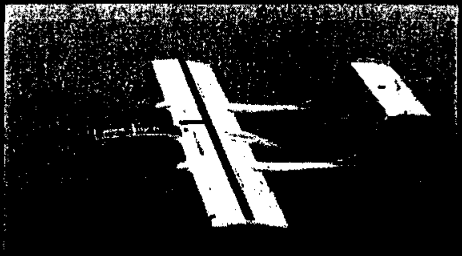

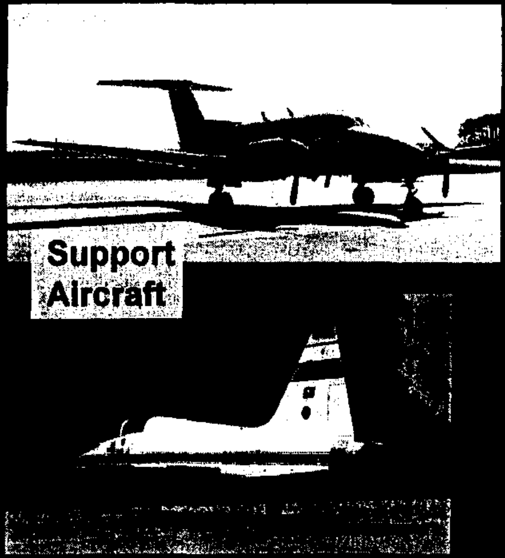

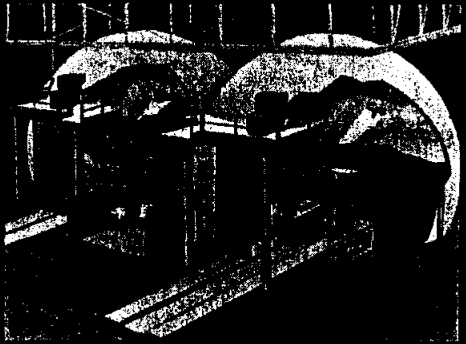

Differential Motion Simulator (DMS)

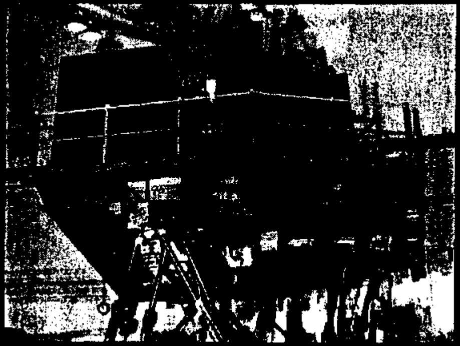

Visual Motion Simulator (VMS)

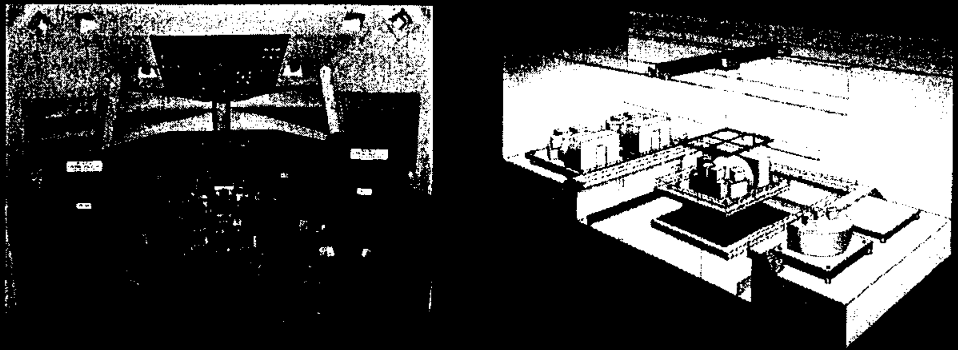

Cockpit Motion Facility (CMF)

Langley Contributions to the Boeing 777

- Computational aerodynamic methods
- Wind-tunnel tests for performance analysis
- Flutter clearance tests
- Advanced flight deck
- Digital data system
- Fly-by-wire flight controls
- Lightweight composite structures
- Tire durability testing

Langley Contributions to the C-17

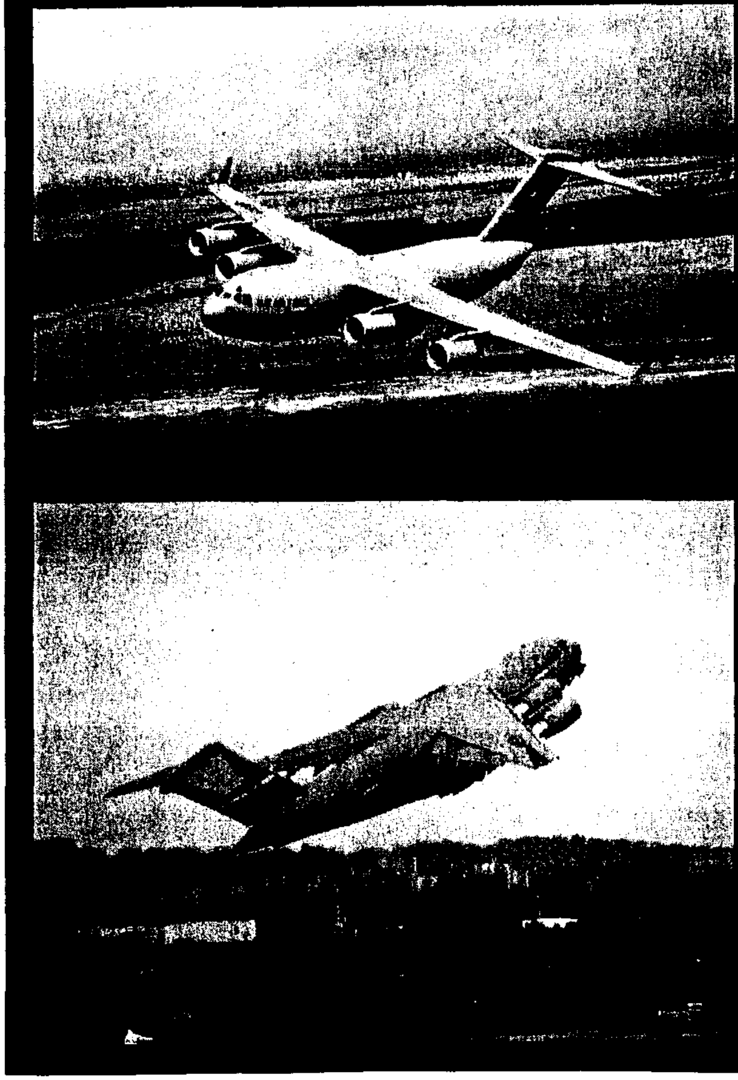

- Externally blown flap concept
- Winglets
- Supercritical wing
- Advanced flight deck
- Composite materials
- Fly-by-wire flight controls
- “T-tail deep stall” avoidance

Space Access and Technology Synergy with Aeronautics

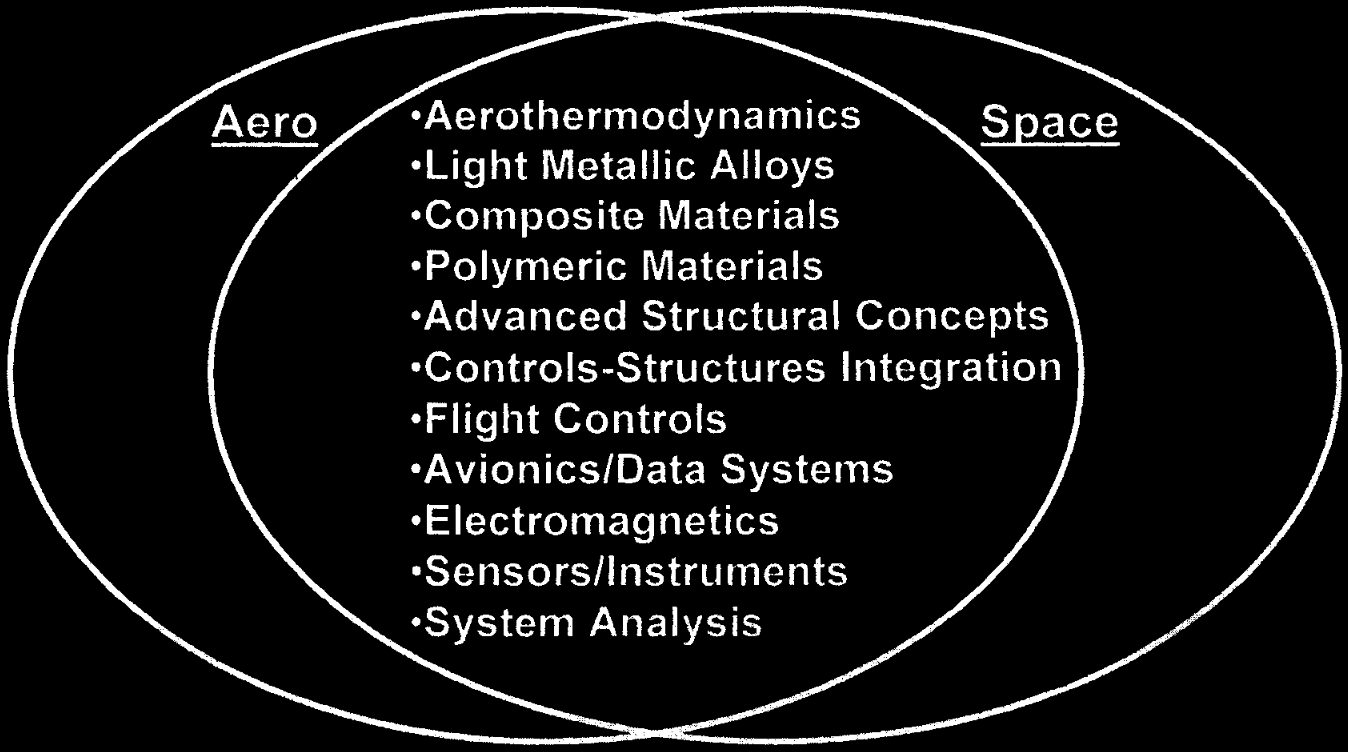

Aero

Space

- Aerothermodynamics
- Light Metallic Alloys
- Composite Materials
- Polymeric Materials
- Advanced Structural Concepts
- Controls-Structures Integration
- Flight Controls
- Avionics/Data Systems
- Electromagnetics
- Sensors/Instruments
- System Analysis

MAJOR TECHNICAL AREAS OF EXCELLENCE AT LANGLEY

(where we are publishing/making a "value-added" contribution as opposed to managing programs or conducting tests for others)

Strong Areas

- Polymer chemistry/matrices for composites etc.
- Crack propagation/growth/stress inducement
- Solid state lasers
- Instrumentation development/deployment/utilization--atmospheric science measurements from space/aircraft
- Aerothermodynamics
- Scramjets
- High reliability software
- Aeroacoustics
- Unsteady aero/aeroelasticity/TDT
- Controls including smart structures/materials
- Materials technology
- Computational sciences
- Radiation effects/shielding

TECHNOLOGIES CRITICAL TO FUTURE OF NASA/LARC

- Structures/materials
  e.g. nanotechnology, fullerene carbons, metal-matrix composites, diamond coatings, fabrication-by-light
- Multidisciplinary optimization from "cradle-to-grave"
  e.g. minimization of total life cycle costs, nonlinear "all up: systems analysis
- Intelligent agents--conversion of information/data to (targeted) knowledge, 3-D multisensory "visualization"
- Miniature/micro instrumentation/sensors/actuators with application to "health monitoring," brilliant materials and atmospheric sciences
- In computational sciences - orders of magnitude reductions in overall solution time (problem formulation to result analysis)
- Software "surety" (security, reliability, safety, etc.)
- Creativity/invention

THOMAS JEFFERSON NATIONAL ACCELERATOR FACILITY AND THE APPLIED RESEARCH CENTER

Amy Wilkerson

Applied Research Center
12050 Jefferson Avenue, Suite 713
Newport News, VA 23606

Telephone 757-269-5760
e-mail alwilker@AS.WM.EDU

Amy Wilkerson

Thomas Jefferson National Accelerator Facility and The Applied Research Center

Presented by Amy Wilkerson, College of William and Mary, Williamsburg, VA

Jefferson Lab

Jefferson Lab is the youngest of four major basic research facilities in High Energy and Nuclear Physics in the United States, and provides a scientific instrument and research opportunities that are unique in the world. Built, managed, and operated by SURA (Southeastern Universities Research Association) for the Department of Energy, the Thomas Jefferson National Accelerator Facility (Jefferson Lab) makes possible the research of an international user community into how nucleons are built from quarks and gluons, and how this structure leads to the standard nucleon-based picture of the nucleus of ordinary matter. Copious physics data of unprecedented precision are providing new insight into the structure of nucleons and attest to the unique beam quality. The performance of the enabling accelerator technology made Jefferson Lab a key partner in the construction of the Spallation Neutron Source; and JLab's Free Electron Laser (FEL) and related developments hold high promise beyond science in defense, security, health and manufacturing.

Jefferson Lab is a valued contributor to scientific education, and a major resource to the local, regional, and national education community. Our Science Education programs and partnerships are designed to advance science learning at every level and especially to address the urgent need to improve the representation of minorities and women in our nation's science and engineering workforce.

Our unique research environment and expertise in science, math, and technology create the basis for extraordinary educational opportunities that are solidly grounded in the Laboratory's scientific programs. Over a third of the Laboratory staff and many of the Lab's scientific users participate as mentors and career role models, interacting on a regular basis with the students and teachers.

Jefferson Lab will be holding sessions designed for teachers during NEW 2003.

Applied Research Center

The Applied Research Center or ARC, is the physical location for a unique partnership among Christopher Newport University, the College of William and Mary, Hampton University, Norfolk State University, Old Dominion University and the Department of Energy's Thomas Jefferson National Accelerator Facility (Jefferson Lab). The partnership's goals are 1) to increase the quality of research and education, 2) to investigate complex problems identified by industry; and 3) to stimulate new economic growth and employment. This flagship building, constructed by the City of Newport News' Economic Development Authority, marks the start of a 200-acre research park and is a symbol of cooperation and encouragement of local and regional business development. The ARC houses 27 state-of-the art laboratories, office space, computer facilities and a technical library focused on concentrating the region's multidisciplinary materials processing resources. Classroom courses can be taught using distance-learning technologies so students and faculty can stay in the building, minimizing Interruptions to their research. The ARC is also home to high-tech business start-ups, a venture capital firm, and high-tech business support services.

The ARC will be providing tours for the participants of NEW 2003.

KEEP – KENTUCKY ELECTRONICS EDUCATION PROJECT, MICROELECTRONICS AS A THEME IN MATH AND SCIENCE

Janet K. Lumpp

Electrical and Computer Engineering Department
University of Kentucky
453 Anderson Hall
Lexington, Kentucky 40506-0046

Telephone: 859-257--4985
e-mail jklumpp@engr.uky.edu

Janet K. Lumpp

KEEP – Kentucky Electronics Education Project, Microelectronics as a Theme in Math and Science

Janet K. Lumpp

Electrical and Computer Engineering Department, University of Kentucky,
453 Anderson Hall, Lexington, KY 40506-0046 jklumpp@engr.uky.edu

Key Words: electricity, electronics, circuit boards, components, patterning, etching, soldering

Prerequisite Knowledge: basic knowledge types of materials, the procedures below are used in classroom and workshop settings to introduce beginners to microelectronic assembly methods

Objectives: to learn basic circuit assembly skills, to learn about conductors, nonconductors, components, and solder, to increase background knowledge of teachers in the area of electronics

Equipment: (Suppliers listed under References)

1. Electronics Assembly Kit (included in workshop registration)
    a. Scotchbrite pad, clothing iron, wood board, Sharpie marker
    b. Hand drill, #69 drill bits, small screwdriver
    c. Soldering iron and stand, wire cutters, needle nose pliers, wire stripper
    d. Solder, desolder braid
    e. Digital multimeter
2. Circuit Materials
    a. Copper clad printed circuit board – 1 ounce, 1 sided
    b. Press and Peel Wet transfer paper
    c. Electrical schematic and layout pattern
    d. Components
3. Etching Setup
    a. Sodium persulfate salt
    b. Scale
    c. Pyrex glass dish
    d. Heat source – hotplate, Bunsen burner
    e. Thermometer
    f. Tweezers or tongs

Introduction:

Microelectronic materials, assembly technologies, and design guidelines span a wide range of topics in chemistry, physics, mathematics, and environmental science, and represent a variety of career opportunities in engineering, manufacturing, and R&D. The Kentucky Electronics Education Project is the education component of two NSF research grants aimed at introducing pre-college students to microelectronics. Working with middle school and senior high school teachers, we are developing curriculum materials and classroom activities using microelectronics as a theme to teach basic concepts in chemistry, math, and physics. Topics include copper etching and plating, semiconductors, insulators, conductors, energy conversion, heat transfer, materials properties, dimensions, routing, soldering, and component types. The emphasis is not vocational training, rather it is the use of a real world example as a theme to integrate basic principles from different disciplines. Activities to date have included classroom circuit building projects, fieldtrips, and teacher workshops. Middle school and high school students have successfully patterned, etched, drilled, and soldered working circuits and enthusiasm is equally distributed among boys and girls. The long term goals are to serve as a resource for school teachers, recruit students into engineering and science careers, and increase public awareness of the exciting advancements in microelectronics.

Procedure:

Instructions for Making Printed Circuit Boards

The process presented here is based on an article by Larry Ball in Electronics Now[1]. Several students at in the Electrical and Computer Engineering program contributed to detailed instructions below. Following the steps below will help you build working circuits, however, it is not completely failsafe and some errors and touch ups are generally required.

Overview

Printed Circuit Boards (PCBs) start out with copper on one or both sides. The continuous layer of copper must be divided into conductive wires separated by insulating spaces. Many of the steps described below are dedicated to transferring the pattern of conductive wires and pads to the PCB. The circuit pattern is drawn using standard features based on the components used and the connections specified by the electrical schematic.

The technique presented here takes the circuit pattern printed on special toner transfer paper and irons that pattern onto a clean copper surface. A chemical etching solution dissolves the exposed copper and the toner protects the copper lines that become the circuit wires. After etching it is necessary to drill holes in the board for the component leads to pass through the board. Finally, the component leads are soldered to the copper wire lines to complete the electrical circuit.

Several common pitfalls will be discussed along with repair methods. The most important step is to CLEAN THE COPPER SURFACE thoroughly. A clean surface improves the adhesion of the toner to the board, which in turn increases the quality of the etched board. If conductor lines are etched through (making an open circuit) then it is necessary to solder a jumper wire over the gap. All of these issues will be covered in the following pages.

Pattern Preparation

For the circuits built during the workshop, we have already prepared the patterns using a software program called WinBoard by IVEX[2]. You can create your own patterns from a schematic using the software or by hand using templates. Templates are necessary to match the circuit pattern to the leads on the components. For example, an 8 pin DIP IC package must match a set of eight holes properly spaced out on the board and the conductor lines must connect the proper pins to the other circuit components. Conductor lines and spaces should be as large as possible to increase the odds for successful pattern transfer and etching. Wherever possible, conductor lines and spaces should be 30-50 mils wide (1 mil = 0.001 inch = 0.025 mm = 25.4 μm). Smaller lines will not transfer and etch reliably. A typical via (donut) hole size is 70 mils outer diameter and 30 mils inner diameter. It is permissible to pass conductor lines under components using the component as a bridge over the conductor line. Lines can also pass between the leads on an IC chip, such as a DIP, by making the conductor line narrower to prevent a short circuit connection to the adjacent via hole donuts. Rub on lines, donuts, and standard component templates can be purchased from electronics suppliers or catalogs. One other option is to have a prepared drawing that can be photocopied onto the toner transfer paper.

It is also useful to have a box drawn around the circuit pattern that corresponds to the size of the circuit board. During the iron on step the box outline helps align the board and pattern.

Pattern Printing

The toner transfer paper is somewhat like a decal. The features on the paper are transferred to the circuit board surface and the backing paper is soaked off in water. Print onto the shiny side of the Press and Peel Wet paper. It is necessary to make a VERY DARK print on the toner transfer paper with a large amount of toner. The toner will protect the copper during chemical etching so more toner ensures better etching resolution. Refer to the instructions on the toner transfer package. In general, a dark print can be accomplished by *increasing the print density* on a laser printer or by *increasing the darkness* on a photocopier. If the open white areas become gray, that is OK. The chemical etchant will etch through this thin layer of toner.

Placing several patterns on a page will help conserve the toner transfer paper. After printing the individual patterns can be cut apart in preparation for ironing onto the board.

Board Cleaning

A CLEAN COPPER SURFACE IS CRITICAL. Copper forms an oxide coating when exposed to air and humidity exactly like the darkening of pennies and green coloring of a copper roof or the Stature of Liberty. The toner *will not adhere* to the copper oxide and it is therefore critical to *remove this layer* before ironing on the toner transfer printout. Scotchbrite scouring pads are used to scrub the oxide layer off of the copper. Press firmly and scrub for at least one minute. Scrub in a circular motion in the center of the board and parallel to the edges of the board. Fine black dust should come off during the scrubbing process. Scratches on the copper from the scrubbing process are OK. The copper should look bright and pink in color.

After scrubbing thoroughly, rinse the board with water and dry with a paper towel. Hold the clean board by the edges to prevent any fingerprints on the surface. Fingerprints contain oil that will prevent the toner from sticking to the surface. If the surface does become soiled, scrub again, rinse and dry. Iron on the pattern *immediately* after cleaning.

Iron On Pattern Transfer

The toner transfer pattern is bonded to the copper by heat and pressure using a clothing iron. Preheat the iron in the no-steam mode and set at the *beginning of the steam range*. Place the clean copper board on a heat safe surface such as a wooden board with the copper facing up. Place the toner transfer paper face down on the board aligning the edges of the board with the box outline on the pattern. Press down firmly with the iron and hold in place for 60 seconds. Move the iron every 60 seconds for a total of five minutes to ensure even heating. DO NOT allow the iron to slide as it will smear the toner and blur the pattern. Heat, pressure, and time are necessary to melt the individual toner particles into a continuous black coating on the copper surface.

After ironing, place the board in a dish of water with the toner transfer paper facing up. Allow the board to soak until the paper floats up off the circuit board, approximately five minutes. The result should be a clean piece of paper and a complete black pattern bonded to the copper surface. If some pieces of toner are not well bonded to the copper, they can be repaired prior to etching.

Pattern Touch Up

If there are major errors in the pattern - missing lines, blurring, and misalignment of the pattern and board - then it may be necessary to scrub the board clean and iron on an new pattern. Small errors can be repaired by drawing the missing sections with a permanent Sharpie marker. Rub on lines and donuts can also be used to repair patterns.

At this point it is also useful to write initials or some other marking on an open area of the pattern to identify whose board is whose. Using the permanent marker make dark letters by going over the letters at least twice. Dark letters will etch better just like the dark toner will protect the conductor lines.

Etching

Several hobby class etchants are available in electronics shops and catalogs. The ferric chloride solution or anhydrous solid that you can dissolve in water will etch copper quickly but is more expensive. The less expensive alternative is sodium persulfate sold as a white crystalline powder you dissolve in water. Etchant solutions are CORROSIVE and should be treated as hazardous materials. WEAR GOGGLES AND GLOVES when working with the etchant powders and solutions. Mix the solution according to the directions on the container. For sodium persulfate the ratio is 1/2 pound per gallon. Tap water is fine or distilled water. Fresh solution will etch more quickly and a solution that has been sitting for several weeks may not etch well. Heat accelerates the etching process and sodium persulfate solution etches effectively at temperatures up to 70°C. Using a Pyrex glass container, the etchant can be heated with a hotplate or Bunsen burner with a thermometer for temperature monitoring. Professional etching tanks with heaters and agitators are also available for approximately $120 and hold 1.5 gallons of solution. Depending on the temperature of the etchant and the area of the circuit board, etching time varies from 20-60 minutes. Circuit boards should be placed in the etching tank using tweezers or tongs so that the copper is exposed to the etchant without other boards overlapping. Stir the etchant occasionally to bring fresh solution in contact with the copper.

Initially it is difficult to observe any progress in the etching process. The copper color changes slightly and the scratches disappear. Eventually the copper becomes thin enough to allow the underlying board material to show through and the edges of the board come clean first. The solution turns blue-green as the copper metal is converted to copper sulfate in solution. The etching process is complete when the visible copper is gone and the only remaining features are the black pattern lines. Under these lines are the copper conductor wires that will connect the electrical components. Etched boards should be rinsed in clean water and dried with a paper towel.

Copper Etching Reactions

The circuit board etching step takes the solid copper metal from the PCB into solution as copper ions Cu^{+2}. The chemical reaction causing the metal to dissolve is a corrosion reaction involving the persulfate ion and the copper atoms on the board. The sodium persulfate crystals ($Na_2(SO_4)_2$ or $Na_2S_2O_8$) are a stable salt of persulfuric acid ($H_2S_2O_8$)[3]. When the sodium persulfate salt is dissolved in water, the sodium is present as Na^{+1} ions and the persulfate ion is present as $S_2O_8^{-2}$ ions as shown in Equation 1. The persulfate ion is a powerful oxidant that oxidizes the metallic copper on the circuit board and converts it to copper ions in solution as shown in Equation 2. If the water in the solution is allowed to evaporate, the copper will precipitate as $CuSO_4$ as shown in the products of Equation 2. The persulfate ion can also hydrolyze into peroxy monosulfate ion (HSO_5^{-1}) which then converts to hydrogen peroxide (H_2O_2) and oxygen (O_2) byproducts. These subsequent reactions cause the etching bath to deteriorate over time. It is important, therefore, to store the etchant in its stable salt form and mix up fresh etchant solution as needed.

$$Na_2S_2O_8 \rightarrow 2Na^{+1} + S_2O_8^{-2} \qquad \text{(Eqn. 1)}$$

$$Na_2S_2O_8 + Cu^0 \rightarrow CuSO_4 + Na_2SO_4 \qquad \text{(Eqn. 2)}$$

$$Cu^0 \rightarrow Cu^{+2} + 2e^- \qquad \text{(Eqn. 3)}$$

Equation 3 shows the copper metal dissolving off of the circuit board and into solution as the copper atom loses two electrons to become a copper ion. A loss of electrons is an oxidation reaction and making the copper an anode that supplies electrons[4]. A gain of electrons is a reduction reaction and a cathode receives electrons. Two electrons are required to make one copper ion and the persulfate ion has two extra electrons. In Equation 2, one mole of sodium persulfate etchant can dissolve one mole of copper, however, the deterioration of the solution discussed above makes the practical etching capacity lower.

The etching solution described in the Instructions for Making Printed Circuit Boards handout is mixed at ½ pound per gallon and heated to 40-70°C. Higher concentrations of etchant are possible but require higher temperatures to keep the salt from precipitating out of the solution.

Via Hole Drilling

A hole must be drilled for each component lead. Small hand drills work best because they are easy to control. With practice, a power drill such as a Dremel tool can be used to drill holes faster. WEAR GOGGLES while drilling because the fine drill bits snap easily. Place the circuit board on a piece of scrap wood to protect your table surface. Hold the drill perpendicular to the board and try to drill straight through not at an angle. Refer to the layout pattern to make sure all holes are drilled. The #69 drill bit works well for most through hole component leads, however, you may also need some larger holes for mounting a battery clip. A careful job of drilling will make it easier to insert components and prevent the awkward job of drilling holes in a partially assembled board.

Toner Removal

The remaining toner should be scrubbed off with the Scotchbrite pad or rinsed off with acetone to reveal the underlying copper. The copper must be exposed to allow the solder to make contact. Toner removal should be done just before soldering so that the copper does not oxidize.

Component Insertion

Components are inserted from the blank side of the board with the leads sticking out through the copper donuts on the backside. The leads on axial lead components must be bent into a U shape and three-lead components need to be separated into a tripod shape. The *orientation of components* is CRITICAL to the operation of the circuit. All components have a specific orientation in a circuit with the exception of resistors and some capacitors. The schematic, layout, and component placement drawings will help you determine the correct orientation for each component. For example, transistors are usually drawn as a half circle with the flat side facing one direction and LEDs are drawn with one black side indicating the shorter lead. Integrated circuit chips are easy to misalign by 180 degrees. The top of the chip is marked with a half circle notch or a white stripe, or pin number 1 is marked with a circle. For example, if power is supposed to go to pin 1 and the chip is in backwards, the power might be going to pin 5 or 8. The circuit will certainly not work as designed and the chips may be damaged if powered up incorrectly. Attention to detail will save debugging time.

After insertion, the leads may be bent slightly to keep the component from falling back out of the holes. Bending the leads is called clinching. Do not trim the length of the leads until after soldering. In general, you can insert a few components at a time, clinch the leads, solder, trim the leads and then insert a few more components. The short pieces of wire trimmed from components are useful for repairing open circuits where the copper has been etched through. Keep a few pieces until you are done debugging and repairing a circuit.

Soldering Safety and Technique

A soldering iron is a simple direct electrical heating element designed to melt solder alloys. Inexpensive soldering irons plug directly into a wall outlet and heat to a set temperature. More elaborate soldering systems allow the user to vary the power or set the maximum temperature. Different size and shape tips are available for soldering various types of components.

The hot tip exposed to air tends to build up an oxide coating that is detrimental to forming a good quality solder joint. Therefore, it is necessary to practice good tip cleaning habits and proper soldering technique. When a hot tip is sitting in the soldering iron stand it should be coated with solder to prevent oxidation of the tip. This is called "tinning" the tip. Always leave the tip tinned when the soldering iron is not in use. A tinned tip looks shiny like a silver mirror. Prior to making a solder joint, the excess solder is wiped from the tip using a damp sponge. Most soldering iron stands come with a small piece of sponge and a tray to keep the sponge in place.

When making a solder joint it is important to heat both the copper conductor line and the component lead so that the solder will make good contact with both surfaces. Hold the tip firmly against both the copper and the lead, and then bring the solder wire in to the joint area. Allow a small amount of solder wire to melt onto the tip, copper and lead. Pull the solder wire away first, and lastly remove the soldering iron tip from the solder joint. (If you pull the iron away first, the solder joint will solidify with the solder wire attached to it. The soldering iron can be used to remelt the solder to detach the solder wire.) Continue on to make another solder joint or tin the tip and place the iron back on the stand. You will see and smell a small amount of smoke when the solder wire melts. The smoke comes from the flux material in the solder wire. The molten solder at the solder joint quickly cools and becomes a solid piece of metal.

Soldering Steps

1. Wipe excess solder onto the damp sponge.
2. Hold the tip against the copper conductor line and the component lead.
3. Bring the solder wire into the hot copper, lead and soldering iron tip.
4. Melt a small amount of solder.
5. Remove the solder wire from the joint area.
6. Remove the soldering iron from the joint area.
7. Make another solder joint using steps 2-6 *or* tin the tip and place the iron in the stand.
8. Wash your hands when you are done soldering to prevent ingestion of lead.

Inspecting Solder Joints

A good solder joint makes a cone shape around the component lead and covers the via hole "donut" area on the copper conductor line. Too much solder at the joint will have a ball shape and may form a bridge to other solder joints nearby. Solder bridges are short circuits that will change the performance of the circuit and must be repaired. Too little solder at the joint will not make the smooth cone shape and may not make a complete connection between the copper and component. Inadequate heating of the copper and lead results in a "cold joint" that may look alright but be an open circuit.

Repairing Solder Joints

One of the simplest debugging tools is to touch up the solder joints. Cold joints can be repaired by remelting the solder at the joint using a hot soldering iron tip. Solder can be added to the joint by repeating the soldering steps. Solder bridges can be broken by remelting the solder. Excess solder can be removed using a solder wick (see desoldering below).

Desoldering

Sometimes it is necessary to remove a soldered component in order to replace it with another component or to reverse the orientation of a misplaced component. In order to remove a component, the solder joints must be eliminated by melting the solder with a soldering iron and removing the molten solder. Two common techniques for removing molten solder are solder wick and desoldering pumps. Solder wick is a braid of copper wire with flux that will attract the molten solder away from the joint. Solder wick is used by laying the solder wick over the solder joint and heating the wick and joint with the soldering iron. The copper colored braid will turn to the silver color of the solder as the molten solder is drawn up into the braid. Remove the braid and iron to inspect the joint. After a section of braid has been used it can be cut off with wire cutters and discarded. A desoldering pump sucks the molten solder away from the joint. The solder is heated with the iron, then the pump opening is brought close to the joint and triggered to pull up the molten solder. Manual desolder pumps operate by depressing a spring-loaded plunger and then releasing the plunger to create a short burst of suction. The pump has to be reloaded for each joint that needs to be desoldered. Electric pumps reload themselves automatically or use a small vacuum pump to generate the suction.

Resoldering

Copper surfaces and components can be soldered several times before the copper is destroyed or the component is damaged by excessive heat. Once the copper conductor line is damaged, it is necessary to add a jumper wire to connect the remaining copper line to the component lead. A damaged component must be replaced with a new one.

About Solder Joints

Solder joints serve two important purposes in electronic circuits. On the one hand, the solder joint works as an adhesive bonding the components to the circuit board. On the other hand, the solder joint forms a short circuit connection between the copper conductor line and the component lead to complete the circuit path. Both jobs are critical to the performance of the circuit. If components fall off the board or are not electrically connected, then the circuit fails. A third job performed by solder joints in more advanced circuit assemblies is heat transfer. Heat generated by the integrated circuit travels through the solder joint to the circuit board to keep the IC cool. The choice of a solder alloy and the soldering technique involve careful study of the properties of the solder, such as, mechanical strength, thermal conductivity, electrical conductivity, and melting point. All of these properties vary with different alloy compositions depending on the specific elements and proportions of the elements in the alloy. The most common solder alloys are combinations of lead (Pb) and tin (Sn). Since lead is known to be toxic, many new alloys have been developed which are lead free.

Circuit Board Processing Steps

1. Prepare the pattern on the iron on transfer paper.
2. Trim the pattern to the size of the board.**

**If you will be etching the same day as ironing on the pattern, you may mix and preheat the etchant at this point (Steps 15 and 16).

CLEAN IMMEDIATELY BEFORE IRONING.

3. Clean the copper surface thoroughly with a Scotchbrite pad.
4. Wash the board in water and dry.
5. Preheat the iron to the beginning of the steam setting without steam.
6. Prepare a tray of water.
7. Place the circuit board on the wooden board with copper facing up.
8. Place the pattern face down on the copper.
9. Press firmly with the hot iron for 5 minutes moving every 1 minute. DO NOT slide the iron.
10. Place the circuit board in the tray of water with the paper facing up.
11. Wait for the paper to float off the board.
12. Dry the board.
13. Inspect the pattern and repair any missing lines with the permanent marker.
14. Label the circuit board with your initials if you are processing multiple boards.

WEAR GOGGLES AND GLOVES WHEN WORKING WITH ETCHANT.

15. Mix the etchant powder in water at the proper ratio.
16. Preheat the etchant solution to 40-70°C.
17. Place the patterned circuit boards into the etchant bath.
18. Stir occasionally and monitor the temperature.
19. Remove the etched boards, rinse with clean water, and dry.

WEAR GOGGLES WHILE DRILLING.

20. Drill holes.

21. Scrub off remaining toner with Scotchbrite pad or rinse off with acetone.
22. Preheat soldering iron.
23. Wet soldering iron sponge.
24. Insert components, clinch, solder, and trim leads.
25. Test circuit.
26. Troubleshoot and repair as needed.

Comments:

The procedures described above have been used successfully with teachers and students over the past four years. While they may seem unsophisticated when compared to industrial manufacturing methods, the basic steps parallel the steps used in commercial PCB fabrication and therefore serve as a real world example to connect students to the technology. For example, the iron-on process provides the same etch resist as photoresist, the etchant is a lower concenctration of a commercial etching bath, and hand soldering demonstrates the use of flux and the roles of solder in circuit assembly. Once the electrical schematic has been converted to an accurate layout pattern, circuits can be built in a few hours providing a sense of accomplishment for teachers and students. Tremendous pride and enthusiasm exude from participants who “made it themselves” in a workshop or classroom activity.

During teacher workshops we also review basic concepts on properties of materials, resistance, voltage, current, component types, circuit layout, solder and flux. Along with resources on all of the procedures, we also provide several lesson plans emphasizing the relevant National Science Standards and connections to mathematics. One of the circuits built in the workshops and classrooms is an electronic dice that displays a random number between one and six. Clearly, the circuit is useful for lessons on statistics and games of chance. Other lesson plans develop graphing skills, unit conversions, density and area calculations, and understanding circuit diagrams.

KEEP is well on its way to accomplish the goals of educating teachers regarding electronic assembly technologies and properties of electronic materials, developing curriculum materials, and organizing hands-on projects. The overall objective of KEEP is to encourage young students to consider technical and engineering careers.

References:

Supplies

The vendors listed below sell supplies that are consumed during circuit assembly.

Vendor	Products
Injectorall Electronics Corporation 110 Keyland Court Bohemia, NY 11716 800-878-7227 FAX 516-563-3389 www.injectorall.com	Sodium persulfate: 1/2 pound and 10 pound bottles of salt powder. 1 ounce copper printed circuit boards.
Techniks Inc. PO Box 463 Ringoes, NJ 08551 908-788-8249 www.techniks.com	Press and Peel Wet transfer paper: packs of 5, 10, 20 or 100 sheets. Fine gauge drill bits.
Chaney Electronics PO Box 4116 Scottsdale, AZ 85261 480-451-9407	1 ounce copper printed circuit boards. Project kits.
Jameco Electronics 1355 Shoreway Road Belmont, CA 94002 1-800-831-4242 www.jameco.com	Needle nose pliers, wire stripper, wire cutter, screwdriver Components
Electronix Express 365 Blair Road Avenel, New Jersey 07001 Phone 1-800-972-2225 www.elexp.com	Multimeter, soldering iron, soldering iron stand, solder, desolder braid
Fargo Enterprises 301 County Airport Rd. #105 Vacaville, CA 95688 707-446-1120 www.micro-tools.com	Fine gauge drill bits.

This research work was based on support from the National Science Foundation, Grant No. ECS-9702108 and DMR-9809686.

Bibliography:

---

[1] Larry Ball, "Make Your Own PC Boards Using Toner-Transfer Products", Electronics Now, Vol. 68, No. 8, August 1997, pp. 48-51.

[2] www,ivex.com WinBoard can be downloaded for FREE with a limit of 100 pins.

[3] C.F. Coombs, Jr., Printed Circuits Handbook, McGraw-Hill, New York, 1996.

[4] A pneumonic for remembering oxidation and reduction is: Leo the lion says Gerrr. LEO = Loss of Electrons is Oxidation. GER = Gain of Electrons is Reduction.

SMART MATERIAL ACTUATORS (2^{nd})

Kyo D. Song

Won J. Yi*

Sang-Hyon Chu*

and

Walter Golembiewski

Department of Technology
Center for Material Research
Norfolk State University
700 Park Avenue
Norfolk, Virginia 23504

Telephone: 757-823-8105
e-mail ksong@nsu.edu

*ICASE
NASA Langley Research Center

Kyo D. Song

Smart Material Actuators (2^{nd})

National Educators' Workshop
San Jose state University, CA
October 13 - 16, 2002

Kyo D. Song, Won Yi*, Sang-Hyon. Chu*, and Walter Golembiewski
Department of Technology, Center for Material Research, Norfolk State University
*ICASE, NASA Langley Research Center

Key Words: Piezoelectric, Unimorph, Smart Materials, THUNDER and Actuators

Prerequisite Knowledge: Basic knowledge of electronics, electromagnetic wave propagation, smart materials, rectenna operations

Objective: To demonstrate THUNDER actuators by a microwave power.

Equipment and Materials:
1. Anechoic chamber
2. Narda X band horn antenna model 601A (8.2 - 12.4GHz)
3. JPL 6 x 6 rectenna array
4. Hewlett Packard 8684B signal generator (5.4 - 12.5GHz)
5. Logi Metric Amplifier
6. Adjustable recycle time delay relay (HDFA Series by Amperite)
7. Hameg Instruments Oscilloscope (HM1507 150MHz 200Ms/s Analog/Digital)
8. Tekronix DMM916 (Analog/Digital Multimeter)
9. Resistors
10. THUNDER (Thin Layer Composite Unimorph Ferroelectric Driver and Sensor)
11. Coaxial cables and wiring fixtures

Introduction:

The concept of microwave-driven smart actuators is envisioned as the best option to alleviate the complexity associated with hard-wired power feed and control circuit. In addition to that, the simplicity of a microwave-driven actuator system can reduce a total weight and fabrication cost of the system. A proof of concept experiment using smart materials such as THUNDER (Thin Layer Composite Unimorph Ferroelectric Driver and Sensor) and paper actuators have been setup and demonstrated by using a microwave. Such advance system will produce a revolutionary class of smart devices that integrated sensors, actuators, and smart flight control as well as biologically-inspired systems.

Experimental Procedure:

An experiment was set up to actuate THUNDER actuators using a microwave source as shown in Fig. 1. A combination of signal generator and amplifier provided 20 W of microwave power to a Narda horn antenna at a frequency setting of 8 GHz. The 20 W microwave power irradiated at a JPL (Jet Propulsion Laboratory) 6 x 6 rectenna array. The rectenna, which is a rectifier and an antenna, converts the microwave power into DC power. The 6 x 6 rectenna array with the required wiring fixtures is inside an anechoic chamber as shown in Fig. 2. All other items listed in the equipment and material section were externally connected to the horn antenna and the rectenna via a backplate at the rear of the chamber. The Narda horn antenna is connected to the amplifier by a coaxial cable, and the signal generator is connected to the amplifier by a separate coaxial cable. The 6 x 6 rectenna array is connected to the exterior of the anechoic chamber by means of a dual output BNC connector. The output of rectenna fed to outside of the chamber, and either measured its output by a multimeter or connected to THUNDER actuators.

THUNDER is a ferroelectric device made of multiple layers of materials, typically stainless steel, aluminum and PZT (Lead Zirconate Titanate) piezoceramic. These layers of materials are sandwiched together with an adhesive bond. A piezoceramic material is composed of randomly oriented crystals or grains. By applying electrodes to the ceramic and a strong DC electric field, the dipoles are aligned in the direction of the electric field. By aligning in this manner, the smart material will have a permanent residual polarization. The result of this polarization is a change in the geometric dimension. Through the piezoelectric effect, THUNDER has the capability to expand or contract, based on the polarity of the voltage applied. When the applied voltage is positive, THUNDER will flatten, and if the applied voltage were negative, the THUNDER arches.

Comments:

The typical spatial distribution of the microwave power density on the rectenna is measured at distances from the horn inside of the anechoic chamber as shown in Fig. 3. As a result, the average power density of a 20 W microwave at 8.5 GHz is approximately 5 mW/cm^2. In this experiment, the 20 W microwave power was converted into a measured 230 V DC by a digital multimeter as shown in Fig.4. The estimated current being produced from the 6 x 6 rectenna array was 3.8mA. This was computed using various measured resistor values and the measured voltage across each resistor. The area exposed to microwave is approximately 2500 cm^2 that gives 60% efficiency of the microwave power at the target. The dimension of the 6 x 6 rectenna is 12 cm by 12 cm. The irradiance of the microwave power on the recetenna is measured as 7 mW/cm^2. Therefore, the power irradiated on the recetenna will be approximately 1.0 W. Based on this calculation, an efficiency of the rectenna is calculated as 87%.

The THUNDER used for the test produced 7.62 mm maximum displacement from 230 V DC output of the rectenna. Fig. 5 shows the displacement levels of THUNDER actuator according to the voltages fed from the 6 x 6 patch rectenna array. A higher voltage output than 230 volts is expected by increasing the beam power. The test of the 6 x 6 patch rectenna was limited by the capacity of the 20 W tunneling wave tube amplifier (TWTA) used.

Currently, a 200 W TWTA is under installation and expected for higher voltage output from the 6 X 6 patch rectenna as predicted in Fig. 6. High voltage output is determined by the number of density and breakdown voltage of Schottky barrier diodes in a rectenna array, the beam power, the frequency, and distance.

References:

1. T.K.Wu, "Multiband FSS," in T. K. Wu (Ed.), *Frequency Selective and Grid Array,* John and Wiley & sons, New York, 1995.
2. W. Schneider, J. Moore, T. Blankney, D. Smith, and J. Vacchione, "An Ultra-Lightweight High Gain Spacecraft Antenna," *IEEE Antennas Progagat. Int. Symp.*, Seattle, WA, June, pp. 886-889, 1994.
3. T. H. Lee, R. C. Rudduck, T. K. Wu, and C. Chandler, "Structure Scattering Analysis for Sea Winds Scatterometer Reflector Antenna Using Extended Aperture Integration and GTD," *IEEE Anetnnas Propagat. Int. Symp.*, pp. 890-893, Seattle WA, June 1994.
4. W. C. Brown, et al., *US Patent 3 4346*78, Mar. 25, 1969.
5. W. C. Brown, "Experiments involving a microwave beam to power and position a helicopter," *IEEE Trans. Aerosp. Electron. Syst.*, Vol AES-5, No. 5, pp. 693-702, 1969.
6. W. C. Brown, "Solar Power Satellite Program Rev. DOE/NASA Satellite Power System Concept Develop. Evaluation Program," *Final Proc. Conf.*800491, 1980.
7. J. Schlesak, A. Alden and T. Ohno, "A microwave powered high altitude platform," IEEE MTT-S Int. Microwave Symp. Dig., pp. 283-286 1988.
8. W. C. Brown, "Design study for a ground microwave power transmission system for used with a high-altitude powered platform," *NASA Final Contractor report 168*344, Raytheon Rpt. PT-6052, 1983.
9. NASA JPL, "Patch Rectenna for Converting Microwave to DC Power," *NASA Tech Briefs*, Vol. 21, January, p. 40, 1997.
10. Brown, W. C., Draft of Paper Prepared for Presentation at the 8th Biennial SSI/Princeton Conference on Space Manufacturing, May 6-9, 1987.

Bibliography:

Dr. Kyo D. Song is a P.I. of Smart Materials Research funded by NASA LaRC. He has been involved in many research projects, such as: Hypersonic Flow Research, Testing high temperature materials for Scram-jet Engine Components, Study on effects of atomic oxygen on space materials, and Smart materials research for Next Generation Space Telescope (NGST) under NASA supported grants. Dr. Sang-Hyon Chu is a staff scientist of ICASE at NASA Langley Research Center. His current research in NASA focuses on development of smart sensor based on bioinorganic nanoparticles. Dr. Won Yi is working as a research scientist at NASA Langley Research Center. His specialized area is high voltage, pulse power, and lasers. Dr. Golembiewski is an Associate Professor working at Computer Technology. He has considerable experience in the design and testing of circuitry and communications.

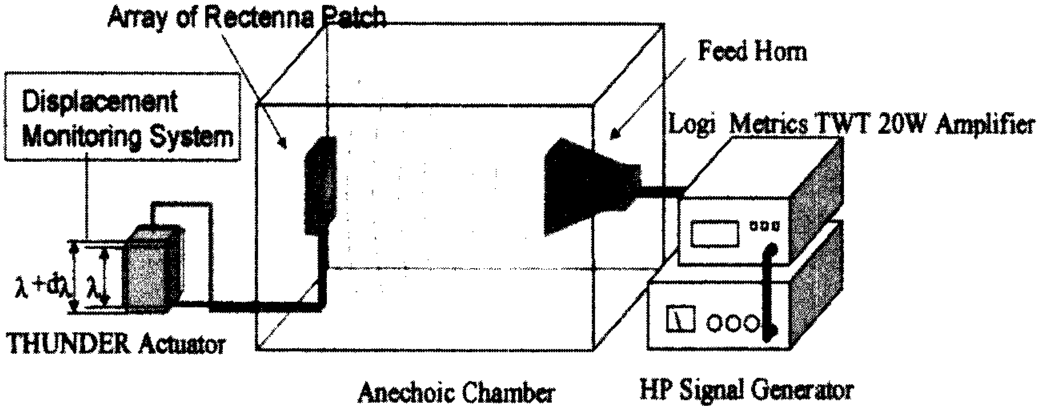

Fig. 1. Schematic of experimental set-up.

Fig. 2. 6 x 6 rectenns located in the Chamber

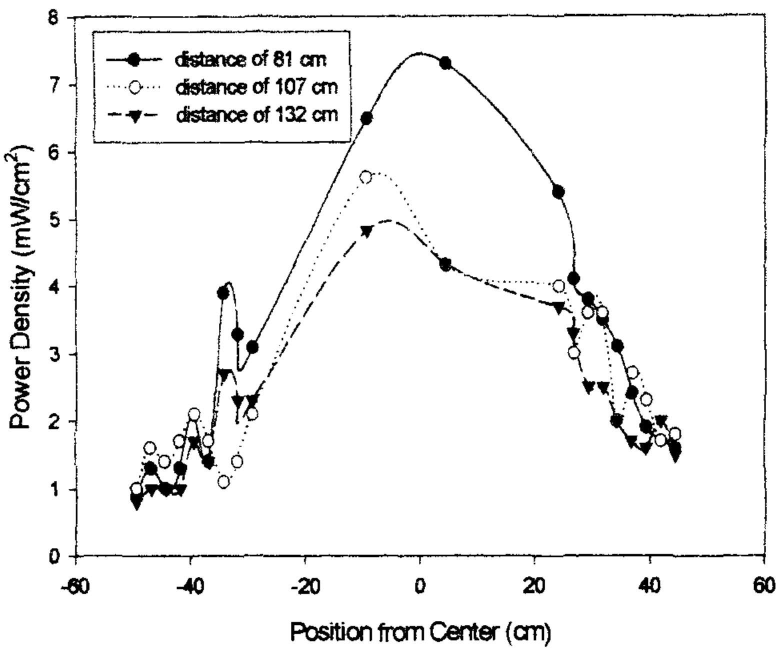

Fig. 3. Microwave Power Density Distribution along Distances.

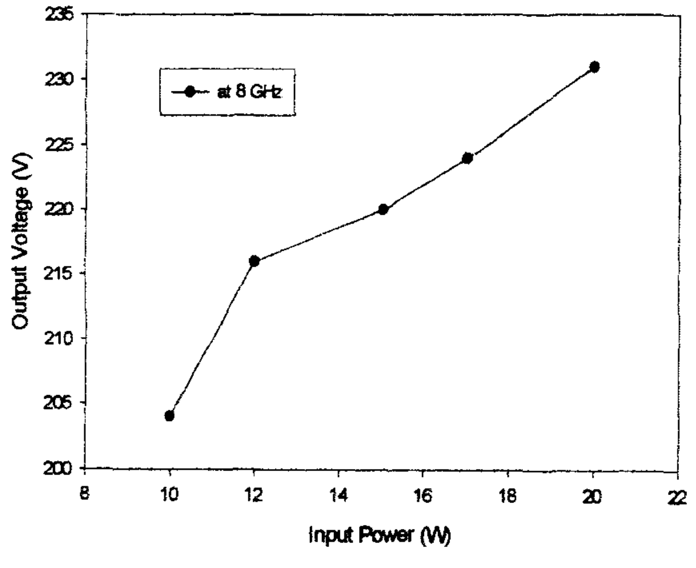

Fig. 4. Input Power Dependent DC Output Voltage from a 6 x 6 Patch Rectenna.

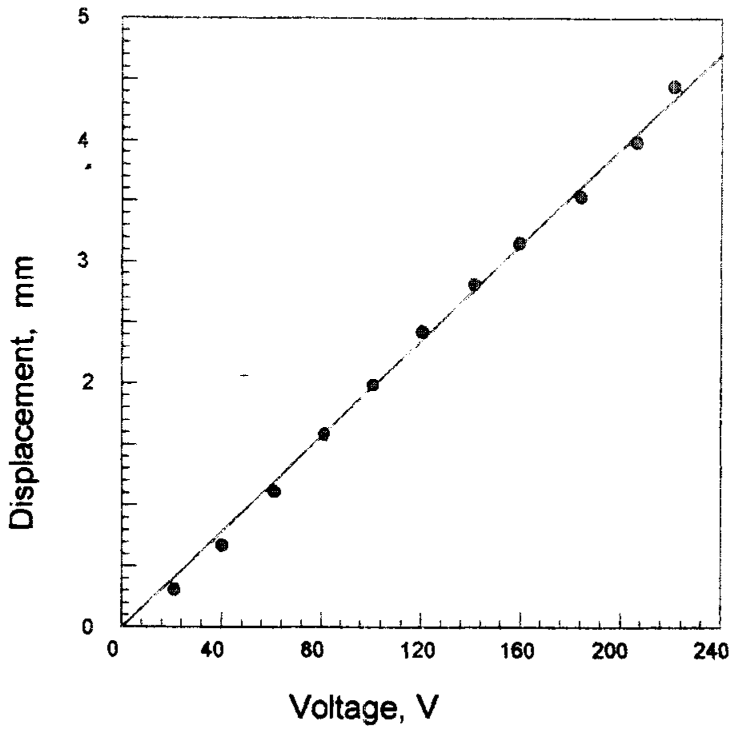

Fig. 5. Displacement of THUNDER actuator.

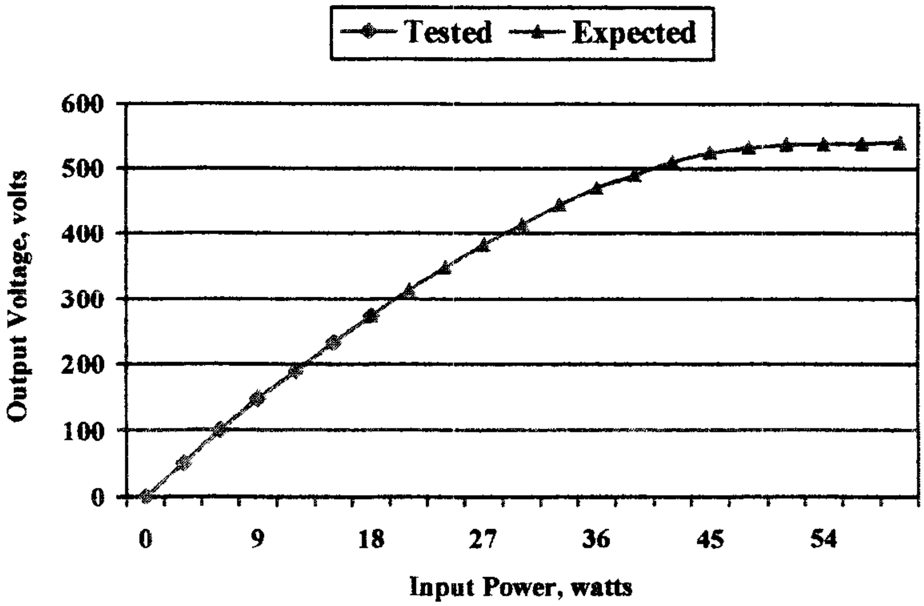

Fig. 6. Output Voltage from a 6 x 6 rectenna patch
in terms of input power of a microwave.

NUMERICAL AND PHYSICAL MODELING OF TUBE HYDROFORMING

G. T. Kridli

and

E. A. Orady

Department of Industrial and
Manufacturing Systems Engineering
University of Michigan-Dearborn
Dearborn, Michigan 48128-1491

Telephone
e-mail gkridli@engin.umd.umich.edu

Numerical and Physical Modeling of Tube Hydroforming

G. T. Kridli and E.A. Orady
Department of Industrial and Manufacturing Systems Engineering
University of Michigan-Dearborn
Dearborn, Michigan 48128-1491

Key Words: Tube hydroforming, finite element analysis, thickness distribution.

Prerequisite knowledge: Basic knowledge of finite element analysis and the use of a finite element modeling tool (i.e. DYNAFORM); mechanical properties of materials; strength of materials.

Objective: To understand the effect of hydroforming pressure and end feed on the thickness distribution and the success of the process in producing defect free components, and to correlate experimental results with numerical model results.

Equipment:
The hydroforming press used in this experiment was acquired through funding from the Education Foundation of the Society of Manufacturing Engineers. DYNAFORM is provided as an in-kind gift from Engineering Technology Associates (ETA).

1. Interlaken servo-hydraulic press
2. Hydroforming dies
3. Unitest data acquisition and machine control software
4. Welded stainless 302-L steel tubes: 7.9 to 8.0 inch long, 2.0-inch outer diameter.
5. DYNAFORM and LS-DYNA
6. Micrometer

Introduction:

Tube hydroforming is a manufacturing process in which an internal hydraulic pressure is applied to transform either a straight or a pre-bent tubular blank into a structural component with different or varying cross-sectional shapes along its length. High pressure tube hydroforming is the most common form of the tube hydroforming process in which a tubular blank is placed in a closed die and the internal hydraulic pressure forces the tube to conform to the shape of the die cavity. In order to reduce thinning in the tube wall, the tube ends are fed into the die cavity by the use of hydraulic cylinders [1]. Punches may also be mounted in the die to pierce holes in the tube wall during the forming operation. A schematic of the loading scheme is shown in Figure 1 with F_e denoting end feed and P denoting the internal pressure for a tube with radius r, wall thickness t, and length l.

The process is being used or is being considered for making a wide range of components for both automotive and non-automotive applications. Pressure levels over 50,000 psi are sometimes used to produce industrial size parts; however, most parts are typically produced at pressure levels under 50,000 psi. Automotive parts currently under development or in production include seat frames, engine cradles, rails, exhaust manifolds, and space frame components. Interest in the tube hydroforming process by the automotive industry is due to the possibility of replacing many multi-piece stamped and welded assemblies in body, frame, or chassis components with one-piece hydroformed components. Thus, there is a great potential for not only weight saving, but also for tooling and labor cost saving that may occur due to the elimination of multi-stage stamping and assembly processes through part consolidation. A draw back of the process is the need for expensive tooling (dies and presses) that can provide and sustain the require forming pressures. Thus, numerical simulation is needed in order to reduce the production cost.

The two most likely defect modes in this process include tube bursting and wrinkling. Tube bursting occurs when the tube cannot support the tensile load produced by the internal pressure; once the tube bursts, splitting occurs near the burst area due to excessive deformation. Tube wrinkling is caused by excessive compressive force generated by end feeding. Either of these two modes of failure results in an unusable product [2].

In this exercise, tubes are formed in the laboratory, under different processing conditions, to demonstrate the different modes of failure, and the conditions that can lead to defect free hydroformed parts. Numerical modeling of the tube hydroforming process is conducted using the finite element tool DYNAFORM, and the model is analyzed using the finite element analysis code LS-DYNA. The hydroformed tubes are cut into sections, and thickness measurements are made along these sections. The physical test results are then compared with the numerical results. Students completing this exercise learn to identify the effects of processing parameters on the final product, and are introduced to numerical modeling tools for metal forming.

Procedure:

The class is divided into two halves and conducts this exercise over two laboratory sessions. In each lab session, half of the students work on the physical model of tube hydroforming and the other half works on the numerical model. In the lab, the students run different tests in order to determine the conditions under which the tube fails (i.e., bursts or wrinkles) for simple part shapes, using the die shape and size shown in Figure 2. Following are the experimental and the numerical procedures used for conducting this exercise.

Experimental Procedure:

1. Observe the safety instructions posted in the lab and make sure to wear safety glasses.
2. Start-up the hydroforming machine control and data acquisition program and select test builder from the "Test" menu.
3. For the first tube, set the internal pressure level to 14,000 psi
4. Set the end feed to 0.3 in for each end.
5. Install the tube in the die with the weld line aligned parallel to the parting line.
6. Turn the hydraulics on to form the part, and once the die opens turn off the hydraulic pump.
7. Remove the part from the machine and label it.
8. Repeat steps 3 to 7 for another tube with the weld line aligned at 45 degrees to the parting line of the die set.
9. For the third tube, change the pressure to _8,000 psi_ and the end feed to _0.7 inch_ for each end, then repeat steps 5 through 7.

Numerical Procedure:

1. Import the provided die and tube drawings (in IGES format) into you modeling tool (DYNAFORM).
2. Using a surface mesh, auto-mesh the die using shell elements with maximum element size 0.6 inch and minimum element size of 0.4 inch
3. Define the meshed die as tool in the "Define Tools" menu.
4. Define the tube material properties using piecewise stress-strain data. (Mat. No. 24 in DYNAFORM)
5. Mesh the tube using Belytschko-Tsay shell elements with element size of 0.1 inch.
6. Define the pressurization curve as a linearly increasing pressure up to 14,000 psi
7. Define the end feed curve for each end as linearly increasing up to 0.3 inches
8. Run the analysis and obtain the thickness distribution in the hydroformed tube.

To introduce the students to metal forming analysis, each group of students conducts an experiment that yields a defect free part (Figure 3), as well as a pressure and end feed combination that causes bursting (Figure 4) or wrinkling (Figure 5) of the tube. Data from all student groups is then compiled and distributed to all groups. The students use the data to develop a two dimensional processing map for bursting and wrinkling and identify the safe forming zone similar to Figure 6. Each student group cuts the defect free tube into sections perpendicular to its axis of rotation and measures the thickness along the cut line using the micrometer. The numerically predicted thickness distribution at the location of the cut is then obtained from the results of the numerical model. A plot of the experimental results and the numerically predicted results is then generated and the results are compared; a sample plot is provided in Figure 7.

Comments:

The tubes are most likely to burst near the weld line due to the physical and metallurgical characteristics of the material near the weld line. Thus by aligning the weld parallel to the parting lines of the die, the weld and the adjacent material experience the least amount of deformation since they contact the die walls at early stages of the hydroforming process. When the weld is aligned at 45 degrees to the parting line of the die, it is located in the zone that experiences the highest level of deformation, thus bursting is likely to occur near the weld.

The tube begins to deform plastically once the internal pressure causes a hoop stress level (σ_h) that is greater than the yield strength of the material according to the relationship shown in equation (1)

$$P = \frac{\sigma_h t}{r} \qquad (1)$$

According to equation (1), the internal pressure is directly proportional to the tube wall thickness and hoop stress, and is inversely proportional to the tube radius. The internal pressure in the tube will increase at the early stages of deformation (due to strain hardening of the tube material), reaching a peak, then decreases as the tube expands further [2]. If the applied pressure exceeds the peak pressure, the tube bursts. Thus, the pressure level at the onset of bursting may be calculated using equation (2)

$$\frac{dP}{dr} = 0 \tag{2}$$

The pressure at the onset on wrinkling is typically related to the axial stress in the tube, which is a function of the effective flexural rigidity of the tube, the effective modulus of the tube, the tube radius, and the tube wall thickness. The properties of the tube material, such as strength coefficient, strain hardening exponent, elongation to fracture, and anisotropy, will result in different processing maps for different tube materials.

References:

1. Ahmetoglu, M., and Altan, T., "Tube hydroforming - state-of-the-art and future trends," *SAE technical paper number 1999-01-0675*, 1999.
2. Xia, Z.C., "Failure Analysis of Tubular Hydroforming," *MED-Vol. 11, Proceedings of the ASME Manufacturing in Engineering Division – 2000*, pp. 641-648.

Biography:

G.T. Kridli is an Assistant Professor of Industrial and Manufacturing Systems Engineering at the University of Michigan-Dearborn. He received his Bachelor's and Master's degrees in Mechanical Engineering from the University of Miami, and his Ph.D. from the University of Missouri-Columbia. He teaches graduate and undergraduate manufacturing and materials related courses. His research and teaching interests include manufacturing process modeling and analysis, lightweight material processing, and material characterization. He is a member of SME, and SAE.

E.A. Orady is a Professor of Industrial and Manufacturing Systems Engineering at the University of Michigan-Dearborn. Dr. Orady has both industrial and academic experience in manufacturing engineering. He has been teaching manufacturing courses for undergraduate and graduate manufacturing programs for over 30 years at UM-D and other universities in North America and the Middle East. He has developed over 12 courses in the manufacturing area. Dr. Orady has over 80 papers in manufacturing field published in journals and national and international conference proceedings. In addition, Dr. Orady wrote four chapters in books including a chapter in the Tool Design Handbook published by SME. He is an active member in several professional organizations including SME, ASME, IIE and member of the USA Technical Advisory Committee for ISO-Robots Manufacturing Environment. He is the Associate Editor-In-Chief for the International Journal of Science and Technology (IJST). Dr. Orady contributed in organizing several conferences for AMSE and IEEE. Dr. Orady is a reviewer and reader for many professional journals and research funding organizations such as SME and NSF.

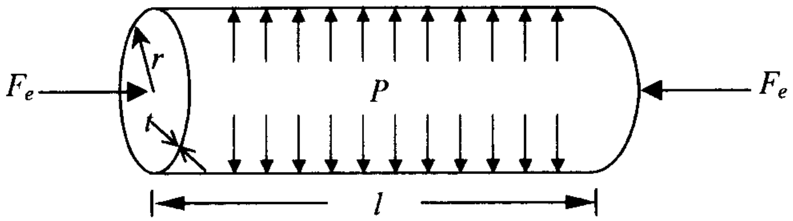

Figure 1. Loading Scheme in High Pressure Tube Hydroforming

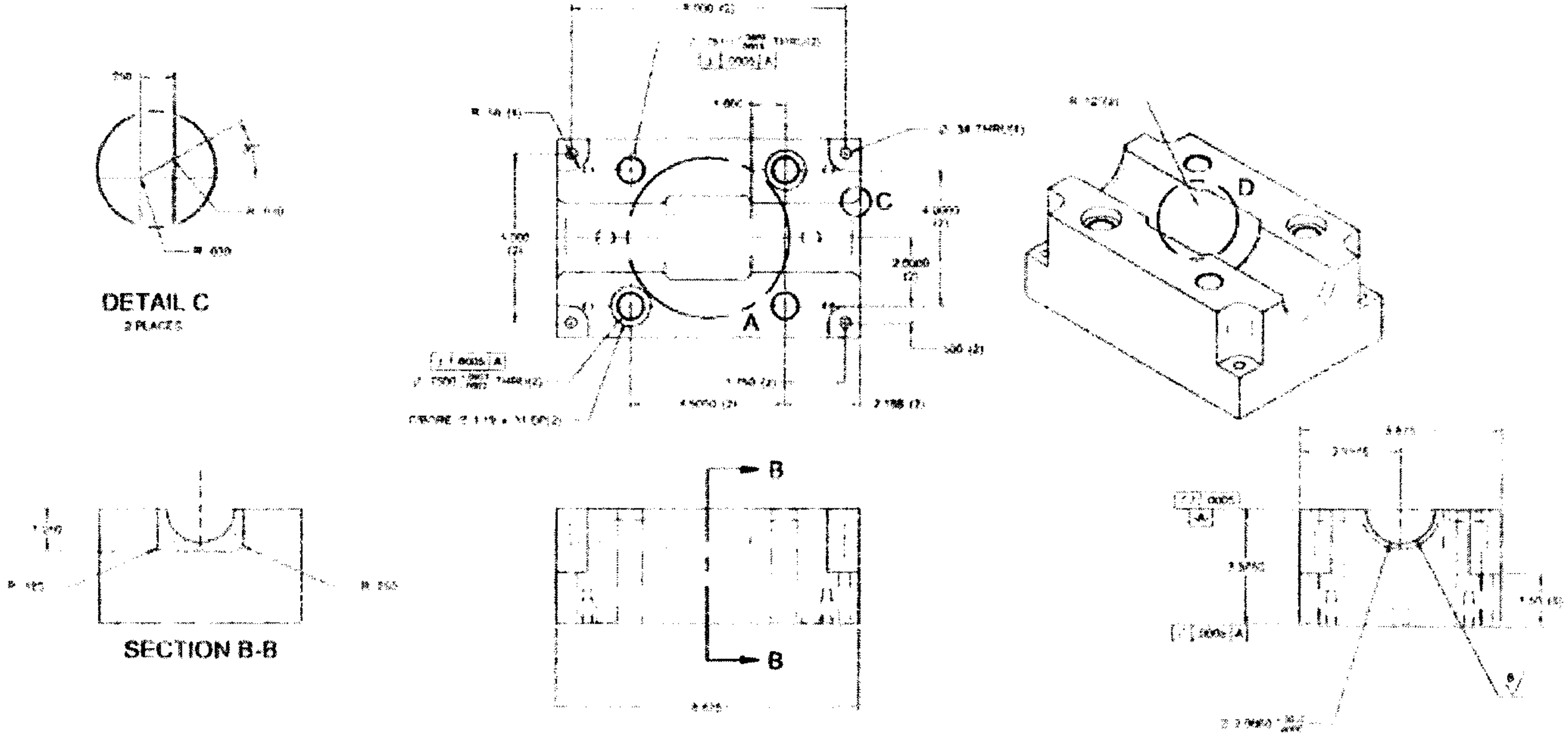

Figure 2. Dimensioned Drawing of Die used in the Experiments

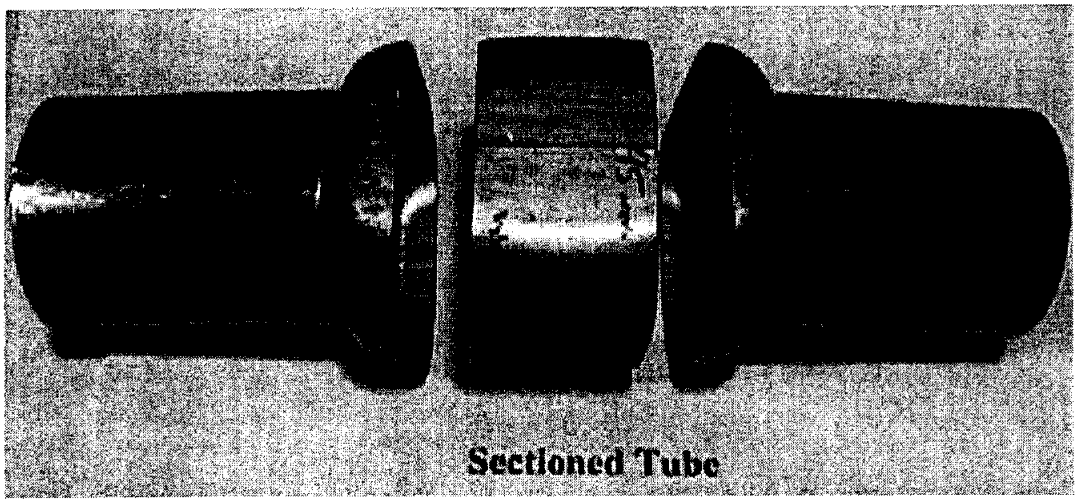

Figure 3. Image of Sectioned Tube Hydroformed without Defects

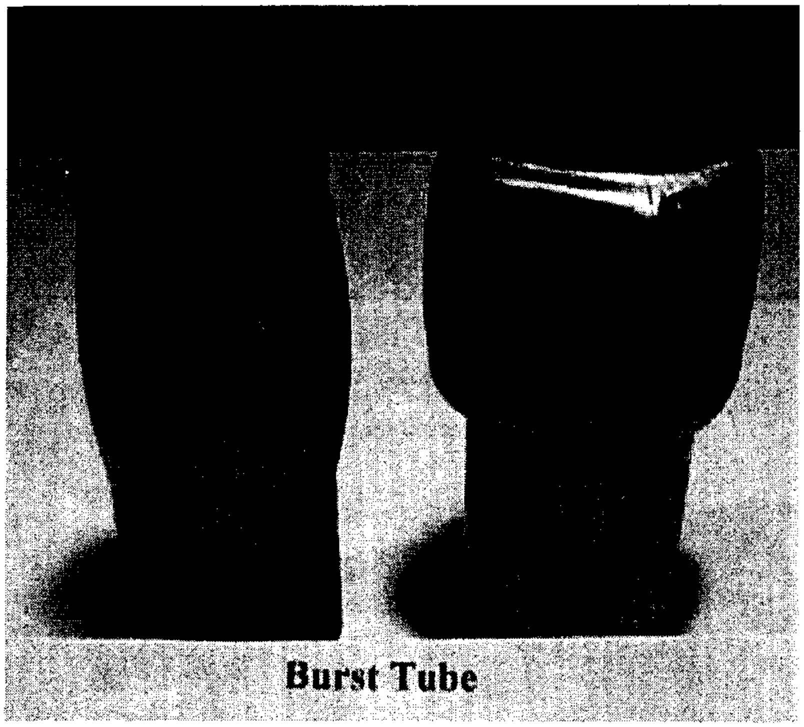

Figure 4. Burst and Split Tubes due to High Levels of Internal Pressure (Seamless Al 6061-T6 tube on the Left and Welded 304-L Stainless Steel Tube on the Right)

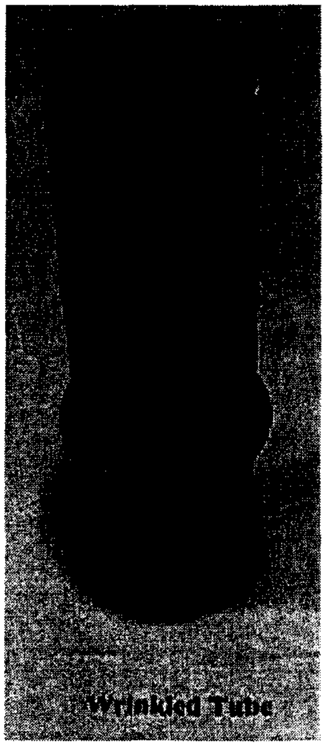

Figure 5. Wrinkled Tube due to Excessive End Feed

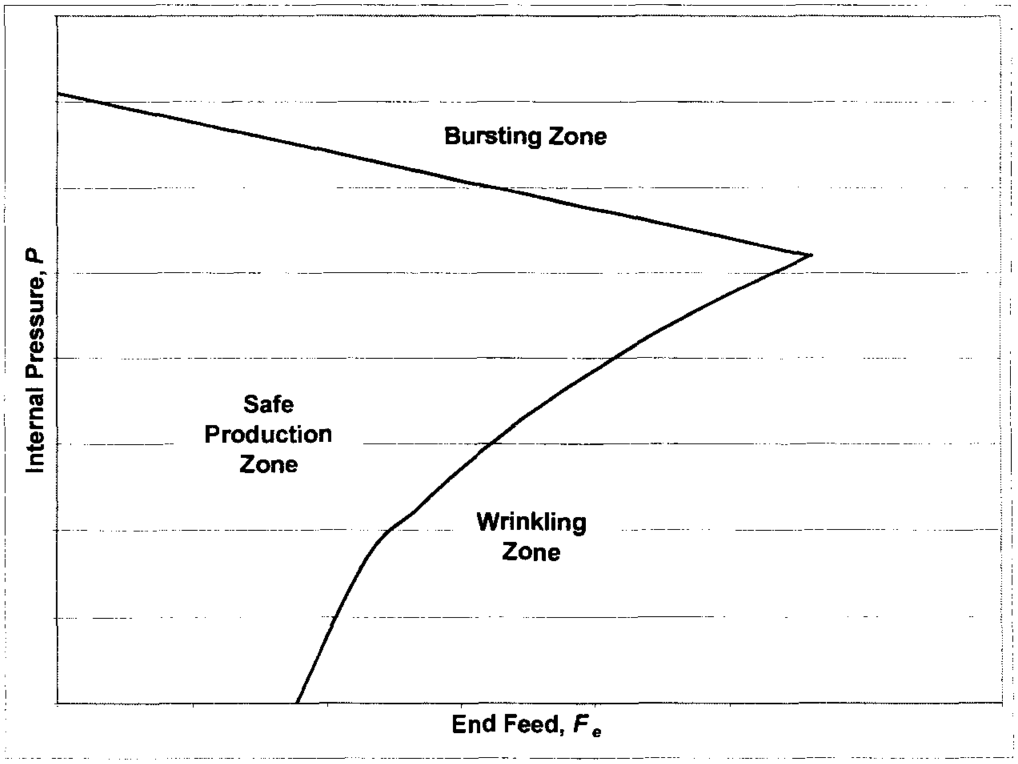

Figure 6. Sample Processing Map for Tube Hydroforming

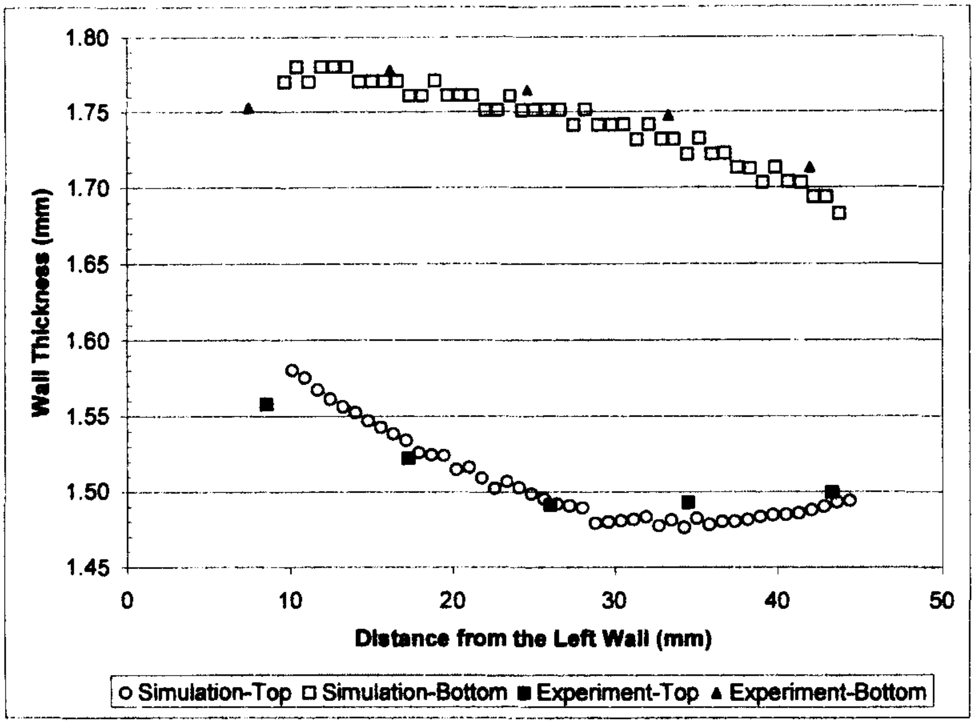

Figure 7. Sample Thickness Distribution Plot showing Experimental and Numerical Results (left wall refers to the side of the tube between the 0.125 corner radii shown in Figure 2 Section B-B)

THE FUNDAMENTALS OF VARIATION: AN INEXPENSIVE AND ELEGANT EXPERIMENT FOR ENGINEERING STUDENTS

Linda Vanasupa
Materials Engineering

and

Heather Smith
Statistics

California Polytechnic State University
San Luis Obispo, California 93407

Telephone 805-756-1537
e-mail lvanasup@calpoly.edu

Linda Vanasupa and Jim Gardner

The Fundamentals of Variation: An Inexpensive and Elegant Experiment for Engineering Students

Linda Vanasupa
Materials Engineering

Heather Smith
Statistics
California Polytechnic State University
San Luis Obispo, California

Key Words: Statistics, variation, measurement, control charts, measurement error, and precision.

Prerequisite Knowledge: *Students:*Basic knowledge of the normal probability curve, the significance of its standard deviation and mean values. *Instructor:* Basic knowledge of control charts and how they are used.

Objective: To demonstrate the variation that exists in measurements and to illustrate the quantitative impact that variation has on the precision of the measurements.

Equipment and Materials:

1. 8 micrometers capable of measuring to 0.0001" (2.5 micrometers)~$35 each
2. 8 virtually identical products whose thickness can be measured with a micrometer [we used polymeric dog-bone tensile specimens]~$4 each
3. 2 blank control charts [see text for details]
4. 1 blank data table [see text for details]

Introduction:

One of the concepts that is difficult for beginning engineering students to grasp is the idea that measurements are not exact numbers; i.e., they contain variation. When making repeated measurements, a student will often experience great discomfort when a second measurement of the same item yields a different result. Although measurement variation is natural and expected, students often suspect that something is "wrong" when they encounter variation in their measurements. We have designed this experiment to demonstrate the reality of variation and instruct students on how to compute its quantitative impact on the measurements results. The experiment is also aimed at getting the students to identify possible sources of variation, design means of minimizing the variation from the different sources and interpret the meaning of the resulting measured value.

Procedure:

(a) Divide the class into eight groups

In our course, we create eight groups of three students each. The number of students per group is not critical, but you should have at least six groups in order to demonstrate the variation effectively.

(b) Distribute micrometers and specimens

Each group should be given a micrometer and a specimen to measure. In our case, we used polymer dog-bone tensile specimens.

(c) Give introductory remarks to students on measurements

These remarks include the following key points:

- Engineers often solve problems by designing or altering an existing design (it could be a design of a *product*, like a gear, or a design of a *process*, like the induction hardening process used to harden the teeth of the gear)
- Engineers often measure *product specifications* or *processes*
- Engineers often rely on measured values to make decisions
- Measurements contain variation (i.e., numeric uncertainty)
- It is important to know how much variation exists, so that the precision of a measured value (such as tensile strength) can be estimated
- A control chart is a tool that is used to keep track of the variation in processes and product specifications during manufacturing

(d) Explain the source of the specimens

The instructor points out that all specimens came from the same batch. In our case, they came from the same batch of injection molded tensile specimens. (Please see the comments below to select the proper specimens.)

(e) Give a tutorial on using the micrometers if needed

Make sure the students know how to use the clutch feature so that they do not over-tighten the micrometers during measuring.

(f) Instruct the students to take three thickness measurements

State that all measurements should be reported to the nearest 0.0001" (or smallest metric value possible with the micrometers). Each group is to take three separate measurements. Tell the groups that they must completely set down the specimen and the micrometers between measurements. This instruction is to ensure that the students don't simply take a repeated measurement in one identical spot. Do not instruct the students further on how to take measurements (see comments below for the purpose). This process should take about 10 minutes.

(g) Have the students record their data on the table

The data table should be large enough for the class to read and posted on the wall. A transparency is sufficient, but less desirable. The data table should have the following format:

Group:	1	2	3	4	5	6	7	8
x_1								
x_2								
x_3								
$\bar{x}$(*mean*)								
R(*range*)								

Each group should record the results of the three measurements to the specified number of decimal places. Each group should also compute the mean thickness, $\bar{x}$, and the range, R:

$$\bar{x} = \frac{x_1 + x_2 + x_3}{3}, \qquad R = (x_{\max} - x_{\min})$$

(h) Compute the values for the control charts
At this point, it is best to explain the idea of a control chart (see the Comments section on background information on control charts). Emphasize that in a real manufacturing situation, the x-axis of the chart would have a greater relevance to the process (for example, the x-axis may represent the shift during which the measurements were taken). However, for this experiment, the x-axis is simply the group designation. First compute the grand mean (the mean of all the group means) and the mean range:

$$\bar{\bar{x}} = \frac{1}{8}\sum_{i=1}^{8} \bar{x}_i, \qquad \text{and} \qquad \bar{R} = \frac{1}{8}\sum_{i=1}^{8} R_i$$

Next, compute the control limits for the two charts. The upper chart is for the mean thickness values and is called an "x-bar chart" to indicate that it represents a plot of the mean thickness $\bar{x}$.
The lower chart is for plotting the range statistics.
For the x-bar chart:

$$LCL = \bar{\bar{x}} - 1.023 \cdot \bar{R}, \text{ and } UCL = \bar{\bar{x}} + 1.023 \cdot \bar{R}$$

For the R chart:

$$LCL = 0, \text{ and } UCL = 2.574 \cdot \bar{R}$$

(i) Plot the values on the control charts
For each chart, plot the upper control limit, the grand mean, and the lower control limit. Then have the students add their mean and range values to the appropriate chart. Your x-bar chart should look something like this:

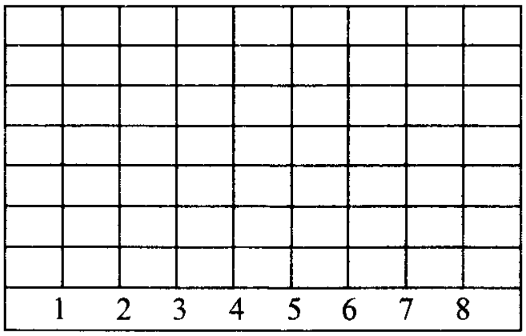

Your chart will have numbers on the y-axis, of course. You will also have the means of the thickness that are plotted by the 8 groups of students.

Make sure that the R-chart is plotted beneath the x-bar chart so that both completed charts can be viewed and discussed at the same time.

(j) Discuss the meaning of the results

The instructor points out the important features in the results. The discussion will depend on what the results are. For example, if it turns out that one or more of the means lies outside of the control limits, it gives the instructor the opportunity to discuss the implications. As another example, all of the means may be well within the control limits, yet the R-chart may have one or more outages (i.e., data points outside of the limits).

(k) Identify the sources of variation

The instructor leads a discussion with the class on what might cause variation during the measuring process. It is best to allow the students to discuss the sources within their group for about a minute and then ask groups to volunteer their answers. You will end up with a list of sources that generally fall into two categories: 1. Variation due to the measuring process, 2. Variation due to real differences in the product.

(l) Compute the margin of error from an estimate of the thickness and discuss its meaning

If it is the case that all of the points on the R-chart were within the limits, the average R can be used as a reliable estimate for the standard deviation. In this case, you can compute the margin of error associated with the measurement of a single observation,

$$\text{standard deviation} \cong \frac{\overline{R}}{1.693}, \text{ and margin of error} \cong 3 \cdot \overline{R}/1.693$$

The value to report as the measured value would be

$$\overline{\overline{x}} \pm \text{margin of error}$$

In other words, a measured value cannot be known more accurately than the margin of error.

Comments:

Choosing specimens to measure

It is very important that you choose specimens whose thickness varies more than the resolution of the micrometers. The polymeric specimens tend to vary more than 0.001" from top to bottom of the sample and from sample to sample. Initially we chose cold-rolled brass. However, the problem with the brass was that the thickness varied on the order of 0.0001". With such small variation, the experiment is quite dull and uninformative.

Withholding specific directions on the measuring process

It is best not to give the students more specific directions on measuring beyond the fact that they should measure the thickness three times. The reason is that you are allowing them to introduce all sorts of variation into the measuring process. When the group later develops reasons for the variation in the measurements, they will realize that the measuring process itself was non-standardized and caused some variation.

Explaining the meaning of the control chart

Students with background knowledge of the normal distribution will be able to grasp the concept of a control chart. It is helpful to review the meaning of control charts before using them in this experiment. An excellent reference for the instructor is the text by Devore and Farnum [1]. The instructor can also download a layman's explanation of control charts by the authors [2]. The equations for the upper and lower limits are based on the three measurements for each group.

Minimizing the variation

After the students identify why variation exists, it is a good exercise to ask the students to come up with ways of minimizing the variation. The students will come up with appropriate solutions like "develop a set of standard operating procedures for measuring."

Computing and interpreting the margin of error

This portion of the experiment helps the students to understand that when they report the result of a measurement, there is inherent uncertainty in the value. This is true even if the reported value is an average. If one of the data points for R lies outside of the upper and lower limits, using $\overline{R}$ will not reliably estimate the standard deviation. If the reason for the outlying condition is known (e.g., one group reported the measurement incorrectly), you can ignore the outlying data point, recomputed $\overline{R}$ and use it in your calculations for the standard deviation. However, if the reason is not known, you should not eliminate the data point.

Altering the exercise

If you would like to change parts of the exercise, you may want to consult the equations in Devore and Farnum [1] so ensure that you are using the right computational values. All the equations in this paper are appropriate only for the conditions that are described in the experiment.

References:

[1] J. Devore and J. Farnum, *Applied Statistics for Engineers and Scientists*, Duxbury Press, Pacific Grove, California (1999).

[2] www.calpoly.edu/~lvanasup. Modules for statistics can be downloaded from this site.

Acknowledgements:

We would like to gratefully acknowledge the students who have dutifully tested our module. This work was supported in part by a grant from the National Science Foundation (NSF Grant#DUE-9952609).

Biographies:

Linda Vanasupa is a professor in the Materials Engineering Department at Cal Poly. Her bachelor's degree is in metallurgical engineering from Michigan Technological University (1985). Her M.S. and Ph.D. degrees are from Stanford University (1987 and 1991) in materials science and engineering. She teaches courses and laboratories in electronic materials, microelectronics processing, and a variety of materials engineering subjects

Heather Smith is a lecturer in the Statistics Department at Cal Poly. She holds degrees from the University of Florida (B.S., Statistics, 1986) and Florida State University (M.S., Statistics, 1989). Ms. Smith's professional experience includes extensive consulting to the metallurgy industry. She continues to act as a consultant while also teaching computer-based courses in statistics for engineering students at Cal Poly. Her professional affiliations include the American Statistical Association. She and Linda Vanasupa have collaborated on a number of interdisciplinary efforts involving the integration of statistics into engineering laboratories.

THE AMAZING PROPERTIES OF MATERIALS

Daniel P. Vigliotti

James B. Alcorn

Nicole A. Neumeyer

D. R. Cyr

A. C. Rodriguez

C. N. Farrell

and

L. A. Leininger

National Institute of Standards and Technology
Materials Reliability Division
325 Broadway-360
Boulder, Colorado 80303-3328

Telephone: 303-497-3351
e-mail vigliotti@boulder.nist.gov

Daniel P. Vigliotti

The Amazing Properties of Materials[*]

Vigliotti, D. P., Alcorn, J. B., Neumeyer, N. A., Cyr, D. R., Rodriguez, A. C.,
Farrell, C. N., Leininger, L. A.
Materials Reliability Division
National Institute of Standards and Technology
Boulder, CO 80305-3328

Key Words: amorphous; anneal; crystalline; coefficient of friction; drop test; hysteresis; neoprene rubber; rate of restitution; stress opticon

Prerequisite Knowledge: The presenter should be familiar with general knowledge of mechanical testing and materials science.

Objective: The purpose of this presentation is to introduce educators to a demonstration that will expose students in grades seven through twelve to a variety of mechanical tests that will allow them to observe certain unexpected properties of materials.

List of Equipment:

1. Stress-Opticon Kit**
2. Drop-Test Tower
3. Steel Ball
4. Veneer Strips
5. Neoprene Rubber Ball
6. Nosorex** Rubber Ball
7. Silly Putty**
8. Tin Rod
9. Coat Hanger
10. Rubber Band
11. Annealed Copper Tubing
12. Shape-Memory Alloy (Nitinol**)

List of Demonstrations:

1. Amorphous vs. Crystalline Materials
2. Drop Test
3. Happy and Unhappy Balls
4. Elastic Deformation vs. Permanent Deformation
5. Work Hardening of Materials
6. Dependence of Materials on Rate of Deformation
7. Shape-Memory Alloy
8. Stress-Opticon

Introduction:

Materials may react in different ways to a given physical stimulus. The experiments described in this paper demonstrate several properties of materials.

** Because the C.A.R.E. kit contains these specific products, trade names contained herein are used only to identify the material used in this research. Such identification does not constitute recommendation or endorsement by NIST of these materials or of their manufacturers.

The experiments will include the use of materials such as Silly Putty, annealed copper tubing, and shape-memory wire. A drop test will demonstrate how methods of manufacturing can increase the strength of certain products. A stress-opticon will be used to demonstrate the techniques of stress analysis and the effects of stress concentration.

Other areas explored include strength and hardness, rate dependence, metal memory, and elastic and permanent deformation. Students will be able to participate in demonstrations of some mechanical principles and determine the behavior of structural elements using visual and audible means.

Experiments:

1. Amorphous versus Crystalline Materials

Most materials are classified as either amorphous or crystalline. Crystalline materials consist of atoms arranged in regular arrays or patterns. These patterns form separate crystals that build upon one another to eventually form a mono- or polycrystalline material. The shape and orientation of individual crystals determine the unique physical properties of a material. An example would be steel or hard plastic.

Most amorphous materials have no regular repeating structure. Common examples of amorphous materials are glass and Silly Putty. There are no naturally occurring amorphous metals in nature. All amorphous materials have the ability to change shape without having any direct outside force applied except gravity. Different materials change shape at different rates, and often only at elevated temperatures. For example, at room temperature the atoms in glass take many decades to shift and to experience a change in shape of the glass material under the action of gravity.

The properties that make a material either crystalline or amorphous can be used to explain the reactions and activities displayed by each material.

Silly Putty

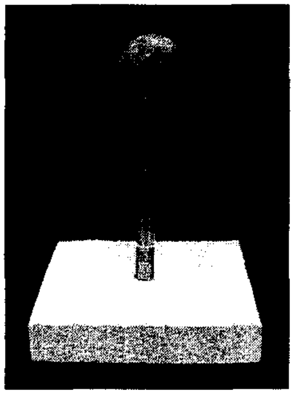

Figure 1: Silly Putty on pedestal.

To demonstrate how amorphous solids change shape without intervention from any outside contact forces such as pushes or pulls, place a ball of Silly Putty on the pedestal. (See Figure 1.)

The Silly Putty will begin to flow over the pedestal like a viscous liquid because it has no defining internal crystalline structure to maintain its original shape. This process can be observed after several minutes. (See Figure 2.)

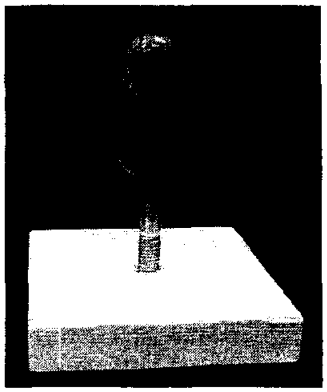

Figure 2: Silly Putty running down pedestal.

There is one outside, non-contact force always working to change the shape of amorphous materials. You can ask your students if they can name this force. This outside force is the force of gravity.

Tin Rod

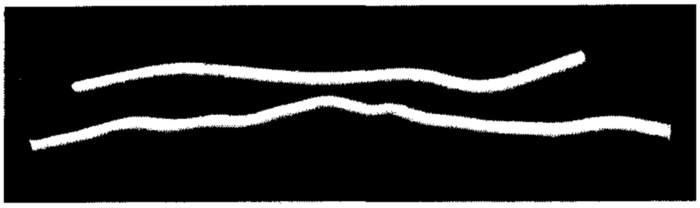

Figure 3: Tin rods.

If a crystalline material is deformed enough, the mutual orientation of the crystals is altered. Depending on the material, the change in orientation of the crystals in a material being deformed can be audible. Tin is one such material. (See Figure 3.) If you quickly bend and unbend a piece of tin rod repeatedly, you will be able to hear a cracking sound. This sound is due to the unique and complex crystal structure of tin that allows the crystals to hold together as they crack against one another rather than changing shape and sliding past each other, as do the crystals in most other materials. **(Caution: When bending the rod, do not bend it completely in half as this may cause it to break.)** When you bend common copper or steel wire in the same way, there is usually sound being produced at the region of bending, but it occurs at frequencies too high for human ears to hear.

2. Drop Test

This experiment will demonstrate the importance of using a combination of materials for strengthening composites. Composite materials gain their strength by combining two or more separate materials to obtain characteristics that would not exist in the individual materials only. This is an instance where the whole is greater than the sum of its parts. The anisotropic properties of the separate materials contribute to the strength of the composite material. This implies that the properties of a material may be different when measured in different directions. A common example of this is plywood. The fibers in the first layer of wood run in one direction, while the fibers on the second layer of wood run perpendicular to those of the first layer. The same material is present in both layers. By simply rotating the direction of the fibers in the material with respect to the applied forces, the strength properties will change.

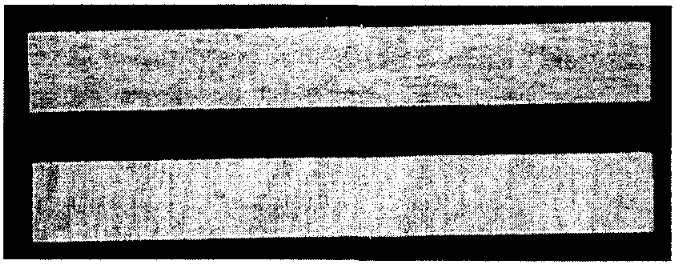

Figure 4: Longitudinal and transverse-grain veneer strips.

Veneer samples will be used to show the strength of composite materials. There are two types of veneer samples in the kit (see Figure 4); one with the grain running the length of the sample (longitudinal), and the other with the grain running across the sample (transverse).

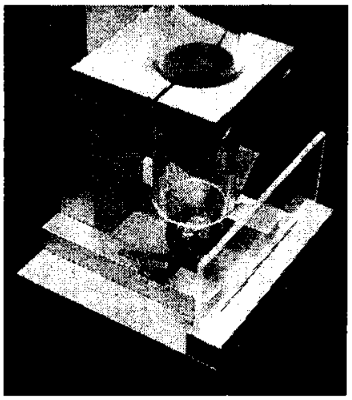

Figure 5: Broken veneer strips.

Begin the experiment by showing the students the different samples of grain orientations. Tape two strips that have transverse grain together and drop the ball onto them. They should easily break. (See Figure 5.) Take another two veneer strips: a longitudinal-grain and a transverse-grain sample and tape them together using double-sided tape. Drop the ball again. This time the sample should remain intact. (See Figure 6.) The combined contrasting grain structures strengthen the veneer. While the transverse grain prevents breakage in one direction, the longitudinal grain prevents breakage in the perpendicular direction; thus allowing the composite specimen of two separate parts to add their strengths along two different directions, allowing them to withstand a higher impact than either could alone.

Figure 6: Unbroken veneer strips.

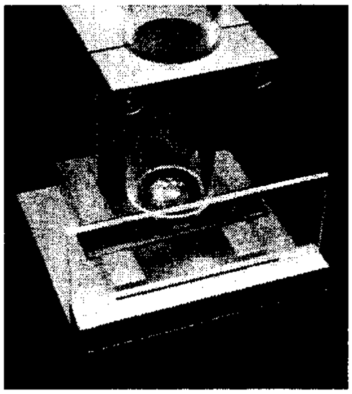

Figure 7: Unbroken pine strips wrapped in nylon.

The pine veneer strips further illustrate the strength of different grain orientations. Drop the ball on the uncoated pine veneer and it should break. Now, have the students examine the pine strips coated with the nylon fabric. Have them take note of the crossing grains and discuss their importance. This time when the ball drops, the specimens should remain intact. (See Figure 7.) The fibers in the nylon, which run in different directions, strengthen the sample, making it more resistant to breakage. By proper design of composite material with fibers laid out in different directions and using strong adhesives to join them, tough materials can be made. They can be used in automobiles, airplanes, and other applications to provide strong structures with less weight than that of steel.

3. Happy and Unhappy Balls

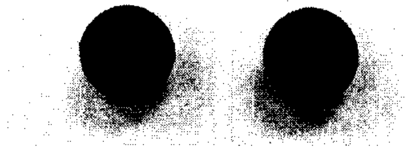

Figure 8: Happy and Unhappy balls.

Hysteresis, friction, and restitution are three physical properties found in the experiment involving the rubber balls. Hysteresis is a material's resistance to deformation when forces are applied. The higher the hysteresis, the less willing the material is to change. Friction is a force that resists the relative motion of two bodies in contact. Restitution is defined as the act of returning to, or recovering from, a former state.

The two balls used in this experiment appear to be identical (See Figure 8). However, one ball is made of a rubber compound known as Nosorex, and the other is made of neoprene rubber. The difference in material make-up accounts for three differences in physical properties between the two balls. At room temperature, the ball made from Nosorex, the unhappy ball, has a high coefficient of friction, high hysteresis, and a low rate of restitution. The ball made from neoprene rubber, the happy ball, has a low coefficient of friction, low hysteresis, and a high rate of restitution. The unhappy ball rolls slower, takes longer to return to its original shape, and barely bounces in comparison to the happy ball.

To begin this experiment, have the students bounce both balls. Watch the happy ball bounce, while the unhappy ball does not. The properties of the two balls will change with temperature. Demonstrate this by placing each ball in a separate glass of ice-cold water and allow them to chill for a few minutes. Once chilled, immediately take out both balls and bounce them again. Notice the unhappy ball now bounces and the happy ball does not bounce as high as it did before being placed in ice water. Let the balls return to room temperature and observe the changes and rate at which each ball returns to its original shape. We learned that the same changes in temperature can actually have opposite effects on two different materials.

Another property can be observed by rolling the two balls down an incline. Due to friction, the unhappy ball rolls more slowly than the happy ball.

4. Elastic Deformation verses Permanent Deformation

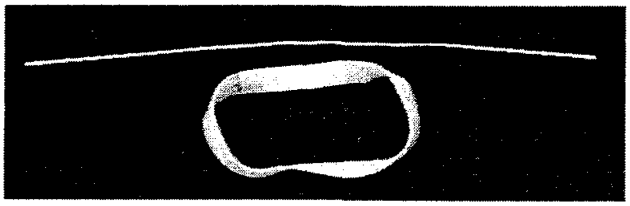

Figure 9: Coat-hanger and rubber band.

Ductile materials are those that have the ability to change shape without breaking, such as the coat-hanger material and rubber band. (See Figure 9.) Some ductile materials are also elastic. Elasticity describes the ability of an object to be deformed, and then naturally return to its original shape. Remember that not all ductile materials are elastic; some have the ability to be deformed, yet are unable to return to their original shape. Demonstrate elasticity by stretching out a rubber band and allowing it to contract. Demonstrate a non-elastic ductile material by bending the copper tubing provided, which will not return to its original shape. Some materials, such as glass, are brittle and thus are resistant to deformation beyond a very small limit. Instead, these materials fracture when subjected to deformation beyond a very small limit.

A material may demonstrate each of these three properties at different times. One example would be coat-hanger material. To demonstrate the elasticity of a steel coat hanger, slightly bend it and watch it spring back to its original shape. Continue bending the coat hanger further and the molecular bonds and crystal structure will start to adjust to the applied force by undergoing deformation. Beyond some point, the material will no longer return to its original shape, but will remain permanently deformed. Finally, if the material is bent too many times, a fatigue crack will develop and the material will embrittle, and will fracture into two pieces.

5. Work Hardening of Materials

Cold working is a term used to describe the process of working on a piece of metal without using heat. Work hardening occurs when cold working is used to harden or strengthen a metal. As a piece of metal is work hardened, it becomes stronger and less ductile. Relative movements of the atoms that compose each individual piece of metal can explain this effect. Due to the process of work hardening, a material that is bent can no longer return to its original shape. (See Figure 10.)

Figure 10: Annealed copper tubing.

For example, an annealed piece of copper refrigerator tubing is composed of atoms that return to their unstrained states in the lattice through the annealing process. When the tube is bent by hand the atoms are dislocated from their equilibrium positions in the lattice. This creates crystal defects called dislocations. The dislocations overlap and lock into one another, making it difficult to bend the copper metal back to its original shape. The process of bending is a form of cold working, because the locked crystal structure that is formed makes the copper metal stronger and more difficult to bend again.

As an experiment, have a student bend a straight piece of annealed copper tubing into an arc. Then have the student bend the tubing straight again. Explain that the student must observe how much force must be exerted when bending the tube in both directions. It should take considerably more force to bend the tube back to the original straight position, and it should be very difficult to return the tubing exactly back to its original straight position. The result of work hardening requires this additional force. An important appreciation of work hardening is in the forging of materials by hitting them with hammers, to make tough steel tools or other objects.

6. Dependence of Materials on Rate of Deformation

Deformation-rate dependence of a material explains how the rate at which the material is pulled apart affects whether the material will snap apart in a brittle fashion (high rate of deformation), or stretch and bend easily (slow rate). When the rate of deformation is increased, materials are more likely to snap, (see Figure 11,) whereas when materials are pulled at a slower rate, they are more likely to stretch before they break, or even stretch a great deal without breaking. (See Figure 12.)

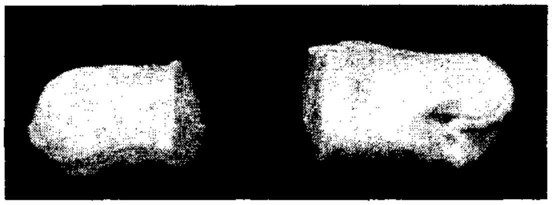

Figure 11: Snapped Silly Putty, deformed at a high rate, resulting in breakage.

Figure 12: Stretched out Silly Putty, greatly deformed at a low rate, without breaking.

Use a piece of Silly Putty to demonstrate this experiment. First pull it apart quickly enough to break it; and then pull apart a piece slowly, deforming it significantly without breaking it. Explain the differences in the outcomes. An application of this is that a bar of steel can be drawn out into a long rod or even wire, if the bar is not pulled too rapidly. If the rate of the pull is too large, the rod will just break, instead of allowing itself to be pulled into wire.

7. Shape-Memory Alloy

Figure 13: Shape-Memory Alloy.

Shape-memory metals can spring back to (or remember) their original shape when the shape of the metal is changed. An example of this is the alloy of nickel and titanium called Nitinol. (See Figure 13.) A piece of Nitinol wire, when placed in cold water will bend due to the decrease in its temperature, and will straighten back to its original shape if returned to its original temperature.

This is due to a solid-state phase change or a kind of crystal lattice, where the change in shape is due to changes in the crystal structure of the metal. At cold temperatures the atoms move easily and the crystals can be deformed, thus bending the metal. When the deformed crystal is exposed to high temperatures it changes to the original crystal structure and returns to its original shape. This reaction happens more quickly at extreme temperatures. For instance, when placed in boiling water the metal will snap back immediately. In water that is only lukewarm, the reaction will take more time.

Perform this experiment by first placing the Nitinol wire in cold water and then in very hot water **(Caution: do not stand too close when the metal is placed in the hot water, as the wire springs back to shape very rapidly.)**

As a related topic, explain that Nitinol alloy is used to deploy satellite antennas in space, to move robotic arms, to open and close greenhouse windows, and in heat engines. This is useful when we want to avoid having to mechanically push or pull things. If you shine a heat lamp on a properly designed structure, at different points, you can make the structure move in different desired directions. You can make it move slowly or rapidly, by using a dim or a bright heat lamp.

8. Stress-Opticon

The miniature photoelastic laboratory is used to demonstrate stress analysis and stress concentration, mechanical principles, and the behavior of structural elements. (See Figure 14.) The kit allows you to compare similar loads on different types of specimens, just as stress tests are performed, by engineers, on models of trusses, arches, frames, and other structures. This allows for a colorful way to identify the locations of weak and strong points within a design.

Photoelasticity is an accurate method of stress analysis and involves viewing a transparent model of a structure through a field of polarized light and interpreting the fringe patterns (colored bands), to determine the locations and magnitudes of stresses in the model. The light from a source passes through a polarizer, the transparent model, the second polarizer (acting as an analyzer), and finally to the viewer. Any type of light source will suffice for this experiment but brighter light, red filters, or a magnifying glass can be used to see the finer details of the fringes.

Both the color and number of these fringes are directly related to the amount and mode of the load placed on the specimen. Red represents the areas under the greatest stress and violet represents areas under the least stress. As the stress increases, the number of fringes within a length will also increase but the pattern will keep its general form. The new bands will appear at the points of highest stress, usually the boundaries, and will crowd the earlier appearing fringes toward the inside of the model.

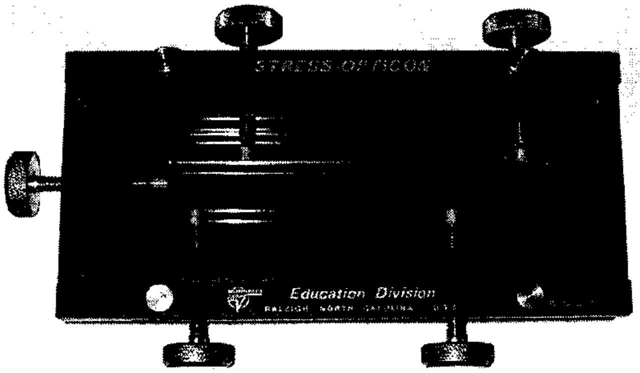

Figure 14: Stress-Opticon

The Stress-Opticon is easy to use and light enough to pass throughout small classrooms. It can also be paired with an overhead projector when larger groups are present. Its simple design consists of the following elements:

- Aluminum frame
- Five T-nuts with nylon-footed loading screws
- Two polarizers with built-in quarter-wave plates
- Three photoelastic models (beams)

The screws should already be loaded into the frame; simply add the polarizers and the model. Apply several different types of loads and observe their stresses.

One type of load can be changed to another without ever touching the model by hand. Place the model in the center of the kit and use the loading screw opposite the support block to clamp one end of the beam. Slide the polarizers into place, with the white dots facing outward, one on top, and one underneath the model. The clamping screws may need to be loosened. Once the polarizers are in place, tighten the clamping screws and apply a load to the beam. When changing loads, remember not to remove the polarizer, simply tighten the model down and rearrange the screws one at a time so it does not drop.

Since the loading screws slide within the frame of the kit, there are a wide variety of loads to experiment with. We will cover seven types, (a-g). There are two other models included in this kit: one with a hole in the middle, and one with segments of varying width. Besides using the following seven tests, replace the first model with either of these other models to demonstrate how different characteristics can alter a structure's behavior under stress. Ask students to figure out different areas of engineering that require the use of each type of model or load. Why are some loads, or areas of the load, unaffected by the type of beam used while others are changed completely?

(a) Cantilever Bending

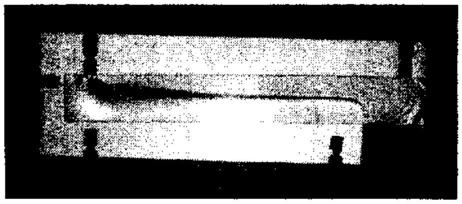

Figure 15: Cantilever bending.

By tightening the appropriate loading screw, clamp one end of the model to the top of the supporting block and add a load to the top of the opposite, free end. The corner under this free end has to be a zero-stress area and should not be colored. The end screw and the two loading screws underneath the model should be lowered so that they are not in contact with the beam. (See Figure 15.)

(b) Simply Supported Beam

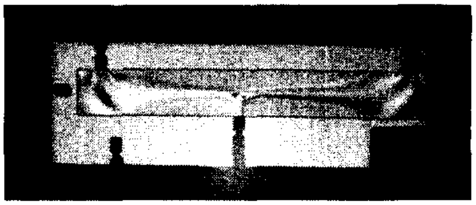

Figure 16: Simply supported beam.

Using the cantilever-bending load, add a single support to the bottom of the beam. Position it slightly off center so that it is supporting the beam. Loosen the top screws and tighten the bottom loading screw until the beam no longer touches the supporting block. The ends of the beam should show zero stress. The area directly above the bottom screw, where there is the most bending, shows the greatest stress. (See Figure 16.)

(c) Constant-Moment Beam

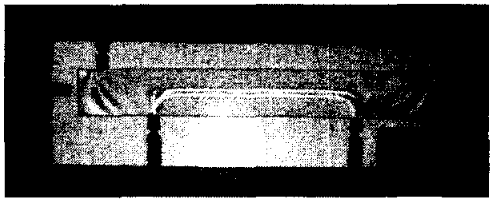

Figure 17: Constant-moment beam.

Using the cantilever-bending load again, add two points of support to the bottom of the beam. These supports should be set apart at equal distances from the ends of the beam. (See Figure 17.) Tighten them and loosen the top screws until the beam no longer touches the supporting block. The area between these two supports will undergo a constant bending so that the load is evenly dispersed along the upper and lower surfaces of the beam. Because the load is constant, the fringes will be parallel to the sides of the model.

(d) Statically Indeterminate Beam

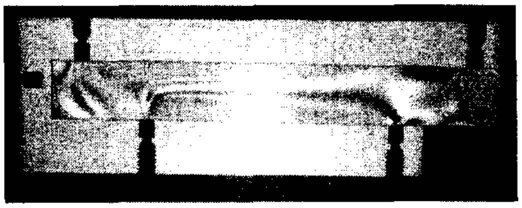

Figure 18: Statically indeterminate beam.

Clamp the model to the supporting block and adjust the two bottom screws so they just barely come into contact with the beam. The beam will slightly discolor when there is contact. Apply the upper load with the loading screw opposite the supporting block.

Even when this load is known, it turns out that the forces at the supports cannot be theoretically determined because of the beam's deformation. This is why the beam is described as statically indeterminate. (See Figure 18.)

(e) Column Loading

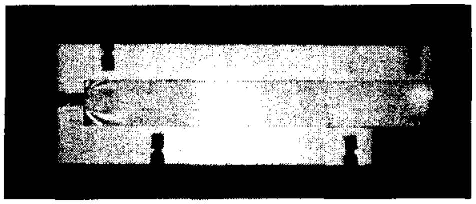

Figure 19: Column-loading beam.

Clamp the model to the supporting block and back all other loading screws away from the beam. Lightly apply a load with the end screw positioned at the center of the beam. Slowly release the support screw as you tighten the end screw. The column is now centrally loaded from one end. The high stress seen at the end screw diffuses throughout the column. The irregular stress seen at the opposite end indicates that the surfaces of the end plate and the beam are not perfectly smooth, parallel, and friction free. (See Figure 19.)

(f) Eccentrically Loaded Column

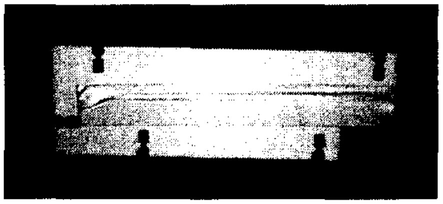

Figure 20: Eccentrically loaded beam.

Clamp the model to the supporting block and back all other loading screws away from the beam. Apply a load with the end screw positioned no longer at the center, but at the bottom corner. Back the support screw away from the beam so it is no longer touching it. Observe the effects of a central load as well as a bending moment at the end of the column. (See Figure 20.)

(g) Opposed Concentrated Forces

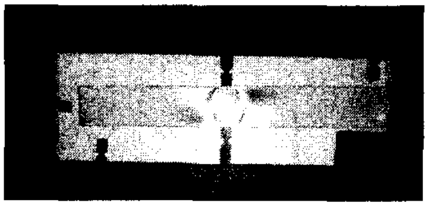

Figure 21: Opposed concentrated forces.

Place two loading screws as exactly as possible located directly opposite each other on the beam. This is an example of St. Venant's principle, which states that when forces are locally balanced, the stresses induced decrease rapidly with the distance away from the load application. The stresses essentially disappear in a distance approximately equal to the depth of the beam. (See Figure 21.) (This load is also useful for holding a beam while changing loads in these experiments or for adjusting the vertical position of the beam.)

When civil engineers want to design a roof over a big stadium, or a big steel bridge, they can make a small model with photoelastic material. By using these methods to find where the greatest stresses appear under loading, the engineers can strengthen those areas. They can save unnecessary expense by designing low-stress areas with less material. The best design will have all the parts of the structure at about the same stress, so that all parts are equally important and nothing is unnecessarily wasted.

Where to obtain resources:

NIST technical divisions manufactured some materials in this kit, and others are available from the following suppliers. NIST does not specifically endorse any of the following suppliers; others may be found to offer products that may serve just as well as those mentioned.

- Hearlihy & Company, 714 W. Columbia Street, Springfield, OH 45504 1-800/622-1000
- Modern School Supplies, Inc., P.O. Box 958, Hartford, CT 06143 1-800/243-2329
- RETCO Alloy Co., 880 Estes Avenue, Elk Grove Village, IL 60007 1-800/722-3307
- PITSCO, Inc., 1002 E. Adams, P.O. Box 1708, Pittsburgh, KS 66762 1-800/835-0686
- Midwest Products, Co., 400 S. Indiana Street, P.O. Box 564, Hobart, IN 46342 1-800/348-4397
- Local craft shops and hardware stores

Acknowledgments and Contacts

Special thanks to Career Awareness and Resource Education (CARE) Coordinator, Phyllis Wright for her remarkable dedication to the program and for furnishing this kit. This Materials Science kit is available from the CARE program office at NIST, Boulder, CO. The CARE program was established in 1979 to promote interest and awareness in math and science. Awareness and exploration of science is encouraged through science kits, videos, field trips, and presentations by the scientific staff.

Phone: 303/497-3351 E-mail vigliotti@boulder.nist.gov
Phone: 303/497-3244 E-mail phyllis.wright@nist.gov

RECYCLING WASTE PAPER

Edward L. Widener

School of Technology
Mechanical Engineering Technology
Purdue University
Knoy Hall, Room 119
West Lafayette, Indiana 47907-1317

Telephone: 765-494-7521
e-mail elwidener@tech.purdue.edu

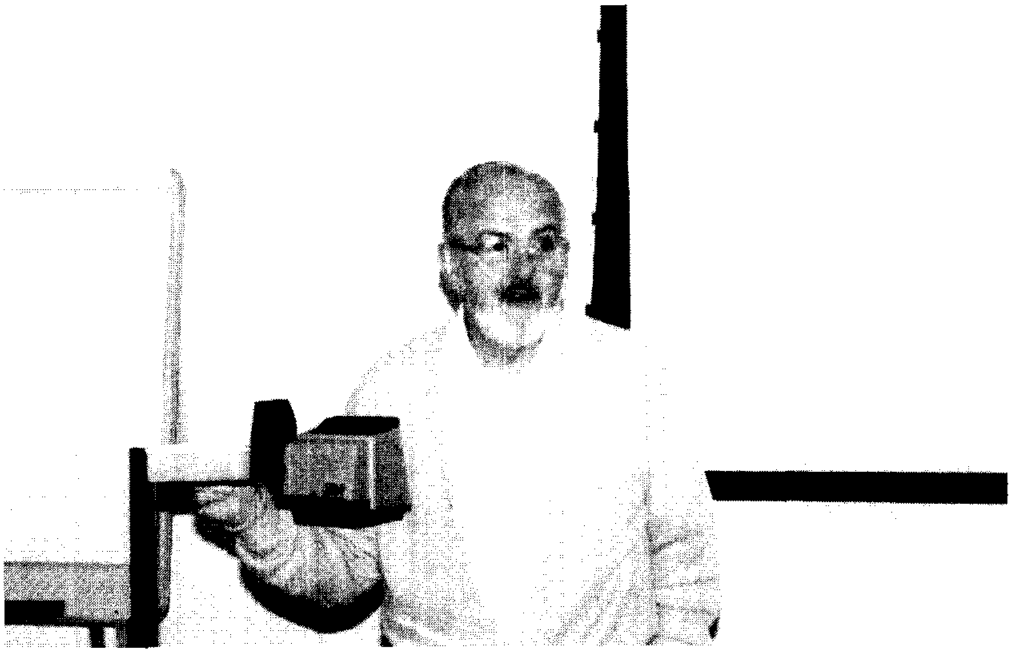

Edward L. Widener

Recycling Waste Paper

Edward L. Widener
Purdue University-Mechanical Engineering Technology
West Lafayette, IN 47907

Key Words: beaters; bleaches; cellulosics; dyes; groundwood; non-woven webs; pulps; secondary fibers; wet- strength resins.

Prerequisite Knowledge:

1) Chemical pulping (sulfate, sulfite, soda processes)
2) Paper grading (stationery, tissues, newsprint, boxboard, magazines)
3) Pulp pricing
4) De-fibering (beaters, hydro-pulpers, blenders)
5) Hydrogen bonding (Van der Waal force)

Objective: To convince consumers and voters that recycling waste papers is economically feasible and ecologically desirable.

Abstract:

In view of popular "AlGoreRhythms" for Ecology and Conservation, a basic Materials and Process Lab will include "Pulp and Papermaking". This involves botany, cellulose chemistry, engineering mechanics, noise and vibration, erosion and corrosion, lubrication and quality control. Employment opportunities for engineers and technologists are obvious.

Start by contrasting starch and cellulose isomers. Explore natural processes of termites, wasps, camels, and cows. Compare the strong covalent bonds between cellulose mers and the weak hydrogen bonds between paper fibers. Describe the huge (80%) capital investment in pulp making: trees, rivers, debarkers, chippers, cookers, bleaches, washers, web-formers, dryers, and balers. Describe the complex operations of paper making and product converting: beating, blending, cleaning, refining, dyeing, sheet forming, pressing, drying, trimming, slitting, and winding. Move over to secondary operations of embossing, printing, plying, slitting, sawing, packaging, sterilizing, warehousing, order filling, and shipping. Then note that paper making and converting have only added some 20% to our pulp investment. So, we conclude recycled paper could cost 80% less. This compares favorably with 95% savings reported for recycled aluminum.

Simple demonstrations of easily recycled waste papers come next. Sort scrap papers by type (consumer products, office grades, newsprint, cardboard, and magazine). Tear a four-gram sample into "postage stamp" pieces, drop into a quart jar of tap water, then soak and shake. Generally, more vigorous agitation is required by choppers, mixers, or blenders. Look for colors, fish-eyes, and shreds. Form a handsheet by pouring slurry through a wire strainer and dewatering with a flat dish. Pour more slurry to make a thicker handsheet. Dry such sheets in sunshine or on a hot plate, then inspect for

"contraries". Use reflected light for thick sheets, transmitted light for thin ones. Test your sheets for tensile pull and tear strength.

Equipment:

1) Waring Blendor® – 120 v, 60 Hz, stainless steel canister.
2) Sunbeam Griddle® – 120 v, 60 Hz, coated surface
3) Ciba-Geigy® Scoop and Press – stainless steel pans.
4) Weight scales-beam balance or spring type
5) Coffee Pot, with temperature control
6) Containers (glass or plastic)
   a. Graduated cylinder or beaker (100-1,000 ml)
   b. Battery jars or cut off jugs (gallon)
7) Bleaches (hypochlorite or peroxide)
8) Dissecting needle (biology probe)
9) Spatula (pallet knife)

Introduction:

The U.S. still has over 70% of those forests existing at Columbus' time. Some 50% of New York State is forest, a renewable raw material. Lumber, pulp, paper, plastics, and fuel industries represent major job opportunities for mechanical engineering technologists in production, process, and maintenance. Yet, our materials labs tend to neglect non-metals, especially common cellulose.

Pulp and paper production requires vast amounts of air, energy, and water. Surging demands threaten to outstrip our plantations or degrade our environment, despite ingenious genetics and fiber conservation cited by ecologists.[1] Paper consumption, estimated at 110-million annual tons, needs some 2.1 acres per person.

Perhaps 80% of papermaking energy is invested in pulping cellulose, a natural polymer. Commercial supplies of wood, bagasse, cotton and flax are valued as "bio-mass" assets; however, enterprises seldom salvage waste paper and cardboard from "trash." A basic experiment in the Materials Lab uses simple equipment to make crude handsheets. Students classify secondary fibers, identify contraries, and estimate savings.

By weight, solid wastes are about 50% paper and increasing three times faster than U.S. population. Crowded dumps and smoky incinerators are now unacceptable. Recycling of "pre-consumer" waste (mill-broke, rejects, trim) approaches 25% of "consumer-products." The challenge is to salvage "post-consumer" waste.[2] The public can be educated and motivated to segregate marketable grades and to accept the subsequent products.[3]

Terms:

A special pulp and paper vocabulary has evolved. Units are U.S., rather than S.I. Color is specified by <u>hue, strength and brightness</u>, with <u>metamerism</u> from light-heat-humidity. <u>Fast</u> means permanent. <u>Wires</u> and <u>felts</u> are machine <u>clothing</u> and <u>white water</u> is recycled machine drainage. <u>Fines</u> are fiber particles and <u>broke</u> is sheet scrap. <u>Converting</u> is the subsequent area for processing. <u>Glassine</u> is film from hard calendering. Fibers are <u>floc</u>, <u>staple</u>, <u>fibrid</u>, <u>fibril</u>, and <u>tow</u>. <u>Non-wovens</u> are formed on <u>cylinders</u> and fourdriniers. Couching and picking affect sheet morphology. Deinking and bleaching affect secondary fiber's softness and tenacity. MIT fold (fatigue), Elmendorf impact (tear), Mullen burst (strength), Patterson punch (puncture), Taber bend (sheet stiffness), Finch stirrup (edge tear), and Canadian Standard Freeness (drainage) are properties. Measurements include caliper (thickness), basis weight (density in pounds avoirdupois per ream), denier (grams per 9000m of yarn), sheet appearance (holes), feel (smoothness or drape), and absorbance (wicking).[4] TAPPI is the Technical Association of the Pulp and Paper Industries.

Pulp Grades:

Pulps are classified by manufacturing process, timber source, or color:

1. Sulfite, made with sodium or calcium bisulfite, needs cleanup of plant waters; it is expensive and soft
2. Sulfate (Kraft) made with sodium sulfide and hydroxide; needs air cleanup; it is strong and cheap
3. Soda, made with sodium hydroxide, is cheaper than sulfite
4. Semi Chemical has partial digestion and steam explosion
5. Mechanical Groundwood (sawdust or wood flour) is weakest, cheapest, and harshest[5,6]

Timbers are hardwoods (deciduous; harsher and cheaper) or softwoods (coniferous and evergreen; softer and costly) from the North (slow growth; thin, supple fibers) or from the South (fast growth; thick, harsh fibers). Northern softwoods give the best pulp quality.

Colors are white (fully bleached), tan (semi-bleached), or brown (unbleached). Bleaching enhances softness but hurts strength.

Prices of virgin pulp may range from \$300-\$800 per short ton (more for metric tonne) compared to recycled fibers at \$30-\$300. A typical mill (using \$2,000,000 of pulp/month) could save \$100,000/month with 25% recycled "secondary fiber," priced 20% less. Some cardboard plants run 100% recycled boxes, bought from local stores and scrap dealers. This is big business.[7]

Procedure:

In the mills, baled pulp and paper are hydrated and defibered to make "handsheets" for quality control tests, according to TAPPI Standard # T-200. The conventional agitators (Valley Beater®, British Std. Disintegrator®) often take several hours. However, a Waring Blendor® takes 30-60 seconds, without presoaking! Such blending involves intense fluid-shear in a 4-lobed canister, as 4 vortexes impinge. Thus, fiber clumps are unrolled, rather than shortened to "fines" by some impeller- blades. Note: the popular "Ultimate Chopper ®" (by Black & Decker) uses 2-horizontal slicers, which make "fines" and weaken "handsheets."

Commercial labs make handsheets with vacuum boxes (Valley Sheet- Mold®) and steam radiators (Williams Sheet-Dryer®).[8] Waste paper dealers use conventional lab filtration setups (Ehrlenmeyer flask, with Büchner funnel and filter paper) requiring a vacuum-pump or eductor-nozzle (tap-water runs to sewer).[9] However, the pocket-sized "scoop and press" (Ciba-Geigy Color Sampler®) can make 3" diameter sheets quickly and easily. Thinner sheets are made by diluting the pulp-slurry (to lower consistency).

A typical recipe: a) Tear a tab card (3 1/4 " x 7 3/8 " x 7-mil thick) into "postage-stamp" pieces; b) Drop into canister, with 500ml. water (70 F); c) Blend at low-speed for 30 sec; d) Pour slurry into shallow bowl, looking for complete defibering of "pulp bundles;" e) Dewater the "pulp-patty", so the new sheet stays on the press pan rather than the screen-knuckles); f) Dry the handsheet on the griddle; g) Use the lid to keep the sheet flat and help visual inspection; h) View thick sheets by reflected light, to find "contaminants" (flakes of clay, specks of foil or film); i) View thin sheets by transmitted light, to find buried contraries (wet-strength clumps); j) Detect tiny balls of pernicious latex or tar with a hot needle; pull a filament like a spider web; k) Test any dyes and wet-strength for "bleachability;" l) Reduce pulping time, using hot water (180°F)

Students can be trained to write formal proposals to mill-management, detailing each step: a) Find the consistent monthly plant tonnage of available waste-paper grades; b) Find the location and cost of baler; c) Select personnel to collect waste and operate equipment; d) Select reliable dealers and establish scrap prices; e) Plan all shipments, ensuring plant security; f) Estimate earnings and equipment payoff, including savings of trash service. Otherwise busy bosses may ignore casual suggestions.

Recycle Samples:

1. Newspapers- plain, printed or colored
2. Magazines- pages only; no covers or staples; no coatings of clay or latex
3. Envelopes and Stationery- white, colored, unbleached, no glassine windows or latex labels.
4. Creped wadding- facial, bathroom, towel, napkin tissues; white, pastel or deep-dyed; plain or wet strength
5. Computer scrap- printouts or tab cards; no carbons: white or pastel
6. Kraft sulfate- bags or wrappers; unbleached or semi-bleached
7. Boxboard- linerboard or corrugate; unbleached or semi bleached; gray or brown.[10,11]

References:

1. Osborne, M.J. "Energy Audit," TAPPI Journal, Vol. 60, No.8, Atlanta, GA, Aug. 1977, p. 12 and 81.
2. Dane, Sally, "The National Buyers Guide to Recycled Paper," EE Handbook, Washington, DC, 1973.
3. NCRR, "Fact Sheet," No. FS-1972-12, Washington, DC, 1972.
4. APPA, The Dictionary of Paper, 2nd ed., G. Banta Pub. Co., Menasha, WI, 1951.
5. "Marketing Trends," (Price List), Paper Trade Journal, Vance Pub. Co., New York, NY, bi-weekly.
6. E.I. du Pont, The Manufacture and Dyeing of Paper, Orchem Dept., Wilmington, DE, 1963.
7. "New Secondary-Fiber Pilot-Plant" (WMU, Kalamazoo, MI), TAPPI Journal, Vol. 60, No.8, Aug. 1977, p.25
8. TMI Catalog, 6th ed., Amityville, L.I., NY, 1976.

9. API, "Guidelines for Determining Recyclabilty of Paper Stock," Paper Stock Conservation Committee, New York, NY, 1975.
10. NARI, "Paper Stock Standards and Practices," Circular #PS-74, New York, NY, 1974.
11. Casey, James P., "Pulp and Paper," 2 volumes, Interscience Pub., NY. (1952).

Biography:

Professor Widener has taught at Purdue University since 1978, concentrating on mechanics, materials, recycling, and communicating. Ed was in Malaysia from April 1995-June 1996, teaching Metals Lab for new technology teachers. Memberships include ASEE, ASME, ASM, ISA, and TAPPI. A registered P.E. in New York and Indiana, he was ABET-accreditation visitor from 1983-1990; and NSF lab grants reviewer in 1989& 1990. Between 1994-1997 he had night classes in Indianapolis, IN (IUPUI) & Danville, IL (Jr. College). Degrees from Purdue are BS '49 (physics) & BS '51 (ME); his MSEM '62 (Hydraulics) is from Univ. of Kansas. Between 1952-1978, Ed was a process or project engineer for Continental Group, Baker-McHenry-Welch, Kimberly-Clark, E.I.DuPont, Union Carbide, & U.S. Steel. In WW II he was U.S. Navy S1/c, aboard light cruisers Vicksburg & Astoria.


Dura
Kote

WEAR OF ADVANCED CERAMICS

Said Jahanmir

Ceramics Division, Materials, Room B 360
National Institute of Standards and Technology
100 Bureau Drive, MS 8520
Gaithersburg, Maryland 20899-8520

Telephone 301-975-3671
e-mail said.jahanmir@nist.gov

Said Jahanmir

WEAR OF ADVANCED CE

Mild to Severe Wear Tra

Said Jahanmi

National Institute of Standards and Techn

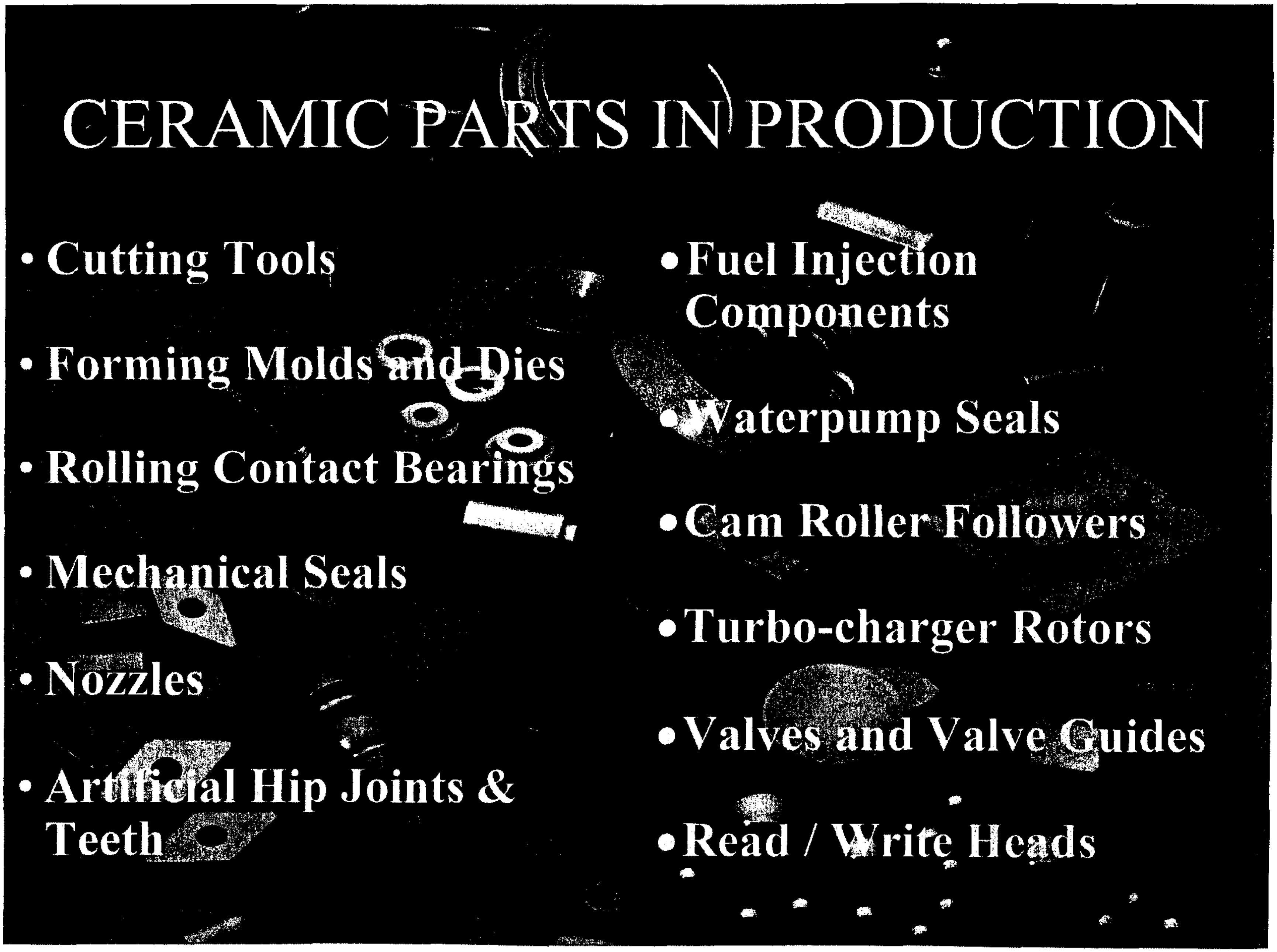

CERAMIC PARTS IN PRODUCTION

- Cutting Tools
- Forming Molds and Dies
- Rolling Contact Bearings
- Mechanical Seals
- Nozzles
- Artificial Hip Joints & Teeth
- Fuel Injection Components
- Waterpump Seals
- Cam Roller Followers
- Turbo-charger Rotors
- Valves and Valve Guides
- Read / Write Heads

ADVANCED STRUCTURAL CERAMICS

Silicon Nitride
- Sintered
- Hot Pressed
- Reaction Bonded
- Sintered Reaction Bonded
- Hot Isostatically Pressed

Silicon Carbide
- Sintered
- Hot Pressed
- Reaction Bonded (Siliconized)
- [illegible]

Alumina
- [illegible]

Zirconia
- Cubic
- Tetragonal
- [illegible]

Sialon
- Sintered
- Hot [illegible]

Wear Transition Diagram for Alumina

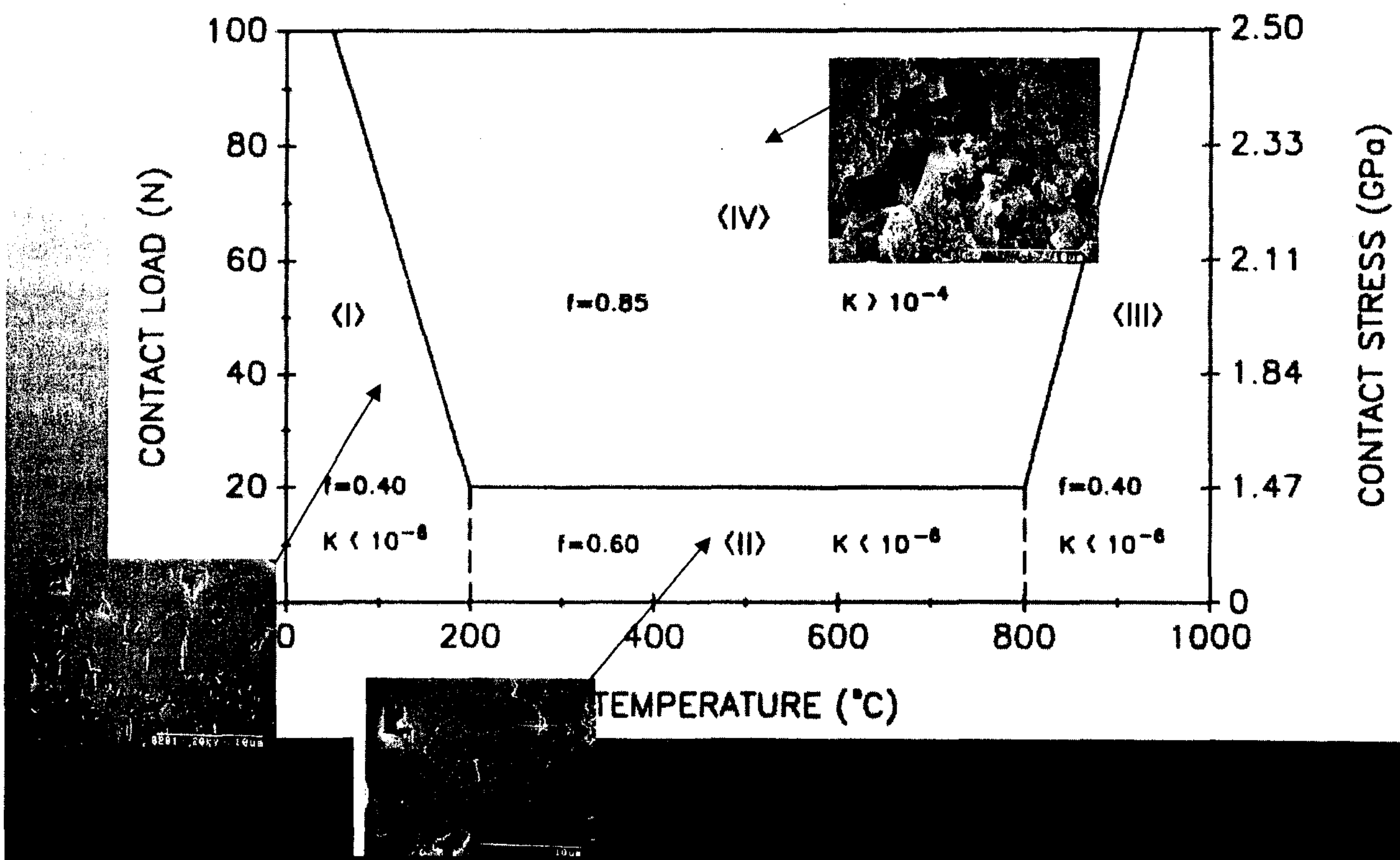

Wear Transition Diagram for Silicon [illegible]

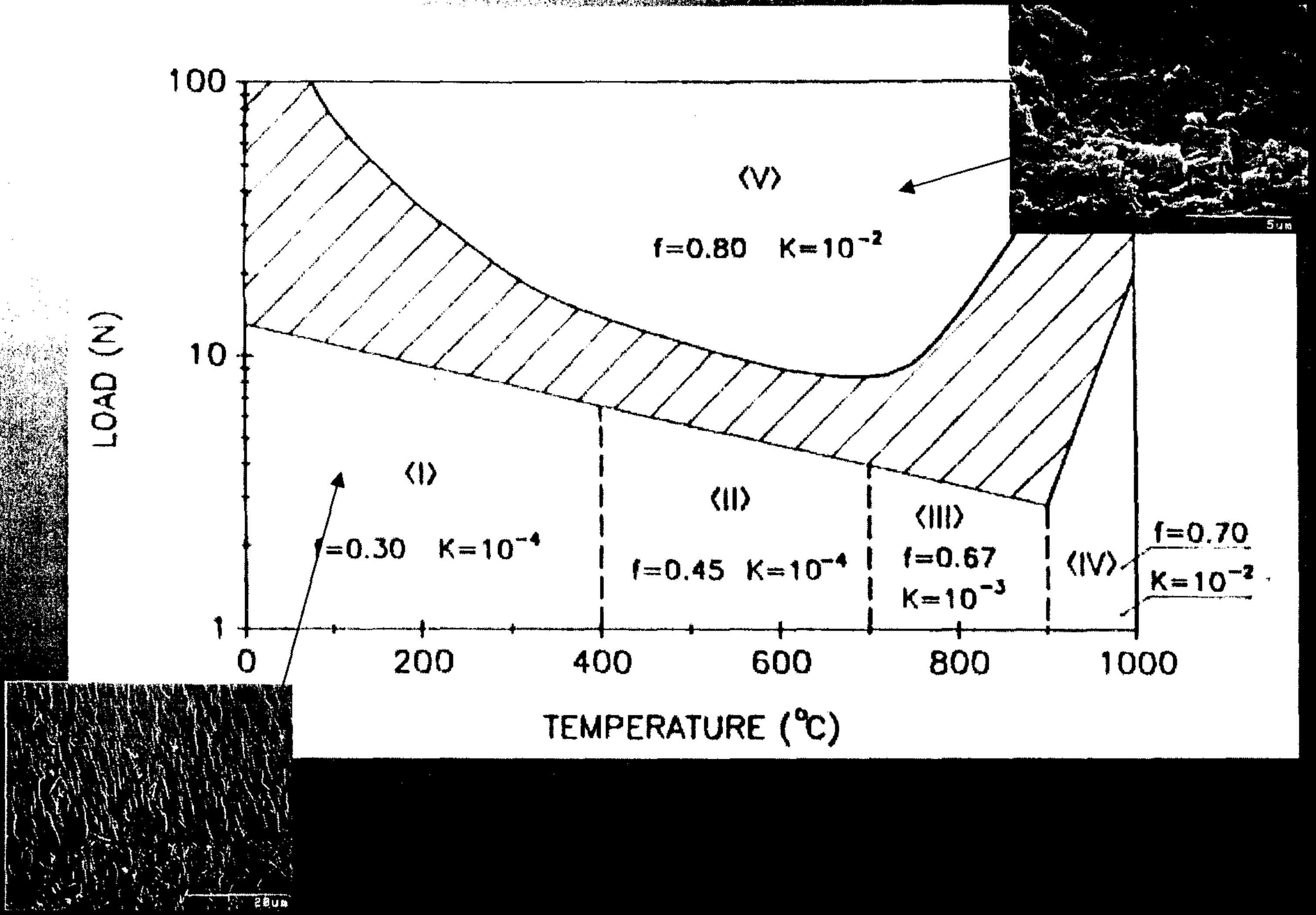

Wear Transition Diagram for Silicon [illegible]

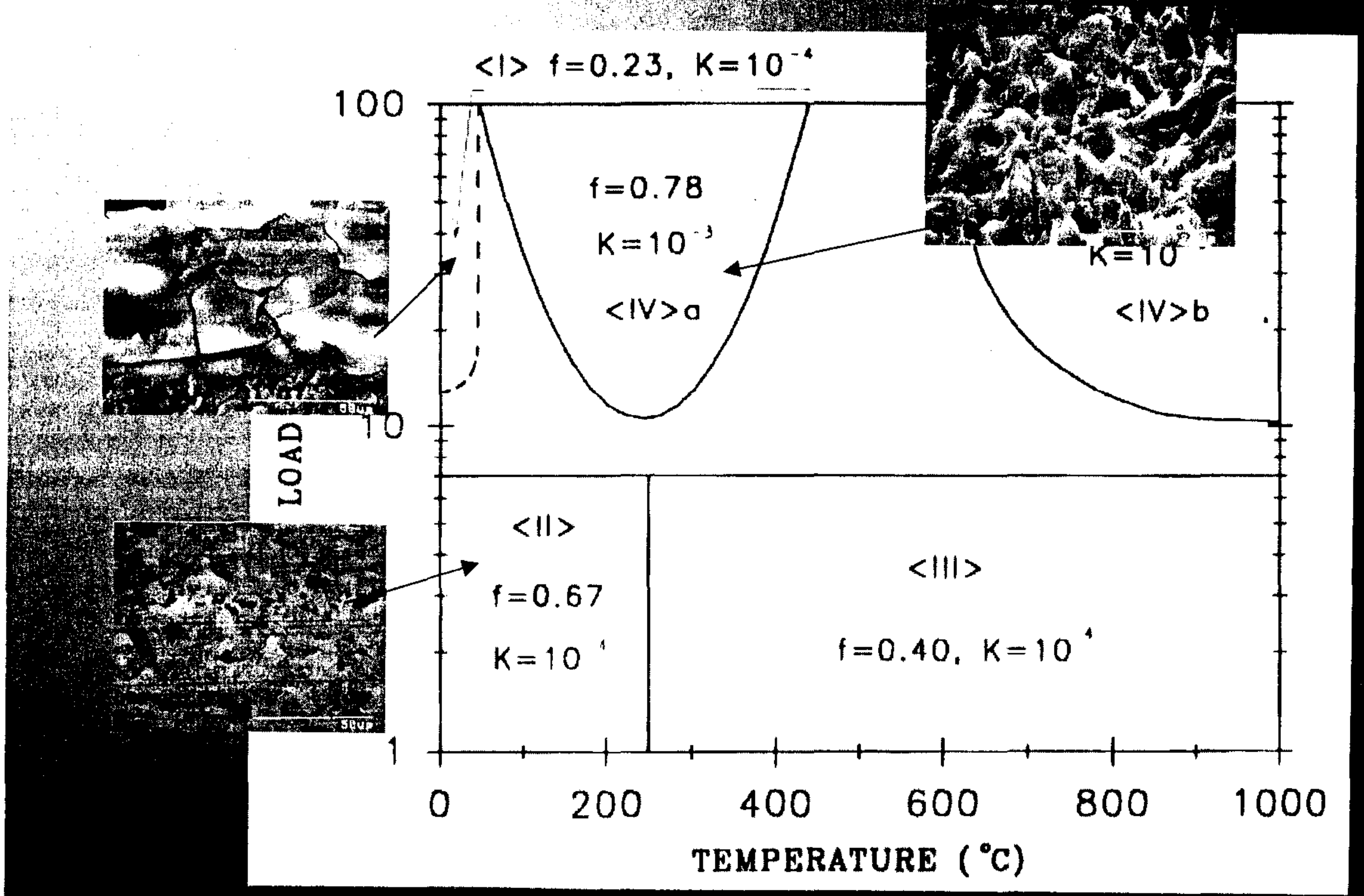

Wear Transition in Alumina (AD 995) Under [illegible]

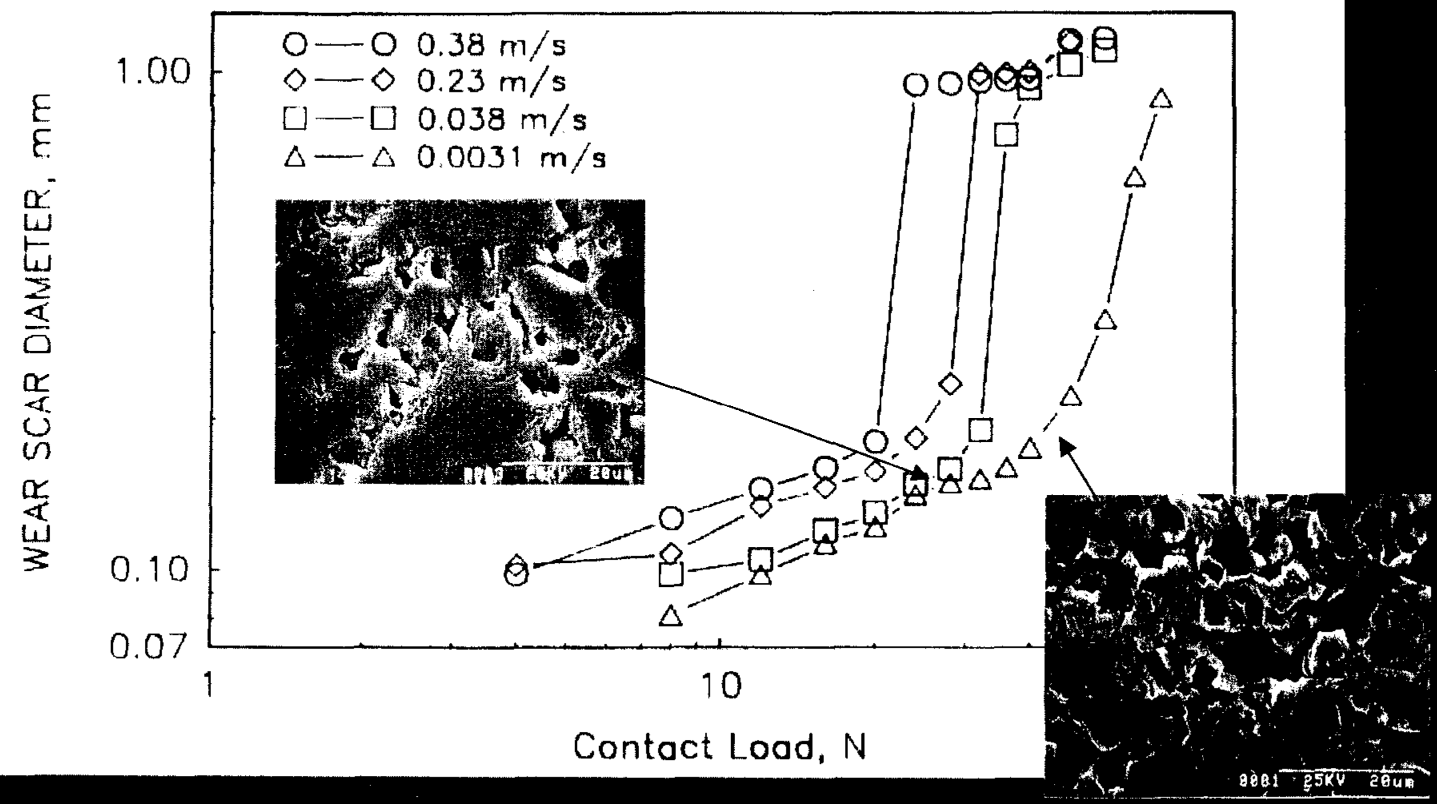

Reduction in Wear of Silicon Nitride

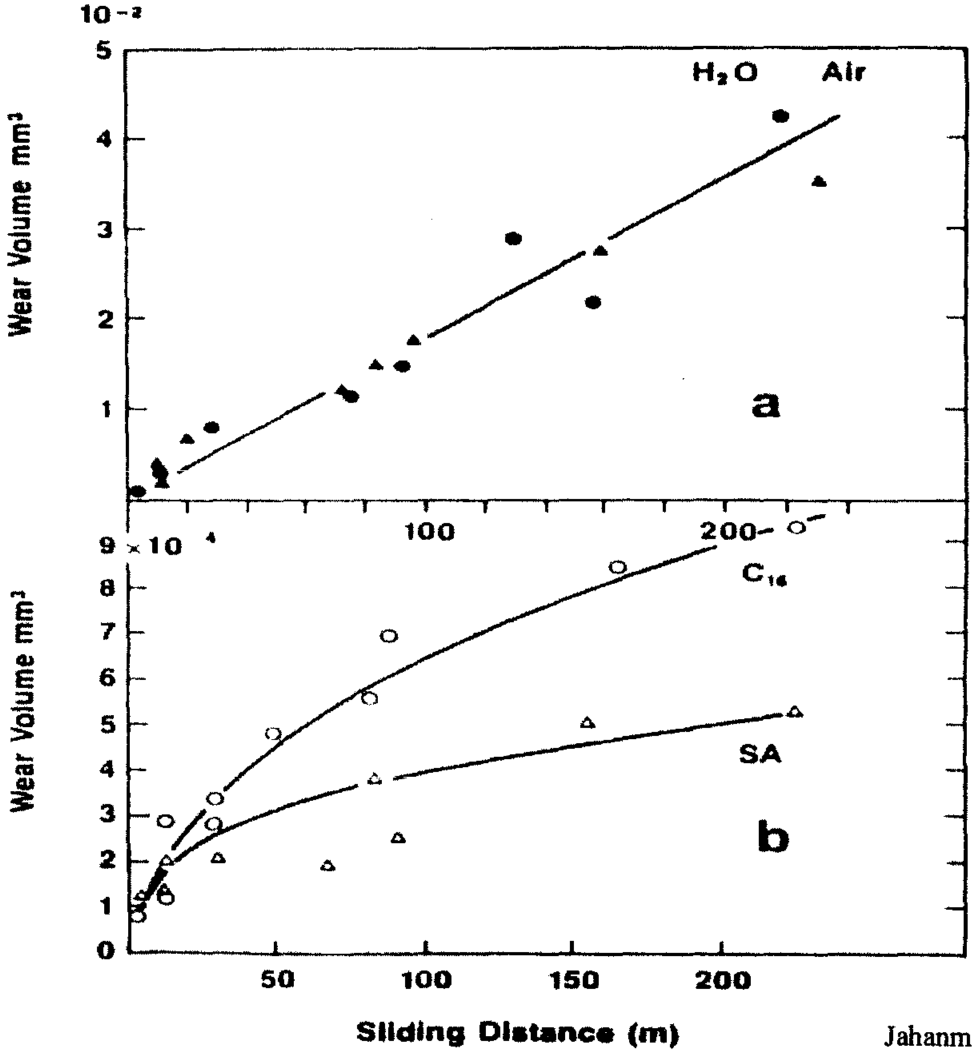

Jahanmir et al.

Damage Formation in Hertzian [illegible]
Brittle vs. Quasi-Plastic Behavior

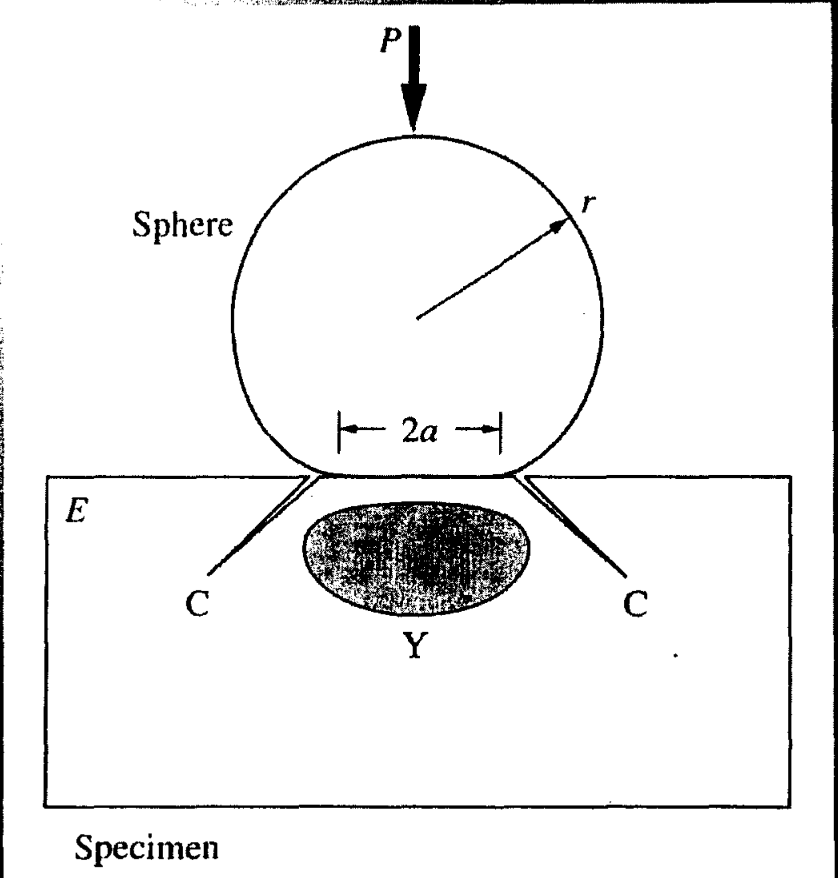

Contact Damage Modes: Three Different

(a)

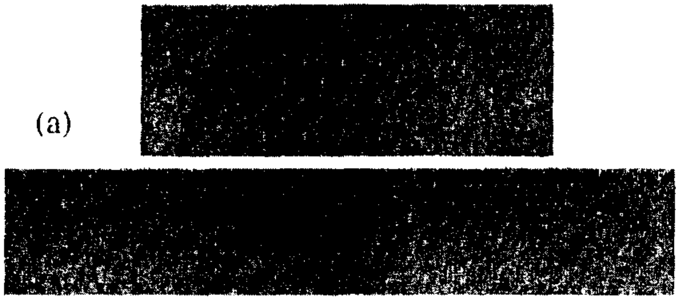

Cone Cracking

Brittle Behavior

Mixed Mode

(b)

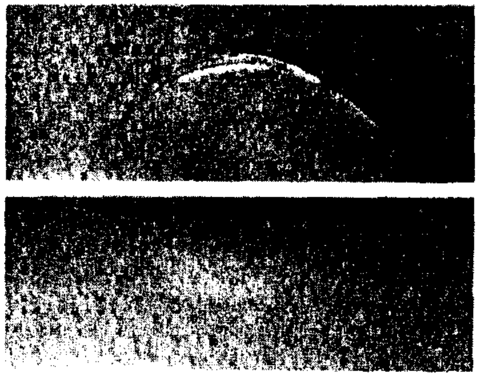

(c)

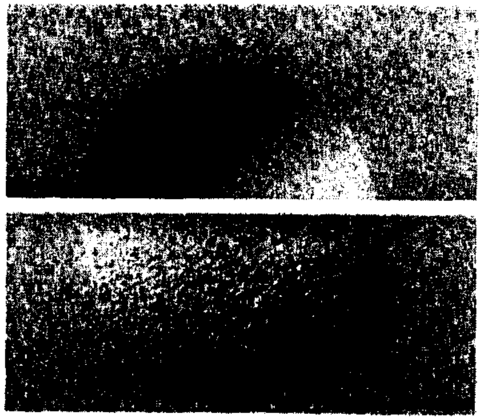

Critical Load for Onset of Cone [illegible]

$P_c / r = AT^2 / E$

P_c -- critical load for onset of cone cracking

r -- radius of ball in contact with a flat surface

T_c -- fracture toughness (i.e. K_{IC} assuming [illegible] toughness)

E -- modulus of elasticity

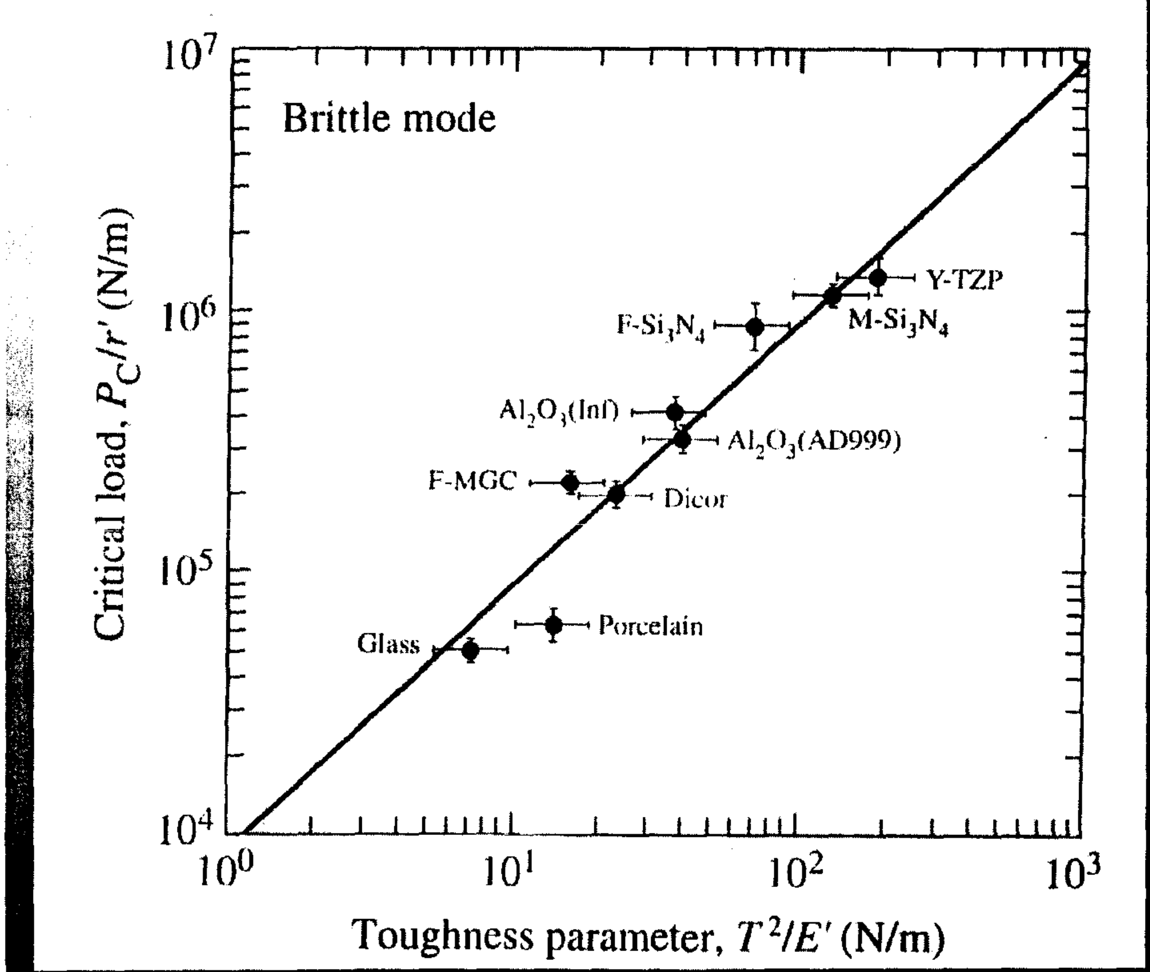
Brittle mode
Critical load, P_C/r' (N/m)
Toughness parameter, T^2/E' (N/m)
10^4
10^5
10^6
10^7
10^0
10^1
10^2
10^3
Y-TZP
M-Si_3N_4
F-Si_3N_4
Al_2O_3(Inf)
Al_2O_3(AD999)
F-MGC
Dicor
Porcelain
Glass

Critical Load for Onset of Quasi

$P_Y / r^2 = DH(H/E)^2$

P_Y -- critical load for onset of plastic yield
H – hardness
E – elastic modulus

Dimensionless constant D related to Poiss
Experimental value D = 0.85

[illegible]

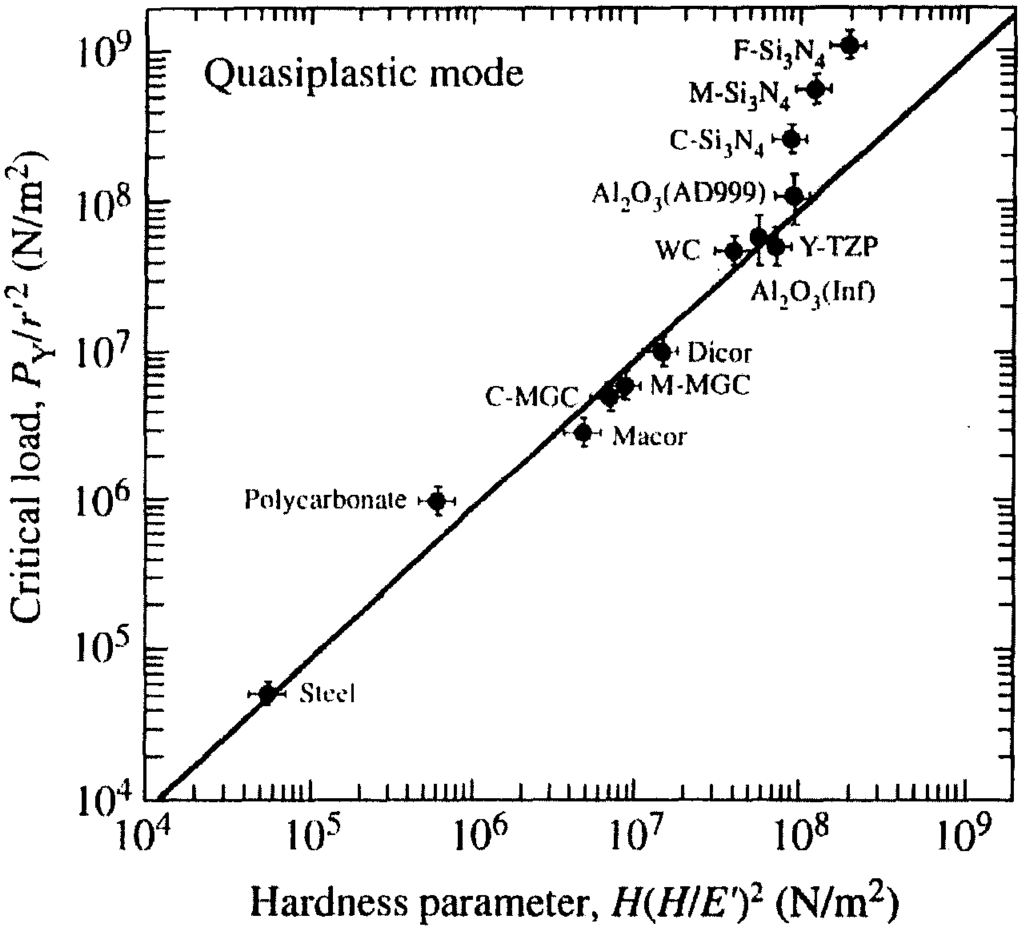
Quasiplastic mode
F-Si_3N_4
M-Si_3N_4
C-Si_3N_4
Al_2O_3(AD999)
WC
Y-TZP
Al_2O_3(Inf)
Dicor
M-MGC
C-MGC
Macor
Polycarbonate
Steel
Critical load, P_Y/r'^2 (N/m^2)
10^4
10^5
10^6
10^7
10^8
10^9
Hardness parameter, $H(H/E')^2$ (N/m^2)

Transition from Brittle to Quasi Pl

$P_Y / P_C = (D/A)\,(H/E)\,(H/T)$

Brittle if $P_Y / P_C > 1$

Quasi Plastic if $P_Y / P_C < 1$

Strong dependence on Hardness

[illegible]

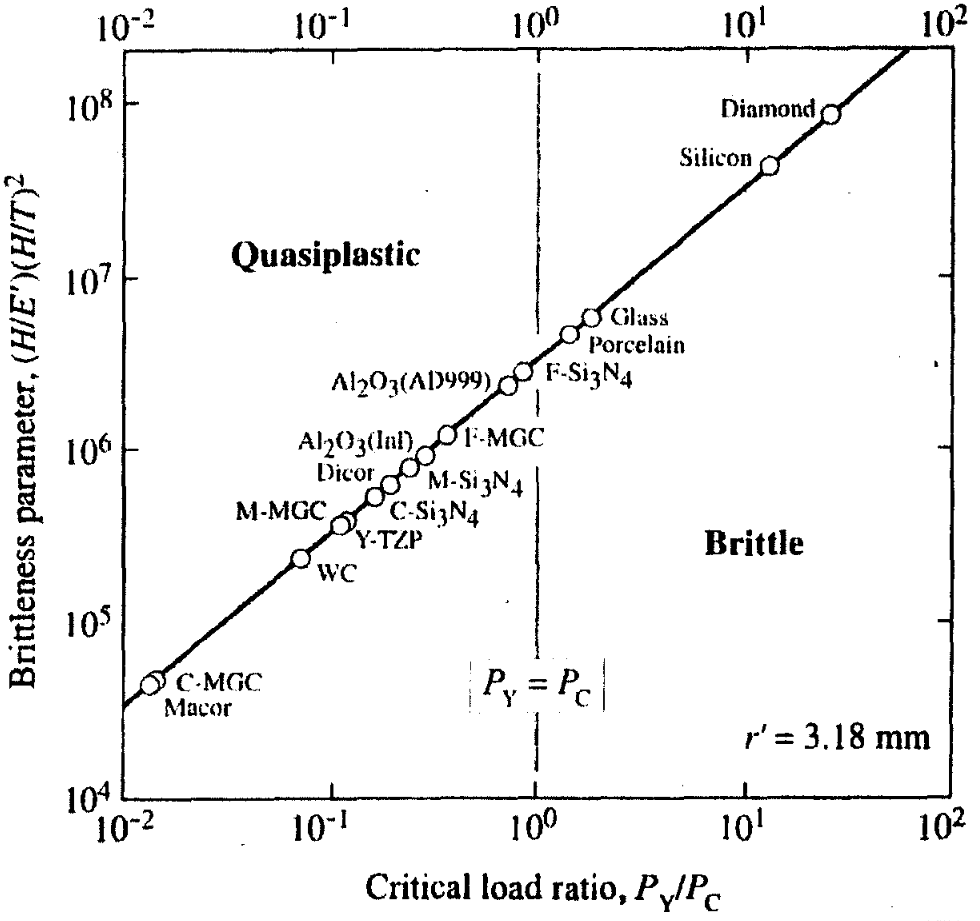
10^-2
10^-1
10^0
10^1
10^2
10^8
10^7
10^6
10^5
10^4
Brittleness parameter, (H/E')(H/T)^2
Critical load ratio, P_Y/P_C
Quasiplastic
Brittle
Diamond
Silicon
Glass
Porcelain
F-Si3N4
Al2O3(AD999)
Al2O3(Inl)
F-MGC
Dicor
M-Si3N4
M-MGC
C-Si3N4
Y-TZP
WC
C-MGC
Macor
P_Y = P_C
r' = 3.18 mm

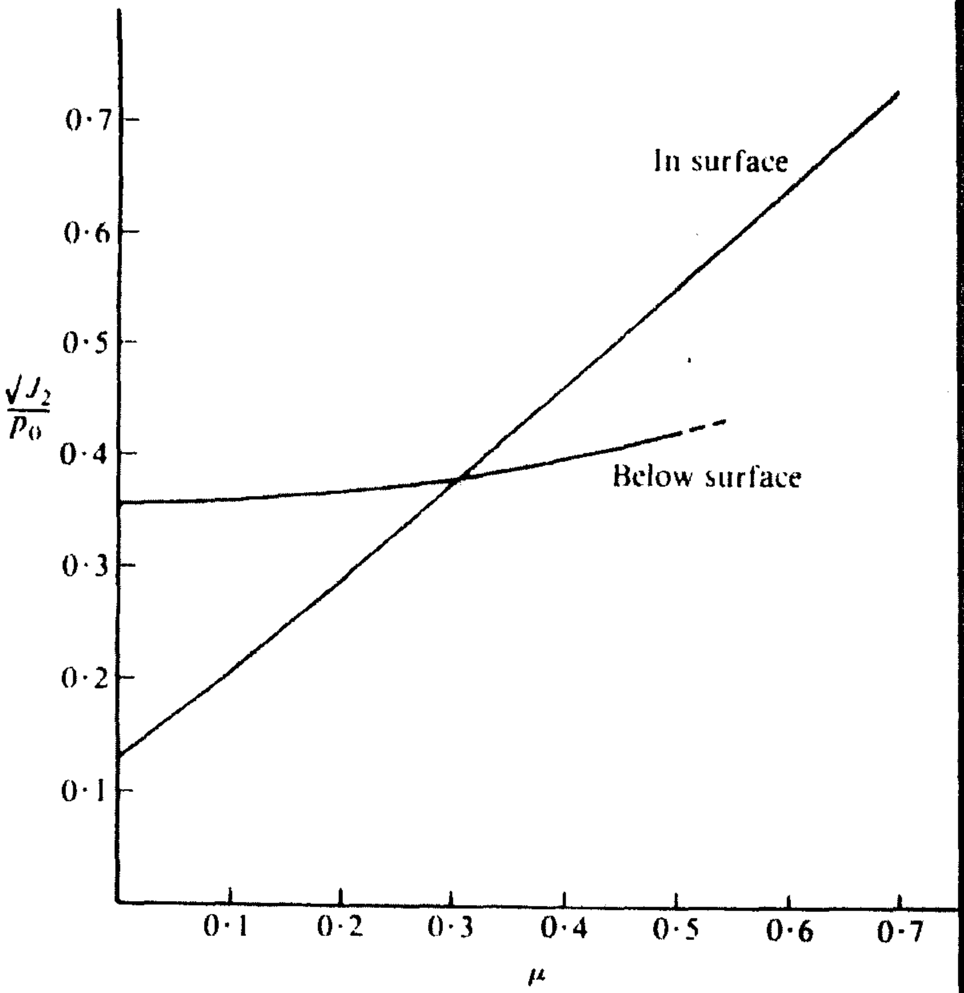
$\frac{\sqrt{J_2}}{p_0}$
0·1
0·2
0·3
0·4
0·5
0·6
0·7
In surface
Below surface
0·1
0·2
0·3
0·4
0·5
0·6
0·7
μ

Transition Load for Quasi Plasticity [illegible]

$P_Y / r^2 = DH(H/E)^2 f(f)$

D depends on Poisson's ratio
D decreases from 0.89 to 0.76 as Poison's ratio in[illegible]

Experimental value D = 0.85 [Rhee et al.] [illegible]
average Poison's ratio of 0.22.

Function f(f) is not sensitive to f for 0 < f < 0.3 [illegible]
Variations in P as the location yield moves to the [illegible]

[illegible]

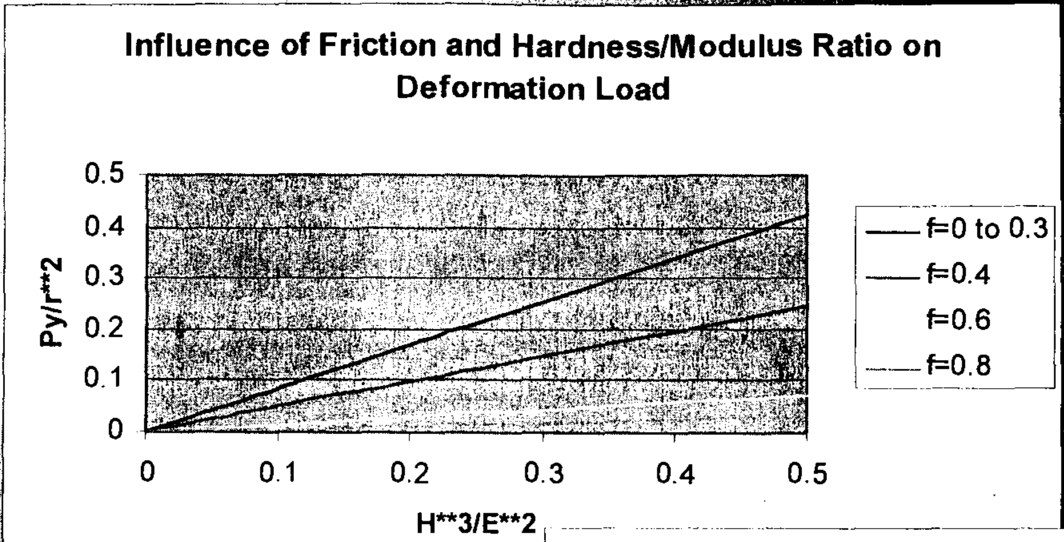
Influence of Friction and Hardness/Modulus Ratio on Deformation Load

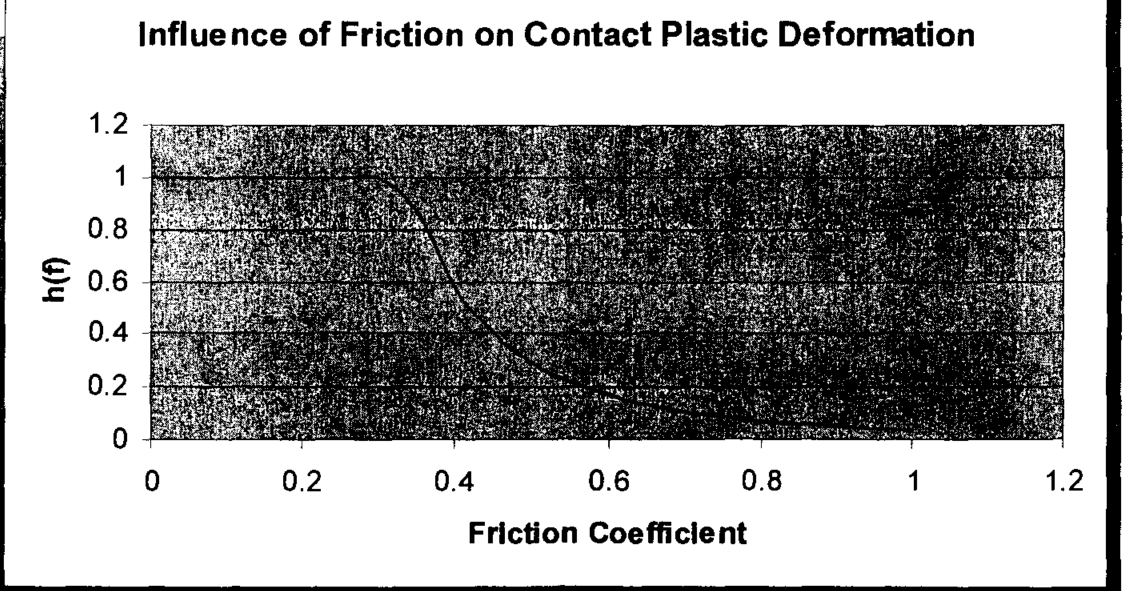
Influence of Friction on Contact Plastic Deformation

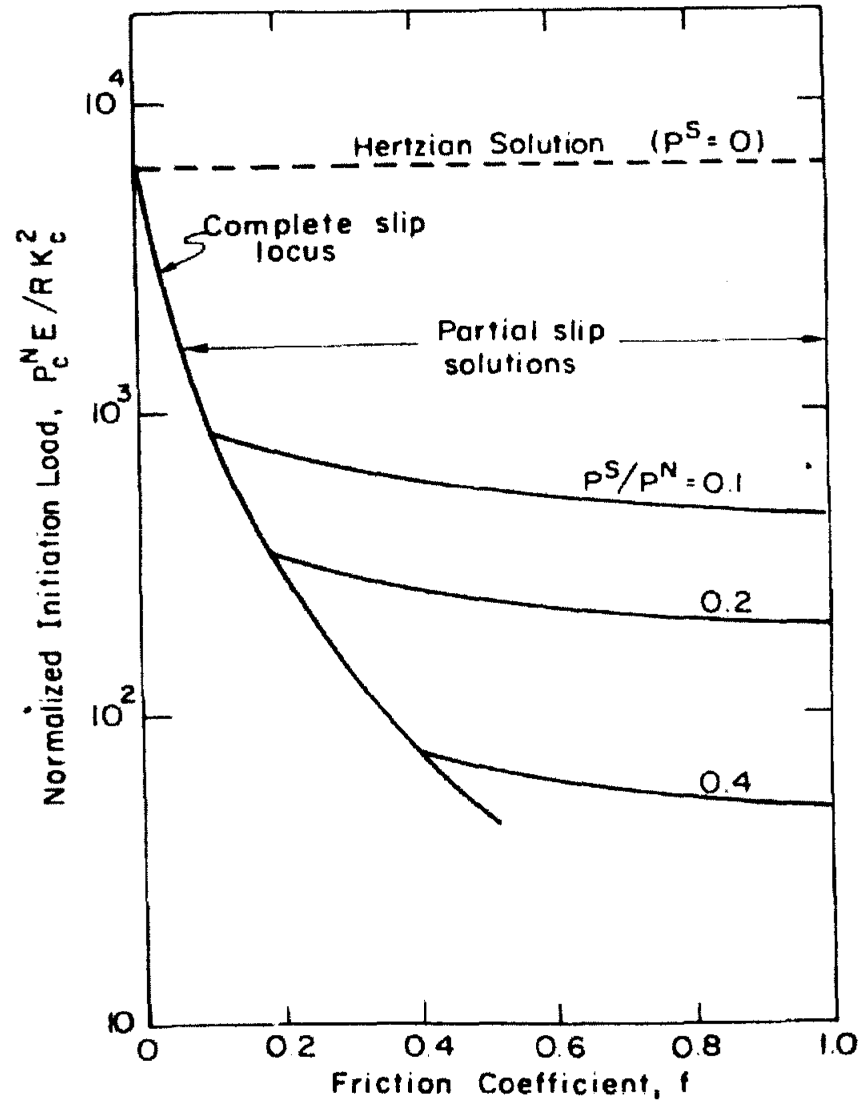
Hertzian Solution $(P^S = 0)$
Complete slip locus
Partial slip solutions
$P^S/P^N = 0.1$
0.2
0.4
Normalized Initiation Load, $P_c^N E / R K_c^2$
10^4
10^3
10^2
10
0
0.2
0.4
0.6
0.8
1.0
Friction Coefficient, f

Transition Load for Brittle Behavior [illegible]

$P_c / r = A\, g(f)\, K_c^2 / E$

A is approximately 7.5 x 10^3, close to value [illegible] at al.

Although an explicit equation was not provided [illegible] Evans, the form of this relationship can be [illegible]

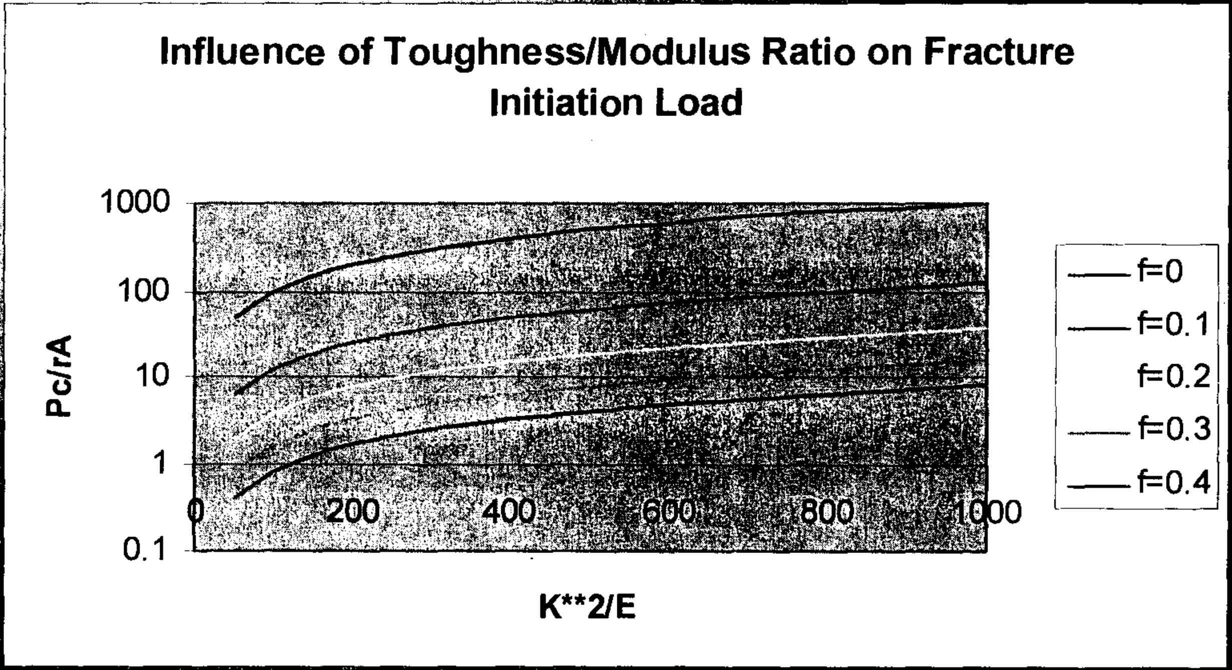
Influence of Toughness/Modulus Ratio on Fracture Initiation Load
Pc/rA
1000
100
10
1
0.1
0
200
400
600
800
1000
K**2/E
f=0
f=0.1
f=0.2
f=0.3
f=0.4

Transition from Brittle to Quasi Plasticity [illegible]

$P_Y / P_C = (D/A)(H/E)(H/T)^2$ [illegible]

Brittle if $P_Y / P_C > 1$
Quasi plastic if $P_Y / P_C < 1$

$h(f) = (1 + B f)^3$ for 0 [illegible]
$h(f) = (1/27)(1/f + B)^3$ for $f > 0.5$

[illegible] promoted [illegible]

Mechanical Properties [illegible]

Mechanical Properties	Alumina Coors AD 998	Alumina Coors AD [illegible]
Vickers Hardness (GPa)	15.0	[illegible]
Elastic Modulus (GPa)	345	[illegible]
[illegible]	[illegible]	[illegible]
[illegible]	[illegible]	[illegible]

Effect of [illegible]
For Several [illegible]
R-Curve Behavior

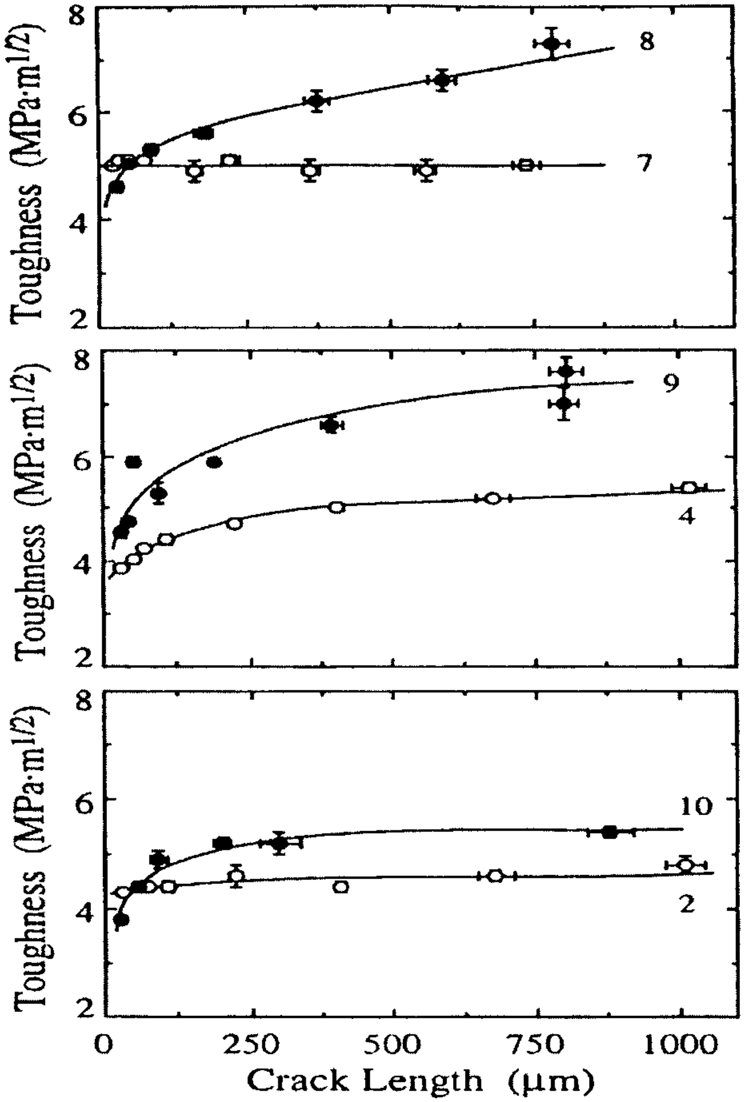

Transition Loads for Brittle and [illegible]
(at Room Temperature)

	Transition Load Expt. (N)	f	P_y^0 (N)	[illegible]	[illegible]
Alumina (AD 998)	20	0.60	920	[illegible]	[illegible]
Alumina (AD 995)	60	0.10	1240	[illegible]	[illegible]
Silicon Nitride [illegible]	10	0.30	2570	[illegible]	[illegible]
[illegible]	[illegible]	[illegible]	[illegible]	[illegible]	[illegible]

SUMMARY

- Wear transition to microfracture mode [illegible] practice
- Mechanics analysis and experimental data [illegible] predict the onset of transition
- Transition to microfracture mode of wear [illegible] brittle fracture or quasi plasticity
- [illegible]

A MATERIALS CONCEPT INVENTORY FOR INTRODUCTORY MATERIALS ENGINEERING COURSES

Stephen Krause

J. Chris Decker

Justin Niska

and

Terry Alford

Department of Chemical and Materials Engineering
Arizona State University
Arizona State University
Tempe, Arizona 85287-6006

Telephone: 480-965-2050
e-mail skrause@asu.edu

and

Richard Griffin

Department of Mechanical Engineering
Texas A&M University
College Station, Texas 77843

Telephone: 409-845-9779
e-mail rgriffin@mengr.tamu.edu

Stephen Krause

A Materials Concept Inventory for Introductory Materials Engineering Courses

Stephen Krause, J. Chris Decker, Justin Niska, Terry Alford and Richard Griffin*

Department of Chemical and Materials Engineering, Arizona State University, Tempe, AZ 85287, E-mail: skrause@asu.edu
*Department of Mechanical Engineering, Texas A&M University,
College Station TX 77843, E-mail: rgriffin@mengr.tamu.edu

Key Words: assessment, concept inventory, interactive engagement, teacher-centered learning, student-centered learning

Prerequisite knowledge: college chemistry and college physics

Introduction

Over the last two decades new theories of learning and associated methods of teaching have been emerging in the fields of science, math, engineering, and technology. The new methods have demonstrated that, compared to teacher-centered lecturing, using a more a hands-on, inquiry-based, student-centered model of education increases a student's knowledge and conceptual understanding of a subject. To compare the differences between the new and old methods, new assessment tools are being created to measure students' conceptual knowledge as well as to understand what preconceptions and background limitations students have when entering a class.

One of the most widely used and influential assessment tools is the Force Concept Inventory (FCI) created by Hestenes[1,2] et al, and tested broadly by Hake[3] for students in high school and college physics classes. A concept inventory questionnaire utilizes a series of multiple-choice, frequently illustrated questions, based on qualitative, concept-oriented problems on a particular subject. It measures deep understanding and conceptual knowledge of a subject rather than a student's ability to solve problems by memorizing facts or by just solving equations. The results have been compared to the performance of students in classes with different teaching methods to determine teaching effectiveness. Over more then a decade, the FCI has shown quite clearly that, the application of new methods of teaching based on education reform is, indeed, more successful in developing conceptual knowledge. Hake's[3] findings indicated that students using reformed methods with "interactive engagement" significantly increased their gain in conceptual knowledge compared to courses taught with traditional, teacher-centered lecture courses.

Application of concept inventory assessment tools is beginning to be applied to engineering subjects, partly as a result of the new EC 2000, continuous self-improvement process implemented by the Accreditation Board of Engineering (ABET[4]). ABET's guidelines establish that, for an engineering program to be accredited, its must have in place a system of continuous evaluation and improvement so that it "demonstrates (the) achievement of... objectives and uses the results to improve the effectiveness of the program."

As part of a project on innovative education in engineering, D. Evans and others in the NSF-sponsored Foundation Coalition[5] are developing concept inventory assessment tools similar to the FCI. As part of this process, a concept inventories test for the subject "materials science and engineering" is being developed and is called the Materials Concepts Inventory (MCI). This paper reports on the development of a MCI and the results that have been obtained so far. The concepts covered by this test emphasize principles that govern concepts on the relationships between structure, processing and properties of engineering materials. A secondary emphasis is on understanding how effectively background educational concepts were developed in earlier courses.

Background and Methodology

In 1985 Hestenes[1,2] and colleagues set out to understand what students knew about physics, and what they were getting out of taking physics courses. To this end they set out to create a test that would evaluate students' understanding of the concepts covered in physics. The test would have to be developed such that the questions investigated students' conceptual understanding of the fundamentals of Newtonian mechanics. The questions had to be simple enough so that students who had never taken a physics course could understand them, and yet were sufficiently content rich so that students who were well experienced in physics would still be challenged. The end result of their work was the Force Concepts Inventory (FCI), a test that has now gained national acceptance as an assessment tool for physics teachers and their classes.

The results of Hestenes[1,2] et al from their original research using the FCI established three main points, "1) Commonsense beliefs (of students) about motion and force are incompatible with Newtonian concepts in most respects, 2) conventional physics instruction produces little change in these beliefs, and 3) this result is independent of the instructor and the mode of instruction." Their conclusions from these findings were that, "to induce significant conceptual change, a well-designed and tested instructional method is essential," and that teaching to solve each individual misconception students had would be unsuccessful.

Following in Hestenes[1,2] et al's footsteps Hake[3] set about to test the effectiveness of the new "Interactive Engagement" (IE) teaching style and to compare it to the classical teacher-centered, lecture-based instructional method. Hake[3] collected FCI scores of over 6500 students from physics courses in high school and college nationwide and computed the average normalized gains between their pre and post-test scores. He took this as a rough indicator of how much students had learned from their physics course. He then broke that data into two sets, students who had been taught in courses, which used little or no Interactive Engagement, and those which used substantial Interactive Engagement methods. His results from courses not taught with the Interactive Engagement method had significantly lower gains in understanding (23%) then those that did employ Interactive Engagement methods (48%). These findings strongly suggest that courses employing the Interactive Engagement method are more effective in teaching students then those courses that do not use these methods. The results of Hake's[3] work has provided a strong incentive for incorporating Interactive Engagement in the teaching of physics.

The general principles utilized by Hestenes[1,2] in the development of the FCI were applied in the development of the MCI. A team of undergraduates, a graduate student, and faculty utilized a variety of resources in the MCI development. Broad general categories of materials concepts and their course linkages were delineated from the content contained class syllabi and in introductory materials science and engineering textbooks. Multiple choice questions on the categories defined were:

Concept Categories
Phase Diagrams & Solubility
Atomic bonding
Electronic structure
Atomic arrangement & Crystal structure
Defects & Microstructure
Reactions & Units
Macroscopic mechanical properties

Table 1 displays the seven key materials concept categories covered in the introductory to materials course.

After key concepts had been determined, the next stage in the creation of the test was to determine what the level of students' prior conceptual knowledge of the subject matter. The average student taking the introduction to materials course is a college sophomore with two to three semesters of experience. These students typically have taken two semesters of college level chemistry, one to two semesters of physics, one to three engineering oriented math courses, and a multitude of high school level math and science courses. From these courses it was determined that some of the concepts covered by the introductory materials course were covered in some of the students' previous courses, but usually only in passing and not in-depth. Thus, it was determined that on the concept inventory a fraction of the questions would not only be created to cover key concepts, but be presented in a manner that students would have been exposed to them in previous courses.

A literature survey was initiated to help the team determine the following, 1) the difficulty level of the questions, 2) how other researchers had created their questions and "distractor" answers, and 3) the guidelines in creating such concept inventories. From the survey the team found concept inventories in thermodynamics, chemistry, and mechanics, along with corresponding data from then and articles on the pros and cons of them. The results of the surveys helped guide the team in the creation of the MCI.

To establish a set of questions and realistic distractor answers the team began a series of weekly interviews and "intuition quizzes" with students from a current – spring semester 2002 – introduction to materials course. In this system the team created weekly short answer, open-ended questions, or multiple choice quizzes that covered what was being taught in the introductory materials course that week. These questions were then given to students at the beginning of class and the answers evaluated by the team. The other portion of understanding what the students knew was weekly volunteer interviews performed by the class instructor and at least one student assistant. In these interviews volunteer students would meet with the instructor and discuss what they were learning that week, and any feedback they had on how the class was going. Then the students were asked some brief questions on the future class content to see what, if anything, the students knew about that subject already. The results of these interviews, along with the quizzes and short answers, and the project teams' own experiences in the field helped to create a multitude of possible concept test questions, and realistic distractor answers.

With a large pool of questions and answers created, the test was created. The team established two criteria before selecting what questions were to be placed on the test, 1) that roughly 1/3 of all the questions were in a form that students would have had previous exposure to them in preceding courses, and 2) that two to six questions would be based on each of the seven primary concepts covered in the course. To meet the first criteria it was determined that a majority of students would have been exposed to several of the primary concepts in their previous chemistry courses, and to a lesser, and surprising, extent, their geometry courses. The distribution of the questions into their primary concept category and broader course categories can be found in tables 2a and 2b below.

Primary Intended Category	**Number of Questions**
Chemistry	8
Materials	16
Geometry	2

Table 2a. The three main categories of all the questions asked in the alpha MCI and the number of questions found in each category

Concept Category	**Number of Questions**
Phase Diagrams & Solubility	2
Atomic bonding	4
Electronic structure	3
Atomic arrangement & Crystal structure	2
Defects & Microstructure	6
Reactions & Units	3
Macroscopic mechanical properties	6

Table 2b. The seven materials concept categories, and how many questions each category contained

After the alpha MCI created it was decided that it would be tested in the summer session of the introductory materials course. The number of participants in the summer session is considerably smaller then regular fall and spring sessions – roughly 15 in summer compared to multiple classes in excess of 50 per class in fall and spring. For this test 13 students participated in the entrance exam given in the first week of lecture and 12 participated in the exit exam given in the last week of lecture. Only nine students took both exams while the other students either withdrew from the class after the first few days or added the class after the initial exam had been given. To create a source of motivation for the students and validity for the test, the students were informed that the test was given the weight of a regular homework assignment. The test was then administered, allowing the students 30 minutes to finish the 26-problem multiple-choice test. In the analysis of the results we have removed four poorly worded or ambiguous questions as determined by post-test discussions.

Results

A summary of the results is shown in the following tables. The results of the 3 student groups are in section 1. Group 1 consisted of students who only took the entrance exam and subsequently withdrew or didn't take the exit exam. Group 2 consisted of the students who only took the exit exam. Group 3, upon which the data was be based, consisted of students who took both the entrance and exit exams. The results are listed as a percentage out of 100% possible, where each question had equal value.

Group 3	**Entrance Exam**		**Exit Exam**
Number of Students	9		9
Mean	35.90		45.30
Median	34.62		42.31
Mode	30.77		42.31
Standard Deviation	10.26		12.13
High	50.00		69.23
Low	19.23		26.92

Table 1 Displays the results obtained from group 3, the only students who completed both the entrance and exit exams

Group 1	**Entrance Exam**
Number of Students	4
Mean	20.19
Median	17.31
Mode	11.54
Standard Deviation	9.58
High	34.62
Low	11.54

Table 3 Displays results from group 1, students who only took the entrance exam

Group 2	**Exit Exam**
Number of Students	3
Mean	33.33
Median	30.77
Mode	30.77
Standard Deviation	6.54
High	42.31
Low	26.92

Table 4 Displays results from group 2, students who only took the exit exam

Section 2 below presents the results from the gain per category from the test for Group 3, and the total gain on the test. Also, the gains from the questions with the highest and lowest gains per category are displayed. All gains were calculated using Hake's[3] model of normalized gain, and all data listed is in percentage form.

Category	Number of Questions	Average Normalized Gain <g>	Highest question gain <g>	Lowest question gain <g>
Chemistry	8	17.65%	50%	-60%
Geometry	2	50%	100%	0%
Materials	16	12.37%	44.44%	-100%
Total	26	14.66%	100%	-100%

Table 5 displays each category from the alpha MCI's normalized gain along with the highest and lowest individual question gain from that respective category

Finally, Table 6 shows the individual scores of the students from Group 3 listed along with the corresponding score received on the final exam. Following this is the statistical correlation between final exam score and student gain. All statistical calculations were done using the statistical package on the TI-83 graphing calculator, specifically the "LinRegTTest," and the "ANOVA" programs.

Student	Entrance Exam Score	Exit Exam Score	Students Gain <g>	Final Exam Score
S1	19.23%	46.15%	28%	90%
S2	23.07%	30.77%	8.33%	83%
S3	30.77%	42.31%	13.63%	70%
S4	30.77%	50.00%	22.72%	84%
S5	34.62%	42.31%	9.52%	82%
S6	42.31%	26.92%	-21.05%	75%
S7	46.15%	57.69%	16.67%	85%
S8	46.15%	42.31%	-5.56%	77%
S9	50.00%	69.23%	29.41%	82%

Table 6 displays each student from group 3's initial and final alpha MCI score, along with that students final exam score

Linear Regression		**ANOVA**	
Y =	78.4722 + .2139x	**MS_{factor} =**	21792.83
R^2 =	33.96%	**MS_{error} =**	149.951
R =	58.27%	**F =**	145.33
		$f_{.05,1,7}$ =	5.59

Table 7 displays the linear equation for the relationship between students gain and final exam score, where Y is the final exam score and X is the students gain. Also the R-value, along with the F ratio, was tested for significance of regression.

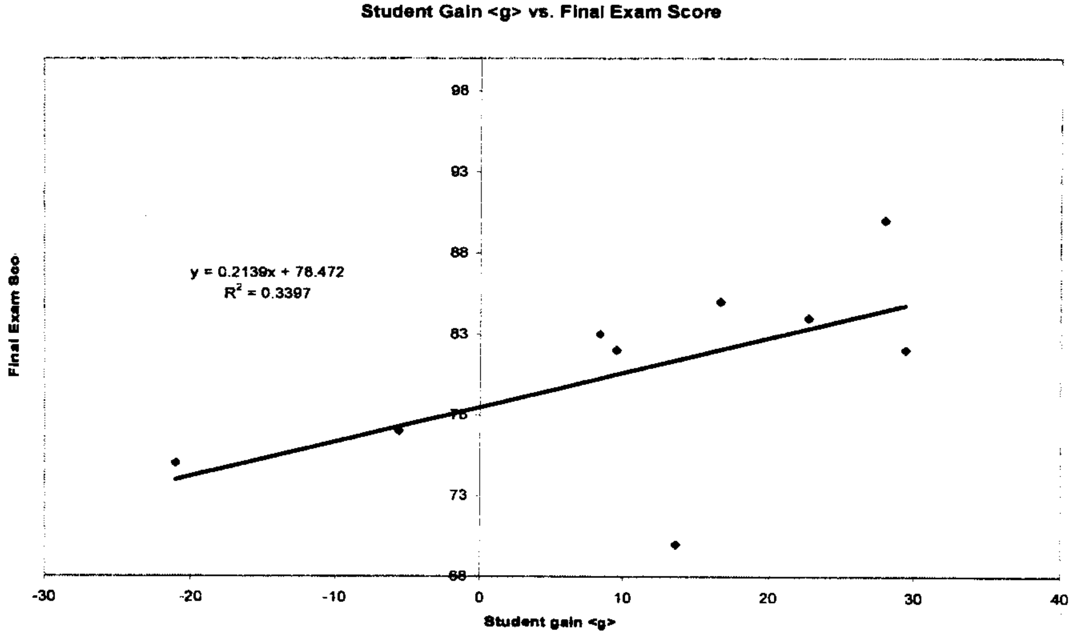

Figure 1 Shows the data points from the students' along with the predicted linear regression equation relating the students' gains on the alpha MCI to their final exam score, along with the R^2 value

Discussion

When the results of the alpha MCI are compared to a circuits phase concept inventory project by Lakdawala et al[8], we find surprising similarities. After a full semester of instruction, the students in both studies demonstrated only 45% - 50% knowledge of the concepts associated with the course. Also, both studies had similar standard deviations, or spreads, indicating a similar range of distribution scores. One of the main differences however, was that the alpha MCI test contained roughly 33% of prior knowledge questions, whereas the Lakdawala[8] et al alpha-circuits test had nearly

60% prior knowledge questions. This is probably the reason why the entrance exam scores by the materials students were nearly 10% lower than the circuits concepts inventory student scores. This difference in entrance exam scores can also be explained by the small differences in net gain by the students in both studies. Both classes ended up understanding generally the same fraction of concepts, yet one class seemed to have gained more knowledge.

The gain the students' knowledge in this study is relatively small compared to other research. According to Hake's[3], our gains indicated that the MCI gain fall into the "low-g" category, as its normalized gain was less then 0.3. Medium gain is 0.3 to 0.7 and high gain is greater than 0.7. Two of the possibilities for this "low-g" gain are, a) the course was not taught using a more student-centered, hands-on approach, using "Interactive Engagement" in teaching, and b) some of the test questions were too difficult for the students, as exemplified by one test question having a -100% gain, and others with large negative gains.

The two possibilities for the "low-g" score could also be related, based on the robust and groundbreaking physics education research by McDermott[9]. His findings established that, students answering similar questions, with one of qualitative nature and the other of a quantitative nature, got the quantitative question correct nearly seven times more frequently. This finding indicates that, because of the teaching method employed, students may have learned and studied more to answer the quantitative questions while paying less attention to the concepts behind them.

The results were examined to find if this was the case for the MCI by comparing the gains of Group 3 students to their final exam scores. The results show that there is a significant relationship between student gains and final exam scores but, as the R^2 value indicates, the linear relation is poor. The poor fit can, to some extent, be attributed to student S3 score, which is an outlier. After finishing the final exam, S3 reported immediately to the professor that he had suffered a "panic attack" during the test, thus partially explain his performance. When the S3 is removed from the fit, the R^2 value more then doubles to 72.41%.

This correlation results in some questionable conclusions. One is that, a student who gains no fundamental conceptual knowledge (as measured by the MCI) after completing the class, can still pass the class and get a high C. Even students who *lose* conceptual knowledge would still be able to get a C grade. An explanation for these conclusions is that the students perform better on quantitatively based questions than on the MCI qualitatively based questions. This would explain how students could do well on their final exams, but still have limited MCI gains.

Summary and Conclusions

An alpha version of a materials concept inventory test has been created for the field of materials science and engineering and tested an alpha version. To create the test, an extensive literature survey of current assessment tools in science, math, and engineering disciplines. A substantial program to solicit student feedback was initiated including weekly short answer and multiple choice quizzes as well as weekly interviews. Once the MCI was created it was administered to a summer session of the introductory materials course of 13 students. At the end of the summer session it was again administered to the 12 people still in the class. The data from these two tests were then assessed and reported in this paper.

Initial exam scores of 35.9% were 15.8% higher then a completely random distribution of 21.3%, and the exit exam scores were moderately higher at 45.3% correct. Exit exam results and their spread were similar to a comparable study by Lakdawala et al at Old Dominion, though gains were different because of the difference in initial scores, which was attributed to the fact that only roughly 33% of the questions were based on students' prior courses whereas Lakdawala[8] et al used approximately 60%. Next, results were compared to the extensive FCI study performed by Hake[3], where it was determined that our course would only be considered a "low-g" course because of the 14.7% gain from the semester. Hake[3] defines "low-g" as a gain of less then 0.3, medium gain as 0.3-0.7, and high gain as 0.7 and greater.

Finally, the correlation between MCI gain and final exam scores from the course was examined. Using a combination of statistical packages it was concluded that there *was* a linear correlation, but a poor one, 33.96%. After taking out one outlying score the fit more then doubled to 72.41%. It was still felt that the fit wasn't indicative of how students would perform because, the correlation seemed to suggest a student who made no gain after completing the course would still be able to pass the class and get a high C – 78% - on the final exam. This was attributed to the differences in teaching and testing methods employed, where the MCI understanding was of qualitative concepts whereas the final exam was more quantitative in nature. These findings were further supported by McDermott's[9] results which indicated that students do seven times better on quantitative versus qualitative questions. From these limited results it is suggested that an "Interactive Engagement," student-centered, teaching mode could increase conceptual knowledge of students. However, it is cautioned that this suggestion is based on limited data. There is a need for wider discussion and testing of the Materials Concepts Inventory.

Future actions

We are revising, and hopefully improving, the MCI by removing some questions and revising others in the alpha version. It was felt that some questions were either poorly stated or used mixed concepts. This was not fully realized until after the initial exam had been given, so they were left on the exit exam to keep a uniform test. However, these questions were not included in the results. After the revisions are complete, we plan to administer the MCI to a wider sample population of students in the fall semester of 2002. Further discussions with other faculty and increased data from beta testing will serve as a guide for future modification and validation of the MCI.

References

1. Hestenes, David, Wells, Malcolm, Swackhamer, and Gregg (1992). "Force concept inventory." *The Physics Teacher*, 30(3): 141-151
2. Hestenes, David, Wells, and Malcolm (1992). "A mechanics baseline test." *The Physics Teacher*, 30:159-166

3. Hake, Richard R (1998). "Interactive-engagement versus traditional methods: A six-thousand survey of mechanics test data for introductory physics courses." *American Journal of Physics* 66(Jan): 64-74
4. ABET (2001). "Criteria for Accrediting Engineering fields," Engineering Accreditation Commission
5. Thermodynamics Concept Inventory
6. Mechanical Concept Inventory
7. Integrated Physics and Chemistry Modeling Workshop, Arizona State University (2001) "Student Preconceptions and Misconceptions in Chemistry" http://www.daisley.net/hellevator/misconceptions/misconceptions.pdf, version 1.35
8. Lakdawala, Zahorian, Gonzalez, Kumar H., Leatherum Jr. (2002). "Proceedings of the 2002 American Society for Engineering Education Annual Conference & Exposition." American Society for Engineering Education
9. McDermott, L., (2001) "Physics Education Research: The key to student learning, Oersted Award Lecture," presented at the Winter 2001 Meeting of the American Association of Physics Teachers, http://www.phys.washington.edu/groups/peg/Oersted.pdf

USING MICROMECHANICS TO PROBE DAMAGE INITIATION IN COMPOSITES

Gale A. Holmes

and

W. G. McDonough

National Institute of Standards and Technology
Polymers Division
Gaithersburg, Maryland 20899-8543

Telephone 301-975-5280
e-mail holmes@enh.nist.gov

Gale A. Holmes

Using micromechanics to probe damage initiation in composites

G. A. Holmes and W. G. McDonough
National Institute of Standards and Technology, Polymers Division
Gaithersburg, Maryland 20899-8543

Abstract

Predicting the failure behavior of composite structures is an area of research that is growing in importance with the increased use of composites in structural applications. As a result, the development of computational models that predict damage accumulation in these anisotropic structures prior to failure has become a critical goal of this research area. To date, only phenomenological anisotropic damage models have been developed. However, the success of these models in reproducing experimentally observed composite failure behavior and recent theoretical advances by Phoenix on the chain-of-bundles modeling approach suggest that the development of a predictive damage accumulation model that uses input data from experimental data may be feasible.

This presentation will discuss the experimental methodologies that must be developed to provide input for such a model. In addition, experimental observations of factors that control the nucleation of critical flaws in unidirectional composites will be presented. Also, data showing how localized failure behavior changes with local changes in fiber volume fraction will be discussed.

KEYWORDS: Composite Materials, Failure Analysis, Fracture, Damage, Multi-fiber

---

1 Introduction

Damage accumulation and failure behavior are of critical importance when designing composite structures. From a design perspective, the strength prediction of a material and evolution of damage in the material when it is exposed to environmental conditions, temperature fluctuations, and mechanical stresses are critical parameters that must be quantified in order to predict its service life and usefulness. Unlike traditional materials, which are homogeneous, the multiphase and laminated structure of composites precludes the determination of damage evolution in a simplistic manner. It is generally accepted that a composite's strength, fracture toughness, and fatigue life are strongly influenced by local characteristics that cannot be integrated or averaged over the structure [1]. Hence, the major technical challenges to developing a predictive computational failure model for composites are (1) the identification of the critical micromechanics properties that control failure initiation and propagation, (2) the development of test methodologies for measuring these properties, and (3) the development of suitable mathematical expressions that incorporate these measured parameters in a macroscopic failure model.

Computational models almost exclusively use the chain-of-bundles modeling approach to incorporate micromechanics parameters into the prediction of composite failure behavior. These models attempt to predict a composite's strength and failure behavior (via, Monte Carlo simulations) by quantifying the magnitude of stress overload in adjacent fibers surrounding a fiber break and accounting for the fiber break configurations that arise at the microscopic level.

As an example, the 3-D chain-of-bundles model proposed by Phoenix [2] has the following general form for calculating the strength of a lamina, $H_{m,n}\{\sigma\}$:

$$H_{m,n}\{\sigma\} \approx 1 - \exp\left\{ -\left(\sigma \middle/ \sigma_{m,n}^{\{k^*\}} \right)^{k^* \rho} \right\}$$

Of particular interest in the above expression for the lamina strength is the dependence of the shape ($k^* \rho$) and scale parameters ($\sigma_{m,n}^{\{k^*\}}$) of the Weibull distribution function on the k^* variable. The explicit definition of these parameters and the explicit form of $\sigma_{m,n}^{\{k^*\}}$ can be found in the Phoenix article. Of particular interest in this discussion is the functional dependence of the k^* variable. For a particular composite, k^* reflects the number of adjacent fiber breaks that must exist before catastrophic failure of the composite occurs. Experimental data suggests that k^* is dependent on micromechanics type parameters.

As an example, Fuwa *et al.* [3] in 1975 changed the failure behavior of a unidirectional carbon fiber lamina from brittle to brush-like by undercuring the matrix. In 1991, Drzal's research group [4] altered the failure behavior of glass fiber composites by treating bare E-glass fiber with the industrial sizing agent γ-aminopropyl trialkoxysilane. The failure behavior changed from ductile to brittle with the introduction of the sizing agent. In addition, the interfacial shear strength (IFSS) was observed to increase by 25 % with the incorporation of the sizing agent. Noting that the microscopic failure behavior associated with fiber fracture changed from debonding only to debonding with matrix crack formation, he speculated that the observed macroscopic failure behavior changes were related to the changes observed at the microscopic level.

In related research, Holmes *et al.* [5] have shown, using self-assembled monolayer technology, that the IFSS can be reduced by 30 % by coating the glass fibers with mixtures of bonding and non-bonding silane coupling agents. However, unlike the change in microscopic failure behavior observed with the reduction in IFSS observed between glass fibers treated with γ-aminopropyl trialkoxysilane and bare glass fibers, no failure behavior change was observed when the IFSS is reduced by the incorporation of the non-bonding coupling agent. However, when the glass fiber is treated with 100 % non-bonding silane coupling agent the failure behavior associated with fiber fracture changes from debonding with matrix crack formation to debonding only. Depending on how the non-bonding silane coupling agent is deposited, the IFSS drops from 40 % (industrial deposition process) to 90 % (self assembled monolayer deposition process). These results suggest that the IFSS and toughness of the fiber-matrix interphase region are important factors in controlling failure initiation and propagation in fibrous composites.

A Weibull formulation has also been used with some success to model the complex failure behavior of composites subject to mechanical induced deformations [6]. Specifically, the stiffness reduction caused by the deformation is modeled using the Weibull formulation for the damage variable, ω. The expression for modeling the reduction in stiffness, E, in these models has the following form:

$$E\{\omega\} = (1-\omega)E = \left(\exp\left[-\left({}^{\varepsilon}\!/_{\varepsilon_o} \right)^m \right] \right) E$$

The use of the Weibull function in both expressions and the referenced experimental data suggests the possibility of incorporating micromechanics parameters in composite damage models. Definition of the remaining variables can be found in the referenced article.

The research results in this paper will focus on understanding how failure initiation occurs in unidirectional composites composed of glass fibers treated with an amine silane coupling agent. The spacing between fibers and hence their interaction will be controlled by using 2-D multi-fiber test specimens. Adhesion at the fiber-matrix interphase will be restricted to covalent bonding molecular forces by using self-assembled monolayer technology to deposit the amine silane-coupling agent and thereby eliminating contributions to adhesion by mechanical interlocking.

2 EXPERIMENTAL

2.1 Fiber-Preparation.

The E-glass fibers used in this investigation were coated with 11-aminoundecyl silane (11-AUS). This silane has the same functional group for bonding to epoxy resin as γ-aminopropyl trichlorosilane (γ-APTCS) and γ-aminopropyl trialkoxysilane (γ-APTAS), where the alkoxy group is most often methoxy (γ-APTMS) or ethoxy (γ-APTES). 11-AUS, γ-APTCS, and γ-APTMS were used in a larger study to quantify the mechanical response of the fiber interphase-matrix interphase interface to fiber fracture and covalent bonding. The synthesis of the relevant compounds can be found in that research [7].

A 30 cm long tow was cut from a spool of E-glass fibers (from Owens-Corning,* average fiber diameter of 15 μm) previously shown to be bare with no processing aids by X-ray photoelectron spectroscopy (XPS) [8]. The tow was washed with acetone (spectrophotometric grade) and vacuum-dried at 100 °C for 2 h and cooled prior to use. The washed E-glass fibers were coated with 11-bromoundecyl trichlorosilane (11-BrUTCS) by dissolving 0.3 % mass fraction of 11-BrUTCS into hexadecane. The acetone-cleaned fibers were immediately immersed in the silane solution. The vial was then placed in an oven and heated to (40 to 50) °C for (4 to 6) h. The coated fibers were then withdrawn from the solution and carefully rinsed with methylene chloride, followed by acetone.

The bromine groups on the 11-BrUTCS treated E-glass fibers were then converted to an azide group by placing the treated fibers in a supersaturated solution of NaN_3 in dry N,N-dimethylformamide (1.5 g in 100 ml) with continuous stirring. After 24 h the azide-terminated fibers were rinsed with distilled water and converted to amino-terminated fibers by placing the fibers for 24 h in a lithium aluminum hydride solution (0.2 mol/L in tetrahydrofuran). The amine-terminated fibers were then placed in a 5 % mass fraction of hydrochloric acid solution for 5 h to complete the hydrolysis of the aluminum complex. The fibers were then rinsed with distilled water, followed by acetone, and then placed in triethylamine for 24 h to convert the terminal $-NH_3^+$ groups into $-NH_2$ groups. The coated surfaces were then dried for 1 h.

2.2 Multi-Fiber Fragmentation Test (MFFT) Specimen Preparation

The molds for preparing single fiber fragmentation test (SFFT) specimens were made with silicon rubber (General Electric) following the procedure described by Drzal and Herrera-Franco [[9]]. All molds were post cured at 150 °C and rinsed with acetone prior to use.

E-glass filaments were then placed on a multi-fiber-positioner (MFP) originally described by Wagner and Steenbakkers [10]. Using the MFP, a planar array of eight fibers were placed within 3 fiber diameters of each other. The fibers were then aligned

---

* Certain commercial materials and equipment are identified in this paper to specify adequately the experimental procedure. In no case does such identification imply recommendation or endorsement by the National Institute of Standards and Technology, nor does it imply necessarily that the product is the best available for the purpose.

and suspended into the silicone molds. The fibers were temporarily fixed in place by pressing them onto double-stick tape. Small strips of double-stick tape were placed over each set of fiber ends to hold them in place until the fiber was permanently mounted with 5-min epoxy (see Figure 1).

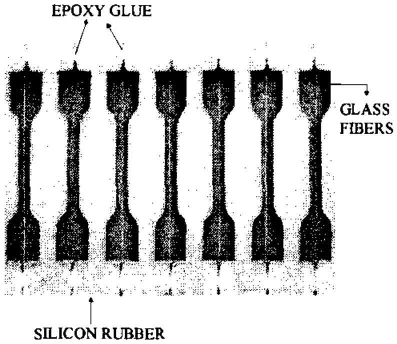

Figure 1. Molds for preparing MFFT specimens.

The MFFT specimens were prepared with an epoxy (diglycidyl ether of bisphenol A, DGEBA, Epon 828, Shell) cured using meta-phenylenediamine (m-PDA, Fluka Chemical). One hundred grams of DGEBA and 14.5 g of m-PDA were weighed out in separate beakers. To lower the viscosity of the resin and melt the m-PDA crystals, both beakers were placed in a vacuum oven (Fisher Scientific Isotemp Vacuum Oven, model 281 A) set at 65 °C. After the m-PDA crystals were completely melted, the silicone rubber mold containing the fibers were placed into another vacuum oven (Fisher Scientific Isotemp Vacuum Oven, model 281 B) that was preheated to 75 °C at –20 kPa, for 20 min. This last procedure dries the mold and minimizes the formation of air bubbles during the curing process. Approximately 9 min before the preheated molds were removed from the oven, the m-PDA is poured into the DGEBA and mixed thoroughly. The mixture was placed into the vacuum oven and degassed for approximately 7 min. After 20 min, the preheated molds were removed from the oven and filled with the DGEBA/m-PDA resin mixture using 10 ml disposable syringes. The filled molds were then placed into a programmable oven (Blue M, General Signal, model MP-256-1, GOP). A cure cycle of 2 h at 75 °C followed by 2 h of post curing at 125 °C was used.

2.3 MFFT Apparatus

The fiber fragmentation tests were carried out on a small hand operated loading frame similar to that described by Drzal [9] mounted on a Nikon Optiphot polarizing microscope (see Figure 2). The image was viewed using a CCD camera (Optronics LX-450 RGB Remote-Head microscope camera) and monitor (Sony, PVM-1344Q). Before the test, the fiber diameter was measured with an optical micrometer (VIA-100 from Boeckeler) attached to the video system. The sample was scanned by translating the loading frame under the microscope with a micrometer. The position of the load frame is monitored by an linear variable differential transformer (LVDT) (Trans-Tek, Inc. model 1002-0012) connected to an A-to-D board (Strawberry Tree, Inc.) in a computer. To measure fragment lengths or other points of interest in the sample, the location was aligned with a cross hair in the microscope as seen on the video monitor, and the position of the LVDT was digitized into the computer. The standard uncertainty in relocating a point reproducibly is ± 1.1 μm. The load is also monitored during the experiment using a 2,224 N (500 pounds) load cell connected to a bridge (load cell and AED 9001A bridge, Cooper Instruments). The expected standard uncertainty of the load measurements is 3 % of the load. The bridge is attached to the same computer via a serial connection. A custom program was developed to continuously record changes in the load and displacement.

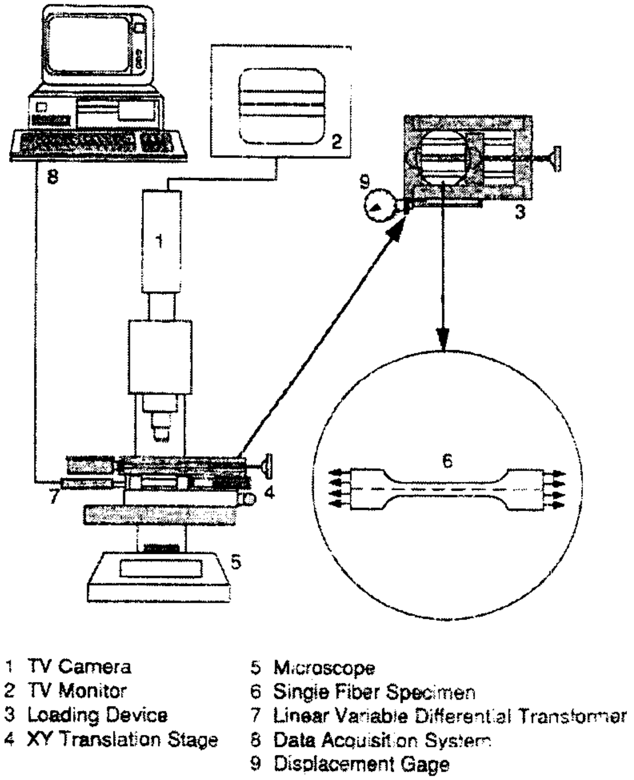

Figure 2. Schematic of Multi Fiber Fragmentation Test Machine

2.4 MFFT Testing Protocol

The MFFT specimen was loaded in tension by the sequential application of step-strains. The average application time of each strain step was (1.1 ± 0.2) s and the average deformation was (14.5 ± 3.1) μm, where the number after the "±" sign represents one standard deviation about the mean value. The delay time between the application of successive step-strains was 10 min [8].

3 Results and Discussion

3.1 Fiber-Fiber interactions between non-touching fibers

In the fracture pattern shown in Figure 3, all fiber breaks are non-aligned (not vertically aligned), even though the fibers are spaced 2 to 4 fiber diameters apart. These staggered breaks are similar to the fracture patterns investigated computationally by Sastry and Phoenix (see Figures 6 and 9 in reference [11]).

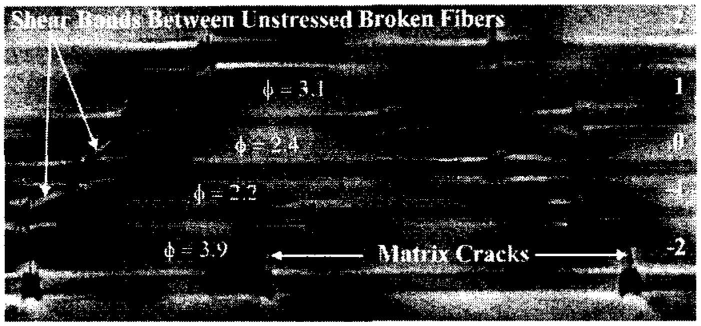

Figure 3. Optical micrograph using crossed polarizers of fiber break (seen as dark regions in fibers) patterns from E-glass/DGEBA/m-PDA 2-D multi-fiber array 24 h after removing stress. The interfiber spacing is denoted by ϕ. Fiber numbers (right side of figure) conform to the convention used by Sastry and Phoenix research (references [11] and [12]).

In Figure 3, the non-aligned breaks appear to be located approximately 45° from the adjacent break. In connection with these non-aligned breaks intense shear bands are located in the matrix between the fiber breaks. These shear bands persists long after the stress in the viscoelastic matrix relaxes. Data taken during the test, where the specimen is under tension, also indicates the existence of these shear bands between the tip of the matrix cracks (see Figure 4). In an attempt to clearly show the shear bands emanating from the crack-tips the {2} fiber is not shown in Figure 4.

At present, we speculate that the origin of these shear bands resides in the fact that the matrix cracks are essentially penny shaped cracks [13]. It is known that penny shaped cracks subjected to uniaxial tensile loads generate 45° deformation shear bands that form relative to the tensile axis at the crack-tip. The deformation bands emanating from the crack tips in Figure 4 may be related to this phenomenon. The influence of these bands on fracture initiation in the adjacent fiber is not currently known. However, the occurrence of three non-aligned fiber break clusters with identical shapes in the top three fibers in Figure 4 may reflect a deflection of the stress concentration factor in the adjacent fiber fragments in a manner different than that described by Hedgepeth and van Dyke [14]. Hedgepeth and van Dyke assumed composite failure to occur by a single, perfect transverse line of fiber breaks caused by the increased probability of failure in the region of the adjacent fiber directly across from the initial fiber break (overstressed region).

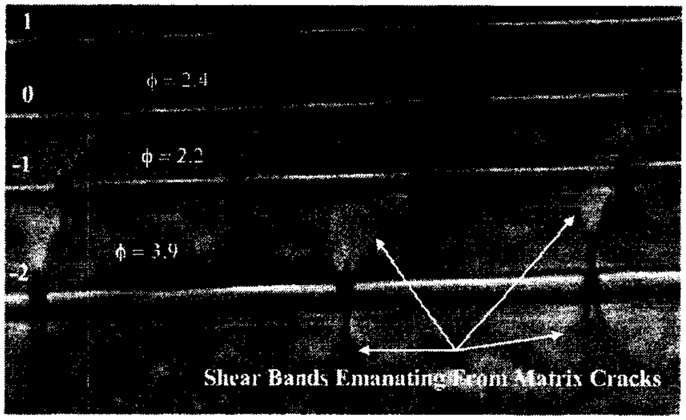

Figure 4. Optical micrograph of fiber break (seen as dark regions in fibers) patterns from E-glass/DGEBA/m-PDA 2-D multi-fiber array (stressed). The interfiber spacing is denoted by ϕ. Fiber numbers (left side of figure) conform to Sastry and Phoenix research (references [11] and [12]). The {2} fiber is not shown.

3.2 Fracture surface caused by matrix cracks

In Figure 5, the critical flaw generated by the fracture of fiber 3 interacts with a preexisting matrix crack that was generated prior to complete failure of the specimen by the fracture of the −1 or −2 fiber or both. Observe that the matrix crack is non-symmetrical, suggesting that a surface flaw may have caused the failure of the −1 or −2 fiber. Optical measurements indicate that the plane of the preexisting matrix crack and the critical flaw differ by less than 1 fiber diameter. The presence of the preexisting matrix crack suggests that the critical flaw is generated by the coalescence of matrix cracks rather the growth of preexisting matrix cracks.

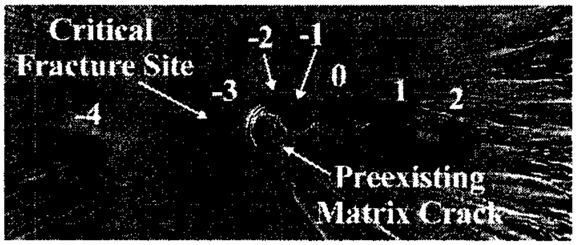

Figure 5. Close-up view of fracture surface from multi-fiber test specimen. The fibers are numbered according to the convention adopted by Sastry and Phoenix ([12]), with only 7 of the 8 fibers shown.

3.3 Fiber-Fiber interactions between touching fibers

Figure 6 shows the interaction between touching fibers such as those typically found in high fiber volume fraction composites. Although matrix crack formation has been suppressed, there are two instances where the energy released by the fractured fiber has caused the adjacent fiber to fragment. These fiber breaks are labeled as fiber breaks with no fiber-matrix debonding and are barely visible in the unstressed state.

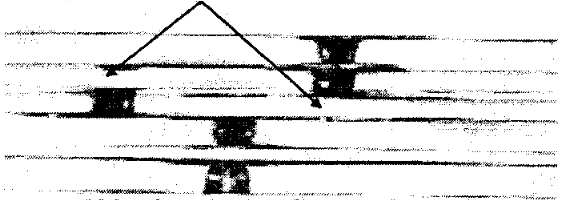

Fiber breaks with no fiber-matrix debonding - unstressed

150 micrometers distance between asymmetric pair of fiber breaks.

Figure 6. Unstressed optical image of fiber break (seen as dark regions in fibers) pattern from E-glass/DGEBA/m-PDA 2-D multi-fiber array with fibers closely spaced.

In Figure 7, the specimen was restressed to clearly show the existence of the fiber breaks. The impact of these closely spaced breaks on critical flaw initiation must still be determined.

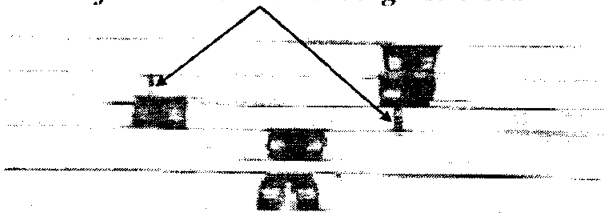

Fiber breaks with no fiber-matrix debonding - stressed

Figure 7. Stressed optical image of fiber break (seen as dark regions in fibers) pattern from E-glass/DGEBA/m-PDA 2-D multi-fiber array with fibers closely spaced.

4 Conclusions

Imaging results on the model composites of DGEBA/m—PDA resin and E-glass fiber coated with alkylamine silanes indicate that matrix cracks do not grow to a critical flaw size but coalesce with existing matrix cracks to form critical flaws. In regions of high fiber volume fraction, matrix crack formation is suppressed. However, the close proximity of the fibers and the dynamics of the fiber-fracture process can induce failure of adjacent fibers. These results suggests that the k^* variable used by Phoenix in the chain-of-bundles model may have a functional dependence on interfiber spacing.

5 References

[1] Daniel, I. M. and Ishai, O., Engineering Mechanics of Composite Materials, (Oxford University Press, Inc., 1994)

[2] Smith, R. L., Phoenix, S. L., Greenfield, M. R., Henstenburg, R. B., and Pitt, R. E., Proc. Royal Soc. London Series A - Mathematical Physical and Engineering Sciences, **388**, 353 (1983).

[3] Fuwa, M., Bunsell, A. R., and Harris, B., J. Mater. Sci, **10**, 2062 (1975).

[4] Drown, E. K., Al Moussawi, H., and Drzal, L. T., Journal of Adhesion Science and Technology, **5**, 865 (1991).

[5] Holmes, G. A., Feresenbet, E., and Raghavan, D., Proceedings of the 24th Annual Meeting of the Adhesion Society, 2001, p. 62.

[6] Agaram, V., Bilkhu, S., Fidan, S., Botkin, M. E., and Johnson, N. L., Proceedings of the Advanced Composites Conference and Exhibition, 1997, p. 181.

[7] Holmes, G. A., Feresenbet, E., and Raghavan, D., Composite Interfaces, (2002).

[8] Holmes, G. A., Peterson, R. C., Hunston, D. L., and McDonough, W. G., Polymer Composites, 21, 450 (2000).

[9] Herrera-Franco, P. J. and Drzal, L. T., Composites, 23, 2 (1992).

[10] Wagner, H. D. and Steenbakkers, L. W., J. Mater. Sci., **24**, 3956 (1989).

[11] Sastry, A. M. and Phoenix, S. L., SAMPE J., **30**, 61 (1994).

[12] Sastry, A. M. and Phoenix, S. L., J. Mat. Sci. Lett., **12**, 1596 (1993).

[13] Anderson, T. L., Fracture Mechanics: Fundamentals and Applications, 1st. Ed., (CRC Press, Inc., Boca Raton, Florida, 1991), p. 308.

[14] Hedgepeth, J. M. and van Dyke, P., J. Comp. Mat., **1**, 294 (1967).

DISCOVERING THE SOURCE OF PROPERTIES IN ALLOYS: METALLOGRAPHIC EXAMINATION

David V. Niebuhr

Assistant Professor of Materials Engineering
California Polytechnic State University
San Luis Obispo, CA 93407

Telephone 805-756-7163
e-mail dniebuhr@calpoly.edu

David V. Niebuhr

Discovering the Source of Properties in Alloys: Metallographic Examination

David V. Niebuhr
Assistant Professor of Materials Engineering
California Polytechnic State University
San Luis Obispo, CA

Key Words: Metallography, microstructure, optical microscopy, ferrous alloys, non-ferrous alloys

Prerequisite Knowledge: Understanding of basic chemistry, introductory materials science (crystallography, light microscopy, phase diagrams, etc.) and a strong problem solving ability.

Objective: This laboratory exercise will relate how microstructures determine the physical and mechanical properties of metals. Common engineering structures are used to show how materials are relevant and important to everyday life.

Equipment:

The lab can be performed using the pictures included in this write-up. The much better alternative is to obtain samples similar to those listed and create metallographic mounts. Therefore the required components include: a light microscope, filar eyepiece, ruler, calculator and the following samples:

1. Steel reinforcing bar
2. High strength steel bolt
3. Carburized gear tooth w/ pearlitic structure
4. Carburized gear tooth w/ martensitic structure
5. Carburized gear tooth w/ decarburized surface structure
6. Gray cast iron
7. Nodular cast iron
8. Thermal sprayed coating (any source)
9. Electrolytic tough pitch copper
10. Titanium 6Al 4V compressor blade
11. Single crystal turbine blade (or 718 nickel alloy)

It is noted that some of these samples may be difficult to obtain, in which case the material should be obtained and the function of the component explained in generic terms. This list can also be edited (reduced) without adversely affecting the lab as a whole.

Introduction:

"Structure determines properties," is a common saying in our introductory course in materials engineering. Students are introduced to the idea that all materials have a microstructure and that these structures can be simple or very complex. The goal of this experiment is to observe common engineering materials and to deduce the properties that are a result of the microstructures.

Using the light microscope you will observe 11 metallic samples. Each sample has been polished and etched (with a chemical) to make its microstructure observable. From looking at the microstructure you will be able to characterize the materials. Using your newfound knowledge of materials engineering and some deductive reasoning answer the questions listed in the lab. It may help to read through the whole lab and to observe all the specimens before attempting to answer the questions.

(One of the goals of the lab is to integrate knowledge and apply a knowledge base to explain and characterize different materials. I have attempted to make the questions general enough that most 2nd year engineering students can answer them.)

Procedure:

Image each of the samples under the light microscope (or observe the micrographs included in this text). Adjust the focus and light intensity to obtain a clear image. Be sure you are looking at the sample and not the medium in which it is mounted. After observing the microstructure answer the questions. The answers will be found in the lab text and through your own application of basic engineering principles.

I. Ferrous Alloys

Steel

For many engineering applications steel is the number one material for the job. Steel is so popular because the properties can vary so widely depending on alloy content and heat treatment. Steel can be hard and brittle or soft and ductile and anywhere in between. The name 'steel' implies a mixture of iron with other elements. Iron exists in two allotropic forms: body centered cubic (BCC) at temperatures up to 727°C and face centered cubic (FCC) from 727°C to 1200°C. The ability of iron to exist as two different structures is what makes it such a versatile material. Unalloyed iron is very soft and ductile, having a tensile strength of only 15 ksi whereas a 4340 alloy steel can have a tensile strength exceeding 200 ksi!

The principal alloying element is carbon. Carbon is an interstitial element, which means it exists in the spaces between the much larger iron atoms. The interstitial atoms include B, O, N, C, and H. Of these 5, carbon is the most valuable and universally associated with steel. Carbon is only soluble up to 0.02 wt.% in BCC iron but can be dissolved in amounts up to 2% in FCC iron. Because carbon is virtually insoluable in BCC iron it forms a separate phase. This phase is known as *cementite* and has a composition of Fe_3C. Cementite is hard and brittle. *Ferrite* or alpha iron are the names given to bcc iron and can be used interchangeably. *The distribution, size and quantity of the cementite phase in bcc (alpha) iron determines the mechanical properties.* There are also several substitutional elements that are added to steel to improve its strength and toughness. These include but are not limited to Ni, Cr, Mo, V, and Mn. Strength can be thought of as the amount of force required to fracture the steel whereas toughness is the amount of energy absorbed by the material during fracture.

The phases or microstructure present at room temperature depend on the alloy composition and cooling rate. To heat treat steel we first heat it above the transformation temperature, to around 830°C. At this high temperature the iron reverts back to FCC and the alloying elements go into solution. This FCC phase of steel is known as *austenite*. In plain carbon steels and most alloy steels austenite is unstable below 727°C. The cooling rate will determine the structure the austenite transforms into. For simplicity we will focus on two cooling rates: slow cooling in air and rapid cooling in water.

If we cool slowly the carbon will be rejected from the ferrite as it transforms from austenite (Figure 2). Carbon will segregate to form alternating layers or lamellae of the two phases: ferrite and Fe_3C. This microstructure is known as *pearlite*. **Sample 1** is a reinforcing bar that is used in concrete structures. Look at the sample and notice the islands of pearlite (dark) surrounded by ferrite (light). If you look closely you can see the lamellar structure. (Questions 1 & 2) Eutectoid steels (0.8% C) are often used for railroad tracks. The structure is 100% pearlite (as predicted from the Fe – Fe_3C phase diagram). Pearlite is chosen because it is neither too hard (must resist fatigue cracking) nor too soft (must resist deformation from high loading). (Question 3)

Now lets consider water quenching our austenite. If we quench our sample in water the carbon does not have time to diffuse. Rather carbon is trapped in the lattice as it transforms from FCC to BCC. The carbon's inability to diffuse causes a distortion in the lattice and the resultant structure is body centered tetragonal. This diffusionless transformation of iron into a single phase is the martensite reaction and the product is *martensite*. Martensite is very hard (up to 65 Rc) and brittle. As-quenched martensite has very few engineering applications. If however we *temper* the martensite we can regain toughness with only a small loss in strength. Tempering involves heating the martensite to around 500°C for 20 minutes or so. This allows for the diffusion of carbon and an overall relaxation of the lattice. The resulting structure is a fine dispersion of carbide in ferrite and is known as *tempered martensite*. **Sample 2** is a high strength aircraft bolt. It is composed of 4340 steel in the quenched and tempered condition. 4340 is a very hardenable steel in that water quenching is not required to obtain martensite. (Question 4). In general alloy steels can form martensite at slower cooling rates than plain carbon steels.

Sample 3 is a gear tooth from a machine. The function of a gear is to transmit force in an efficient way. (Question 5) Gears are generally made from low carbon or alloy steel (Carbon = 0.10 %- 0.25%). Typical grades include 1018, 1117 and 8620. The surface of the gear is hardened by the addition of carbon, this is known as case-hardening. The case has a thickness of 250 μm to over 1 mm and can have a structure of martensite or pearlite depending on the cooling rate. Sample 3 was slow cooled following the carburizing process. The core of the gear is pearlite and ferrite. Case hardening is achieved by heating the gear to a high temperature (800°C and higher) in a reducing atmosphere of CO and H_2. This allows carbon to diffuse into the lattice, which is FCC at this temperature. Recall that FCC has a much higher solubility limit of carbon than BCC. A generic carburizing reaction is $CO + H_2 \leftrightarrow \underline{C} + H_2O$ where $\underline{C}$ denotes carbon in solution. Other gasses can be used as a source of carbon (methane, propane, etc.). (Question 6) **Sample 4** is a gear tooth that also underwent a carburizing process but was water quenched following diffusion of C. Look at the structure of the sample and how it differs from Sample 3. (Question 7) **Sample 5** is another machine component that was case hardened. This component was exposed to air at temperatures exceeding 500°C. The structure has changed and as a result is more inclined to wear under sliding contact conditions. (Question 8)

Cast Iron

To this point we have discussed steel, which is an iron alloy which contained less than 1.2 % carbon. If we now increase the carbon content to between 2 and 4 % we create a new structure called *cast iron*. As the name implies they are intended to be cast into the desired shape rather than being worked in the solid state. Cast irons are used for thousands of engineering applications. There are several types of cast iron, which are created by varying heat treatment and alloying elements. **Sample 6** came from the block of a 350 Chevrolet engine. Look at the microstructure and notice that carbon is present in the form of graphite flakes. This type of cast iron is denoted *gray cast iron* and contains silicon to promote the formation of graphite as opposed to iron carbide (Fe_3C). (Fe_3C is considered a metastable phase of carbon, the true equilibrium phase of carbon is graphite) The sample has been prepared so that half is as-polished and half is etched. The as-polished half appears as graphite flakes in a white matrix. When we etch the sample with 2% nitric acid the pearlite matrix is exposed. If you look close you can see the lamellar structure of the pearlite. (Question 9)

The brittle nature of gray cast iron lead to the development of *nodular* or *ductile cast iron*. By adding small amounts of magnesium or cerium to the molten cast iron favorable nucleation sites are created. These nucleation sites allow the graphite to precipitate into a spherical shape. **Sample 7** is a part of an automotive crankshaft, it consists of graphite spheres in a matrix of pearlite and ferrite. The spheres of graphite give the ductile iron greater strength and toughness. The tensile strength of this sample is around 80 ksi as compared to 35 ksi for the gray cast iron. Depending on the heat treatment tensile strengths of up to 120 ksi can be achieved. (Question 10) The production of ductile iron has seen a steady increase in recent years whereas gray cast iron production is on a steep decline.

Plasma Sprayed Coatings

Plasma spraying is a process for creating unique coatings which may otherwise be difficult to produce. In this process a gas (usually N_2 and H_2) is ionized by a large power input (100-200 kW). The result is a plasma which consists of electron-stripped ions and a large current flow (300-400 amps) (Figure 1). The resulting plasma has a temperature of 6000° C to 20,000° C and travels at speeds exceeding Mach 1. Metal or ceramic powders are injected into the gas stream (commonly referred to as the *plume*) and accelerated toward the surface to be coated. The molten particles build up the coating one 'splat' at a time. The plume temperature is controlled by the applied voltage and by the gas flow rate. Plasma spraying can be done in ambient conditions or in an inert atmosphere to prevent oxidation of the molten particle (Question 11). **Sample 8** is a coating of Fe and Cr sprayed in ambient conditions. The coating consists of iron and chrome 'splats' plus a certain volume of oxidized metal and porosity. Porosity is minimized with optimized plume conditions (not too hot or cold). The coating is used to prevent abrasive and erosive wear in paper making machinery. The coating must survive a sulphuric acid environment plus impingement of abrasive particles (Question 12).

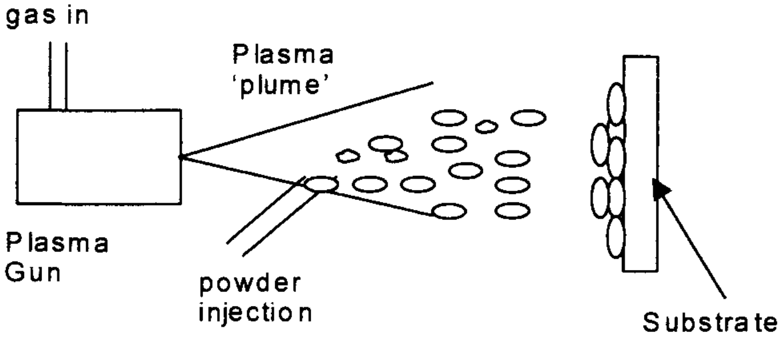

Figure 1. Schematic of plasma spray system

II. Non-ferrous alloys

ETP Copper

Unalloyed copper is an important engineering metal. Because of its high electrical conductivity it is used extensively in the electronics industry. Copper also has excellent resistance to corrosion and high ductility, which allows for very fine wire to be created. Electrolytic tough pitch (ETP) copper is 99.9% pure. The remaining impurity is mainly oxygen. **Sample 9** shows the structure of ETP copper. Oxygen is almost insoluable in copper. When the copper is cast the oxygen combines to form a Cu_2O eutectic compound. The eutectic composition has the lowest melting temperature thus, it is the last to solidify. The Cu_2O segregates to the grain boundaries upon solidification. When copper is etched the oxides are revealed. The black areas are porosity, which is revealed by going in and out of focus while observing the microstructure. Oxygen free copper would appear all white under the microscope as no phase would be present to 'decorate' the grain boundaries (Question 13). Oxygen free copper is more expensive but has a higher electrical conductivity than ETP copper.

Titanium 6Al 4V

Titanium is also a very important engineering material. Titanium has been recognized as an element for 200 years, but only in the last 50 years has the metal gained strategic importance. Titanium has wide spread uses ranging from chemical processing equipment to surgical implants and prosthetic devices. However, aerospace applications, including structural components and jet engines, still account for the largest share of titanium alloy use.

Titanium, like iron, is an allotropic material. This means that it exists as two different crystal structures depending on temperature. From room temperature up to 883°C the structure is hexagonal close packed (HCP) and is denoted as *alpha.* Above 883°C the structure transforms to BCC and is denoted as *beta.* Alloying elements can be added that change the transformation temperature or even make beta iron stable at room temperature. This ability to manipulate the crystal structure gives titanium tremendous versatility. Complex variations in microstructure are possible. This yields a wide range of properties where yield strength can range from 70 ksi to 250 ksi! This is strength comparable to alloy steel but with only 60% the density.

A jet engine in the modern commercial airplane is quite an engineering marvel (Figure 2). **Sample 10** is a compressor blade from a jet engine. Figure 3 is a cross section of a modern jet engine. Notice the compressor blades are on the front or 'cool' side of the engine. The compressor blades guide air into the combustion chamber or 'burner can' where fuel is injected and ignited. This creates a stream of hot compressed gas which turns the turbine blades and then exits the rear of the engine. The titanium alloy contains 6% aluminum and 4% vanadium. The aluminum stabilizes the alpha phase and adds ductility and reduces density. Vanadium stabilizes the beta phase allowing it to exist at room temperature. Observe the microstructure, the white slightly elongated grains are α phase while the darker grains are equiaxed β phase. This combination of alpha and beta yields a tensile strength of 160 ksi. The compressor blades must endure thousands of hours of centrifugal forces and various foreign object impingement (hail, gravel, birds). (Question 14 & 15)

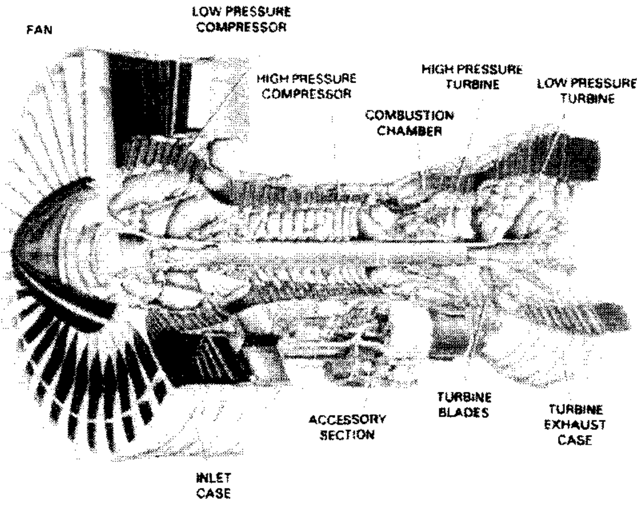

Figure 2. Cross-section of a 94 inch fan blade Pratt and Whitney 4000 axial flow turbine jet engine. (*Courtesy of Pratt & Whitney*)

Nickel alloy

Nickel based super alloys are used in high temperature environments. Nickel, unlike steel, maintains its strength to temperatures exceeding 2000° F and has excellent resistance to corrosion. Steel on the other hand has very little strength at temperatures above 1000°F and poor corrosion resistance. **Sample 11** is a turbine blade from a jet engine. Recall that the turbine blades rotate as a result of hot compressed gasses. The turbine blades rotate at several thousand RPM, so they must endure both high temperature (2000° F) and centrifugal forces. Commercial aviation fuel contains sulfur, which is corrosive to nickel at elevated temperatures. To improve the corrosion resistance of the nickel the surface is alloyed with aluminum to form a nickel-aluminum intermetallic compound. Even with this protective coating some turbine blades will fail due to hot corrosion. Sample 11 was removed during a routine engine rebuilding and did not fail in service. (Question 16)

Creep is the phenomena of deformation at elevated temperatures. There will be some increase in the size of the turbine blade due to thermal expansion, which is accounted for. Nickel is resistant to creep thanks to second phase particles that prevent grain boundary sliding. In order to maintain long term creep resistance the nickel is cast into a single crystal. Certain directions i.e. <110>, <001>, etc. have higher strength and resistance to deformation because of the way the atoms are arranged. Recall that polycrystalline materials are for the most part isotropic, (meaning they have similar properties in all directions) this is due to the fact that the grains are oriented in different directions and the net result is an averaging of the properties. By using a single crystal the direction of greatest strength can be grown and oriented in the direction of greatest stress. (Question 17)

Nickel is a very versatile metal, but it is expensive which limits its applications to those that can justify the expenditure.

You have now completed the lab! You should have found all the answers or deduced them from your engineering background. From looking at the different microstructures you can see how diverse metals can be. The one common theme that must be remembered is that *structure determines properties*.

Question Sheet

1. Estimate the % pearlite in sample 1 and then determine the total carbon content.
2. Given that pearlite consists of ferrite and Fe_3C what type of mechanical properties would you expect (i.e. low strength, brittle, ductile, etc.)?
3. Name the other major reason why a rail steel must have a minimum hardness (Rc =30) (it can't be too soft)
4. What is the difference between hardness and hardenability?
5. What properties are important in a gear that would justify the expense of case hardening?
6. For samples 3 and 4 measure the carburization depth using the filar eyepiece. For sample 5 measure the depleted region.
7. How does the microstructure of the case in Sample 4 differ from that of Sample 3? What is the advantage of having said microstructure in Sample 4?
8. What has happened to sample 5? What is different about its microstructure and why did it occur?
9. From looking at the microstructure of cast iron speculate as to why it fractures in a brittle manner.
10. How could the matrix of the ductile iron be altered to attain even greater strength (Think microstructure as a function of heat treatment)?
11. Describe the coating microstructure. What is the nominal thickness?
12. How might the plasma spray process be used in the repair of worn parts? (This process is very common in the aircraft industry)
13. How does the presence of oxygen affect the electrical conductivity of copper? Why?
14. What type of properties would be important for a jet engine component?
15. Titanium alloys are said to be notch sensitive. What does this mean?
16. Measure the thickness of the aluminum/nickel coating.
17. What is missing in the microstructure of the single crystal turbine blade that was present in the other samples?

Answer Sheet

1. Estimate the % pearlite in sample 1 and then determine the total carbon content.

   There is roughly 50% pearlite in the microstructure. Carbon content is therefore 0.50 x 0.8 wt% C in pearlite, which equates to 0.4 wt.% total carbon in the steel. Therefore the rebar sample is probably a 1040 steel.

2. Given that pearlite consists of ferrite and Fe_3C what type of mechanical properties would you expect (i.e. low strength, brittle, ductile, etc.)?

   Pearlite can be thought of as a composite which derives its strength from both the ductile ferrite (matrix) and hard, brittle cementite (hardener). The net properties consist of moderate strength (100 ksi yield strength), good ductility (elongation = 20-30%) and good toughness and wear resistance.

3. Name the other major reason why a rail steel must have a minimum hardness (Rc =30) (it can't be too soft)

   The rail must resist sliding (abrasive) wear from the wheel. In general greater hardness equates to greater wear resistance. If the rail is too hard however, there will be greater susceptibility to rolling contact fatigue. Thus a balance is achieved by utilizing 100% pearlite.

4. What is the difference between hardness and hardenability?

   Hardness is a mechanical property that measures a material's ability to resist deformation. Hardness is proportional to tensile strength in most cases. Hardenabilty is the ease at which martensite forms during the cooling process. A 1020 steel has low hardenabilty because even water quenching will not produce 100% martensite whereas a 1-2 inch thick 4340 steel will form martensite when air cooled.

5. What properties are important in a gear that would justify the expense of case hardening?

   A gear needs to be tough but wear resistant. By carburizing the surface a hard, brittle structure is created. The high hardness equates to high sliding wear resistance. The majority of the gear is a pearlitic structure, which has good toughness (resistance to fracture) and machinabilty.

6. For samples 3 and 4 measure the carburization depth using the filar eyepiece. For sample 5 measure the depleted region.

   The values will vary depending on the samples.

7. How does the microstructure of the case in Sample 4 differ from that of Sample 3? What is the advantage of having said microstructure in Sample 4?

   Sample 3 was slow cooled after carburization resulting in a pearlitic matrix. Sample 4 was quenched in water following carburization, which formed a high carbon martensite. Martensite is much harder than pearlite and will be a more wear resistant structure.

8. What has happened to sample 5? What is different about its microstructure and why did it occur?

   Sample 5 was exposed to an oxidizing atmosphere at an elevated temperature. The result is decarburization. Carbon in solution diffused and formed CO or CO_2 *and left the system. The resulting structure is soft, ductile ferrite. Wear resistance will be severally reduced.*

9. From looking at the microstructure of cast iron speculate as to why it fractures in a brittle manner.

   The cast iron contains a large volume of graphite flakes. Graphite being very brittle is a non-load bearing structure and will act as a site for crack initiation. The shape of the flakes creates stress risers, which exacerbate the overall brittle nature of the material.

10. How could the matrix of the ductile iron be altered to attain even greater strength (Think microstructure as a function of heat treatment)?

    Upon solidification the graphite will form as spheres in a matrix of austenite. The austenite will transform into pearlite, bainite, or martensite depending on cooling rate. A matrix of bainite would provide higher strength than pearlite. (You may want to mention austempering at this point) Austempering is performed by quenching the cast iron to a temperature just above the martensite start temperature and holding. The transformed structure is a mixture of austenite and ferrite, dubbed 'ausferrite.' Ausferrite has toughness and strength comparable to cast steel.

11. Describe the coating microstructure. What is the nominal thickness?

    The structure consists of 'splats' of metal and oxide layers (gray regions). The coating is built up one splat at a time and can be thought of as a composite of metal and metal oxide. The coating thickness will depend on the sample.

12. How might the plasma spray process be used in the repair of worn parts? (This process is very common in the aircraft industry)

    Components that have worn and are outside of tolerance can be built up again by the thermal spray process. Using powder or wire feed stock of the parent material the component is coated and then machined or ground to final dimension. This process is much less expensive than total replacement of the component.

13. How does the presence of oxygen affect the electrical conductivity of copper? Why?

    Oxygen reduces the conductivity by forming copper oxides (Cu_2O). The copper oxides cause a discontinuity in the lattice, which scatters electrons. In general any impurity added to a pure metal will reduce the electrical conductivity.

14. What type of properties would be important for a jet engine component?

    A jet engine component needs to be light weight, strong, tough, and corrosion resistant. Price and ease of manufacture are also considerations.

15. Titanium alloys are said to be notch sensitive. What does this mean?

    Notch sensitivity occurs when small surface discontinuities or changes in geometry allow fracture at stresses considerably lower than what would be predicted in a tensile test of a near perfect sample. For this reason surface finish is very important and care is taken to avoid designs which have inherent stress concentrations.

16. Measure the thickness of the aluminum/nickel coating.

    The coating thickness will vary depending on the sample.

17. What is missing in the microstructure of the single crystal turbine blade that was present in the other samples?

    There are no grain boundaries as the sample is a single grain.

Appendix

Photomicrographs of the samples

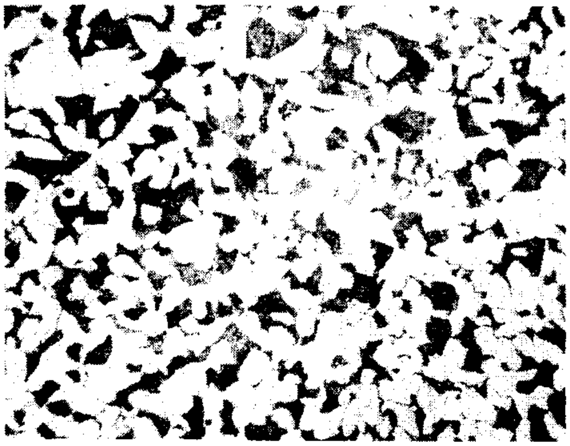

Sample 1. Steel reinforcing bar, 400x, Nital etch.

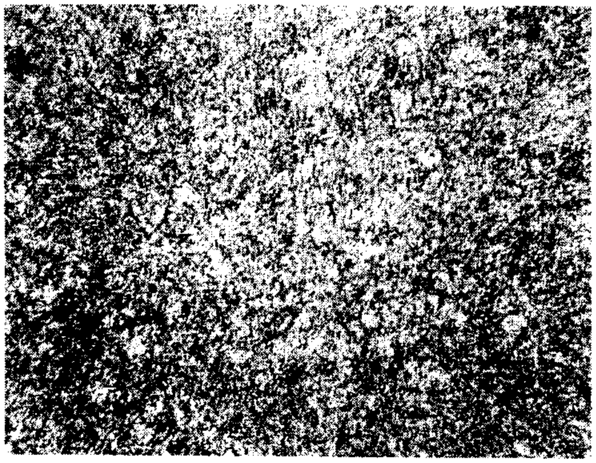

Sample 2. High strength bolt, 400x, Nital etch

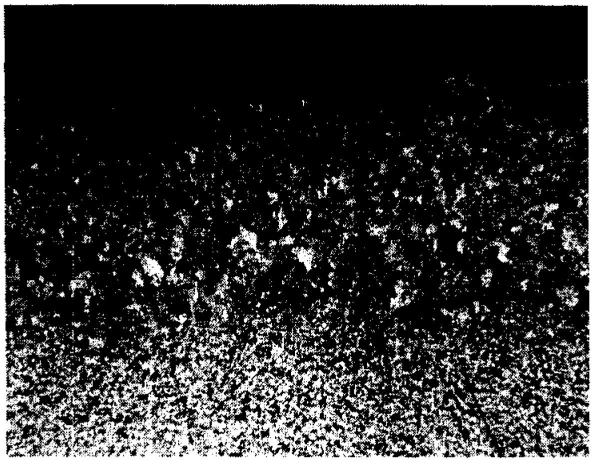

Sample 3 Carburized gear tooth, air cooled 400x, Nital etch

Sample 4 Carburized gear tooth, quenched, 400x, Nital etch

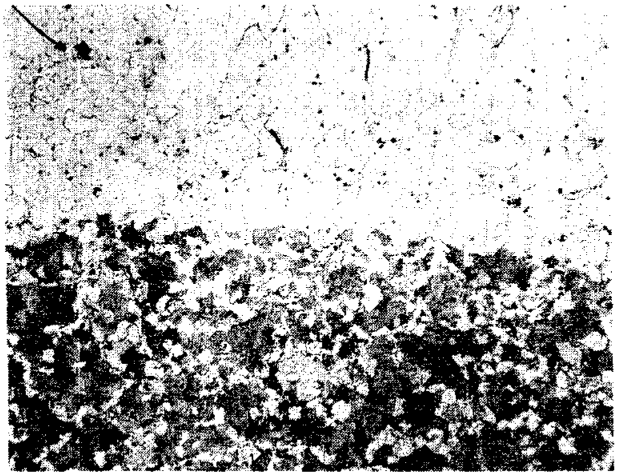

Sample 5 Decarburized gear tooth, 400x, Nital etch

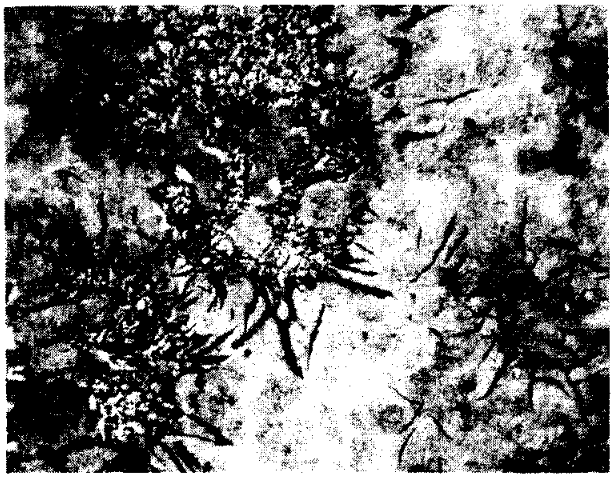

Sample 6 Gray cast iron, 400x, Nital etch

Sample 7 Nodular cast iron, 400x, Nital etch

Sample 8 Fe-Cr plasma sprayed coating, 200x

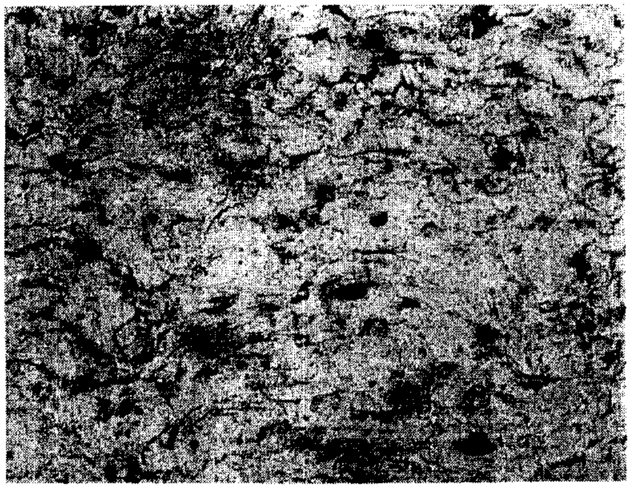

Sample 8 Fe-Cr plasma sprayed coating, 400x

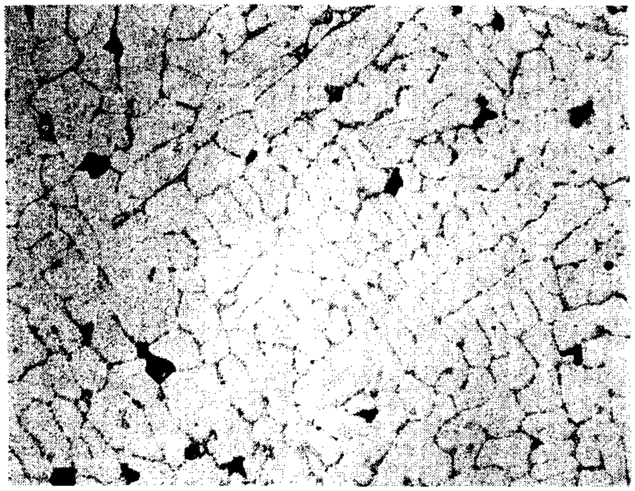

Sample 9 ETP copper, 400x, $NH_4OH + H_2O_2$ etch

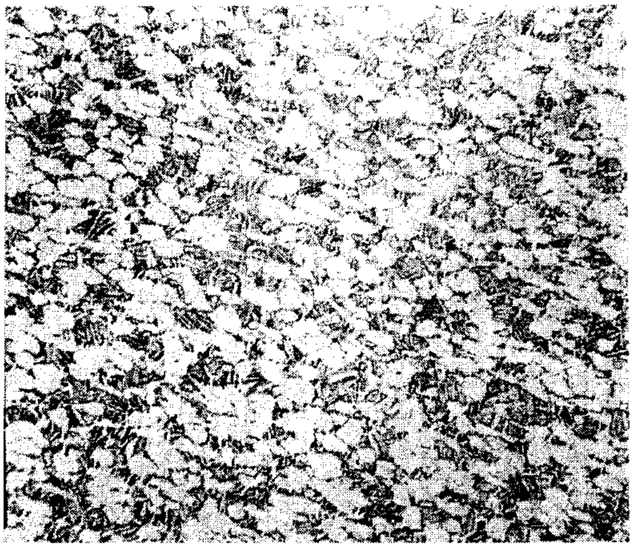

Sample 10 Titanium 6Al4V compressor blade, 400x, Kroll's etch

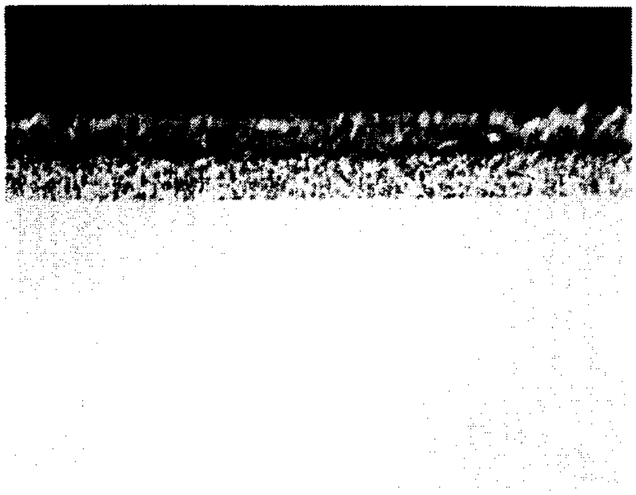

Sample 11 Nickel alloy turbine blade, 400x

Biography:

David Niebuhr is currently an assistant professor at Cal Poly State University in San Luis Obispo, CA. He has a B.S. from Cal Poly, SLO and a Ph.D. from the Oregon Graduate Institute in Portland, Oregon. His research interests include tribology, failure analysis, and materials characterization.

OXYGEN DIFFUSION INTO TITANIUM

Mike L. Meier

Aaron Broumas

and

Nick Degnan

Department of Chemical Engineering and Materials Science
University of California, Davis
Davis, California 95616

Telephone: 530-752-5166
e-mail mlmeier@ucdavis.edu
abroumas@aol.com
nmdegnan@ucdavis.edu

Mike L. Meier

OXYGEN DIFFUSION INTO TITANIUM

Aaron P. Broumas, Nick M. Degnan, Michael L. Meier

Department of Chemical Engineering and Materials Science
University of California, Davis

Key Words: titanium, oxidation, microhardness, diffusion, solid solution strengthening, activation energy

Prerequisite Knowledge: basic knowledge of diffusion processes and hardness

Objective: to measure D_o and the activation energy for diffusion of oxygen into titanium

Equipment:

1. Ovens capable of reaching 900°C
2. Metallographic specimen preparation equipment
3. Microhardness tester
4. Optical or scanning electron microscope

Introduction:

Titanium is well known for its excellent resistance to corrosion primarily due to a passive oxide layer at the surface. When exposed to air at elevated temperatures, 300°C or more, this oxide layer will grow and simultaneously oxygen will diffuse into the metal. The oxygen atoms that do diffuse into the metal can occupy both interstitial and substitutional sites, making the material harder, and since the concentration of oxygen at the surface would be greater than concentration deeper into the metal it should be harder near the surface and softer in the interior. The correlation between the concentration profiles and hardness profiles suggests that microhardness testing can be an effective tool in studying the oxygen diffusivity in titanium.

The governing differential equation for diffusion, known as Fick's second law, is:

$$\frac{\partial C}{\partial t} = D\frac{\partial^2 C}{\partial x^2} \tag{1}$$

where D is the diffusivity and C is the concentration of the diffusing species [1]. The solution to this differential equation, where surface concentrations are held fixed and the diffusion medium is infinitely long, generates the concentration profile described by the equation

$$\frac{c - c_o}{c_s - c_o} = 1 - erf\left(\frac{x}{2\sqrt{Dt}}\right) \tag{2}$$

where c_o is the concentration at infinity, c_s is the concentration at the surface, x is the distance from the surface, and t is the time.

Rosa [2] has proposed using the following dimensionless correlation between hardness and oxygen concentration,

$$\frac{H - H_o}{H_s - H_o} \propto \frac{c - c_o}{c_s - c_o} \tag{3}$$

where H refers to point hardness values, H_o refers to hardness values at infinity, and H_s refers to hardness values at the surface. Substitution into equation 2 gives

$$\frac{H - H_o}{H_s - H_o} \propto 1 - erf\left(\frac{x}{2\sqrt{Dt}}\right). \tag{4}$$

By measuring the hardness values from the surface of the metal inward, a hardness profile that is scaled to the concentration profile can be generated. This means that instead of using complicated and expensive analytical machines to measure the oxygen concentrations directly, a microhardness tester can be used to measure these hardness profiles and ultimately to determine the diffusivity.

This experiment involves determining the activation energy and diffusion rate of oxygen into titanium from a series of microhardness profiles. Several aspects presented in materials science courses are ultimately covered in this experiment, three of which are high-temperature oxidation, diffusion, and solid-solution hardening. The goal of this experiment is to provide upper-division materials science laboratory courses with a relatively inexpensive procedure for measuring the diffusivity coefficients and activation energies while emphasizing fundamental issues of materials science.

Procedure:

Material

Commercially pure, 0.75-inch (19 mm) diameter titanium rods were used in this experiment. Pure titanium was used to avoid issues related to the presence of other alloying elements and, since it is an α alloy, there won't be any α-case to complicate matters.

Heat Treating

The temperature range used in this study range from 700 to 800°C. At roughly 890°C, titanium transforms from a close-packed hexagonal α-phase to a body-centered cubic β-phase, which remains stable to the melting temperature 1670°C. By limiting the temperature of the metal to just a single phase region during annealing, in this case the α-phase, we did not have to take into account the different diffusivities for the α and β phases and the moving α-β phase interface.

The 0.75-inch (19 mm) diameter titanium pieces were cut into 0.75-inch (19 mm) long pieces and degreased with acetone and ethanol rinses. The samples were annealed in air at temperatures and times shown in table 1.

Table 1. Annealing temperatures and times.

Sample #	1	2	3	4	5	6	7
Temperature [C]	700	700	700	700	700	750	800
Time [hr]	20	50	100	200	500	100	100

Metallography

The annealed pieces were sectioned and mounted in Epomet mounting material, which is considerably harder than most mounting materials. This choice provided excellent edge retention, which is vital for accurate hardness data. The mounted specimens were then polished using 240, 320, 420, and 600 grit SiC abrasive papers, followed by intermediate polishing using 6 and then 3-micron diamond paste and finally 0.05 micron alumina on a vibratory polisher.

Microhardness Testing

A Kentron Micro Hardness Tester, equipped with a Knoop indenter, was used to measure hardness of the prepared specimens. Indentions were made using 100 grams load and a dwell time of 90 seconds, beginning from 30μm from the edge of the sample, approximately the width of one indentation. Additional indentions were made in increments of 25.4 μm toward the center until a depth of roughly 3 mm. A diagonal pattern was used so that many closely spaced readings, relative to the surface, could be made.

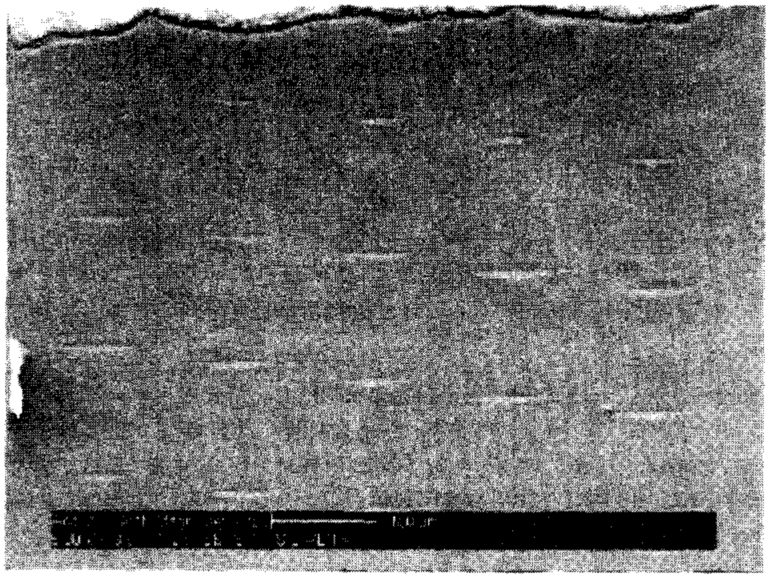

Figure 1 SEM image showing the microhardness indentations of a sample annealed at 800°C for 100 hours. Smaller indentations indicate higher hardness.

Results:
Figure 1 shows typical microhardness indentions. Note that the excellent edge retention made it possible to make measurements very close to the surface. Also note the diagonal pattern used. By distributing these indentations horizontally it was possible to space them close together vertically.

Microhardness Profiles as a Function of Time
The hardness profiles for the samples heat treated at 700°C and for times up to 500 hours are shown in figure 2. H_o was calculated by averaging the flat-line portion of the hardness profiles and was determined to have a value of 47.2 KHN. H_s and the diffusivity coefficient, D, were determined simultaneously by utilizing the "solver" utility in Excel and were determined to be 184.0 KHN and 1.14×10^{-11} cm^2/sec respectively. The constraining factor for the solver application was minimization of the sum of the square of the differences between calculated and experimental hardness values. The resulting fit between the data points and the calculated profile yielded a root mean square error in the range of 3.7 to 6.5 KHN.

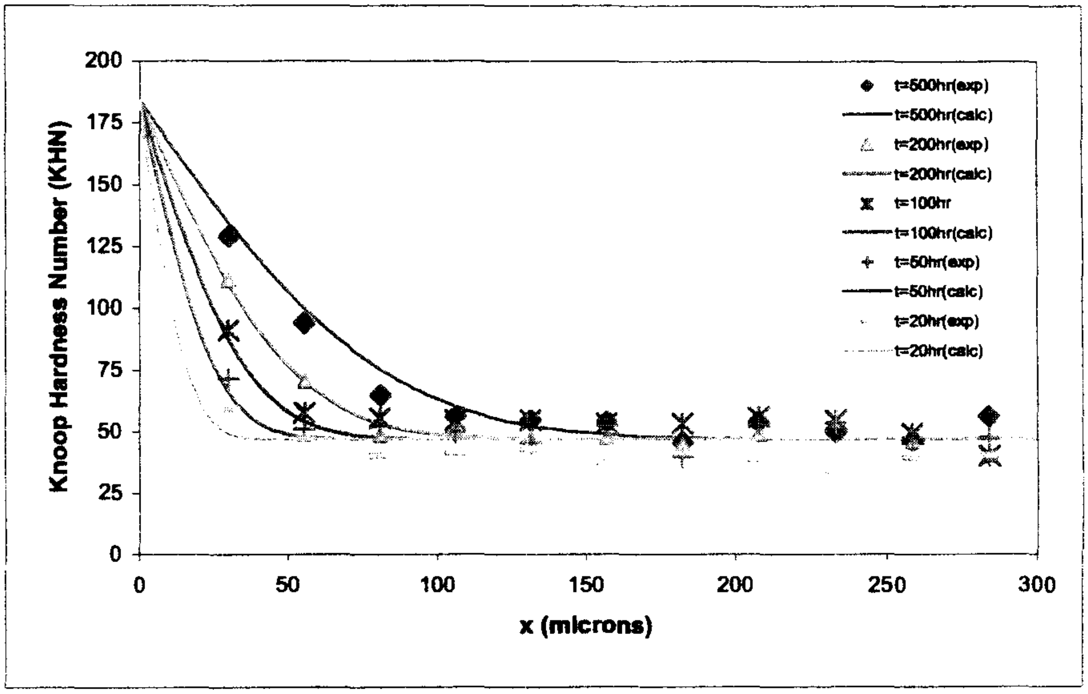

Figure 2 Microhardness profiles for samples annealed at 700°C

Microhardness Profiles as a Function of Temperature
In order to determine the activation energy of the system, annealing was done at three different temperatures, 700, 750 and 800°C and the annealing times were 100 hours each. The hardness profiles for two of these three samples are shown in figure 3.

Unfortunately, at the beginning of this series of microhardness tests the indenter was damaged. A new indenter was borrowed from another laboratory, but when it was used to test a calibration standard the lengths of the indentations were half of what they should have been. Therefore, a correction factor of 2 was used in these measurements. A new indenter will be purchased and these measurements will be repeated.

Values for H_0 and H_s found from the 700°C profiles were carried over to the 750 and 800°C profiles. Again, the "solver" component in Excel was used to determine values of D for these profiles. The resulting fit between the data points and the calculated profile was excellent, with a root mean square error of 4.5 to 5.5 KHN. The diffusivity coefficients, D, for the 750 and 800°C profiles, were 3.44×10^{-11} and 9.76×10^{-11} cm^2/second respectively.

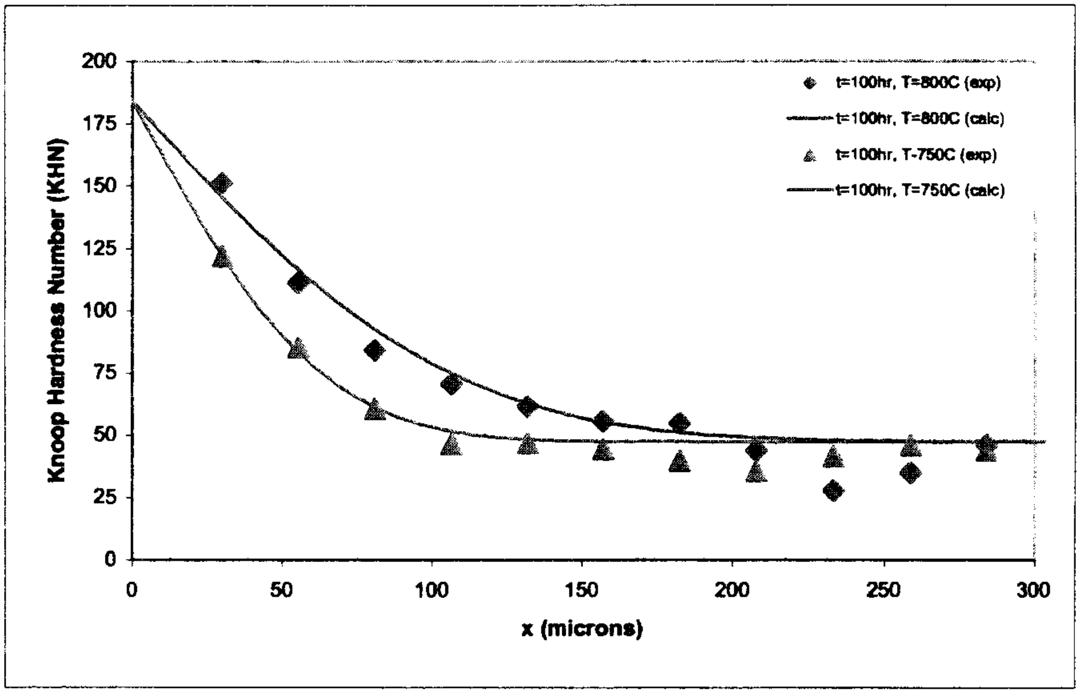

Figure 3 Microhardness profiles for samples annealed at 750 and 800°C for 100 hours.

Analysis of the Activation Energy

The experimentally determined activation energy for oxygen diffusion in α-titanium was found to be 186 kJ/mol. The slope of lnD vs. 1/T was used to determine this value, and the linear equation that fits the three data points is shown in figure 4. The activation energy is in the range reported in the literature.

Discussion:

Microhardness Profiles

The hardness profiles generated by this experiment look just like concentration profiles. In fact, the correlations suggested by equations 3 and 4 are indeed reinforced by the plots shown in figures 3 and 4. Variables such as activation energies and diffusion coefficients found through hardness testing can be used to predict the hardness values and therefore the relative concentration of oxygen at other temperatures, times, and depths.

The Stability of the Value of H_o

H_o is the initial hardness of the material, before any oxygen diffusion has taken place. H_o, however, can change due to other factors, such as recrystallization and grain growth. In this work annealed titanium was used to avoid this problem. Our results showed that for heat treatments done at 700°C and higher, and 20 hours and longer, the value of H_o did not change. It is possible that if this experiment is extended to lower temperatures and shorter times that it could change.

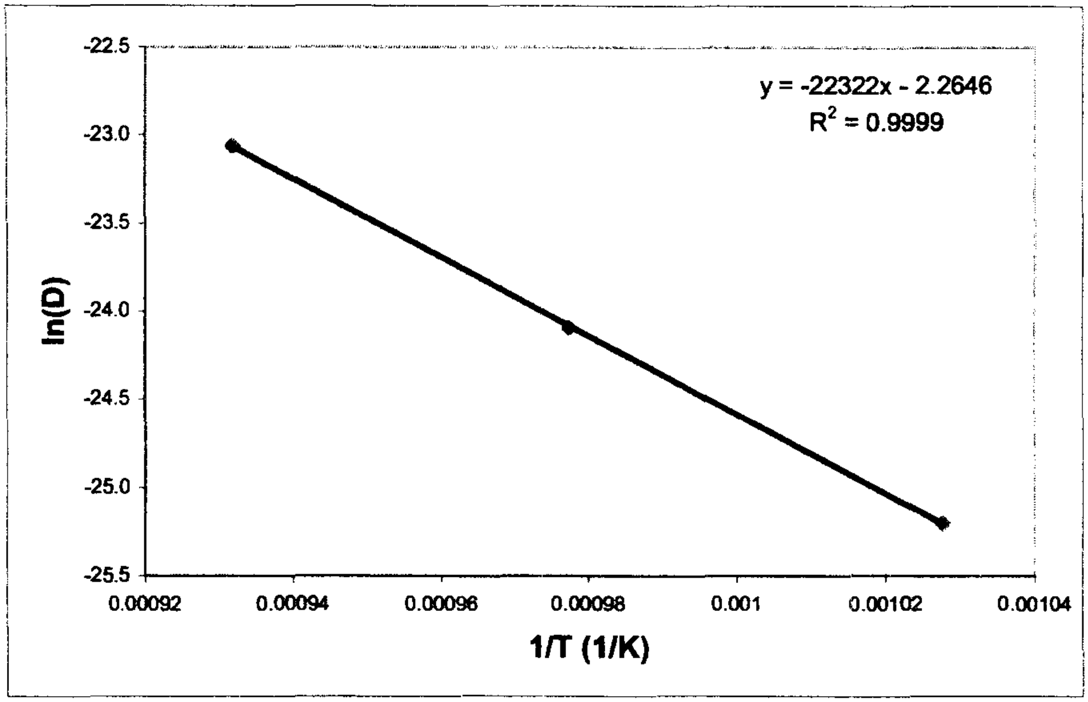

Figure 4 Arrhenius plot of the diffusivity

Using Solver to Find H_s and D

Using the solver capability of spreadsheets helped us to determine the hardness value at the surface, H_s, and the diffusion coefficients, D. These values, along with the value of H_o, were used in equation 4 to calculate the profiles. Using this numerical approach was necessary. It was not possible to measure H_s for the reasons mentioned below. We were concerned about the possibility that this approach could lead to multiple solutions. However, we had only two unknowns in a single equation, and we had 7 sets of data and a total of over 140 data points. The results turned out to be very reasonable and the RMS error for all 7 data sets was around 5 KHN, which is about the same as the scatter in the data.

The hardness value at the surface would have been impossible to obtain since it would need an indentation right at the surface. The diamond-shaped indentions were roughly 25 μm wide, and our best attempt to place the indenter close to the edge would generate fractures that would reach the edge. The best way to solve this problem was to allow approximately 30 μm of relief from the edge. The surface hardness determines where the profiles begin, but the diffusivity coefficient greatly influences the shape of the curve. The values for D and H_s were automatically adjusted so that the calculated profiles fit as close as possible with the experimental data points. Minimizing the sum of the difference between the calculated hardness (equation 4) and the experimental hardness for the profile(s) in each temperature group at fixed distances led to values for H_s and D. For the cases of the 750 and 800°C, the value for H_s found with the 700°C profiles was used since it already provided the best fit for five profiles. The value of D was determined numerically for each temperature.

Activation Energies
The activation energy found in this experiment is within the range of other values cited in the literature [2,4-7] and is very close to the value of Ti tracer diffusivity [8]. This suggests that the diffusion of oxygen in α-Ti occurs by a substitutional vacancy mechanism.

The table below lists the activation energies reported for earlier microhardness-based diffusivity studies as well as for other methods, including the tracer diffusivities for pure titanium.

Table 2. Activation energies for the diffusivity of oxygen in titanium.

Investigator	**Alloy**	**Method**	**Activation Energy kJ/mol**	**Year and Reference**
Present work	CP – Ti	Microhardness	186	2002
Gupta and Weinig	Ti-0.2^{a}% O-based alloy	Internal friction	188	1962 [3]
Pratt et al	Ti-3.5^{a}%O	Internal Friction	201	1954 [4]
Roe et al	Ti75A	Microhardness	140	1960 [5]
Rosa	CP – Ti	Microhardness	203	1970 [2]
Revyakin			150	1954 [6]
Tracer Diffusivity				
Dyment et al	α - Ti^{44}	Tracer	173	1968, [7]

The experimental methods used in several of the investigations listed in table 1 were quite complex, requiring very expensive analytical machines. Our experiment shows how hardness testing can be used as an inexpensive method of determining the activation energies.

Other Factors
All of the heat treatments were done in air, and while this might better represent typical service conditions, air contains four times as much nitrogen as oxygen. Nitrogen diffusion has been addressed in other studies [8]. The activation energy of nitrogen

diffusion is similar to that for oxygen but its diffusion rate in the present temperature range is a factor of 4 lower than for oxygen. In general nitrogen does not seem to concern people as much as oxygen, perhaps because a thick layer of TiO_2, not TiN, forms on the surface, and because of the lower diffusion rate. The matter was also not addressed here so that we could concentrate on a phenomenon that could be presented in a classroom setting.

One other factor that influences the results of these types of studies is the effect the oxide itself has on the diffusivity. Once the oxide forms the value of c_s changes from that of air to that of the oxide. Since the oxide forms immediately, c_s probably never was equal to the oxygen concentration of air. This means that c_s was probably constant and therefore H_s was probably constant.

Conclusions:

The results obtained here are similar to those reported in the literature. This experiment also incorporates a number of fundamental concepts, such as diffusion, solid solution strengthening, phase diagrams and practical skills such as heat treating, metallography, microhardness testing and data reduction. It is also a relatively inexpensive experiment that can be done as a group experiment. All of these factors make it very attractive as an experiment for the teaching laboratory.

It should be noted that the linear correlation may not be the best approximation. Data showing hardness as functions of oxygen concentration in pure titanium shows a slight nonlinear (concave down) relationship [9]. The nonlinear might not be enough to change the results significantly but a new analysis should be attempted. It would be interesting to split the students into two groups, ask each to use one of these approaches, and then compare the results and debate the merits of each.

This experiment required us to find new ways to analyze the data. The "solver" capabilities of the Excel spreadsheet allowed us to solve for multiple unknowns using regression, which is not common in undergraduate education.

An interesting side-benefit of this experiment is that all of the specimens one would need to conduct an experiment on the kinetics of grain growth of titanium are already prepared. All that has to be done is to etch the samples and measure the grain sizes.

Finally, similar experiments could be developed for other systems. We have shown here is that in certain cases microhardness testing can be used to investigate the diffusivity of materials.

References:

1. D. Porter and K. Easterling, Phase Transformations in Metals and Alloys, Second Edition, Chapman and Hall, 1992, p. 71.

2. C. J. Rosa, Oxygen Diffusion in Alpha and Beta Titanium in the Temperature Range of 932° to 1142°C, Metallurgical Transaction, Vol.1 September, 1970, pp. 2517-2522.

3. D.Gupta and S. Weinig, *Acta Met*, 1962, vol. 10, p. 292.

4. J. N. Pratt, W. J. Bratina, and B. Chalmers: *Acta Met.*, 1954 vol. 2, p. 203.

5. W.P. Roe, H. R. Palmer, and W. R. Opie: *Trans. ASM*, 1960, vol. 52, p.191.

6. A. V. Revyakin: *Izv. Akad. Nauk* SSSR, *Tekh. Nauk Met. i Topliva*, 1961, p. 113.

7. F. Dyment and C.M. Libanati, *J. Mager Sci*, vol. 3, no. 4, 1968, p. 349.

8. R. J. Wasilewski, Diffusion of Nitrogen and Oxygen in Titanium, Journal of the Institute of Metals, Vol. 83, Institute of Metals, 1954-55, pp. 94-104.

9. R. Boyer, G. Welsch, and E. W. Collings, Materials Properties Handbook: Titanium Alloys, Eds., ASM International, 1994, pp.148-149.

Biographical Information:
Aaron Broumas is in his senior year at the University of California, Davis and is double-majoring in chemical engineering and materials science. He is working as an intern in Materials Science Central Facilities and is proficient in metallography, specimen preparation techniques, scanning electron microscopy and EDS and is learning x-ray diffraction and other materials characterization techniques. Aaron is also helping users of the facility and is a principal operator of our two scanning electron microscopes. He is also engaged in the analysis of dust samples collected over Puerto Rico and in the northern deserts of China.

Nick Degnan is a junior at the University of California, Davis double-majoring in mechanical engineering and materials science. He is working as an intern in Materials Science Central Facilities learning metallography, specimen preparation techniques, optical microscopy, scanning electron microscopy and EDS. He is also engaged designing and building a laser diffraction demonstrator for use in class, rebuilding laboratory equipment and assisting users of the facility.

Michael L. Meier received his B.S. in Materials Engineering from North Carolina State University in 1979 and his M.S. (1986) and Ph.D. (1991) in Materials Science and Engineering from the University of California, Davis. After a two-year post-doctoral research at the Universität Erlangen-Nürnberg in Erlangen, Germany he returned to UC Davis where he is now the director of Materials Science Central Facilities, a materials characterization facility, and is very active in developing the laboratory teaching program.

STATISTICAL PROCESS CONTROL: THE MANUFACTURER'S BEST FRIEND

Ransom West Douglas

Program Director, Design Technology
Norfolk State University
700 Park Avenue
Norfolk, Virginia 23504

Telephone: 757-823-8833
e-mail rdouglas@nsu.edu

Ransom West Douglas

Statistical Process Control: The Manufacturer's Best Friend

Ransom West Douglas
Program Director, Design Technology
Norfolk State University
Norfolk, Virginia

Key Words: Control charts, continuous improvement, flow chart, process capability, and process improvement.

Prerequisite Knowledge: Basic statistical concepts, variations, phases of statistical application, and tools of statistical process control.

Objective: To demonstrate the application of non traditional SPC techniques in monitoring and controlling manufacturing processes involving lower production rates and smaller lot sizes.

Introduction: Improvement of product quality in a manufacturing outfit utilizing dual methods. Hidden causes for poor quality are identified through the use of a flow chart to provide the basis for problem analysis. Traditional control charts for variables are not suitable under certain manufacturing environment, thus necessitating the application of non-conventional methods involving pre-control charts.

Procedure: Lower production rates and smaller lot sizes create a unique problem for the use of traditional SPC techniques. In this environment, there exist insufficient data to estimate the control limits, process mean, and the process spread. To overcome this problem, pre-control and short run charts are recommended as they are appropriate for high capability processes. The pre-control chart is divided into five regions (fig. 1).
The central green region, two yellow regions, one on each side of the green region, and two red regions on the outer side of the yellow regions. This chart is used instead of the traditional process control chart when the process spread (6σ) is less than 70% of the blue print tolerance
or $6\sigma/(USL - LSL) = 0.7$
$Cp = (USL - LSL)/(6\sigma) = 1/0.7 = 1.429$
$USL - LSL = 6*1.429 = 8.57\sigma$
Therefore, specification limits are $8.57/2 = 4.3\sigma$ away from the process mean. The green region covers the ±50% of the tolerance, making the boundaries of the green region equal $\pm 2.15\sigma$ away from process mean. Each section of the yellow region is ½ as wide as the green region. The green plus the yellow regions cover the full width of the blue print tolerance. The red region indicate the out of specification region.

Please refer to the four rules of a pre-control chart on (fig.2).
The assumptions of a pre-control charts are as follows:

1. That the process follows a normal distribution
2. That the process is highly capable, cp = 1.429
3. That the specification limits are ± 4.3σ
4. That the green region is bounded by ±2.15σ with an area of 96.84% of the normal distribution.
5. That the probability of a part falling in one of the 2 yellow regions is 1.58%
6. Thus , the probability of both the parts falling in the green region is 93.8%. The probability of a part falling in the green and the other in the yellow is .9684*.0158 = 0.0153.

Comment: In today's turbulent business environment where manufacturers of products are increasingly expected to improve the quality of their products, demands use of appropriate SPC tools. However, care must be taken to select the tools for a given manufacturing outfit. Job shop manufacturing environment would be more suitable for the use of pre-control SPC techniques. In a case study carried out at a defense contractor's, to be shared with participants, it was found that pre-control charts are appropriate for use in a case of lower production rates and smaller lot sizes resulting in cycle-time reduction.

References:

1. Gerald M. Smith, Statistical Process Control and Quality Improvement, 4th Edition, pp. 301 – 306.
2. J.M. Juran & Frank M. Gryna, Quality planning and Analysis, 3rd Edition, pp. 391 –400.

Biography:

Ransom West Douglas is a consultant in manufacturing technologies and integrated logistics systems. He had worked for Union Carbide, refineries, petrochemical plants in the capacity of Head, Project Control. He earned a BBA at the University of Texas in Austin, MBA at Golden Gate University in San Francisco, and a Doctorate degree at the George Washington University in Washington, DC. He is the program director for Design Technology program at Norfolk State University.

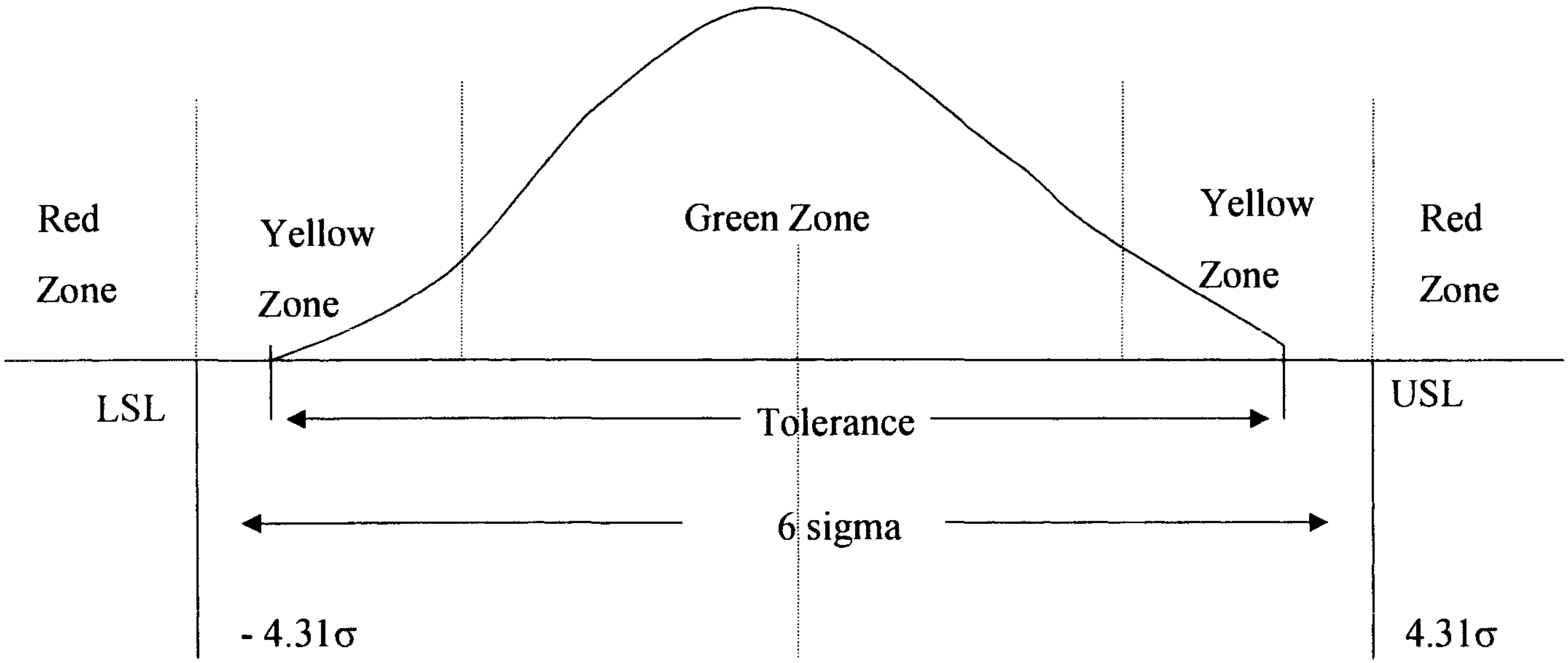
Red
Zone
Yellow
Zone
Green Zone
Yellow
Zone
Red
Zone
LSL
Tolerance
USL
6 sigma
- 4.31σ
4.31σ

Measurement	Zone	Decision
A	Green	Run_(B not needed)
A	Yellow	Check the next piece
B	Green	Run
A	Yellow	Check the next piece
B	Yellow	Adjust or correct: A and Bin the same yellow zone, x is out of control. A and Bin opposite yellow zones, the range, R, is out of control and variation has increased.
A	Red	Adjust or correct

MATERIALS FOR NEW DESIGNS, AND DESIGNING NEW MATERIALS

Leonard W. Fine

Department of Chemistry
Columbia University in the City of New York
Havemeyer Hall
New York, New York 10027

Telephone: 212-854-2017
e-mail fine@chem.columbia.edu

and

Sam Miller

Advanced Application Engineering
GE Plastics
Pittsfield, Massachusetts 01201

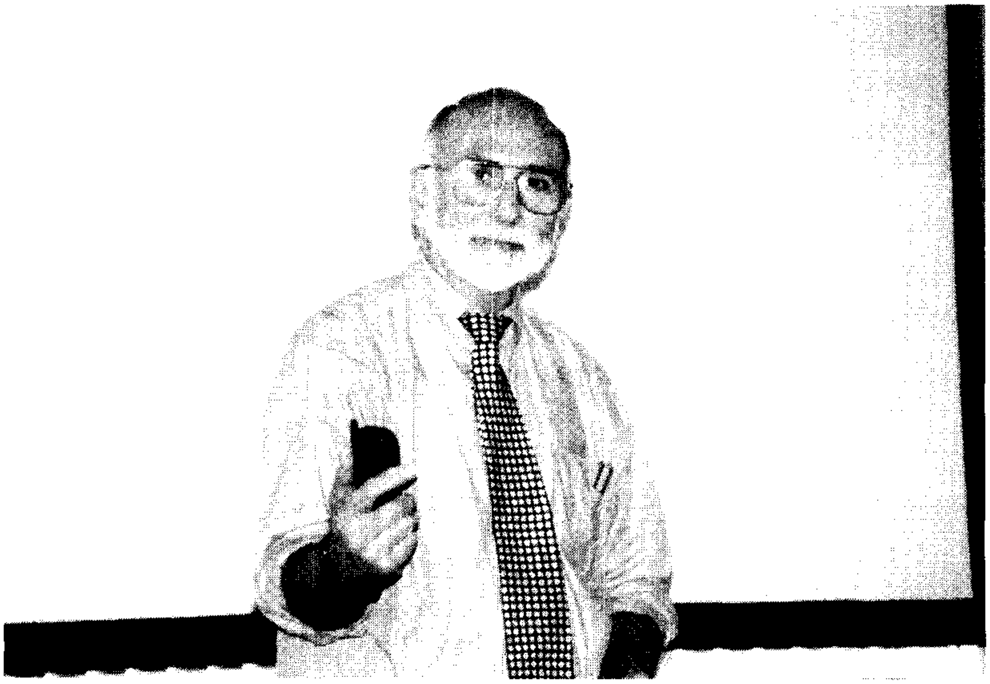

Leonard W. Fine

“MATERIALS FOR NEW DESIGNS, AND DESIGNING NEW MATERIALS.
Paradigms Lost and Paradigms Found in the Changing World of Engineering Plastics”

Leonard W. Fine, Department of Chemistry, Columbia University, New York, NY 10027
and Sam Miller, Advanced Application Engineering, GE Plastics, Pittsfield, MA 01201.

Abstract

For those of us who will have spent most of our professional lives in the second half of the 20th century, we cannot fail to see that entire century as a world of transformations. Everything changed! And the rate of change accelerated through the century. For scientists and technologists, if there ever were classical textbook models for creating, designing, and building principles and practices for engineering the future, they have been transformed by the accelerating rate of change that is the benchmark of our times. And nowhere is that better illustrated than in the changing world of engineering plastics. This brief lesson from history suggests how some ideas and some things, and some ideas *about* things, have come together at the interface between research and education, and between teaching and learning.

Introduction

Paradigm! The word Thomas Kuhn used to describe the intellectual order driving a scientific field or activity that is overthrown, convulsing, or shifting during a period of change. For my generation of scientists – growing to Manhood in the ‘60s under the impact of “The Structure of Scientific Revolutions (1962)” it is hard not to recognize parallels in technology. An existing order has the stability of a well-built model which gives us comfort with the understanding it brings. We know how things work or at least, are expected to work. A model! Sometimes mathematical. Sometimes economic. Sometimes scientific. Philosophical. Models help us understand.

Kuhn will be remembered for teaching us ....

1) that the processes of discovery and invention are intimately embedded in a larger framework of human activity.
2) that discoveries and inventions are the product <u>not</u> of some plodding rational process but of human ingenuity intermingled with politics and personality.
3) That science and technology are in the end social processes.

In the plastic century that opened in 1902 with the invention of Bakelite, we have moved from a technics based on production and producers to one of consumption and consumers. The change-over has suddenly become evident.

The implications for R&D in engineering plastics are timely to consider. Long before Bakelite, Adam Smith, the moral philosopher on whose ideas most modern economic theories were built, recognized that...“the fitness of any system or machine to produce the end for which it was intended, bestows a certain propriety and beauty upon the whole, and renders the very thought and contemplation of it agreeable.” Adam Smith taught us that utility is one of the principal sources of beauty! But something has happened to Adam Smith's economic model that reduced science and invention to practiced technology in the market place. In spite of what Ecclesiastes teaches, there is something new under the Sun. The price and the profit are coupled to the aesthetic. And the driver of design has become the consumer – no longer, the producer – of products.

From the Model T to the Mac

Ford's Model T was revolutionary for its mass production methods. At the same time, a demanding public required rubber on the road that lasted for thousands of miles and the conveniences provided by of an assortment of Bakelite knobs, widgets, parts - in any color you wanted as long as it was black.

Half a century later, Steve Jobs and Steve Wozniak launched Apple Computer and hoped to fulfil a similar dream, revolutionizing the modern counterpart to the car, the computer. The Apple II that emerged a year later was the first ever commercial computer. It included color graphics for the first time, sported the Apple II DISK which was (at the time) the cheapest and easiest-to-use floppy drive available, and became the data storage device of choice among most scientists and technologists, especially the university crowd. And it had an all plastic chassis, keys, and keyboard.

In 1984, Apple Computer launched the Macintosh, featuring a user-friendly interface with a high-definition screen, a mouse, and an integrated monitor and disk drive. The look was created not by scientists and engineers but rather by artists and designers. By product designers! And the Mac sported a radically different look (from the angular predecessor and competitor). There was something softer about the Mac. It had flowing lines, was a warm cream-color, and had the now classic icon-driven graphics interface. The Powerbook was launched in 1991. The PowerMac in 1994.

Somewhere along the way Steve Jobs was forced out of the company he founded, in 1985, by successors who tried and failed to keep market share in the face of Microsoft, Windows and the PC. But without a doubt, plastics had a market. In 1996, Steve Jobs returned to rebuild the nearly moribund Apple Computer. His genius insight? To take all his "geek" computer and software engineers out of their backroom hangouts and move them into the front room where their customers hung out. He hired an industrial designer named Jonathan Ive and, as they say, the rest is history: the iMac; the iBook; the G3. Three computers that collectively sounded the death knell of the anonymous and essentially alienating dull-colored box and in its place a cool-looking design with an identifiable character that was understandable and familiar to the potential customer/user. It was the first computer to have stylistically influenced and launched the design of families of products from tasking lamps to desk accessories. The paradigm had clearly shifted.

Baekeland and Bakelite

Long before there was polycarbonate, engineering plastics, or even"plastics," there was Bakelite, the invention (discovery) of an accomplished, well-trained Belgian chemist, one Leo Hendrik Baekeland. Trained and educated in his native country, at age 28 he already found himself Lecturer in Chemistry at the University of Ghent (1887). Shortly after that, as a (now) rich and successful entrepreneur for having sold an improved photographic paper invention to George Eastman (1899). While dabbling in his garage chemistry laboratory at his home in the Bronx, he turned his attention to reactions of phenol and formaldehyde.

It was well-known at the time that phenol and formaldehyde would react but produce a hard, black, intractable and insoluble material that defied analysis. Baekeland reasoned that if he could vary the conditions and the quantities, and come up with a way of applying a coating to wood or wire, he might find a substitute for shellac, other varnishes, and insulating wire coatings. In a series of experiments in mid-1907, Baekelund learned how to manipulate the phenol-formaldehyde reation to produce a varnish and a solid, moldable resin. By 1908, with patent in hand, he announced to the world his discovery:

> "It makes excellent billiard balls of which the elasticity is close to that of ivory, in short, it can be used for similar purposes like knobs, buttons, knife handles… and many more applications for engineering purposes.

By 1910, Baekelund had established the General Bakelite Corporation and the large scale production of this new, synthetic material. During the next 25 years, a generation of independent, entrepreneurial molders and extruders began doing what Grant Austen did in the fictional (1955) novel, "Cash McCall:." He started a company in a barn with a rebuilt hydraulic press, spooning a carbolic-smelling powder into the cavity before bringing the hot plattens together. When the press opened, a miracle had taken place. The powder had miraculously become the socket for an electric light bulb and he was in business.

Central to Grant Austen's success was a powerful logical structure connecting the four elements of polymer science: processing – structure – properties – performance. Essentially all polymer materials on their way from molecule to product undergo one or more processing steps: spinning; molding; casting; forming. It is generally accepted that final material properties can vary drastically and dramatically with processing history. Design of processing equipment is itself a major industrial undertaking.

Thomas Kuhn and His Paradigm

It is interesting to speculate on the relative importance of new concepts and new tools in the progress of science and technology. Design has clearly become a force for change: a way to enhance performance; a way to drive science and technology; and a way to create prosperity; maybe even the means to sustaining cultural advantage… or creating cultural advantage… in a competitive world

In the early decades of the 20th century, PRODUCTION was the important focus; NOW, it is clearly CONSUPTION. Of course, production and consumption go hand-in-hand with the difference being which is in the driver's seat – the original materials supplier (PRODUCTION) or the object-makers (CONSUMPTION). The paradigm has shifted. The relationship between users' needs and desires and the object are at the heart of our experience in our early 21st-century world. DESIGN is still the thing! But now we are all included on the design team – consumers, producers, designers… and scientists and technologists – all shaping our worldly experience. Objects of desire (or necessity) can boldly announce that design is more than just a lifestyle issue. Design is a force for change: a way to enhance industry performance; a way to drive science and technology; and a way to create prosperity; maybe even the means to sustaining cultural advantage in a competitive world… or creating cultural advantage.

Kuhn rescued our understanding of science and technology from the mundane mechanical world of determinacy. He taught us why science and technology are exciting and unpredictable, getting beyond the "method" of science and the mechanical reduction of science to engineering practice. Kuhn taught us "The Structure of Scientific Revolutions."

References

1) The Structure of Scientific Revolutions (1969), by KUHN, Thomas S.
2) Pioneer Plastic: The making and Selling of Celluloid (1983), by FRIEDEL, Robert
3) American Plastic: A Cultural History (1997), by MEIKLE, Jeffrey L.
4) Three Hundred Years of Industrial Design (2000), by HEATH, Adrian and Ditte, and JENSEN, Aage Lund.
5) Design of the 20th Century (1999), by FIELL, Charlotte and Peter.

BEAMS IN BENDING: AN INSTRUMENTED CLASSROOM DEMONSTRATOR

Richard B. Griffin(1)

Led Klosky(2)

Reid Vander Schaaf(2)

(1)Department of Mechanical Engineering
Texas A&M
College Station, Texas 77843

Telephone: 409-845-9779
e-mail rgriffin@mengr.tamu.edu

(2)Civil & Mechanical Engineering
United States Military Academy
West Point, New York 10996

Richard B. Griffin

Beams in Bending; an Instrumented Classroom Demonstrator

Dr. Richard Griffin[1], Faculty
Dr. Led Klosky, Faculty
Capt. Reid Vander Schaaf, Faculty
Civil & Mechanical Engineering
United States Military Academy
West Point, NY 10996

Abstract

In mechanics and/or material classes, students often struggle with the concept that both material properties and geometry may affect a materials response. A four-cantilever beam setup has been designed and developed to illustrate the effect that geometry and modulus of elasticity have on the strain measured in a beam. There are three aluminum beams and one steel beam contained in the fixture. The four beams are 1 in. x 1/8 in. (steel), 1 in. x 1/8 in. (Al), 1 in. x ¼ in (Al), and ¼ in. x 1 in. (Al) and about 16 inches long. Weights are hung from the end of the beam, and strain gauges are located 1 ½ in. from the fixed end of the cantilever. The strain is measured as each load is placed on the cantilever beam.

A comparison may be made between steel and aluminum at 1/8 in. in thickness, and the effect of material property is demonstrated. Then, the 1/8 in. aluminum can be compared to the ¼ in. thick aluminum beam, and now the effect of geometry can be observed. Finally, the fourth beam is turned on edge so that the 1-in. height is vertical, and a very dramatic effect on strain is observed. The unit can be brought to class and used for either in class demonstrations or can be made available for students to experiment with during, after, or before class.

---

[1] Dr. Griffin was on sabbatical leave at the United States Military Academy during the 2001- 2002 academic year. He has returned to Texas A&M University, MEEN Dept.-3123, College Station, TX 77843.

Key Words: mechanics of materials, strength of materials, beam bending, cantilever beam, and material properties

Prerequisite Knowledge

Physics, statics, stresses and strains in beams, and strain gauges

Objective

This in-class demonstration enables a student to understand and compare the significance of geometry and material properties in the behavior of a beam under load.

Equipment

1. Beams of various sizes see Table 1.

Table 1. Dimensions, moduli, and moments of inertia for different beams.

	Material	Size, in. (l x w x h)	Modulus, psi	$I = bh^3/12$, in^4
1	Steel (1018)	16 ½ x 1 x 1/8	30×10^6	0.1628×10^{-3}
2	Aluminum (6061T6)	16 ½ x 1 x 1/8	10×10^6	0.1628×10^{-3}
3	Aluminum (6061T6)	16 ½ x 1 x 1/4	10×10^6	1.302×10^{-3}
4	Aluminum (6061T6)	16 ½ x 1/4 x 1	10×10^6	20.83×10^{-3}

2. Fixture for supporting the beams
3. Load supporting fixture
4. Weights
5. Strain gauges
6. Strain measuring equipment
7. Dial indicators (optional)

Cost depends on availability of strain measuring equipment. If you have access to the strain measuring equipment, then the estimated cost would be about $50.00 in materials and about three days of machine room time. The strian mesuring components for installation in a computer that uses LabView™ are about $1000 per module.

Introduction

Using demonstrations in the classroom helps those learners who need something physical to connect theory with what is actually happening. Over the past several years the authors have developed a number of classroom demonstration devices.[1, 2, 3, 4, 5] In mechanics and materials classes students often struggle with the concept that an object's response to a load is controlled by either a material property or the geometry of the situation. The cantilevered beam device (CBD) described in this paper was developed to demonstrate these differences. The CBD has been successfully used in a mechanics of materials class, where the device is brought to the classroom for demonstration or to have available for student's to experiment with. The current unit, shown in Figure 1, uses four beams, which are listed above in Table 1. Three of the beams have the 1-inch dimension horizontal, while the fourth has the 1-inch dimension in the vertical direction. If beams number 1 and 2 are compared, then the effect of material property may be demonstrated, while if numbers 2, 3 and 4 are compared the effect of geometry may be shown. The details of the device and its operation will be described in the following sections of the paper.

Description of Device

The drawings for the cantilever beam device are shown in Figure 1. Typically,

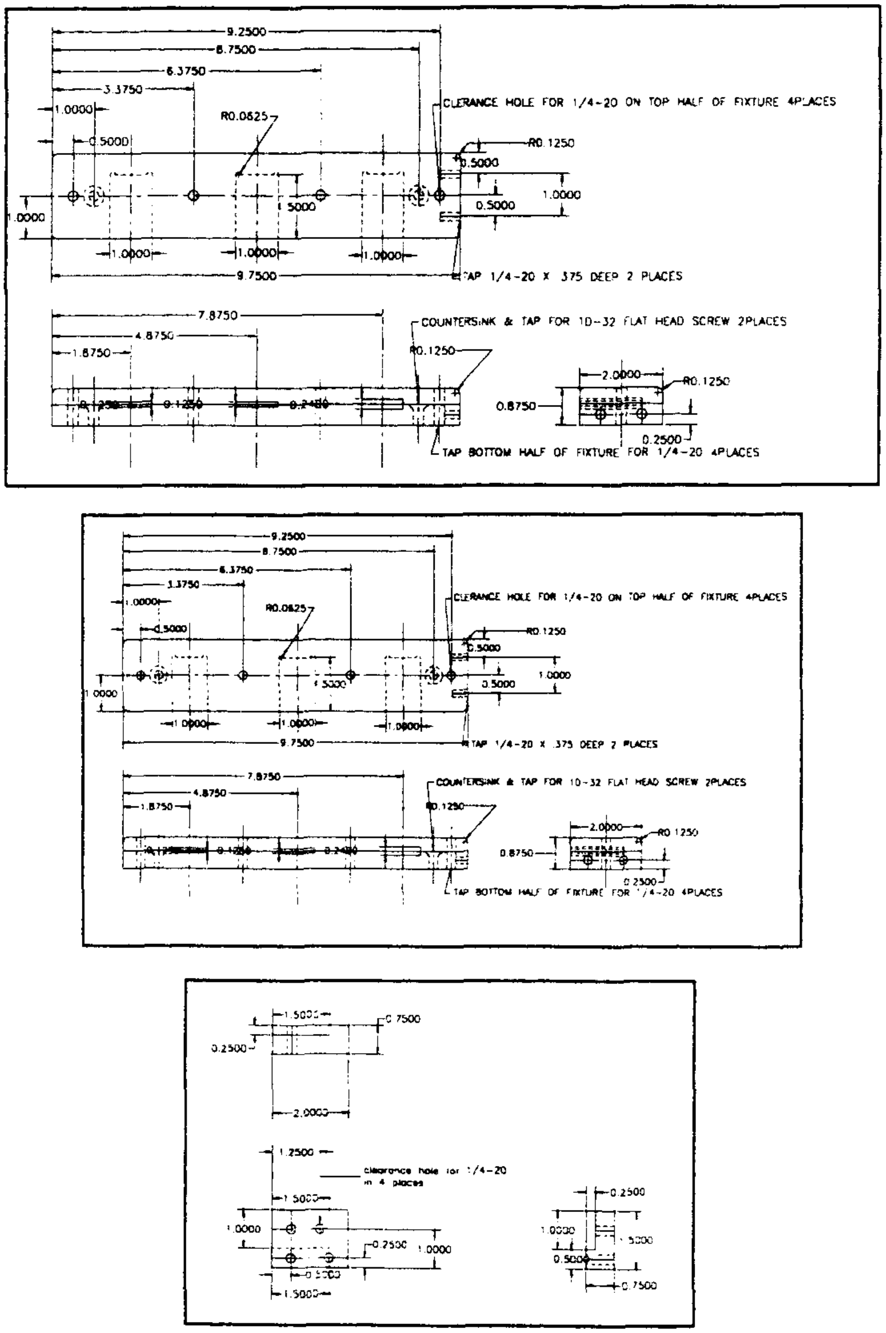

Figure 1. Drawings for the cantilever beam device.

a 1-lb. weight has been used for the load. Figure 2 shows the setup in the classroom. The midpoint for the strain gauges is located 1 ½ in. from the fixed end of the cantilever. The strain readings vary from about 190 με for the steel to about 600 με units for the aluminum. Figure 3 shows the students gathered around the unit in the classroom.

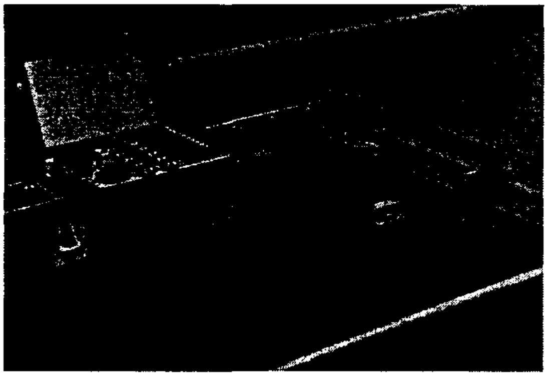

Figure 2. Cantilever beam setup in the classroom.

Figure 3. Students gathered around the cantilever beam demonstration device.

Theory

One of the fundamental concepts in any introductory course in solid mechanics is the effect of geometry and material type on the behavior of beams in bending. For each of the beams shown, the shear and moment diagrams can be drawn by the students, allowing them to find the moment, M, at the location of the strain gage. The students should be led to noticing that the moment is unaffected by either the material type or the beam shape. This is because they are part of the force system, and are not stresses. The operative equation for computing the normal stress, σ, in the direction of the strain gage (placed in the long direction on the beam), is:

$$\sigma = \frac{Mc}{I} \qquad \text{Equation 1}$$

where I is the moment of inertia, $(1/12)^* bh^3$, and c is the distance from the neutral axis to the strain gage. Of course, stress is not strain, and σ must then be converted to strain, or microstrain depending on the strain readout device. This conversion is simply:

$$\mu\varepsilon = \frac{\sigma}{E} * 1000 \qquad \text{Equation 2}$$

Thus, students should be able to first draw the shear and moment diagrams for the real system they see, and then predict the resulting stresses and measurable strains. Additionally, it is possible for the students to predict and then measure deflections at various points on the beam based on widely-published beam deflection equations.

Results

Having the students calculate the expected change in strain after taking a strain reading on the first beam with the one-pound weight on it, is a very effective way to get the students to understand how much and why the material and the geometry of the beams in important. When comparing the strain readings made between steel and aluminum at 1/8 in. in thickness, we predict the strain in the aluminum will be three times higher, and the device demonstrates this, with a reading of approximately 190 με for the steel, and 600 με for the aluminum, see Table 2. Then, the effects of geometry can be observed by comparing the 1/8 in. aluminum to the ¼ in. thick aluminum beam. We predict a reading eight time higher in the ⅛ inch beam, which the model illustrates with a reading of 600 με verses 72 με. Finally, the fourth beam is turned on edge so that the 1-inch height is vertical, and a very dramatic effect on strain is observed. The strain reading is one sixteenth of that on the flat ¼ in. beam (beam 3), and 1/128 of the strain experienced by the 1/8 in. flat beam (beam 2).

Table 2. Approximate strain values for the CBD.

Beams	Strain Values (με)
Steel: 1/8 in. thick	190
Aluminum: 1/8 in thick	600
Aluminum: ¼ in. thick	72
Aluminum: 1 in. thick	4

Discussion

In discussing the experiment with the students, Equations 1 and 2 can be used, and written as follows.

$$\varepsilon = \frac{\mathrm{Mc}}{\mathrm{IE}} \qquad \text{Equation 3}$$

If a comparison is made between steel and aluminum (1/8 in.) then the ratio of Equation 3 is about 1/3, which is what Table 2 illustrates. This clearly shows the effect of material properties. Similarly, if the ratio of steel and aluminum (1/4 in.) is considered then the ratio of the equations is about 1/8, which Table 1 illustrates. The questions can be posed to the students, and then the students may test their responses using the CBD.

Alternatively, it is possible to measure the deflections and compare them with calculated values. or ask where would the loads need to be located for steel and aluminum to have the same maximum deflections. A wide variety of questions may be posed and the answers tested for.

Assessment

In fall 2002, 87 students were asked to assess the inclass CBD activity. Table 3 gives their numerical responses to the question, "Should we keep the activity or send it to the scrap heap?" The scale was 1 to 5 with 5 being high and 1 being low. Another question asked the students, "Did the classroom demonstration make any difference in your understanding of the activity (CBD)?" Fifty-one (51) responded yes, twenty-six (26) responded no, and eight (8) students responded with somewhat. From this brief analysis, 79% rated the experiment 32 or higher on the 1 to 5 scale, while 69% said either yes or somewhat to making a difference in their understanding of the CBD demonstration.

Table 3. Student evaluation for CBD activity.

No. of Students	Points
45	> or = 4
24	3
18	< or = 2

Conclusions

A cantilever beam setup has been designed and built that demonstrates the effect of material properties and geometry for steel and aluminum beams. The system is simple to use and may be brought to the classroom. The CBD provides students with a visual way of observing the effect of the modulus of elasticity and the effect of geometry.

Acknowledgements

The authors would like to thank Rich Ellingsen from West Point for the construction of the unit and the AutoCAD drawings. RBG would like to thank Texas A&M University and the United States Military Academy for supporting his sabbatical leave.

---

[1] Griffin, R. B., Cornwell, L. R., Yapura, C., Krishnan, S., and Hallford, J., "Use of a Four-Point Bend Apparatus to Determine the Modulus of Elasticity," National Educators Workshop Update 98, Brookhaven, NY, 1-4 November, 1998.

[2] Griffin, R. B., Ragupathi, P., Johnson, E., "Development of a Thermal Conductivity Experiment for Use in Class," ASEE, Seattle, WA, 1998.

[3] Yapura, C. L. Richard Griffin, R. B., Lagoudas, D. L., "Mechanics of Materials Experiments Via the Internet," National Instruments Week, Austin, TX, Aug. 1999.

[4] Griffin, R. B., and Terrill, L., "Measurement of Viscosity: Classroom Demonstration," Journal of Materials Education, Vol 21 (3 & 4), pp. 169- 174, 2000.

[5] Vander Schaaf, R., and Klosky, L., "Enhancing Introductory Mechanics using Physical Models," ASEE Zone 1 Meeting, West Point, NY, April 5-6, 2002.

COMPOSITE BEAR CANISTER

W. Richard Chung

Department of Chemical & Materials Engineering
San Jose State University
San Jose, California 95192-0082

Telephone 408-924-3927
e-mail wrchung@email.sjsu.edu

and

Steve Jara

and

Susan Suffel

NASA-Ames Research Center
Moffett Field
California 94035-1000

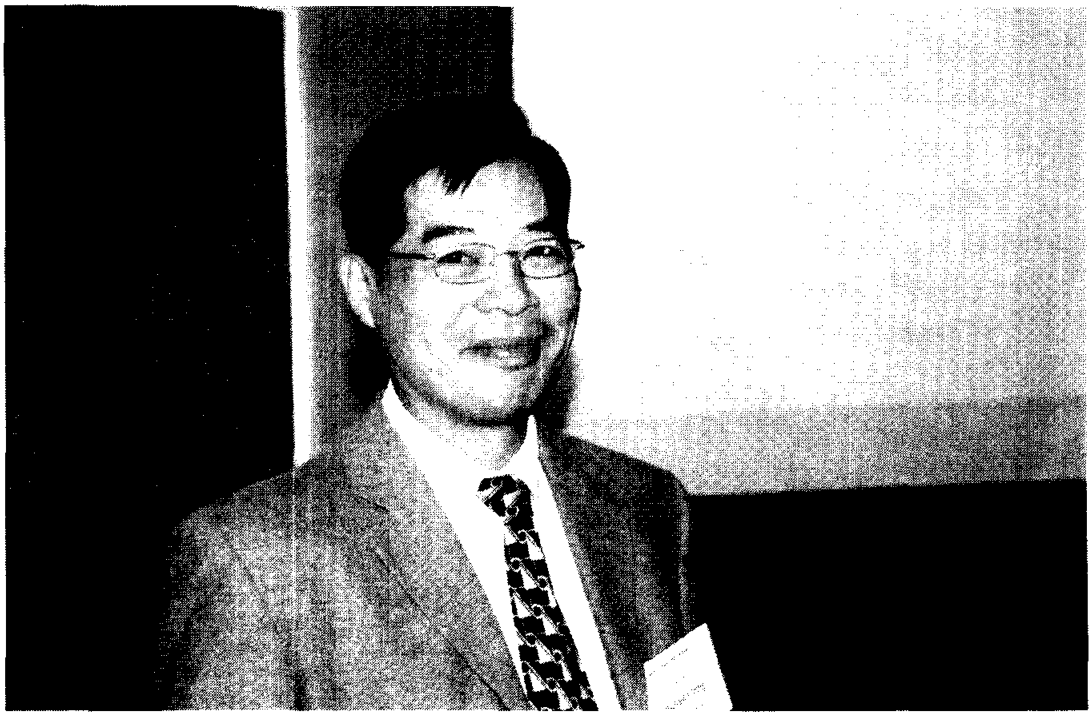

W. Richard Chung

Composite Bear Canister

W. Richard Chung, Department of Chemical and Materials Engineering, San Jose State University, San Jose, CA 95192-0082

and

Steve Jara and Susan Suffel, NASA-Ames Research Center, Moffett, Field, CA 94035-1000

Abstract

To many national park campers and mountain climbers saving their foods in a safe and unbreakable storage container without worrying being attacked by a bear is a challenging task. In some parks, the park rangers have mandated that park visitors rent a bear canister for their food storage. Commercially available bear canisters are made of ABS plastic, weigh 2.8 pounds, and have a 180 cubic inch capacity for food storage. A new design with similar capacity was conducted in this study to reduce its weight and make it a stiffer and stronger canister. Two prototypes incorporating carbon prepreg with and without honeycomb constructions were manufactured using hand lay-up and vacuum bag forming techniques. A 6061-T6-aluminum ring was machined to dimensions in order to reinforce the opening area of the canister. Physical properties (weight and volume) along with mechanical properties (flexural strength and specific allowable moment) of the newly fabricated canisters are compared against the commercial ones. The composite canister weighs only 56% of the ABS one can withstand 9 times of the force greater. The advantages and limitations of using composite bear canisters will be discussed in the presentation.

EDUCATIONAL OUTREACH PROGRAM SUMMARY

Charles R. Hayes

Executive Director
ASM International Foundation

Telephone 800-336-5152 extension 5506
e-mail crhayes@asminternational.org

ASM International Foundation

Educational Outreach Program Summary

MATERIALS CAMP

- Weeklong residential, hands-on learning.
- Have a lot of FUN while becoming a "science detective" conducting a failure analysis investigation
- High School students entering Junior or Senior year in the fall
- Pre-requisites: chemistry, physics, algebra II
- "Teach the Teacher" program for High School math / science teachers, held at University Michigan-Ann Arbor
- FREE tuition, housing, meals, extra-curricular events
- Competitive application process
- Locations in Seattle, Cleveland and Toronto in 2003
- World class all-volunteer faculty "Materials Mentors

K-12 TEACHERS

- "Living in a Material World": $500 grants for use in classroom materials projects
- High School Teachers MATERIALS CAMPs: Learn to use FUN, hands-on activities in math & science courses, focusing on materials
- "Fun in Metals": a lively and entertaining video that introducing materials to the young and young at heart

COLLEGE

- 40 + Undergraduate scholarships from full tuition to $500
- "LeaderShape" full scholarships: week-long leadership training emphasizing ethics
- Metallurgy / Materials Yearbook: list all colleges/universities that offer undergraduate and graduate degree programs in materials, ceramics and polymers. Complete "Who's Who.."faculty directory
- "QuickNotes": concise study guide on materials engineering
- ASM Student Chapter grants

SCIENCE FAIRS

- 500 awards to "best Materials Project" world-wide distribution
- Top 3 winners receive major cash grants and are invited to attend a MATERIALS CAMP

MORE INFORMATION:

- Chuck Hayes, Executive Director
- www.asminternational.org/foundation
- Phone: 1-800-336-5152
- Fax: 440-338-4634

UNDERSTANDING MOTOR OPERATION BY BUILDING A SINGLE-POLE PULSE ELECTRIC MOTOR

John A. Marshall

School of Applied Science
University of Southern Maine
Gorham, Maine 04038

Telephone 207-780-5447
e-mail jmarshal@usm.maine.edu

Understanding Motor Operation

by

Building an Single-Pole Pulse Electric Motor

Dr. John Marshall
University of Southern Maine
Gorham, ME 04038

Key Words: Conductors, insulators, enamel, magnetism, electromagnet, motor principles.

Prerequisite Knowledge: Basic knowledge of electricity and magnetism.

Objective: To understand basic electric motor principles and the materials needed to convert electricity and magnetism into motion.

Equipment:

- One 'D' cell alkaline battery
- One wide rubber band
- Two three inch lengths of heavy gauge copper wire
- One rectangular ceramic magnet
- Heavy gauge magnet wire
- Fine sandpaper
- Needle-nosed pliers

Introduction:

This is a tremendous activity, originally developed by Beakman's World, which I have perfected over the past ten years of teaching motor principles at the university level. Standard *Radio Shack* materials can be used. Heavy gauge copper wire is used to fabricate the coil cradle, and the cradle is attached to a standard "D" size battery with elastic bands. After winding the motor coil, we remove insulation from two locations with sandpaper and assemble the device.

When the un-insulted parts of the coil make contact with the cradle, current flows through the coil, making it into an electromagnet. Since magnets attract, the coil attempts to align itself with the magnet. However, when the coil turns to face the magnet, contact is broken, and the magnetic field collapses. Inertia causes the coil to continue around until contact is reestablished and the process repeats itself. In other words, the motor revolves continuously.

Procedure:

1. Start about 3 inches from the end of the magnet wire and wrap it seven times around the battery. Remove the battery and cut the wire, leaving a three-inch tail opposite the original starting point. Wrap the two tails around the coil so that the coil is held together and the two tails extend perpendicular to the coil.
2. On one tail, use fine sandpaper to completely remove the insulation from the wire. On the other tail, lay the coil down flat and lightly sand off the insulation from the top half of the wire <u>only</u>.
3. Using needle-nosed pliers, bend the two heavy copper wires. Form a cradle on one end that will hold the coil, and form a loop on the other end that will contact the battery.
4. Use a rubber band to hold the loop ends to the terminals of the "D" cell battery.
5. Stick the ceramic magnet on the side of the battery between the attached copper wires.
6. Place the coil in the cradle formed by the ends of the paper clips. You may have to give it a gentle push to get it started, but it should begin to spin rapidly.

Comments:

Balance is important, so be sure to center the two tails on either side of the coil.

If it doesn't spin, check to make sure that all of the insulation has been removed from the wire ends.

If it spins erratically, make sure that the tails on the coil are centered on the sides of the coil.

References:

Beakman's Electric Motor
Beakman's World Show

Bibliography:

Dr. JOHN ALLEN MARSHALL taught senior high school prior to receiving his Ph.D. from Texas A&M University. He has nineteen years of university teaching experience, and is currently the Coordinator of the Industrial Power and Control curriculum and laboratories as well as the Internship Coordinator for the University of Southern Maine's Department of Technology.

EXPERIMENTS WITH AN AC-DC DROPPING VOLTAGE WELDING POWER SOURCE

Carlos E. Umaña

Department of Materials
School of Mechanical Engineering
University of Costa Rica
San Jose, Costa Rica

Telephone: 506-207-4548
e-mail caruma@terraba.fing.ucr.ac.cr

EXPERIMENTS WITH AN AC-DC DROPPING VOLTAGE WELDING POWER SOURCE

Carlos E. Umaña
Consultant Engineer
San José, Costa Rica

KEY WORDS: Plasma, arc length, arc blow.

PREREQUISITE KNOWLEDGE: The students should be familiar with welding equipment and instruments for electrical measurements.

GENERAL OBJECTIVE: To familiarize students of a welding course with the arc behavior and the basic parameters of arc welding power sources.

SPECIFIC OBJECTIVES:

1. To experimentally obtain the characteristic voltage-current curves of a welding power source.
2. To demonstrate the arc blow effect.
3. To show the heat distribution between electrodes for AC versus DC mode operation.
4. To establish the heat distribution between electrodes for DC mode operation.

EQUIPMENT AND SUPPLIES: (See figure 1)

1. An AC-DC dropping voltage welding power source
2. Welding helmets, preferable auto darkening helmets
3. Two carbon electrodes about 1/4 inch diameter
4. Two stands and clamps to hold the carbon electrodes
5. Rubber bands to be used as electrode insulators
6. Two voltmeters
7. A clamp-on current meter
8. A plastic ruler
9. A magnet

PROCEDURE: (See figure 1)

PART 1.

1. Set up the connections as shown in figure 1.

2. Make sure the welding power source is off.
3. Set the welding power source to AC mode.
4. Alien and hold the electrodes with the clamps on the stands. Use rubber bands to isolate the electrodes from the clamps.
5. At least four students are required to run the experiment. Student 1 will be in charge of turning on and off the power source and taking the open circuit voltage (OCV) readings. Student 2 will take care of the clamp-on current readings. Student 4 will make the arc voltage readings and student 4 will be the leader who gives the instructions during the experiments and handle the electrodes to make the short circuit and start and end the arc.
6. Set the nominal current on the power source. It is recommended to use the following currents: 40, 60, 80 and 100 amperes.
7. With a plastic ruler set the required arc length by relocating the stands. It is recommended to use the following arc lengths for each nominal current: 6, 10, 12 and 15 mm.
8. Students who will face the arc should cover their faces with welding helmets before turning on the power source. Student 4 will execute step 10 to step 13
9. Give order to turn on the power source and ask for an OCV reading.
10. Tilt one stand until electrodes make contact with each other and ask for a short circuit current (I_{sc}) reading. Make sure the stand does not slip.
11. While the arc is on, return the stand to its normal position and ask for simultaneous current and arc voltage readings. Use a table like the one shown in Table 1 to collect the data.
12. Separate the electrodes and turn off the power source.
13. Repeat from step 7 until all arc lengths have been tested.
14. Repeat from step 6 until all nominal currents have been tested.

PART 2.

1. On the AC mode set the welding power source to the highest nominal current used before.
2. Set an arc length to about 8 mm.
3. Cover faces with welding helmets and give order to turn on the power source.
4. Tilt one stand until electrodes make contact with each other, then return the stand to its normal position while the arc is on.
5. Bring the magnet close to the arc and observe the arc behavior.
6. Observe and compare the incandescence intensity on both electrodes.
7. Change to the DC mode and set the welding power source to the highest nominal current used in part 1.
8. Repeat from step 2 to step 6.

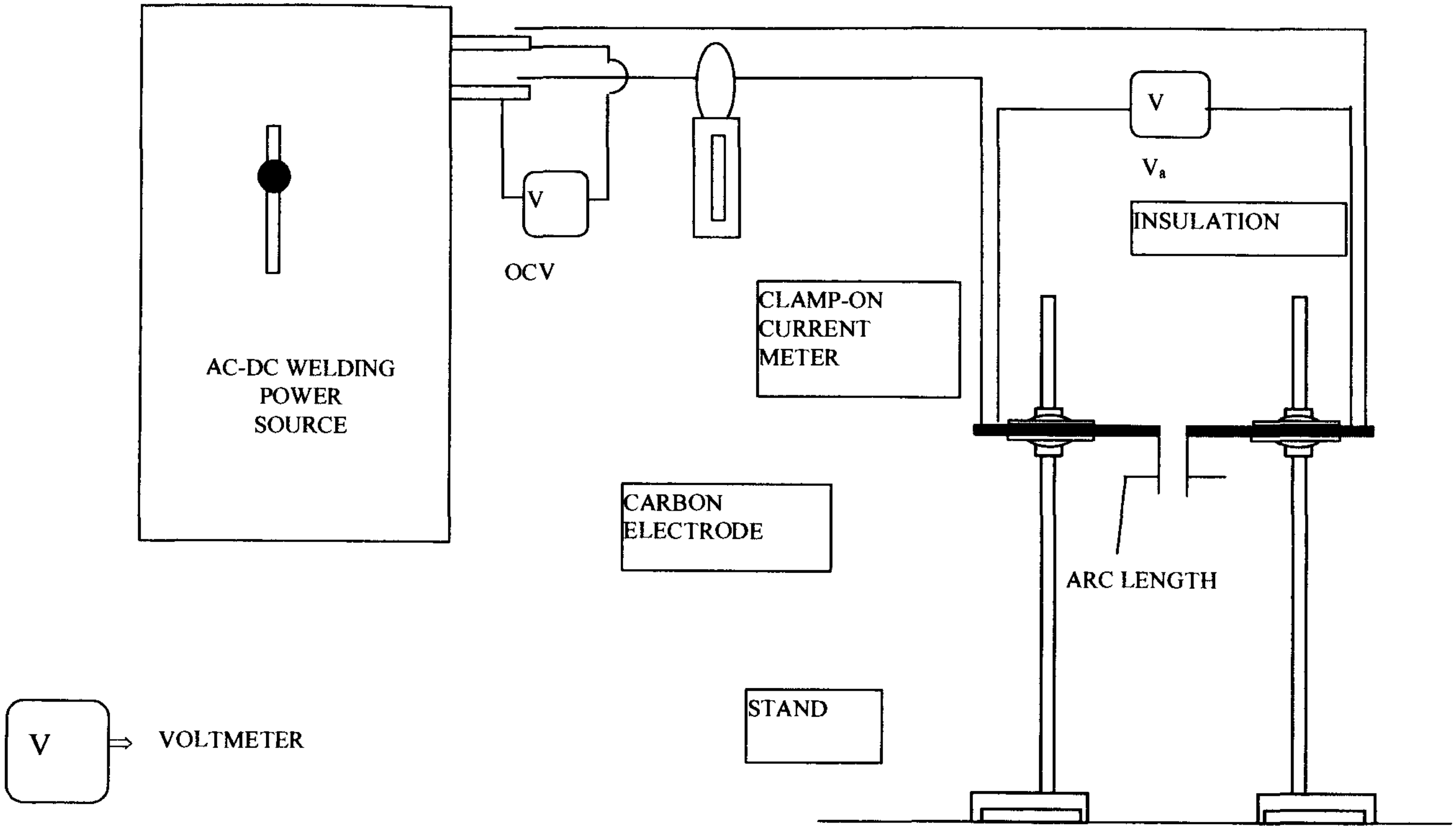

Figure 1. Experimental arrangement.

TABLE 1

I_n [A]	L [mm]	V_a [volts]	I_a [A]	I_{sc} [A]
40	6			
	10			
	12			
	15			
60	6			
	10			
	12			
	15			
80	6			
	10			
	12			
	15			
100	6			
	10			
	12			
	15			

RESULTS AND DISCUSSION:

For every nominal current plot the OCV at zero current and the average short circuit current at zero voltage. Also plot V_a versus I_a and trace curves as shown schematically in figure 2. Each curve simulates the actual manual welding operation and describes how the machine reacts to a variation of arc lengths. The shorter the arc the higher the current and viceversa. Curves are steeper for lower nominal currents.

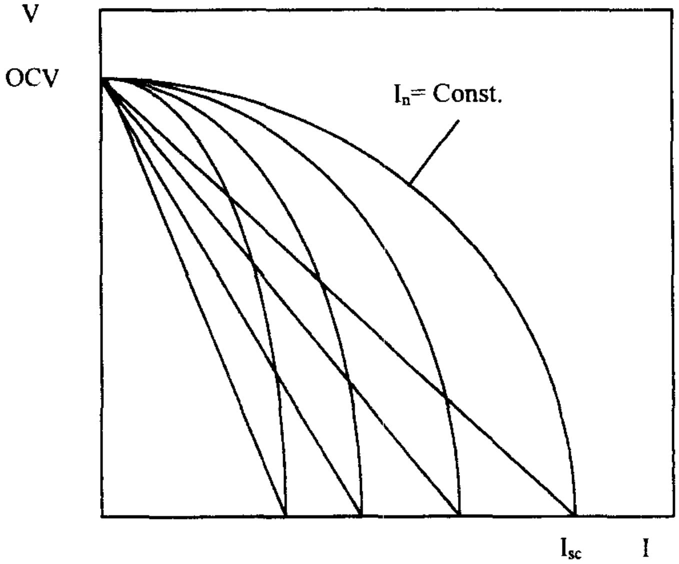

Figure 2. Schematic dropping voltage-current curves.

The magnet test shows how the DC arc can be affected by a magnetic field. This effect makes the welding process difficult and increases the possibility of weld defects.

For AC current heat distribution is uniform in both electrodes. Both show the same incandescence intensity. On the other hand for DC mode the anode or positive electrode generates more heat than the cathode (-) as can be deduced from differences in incandescence intensity between electrodes. This result only applies to carbon electrode arc in air and should not be taken as a rule, the anode is not always the hottest electrode due to the fact that heat distribution between anode and cathode depends on the kind of electrodes and the type of atmosphere. As can be deduced from these experiment, polarity is therefore a very important parameter in DC welding processes.

INSTRUCTOR NOTES:

Extreme precautions should be taken in order to avoid accidental eye arc exposure and burns caused by touching hot electrodes.

REFERENCES:

1. The Procedure Hand book of Arc Welding, The Lincoln Electric Company:, 12th ed., 1973.
2. Metals Handbook, Vol. 6, ASM, 8th ed., 1971.

ACKNOWLEDGMENTS:

The author wishes to thank Prof, Allan Bloomfield for reviewing the grammar and vocabulary of this paper.

SCIENCE BUDDIES

Gina Han

Program Director
Science Buddies
The K. L. Hess Family Charitable Foundation
Carmel, California 93921

Telephone: 408-773-8882
e-mail gina@sciencebuddies.org

SCIENCE
BUDDIES

Abstract for National Educators Workshop

FACT: Did you know that California students tied for dead last among the 50 states in the most recent national assessment of science education?

Science Buddies is a peer e-mentoring program for Bay Area middle and high school students with a fun, hands-on approach to science and access to science-related career role models. The goal is for students to complete a science fair project and to enter it in a local science fair.

How Science Buddies is unique:

1. PEER mentoring: Students help other students. High school "Mentors" are trained to take the lead in guiding the less experienced student who does the actual project. The team "Advisor" (usually a science professional) serves as backup and sometimes takes a more active role when necessary.
2. CONVENIENT e-mentoring: All team interaction takes place via an online message board monitored by Science Buddies staff. Check in anytime, anywhere there's Internet access.
3. FRAMEWORKED: The interactive Web site leads students through a step-by-step project framework, places how-to information at their fingertips, and provides samples.

Each Advisor is matched with a student team (a middle schooler and a high school Mentor) interested in the Advisor's area. The Advisor helps them refine a topic suitable to their skill level that leverages the Advisor's background.

What Science Buddies looks for in Advisors:

- Desire to foster interest in the sciences at a pivotal age.
- Wish to give back to the community in a way that doesn't take a lot of time but has high value.
- Has a science or engineering background by education and/or profession.
- Accesses the Internet and email on a regular basis.

For more information, visit www.sciencebuddies.org.

Contact:

Gina Han, Program Director
gina@sciencebuddies.org

REPORT DOCUMENTATION PAGE

Form Approved
OMB No. 0704-0188

1. REPORT DATE *(DD-MM-YYYY)*
01- 05 - 2003

2. REPORT TYPE
Conference Publication

3. DATES COVERED *(From - To)*

4. TITLE AND SUBTITLE
National Educators' Workshop: Update 2002

Standard Experiments in Engineering, Materials Science, and Technology

5a. CONTRACT NUMBER

5b. GRANT NUMBER

5c. PROGRAM ELEMENT NUMBER

6. AUTHOR(S)
Compiled by: Prior, Edwin J.;

Jacobs, James A.; and Chung, W. Richard

5d. PROJECT NUMBER

5e. TASK NUMBER

5f. WORK UNIT NUMBER
772-30-10-32

7. PERFORMING ORGANIZATION NAME(S) AND ADDRESS(ES)
NASA Langley Research Center
Hampton, VA 23681-2199

8. PERFORMING ORGANIZATION REPORT NUMBER
L-18298

9. SPONSORING/MONITORING AGENCY NAME(S) AND ADDRESS(ES)
National Aeronautics and Space Administration
Washington, DC 20546-0001

10. SPONSOR/MONITOR'S ACRONYM(S)
NASA

11. SPONSOR/MONITOR'S REPORT NUMBER(S)
NASA/CP-2003-212403

12. DISTRIBUTION/AVAILABILITY STATEMENT
Unclassified - Unlimited
Subject Category 23
Availability: NASA CASI (301) 621-0390 Distribution: Standard

13. SUPPLEMENTARY NOTES
An electronic version can be found at http://techreports.larc.nasa.gov/ltrs/ or http://ntrs.nasa.gov/

14. ABSTRACT

This document contains a collection of experiments presented and demonstrated at the National Educators' Workshop: Update 2002 held in San Jose, California, October 13–16, 2002.

15. SUBJECT TERMS
Materials; Experiments; Education; Structures; K–12; Materials science; Composites; Plastics; Nanomaterials; Metals; Testing; Ceramics; Polymers; Optical materials; Materials curriculum; Early aviation; Future aviation

16. SECURITY CLASSIFICATION OF: a. REPORT	b. ABSTRACT	c. THIS PAGE	17. LIMITATION OF ABSTRACT	18. NUMBER OF PAGES	19a. NAME OF RESPONSIBLE PERSON / 19b. TELEPHONE NUMBER *(Include area code)*
U	U	U	UU	600	STI Help Desk (email: help@sti.nasa.gov) (301) 621-0390